



**HAL**  
open science

## Structure-property relationship for kinetics of the amines-CO<sub>2</sub> reaction in aqueous solutions

Gabriel Couchaux

► **To cite this version:**

Gabriel Couchaux. Structure-property relationship for kinetics of the amines-CO<sub>2</sub> reaction in aqueous solutions. Food and Nutrition. Université de Lorraine, 2013. English. NNT : 2013LORR0206 . tel-01750507

**HAL Id: tel-01750507**

**<https://hal.univ-lorraine.fr/tel-01750507v1>**

Submitted on 29 Mar 2018

**HAL** is a multi-disciplinary open access archive for the deposit and dissemination of scientific research documents, whether they are published or not. The documents may come from teaching and research institutions in France or abroad, or from public or private research centers.

L'archive ouverte pluridisciplinaire **HAL**, est destinée au dépôt et à la diffusion de documents scientifiques de niveau recherche, publiés ou non, émanant des établissements d'enseignement et de recherche français ou étrangers, des laboratoires publics ou privés.



## AVERTISSEMENT

Ce document est le fruit d'un long travail approuvé par le jury de soutenance et mis à disposition de l'ensemble de la communauté universitaire élargie.

Il est soumis à la propriété intellectuelle de l'auteur. Ceci implique une obligation de citation et de référencement lors de l'utilisation de ce document.

D'autre part, toute contrefaçon, plagiat, reproduction illicite encourt une poursuite pénale.

Contact : [ddoc-theses-contact@univ-lorraine.fr](mailto:ddoc-theses-contact@univ-lorraine.fr)

## LIENS

Code de la Propriété Intellectuelle. articles L 122. 4

Code de la Propriété Intellectuelle. articles L 335.2- L 335.10

[http://www.cfcopies.com/V2/leg/leg\\_droi.php](http://www.cfcopies.com/V2/leg/leg_droi.php)

<http://www.culture.gouv.fr/culture/infos-pratiques/droits/protection.htm>



# THESE

Pour l'obtention du grade de  
**Docteur de l'Université de Lorraine**

Spécialité : Génie des procédés et des produits

Soutenue le 24 octobre 2013 par

**Gabriel Couchaux**

## **Relation Structure-Propriété pour la Cinétique de la Réaction Amine-CO<sub>2</sub> en Solution Aqueuses**

### **Jury :**

Pr. Manuel Ruiz-Lopez	Président
Pr. Walter Fürst	Rapporteur
Pr. Didier Villemin	Rapporteur
Pr. Lionel Estel	Examineur
Dr. Mohamed Kanniche	Examineur
Pr. Danielle Barth	Directrice de thèse
Dr. Julien Grandjean	Promoteur IFP Energies nouvelles

**École doctorale : RP2E**



## **PhD Thesis**

Presented by

**Gabriel COUCHAUX**

*MSc in Analytical Chemistry of the UNIVERSITY of POITIERS*

In partial fulfillment of the requirements for the degree of

**Doctor of Philosophy**

Speciality: Process and product engineering

---

# **Structure-Property Relationship for Kinetics of Reaction between Amines and Carbon Dioxide in Aqueous Solutions**

---

*Defended on October 24<sup>th</sup>, 2013 in front of a jury composed of*

President	Pr. Manuel RUIZ-LOPEZ, director of research (SRSMC, University of Lorraine, Nancy)
Reviewers	Pr. Walter FÜRST, professor (ENSTA-Paris Tech, Paris) Pr. Didier VILLEMIN, professor (LCMT, ENSICAEN, Caen)
Examinators	Pr. Lionel ESTEL, professor (LSPC, INSA Rouen, Rouen) Dr. Mohamed KANNICHE, researcher-expert (EDF, Chatou)
Advisors	Pr. Danielle BARTH, professor (LRGP, University of Lorraine, Nancy) Dr. Julien GRANDJEAN, research engineer (IFP Energies nouvelles, Solaize)

Work prepared at **Laboratory Reaction and Process Engineering** (UMR 7274 CNRS of the UNIVERSITY of LORRAINE, Nancy, France) and at **IFP Energies nouvelles** (Solaize, France)



*«Shoot for the moon. Even if you miss, you will land among the stars. »*  
*«Il faut viser la lune car même en cas d'échec on atterrit dans les étoiles. »*

Oscar WILDE

*To my family*



## REMERCIEMENTS

Bien qu'une thèse soit un exercice qui nécessite une importante implication personnelle, elle résulte également de la contribution d'un grand nombre de personnes. Je souhaite dans cette partie adresser mes plus sincères remerciements, dans ma langue maternelle, aux principales personnes qui m'ont soutenu tant professionnellement que personnellement et qui ont contribué à faire de ce travail ce qu'il est.

D'abord je souhaite remercier Lionel ESTEL, Walter FÜRST, Mohamed KANNICHE, Manuel RUIZ-LOPEZ et Didier VILLEMEN, membres du jury de thèse, pour avoir accepté d'évaluer ce travail, pour votre ouverture et pour la pertinence de votre évaluation et de vos remarques.

Je souhaite remercier Denis GUILLAUME et Alain METHIVIER pour m'avoir donné une chance de prouver ma valeur en m'accueillant au sein de la direction catalyse et séparation et du département séparation d'IFP Energies nouvelles de Solaize. Je vous remercie également pour votre accessibilité, votre écoute, l'intérêt que vous avez pour les thésards et vos précieux conseils notamment pour la recherche d'emploi.

Je souhaite remercier Danielle BARTH, ma directrice de thèse, ainsi que Julien GRANDJEAN et Marc JACQUIN, mon promoteur et co-promoteur de thèse. Vous m'avez quotidiennement appris le métier de chercheur en me présentant aussi bien la satisfaction que l'on peut en tirer et les difficultés que l'on peut rencontrer. J'ai beaucoup appris de vous et vous en suis éternellement reconnaissant. Je vous remercie d'avoir cru en moi et espère avoir été à la hauteur de vos espérances !

Je souhaite remercier Corinne SAGNARD et Olivier DELPOUX, les encadrants de mon précédent stage pour m'avoir préparé à la recherche et pour m'avoir soutenu dans cette démarche. Vous m'avez permis de relever plus sereinement ce défi que représente un doctorat.

Je souhaite remercier Mohamed RIFAI, Alexandre FONTENAY et Virgil CREPIN LISSASSI, tous les trois stagiaires dont les travaux ont été ici essentiels. Je vous remercie pour votre sérieux, votre implication et d'avoir été indulgent avec mon encadrement qui n'en était encore qu'à ses débuts !

Je souhaite remercier mes collègues du laboratoire solvants de m'avoir accueilli parmi vous et pour l'aide que vous avez pu m'apporter. Laétitia GIRAUDON pour ton soutien au début et tout au long de ces trois années ; Monique PRIGENT pour ta bonne humeur bretonne quotidienne et ton goût prononcé pour la métrologie ; Leslie BONNARD pour ta joie, ton naturel et tes pas de danse maintenant célèbres ; Laurent RENAUDOT pour tous les débats et les conversations intéressantes ; Fabrice PAILLE pour tes visites du soir et pour ces bons moments passés avec le Titrino ; Thierry HUARD pour l'aide que tu m'as apporté pendant les réunions et les randonnées passés ensemble ; et Pierre-Louis CARETTE pour l'important soutien que tu me communiquais régulièrement (et même encore aujourd'hui !).

Je souhaite remercier les collègues des autres divisions pour m'avoir aidé sur les sujets connexes ; Pascal DUCHENE sur la modélisation et l'explication de la résolution de modèles algébriques-différentiels ; Aziz FARAJ sur les aspects statistiques, pour ta pédagogie, ta passion et pour avoir prouvé que l'intelligence est bien collective ; Nicolas LALOUE pour les aspects procédés, pour ton soutien et m'avoir rappelé que les présentations sont aussi des moments de plaisir ; Javier PEREZ-PELLITERO pour ton apport considérable sur le nouveau descripteur et pour avoir permis de m'initier à la modélisation moléculaire ; Théodorus de BRUIN pour ton aide apportée dans le calcul de la valeur de descripteurs standards ; Bruno DELFORT et Dominique PICQ pour votre aide en chimie organique ; et Lionel MAGNA pour les discussions intéressantes sur l'encombrement stérique et les aspects QSAR.

Je souhaite remercier tous les collègues du département séparation pour votre accueil et votre bonne humeur quotidienne. Sandra pour les discussions sur les voyages, murders et autres qui vendaient du rêve ; Emmanuelle pour ta patience compte tenu de certain de tes collègues de bureau ; Danielle pour ton soutien et les discussions au café plus que mémorables ; Elsa pour toutes les conversations intéressantes ; Delphine pour avoir pu sauver mon orchidée ; Patrick pour m'avoir entraîné dans les peslerberie, j'espère un jour dépasser le maître ; Anthony pour les conversations intéressantes sur les mangas et ton soutien, j'espère vraiment être à la hauteur de ce que tu pensais de moi ; Alexandre pour ton humour taquin quotidien et ton soutien, prend bien soin de mon ancien bureau ; Jean-Pierre REYT pour la bonne humeur que tu apportes notamment au café ; Jean-Pierre COURCY pour les discussions sur le 7<sup>ème</sup> art ; Marc pour les débats intéressants et pour avoir su mettre ton grain de sel . Je remercie également Aurélie, Sonia, Christine, Morgane, Catherine, Karin, Michel, Arnaud, David, Philibert et Fabien avec qui je garde aussi en souvenir d'excellents moments.

Je souhaite remercier mes collègues de bureau. Sophie je te remercie pour tout ce que tu as pu faire pour moi (et ça fait beaucoup de choses !) et tous les souvenirs qu'on a pu laisser dans ce bureau (des chants de Noël jusqu'à la manivelle du store). Claire je te remercie pour ces bons moments et d'avoir veillé sur moi bien que je n'ai pas toujours respecté tes consignes en partant plus tard que prévu. En fin de compte, je dois surtout vous remercier d'avoir su tolérer mon humour auquel vous étiez particulièrement exposées (surtout à la fin !).

Je souhaite remercier Sébastien, Emmanuel, Didier BERNARD, Didier ESPINAT, Olivia, Michèle, Christophe, Jérémie et Ludovic. Vous avez tous contribué à m'aider soit en assouvissant une partie de ma curiosité, ou en m'aidant à m'installer sur Lyon ou simplement en créant des petits moments spéciaux qui ont beaucoup compté pour moi.

Je souhaite remercier les secrétaires, Nathalie, Sandrine, Sylvie et Valérie pour votre soutien, votre aide dans mes démarches administratives, votre bonne humeur et pour avoir su supporter mes visites parfois maladroitement.

Je souhaite remercier tous les étudiants stagiaires, en alternances, thésards et post-doc ! D'abord LE post-doc j'ai nommé Romain, alias RR. Je te remercie pour tous ces bons souvenirs, notamment concernant tes talents de commentateur sportif mais aussi pour m'avoir demandé de participer à tes expériences nocturnes à hautes températures !

Je souhaite remercier les nombreux « anciens ». Marco pour tes précieux conseils avant ton départ ; Vincent pour toutes tes anecdotes croustillantes, tes conseils de rédaction de thèse, ta définition de la fin de thèse et pour m'avoir permis de m'intégrer parmi les thésards ; Edder pour avoir été assez loco pour que je sois ton co-voitureur pendant ta dernière année de thèse et pour toutes les références croustillantes que tu m'as indiqué ; Nabil pour ta bonne humeur, tes visites et pour m'avoir fait profiter de ancienneté de ta confiance sans qu'il y ait anguille sous roche ; Laure et Lin pour m'avoir m'aidé quand j'avais besoin d'un coup de main ; Jérémy pour ton art de la présentation, ton calme légendaire, ta sportivité insoupçonnée (particulièrement au badminton) et nos conversations passionnées ; Lilia pour m'avoir initié à la salsa ; Bertrand pour tes accompagnements à la guitare avec les PHD .

Je souhaite remercier les collègues de la promo 2013. Alexandre pour cette complicité créée pendant 3 ans, les discussions passionnées sur divers sujets notamment dans la voiture, mon initiation à la batterie et à D3 et pour le soutien mutuel tout au long de ces 3 années ; Caroline pour avoir présidé cette belle bande de thésards pendant un an et su être à l'écoute des autres, pour m'avoir invité pour des événements qui te tenait à cœur et pour ta franchise ; Maria et Rim pour les bons moments passés ensemble notamment à l'ADIFP et pour m'avoir permis de découvrir la Norvège ; Emanuelle, Thibault et Guillaume pour la pause de 18h, les divers trips avec chacun d'entre vous et notre soutien mutuel en dernière année .

Je souhaite remercier les « p'tis jeunes ». Yoldès pour ta gentillesse, ton soutien et ta patience avec Marc ; Camille GOUEDARD pour ta gentillesse et surtout toutes les crises de rire tant plébiscitées ; Cécile pour tes coups de téléphone, ton apprentissage de l'art de déranger les autres et de leur mettre la pression ; Camille MORIN pour ces nombreux souvenirs notamment celui dans le sud ; Déborah pour toutes les niaiseries que j'ai aimé partagé et pour savoir prendre soin de Jérem ; Alban pour ton idéalisme, ton ouverture, pour ton esprit musical que je partage, le skol, la viking attitude et ton aide diabolique à la fin de la thèse ; Régis pour la légende de l'ESPCI et les anecdotes croustillantes notamment sur le TIC et ton esprit festif.

Je remercie également, Léa, Stefânia, Laure BRACONNIER, Laure BOURSIER, Taha, Fouad, Vincent L., Vincent G., Anthony, Fabien, Agnès, Florine, Ferdaous, Sofia, Joachim, Benoît, Marie Lou pour tous ces bons moments.

Je souhaite remercier Pauline, Thierry, Patrice, Nicolas et Daniel pour les bons moments passés avec Zik à la Raf à faire sonner les murs de la raffinerie et en mémoire de nos fameuses performances !

Je souhaite enfin remercier ma famille et Céline qui m'ont toujours soutenu et encouragé à poursuivre dans cette voie qui m'a toujours passionné. Sans vous, ne serait-ce qu'envisager de faire une thèse n'aurait pas été possible et j'espère que je peux vous rendre fier aujourd'hui.

A vous tous et ceux que j'ai pu oublier je vous suis éternellement reconnaissant.

J'ai vécu grâce à vous une des meilleures expériences de ma vie.

Je vous souhaite le meilleur pour la suite !

# Table of contents

---

TABLE OF CONTENTS .....	I
TABLE OF FIGURES .....	VII
TABLE OF TABLES .....	XV
NOMENCLATURE.....	XXI
CHAPTER I : GENERAL INTRODUCTION.....	1
CHAPTER II : STATE OF THE ART.....	3
1 Global warming .....	3
2 Carbon capture and storage.....	6
2.1 Storage .....	6
2.2 Transport.....	7
2.3 Capture.....	7
3 Amine scrubbing capture process.....	13
3.1 Description of the process.....	13
3.2 Natural gas treatment .....	14
3.3 Performance of the process .....	15
3.4 Choice of the solvent .....	16
3.5 Conclusion .....	17
4 The amine – carbon dioxide reaction .....	18
4.1 Definitions.....	18
4.2 Instantaneous reactions .....	19
4.3 Kinetically limited reactions .....	19
4.4 Conclusion .....	24
5 Experimental techniques .....	24
5.1 Measurement of CO <sub>2</sub> absorption flow rate .....	24
5.2 Rapid mixing methods .....	25
5.3 Conclusion .....	26
6 Methods for data treatment .....	26
6.1 Numerical method.....	26

6.2	Analytical method.....	26
7	Conclusion.....	27
<b>CHAPTER III : CRITICAL REVIEW OF THE LITERATURE .....</b>		<b>29</b>
1	Stopped-flow data.....	29
2	First order kinetic constants .....	32
3	Effect of the concentration .....	33
3.1	Analysis of the raw data.....	33
3.2	Tertiary amines .....	35
3.3	Primary and secondary amines .....	38
3.4	Multi-amines .....	48
4	Effect of temperature .....	50
4.1	Statistical compensation.....	51
4.2	Physico-chemical compensation.....	52
5	Conclusion and scope of this work.....	54
<b>CHAPTER IV : METHODOLOGY .....</b>		<b>57</b>
1	Experimental techniques .....	57
1.1	Stopped-flow technique .....	57
1.2	Acid-base titration.....	60
2	Characterisation of apparent kinetic constants .....	64
2.1	Numerical method.....	65
2.2	Analytical method.....	74
2.3	Experimental optimization.....	77
2.4	Method of data treatment .....	84
2.5	Uncertainty of the apparent kinetic constant .....	85
3	Characterisation of the constants of the kinetic model .....	85
3.1	Semi-empirical model.....	86
3.2	Uncertainty of the constants of the kinetic model.....	88
4	Design of experiments .....	89
4.1	General features .....	89
4.2	Tertiary amines .....	90
4.3	Primary and secondary amines .....	92
4.4	Multi-amines .....	98

5	Conclusion.....	99
<b>CHAPTER V : INTERPRETATION OF EXPERIMENTAL RESULTS...101</b>		
1	Overview .....	101
1.1	Definitions.....	101
1.2	Amines of the class A .....	102
1.3	Amines of the class B .....	102
2	Tertiary and sterically hindered secondary amines .....	104
2.1	Comparison with results from literature .....	104
2.2	Alkanolamines .....	105
2.3	Alkylamines .....	108
2.4	Other tertiary amines.....	110
2.5	Secondary amines .....	112
2.6	Conclusion .....	113
3	Primary amines .....	114
3.1	Effect of the basicity .....	114
3.2	Effect of the steric hindrance .....	118
3.3	Enantiomerism .....	122
3.4	Conclusion .....	122
4	Acyclic secondary amines.....	124
4.1	Change of degree of substitution .....	124
4.2	Effect of the basicity .....	125
4.3	Effect of the steric hindrance .....	127
4.4	Conclusion .....	132
5	Cyclic secondary amines.....	134
5.1	Effect of the basicity .....	134
5.2	Effect of the steric hindrance .....	136
5.3	Conclusion .....	137
6	Multi-amines.....	138
6.1	N,N,N',N'-Tetramethylethylenediamine .....	138
6.2	1-Methylpiperazine .....	139
6.3	Piperazine.....	140
6.4	Conclusion .....	142
7	Discussion .....	142

8	Conclusion.....	146
CHAPTER VI : QSPR MODELLING.....		147
1	General points.....	147
2	QSPR descriptor model.....	148
2.1	Descriptors.....	148
2.2	QSPR model.....	160
2.3	Conclusion.....	169
3	Results.....	170
3.1	Modelling of tertiary and sterically hindered amines.....	170
3.2	Modelling of primary and secondary amines.....	177
4	Discussion.....	188
4.1	Tertiary and sterically hindered amines.....	188
4.2	Primary and secondary amines.....	190
5	Conclusion.....	196
CHAPTER VII : GENERAL CONCLUSION AND PERSPECTIVES.....		199
CHAPTER VIII : BIBLIOGRAPHIC REFERENCES.....		203
CHAPTER IX : APPENDICES.....		213
1	Bibliography.....	213
1.1	Kinetic constants and orders at 25°C.....	213
1.2	Bibliography: variation of $k_{ter1}$ and $k_{ter2}$ with temperature.....	215
1.3	Bibliography: kinetic constants $k_1$ and $k_2$ .....	218
2	Taft constant.....	219
3	Experimental method.....	220
3.1	Determination of CO <sub>2</sub> concentration in aqueous solutions.....	220
3.2	Experimental optimization.....	222
4	Additional information concerning the numerical model.....	226
4.1	Thermodynamic parameters.....	226
4.2	Kinetic parameters.....	227
4.3	Conductivity parameters.....	228
5	Additional information concerning the analytical model.....	230
5.1	Tertiary amines.....	230

5.2	Primary and secondary amines .....	232
6	List of studied molecules .....	236
6.1	Primary amines .....	236
6.2	Secondary amines .....	239
6.3	Tertiary amines .....	243
6.4	Multi-amines .....	246
6.5	Acidic solutions .....	246
6.6	Gas .....	246
7	Kinetic results of each studied amine for each concentration .....	247
8	Thermodynamic and kinetic parameters of each molecule .....	277
9	Molecular descriptors.....	285
9.1	Complete list of molecular descriptors .....	285
9.2	Values of molecular descriptors for primary amines .....	290
9.3	Values of molecular descriptors for secondary amines .....	298
9.4	Values of molecular descriptors for tertiary amines .....	306
10	Nitrogen accessible surface.....	314
10.1	Algorithm to calculate the nitrogen accessible surface.....	314
10.2	Values of nitrogen accessible surface of studied monoamines.....	321
11	QSPR model .....	322
11.1	Justification of the proportion of data in each set.....	322
11.2	Justification of the number of model used.....	323
12	Coefficients of the second order models .....	325
12.1	Kinetic constant $k_1$ tertiary and sterically hindered amines.....	325
12.2	Kinetic constant $k_1$ primary and secondary amines .....	326
12.3	Kinetic constant $k_2$ primary and secondary amines .....	330
13	Results of the QSPR modelling.....	333
13.1	Tertiary and sterically hindered amines.....	333
13.2	Primary and secondary amines .....	335
14	French detailed summary (résumé détaillé en français).....	338



## Table of figures

---

Figure II-1. Greenhouse effect.....	3
Figure II-2. Origin of emissions of carbon dioxide in the atmosphere in 2009 (International Energy Agency, 2011). .....	4
Figure II-3. Envisaged scenarios to reduce emission of carbon dioxide in the atmosphere.(International Energy Agency, 2008) .....	5
Figure II-4. Principle of carbon capture and storage (Total, 2013). .....	6
Figure II-5. Classical oxy-combustion process (Vattenfall, 2013a). .....	9
Figure II-6. Chemical looping combustion process (CLC, 2013). .....	9
Figure II-7. Capture of CO <sub>2</sub> by pre-combustion process (Vattenfall, 2013b). .....	10
Figure II-8. Capture of CO <sub>2</sub> by postcombustion (Zero, 2013). .....	12
Figure II-9. Schematic representation of the amine scrubbing capture process (Capture Ready, 2013). .....	14
Figure II-10. Example of primary (R <sub>1</sub> NH <sub>2</sub> ), secondary (R <sub>1</sub> R <sub>2</sub> NH) and tertiary amines (R <sub>1</sub> R <sub>2</sub> R <sub>3</sub> NH). .....	18
Figure II-11. Apparent kinetic obtain by different authors and experimental technique for diethanolamine at 25 °C in function of the amine concentration (Rinker <i>et al.</i> , 1996). .....	25
Figure III-1. Apparent kinetic constants k <sub>0</sub> vs. molecules studied in the literature. ....	32
Figure III-2. Apparent kinetic constants vs. ethylethanolamine concentration (molecule n°9). Experimental results (black circles) and fit of experimental data (black line) according to Equation 15. T = 25 °C. ....	33
Figure III-3. Values of (k <sub>Am</sub> , n) from Equation 15 for tertiary amines (triangles), primary and secondary amines (circles) listed in Table III-1. Dashed lines represent values of (k <sub>Am</sub> , n) giving the same value of k <sub>0</sub> for [Am] = 100 mol.m <sup>-3</sup> . Setting n=1 for molecules n°5, 6 and 11 gives 5', 6', 11' .....	34
Figure III-4. Experimental apparent kinetic constant vs. 1-Dimethylamino-2-propanol concentration (molecule n°5) (black circles). Fit using affine function (blue line), power law function (black line) and linear function (red line). T = 25 °C. ....	35
Figure III-5. Kinetic constant $k'_{R_3N}$ values vs. tertiary amines pKa (black circles) and optimum estimation of parameters (black line). T = 25 °C. ....	38
Figure III-6. Kinetic constant $k'_{R_3N}$ values vs. tertiary amines pKa (black circles) and tert-Butylethanolamine (11) (red circle). Optimum estimation of parameters (black line). T = 25 °C. ....	39
Figure III-7. Apparent kinetic constant and order (k <sub>Am</sub> , n) for ethanolamines (n°7, 8, 9, 10 and 11) at 25 °C. Continuous lines iso-k <sub>0</sub> represent values of (k <sub>Am</sub> , n) giving the same value of k <sub>0</sub> for .....	40
Figure III-8. Response surface for average relative error below 1 % for k <sub>0</sub> modelled with zwitterion mechanism for piperazine at 30 °C (Rayer <i>et al.</i> , 2011). Projection of response surface on the log <sub>10</sub> (k <sub>NA</sub> ), log <sub>10</sub> (k <sup>'R<sub>2</sub>NH</sup> <sub>Dep</sub> ) plane is indicated by the continuous line. ....	44

Figure III-9. Variation of $\log(k_7)$ with $\log(K_6)$ for some amines studied by Conway <i>et al.</i> (2012a). A linear fit, realized only with cyclic amines indicate a relationship between $\log(k_7)$ and $\log(K_6)$ . Kinetic constant $k_7$ corresponds to the kinetic constant of the carbamic acid mechanism (Reaction 20) and $K_6$ correspond to the inverse of amine dissociation constant ( $K_a$ , Reaction 11).....	46
Figure III-10. Variation of kinetic constant $k_{Am}$ with pKa of molecules n°12 to 14. ....	46
Figure III-11. Variation of $\log(k_7)$ vs. $\log(K_6)$ for n-butylamine (n-BA), n-propylamine (n-PA), isobutylamine (IBA), 3-amino-1-propanol (3-AP), 1-amino-2-propanol (1-AP), monoethanolamine (MEA), sec-butylamine (SBA), 2-aminopropanol (2-AP), ammoniac ( $NH_3$ ), diethanolamine (DEA) and a series of cyclic secondary amines (black diamonds) determined by Conway <i>et al.</i> (2012b). A linear fit, realized only with cyclic amines indicate a relationship between $\log(k_7)$ and $\log(K_6)$ . The kinetic constant $k_7$ corresponds to the second order kinetic constant of the carbamic acid mechanism (Reaction 20) and $K_6$ correspond to the inverse of amine dissociation constant ( $K_a$ , Reaction 11). ....	47
Figure III-12. Calculated free energy of carbamate formation $\Delta G_{e2s}$ vs. logarithm of experimental reaction rate $k_2$ . Reaction rate $k_2$ correspond to the nucleophilic addition of the zwitterion mechanism (Reaction 16) (da Silva and Svendsen, 2007). ....	48
Figure III-13. Variation of $\log(k_7)$ vs. $\log(K_6)$ for piperazine (PZ), piperazine monocarbamate ( $PZCO_2^-$ ), N-methylpiperazine (N-MPIPZ), protonated piperazine ( $PZH^+$ ), cyclic mono-amines (black diamonds), sterically hindered amines (blue circles) and ammoniac (red square). The dashed line represents the linear relationship between $\log(k_7)$ and $\log(K_6)$ for cyclic mono-amines. The kinetic constant $k_7$ corresponds to the kinetic constant of the carbamic acid mechanism (Reaction 20) and $K_6$ correspond to the inverse of amine dissociation constant ( $K_a$ , Reaction 11) (Conway <i>et al.</i> , 2013).....	49
Figure III-14. Relation between Arrhenius parameters for $k_{ter1}$ (a) and for $k_{ter2}$ (b). ....	51
Figure III-15. Relation between Arrhenius parameters for $k_{ter1}$ with confidence ellipse area. ....	52
Figure III-16. Summary of our experimental and model approach to establish a quantitative structure-property relationship. ....	55
Figure IV-1. Stopped-flow CSA-20 equipment without thermostated bath. ....	58
Figure IV-2. Stopped-flow apparatus chart (Ali <i>et al.</i> , 2000). ....	59
Figure IV-3. Experimental set-up for preparation of saturated $CO_2$ solutions. ....	60
Figure IV-4. pH metric curve (blue line) and derivate (red line) obtained by titration of dimethylmonoethanolamine with hydrochlorid acid at $0.1 \text{ mol.m}^{-3}$ .....	61
Figure IV-5. pH metric curves (blue lines) and derivates (red lines). Titration of a mix of 27 g of $[CO_2] = 30 \text{ mol.m}^{-3}$ neutralized with 12 g of $[NaOH] = 100 \text{ mol.m}^{-3}$ by $[HCl] = 100 \text{ mol.m}^{-3}$ .....	62
Figure IV-6. Parity plot between the concentrations of $CO_2$ determined by titration of the theoretical concentrations of $CO_2$ according to Henry's law. ....	62
Figure IV-7. pH metric curves (blue lines) and derivates (red lines)obtained by titration of (a) N,N,N',N'-tetramethylethyldiamine (b) and N,N,N',N'-tetramethylhexanediamine experimental data (black circles), and fit with CurTiPlot (Curtiplot, 2013).....	64
Figure IV-8. Example of conductivity curve as a function of time obtained by stopped-flow technique. $[Monoethanolamine]=40 \text{ mol.m}^{-3}$ and $[CO_2]=4 \text{ mol.m}^{-3}$ before mixing.....	64
Figure IV-9. Density of monoethanolamine as a function of mass fraction. ....	66

Figure IV-10. [Monoethanolamine] = 40 mol.m <sup>-3</sup> and [CO <sub>2</sub> ] = 4 mol.m <sup>-3</sup> before mixing.(a) Conductance as function of time (circle) experimental and (line) modelled. $G_0 = 2 \times 10^{-3}$ m, $t_0 = 3$ ms and $k_0 = 76.7$ s <sup>-1</sup> ( $k_{R_2NH}^m = 5.40$ kg <sup>n</sup> .mol <sup>n</sup> .s <sup>-1</sup> and $n = 1$ ). (b) Evolution of the different concentrations as function of the time. ....	73
Figure IV-11. Conductivity curve as function of time: experimental (circle) and fit with analytical model (continuous line). [Monoethanolamine] = 40 mol.m <sup>-3</sup> and [CO <sub>2</sub> ] = 4 mol.m <sup>-3</sup> before mixing. ....	75
Figure IV-12. Apparent kinetic constant modelled of monoethanolamine with numerical method (NM) (black line), and determined with analytical method (AM) at the initial conditions (blue triangles) and at the final conditions (red squares). ....	76
Figure IV-13. Titration of a solution of [methyldiethanolamine] = 100 mol.m <sup>-3</sup> with [CO <sub>2</sub> ] = 100 mol.m <sup>-3</sup> . pH of the solution as function of the loading in carbon dioxide. Simulation realized using CurTiPlot. ....	78
Figure IV-14. Methyldiethanolamine. (a) Extremum of the ratio of the kinetic contribution of hydroxide ions on the apparent kinetic constant as a function of the concentration of amine. (b) Apparent first order kinetic constants $k_0$ as function of the amine concentration. ....	79
Figure IV-15. (a) Amplitude of the conductivity curve of monoethanolamine as function of the concentration of carbon dioxide. (b) Apparent kinetic constant as function of the concentration of amine. ....	81
Figure IV-16. Conductance of [piperazine] = 1.2 mol.m <sup>-3</sup> with [CO <sub>2</sub> ] = 0.09 mol.m <sup>-3</sup> before mixing as a function of the time. ....	82
Figure IV-17. Flowsheet of the experimental optimization to determine the apparent kinetic constant of the amine-CO <sub>2</sub> reaction. A stands for the amplitude. Symbols +/- respectively indicate a positive effect, no effect or a negative effect of the actions on the signal and kinetic ratios. ....	83
Figure IV-18. Flowsheet which indicates the method followed to treat conductivity curves. ....	84
Figure IV-19. Normal probability plot of data. [Monoethanolamine] = 40 mol.m <sup>-3</sup> and [CO <sub>2</sub> ] = 4 mol.m <sup>-3</sup> before mixing. ....	85
Figure IV-20. Average apparent kinetic constant as function of the amine concentration. Fit realized by least square regression (red dash line) and weighted least square regression (blue dot line). ....	87
Figure IV-21. Parity plot between the apparent kinetic constant $k_0^{Am}$ calculated from the $k_1$ , $k_2$ model vs. experimental apparent kinetic constant of $k_0^{Am}$ . Molecules of the Table III-1. Tertiary amines (red triangles). Primary and secondary amines (black circles). ....	87
Figure IV-22. Optimal value and area of confidence for the kinetic constants $k_1$ and $k_2$ for monoethanolamine. The area of confidence is limited by the ellipse. The interval of confidence calculated on each parameter is indicated by error bars. ....	89
Figure V-1. Kinetic constant $k_1$ as a function of the pKa for amines of the class A (black circles). ....	102
Figure V-2. Kinetic constant $k_2$ as a function of the kinetic constant $k_1$ . Amines of the class A (red triangles), of the class B (black circle), iso- $k_0$ lines (grey lines) and iso-order lines (colored lines). ....	103
Figure V-3. Kinetic constant $k_1$ as a function of the pKa for molecule studied in the literature (black circles) and our results (red circles). ....	104
Figure V-4. Kinetic constant $k_1$ as a function of the pKa for studied acyclic alcanolamines (red circles). Linear estimation realized with molecules 1310, 1311, 1312 and 1313. ....	105

Figure V-5. Kinetic constant $k_1$ as a function of the pKa for studied cyclic alkanolamines (green triangles) in comparison with acyclic alkanolamines (red circles). Linear estimation realized with molecules 1310, 1311, 1312, 1313, 1344, 1343 and 1345.....	107
Figure V-6. Kinetic constant $k_1$ as a function of the pKa for studied acyclic alkylamines (black squares) in comparison with acyclic alkanolamines (red circles) and cyclic alkanaolamines (green triangles). Linear estimation realized with molecules 1310, 1311, 1312, 1313, 1344, 1343 and 1345.....	108
Figure V-7. Kinetic constant $k_1$ as a function of the pKa for studied cyclic alkylamines (grey triangles) in comparison with acyclic alkylamines (black squares). Linear estimation realized with molecules 1310, 1311, 1312, 1313, 1344, 1343 and 1345.....	109
Figure V-8. Kinetic constant $k_1$ as a function of the pKa for studied other acyclic amines (orange diamonds). Linear estimation realized with molecules 1310, 1311, 1312, 1313, 1344, 1343 and 1345.....	110
Figure V-9. Kinetic constant $k_1$ as a function of the pKa for studied other cyclic amines (blue triangles). Linear estimation realized with molecules 1310, 1311, 1312, 1313, 1344, 1343, 1345 and 1351. Second linear estimation realized with molecules 1300, 1301, 1321, 1330, 1331, 1340, 1346, 1350, 1352 and 1353. ....	111
Figure V-10. Kinetic constant $k_1$ as a function of the pKa for studied secondary amines of the class A (purple stars). Linear estimation realized with molecules 1310, 1311, 1312, 1313, 1344, 1343, 1345 and 1351. Second linear estimation realized with molecules 1300, 1301, 1321, 1330, 1331, 1340, 1346, 1350, 1352 and 1353. ...	112
Figure V-11. Kinetic constant $k_1$ as a function of the pKa for studied amines of the class A. Linear estimation realized with molecules 1310, 1311, 1312, 1313, 1344, 1343, 1345 and 1351. Second linear estimation realized with molecules 1300, 1301, 1321, 1330, 1331, 1340, 1346, 1350, 1352 and 1353. ....	113
Figure V-12. Kinetic constant $k_2$ as a function of the kinetic constant $k_1$ for a series of linear primary amines. Alkylamines (black squares), alkanolamines (red circles), benzylamines (brown stars), etheramine (orange diamond) nitrilamine (blue triangle).....	115
Figure V-13. Evolution of kinetic constant $k_1$ (a) and $k_2$ (b) as a function of the pKa of a series of linear primary amines. Alkylamines (black squares), alkanolamines (red circles), benzylamines (brown stars), etheramine (orange diamond) nitrilamine (blue triangle). Regression has been realized without molecule 1100. ....	116
Figure V-14. Kinetic constant $k_2$ as a function of the kinetic constant $k_1$ for a series of derivates from tert-butylamine. Alkylamine (black square) and alkanolamines (red circles).....	117
Figure V-15. Evolution of kinetic constant $k_1$ (a) and $k_2$ (b) as a function of the pKa for a series of derivates of tert-butylamines. Alkylamine (black square) and alkanolamines (red circles).....	118
Figure V-16. Kinetic constant $k_2$ as a function of the kinetic constant $k_1$ for a series of alkylamines (black squares).....	119
Figure V-17. Evolution of kinetic constant $k_1$ (a) and $k_2$ (b) as a function of the Taft constant of a series of alkylamines (black squares). ....	120
Figure V-18. Kinetic constant $k_2$ as a function of the kinetic constant $k_1$ for primary amines. Effect of $\alpha$ and $\beta$ hindrance. Alkanolamines (red circles) and benzylamines (brown stars).....	121
Figure V-19. Kinetic constant $k_2$ as a function of the kinetic constant $k_1$ of two stereoisomerisms. ....	122
Figure V-20. Kinetic constant $k_2$ as a function of the kinetic constant $k_1$ for primary amines. ....	123
Figure V-21. Kinetic constant $k_2$ as a function of the kinetic constant $k_1$ for five series of amines. Alkylamines (black squares), alkanolamines (red circles), benzylamines (brown stars) and nitrilamines (blue triangles).....	124

Figure V-22. Kinetic constant $k_2$ as a function of the kinetic constant $k_1$ for a series secondary amines. Alkylamines (black squares), alkanolamines (red circles), benzylamine (brown star) and nitrilamine (blue triangle). .....	126
Figure V-23. Evolution of kinetic constant $k_1$ (a) and $k_2$ (b) as a function of the pKa for a series of secondary amines. Alkylamines (black squares), alkanolamines (red circles), benzylamine (brown star) and nitrilamine (blue triangle). Regression has been realized without molecule 1200.....	126
Figure V-24. Kinetic constant $k_2$ as a function of the kinetic constant $k_1$ for series of secondary alkylamines (black squares). .....	128
Figure V-25. Kinetic constant $k_2$ as a function of the kinetic constant $k_1$ for series of secondary benzylamines (brown stars) and alkanolamines (red circles). Trend obtained for alkylamines (black).....	129
Figure V-26. Kinetic constant $k_2$ as a function of the kinetic constant $k_1$ for series of secondary nitrilamines (blue triangles). Trend obtained for alkylamines (black), benzylamines (brown) and alkanolamines (red). .....	129
Figure V-27. Evolution of kinetic constant $k_1$ (a) and $k_2$ (b) as a function of the Taft constant of four series of secondary amines. Alkylamines (black squares), alkanolamines (red circles), benzylamines (brown stars) and nitrilamines (blue triangles).....	130
Figure V-28. Kinetic constant $k_2$ as a function of the kinetic constant $k_1$ for two secondary amines. Alkanolamines (red circles).....	132
Figure V-29. Kinetic constant $k_2$ as a function of the kinetic constant $k_1$ for acyclic secondary amines.....	133
Figure V-30. Kinetic constant $k_2$ as a function of the kinetic constant $k_1$ for a series of cyclic secondary amines. Alkyl secondary cyclic amines (grey triangles), 4-hydroxypiperidine (green triangle) and morpholine (blue triangle). .....	134
Figure V-31. Evolution of kinetic constant $k_1$ (a) and $k_2$ (b) as a function of the pKa for a series of secondary cyclic amines. Alkyl secondary cyclic amines (grey triangles), 4-hydroxypiperidine (green triangle) and morpholine (blue triangle).....	135
Figure V-32. Kinetic constant $k_2$ as a function of the kinetic constant $k_1$ for a series of secondary cyclic amines. Derivate of 4-hydroxypiperidine (Green triangles). .....	136
Figure V-33. Kinetic constant $k_2$ as a function of the kinetic constant $k_1$ for all studied secondary cyclic amines. ....	137
Figure V-34. Kinetic constant $k_1$ as a function of the pKa for mono- tertiary amines which do not contain accessible alcohol groups and N,N,N',N'-tetramethylethylenediamine. ....	138
Figure V-35. Kinetic constant $k_2$ as a function of the kinetic constant $k_1$ for a series of secondary cyclic monoamines and 1-methylpiperazine. Alkyl cyclic amines (grey triangles), 4-hydroxypiperidine (green triangle) and morpholine (blue triangle).....	139
Figure V-36. Evolution of kinetic constant $k_1$ (a) and $k_2$ (b) as a function of the pKa for a series of secondary cyclic amines and 1-methylpiperazine. Alkyl cyclic amines (grey triangles), 4-hydroxypiperidine (green triangle) and morpholine (blue triangle). .....	140
Figure V-37. Kinetic constant $k_2$ as a function of the kinetic constant $k_1$ for a series of secondary cyclic monoamines, 1-methylpiperazine and piperazine. Alkyl cyclic amines (grey triangles), 4-hydroxypiperidine (green triangle) and morpholine (blue triangle). .....	141

Figure V-38. Evolution of kinetic constant $k_1$ (a) and $k_2$ (b) as a function of the pKa for a series of secondary cyclic amines, 1-methylpiperazine and piperazine. Alkyl cyclic amines (grey triangles), 4-hydroxypiperidine (green triangle) and morpholine (blue triangle).	141
Figure V-39. Kinetic constant $k_2$ as a function of the kinetic constant $k_1$ for all mono-amines studied. Tertiary amines (red triangles), primary amines (blue circles), acyclic secondary amines (green diamonds), cyclic secondary amines (black stars).	142
Figure V-40. (a) Based-catalyzed hydration mechanism. (b) Zwitterion mechanism for tertiary amines.	143
Figure V-41. Evolution of kinetic constant $k_1$ (a) and $k_2$ (b) as a function of the pKa for the series of tertiary amines and non sterically hindered primary and secondary amines studied.	145
Figure VI-1. Van der Waals surface.	151
Figure VI-2. Projection of the molecule in the z direction.	152
Figure VI-3. Dendrogram of the 110 generic theoretical descriptors. Dashed line indicates a partition of descriptors into 12 classes which correspond to an explicated inertia of 77.0 %.	154
Figure VI-4. Scatter plot of variables of the class 1. Inertia of the class = 91.4 %. Variables are HOMOg, HOMOLUMOg, HOMOaq, HOMOLUMOaq.	155
Figure VI-5. Illustration of the nitrogen accessible surface for the case of trimethylamine.	156
Figure VI-6. (a) Degree of substitution vs. accessible surface for the molecules studied in this work. (b) Relation between accessible surface and Taft constant for alkanolamines.	158
Figure VI-7. Histogram of tertiary amines data for (a) kinetic constant $k_1$ and for (b) the decimal logarithm of kinetic constant $k_1$ .	160
Figure VI-8. On left, one model with 80 % of the molecules in the training set and 20 % in a prediction set. On right, M different models composed each of 60 % of the molecules in the training set, 20 % in the validation set and 20 % in the prediction set.	164
Figure VI-9. Example of distribution of RMSEP of validation for modelling of $\log_{10}(k_1)$ of amines which form carbamates with 68 descriptors.	166
Figure VI-10. Flowchart of the obtaining method of the QSPR first order model.	168
Figure VI-11. Flowchart of the obtaining method of the QSPR second order model.	169
Figure VI-12. Distribution of the RMSEP of the prediction sets of $k_1$ of tertiary and sterically hindered amines (average, $Q_{2.5}$ and $Q_{97.5}$ ) as a function of the number of terms used in the corresponding QSPR model. (a) All results. (b) Zoom between 0 and 40 terms. First order results (black circles), second order results with 24 descriptors (red squares) and second order results with 7 descriptors (green triangles). The number of the modelling is also indicated.	171
Figure VI-13. Parity plot between modelled kinetic constant $k_1$ and experimental kinetic constant of tertiary and sterically hindered amines. (a) First order QSPR model. (b) Second order QSPR model.	174
Figure VI-14. Kinetic constant $k_1$ of molecules of the prediction set of tertiary amines as a function of the pKa. (a) First order QSPR model. (b) Second order QSPR model. Experimental values (black circles) and predicted values (red open circles). The error bar corresponds to the projections of the confidence ellipse on the experimental kinetic constant $k_1$ .	175

Figure VI-15. Parity plot between modelled and experimental apparent kinetic constant of tertiary and sterically hindered amines. (a) First order QSPR model. (b) Second order QSPR model. Error bars correspond to the experimental confidence interval.....	176
Figure VI-16. Modelling of kinetic constant $k_1$ of primary and secondary amines. Average RMSEP and quartiles as a function of the number of terms. (a) All results. (b) Zoom between 0 and 30 terms. First order results (black circles), second order results with 29 descriptors (red squares) and second order results with 16 descriptors (green triangles). The number of the modelling is also indicated. ....	177
Figure VI-17. Parity plot between modelled kinetic constant $k_1$ and experimental kinetic constant of primary and secondary amines. (a) First order QSPR model. (b) Second order QSPR model.....	180
Figure VI-18. Modelling of kinetic constant $k_2$ of primary and secondary amines. Average RMSEP and quartiles as a function of the number of terms. (a) All results. (b) Zoom between 0 and 35 terms. First order results (black circles), second order results with 31 descriptors (red squares) and second order results with 16 descriptors (green triangles). The number of the modelling is also indicated. ....	182
Figure VI-19. Parity plot between modelled kinetic constant $k_2$ and experimental kinetic constant of primary and secondary amines. (a) First order QSPR model. (b) Second order QSPR model.....	185
Figure VI-20. Kinetic constant $k_2$ of molecules of the prediction set of tertiary amines as a function of the kinetic constant $k_1$ . (a) First order QSPR model. (b) Second order QSPR model. Experimental values (black circles) and predicted values (red open circles). The confidence ellipses are represented.....	186
Figure VI-21. Parity plot between modelled and experimental apparent kinetic constant of primary and secondary. (a) First order QSPR model. (b) Second order QSPR model. Error bars correspond to the experimental confidence interval.....	187
Figure VI-22. (a) Experimental kinetic constant $k_1$ and (b) class of tertiary and sterically hindered amines as a function of the value of the dipole $a_q$ . ....	189
Figure VI-23. (a) Experimental kinetic constant $k_1$ and (b) class of tertiary and sterically hindered amines as a function of the value of the HOMO $g$ . ....	190
Figure VI-24. Value of the nitrogen accessible surface as a function of the class of primary and secondary amines. ....	192
Figure VI-25. Kinetic constant (a) $k_1$ and (b) $k_2$ as a function of the nitrogen accessible surface for a series of primary acyclic alkylamines. ....	193
Figure VI-26. Scheme of the different configuration of the conformers results. ....	194
Figure VI-27. Kinetic constant (a) $k_1$ and (b) $k_2$ as a function of the nitrogen accessible surface for a series of secondary acyclic alkylamines. ....	195
Figure VI-28. Kinetic constant (a) $k_1$ and (b) $k_2$ as a function of the nitrogen accessible surface for a series of secondary acyclic alkanolamines. ....	196
Figure IX-1. (a) Scheme of the molar fraction vs. the pH of the solution for the different step of the titration (1, 2, 3 and 4). (b) Titration of a mix of 27 g of $[\text{CO}_2]=30 \text{ mol.m}^{-3}$ neutralized with 12 g of $[\text{NaOH}]=100 \text{ mol.m}^{-3}$ by $[\text{HCl}]=100 \text{ mol.m}^{-3}$ . pH metric curves (blue line) and derivates (red line). Corresponding step 2, 3 and 4 are also indicated. ....	221
Figure IX-2. Limiting molar conductivity vs. molecular mass of alkylammonium of the Table IX-11. ....	229

Figure IX-3. (a) Distribution of RMSEP of prediction for modelling of  $\log_{10}(k_1)$  of amines which form carbamates with 68 descriptors with 250 models (black line), 500 models (blue line), 750 models (green models) and 1,000 models (red line). (b) Same plot with normalized abscissa axis. .... 323

Figure IX-4. Distribution of RMSEP of the the validation set as a function of the number of models. .... 324

## Table of tables

---

Table II-1. Characteristics of industrial flue gases depending on application (Lecomte <i>et al.</i> , 2010). .....	8
Table II-2. Main advantages and weaknesses of the different technologies for CO <sub>2</sub> capture.....	13
Table II-3. Specification of natural gas in function of application.....	15
Table II-4. Economical and production impact of addition of post-combustion unit (Lecomte <i>et al.</i> , 2010). .....	15
Table II-5. Contact time of some experimental techniques (Laurent <i>et al.</i> , 1975).....	24
Table III-1. Name, abbreviation, chemical structure, references of stopped-flow kinetic studies of amine-CO <sub>2</sub> reaction with conductimetric detection, concentration range, temperature range, pKa at 25 °C and references of pKa values. References selected for the rest of this section are indicated in bold. ....	30
Table III-2. Parameters and average relative deviation (ARD) of three models used to fit data of molecule 5 (1-dimethylamino-2-propanol) at 25 °C.....	35
Table III-3. Determination of the factor R which indicates the kinetic contribution of hydroxide ions on molecule n°3 (dimethylmonoethanolamine) studied by Henni <i>et al</i> (2008). T=25 °C.....	37
Table III-4. pKa at 25 °C and Taft constants (Taft, 1976) for molecules n°7 to 11.....	41
Table III-5. Experimental data of k <sub>0</sub> for piperazine determined by Rayer <i>et al.</i> (2011) at 30 °C. ....	43
Table III-6. Corresponding number, structure, value of activation enthalpy and activation entropy determined according to transition state theory for amines of Figure III-15.....	53
Table IV-1. Reactions considered in the numerical model and expression of the thermodynamic constant. Correlations for the thermodynamic constants are given in Chapter IX .4.1.....	68
Table IV-2. Reaction kinetically limited considered in the numerical model and expression of associated rate law. Correlations for the available constants are given in appendix. ....	69
Table IV-3. Studied tertiary alkylamines. ....	90
Table IV-4. Studied tertiary alkanolamines. ....	90
Table IV-5. Studied other acyclic tertiary amines. ....	91
Table IV-6. Studied cyclic tertiary alkylamines. ....	91
Table IV-7. Studied cyclic tertiary alkanolamines. ....	92
Table IV-8. Studied other cyclic tertiary amines.....	92
Table IV-9. Studied primary alkylamines. ....	93
Table IV-10. Studied secondary alkylamines.....	93
Table IV-11. Studied primary benzylamines.....	94
Table IV-12. Studied secondary benzylamines. ....	94
Table IV-13. Studied primary alkanolamines. ....	95

Table IV-14. Studied secondary alkanolamines. ....	95
Table IV-15. Studied primary and secondary amino-ethers. ....	96
Table IV-16. Studied primary and secondary nitrilamines. ....	97
Table IV-17. Studied cyclic secondary alkylamines.....	97
Table IV-18. Studied cyclic secondary alkanolamines. ....	98
Table IV-19. Studied amines derivates from morpholine. ....	98
Table IV-20. Studied multi-amines.....	99
Table V-1. Kinetic constant $k_1$ for molecule 1310, 1311, 1312 and 1313. Comparison with the literature, relative deviation and references. ....	105
Table V-2. Values of pKa and kinetic constant $k_1$ and $k_2$ for the series of linear primary amines. ....	116
Table V-3. Values of pKa and kinetic constant $k_1$ and $k_2$ of the series of derivates from tert-butylamine. ....	118
Table V-4. Value of Taft, pKa and constant and kinetic constant $k_1$ and $k_2$ of the series of alkylamines.....	120
Table V-5. Value of pKa and kinetic constant $k_1$ and $k_2$ of the series of secondary amines. ....	127
Table V-6. Value of Taft constant, pKa and kinetic constant $k_1$ and $k_2$ for the series of secondary alkylamines. ....	131
Table V-7. Value of Taft constant, pKa and kinetic constant $k_1$ and $k_2$ for the series of secondary benzylamines. ....	131
Table V-8. Value of Taft constant, pKa and kinetic constant $k_1$ and $k_2$ for the series of secondary alcanolamines. ....	131
Table V-9. Value of Taft constant, pKa and kinetic constant $k_1$ and $k_2$ for the series of secondary nitrilamines. ....	131
Table V-10. Value of pKa and kinetic constant $k_1$ and $k_2$ of the series of cyclic secondary amines. ....	135
Table VI-1. Examples of some electronic and geometric descriptors. ....	148
Table VI-2. Van der Waals parameters used to calculate the accessible surface (Rappe <i>et al.</i> , 1992). ....	157
Table VI-3. List of descriptors and obtaining method.....	159
Table VI-4. Number of amines and proportion of data in each set for each modelling. ....	164
Table VI-5. Molecules of each prediction set. ....	165
Table VI-6. Results of modelling of tertiary and sterically hindered secondary amines.....	171
Table VI-7. Normalized coefficients of the modelling n° 3. Descriptors which explain more than 80 % of the information are indicated in bold.....	172
Table VI-8. Coefficients of the first order QSPR model for the kinetic constant $k_1$ of tertiary and sterically hindered amines. ....	173

Table VI-9. Average relative deviation and standard deviation of the relative deviation between experimental and modelled value of $k_1$ of tertiary and sterically hindered secondary amines for training and validation set and prediction set of the first and second order QSPR models.....	173
Table VI-10. Relative deviation of the molecules of the prediction set of tertiary and sterically hindered amines for the first and second order QSPR models. ....	174
Table VI-11. Average relative deviation and standard deviation of the relative deviation between experimental and modelled value of $k_0^{Am}$ of tertiary and sterically hindered secondary amines for training and validation set and prediction set of the first and second order QSPR models. ....	175
Table VI-12. Results of the modelling of the kinetic constant $k_1$ of primary and secondary amines. ....	178
Table VI-13. Normalized coefficients of the modelling $n^\circ 2$ . Descriptors which explain more than 80 % of the information are indicated in bold. ....	178
Table VI-14. Coefficients of the first order QSPR model for the kinetic constant $k_1$ of primary and secondary amines. ....	179
Table VI-15. Average relative deviation and standard deviation of the relative deviation between experimental and modelled value of $k_1$ of primary and secondary amines for training and validation set and prediction set of the first and second order QSPR models.....	180
Table VI-16. Relative deviation of the molecules of the prediction set of primary and secondary amines for the first and second order QSPR model.....	181
Table VI-17. Results of the modelling of the kinetic constant $k_2$ of primary and secondary amines. ....	182
Table VI-18. Normalized coefficients of the modelling $n^\circ 2$ . Descriptors which explain more than 80 % of the information are indicated in bold. ....	183
Table VI-19. Coefficients of the first order QSPR model for the kinetic constant $k_2$ of primary and secondary amines. ....	184
Table VI-20. Average relative deviation and standard deviation of the relative deviation between experimental and modelled value of $k_2$ of primary and secondary amines for training and validation set and prediction set of the first and second order QSPR models.....	185
Table VI-21. Relative deviation of the molecules of the prediction set of primary and secondary amines for the first and second order QSPR model.....	185
Table VI-22. Average relative deviation and standard deviation of the relative deviation between experimental and modelled value of $k_0^{Am}$ of primary and secondary amines for training and validation set and prediction set of the first and second order QSPR models.....	187
Table VI-23. Classes for tertiary and sterically hindered amines.....	188
Table VI-24. Classes of primary and secondary amines.....	191
Table IX-1. Chemical structure, number, values of $k_{Am}$ and $n$ for selected data with average relative deviation between model and experimental first order constant $k_0$ on concentration range specified in Table III-1. ....	213
Table IX-2. Second order kinetic constants $k_{ter1}$ and $k_{ter2}$ and average relative deviation between termolecular model and experimental values of $k_0$ from literature data specified in Table III-1.....	215
Table IX-3. Number, value of $k_1$ and $k_2$ and average relative of literature data specified in Table III-1.....	218

Table IX-4. Neutralization of amine solutions with carbon dioxide or hydrochloric acid to neutralize the hydroxide ions contribution.....	222
Table IX-5. First order kinetic constant determined for some tertiary amines with neutralization with hydrochloric acid and carbon dioxide in comparison with literature results. ....	223
Table IX-6. Properties of acids used to maximize the variations of conductance in carbamate forming reaction. CRC Handbook of chemistry and physics, 75 <sup>th</sup> Edition; CRC Press, 1995 (Lide, 1994).....	224
Table IX-7. Results of the pre-study realized to optimize the amplitude. ....	225
Table IX-8. Equilibrium constants. Temperatures T are expressed in K. ....	226
Table IX-9. Kinetic constants. Temperatures T are expressed in K. ....	227
Table IX-10. Limiting molar conductivity at 25 °C. Data available in CRC Handbook of chemistry and physics, 75 <sup>th</sup> Edition; CRC Press, 1995 (Lide, 1994).....	228
Table IX-11. Limiting molar conductivity at 25 °C of some alkylammonium at 25 °C. Data available in CRC Handbook of chemistry and physics, 75 <sup>th</sup> Edition; CRC Press, 1995 (Lide, 1994). ....	228
Table IX-12. Experimental results of primary amines.....	248
Table IX-13. Experimental results of secondary amines. ....	256
Table IX-14. Experimental results of tertiary amines.....	268
Table IX-15. Experimental results of multi-amines. ....	276
Table IX-16. Physico-chemical parameters of primary amines. ....	278
Table IX-17. Physico-chemical parameters of secondary amines.....	280
Table IX-18. Physico-chemical parameters of tertiary amines. ....	282
Table IX-19. Physico-chemical parameters of multi-amines.....	284
Table IX-20. List of descriptors used for QSPR modelling. Descriptors in bold have been retained after a hierarchical clustering analysis.....	285
Table IX-21. Values of the 68 retained descriptors for primary amines. The numbers of the left column indicate the number of the amine. The numbers of the top line indicate the number of the descriptor.....	290
Table IX-22. Values of the 68 retained descriptors for secondary amines. The numbers of the left column indicate the number of the amine. The numbers of the top line indicate the number of the descriptor. ....	298
Table IX-23. Values of the 68 retained descriptors for tertiary amines. The numbers of the left column indicate the number of the amine. The numbers of the top line indicate the number of the descriptor.....	306
Table IX-24. Value of nitrogen accessible surface (NAS) of studied amines. ....	321
Table IX-25. Coefficients and coefficients of standardized variables of the second order QSPR model for $k_1$ of tertiary and sterically hindered amines. ....	325
Table IX-26. Coefficients and coefficients of standardized variables of the second order QSPR model for $k_1$ of primary and secondary amines. ....	326

Table IX-27. Coefficients and coefficients of standardized variables of the second order QSPR model for $k_1$ of primary and secondary amines. ....	330
Table IX-28. Experimental and modelled with the first and second order QSPR models kinetic constants $k_1$ and $k_2$ for tertiary and sterically hindered amines. Molecules in bold are used in the prediction set. ....	333
Table IX-29. Experimental and modelled with the first and second order QSPR models kinetic constants $k_1$ and $k_2$ for primary and secondary amines. Molecules in bold are used in the prediction set. ....	335



## Nomenclature

---

### *Physico-chemical parameters*

[X]	Concentration of the species X	$\text{mol.m}^{-3}$
$\rho_X$	Density of the species X	
$\lambda_X^\infty$	Limiting molar conductivity of the species X	$\text{S.m}^2.\text{mol}^{-1}$
$a_X$	Activity of the species X	
A	Amplitude of the signal	S
C	Value at the steady state	S
$C_X$	Concentration of the species X in a solution (fixed)	$\text{mol.m}^{-3}$
G	Conductance of a solution	S
$k_i$	Kinetic constant of the reaction i	
$k_{-i}$	Kinetic constant of the reverse reaction of i	
$k_i^m$	Kinetic constant of the reaction i expressed in a molality scale	
$k_0$	Apparent kinetic constant	$(\text{s}^{-1})$
$k_0^{\text{Am}}$	Apparent kinetic constant specific to amine-carbon dioxide reaction	$(\text{s}^{-1})$
Ki	Thermodynamic constant	
$m_X$	Molality of the species X	$\text{mol.kg}^{-1}$
$M_X$	Molecular mass of the species X	$\text{g.mol}^{-1}$
$n_X$	Quantity of the species X	mol
$p_X$	Partial pressure of the species X	Pa
Q	Volumetric flow rate	$\text{m}^3.\text{s}^{-1}$
$r_X^i$	Rate of reaction of the species X in the reaction i	
R	Resistance of a solution	$\Omega$
t	Time	S
V	Volume	$\text{m}^3$
$w_X$	Mass fraction of the species X	%

### *Exponents*

i	Initial, for $t = 0$ , at the beginning of a phenomena
f	Final, at the equilibrium, at the end of a phenomena
tot	Total

### *Chemical species*

Am	Amine (primary, secondary or tertiary)
CH <sub>4</sub>	Methane
Cl <sup>-</sup>	Chloride ion
CO	Carbon monoxide
CO <sub>2</sub>	Carbon dioxide
CO <sub>3</sub> <sup>2-</sup>	Carbonate ion
HCl	Hydrochloric acid
HCO <sub>2</sub> H	Formic acid (methanoic acid)
HCO <sub>2</sub> <sup>-</sup>	Formate ion (methanoate ion)
HCO <sub>3</sub> <sup>-</sup>	Hydrogenocarbonate ion (bicarbonate ion)
HO <sup>-</sup>	Hydroxide ion
H <sub>2</sub>	Dihydrogen
H <sub>2</sub> CO <sub>3</sub>	Carbonic acid
H <sub>2</sub> O	Water
H <sub>2</sub> S	Hydrogen sulfide
H <sub>3</sub> O <sup>+</sup>	Hydronium ion
MEA	Monoethanolamine
MOF	Metal Organic Frameworks
N <sub>2</sub> O	Nitrous oxide
N <sub>2</sub>	Dinitrogen
NaOH	Sodium hydroxide
O <sub>2</sub>	Dioxygen
O <sub>3</sub>	Ozone
NO <sub>x</sub>	Nitrogen oxides
N <sub>2</sub> O	Nitrous oxide
R <sub>2</sub> NH	Primary or secondary amine
R <sub>2</sub> NCO <sub>2</sub> <sup>-</sup>	Carbamate ion
R <sub>2</sub> NCO <sub>2</sub> H	Carbamic acid
R <sub>3</sub> N	Tertiary amine
SO <sub>x</sub>	Sulfur oxides

### ***Other abbreviations***

AM	Analytical method
ARD	Average Relative Deviation
CAPEX	Capital expense
CCS	Carbon Capture and Storage
CLC	Chemical Looping Combustion
EUETS	European Union Emissions Trading System
GHG	Green House Gases
MLR	Multiple Linear Regression
NM	Numerical method
OPEX	Operating expense
PLS	Partial Least Square
PLS-GLR	Partial Least Square – Generalised Linear Regression
QSAR	Quantitative Structure-Activity Relationship
QSPR	Quantitative Structure-Property Relationship
RMSEP	Root Mean Square Error of Prediction

## *Chapter I: GENERAL INTRODUCTION*

---

If the age of the earth is compared to one day, the age of humanity is around four seconds and it has been only four milliseconds since the industrial revolution started. During this period, the transformations of human activity and standards of life have been so significant that they are suspected to affect the climate and the environment by the global warming effect. This climate change with a 1°C increase of the average temperature since 1910 is linked to an increase of the carbon dioxide (CO<sub>2</sub>) level in the atmosphere from 280 ppm before the industrial revolution to 379 ppm in 2005 (Contribution of Working Groups I *et al.*, 2008; Lecomte *et al.*, 2010). This human perturbation of the natural equilibrium between CO<sub>2</sub> emissions and absorption and its impact on the climate worldwide scale has accelerated over the last 50 years.

Conscious of its responsibility, the international community has started to undergo policies to ensure sustainable development. Among the different technologies to limit the anthropogenic greenhouse effect, post-combustion process working by amine scrubbing seems to be a timely and efficient way to limit emissions of CO<sub>2</sub> in the atmosphere. However, with traditional amine solvents such as monoethanolamine (MEA), the operating costs to regenerate the solvent and compress the CO<sub>2</sub> represent a considerable energetic penalty.

To reduce these costs, the development of advanced amine solvents is based on screening studies in order to find the best candidate with respect to the thermodynamics, kinetics of the CO<sub>2</sub> absorption and desorption and the chemical stability of the amine solvent. Other important criteria such as corrosiveness, volatility, toxicity, *etc.*, also need to be considered. Numerous studies shed some lights on relationships between amine property and structure (Porcheron *et al.*, 2011).

The objective of this work is to provide a large database of kinetic data on CO<sub>2</sub>-amine in aqueous solution to achieve a comprehensive understanding of structural effects and establish a quantitative structure-property relationship. Our ambition is finally to provide a tool to guide the synthesis and the screening of new amines by predicting their kinetic constants. This work is divided into five main chapters.

Chapter II presents the context of global warming and the different technologies developed to limit emissions of carbon dioxide due to the production of energy and industry. The performances and specifications of an amine scrubbing process depend greatly on the kinetics of reaction between amine and CO<sub>2</sub>. The different reactions have been extensively described in the literature with a great variety of experimental approaches and kinetic models to interpret the data.

A critical review of data from the literature has been realized in Chapter III. This part is particularly important in order to analyse the effect of the concentration and the temperature on kinetic properties. It also helps to determine advantages and weaknesses of each mechanism proposed in order to represent experimental data. At this stage, some relations

between chemical structures and kinetic properties have been observed. According to this in-depth analysis, the objectives and the scope of this work can be clearly defined.

The Chapter IV is fully dedicated to the description of the experimental approach used in this study. We first describe experimental techniques to obtain the kinetic constants and others complementary information. Then the method followed to extract apparent kinetic constant and kinetic constants are explained. Finally the molecules studied and the reasons of our choice are presented.

The interpretation of results obtained by following the method described in Chapter IV is realised in Chapter V. The results of primary, secondary, tertiary amines and multi-amines are compared. In this chapter, an in-depth analyse of the influence of structural parameters on the kinetic constants is done. These effects are then taken into account to build the structure-property relationship.

In Chapter VI the method followed to set up the Quantitative Structure-Property Relationship (QSPR) model is described. The methodology has been implemented thanks to the analysis of experimental data realized in Chapter V. Then the results associated are presented and we discuss about their performances.

*«We do not inherit the earth from our parents, we borrow it from our children. »*

Antoine de SAINT-EXUPÉRY

## Chapter II: STATE OF THE ART

### 1 Global warming

The greenhouse effect on earth is a natural phenomenon due to the atmosphere. Indeed, greenhouse gases (GHG), naturally present in the atmosphere, absorb a part of the radiation of the sun reflected by the earth's surface as detailed in Figure II-1. While average temperature on earth is around 18°C, it would be only -18°C without greenhouse effect. The main greenhouse gases naturally present in the atmosphere are water (H<sub>2</sub>O), carbone dioxide (CO<sub>2</sub>), methane (CH<sub>4</sub>), nitrous oxide (N<sub>2</sub>O) and ozone (O<sub>3</sub>) (Lecomte *et al.*, 2010).

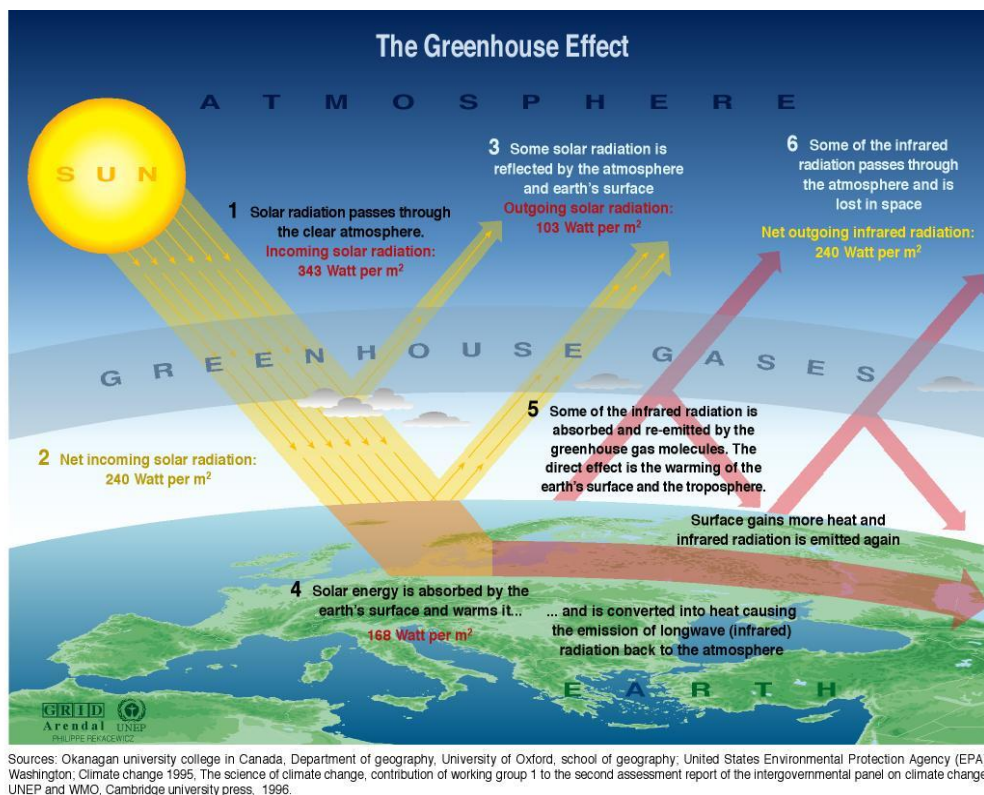


Figure II-1. Greenhouse effect.

Since the beginning of the industrial revolution, humans have used more and more power for their daily activities. Since this time, the main part of this power has been brought by the combustion of fossil fuels which releases in the atmosphere additional greenhouse gases. Numerous studies show that these additional emissions of greenhouse gases have an impact on the environment, especially on global warming.

Most of government officially recognize the correlation between global warming and human-caused GHG and have begun to adopt measures to fight against anthropogenic emissions of greenhouse gases. The most important example is certainly the Kyoto protocol which took place in 1997. The main objective of the protocol is to reduce the emissions of six greenhouse gases: CO<sub>2</sub>, CH<sub>4</sub>, N<sub>2</sub>O, fluorocarbon, chlorofluorocarbon and sulfur hexafluoride.

## 1. Global warming

Among the six main greenhouse gases emitted by humans, emission of carbon dioxide is by far the most important. In 2004, it represented more than 76 % (around 37.2 Gt) of all greenhouse gas emissions related in CO<sub>2</sub> equivalent in the world (Contribution of Working Groups I *et al.*, 2008). This increase of anthropogenic CO<sub>2</sub> emissions results from the increasing needs in energy which is mainly produced by combustion of fossil fuels. This increase of energy demand is related to the increase of world population and global improvement of quality of life, especially in developing countries.

Figure II-2 shows that in 2009 carbon dioxide was mainly (around 60 %) emitted by stationary sources such as electricity generation or industry (International Energy Agency, 2011).

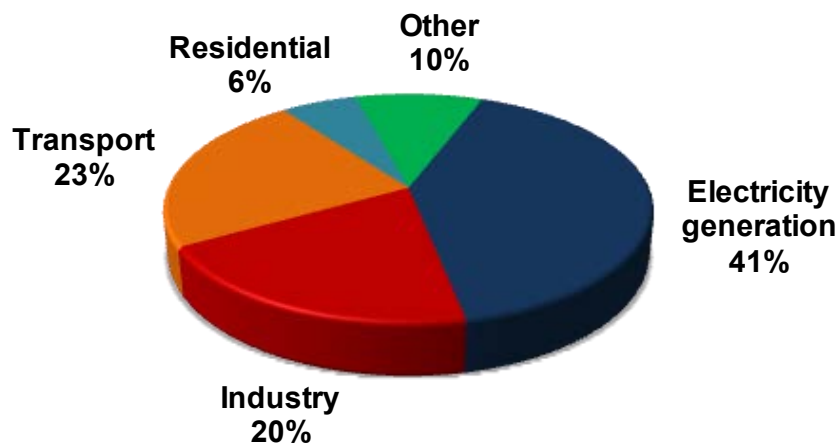


Figure II-2. Origin of emissions of carbon dioxide in the atmosphere in 2009 (International Energy Agency, 2011).

Different options are considered in order to reduce anthropogenic emissions. These considered solutions, summarized by Figure II-3, consist in:

- Controlling the energetic consumption. It represents around 50 % of avoid emissions. It consists in improving energetic efficiency of buildings, vehicles and manufacturing processes, developing public transportation systems, etc.
- Development of renewable energies. This way represents around 21 % of possibility for reduction CO<sub>2</sub> emissions.
- Production of energy using nuclear power stations. It may contribute to 6 % to the reduction of greenhouse gas emissions.
- Capture and storage of carbon dioxide. This option called carbon capture and storage (CCS) could reduce around 20 % of emissions. Contrary to other option, this one could be developed more quickly. It would enable to operate with current installation and to reduce at the same time carbon emissions.

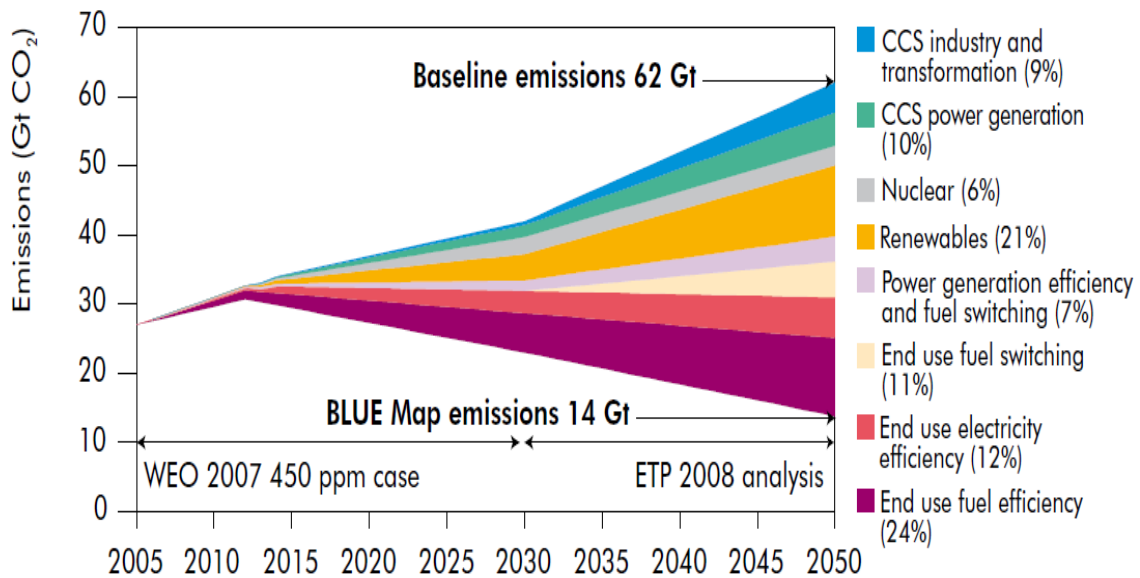


Figure II-3. Envisaged scenarios to reduce emission of carbon dioxide in the atmosphere.(International Energy Agency, 2008)

In 2005, the European Union launched the European Union Emissions Trading System (EU ETS), also known as the European Union Emissions Trading Scheme (Ellerman and Buchner, 2007). Public authorities determine a ceiling level of emission per year for main emitters and attribute a corresponding allowance. At the end of the year, if emitters released in the atmosphere less than permitted they can sell their additional allowance. However if they produce more CO<sub>2</sub> than permitted they must buy missing quotas. Exchange of allowance can be realised over the counter or by trading on the spot market of one of Europe's climate exchanges.

The implementation has been realised in three main phases. During the phase I, between 2005 and 2007, the goal was to establish price and quotas at national levels of the CO<sub>2</sub> market. 12,000 installations which represented 40 % of the European Union emissions were concerned. During phase II, between 2007 and 2012 the protocol Kyoto was enforced and free quotas were provided to emitters. The quotas were attributed with a diminution of 6.5 % in reference with level of emission of 2005. During phase III between 2013 and 2020, emissions beyond quotas have to be paid and restrictions are reinforced and extended in order to reduce by 20 % the CO<sub>2</sub> emissions by 2020 (Commission européenne, 2009).

During the three phases, the price of CO<sub>2</sub> has decreased irregularly from around 20 €/t in phase I (Ellerman and Buchner, 2008) to around 6 €/t on the 4<sup>th</sup> January 2013 (Vitelli, 2013). According to the committee on climate change, even if uncertainties remain, the price of CO<sub>2</sub> should reach between 22 to 30 €/t in 2020 (Committee on Climate Change, 2008). As long as the investment costs shall exceed financial penalties, energy and industrial companies shall not develop CCS.

## 2. Carbon capture and storage

Different technical solutions have been proposed for CCS with their strengths and weaknesses. They differ from their cost, social impact, political and geo-political context of each country. In this context, developed countries have invested many research and demonstration projects since the last decade.

## 2 Carbon capture and storage

The carbon capture and storage chain is composed of three important steps: capture, transportation and lastly, storage in the underground. Each of these steps, represented in Figure II-4, will be developed in the next section. We first mention transport and storage which are not concerned by our study. Moreover, cost for transportation is 1 to 3 €/t of CO<sub>2</sub> for 100 kilometers of pipe and 5 €/t of CO<sub>2</sub> for storage. We describe mainly the step of CO<sub>2</sub> capture which is the most expensive part of CCS (40 to 60 €/t of CO<sub>2</sub>). It also corresponds to the field where research can bring the most important improvements.

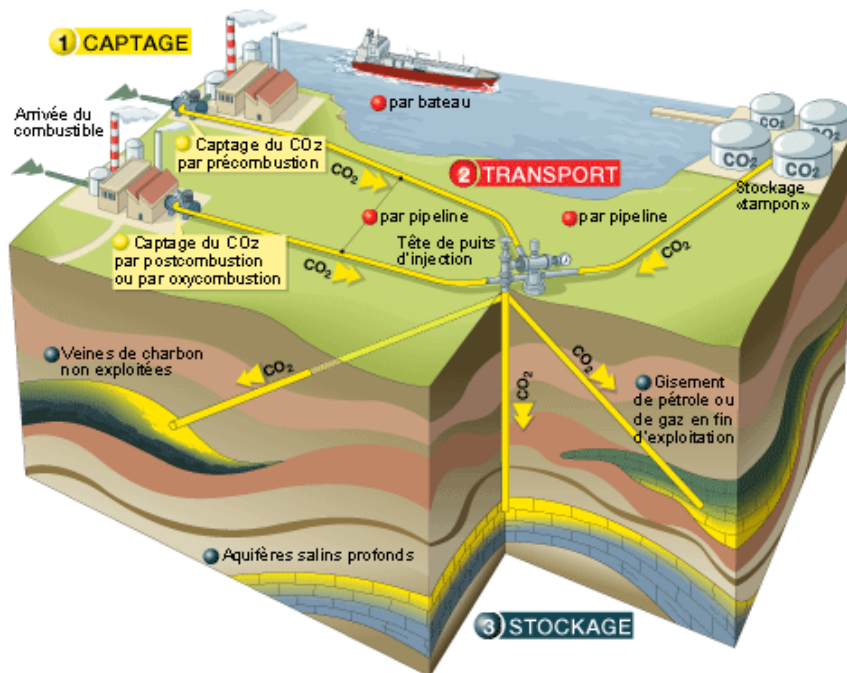


Figure II-4. Principe de carbon capture and storage (Total, 2013).

### 2.1 Storage

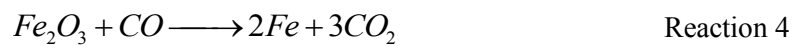
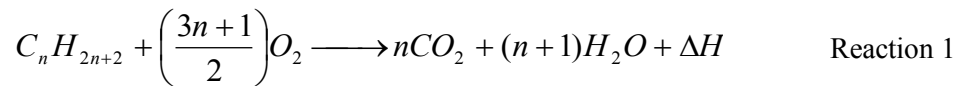
It is well established that CO<sub>2</sub> can be easily trapped in the underground under dense form in porous rocks or by adsorption on coal. Storage is possible from 800 meters depth where CO<sub>2</sub> is in supercritical state (temperature above 31 °C and pressure above 74 bars). Sealing is ensured by the presence of an impermeable layer shield composed by clay above the reservoir layer. Therefore, it is necessary to verify that the chemical action of CO<sub>2</sub> on rocks does not affect impermeability. There are three different kinds of geologic formation where CO<sub>2</sub> can be trapped: deep aquifers, depleted oil and gas reservoirs and unexploited coal seams.

## 2.2 Transport

Transport of CO<sub>2</sub> can be operated by pipelines or by ship. When carbon dioxide is transported by pipelines, it is transported in supercritical state (pressure superior to 74 bars and temperature superior to 31 °C). Studies are also made to transport CO<sub>2</sub> in liquid state by pipelines. In the case of transport by ship, useful for long distance and offshore storage, CO<sub>2</sub> is in liquid phase (temperature of -20 °C and pressure of 20 bars).

## 2.3 Capture

Flue gases have at least three different origins: thermal power plant, cement industry and steel industry. In the case of thermal power plant, the goal is to produce electricity from the reaction of combustion (Reaction 1). In cement works, calcium oxide is obtained by the calcination of calcium carbonate (Reaction 2). In steelworks, coke is first burnt with an air deficiency to get carbon monoxide (Reaction 3). Carbon monoxide reduces iron (III) oxide and forms elementary iron and carbon dioxide (Reaction 4). Table II-1 indicates the main characteristics of the flue gases depending on their origin.



Three different ways of capturing CO<sub>2</sub> can be considered: pre-combustion, oxy-combustion and post-combustion which can be chosen depending on the source of emission. In the following section, we briefly describe the main characteristics of these three options.

## 2. Carbon capture and storage

Table II-1. Characteristics of industrial flue gases depending on application (Lecomte *et al.*, 2010).

		Thermal power plant		Cement industry	Steel industry
	Unit	Natural gas	Coal	Dry process	Blast furnace
<b>Capacity</b>		600 MWe	600 MWe	2,300t/day of clinker	9,700 t/day of cast iron
<b>Flue gas flow rate</b>	Nm <sup>3</sup> .h <sup>-1</sup>	3.3×10 <sup>-6</sup>	1.7×10 <sup>-6</sup>	2.5×10 <sup>-5</sup>	6.0×10 <sup>-5</sup>
	t.h <sup>-1</sup>	4,290	2,210	325	780
<b>Temperature</b>	°C	95-105	85	110	55
<b>Pressure</b>	bar	1	1	1	3
<b>Composition:</b>					
<b>N<sub>2</sub></b>	% vol	75-80	70	65-70	40
<b>O<sub>2</sub></b>		13.5	4	8-10	trace
<b>CO<sub>2</sub></b>		3.5	13.5	15	20
<b>H<sub>2</sub>O</b>		7	11	6-11	15
<b>Others</b>		trace-1	1.5	trace-6	25 (mainly CO)

### 2.3.1 Oxy-combustion

The principle of the oxy-combustion process consists in realizing combustion with pure dioxygen (O<sub>2</sub>). In this way, carbon dioxide just needs to be separated from the water in the flue gas. Two processes have been developed to realize oxy-combustion.

#### 2.3.1.1 Classical oxy-combustion process

In this three step process, represented by Figure II-5, the first operation consists in separating dinitrogen (N<sub>2</sub>) from air to produce dioxygen with 95 % purity (Anheden *et al.*, 2005). There are three processes to product O<sub>2</sub>: adsorption, membranes and cryogenic distillation. With respect to the important flow rate to produce for industries or power plants, cryogenic distillation is often the most adapted but still suffers from important energy penalties due to the compression step (Feron and Hendriks, 2005).

The second step of the process consists in making combustion reaction between the fuel and the oxygen. Specific materials have been developed for the boilers to resist high flame temperature and thermal constraints. An addition of CO<sub>2</sub> and water issue to product of reaction can also be added in the boiler to reduce the flame temperature. There are three kinds of boilers: pulverized coal boiler, circulated fluidized bed and combustion without flame.

Finally the mixture of water and carbon dioxide produced by combustion is easily separated by water condensation after elimination of sulfur oxides (SO<sub>x</sub>) and nitrogen oxides (NO<sub>x</sub>). It may also contain dioxygen in excess. Generally, the carbon dioxide capture this way is quite pure (around 95 %).

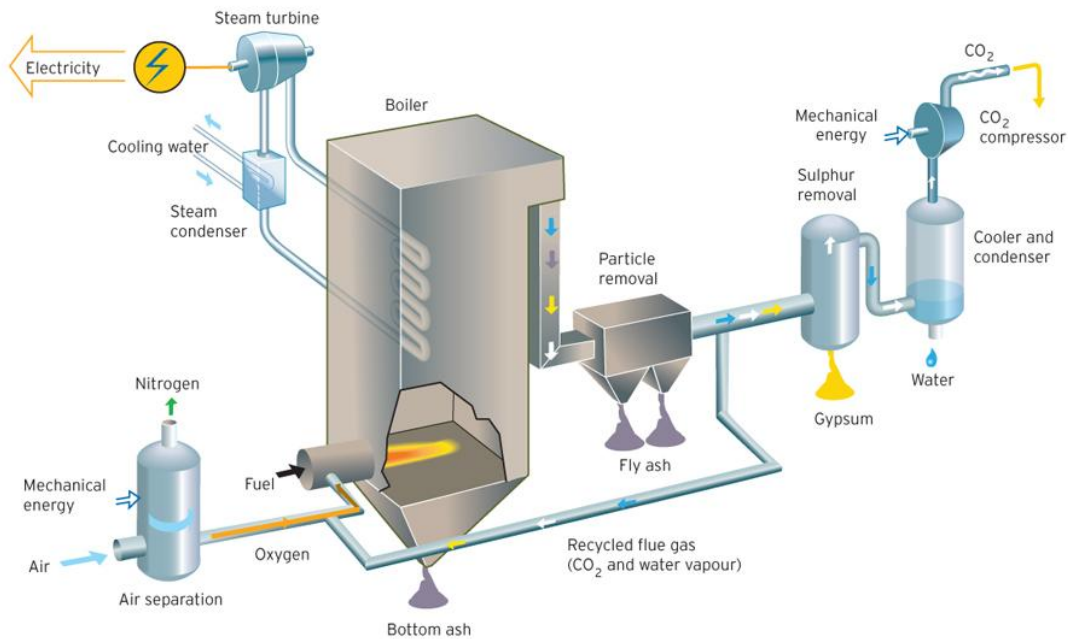
Oxyfuel ( $O_2/CO_2$  recycle) combustion capture

Figure II-5. Classical oxy-combustion process (Vattenfall, 2013a).

## 2.3.1.2 Chemical looping combustion

Chemical looping combustion (CLC) brings oxygen to the fuel by the intermediate of a metal oxide. In a first step, the reduced form of the oxide is oxidized with air in the air reactor. Then the oxidant form is reduced by the fuel in the fuel reactor (Figure II-6). The reaction in the fuel reactor produces only CO<sub>2</sub> and H<sub>2</sub>O which can be easily separated by condensation like in the classical combustion process. Still under development, this process can potentially bring significant reduction of energetic cost for CO<sub>2</sub> capture (Eide *et al.*, 2005).

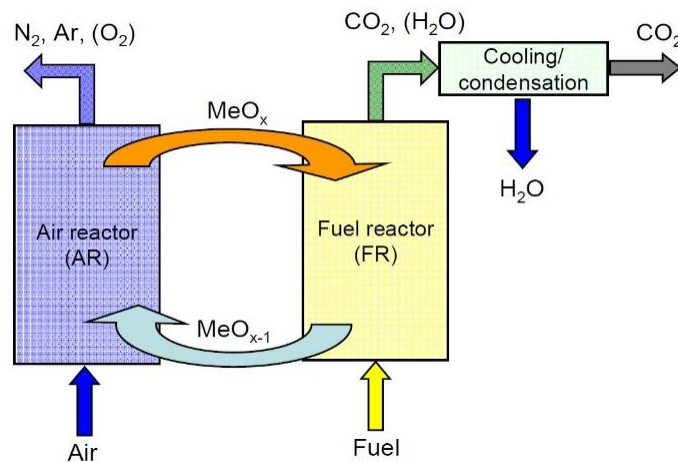
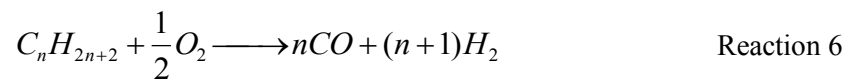
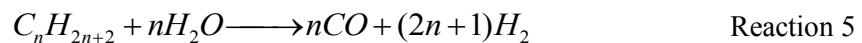


Figure II-6. Chemical looping combustion process (CLC, 2013).

## 2. Carbon capture and storage

### 2.3.2 Pre-combustion

The objective of this process is to transform a fuel into CO<sub>2</sub> and dihydrogen (H<sub>2</sub>) and transform H<sub>2</sub> in electricity and/or heat through a cogeneration plant. The primary fuel (liquid hydrocarbon, natural gas, coal, lignocellulosic biomass), is transformed in a gas mixture of carbon monoxide and H<sub>2</sub> by a steam reforming process (Reaction 5) or a partial oxidation process (Reaction 6) or autothermal reforming process which is a combination of both in the same reactor. This mixture is called syngas. This syngas is then treated by a shift conversion reaction. In this Water Gas Shift reaction, carbon monoxide reacts with water to form carbon dioxide and dihydrogen as shown by Reaction 7. Remaining dihydrogen is burnt with air to produce electricity and/or heat without emission of CO<sub>2</sub> (Eide and Bailey, 2005).



Carbon dioxide is then easily separated from H<sub>2</sub> using chemical solvents (amines) or physical solvents like methanol depending on partial pressure of CO<sub>2</sub>. Other separation techniques like cryogenics or membranes (polyethylene terephthalate) can also be considered (Härtel *et al.*, 1996). However cryogenics still suffers from high energy penalties assigned to a necessary compression step and membranes are not yet ready to be used in a large scale.

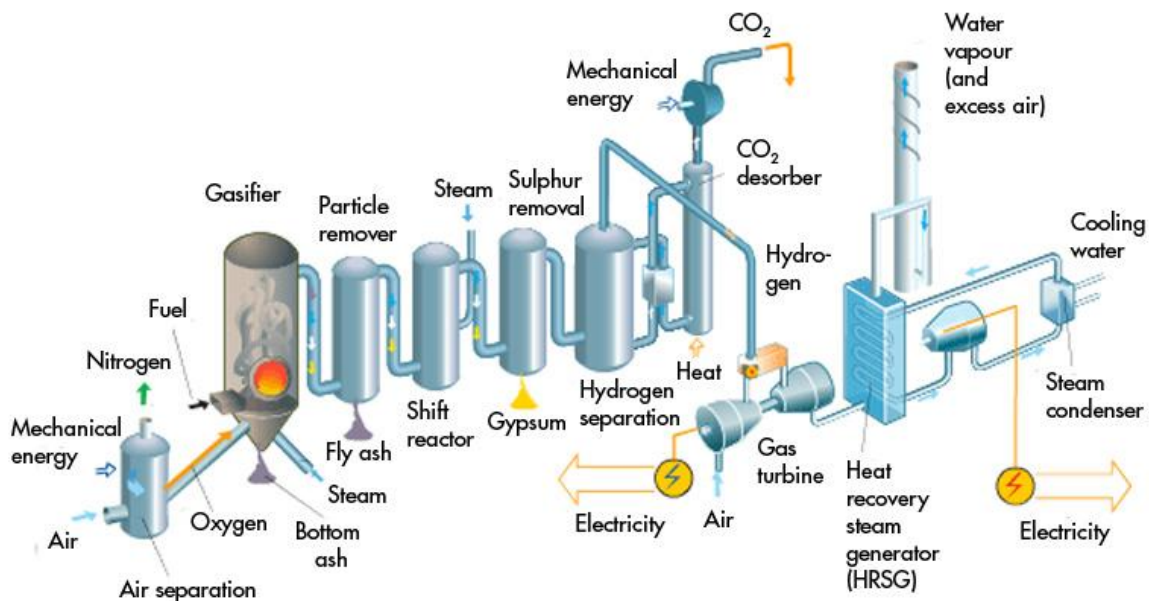


Figure II-7. Capture of CO<sub>2</sub> by pre-combustion process (Vattenfall, 2013b).

### 2.3.3 Post-combustion

The term post-combustion is used when the separation of CO<sub>2</sub> takes place after the combustion. Separation of CO<sub>2</sub> from dinitrogen is necessary to avoid the energetic penalty for compression of the entire flow rate of flue gas. In this sense several methods of separation have been developed. We will present these methods in the next section.

#### 2.3.3.1 Membranes

Separation with membranes uses the property of species to diffuse at different rates through a membrane material to separate CO<sub>2</sub>. This technology takes advantage from important specific area (around 30,000 m<sup>2</sup>.m<sup>-3</sup>). Nevertheless it suffers from high energetic penalties due to the requested compression of the flue gas necessary to compensate for the low partial pressure of CO<sub>2</sub> (Lecomte *et al.*, 2010).

#### 2.3.3.2 Adsorption

Inspired by numerous separation processes, adsorption process is used to separate carbon dioxide. Indeed zeolite and active carbon have a strong affinity with CO<sub>2</sub>. Adsorbents studied more recently as metal organic frameworks (MOF) offer important capacity properties (1 gCO<sub>2</sub>/g of MOF at 32 bars). However, due to the low partial pressure of carbon dioxide in fumes, an important mass of adsorbent is needed. This mass needs to be heated and cooled, which makes it difficult to use in an economical point of view (Lecomte *et al.*, 2010).

#### 2.3.3.3 Cryogenics

As classical cryogenic processes cannot work due to the weak concentration of CO<sub>2</sub> in the flue gas, a method based on antisublimation has been developed. It consists in cooling fumes at least to -78.5 °C at around atmospheric pressure to transform CO<sub>2</sub> in its solid state. In a first step, water is removed by successive thermal exchange until to reach -40 °C. Then fumes are cooled until -120 °C. Two capacities are necessary for this process, one for capturing CO<sub>2</sub> and the other where CO<sub>2</sub> is recovered under pressure in liquid phase. Both reactors operate alternatively. Although this process benefits of good energy efficiency it is yet not ready to be used in the range of flue gas flow rates (Lecomte *et al.*, 2010).

#### 2.3.3.4 Hydrates

Hydrates, which are crystalline structure composed of molecules of water associated to low molecular weight compounds, can also be used to capture CO<sub>2</sub>. Thanks to their particular structure, CO<sub>2</sub> is selectively trapped from N<sub>2</sub> at 5 °C and 25 bar. Indeed, at the same temperature, 250 bar of N<sub>2</sub> is needed to trap this compound. However, the low concentration of CO<sub>2</sub> in flue gases implies to use a compressor which brings important energy penalties. Actually, researches are made to reduce pressure and increase temperature of hydrate formation (Lecomte *et al.*, 2010).

#### 2.3.3.5 Absorption

Absorption consists in dissolving selectively CO<sub>2</sub> in a liquid solvent. There are two kinds of absorption: physical absorption and chemical absorption. In the case of physical

## 2. Carbon capture and storage

absorption, CO<sub>2</sub> does not react with solvent, it is simply dissolved by liquid-vapor equilibrium. In the case of chemical absorption, CO<sub>2</sub> is first dissolved and then it reacts with the solvent. We will only take in interest in chemical solvents which are much more capacitive and adapted to low partial pressure of CO<sub>2</sub> in flue gas (Lecomte *et al.*, 2010).

The flue gas is contacted in an absorption column (absorber) with the solvent, which circulates counter-currently and gets loaded in carbon dioxide. The exhaust gas is released at the top of the absorption column. The rich solvent is transferred in a separation column or stripper where heat and stripping vapor separates CO<sub>2</sub> from the solvent. Carbon dioxide is recovered at the top of the stripper and the lean solvent is reintroduced in the absorption column. This cycle is represented in Figure II-8.

This technology is currently the most mature to capture carbon dioxide in flue gas. Indeed it benefits from the knowledge of mature processes in natural gas treating. Moreover this technology can be adapted on an existing plant. It is also suitable to capture CO<sub>2</sub> on the different emission sources (thermal power plant, cement industry, steel industry, etc). Nevertheless this process suffers from the high energetic cost due to the regeneration of the solvent.

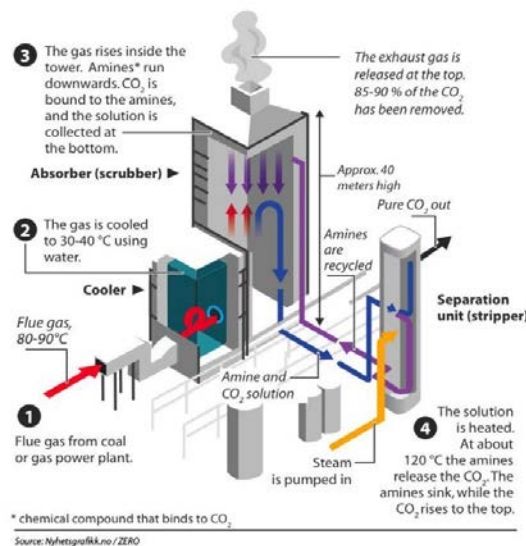


Figure II-8. Capture of CO<sub>2</sub> by postcombustion (Zero, 2013).

### 2.3.4 Conclusion concerning carbon dioxide capture

As shown by Table II-2, each technology used for CO<sub>2</sub> capture presents advantages and weaknesses. Moreover, the source of emission has also an important impact on the selection of the process. Overall, oxy-combustion and pre-combustion technologies, which present good results in term of energetic cost, are still in development and can be considered on grass-root plants. Concerning post-combustion technologies downstream of existing plants, membranes, adsorption, cryogenics and hydrates are still too much impacted by energy penalties or not yet mature to be applied on such a large scale. Finally the post-combustion using absorption seems to be an interesting first-generation technology to reduce carbon dioxide emission. In the next part we will present this technology more thoroughly.

Table II-2. Main advantages and weaknesses of the different technologies for CO<sub>2</sub> capture.

	Advantages	Weaknesses
<b>Oxy-combustion</b>		
Classical	Important thermal efficiency No effluent in the atmosphere	High flame temperature High energy consumption (compressor)
CLC	No energy input needed	Difficulty to find the optimal redox compound No demonstration at large scale
<b>Pre-combustion</b>		
	Synthesis of H <sub>2</sub> (high calorific value) Weak energy to capture CO <sub>2</sub>	Development of an adapted gas turbine necessary
<b>Post-combustion</b>		
Membranes and adsorption	High specific surface	High energy penalties linked to compression
Cryogenics	Excellent energetic performance	Not studied at important scale (maximum 1 t of CO <sub>2</sub> per hour)
Hydrates	Recovering of high pressure CO <sub>2</sub>	Selectivity not guaranteed Energy for compression
Absorption	Most matured process Usable for all CO <sub>2</sub> sources Don't imply huge modification of industrial site	Important energy penalties

### 3 Amine scrubbing capture process

#### 3.1 Description of the process

In the post-combustion flue gases, the principal compounds are N<sub>2</sub>, O<sub>2</sub>, H<sub>2</sub>O and CO<sub>2</sub>. This flue gas is introduced thanks to the fan (also called blower) at the bottom of the absorption column. An amine solution is used as the chemical solvent. The flue gas is contacted counter-currently with the lean amine solution. The absorption column is a packed column in order to increase the area of contact between gas and liquid. CO<sub>2</sub> is absorbed selectively by the amine solution and reacts with the amine to form salts. Generally, the absorption column operates at a pressure close to 1 bar and at temperature between 40 and 70 °C. The objective is generally to capture at least 90 % of the CO<sub>2</sub> present in the flue gas.

The rich amine is pumped from the bottom of the absorber to an amine-amine thermal exchanger to heat the solution with the lean amine coming from the bottom of the stripper. The heated rich amine is introduced at the top of the stripper (also called regeneration column). This column operates at a pressure around 1.5 bars and a temperature around 120 °C. The energy brought by the boiler to regenerate the solution is the sum of three terms: the sensible heat, the enthalpy of reaction and the excess of stripping. The difference of temperature between the top and the bottom of the stripper corresponds to the sensible heat. The enthalpy of reaction is the energy to break the chemical bond between amine and CO<sub>2</sub> in the case of primary and secondary amine or to reverse the reaction between CO<sub>2</sub>, amine and water in the case of tertiary amines. Finally, the excess of stripping is the necessary energy to generate enough steam to desorb CO<sub>2</sub> from the amine. The regenerated solvent (lean amine) is then

### 3. Amine scrubbing capture process

recovered from the bottom of the stripper, cooled through the amine-amine thermal exchanger and introduced at the top of the absorption column.

A schema of this process is represented by Figure II-9. As we previously said, this process is similar to the acid gas removal process in natural gas. The specificities of the latter are presented in the next section.

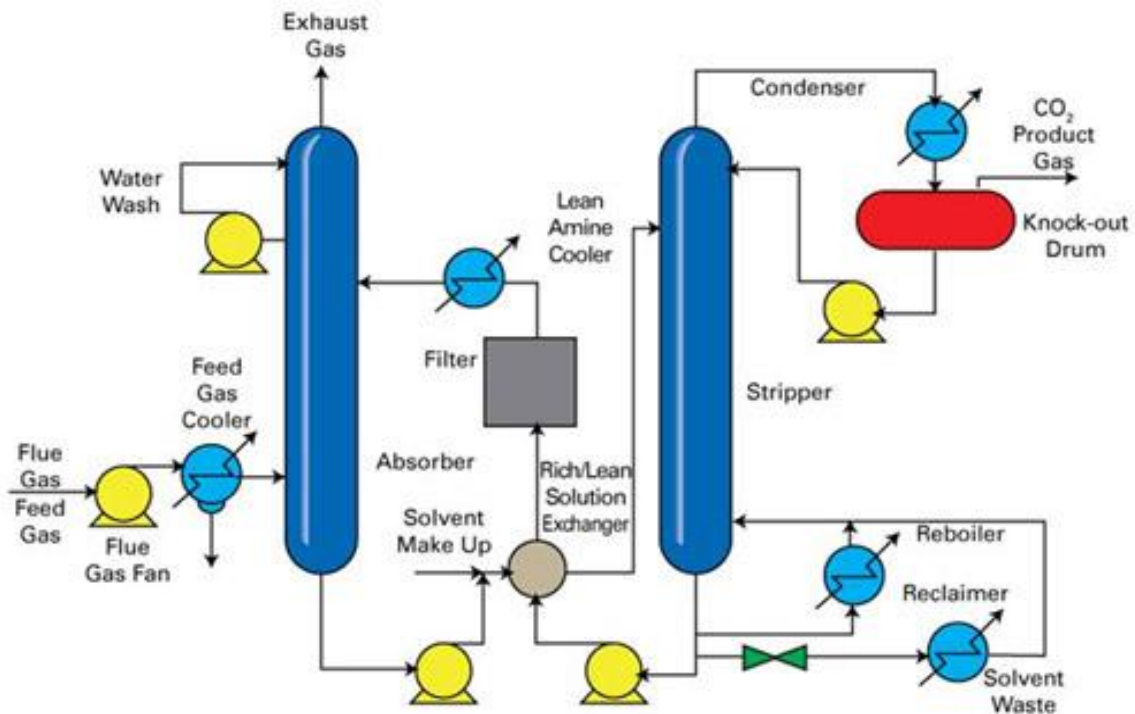


Figure II-9. Schematic representation of the amine scrubbing capture process (Capture Ready, 2013).

### 3.2 Natural gas treatment

For many decades, natural gas has been used as fossil fuel to provide energy to humans. This energy vector is particularly appreciated for its high energy efficiency and the facility of transport (IFP Energies nouvelles, 2013). However natural gas contains impurities such as carbon dioxide (CO<sub>2</sub>), hydrogen sulfide (H<sub>2</sub>S) and others sulfur compounds. These acid compounds have to be partially or totally removed before injection in the pipelines or liquefaction. Specifications on treated gas ensure a constant energetic value and less than 4 ppm H<sub>2</sub>S independently from the composition of the raw gas. In fact, concentration of CO<sub>2</sub> and H<sub>2</sub>S may reach more than 20 % in very sour gases. Moreover, specifications depend on the transportation mode as shown by Table II-3. In most of cases, the acid gas removal process is an amine absorption process, treating the gases at the outlet of the gas field.

The main difference with the CO<sub>2</sub> capture is the operating pressure of the absorption column and its nature. Generally natural gas is introduced in tray or packed absorption column at high pressure (40-100 bars) and temperature ranging between 30 and 70 °C. For pipeline specifications, the absorption of CO<sub>2</sub> has to be limited to keep up to 2 vol. per cent of

CO<sub>2</sub>. In such cases, the difference of reactivity between CO<sub>2</sub> and H<sub>2</sub>S is sought to capture selectively H<sub>2</sub>S which is transformed in elemental sulfur in the Claus process. In the case of production of liquefied natural gas, the solvent have to be enough efficient to purify the natural gas and then to remove almost completely H<sub>2</sub>S and CO<sub>2</sub>.

Table II-3. Specification of natural gas in function of application.

	<b>Production of liquefied natural gas</b>	<b>Transport by pipeline</b>
H <sub>2</sub> S	4 ppm	4 ppm
CO <sub>2</sub>	50 ppm	2 vol. %

### 3.3 Performance of the process

In order to compare performances it is important to consider a reference. In the case of post-combustion, it generally corresponds to a process using monoethanolamine (MEA) to capture CO<sub>2</sub> from coal power plant which offers a thermal power of 1,400 MWth and producing 630 MWe. IFP Energies nouvelles realized this study in 2007 within the framework of the éCO<sub>2</sub> project in association with Alstom. In this process fumes flow is about 2,280 t/h and contains 13.5 molar per cent of CO<sub>2</sub>. It corresponds to the production of around 420 tonnes of CO<sub>2</sub> per hour.

Indeed, MEA benefits of excellent properties of solubility in water, fast kinetics of reaction with CO<sub>2</sub>, good capacity to capture an important quantity of CO<sub>2</sub> in operating conditions and is quite cheap. However this solution suffers from high energy consumption (3.75 GJ/t of CO<sub>2</sub>). It is necessary to use energy which will create 0.6 tonnes of additional CO<sub>2</sub> to capture 1 tonne of CO<sub>2</sub>. Costs associated to the installation of a post-combustion process on the power plant represents a 40 % increase of investment and a 20 % increase of operating costs. Moreover it diminishes electrical efficiency by 10 points the net electricity generation as shown in Table II-4.

Table II-4. Economical and production impact of addition of post-combustion unit (Lecomte *et al.*, 2010).

	<b>Coal power plant</b>	<b><i>Idem</i> + post-combustion unit</b>
Investment cost	710 M€	1,000 M€
Operating cost	66 M€/year	80 M€/year
Net electrical efficiency	45 %	35 %
Net electricity generation	630 MWe	490 MWe

### 3. Amine scrubbing capture process

Capital expense (CAPEX) of the post-combustion process is mainly related to the price of the absorber which represents 30 to 50 % of the investments while operating costs (OPEX) are driven by the regeneration heat (50 to 60 %) and the compression costs of flue gases by the blower (5 to 10 %). The design of the absorber and the cost of the regeneration are mainly driven by thermodynamic and kinetic properties of the solvent.

The principal thermodynamic properties are the enthalpy of reaction and the cyclic capacity of the solvent. The cyclic capacity, defined as the difference of CO<sub>2</sub> loading (number of moles of CO<sub>2</sub> absorbed per kg of solvent) between the lean amine solution and the rich amine solution, is inversely proportional to the solvent flow rate. In the stripper duty, the contribution of sensible heat and the excess of the stripping are directly proportional to the flow rate of the solvent and therefore inversely proportional to the cyclic capacity. In last years, amines with increased capacity have been developed in order to reduce the cost of regeneration (Porcheron *et al.*, 2011).

The kinetics of reaction with CO<sub>2</sub> affects directly the size of the absorber which represents 30 to 50 % of the CAPEX. Indeed, for a given flow rate of solvent and gas and for a given amount of CO<sub>2</sub> to absorb, an amine which reacts faster in a large range of CO<sub>2</sub> loadings requires a smaller column. Moreover, for a given solvent, a poor kinetics would induce increase of the solvent flow rate to reach the required yield of capture in a given height of absorber. Therefore, a great attention has to be paid on kinetics in order to reduce both CAPEX and OPEX.

These elements of design show the importance of the choice of the solvent to reduce the cost associated to CO<sub>2</sub> capture.

#### **3.4 Choice of the solvent**

Generally amines are classified by tertiary or sterically hindered amines on the one hand and moderately hindered primary and secondary amines on the other hand. Tertiary and sterically hindered amines react slowly with CO<sub>2</sub> and require moderate energy of regeneration with high capacities. Other primary and secondary amines react faster but require high energy of regeneration with generally lower capacities than tertiary amines.

In the case of gas treatment, for pipeline application, tertiary or sterically hindered amines are chosen for their high capacity to absorb acid gases and their slow rate of reaction with CO<sub>2</sub> adapted to selective capture of H<sub>2</sub>S. However the case of production of liquefied natural gas is similar to the post-combustion problematic. In those cases a compromise should be made between a good capacity and energy of regeneration brought by the tertiary or sterically hindered amine and a fast kinetic property of reaction dependent on the selected primary or secondary amine.

In order to get an optimum between kinetic and thermodynamic properties which reduces the cost compared to reference MEA, we give here different examples of new technologies which have been developed for CO<sub>2</sub> capture.

### 3.4.1 Ammonia process

Ammonia process consists simply to replace MEA by an ammonia solution. This process benefits from a lower energy regeneration, the low cost of ammonia, a good tolerance to oxygen, low degradation and its capacity to form ammonium sulfite and nitrate in presence of SO<sub>x</sub> and NO<sub>x</sub> which can be used in farming. However it suffers from important loss of volatile ammonia, a slower kinetics in comparison with MEA and an important energetic consumption to cool fumes. The main process using this technology is the Chilled Ammonia Process (Alstom) (Lecomte *et al.*, 2010).

### 3.4.2 Sterically hindered amines

Mitsubishi Heavy Industries and Kansai Electric Power developed a solvent called KS-1 based on a blend of a sterically hindered amine with a fast reacting secondary amine used as an activator. Even if this solvent is 3 or 4 times more expensive than MEA, it enables the operating costs to be reduced significantly insofar as solvent flow, energy of regeneration, solvent degradation, solvent loss and corrosion are decreased. An estimation realized by Mitsubishi indicates that the cost of capture is reduced by around 20 % in comparison with MEA. This process has been tested since the end of the 1990's and other solvents have also been developed (KS-2 and KS-3) (Lecomte *et al.*, 2010).

### 3.4.3 Multiamines

Cansolv Technologies has developed proprietary solvents (DC101 and DC103) based on multiamines. These solvents have a better capacity than MEA and reduce operating costs. Moreover they are very resistant to oxidation, little volatile and achieve capture of CO<sub>2</sub> and SO<sub>2</sub> in the same absorber. Cansolv Technologies also indicate a reduction of 60 % of energy necessary for regeneration in comparison with MEA (Lecomte *et al.*, 2010).

### 3.4.4 Demixing solvent

A demixing solvent has the property to form two or more immiscible phases depending on solvent composition and temperature. This property is particularly interesting on rich solutions. Indeed, at a given CO<sub>2</sub> loading and temperature, phase separation takes place. The lower phase contains the product of the reaction and the upper phase contains the unreacted amine. Phase separation downstream the absorption column leads to regenerate only the lower phase and then reduces the regeneration energy. IFP Energies nouvelles has recently developed solvents DMX-1 and DMX-2. The latter, in comparison with MEA process diminishes the flow of solvent of 40 %, the energy of reboiler of 40 % (2.25 GJ/t of CO<sub>2</sub>) and operating costs of 30 % (Lecomte *et al.*, 2010).

## 3.5 Conclusion

Among the different technologies available for CO<sub>2</sub> capture, amine scrubbing process is the most mature, directly inspired from natural gas treatment. In this process, optimization in terms of energy and costs is mainly driven by the formulation of solvent.

Kinetics of CO<sub>2</sub> absorption by the solvent impacts directly on 30 to 50 % of CAPEX and indirectly on 55 to 70 % of OPEX of the post-combustion capture process. Therefore, the

#### 4. The amine – carbon dioxide reaction

understanding and optimization of this parameter is a key to develop a competitive solvent. In order to understand kinetics of CO<sub>2</sub> absorption by different solvents, we decide to develop a comprehensive structure-property relationship applied to the different structures of amine.

In the next section we present the reactions of carbon dioxide in aqueous amine solutions. After presenting some definitions, a presentation of instantaneous reactions will be done. Then we present mechanisms and rate laws for the other kinetically limited reactions. Finally we present experimental methods to study those reactions and mathematical methods to extract kinetic data in order to have a global comprehension of the relation between the structure of the amine and its kinetic properties.

### 4 The amine – carbon dioxide reaction

In the previous section we have shown the great importance of kinetic properties in the amine scrubbing capture process. In order to study the kinetics of the amine-carbon dioxide reaction, we present first the reactions which take place in aqueous amine solutions. We define the different classes of amines and their mechanisms of reaction with CO<sub>2</sub> as proposed in the literature.

#### 4.1 Definitions

IUPAC define an amine as "compounds formally derived from ammonia by replacing one, two or three hydrogen atoms by hydrocarbyl groups, and having the general structures RNH<sub>2</sub> (primary amines), R<sub>2</sub>NH (secondary amines), R<sub>3</sub>N (tertiary amines)".

As indicated in the IUPAC definition, amines can be classified by their degree of substitution: primary amines (R<sub>1</sub>NH<sub>2</sub>), secondary amines (R<sub>1</sub>R<sub>2</sub>NH) and tertiary amines (R<sub>1</sub>R<sub>2</sub>R<sub>3</sub>NH) as indicated in Figure II-10. Amines are basic and nucleophilic compounds due to the presence of a lone electron pair on the nitrogen atom. These properties as well as other physicochemical properties depend on the nature of substituent R<sub>1</sub>, R<sub>2</sub> and R<sub>3</sub>.

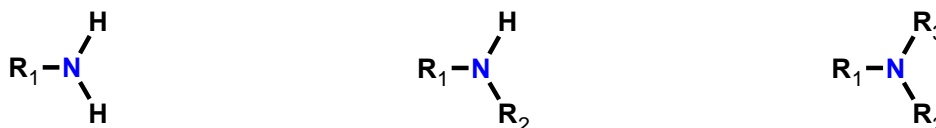


Figure II-10. Example of primary (R<sub>1</sub>NH<sub>2</sub>), secondary (R<sub>1</sub>R<sub>2</sub>NH) and tertiary amines (R<sub>1</sub>R<sub>2</sub>R<sub>3</sub>NH).

In this study we only consider molecules composed of at least one amine function. The rest of the molecule may contain other functional group. For reason of the number of potential amine corresponding to this definition we limit our study by considering atoms of functional groups which are only constituted by atoms of hydrogen, carbon, oxygen and/or nitrogen. We also consider heterocyclic compounds which are not aromatic as piperidine and morpholine.

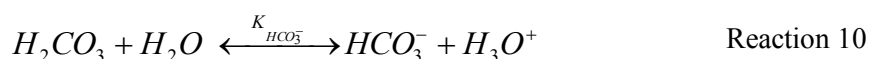
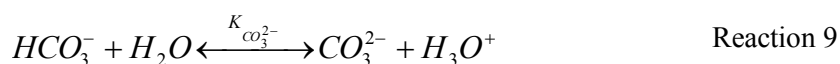
## 4.2 Instantaneous reactions

In this study, we assume that all reactions presented in this section are so fast that they can be considered as instantaneous in comparison with other reactions. Indeed, all the reactions of this section are essentially proton transfer reactions.

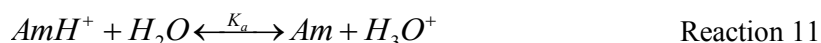
When water is used as solvent, the most common reaction is the reaction of self-ionization of water described by Reaction 8.



Carbon dioxide has one basic form (carbonate ( $CO_3^{2-}$ )), one amphoteric form (hydrogencarbonate or bicarbonate ( $HCO_3^-$ )) and one acidic form (carbonic acid ( $H_2CO_3$ )). For all these species, there are two acido-basic equilibria with conjugated forms as shown by Reaction 9 and Reaction 10.



The last instantaneous reaction which happens is the dissociation of amine in water given by Reaction 11. Contrary to previous reactions, the thermodynamic constant of this one is dependent on the amine.



## 4.3 Kinetically limited reactions

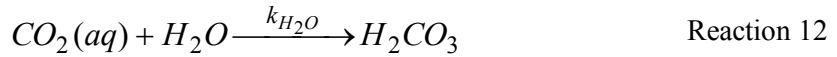
Reaction of  $CO_2$  in aqueous amine solutions can be described by three sets of reactions. The first set of reactions involves carbon dioxide with water or hydroxide ions and is common to all amines. The second set of reactions takes place with tertiary amine. Finally, the third set takes place with primary and secondary amines. In all cases we present only reactions of  $CO_2$  with large excess of amine, and do not take into account inverse reactions.

### 4.3.1 General case

#### 4.3.1.1 Hydration of carbon dioxide

Carbon dioxide in presence of water is hydrated and forms carbonic acid (Reaction 12). Carbonic acid reacts with a basic compound (B) present in solution (Reaction 13). The base B can be an amine, water or a hydroxide ion.

#### 4. The amine – carbon dioxide reaction



Pinsent *et al.* (1956) showed first that Reaction 12 is the limiting step and determined the pseudo-first-order associated rate constant defined by Equation 1 (at 25 °C  $k'_{H_2O} = 2.57 \times 10^{-2} \text{ s}^{-1}$ ). More recently Soli and Byrne (2002) determined the rate of this reaction (at 25 °C  $k'_{H_2O} = 3.06 \times 10^{-2} \text{ s}^{-1}$ ). These values are not identical but have the same order of magnitude. They show that this reaction is very slow compared to hydroxyde-CO<sub>2</sub> and amine-CO<sub>2</sub> reaction described below.

$$r_{CO_2}^{H_2O} = \underbrace{k_{H_2O} \cdot [H_2O]}_{k'_{H_2O}} [CO_2] \quad \text{Equation 1}$$

##### 4.3.1.2 Reaction between carbon dioxide and hydroxide ion

In aqueous basic solution, carbon dioxide reacts with a hydroxide ion to form a bicarbonate ion (Reaction 14).



Rate of this reaction is given by Equation 2. The correlation determined by Pinsent *et al.* (1956) gives  $k_{HO^-} = 8.32 \text{ m}^3 \text{ mol}^{-1} \text{ s}^{-1}$  at 25 °C.

$$r_{CO_2}^{HO^-} = k_{HO^-} \cdot [CO_2] \cdot [HO^-] \quad \text{Equation 2}$$

##### 4.3.2 Tertiary amines

###### 4.3.2.1 Based-catalyzed hydration mechanism

Donaldson and Nguyen (1980) show that tertiary amines (R<sub>3</sub>N) do not react directly with carbon dioxide. Tertiary amines act as "pseudo-catalyst". They accelerate the reaction of hydration of carbon dioxide. For this reason, this mechanism is called based-catalyzed hydration mechanism (Reaction 15).

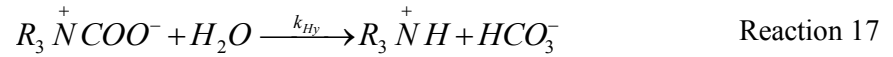


Since concentration of water does not vary too much in kinetic studies and is in large excess, this reaction is generally considered to be first order with respect to amine concentration (Equation 3) with the pseudo-constant  $k'_{R_3N} = k_{R_3N} \cdot [H_2O]$  (Crooks and Donnellan, 1990).

$$r_{CO_2}^{R_3N} = \underbrace{k_{R_3N} \cdot [H_2O]}_{k'_{R_3N}} \cdot [CO_2] \cdot [R_3N] \quad \text{Equation 3}$$

#### 4.3.2.2 Zwitterion mechanism

A two-step mechanism was also suggested by Yu *et al.* (1985). Carbon dioxide reacts first with the amine to form a zwitterion (Reaction 16). The zwitterion is then hydrolyzed by water to form ammonium ions and bicarbonate ions (Reaction 17). As a very instable intermediate, the zwitterion is assumed at a steady state low concentration.



With this assumption, reaction rate of  $CO_2$  is shown in Equation 4. Kinetic constants  $k'_{R_3N}$  and  $k'^{H_2O}_{Hy}$  are explicated by Equation 5.

$$r_{CO_2}^{R_3N} = \frac{[R_3N] \cdot [CO_2]}{\frac{1}{k_{NA}} + \frac{1}{k'^{H_2O}_{Hy}}} = k'_{R_3N} [R_3N] \cdot [CO_2] \quad \text{Equation 4}$$

$$\frac{1}{k'_{R_3N}} = \frac{1}{k_{NA}} + \frac{1}{k'^{H_2O}_{Hy}} \quad \text{and} \quad k'^{H_2O}_{Hy} = \frac{k_{NA} \cdot k'^{H_2O}_{Hy} [H_2O]}{k_{-NA}} \quad \text{Equation 5}$$

In the case of tertiary amines, the overall rate of reaction of carbon dioxide (Equation 6) corresponds to the sum of the contributions of three reaction paths (Reaction 12, Reaction 13 and Reaction 14), and the reaction with the tertiary amine (Reaction 15) or (Reaction 16 and Reaction 17). Based-catalyzed hydration mechanism or zwitterion mechanism both yield to an order of reaction of one with respect to amine.

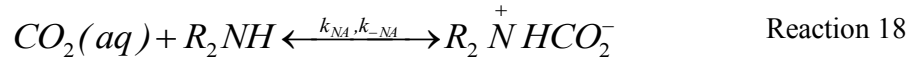
$$r_{CO_2}^{III} = r_{CO_2}^{H_2O} + r_{CO_2}^{HO^-} + r_{CO_2}^{R_3N} \quad \text{Equation 6}$$

#### 4. The amine – carbon dioxide reaction

##### 4.3.3 Primary and secondary amines

###### 4.3.3.1 Zwitterion mechanism

The two-step mechanism proceeding through the formation of a zwitterion as an intermediate has been suggested for the first time by Caplow (1968) and reintroduced by Danckwerts (1979). In the first step, amine reacts with carbon dioxide and forms a zwitterion (Reaction 18). Then zwitterion is deprotonated by a base B (Reaction 19). In these equations  $k_{NA}$  corresponds to the kinetic constant of the nucleophilic addition,  $k_{-NA}$  corresponds to the kinetic constant of the reverse reaction and  $k_{Dep}^B$  corresponds to the kinetic constant of the deprotonation of the zwitterion by a base B.



Versteeg and Vanswaaij (1988) have shown that deprotonation reaction with hydroxide ion as a base is insignificant for unloaded solution. Only amine and water have to be considered as bases for deprotonation of the zwitterion. The rate of the reaction of  $CO_2$  with amine is then given by Equation 7, assuming zwitterion concentration at quasi steady state (Danckwerts, 1979). We simplify this equation as shown by Equation 8 and with  $k_{Dep}^{R_2NH}$  and  $k_{Dep}^{H_2O}$  defined in Equation 9.

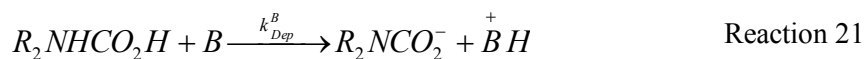
$$r_{CO_2}^{R_2NH} = \frac{[R_2NH] \cdot [CO_2]}{\frac{1}{k_{NA}} + \frac{k_{-NA}}{k_{NA} (k_{Dep}^{R_2NH} \cdot [R_2NH] + k_{Dep}^{H_2O} \cdot [H_2O])}} \quad \text{Equation 7}$$

$$r_{CO_2}^{R_2NH} = \frac{[R_2NH] \cdot [CO_2]}{\frac{1}{k_{NA}} + \frac{1}{k_{Dep}^{R_2NH} \cdot [R_2NH] + k_{Dep}^{H_2O} \cdot [H_2O]}} \quad \text{Equation 8}$$

$$k_{Dep}^{R_2NH} = \frac{k_{NA} \cdot k_{Dep}^{R_2NH}}{k_{-NA}}; \quad k_{Dep}^{H_2O} = \frac{k_{NA} \cdot k_{Dep}^{H_2O}}{k_{-NA}} \quad \text{Equation 9}$$

###### 4.3.3.2 Carbamic acid

Recently McCann *et al.* (2009) proposed a mechanism which is close to the zwitterion model. According to them, the reaction between carbon dioxide and amine forms a carbamic acid (Reaction 20). Carbamic acid is a more stable tautomeric form of the zwitterion according to NMR measurements. Then carbamic acid is deprotonated instantaneously by a base (Reaction 21).



Reaction rate according to this carbamic acid mechanism is given by Equation 10 which has the same expression as the limit case of the zwitterion model when nucleophilic addition is the rate-limiting step.

$$r_{CO_2}^{R_2NH} = k_{NA} \cdot [R_2NH] \cdot [CO_2] \quad \text{Equation 10}$$

#### 4.3.3.3 Termolecular mechanism

Another mechanism which considers that carbon dioxide, amine and base react simultaneously has been suggested by Crooks and Donnellan (1989). This termolecular mechanism (Reaction 22) corresponds to a limiting case of the zwitterion mechanism where the limiting step is deprotonation. This mechanism has been recently supported by molecular modelisation (da Silva and Svendsen, 2004). In this work da Silva and Svendsen (2004) show that energetic levels are in favour of a one step mechanism. In this equation  $k_{ter}^B$  corresponds to the third order kinetic constant of the termolecular mechanism. By analogy with the zwitterion mechanism, termolecular reaction with hydroxide ions is insignificant.



The reaction rate according to this termolecular mechanism is given by Equation 11. Third order kinetic constants  $k_{ter}^{H_2O}$  and  $k_{ter}^{R_2NH}$  correspond to the reaction of  $CO_2$  with respectively one molecule of amine and one molecule of water and two molecules of amine.

$$r_{CO_2}^{R_2NH} = k_{ter}^{H_2O} \cdot [H_2O] \cdot [R_2NH] \cdot [CO_2] + k_{ter}^{R_2NH} [R_2NH]^2 \cdot [CO_2] \quad \text{Equation 11}$$

The overall rate of carbon dioxide reaction for a primary or secondary amine is then given in Equation 12.

$$r_{CO_2}^{I/II} = r_{CO_2}^{H_2O} + r_{CO_2}^{HO^-} + r_{CO_2}^{R_2NH} \quad \text{Equation 12}$$

#### 4.3.3.4 Carbamate hydrolysis

Carbamates ( $R_2NCO_2^-$ ) are more or less stable species in water, depending on their structure. Other things being equal, more a carbamate is sterically hindered less it is stable. Generally they are hydrolyzed by water to form ammonium ion and hydrogencarbonate ion as

## 5. Experimental techniques

show by Reaction 23. This reaction is described as quite slow in comparison with reaction rate of primary and secondary amines (Vaidya and Kenig, 2007). For this reason, authors consider that this reaction does not impact significantly results of other reactions.



### 4.4 Conclusion

In this part we have seen that studying kinetics of reaction between amine and carbon dioxide is complex because of the number of reaction implied. We also notice that different mechanisms have been proposed to explain the same reaction (tertiary amines, primary and secondary amines). We now give a brief description of experimental techniques adapted to kinetic studies.

## 5 Experimental techniques

Experimental techniques for kinetic measurements on amine – CO<sub>2</sub> systems can be classified in two types of equipment at the laboratory scale: measurement of gas-liquid mass transfer rate on the one hand, and in situ measurements of reaction rate after rapid mixing of liquid phases on the other hand. Both types of techniques present advantages and drawbacks for data comparison and the establishment of a structure-activity relationship.

### 5.1 Measurement of CO<sub>2</sub> absorption flow rate

Several kinds of gas-liquid reactors are dedicated to measure the kinetics of CO<sub>2</sub> absorption in amine solutions (Laurent *et al.*, 1975). Each of these equipments based on gas-liquid absorption measurement is characterized by a limited range of contact time or liquid mass transfer coefficient, and thus allows measurements in a given concentration range for appropriate formulations of amine. Since reaction rates of amines with CO<sub>2</sub> vary on several orders of magnitude, none of these equipments is adequate for accurate determination of kinetic parameters in the large experimental domain covered by the great variety of amines. Characteristics of some techniques are indicated in Table II-5.

Table II-5. Contact time of some experimental techniques (Laurent *et al.*, 1975).

Technique	Laminar jet	Cylindrical falling film reactor	Hemispherical falling film reactor	Disc column	Stirred reactor
Contact time (s)	10 <sup>-3</sup> -10 <sup>-1</sup>	10 <sup>-1</sup> -2	0.2-1	10 <sup>-1</sup> -2	0.06-10 <sup>1</sup>

For example, kinetics of absorption by a 30 weight percent of monoethanolamine solution will be studied on a wetted-wall column (Puxty *et al.*, 2010), whereas a 50 weight percent of methyldiethanolamine will be studied on a stirred vessel (Versteeg and Van Swaij, 1988).

These techniques also imply the use of a mass-transfer model to analyze experimental data. This model takes into account the thermodynamic equilibrium, the hydrodynamics of gas and liquid phases, physical solubility, diffusion of reactants and products in the liquid phase to fit measured mass transfer rate. In these conditions, estimation of kinetic constants greatly depends on the different hypotheses of the mass transfer model (Charpentier, 1981; Danckwerts, 1970; Laurent and Charpentier, 1974) which can provide additional source of dispersion on data.

For diethanolamine, which is commonly used in gas treatment, Rinker *et al.* (1996) show that dispersion between second order apparent kinetic constants found by different authors is higher than 50 % as indicated by Figure II-11.

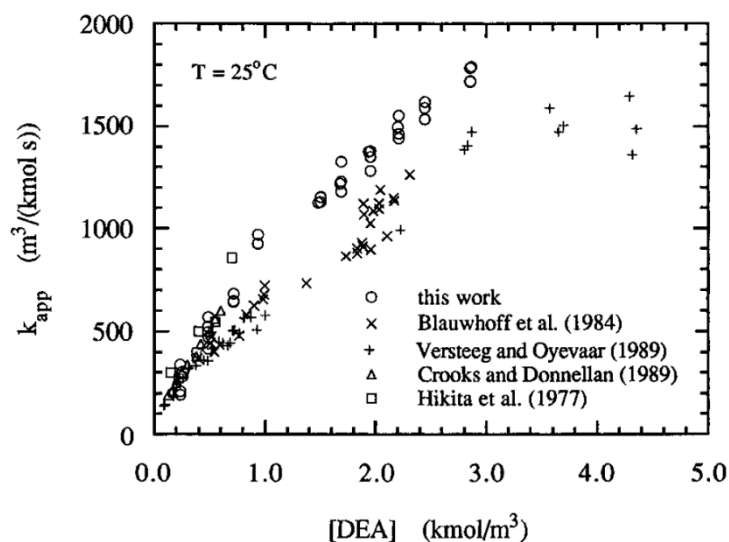


Figure II-11. Apparent kinetic obtain by different authors and experimental technique for diethanolamine at 25 °C in function of the amine concentration (Rinker *et al.*, 1996).

## 5.2 Rapid mixing methods

Rapid mixing methods consist in mixing two reagents in a cell and to measure a physical signal representative to the extent of reaction at this place. There are two kinds of rapid mixing methods: continuous-flow technique and stopped-flow technique. In the case of continuous-flow technique concentration of reagents and products or temperature are measured at different locations downstream of the mixing chamber. In given condition, by changing the rate of flow and then the mixing time, it is possible to determine the extent of reaction and then to determine the kinetic properties. In the case of stopped-flow technique, reagents are rapidly mixed in a cell in such way reaction does not have time to take place during the mixing time. Then the flow is stopped, the measure of a physical signal (generally spectrometric or conductivity measurement) can be related to the evolution of chemical species and the extent of reaction.

The most widely used of rapid mixing techniques for CO<sub>2</sub>-amine studies is the stopped-flow technique. In comparison with mass-transfer techniques, stopped-flow technique

## 6. Methods for data treatment

enables to determine kinetic constant usually ranged between about 0.01 and 1,000 s<sup>-1</sup>, the upper limit corresponding to the inverse of the mixing time which is close to 1 ms. It is then not suited to study kinetics of reaction of fast-reacting amines in industrial conditions. However, kinetic measurements with stopped-flow technique are free from gas-liquid mass transfer limitations. Signal can be directly related to the intrinsic reaction in the liquid phase which makes the method very reproducible. Rayer *et al.* (2011) show that the overall uncertainty on these data are generally around 5 %. Then this method is well fitted to draw quantitative structure activity relationship from the comparison of intrinsic kinetics of reaction of very different amines with CO<sub>2</sub>.

### 5.3 Conclusion

According to the characteristics of the different techniques, stopped-flow seems to be the most adapted to realize a study to understand the relation between structure and kinetic properties. Indeed, this technique is free of gas-liquid transfer and then avoids a potential source of dispersion when kinetic data from different amine are compared. Moreover it covers a large range of reaction rates. We now give a brief description of the methods to determine apparent kinetic constant from results got by stopped-flow technique.

## 6 Methods for data treatment

We distinguish two methods to derive kinetic parameters from stopped-flow data. The choice of the method depends on detection type (conductimetry, spectrophotometry), mechanistic hypotheses and operating condition. We consider advantages and drawbacks of both methods.

### 6.1 Numerical method

The numerical method solves a system of equations which takes into account all chemical species with the reactions and thermodynamic equilibria in which they are involved. Kinetic parameters are optimized to reduce deviation between the model and experimental data. This approach is necessary when spectrophotometric detection is used to follow the reaction (Barth *et al.*, 1981; Barth *et al.*, 1983; Barth *et al.*, 1984; Barth, 1984; Barth *et al.*, 1986) or if operating conditions like CO<sub>2</sub> loading is not compatible with an analytical solution of the model (Conway *et al.*, 2011; Conway *et al.*, 2012a; Conway *et al.*, 2013; Conway *et al.*, 2012b ; McCann *et al.*, 2009; Wang *et al.*, 2011; Xiang *et al.*, 2012).

Although this method is quite exhaustive, results on kinetic constants is still dependant on the mechanistic hypotheses and the thermodynamic model representing non ideal solutions.

### 6.2 Analytical method

Analytical model is the most widespread approach for stopped-flow studies on amine-CO<sub>2</sub> reaction. This approach considers a single irreversible reaction with amine in large excess of first order with respect to CO<sub>2</sub>. Generally, authors operate with a total concentration of amine at least ten times higher than the concentration of carbon dioxide. In these

conditions, the variation of concentration of chemical species depends on the pseudo first order kinetic constant  $k_0$  according to a monoexponential expression. For conductivity stopped flow measurements, the variation of concentrations of ionic species is monitored by the change of conductance in the solution. Conductance  $G$  (S) is the inverse of the electric resistance  $R$  ( $\Omega$ ),  $A$  (S) is the amplitude of the signal,  $k_0$  the pseudo first order kinetic constant,  $t$  (s) is the time and  $C$  (S) is the value of the conductance at the end of the observed reaction. Variation of conductance is then related to the formation of amine salts and to  $k_0$  according Equation 13 (Ali *et al.*, 2000).

$$\frac{1}{R(t)} = G(t) = -A \times \exp(-k_0 \times t) + C \quad \text{Equation 13}$$

The pseudo first order kinetic constant  $k_0$  (also called apparent kinetic constant) is defined as shown by Equation 14. When it is measured in a large excess of amine,  $k_0$  depends on the nature of the amine, the concentration of amine and the temperature.

$$r_{CO_2} = k_0 \cdot [CO_2] \quad \text{Equation 14}$$

## 7 Conclusion

Amine scrubbing process is today the most mature process to reduce anthropogenic emissions of  $CO_2$  in the atmosphere. It benefits from the experience obtained in the field of natural gas treatment. However, it always suffers from important cost penalties directly linked to the solvent properties. Besides thermodynamic properties such as optimal cyclic capacities, kinetics of  $CO_2$  absorption needs to be optimized in order to make the process economically available. This optimization is only possible with a global comprehension of the impact of the structure of the amine on kinetic properties.

Among the variety of amines we limit our study to amine composed of hydrogen, carbon, nitrogen and/or oxygen. Their mechanisms of reaction with  $CO_2$  with the different interpretations proposed in the literature have been presented.

According to the literature, stopped-flow technique is suitable to study amines within a very large range of reaction rate and then is adapted to establish a structure-property relationship. Most of authors determine pseudo first order kinetic constant using the analytical method. Many raw data of pseudo first order available in the literature can be directly compared, without any mechanistical consideration.

For all these reasons it seems very interesting to collect all data obtained in the literature with stopped-flow equipment and analytical method and analyze them. That is why in the next chapter, we will synthesize and discuss about data obtained by this way. This step is particularly important to identify trends and to guide our approach in order to build a structure-property relationship.

*«The constructive critic is a lever of progress. »*

Anonymous

## Chapter III: CRITICAL REVIEW OF THE LITERATURE

---

This section describes our approach to compare data from different authors in order to get an overview on kinetics of amine–CO<sub>2</sub> systems. In the precedent chapter, we have justified the comparison of results from different authors with the stopped-flow technique. Indeed, this technique covers a large range of reaction rates and is quite reproducible. We have also chosen to analyze kinetic data obtained by the monoexponential expression which is the most widespread analytical method to extract kinetic constants from stopped-flow experiments.

This review is based on apparent kinetic constants obtained by the stopped-flow technique and determined with the analytical method. We first compare pseudo-first order kinetic constants  $k_0$  of the different amines at a given concentration and temperature. We then look at the effect of concentration at 25°C for the different amines. In this part we show the influence of various structural parameters on apparent kinetic constant and order of reaction and confront the different mechanisms proposed in the literature with experimental results. We also discuss on the Arrhenius parameters obtained from data at different temperatures. In the conclusion, we define the scope and objectives of our work.

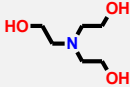
### 1 Stopped-flow data

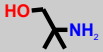
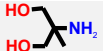
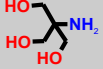
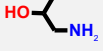
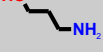
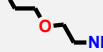
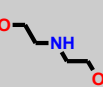
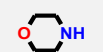
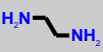
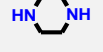
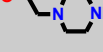
All published pseudo-first order constants (also called apparent kinetic constants)  $k_0$  of amine which were measured on a conductimetric stopped-flow apparatus at 25 °C have been compiled. The data corresponding to these amines and the corresponding references are listed in Table III-1. The concentration range, the temperature range, the pKa at 25 °C and its reference are also indicated.

Some amines have been studied by different authors and, apart from two cases Ali *et al.* (2010) for molecule n°8 (methylethanolamine), and Crooks and Donnellan (1989) for molecule n°18 (diethanolamine), a discrepancy smaller than 25 % between kinetic constants from the different authors is observed on the same amine. After removal of the two latter references, we retain for each amine the study that covers the largest range of amine concentration at 25°C. Corresponding references have been represented in bold in Table III-1.

## 1. Stopped-flow data

Table III-1. Name, abbreviation, chemical structure, references of stopped-flow kinetic studies of amine-CO<sub>2</sub> reaction with conductimetric detection, concentration range, temperature range, pKa at 25 °C and references of pKa values. References selected for the rest of this section are indicated in bold.

Name	Abbreviation	Number	Chemical structure	Authors	Concentration range (mol.m <sup>-3</sup> )	Temperature range (°C)	pKa at 25°C	Reference
Triethanolamine	TEA	1		(Crooks and Donnellan, 1990)	25-176	25	7.76	(da Silva and Svendsen, 2007)
Methyldiethanolamine	MDEA	2		(Crooks and Donnellan, 1990)	25-176	25	8.52	(da Silva and Svendsen, 2007)
Dimethylmonoethanolamine	DMMEA	3		(Henni <i>et al.</i> , 2008)	303-986	25-40	9.23	(da Silva and Svendsen, 2007)
3-Dimethylamino-1-propanol	3-DMAP	4		(Kadiwala <i>et al.</i> , 2012)	350-1,003	25-40	9.54	(Kadiwala <i>et al.</i> , 2012)
1-Dimethylamino-2-propanol	DMA-2-P	5		(Kadiwala <i>et al.</i> , 2012)	238-1,000	25-40	9.50	(Kadiwala <i>et al.</i> , 2012)
Diethylmonoethanolamine	DEMEA	6		(Li <i>et al.</i> , 2007)	197-997	25-40	9.75	(da Silva and Svendsen, 2007)
Monoethanolamine	MEA	7		(Crooks and Donnellan, 1989) (Alper, 1990a; Alper, 1990b) <b>(Ali <i>et al.</i>, 2002)</b>	20-59 28-52 (at 25 °C) <b>5-36</b>	25 5-40 <b>25-40</b>	9.44	(Hamborg and Versteeg, 2009)
Methylethanolamine	MMEA	8		<b>(Ali <i>et al.</i>, 2002)</b> (Ali <i>et al.</i> , 2010)	<b>8-39</b> 20-69	<b>10-35</b> 25-40	9.85	(Hamborg and Versteeg, 2009)
Ethylethanolamine	EEA	9		(Li <i>et al.</i> , 2007)	28-82	25-40	9.89	(Chemicalize, 2012c)
n-Butylethanolamine	NBAE	10		(Ali <i>et al.</i> , 2002)	20-98	10-35	10.00	(Chemicalize, 2012d)
t-Butylethanolamine	TBAE	11		(Ali <i>et al.</i> , 2002)	17-63	10-35	10.12	(Littel <i>et al.</i> , 1990b)

Name	Abbreviation	Number	Chemical structure	Authors	Concentration range (mol.m <sup>-3</sup> )	Temperature range (°C)	pKa at 25°C	Reference
2-amino-2-methyl-1-propanol	AMP	12		(Alper, 1990b) (Ali, 2005)	25-1,486 (at 25 °C) 54-346	5-25 25-40	9.72	(da Silva and Svendsen, 2007)
2-amino-2-methylpropan-1,3-diol	AMPD	13		(Bouhamra <i>et al.</i> , 1999)	25-1,351 (at 25°C)	5-30	9.48	(Chemicalize, 2012b)
2-amino-2-hydroxymethyl-1,3-propanediol	AHPD	14		(Ume and Alper, 2012)	500-2,000	25	8.95	(Chemicalize, 2012a)
1-amino-2-propanol	1-AP	15		(Henni <i>et al.</i> , 2008)	25-82	25-40	9.46	(da Silva and Svendsen, 2007)
3-amino-1-propanol	3-AP	16		(Henni <i>et al.</i> , 2008)	27-61	25-40	10.00	(da Silva and Svendsen, 2007)
2-(2-aminoethoxy)ethanol	DGA	17		(Alper, 1990a)	12-206 (at 25 °C)	5-25	9.46	(da Silva and Svendsen, 2007)
Diethanolamine	DEA	18		(Crooks and Donnellan, 1989) (Ali, 2004) (Li <i>et al.</i> , 2007)	100-1,016 66-519 150-518	25 25-40 25-40	8.96	(da Silva and Svendsen, 2007)
Morpholine	MOR	19		(Alper, 1990a) (Ali <i>et al.</i> , 2010)	3-102 (at 25 °C) 32-130	5-25 25-40	8.49	(da Silva and Svendsen, 2007)
Ethylenediamine	EDA	20		(Li <i>et al.</i> , 2007) (Rayer <i>et al.</i> , 2011)	26-68 20-101	25-40 25-40	9.92	(da Silva and Svendsen, 2007)
Piperazine	PZ	21		(Gordesli and Alper, 2011)	10-100 (at 25 °C)	5-25	9.71-5.41	(Hamborg and Versteeg, 2009)
Hydroxyethylpiperazine	HPZ	22		(Ume <i>et al.</i> , 2012)	2.5-30	25	8.92-3.97	(Hamborg and Versteeg, 2009)

## 2. First order kinetic constants

### 2 First order kinetic constants

According to data in Table III-1, we extrapolate thanks to a power law indicated by Equation 15 in the next part, the value of the apparent first order kinetic constant  $k_0$  of each amine at an amine concentration of  $100 \text{ mol.m}^{-3}$  at  $25^\circ\text{C}$ . Figure III-1 represents  $k_0$  for the different amines.

At the given concentration  $0.1 \text{ M}$  of amine,  $k_0$  varies by more than 4 orders of magnitude. This observation confirms on the one hand the significance of the choice of the amine in the amine scrubbing process and on the other hand, the interest to use stopped-flow technique to screen amines.

Figure III-1 also shows that primary and secondary amines, which form carbamates, react faster than tertiary amines, excepted for AHPD indicated by a green ellipse. Moreover, multi-amines (PZ, HPZ and EDA) are among the fastest amines.

We notice that for an amine concentration of  $100 \text{ mol.m}^{-3}$ , apparent kinetic constant of the fastest molecule is superior to  $1,000 \text{ s}^{-1}$ . This value corresponds to the technical limit for a kinetic measurement with a stopped-flow equipment having a mixing time of  $1 \text{ ms}$ . It indicates that studying this kind of molecules implies to operate at a lower concentration than  $100 \text{ mol.m}^{-3}$ . For a molecule which has a molecular weight of  $100 \text{ g.mol}^{-1}$  and a density of  $10^6 \text{ g.m}^{-3}$ , it corresponds to a weight concentration of  $1\%$ . The study of the reaction between amine and  $\text{CO}_2$  by stopped-flow technique is therefore generally realized in diluted solutions due to the technical limitation of the reaction rate.

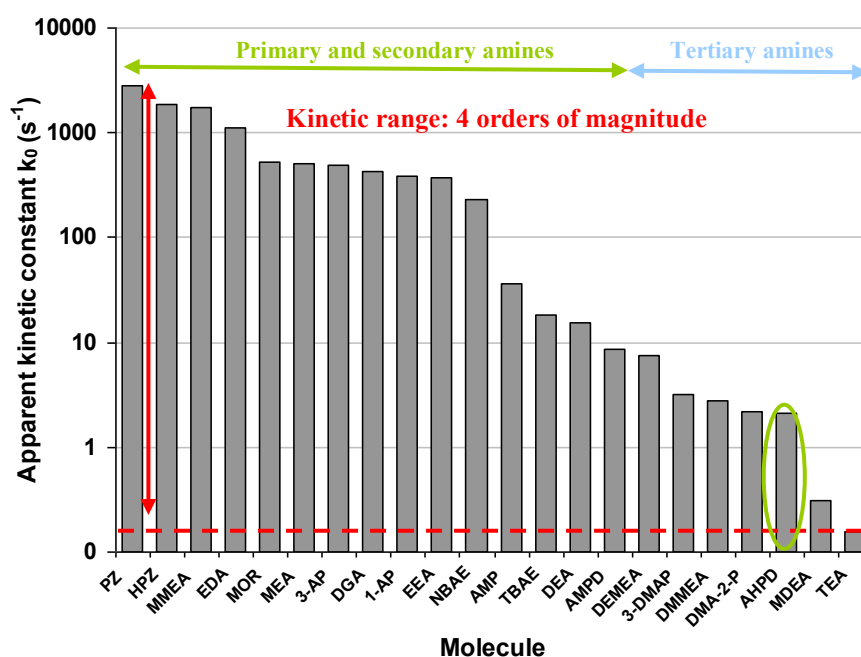


Figure III-1. Apparent kinetic constants  $k_0$  vs. molecules studied in the literature.  $[\text{Am}] = 100 \text{ mol.m}^{-3}$ .  $T = 25^\circ\text{C}$ .

As kinetics depends on concentration, the comparison of pseudo first order constants at a single concentration is limited. We shall now consider the dependency of this constant with concentration for the different amines through the comparison of  $k_{Am}$  et n.

### 3 Effect of the concentration

#### 3.1 Analysis of the raw data

In the chapter II, we showed that several mechanisms are proposed in the literature to explain experimental results. It is well known that the rate law depends on the mechanism of the reaction. In order to analyze the raw data without any mechanistic assumption, we determine the two parameters  $k_{Am}$  and n of the power law model given by Equation 15. The parameter  $k_{Am}$  is an empirical kinetic constant ( $m^{3n} \cdot mol^{-n} \cdot s^{-1}$ ) and n is the apparent order of reaction with respect to amine.

$$k_0 = k_{Am} \cdot [Am]^n \quad \text{Equation 15}$$

Optimal parameters are obtained by fitting variation of experimental pseudo first order constant  $k_0$  as a function of concentration for each amine as indicated by Figure III-2. This figure indicates that for molecule n°9 (ethylethanolamine) optimal value of  $k_{Am}$  is  $4.76 \times 10^{-2} m^{3n} \cdot mol^{-n} \cdot s^{-1}$  and optimal value of n is 1.95.

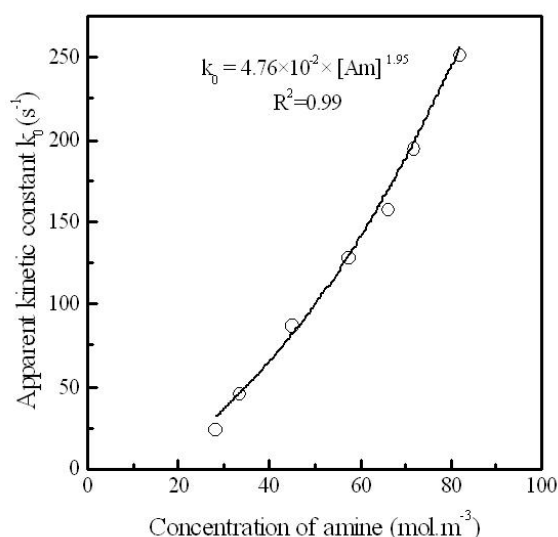


Figure III-2. Apparent kinetic constants vs. ethylethanolamine concentration (molecule n°9). Experimental results (black circles) and fit of experimental data (black line) according to Equation 15. T = 25 °C.

### 3. Effect of the concentration

For all set of data selected in Table III-1, we determine the optimum parameters by this way. The average relative deviation between the experimental constants and this model over all data is 7.3 %. For each amine, parameters  $k_{Am}$  and  $n$  are plotted on Figure III-3. We also represent by continuous lines values of  $(k_{Am}, n)$  giving the same value of  $k_0$  for concentration of amine of  $100 \text{ mol.m}^{-3}$ . This concentration has been chosen because almost all studied amines can be evaluated at this concentration in the operating range available by the stopped-flow technique.

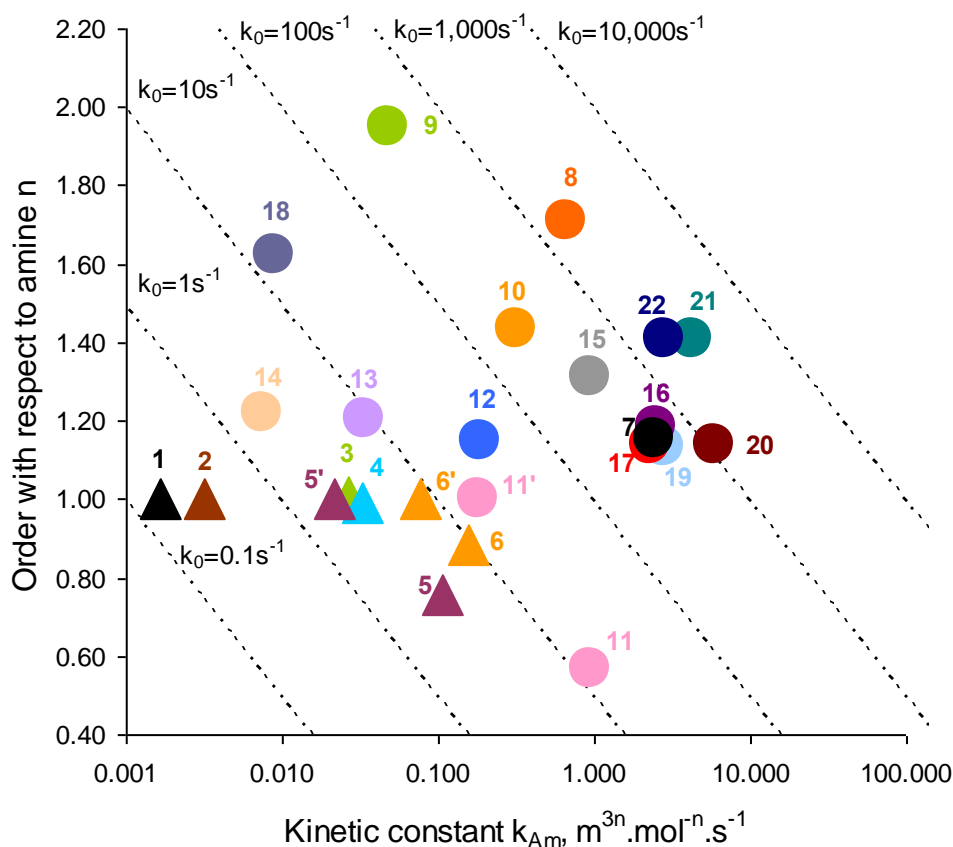


Figure III-3. Values of  $(k_{Am}, n)$  from Equation 15 for tertiary amines (triangles), primary and secondary amines (circles) listed in Table III-1. Dashed lines represent values of  $(k_{Am}, n)$  giving the same value of  $k_0$  for  $[Am] = 100 \text{ mol.m}^{-3}$ . Setting  $n=1$  for molecules  $n^{\circ}5, 6$  and  $11$  gives  $5', 6', 11'$ .  $T = 25 \text{ }^{\circ}\text{C}$ .

We notice that molecules  $n^{\circ}5, 6$  and  $11$  have an apparent order lower than 1. This is in contradiction with the mechanisms proposed in the literature where the order of reaction can only be between 1 and 2 with respect to amine. This result is due to the variation of apparent  $k_0$  with  $[Am]$  which is better fitted by an affine function. For instance, 1-dimethylamino-2-propanol (molecule  $n^{\circ}5$ ) is fitted by the affine model with an average relative deviation of 2.0 %, as shown by Table III-2. An artefact yields to an intercept different from zero and an apparent order inferior to one by fitting variation of  $k_0$  with Equation 15. This intercept comes from the contribution of hydroxide ions which will be described later. This phenomenon is also illustrated in Figure III-4.

Table III-2. Parameters and average relative deviation (ARD) of three models used to fit data of molecule 5 (1-dimethylamino-2-propanol) at 25 °C.

Function	$k_{Am}$	n	Intercept	ARD (%)
Affine: $k_0 = k_{Am} \times [Am] + \text{Intercept}$	$1.77 \times 10^{-2}$	1.00	2.51	2.0
Power law: $k_0 = k_{Am} \times [Am]^n$	$1.06 \times 10^{-1}$	0.76	0.00	3.6
Linear: $k_0 = k_{Am} \times [Am]$	$2.17 \times 10^{-2}$	1.00	0.00	7.3

A representation of each model is given by Figure III-4. In order to be more consistent with rate law proposed in the literature, for molecule n°5, 6 and 11 we force order to n=1 and then consider a linear model. Corresponding values of  $k_{Am}$  with n=1 are indicated by 5', 6' and 11' on Figure III-3.

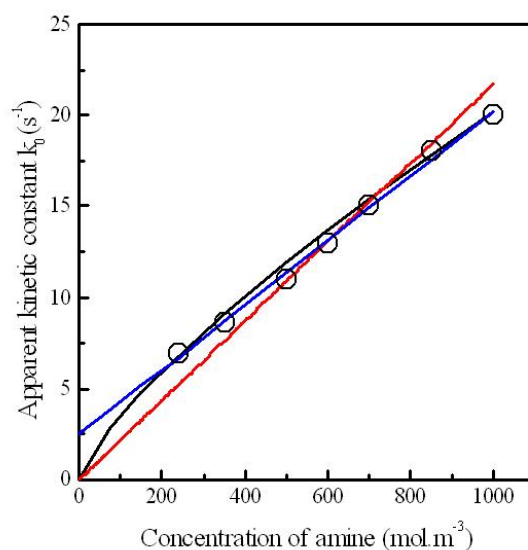


Figure III-4. Experimental apparent kinetic constant vs. 1-Dimethylamino-2-propanol concentration (molecule n°5) (black circles). Fit using affine function (blue line), power law function (black line) and linear function (red line). T = 25 °C.

Values of  $k_{Am}$  and n plotted in Figure III-3 are reported in Table IX-1 in appendix with the average relative deviation between each model and corresponding experimental data.

## 3.2 Tertiary amines

### 3.2.1 Overall observations

If we take into account the corrected order, all tertiary amines, represented by triangles on Figure III-3, have an apparent global order of reaction close to 1 with respect to amine. We also notice that value of the kinetic constant  $k_{Am}$  of each amine increase with the value of pKa of the tertiary amine.

### 3. Effect of the concentration

#### 3.2.2 Confrontation with mechanisms

Base catalyzed hydration mechanism and zwitterion mechanism are both first order mechanisms with respect to amine. Both mechanisms are consistent to explain apparent order of 1 with respect to amine for tertiary amines represented in Figure III-3. When  $n = 1$ , value of  $k_{Am}$  can be assimilated to  $k'_{R_3N}$ , the second order kinetic constant of tertiary amines presented in Chapter II. This kinetic constant varies between  $3 \times 10^{-3}$  and  $10^{-1} \text{ m}^3 \cdot \text{mol}^{-1} \cdot \text{s}^{-1}$  for the studied amines. From this point, we consider the single kinetic constant  $k'_{R_3N}$  to quantify the kinetics of reaction of tertiary amines with  $\text{CO}_2$ .

According to the literature, some authors consider that the kinetic contribution of hydroxide ions is negligible whereas some others consider that it is not negligible. If contribution of hydroxide ions is not negligible, it could have a significant impact in the determination of the kinetic constant  $k'_{R_3N}$ . In the next paragraph we will verify this assumption.

#### 3.2.3 Influence of hydroxide ions

According to Astarita *et al.* (1983), the initial concentration of hydroxide ions (before the reaction with  $\text{CO}_2$  takes place) can be estimated through Equation 16. In this relationship  $[\text{HO}^-]^i$  is the initial concentration of hydroxide ions ( $\text{mol} \cdot \text{dm}^{-3}$ ),  $K_w$  is the water self-ionization constant ( $10^{-14}$  at  $25^\circ\text{C}$ ),  $K_a$  is the amine dissociation constant and  $[\text{R}_3\text{N}]$  is the total concentration of amine ( $\text{mol} \cdot \text{dm}^{-3}$ ).

$$[\text{HO}^-]^i = \sqrt{\frac{K_w}{K_a} [\text{R}_3\text{N}]} \quad \text{Equation 16}$$

The kinetic constant  $k_{\text{HO}^-}$  (Reaction 14) is known and it is possible to estimate kinetic constant of the amine  $k'_{R_3N}$  by fitting. Moreover we also know initial concentration of amine  $[\text{R}_3\text{N}]^i$  and of hydroxide ions  $[\text{HO}^-]^i$ . Then it is possible to determine the ratio R between the initial contribution of hydroxide ions and amine as indicated by Equation 17.

$$R = \frac{k_{\text{HO}^-} [\text{HO}^-]^i}{k'_{R_3N} [\text{R}_3\text{N}]^i} \quad \text{Equation 17}$$

From this expression we determine for molecule n°3 (dimethylmonoethanolamine), which is one of the most studied tertiary amine, the value of the ratio R for each concentration from results got by Henni *et al.* (2008) in Table III-3. When the amine reacts with  $\text{CO}_2$ , the solution become more and more acidic and then the concentration of hydroxide ions diminishes. The factor R corresponds to the maximum contribution of the kinetic contribution of hydroxide ions.

We notice that in this case, the contribution of hydroxide ions is by far non negligible. Indeed, as expressed by Equation 16, the initial concentration of hydroxide ions increases with basicity. Moreover, the dissociation of the amine is more important when the amine solution is diluted. In these cases, the contribution of hydroxide ions represents a larger part of the reaction rate at the initial time.

Table III-3. Determination of the factor R which indicates the kinetic contribution of hydroxide ions on molecule n°3 (dimethylmonoethanolamine) studied by Henni *et al* (2008). T=25 °C.

$[R_3N]^0$ (mol.m <sup>-3</sup> )	$[HO^-]^0$ (mol.m <sup>-3</sup> )	$k'_{R_3N}[R_3N]^0$ (s <sup>-1</sup> )	$k_{HO^-}[HO^-]^0$ (s <sup>-1</sup> )	<b>R</b>
302	2,3	8,0	18,9	2.36
523	3,0	13,8	24,8	1.80
597	3,2	15,8	26,5	1.68
693	3,4	18,3	28,5	1.56
778	3,6	20,5	30,2	1.47
911	3,9	24,1	32,7	1.36
986	4.1	26.0	34.0	1.31

### 3.2.4 Structure-property relationship

Littel *et al.* (1990a) have studied 5 molecules (molecules n°1, 2, 3, 6 and triethylamine) using a stirred cell reactor and observed a correlation between the kinetic constant of the tertiary amine and the pKa called Brønsted relationship. This correlation is indicated by Equation 18. This relationship is quite intuitive. In fact, the reaction between a tertiary amine and carbon dioxide can be considered as a nucleophilic addition initiated by the nucleophilicity of the amine. Other things being equal, the nucleophilicity increases with pKa, yielding to a faster reaction rate.

$$\ln(k'_{R_3N}) = -\frac{-8,171.00}{T(^{\circ}K)} + 1.47 \times pKa + 9.80 \quad \text{Equation 18}$$

In order to confirm this correlation for stopped-flow data, we plot on Figure III-5 values of  $k'_{R_3N}$  as a function of pKa. We outline, as evidenced by Littel *et al.* (1990a) that the logarithm with base 10 of  $k'_{R_3N}$  shows a quasi linear variation with the pKa of the amine according to a Brønsted relationship. We determine the optimal parameters for experimental data and represent this correlation in Figure III-5. The average relative deviation between experimental kinetic constants and correlation is about 33 %.

### 3. Effect of the concentration

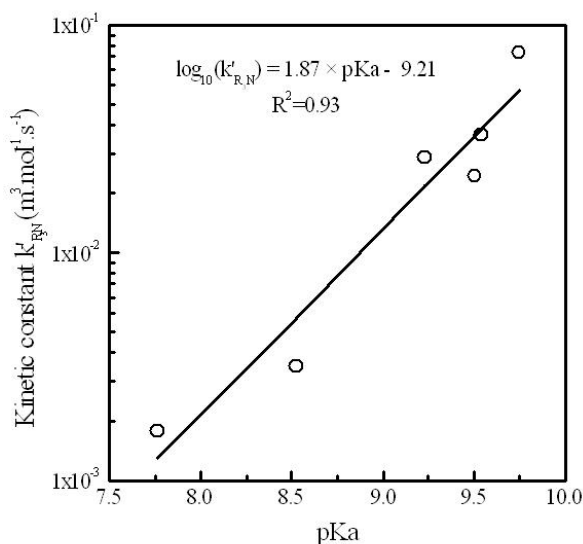


Figure III-5. Kinetic constant  $k'_{R_3N}$  values vs. tertiary amines pKa (black circles) and optimum estimation of parameters (black line). T = 25 °C.

However we shown in the previous part that in some cases, the hydroxide ions have a non negligible contribution on the determination of apparent kinetic constants, yielding to an overestimation of the kinetic constant  $k'_{R_3N}$ . The question can be raised whether the Brønsted relationship is really intrinsic to the amine or affected by the contribution of hydroxide ions which also increases with the basicity of the amine.

### 3.3 Primary and secondary amines

#### 3.3.1 Overall observations

Primary and secondary amines, represented by circles in Figure III-3 have a global order of reaction between 1 and 2 with respect to the amine. Moreover, four main observations can be drawn from these data.

##### 3.3.1.1 Tert-Butylethanolamine

First, we notice that tert-butylethanolamine (molecule n°11) is the only primary/secondary amine which can be fitted with  $n=1$ . This molecule has a 2.3 time higher value of  $k_{Am}$  compared to the fastest tertiary amine (molecule n°6). According to Ali *et al.* (2002), this amine fits the description given by Sartori and Savage (1983) of a severely sterically hindered amine. These authors have suggested that such amines are unable to form a carbamate and then behave as tertiary amine.

We verify that the first order kinetic constant obtain for tert-butylethanolamine follows the trend of the Brønsted relationship proposed for tertiary amines in part Chapter III .3.2.4 as indicated by Figure III-6. Indeed, the relative deviation between experimental data and estimation of tert-butylethanolamine is about 43.8 % and then have the same order of

magnitude that the average relative deviation between tertiary amines with estimation (33 %). As suggested by authors this molecule seems to behave as a tertiary amine.

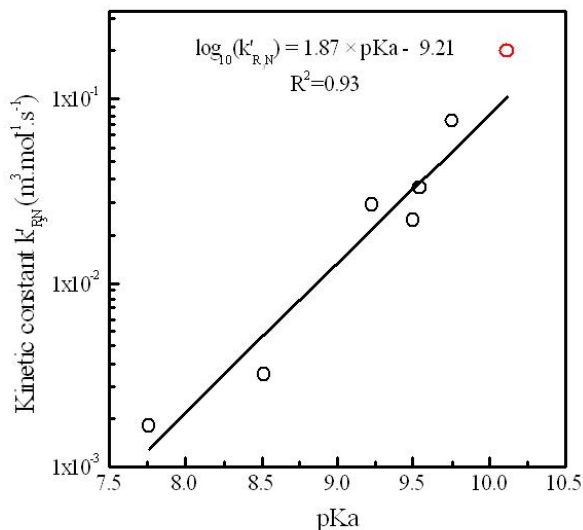


Figure III-6. Kinetic constant  $k'_{R_3N}$  values vs. tertiary amines pKa (black circles) and tert-Butylethanolamine (11) (red circle). Optimum estimation of parameters (black line). T = 25 °C.

Now the question can be raised whether it is consistent to make a difference between primary/secondary amines and tertiary amines. It may be more consistent to consider on the one hand amines which form carbamates and then which behave as most of primary and secondary amines and on the other hand amines which directly form carbonates and then which behave as tertiary amine.

### 3.3.1.2 Sterically hindered primary amines

If we now have a closer look on the series of molecules n°12 to 14, which are all primary amines with an amino group linked to a quaternary carbon and exhibit an order n of 1.2, an increase of the pKa tends to increase the value of  $k_{Am}$ , as it has been already pointed out with tertiary amine. However, these sterically hindered primary amines are faster to react with  $\text{CO}_2$  than tertiary amines having same pKa, as can be seen by comparing molecule n°6 with molecule n°12 (pKa = 9.72 - 9.75) or molecule n°13 with molecule n°5 (pKa = 9.48 - 9.50).

### 3.3.1.3 Comparison between acyclic and cyclic secondary amines

Molecules n°18 and 19 can be compared. Indeed these molecules are both secondary amines with the same number of carbon between nitrogen and the oxygen atoms. Linear diethanolamine (molecule n°18) reacts 10 times more slowly than cyclic morpholine (molecule n°19) at  $100 \text{ mol} \cdot \text{m}^{-3}$  in spite of the fact that diethanolamine is more basic. It reveals that there is an important difference of behaviour between cyclic and acyclic amines.

### 3. Effect of the concentration

#### 3.3.1.4 Series with increasing steric hindrance

Series of monoamines n°7 to 11 corresponds to ethanolamines R-NH-CH<sub>2</sub>-CH<sub>2</sub>-OH with R being with increasing number: hydrogen (n°7), methyl (n°8), ethyl (n°9), n-butyl (n°10) and tert-butyl (n°11). For this series of molecules, the pKa varies between 9.44 and 10.12 with an increasing steric hindrance around the nitrogen group. This variation of pKa and steric hindrance is correlated with significant variations of k<sub>Am</sub> and n.

It is very interesting to notice that the effect of hindrance around the amino group on the order n is not monotonic: starting from 1.2 with monoethanolamine (molecule n°7), it first increases up to a maximum around 2 for ethylethanolamine (molecule n°9), and then decreases down to a value of 1 for tert-butylethanolamine (molecule n°11).

It is also possible to compare k<sub>0</sub> of these amines at a concentration of 100 mol.m<sup>-3</sup>: we see first an increase of the reaction rate from monoethanolamine to methylethanolamine, and an increasing negative effect of hindrance on k<sub>0</sub> as the alkyl substituent of the secondary amine gets longer or more substituted, as k<sub>0</sub> decreases by two orders of magnitude between methylethanolamine and tert-butylethanolamine. These observations are further discussed below with respect to the different mechanisms proposed in the literature.

#### 3.3.2 Confrontation with mechanisms

The series of molecules n°7 to 11 is represented by Figure III-7. Corresponding pKa and steric hindrance quantified by Taft constants are given in Table III-4. A brief description of Taft constant is given in Chapter IX .2 in appendix. We now attempt to explain the evolution of kinetic constant and order with pKa and Taft constant, considering three hypotheses for the reaction mechanism: carbamic acid, zwitterion or termolecular mechanism.

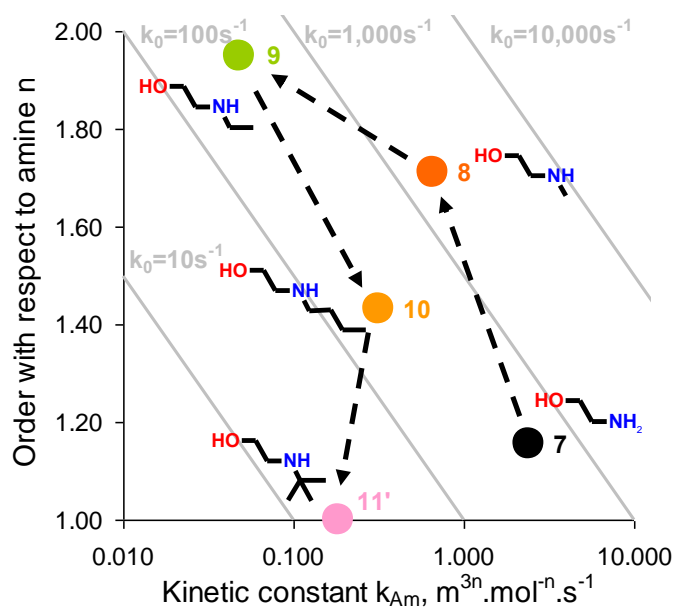


Figure III-7. Apparent kinetic constant and order (k<sub>Am</sub>, n) for ethanolamines (n°7, 8, 9, 10 and 11) at 25 °C. Continuous lines iso-k<sub>0</sub> represent values of (k<sub>Am</sub>, n) giving the same value of k<sub>0</sub> for [Am] = 100 mol.m<sup>-3</sup>.

Table III-4. pKa at 25 °C and Taft constants (Taft, 1976) for molecules n°7 to 11.

Number	Substituting group	pKa	Reference	Taft constant
7	Hydrogen	9.44	(Hamborg and Versteeg, 2009)	0
8	Methyl	9.85	(Hamborg and Versteeg, 2009)	-1.24
9	Ethyl	9.89	(Chemicalize, 2012c)	-1.31
10	n-Butyl	10.00	(Chemicalize, 2012d)	-1.63
11	tert-Butyl	10.12	(Littel <i>et al.</i> , 1990b)	-2.78

### 3.3.2.1 Carbamic acid model

McCann *et al.* (2009) use the mechanism of carbamic acid to explain kinetics of monoethanolamine in loaded solution. Although it is convenient to account for first order kinetics with respect to amine, it cannot be generalized to orders larger than 1.

### 3.3.2.2 Zwitterion model

For monoethanolamine (molecule n°7), apparent order with respect to amine  $n$  is close to 1, which matches either with the nucleophilic addition or the deprotonation by water as the limiting step of the carbamate formation. Iida and Sato (2012) suggest, using *ab initio* calculation, that nucleophilic addition of zwitterion mechanism is the rate-limiting step. However, Kumar *et al.* (2003) assume that deprotonation by water is the limiting step at low concentration of amine. Since monoethanolamine is not sterically hindered, it seems yet difficult to consider a deprotonation as a limiting step. Indeed, deprotonations reactions, which are acid-base reactions, are generally easier than nucleophilic addition, hydration or hydrolysis reaction. For example, at 25 °C the rate constant of the reaction between oxonium ions and hydroxide ions in water is equal to  $1.4 \times 10^{11} \text{ dm}^3 \cdot \text{mol}^{-1} \cdot \text{s}^{-1}$  (Atkins and de Paula, 2006).

With a methyl group on the nitrogen, methylethanolamine (molecule n°8) is slightly more basic and moderately hindered. Apparent order  $n$  is close to 1.7. Consistently with the discussion on the monoethanolamine, this intermediate order for methylethanolamine can be explained by a competition between nucleophilic addition step and deprotonation of the zwitterion by the amine. With an ethyl group as a substituent (molecule n°9), apparent order  $n$  is almost 2 which is consistent with a deprotonation of the zwitterion by the amine as the rate limiting step in the studied range of concentration.

With a n-butyl substituent to the nitrogen atom (molecule n°10),  $n$  is close to 1.4 with a value of  $k_0$  10 times lower than methylethanolamine (molecule n°8) at the same concentration of  $100 \text{ mol} \cdot \text{m}^{-3}$ . Two hypotheses can support this result. We either have a competition between nucleophilic addition step and deprotonation by amine or a competition between deprotonation by water and deprotonation by amine.

### 3. Effect of the concentration

Further increase of steric hindrance for molecule n°11 leads to an apparent order of 1. As we previously showed in Chapter III .3.3.1.1, this molecule behaves as tertiary amines. Yu *et al.* (1985) suggested that zwitterion mechanism occurs for tertiary amines. Nevertheless it is not possible to determine the limiting step (nucleophilic addition or deprotonation by water).

It comes out that the effect of the steric hindrance on the two steps of the zwitterion mechanism can account for apparent orders between 1 and 2 which are observed for primary and secondary amines. However, in most cases, an uncertainty remains on the respective contribution of the two steps of the reaction.

#### 3.3.2.3 Termolecular model

Crooks and Donnellan (1989) explain the reaction of monoethanolamine (molecule n°7) with CO<sub>2</sub> by a single step termolecular mechanism involving amine, water and CO<sub>2</sub> where nucleophilic addition and deprotonation represent one single energy barrier. This hypothesis is supported by *ab initio* calculations of da Silva and Svendsen (2004).

According to the termolecular mechanism, the apparent order equal to 1.7 for methylethanolamine (molecule n°8) is explained by a competition between reaction of CO<sub>2</sub> with amine and water (order 1) and with two molecules of amine (order 2).

For ethylethanolamine (molecule n°9), the order equal to 2 means that the one step reaction of CO<sub>2</sub> with amine and water is negligible in front of one step reaction of CO<sub>2</sub> with two molecules of amine.

Apparent order of 1.4 for n-butyl-ethanolamine (molecule n°10) is explained by the competition between the two single step termolecular reactions as for methylethanolamine.

Order 1 for tert-butylethanolamine (molecule n°11), which does not form carbamate, can be explained by the base-catalyzed hydration mechanism of tertiary amine, which can be seen as an extension of termolecular mechanism for tertiary amine and severely hindered secondary amines.

#### 3.3.2.4 Conclusion

To conclude with this series of primary and secondary amines, the one-step termolecular or the two-step zwitterion mechanisms both explain experimental orders of reaction. The one-step termolecular mechanism can be seen as a particular case of the zwitterion mechanism where the deprotonation step is rate limiting.

On a practical point of view, the choice of one or the other mechanism should be driven by the ability of the model to fit experimental data of  $k_0$  on the studied concentration range and to determine all its kinetic constants.

### 3.3.3 Determination of the kinetic constants

#### 3.3.3.1 Zwitterion model

The zwitterion model for primary and secondary amines has three parameters ( $k_{NA}$ ,  $k_{Dep}^{R_2NH}$  and  $k_{Dep}^{H_2O}$ ) and two variables (concentration of amine and of water) to determine the apparent kinetic constant  $k_0$ . It is generally not possible to extract these three constants due to the small variation of water concentration.

For instance, in the case of 2-amino-2-methyl-1-propanol studied by Alper (1990b), which presents the largest measured range of concentration, the concentration of amine varies between 25 and 1,486 mol.m<sup>-3</sup>, correlated with a variation of water concentration between 55,431 and 48,197 mol.m<sup>-3</sup> according to the Equation 19 where  $\rho_w$  is the density of water,  $M_{Am}$  is the molecular weight of amine and  $M_w$  is the molecular weight of water.

$$[H_2O] = \frac{\rho_w - [Am] \times M_{Am}}{M_w} \quad \text{Equation 19}$$

As the concentration of amine varies more than 60 times, the concentration of water varies only by 15 percent. In order to discriminate contributions of  $k_{NA}$ ,  $k_{Dep}^{R_2NH}$  and  $k_{Dep}^{H_2O}$ , both concentrations of water and amine should vary significantly. Since it is not the case, several sets of kinetic constants can fit variation of  $k_0$  with amine concentration. This is illustrated by the case of piperazine for which experimental results obtained by Rayer et al. (2011) at 30 °C are given in Table III-5.

Table III-5. Experimental data of  $k_0$  for piperazine determined by Rayer et al. (2011) at 30 °C.

[PZ] (mol.m <sup>-3</sup> )	[H <sub>2</sub> O] (mol.m <sup>-3</sup> )	$k_0$ (s <sup>-1</sup> )
20	55,460	341
31	55,409	533
40	55,365	711
52	55,308	939
60	55,270	1,100
80	55,174	1,497
100	55,077	1,910

With these data we calculate with the software Maple<sup>®</sup> the response surface of  $k_{NA}$ ,  $k_{Dep}^{R_2NH}$  and  $k_{Dep}^{H_2O}$  yielding to an average relative deviation below 1 % between the model and

### 3. Effect of the concentration

experimental values of  $k_0$ . This response surface has been obtained for values of constant between  $10^{-5}$  and  $10^5$  using 200 points for each constant on a logarithmic scale. Black points which appear in the Figure III-8, correspond to values of  $k_{NA}$ ,  $k'_{Dep}{}^{R_2NH}$  and  $k'_{Dep}{}^{H_2O}$  that give a prediction of  $k_0$  with an average relative deviation from the experimental data lower than 1 %. The projections of the points on the  $\log_{10}(k_{NA})$ ,  $\log_{10}(k'_{Dep}{}^{R_2NH})$  plane are also indicated represented by the continuous line.

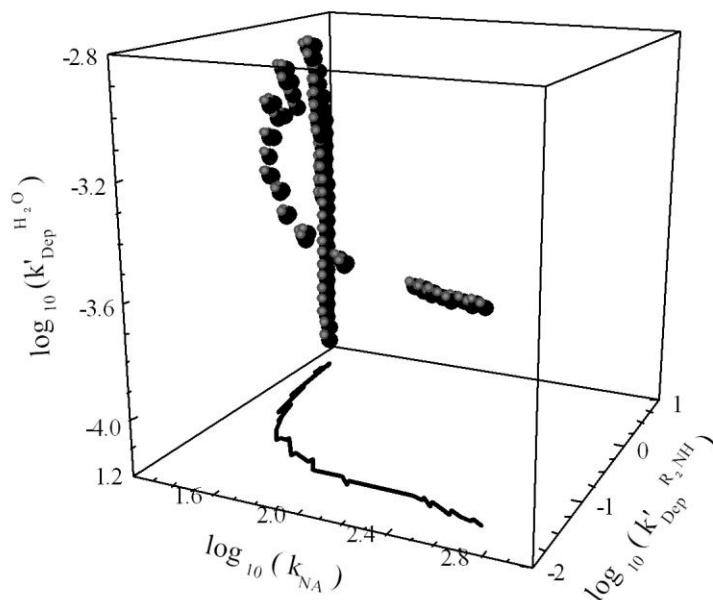


Figure III-8. Response surface for average relative error below 1 % for  $k_0$  modelled with zwitterion mechanism for piperazine at 30 °C (Rayer *et al.*, 2011). Projection of response surface on the  $\log_{10}(k_{NA})$ ,  $\log_{10}(k'_{Dep}{}^{R_2NH})$  plane is indicated by the continuous line.

From this calculation, it is impossible to minimize the average relative deviation giving a single set of kinetic parameters able to represent the reaction of piperazine with  $\text{CO}_2$ . In this case, the response surface of those parameters giving an average relative deviation below 1% stretches between  $10^{1.3}$  and  $10^{2.8}$   $\text{m}^3 \cdot \text{mol}^{-1} \cdot \text{s}^{-1}$  for  $k_{NA}$ , between  $10^{-1.6}$  and  $10^{0.4}$   $\text{m}^6 \cdot \text{mol}^{-2} \cdot \text{s}^{-1}$  for  $k'_{Dep}{}^{R_2NH}$  and between  $10^{-4.1}$  and  $10^{-3.1}$   $\text{m}^6 \cdot \text{mol}^{-2} \cdot \text{s}^{-1}$  for  $k'_{Dep}{}^{H_2O}$ .

In this surface, we identify two areas. The first with low value of  $k_{NA}$  ( $10^{1.3}$   $\text{m}^3 \cdot \text{mol}^{-1} \cdot \text{s}^{-1}$ ) and high value of  $k'_{Dep}{}^{R_2NH}$  ( $10^{0.4}$   $\text{m}^6 \cdot \text{mol}^{-2} \cdot \text{s}^{-1}$ ) corresponds to the nucleophilic addition limiting step. In this area value variation of  $k'_{Dep}{}^{H_2O}$  by a factor of 10 is not sensitive on the resulting  $k_0$ . The second one with an intermediate value of  $k'_{Dep}{}^{H_2O}$  ( $10^{-3.5}$   $\text{m}^6 \cdot \text{mol}^{-2} \cdot \text{s}^{-1}$ ) and a

low value of  $k_{Dep}^{R_2NH}$  ( $10^{-1.6} \text{ m}^6 \text{ mol}^{-2} \text{ s}^{-1}$ ) corresponds to the deprotonation by water limiting step. In this area, variation of  $k_{NA}$  by a factor close to 10 has no impact on  $k_0$ .

Finally it is impossible to determine what the limiting step of the zwitterion mechanism is. We reach the same conclusion for 2-amino-2-methyl-1-propanol (n°12) with n=1 (Alper, 1990b). In the case of a study of an amine with n=2, (ethylethanolamine, n°9, (Li et al., 2007)), kinetic constant  $k_{Dep}^{R_2NH}$  can be determined but other constants are insensitive as they are first order kinetic constant according to the amine concentration.

In overall, it is mathematically impossible to determine a unique set of kinetic constants related to the zwitterion model which would be characteristic of a given amine.

### 3.3.3.2 Termolecular model

With apparent order n between one and two, all data can be fitted by the termolecular mechanism given by Equation 20. Unlike the variety of interpretations associated to the zwitterion model, the fitting of  $k_0$  with the termolecular model yields to one single set of ( $k_{ter}^{H_2O}$ ;  $k_{ter}^{R_2NH}$ ) parameters to characterize each amine.

$$k_0 = k_{ter}^{H_2O} [H_2O][R_2NH] + k_{ter}^{R_2NH} [R_2NH]^2 \quad \text{Equation 20}$$

## 3.3.4 Structure-property relationship

The authors have identified two main effects on the kinetics of reaction of primary and secondary amines with  $\text{CO}_2$ : basicity and steric hindrance, which are illustrated with the following examples.

### 3.3.4.1 Effect of basicity

As same as tertiary amines, the basicity of the amine impacts on the kinetics of the reaction with  $\text{CO}_2$ . A first example is given by Conway *et al.* (2012a) showing a correlation between the second order kinetic constant of the carbamic acid model and the protonation constant of the amine for cyclic amines described with the carbamic acid mechanism (Chapter II 4.3.3.2). This correlation is illustrated by Figure III-9. According to this figure we also notice that monoethanolamine seems to follow the trend of cyclic secondary amines contrary to ammonia and diethanolamine. Indeed these two latest molecules react at least ten times faster than for cyclic secondary amines which have the corresponding value of protonation constant. Contrary to tertiary amines, the effect of basicity has to be considered for a particular series of amines with similar hindrance of the nonbonding electron pair of the nitrogen atom.

### 3. Effect of the concentration

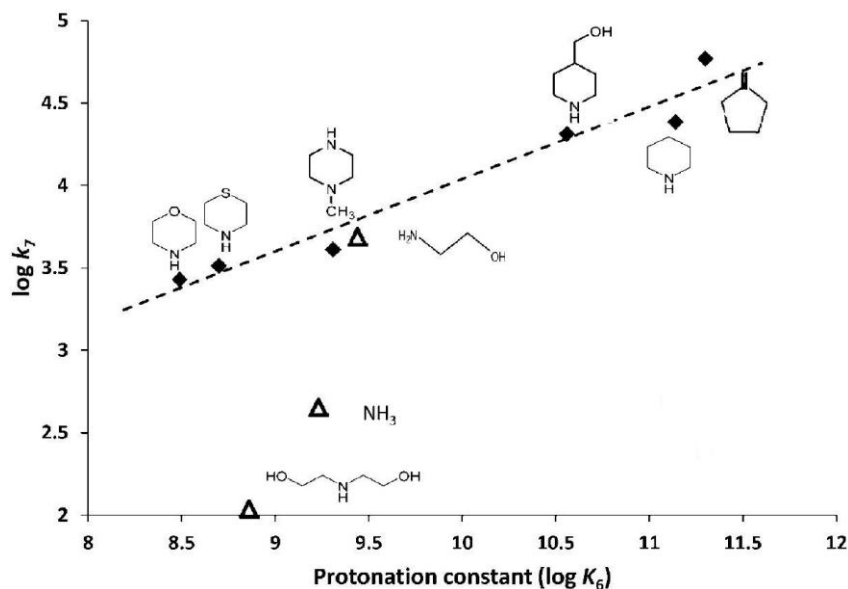


Figure III-9. Variation of  $\log(k_7)$  with  $\log(K_6)$  for some amines studied by Conway *et al.* (2012a). A linear fit, realized only with cyclic amines indicate a relationship between  $\log(k_7)$  and  $\log(K_6)$ . Kinetic constant  $k_7$  corresponds to the kinetic constant of the carbamic acid mechanism (Reaction 20) and  $K_6$  correspond to the inverse of amine dissociation constant ( $K_a$ , Reaction 11).

In fact, another example of the effect of basicity can be seen on sterically hindered primary amines. As we have already noticed, molecules n°12 to 14 show increasing value of  $k_{Am}$  with pKa for and order of reaction is around  $n = 1.2$ . We have also seen that these molecules do not react as tertiary amine. Nevertheless it is possible to observe a trend between kinetic constant  $k_{Am}$  and pKa of these molecules as shown by Figure III-10.

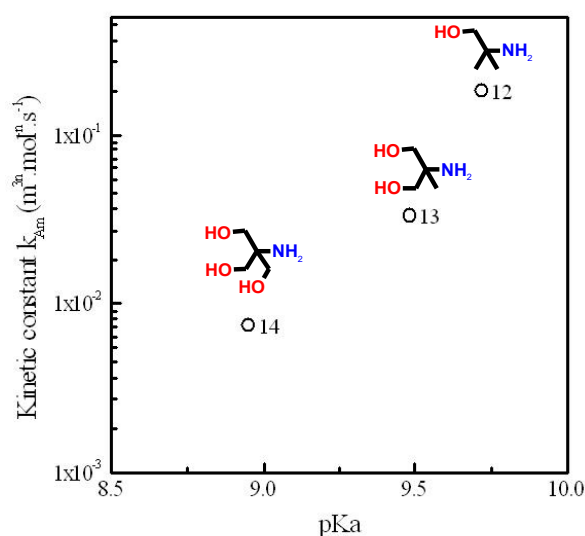


Figure III-10. Variation of kinetic constant  $k_{Am}$  with pKa of molecules n°12 to 14.

## 3.3.4.2 Effect of steric hindrance

In the part Chapter III .3.3.1.4 we have shown that steric hindrance has a preponderant role to explain kinetic parameters. Conway *et al.* (2012b) have studied this effect and obtained the results summarized in Figure III-11. Without a descriptor of the steric hindrance for a molecule which could be calculated for their different linear and cyclic amines, they were not able to find a quantitative relationship between steric hindrance and the kinetics of reaction. However, the negative effect of steric hindrance is clearly observed on the second order kinetic constant of the carbamic acid model of the primary amines represented by red circles. This effect can be illustrated by the comparison between n-BA (n-butylamine) and SBA (sec-butylamine) (pKa = 10.6-10.7) on the one hand and with 1-AP (1-amino-2-propanol) and 2-AP (2-aminopropanol) on the other hand (pKa = 9.6).

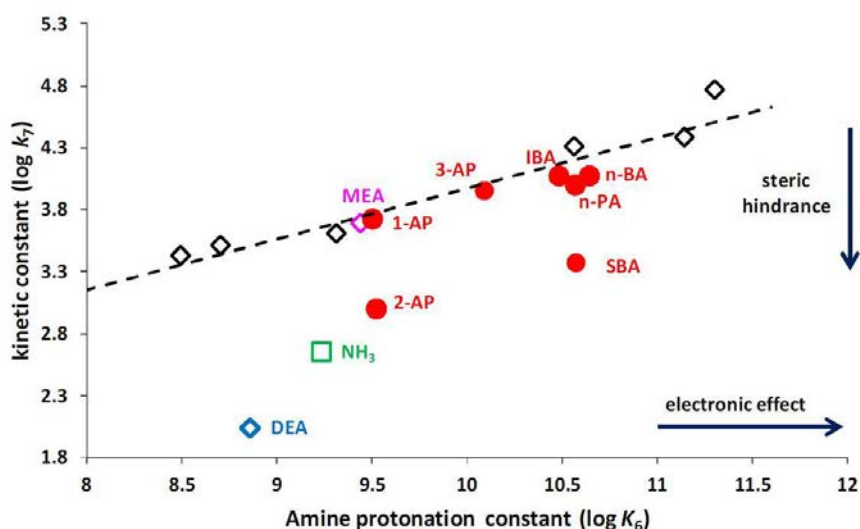


Figure III-11. Variation of  $\log(k_7)$  vs.  $\log(K_6)$  for n-butylamine (n-BA), n-propylamine (n-PA), isobutylamine (IBA), 3-amino-1-propanol (3-AP), 1-amino-2-propanol (1-AP), monoethanolamine (MEA), sec-butylamine (SBA), 2-aminopropanol (2-AP), ammoniac (NH<sub>3</sub>), diethanolamine (DEA) and a series of cyclic secondary amines (black diamonds) determined by Conway *et al.* (2012b). A linear fit, realized only with cyclic amines indicate a relationship between  $\log(k_7)$  and  $\log(K_6)$ . The kinetic constant  $k_7$  corresponds to the second order kinetic constant of the carbamic acid mechanism (Reaction 20) and  $K_6$  correspond to the inverse of amine dissociation constant ( $K_a$ , Reaction 11).

da Silva and Svendsen (2005) calculated the free energy of carbamate formation  $\Delta G_{c2s}$  according to the reverse of the Reaction 23 of Chapter II. It is generally accepted that the stability of the carbamate is related to the steric hindrance of the amine function and then it could be an indirect descriptor of steric hindrance. In their work, they observed that the kinetic constant of the nucleophilic addition in the zwitterion mechanism is decreased with an increased value of the free energy of carbamate formation as indicated by Figure III-12.

### 3. Effect of the concentration

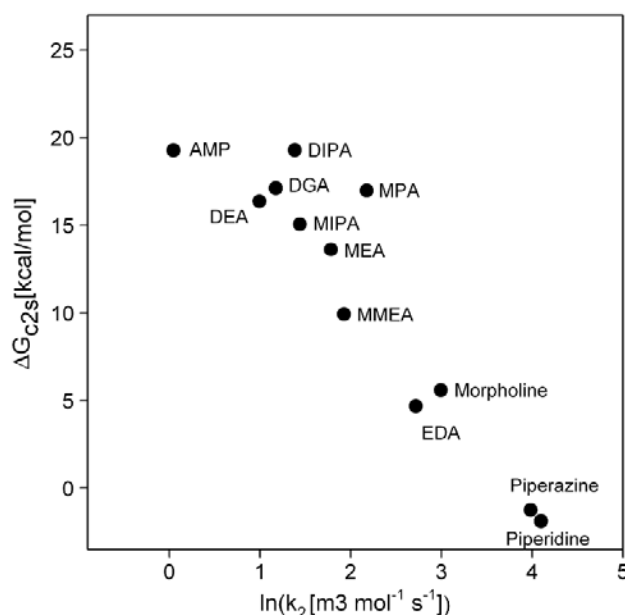


Figure III-12. Calculated free energy of carbamate formation  $\Delta G_{c2s}$  vs. logarithm of experimental reaction rate  $k_2$ . Reaction rate  $k_2$  correspond to the nucleophilic addition of the zwitterion mechanism (Reaction 16) (da Silva and Svendsen, 2007).

### 3.4 Multi-amines

Even though the number of multi-amines studied with the stopped flow technique is still limited, we discuss the case of three molecules having two amine functions.

#### 3.4.1 Derivatives of piperazine

Two derivatives of the piperazine have been studied by Conway *et al.* (2013) and compared with cyclic mono-amines: piperazine (PZ) and N-methylpiperazine (N-MPIPZ). These latter have already been represented in Figure III-9. The comparison obtained by Conway *et al.* (2013) is shown by Figure III-13. We only focus on results got for N-methylpiperazine and piperazine compared with the linear relationship obtained on cyclic amines.

##### 3.4.1.1 N-methylpiperazine

N-methylpiperazine seems to follow the trend obtain with the linear relationship proposed by Conway *et al.* (2013) and then reacts with  $\text{CO}_2$  as a cyclic secondary mono-amine. N-methylpiperazine is indeed a diamine composed of one secondary function and one tertiary function. As we have seen previously, reaction of  $\text{CO}_2$  with tertiary amines is several order of magnitudes slower in comparison with non hindered secondary amines. For this reason, the tertiary amine function of N-methylpiperazine does not contribute to the rate of reaction.

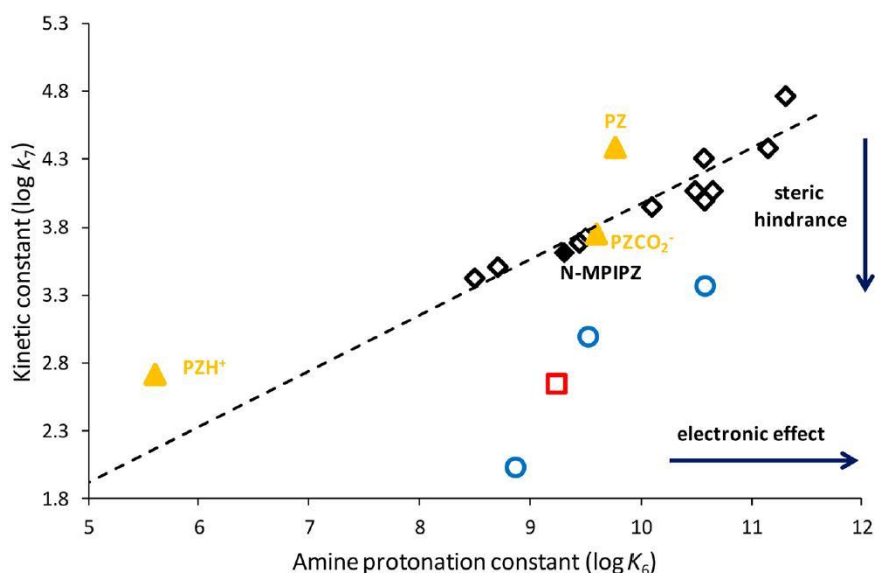


Figure III-13. Variation of  $\log(k_7)$  vs.  $\log(K_6)$  for piperazine (PZ), piperazine monocarbamate ( $\text{PZCO}_2^-$ ), N-methylpiperazine (N-MPIPZ), protonated piperazine ( $\text{PZH}^+$ ), cyclic mono-amines (black diamonds), sterically hindered amines (blue circles) and ammoniac (red square). The dashed line represents the linear relationship between  $\log(k_7)$  and  $\log(K_6)$  for cyclic mono-amines. The kinetic constant  $k_7$  corresponds to the kinetic constant of the carbamic acid mechanism (Reaction 20) and  $K_6$  correspond to the inverse of amine dissociation constant ( $K_a$ , Reaction 11) (Conway *et al.*, 2013).

#### 3.4.1.2 Piperazine

Based on Figure III-13, we observe that free piperazine reacts about three times faster than other cyclic amines having similar values of  $K_a$ .

This result can be explained by an entropic effect related to the number of equivalent functions in the piperazine before it reacts. Then there are at least twice more chances to get in contact with  $\text{CO}_2$  than for an equivalent molecule having just one amino group. Another effect proposed by Conway *et al.* (2013), may be the role of the diamine structure in the stabilization of the intermediate transition state geometries to form the carbamate. This could lead to lower activation energy and faster reaction rates. Finally, the increase of reaction rate can come from the contribution of both entropic and enthalpic effects.

#### 3.4.2 Ethylenediamine

We compare the apparent kinetic constants from stopped flow data between 3-aminopropanol ( $k_{\text{Am}} = 2.15 \text{ m}^{3n} \cdot \text{mol}^{-n} \cdot \text{s}^{-1}$ ) and ethylenediamine ( $k_{\text{Am}} = 5.95 \text{ m}^{3n} \cdot \text{mol}^{-n} \cdot \text{s}^{-1}$ ). Indeed, these molecules have almost the same apparent order  $n \approx 1.15$  and similar values of  $\text{p}K_a$ , respectively 10.00 and 9.92. Moreover they are both linear non hindered primary amine. With a 2.8 factor between the kinetic constant of these molecules, we observe the same effect than for piperazine which are both symmetric multi-amines.

#### 4. Effect of temperature

### 4 Effect of temperature

In order to study the effect of the temperature, it is necessary to determine the kinetic constants of each molecule. As we show previously, in the case of primary and secondary amines, the termolecular model is the only one which describes experimental results obtained in the literature with a single set of parameters. Moreover, in the case of tertiary amines, we notice that the third order kinetic constant  $k_{R_3N}$ , presented in the chapter II, which is also a termolecular mechanism, is comparable to the kinetic constant  $k_{ter}^{H_2O}$  of the termolecular model.

For practical reasons, we replace kinetic constants  $k_{ter}^{H_2O}$  and  $k_{ter}^{R_2NH}$  of the termolecular model by respectively  $k_{ter1}$  and  $k_{ter2}$ , as indicated in Equation 21, and we determine parameters  $k_{ter1}$  and  $k_{ter2}$  of experimental data collected in Table III-1.

$$k_0 = k_{ter1} \cdot [H_2O][R_2NH] + k_{ter2} \cdot [R_2NH]^2 \quad \text{Equation 21}$$

Values of  $k_{ter1}$  and  $k_{ter2}$  at different temperatures are reported in Table IX-2 in Chapter IX .1.2, with average relative error between model and experimental values of  $k_0$ . Deprotonation by amine is not considered ( $k_{ter2} = 0$ ) for amines with  $n = 1$  (molecule n°3, 4, 5, 6 and 11) and deprotonation by water is not considered ( $k_{ter1} = 0$ ) for amines with  $n = 2$  (molecule n°9).

Then we determine parameters of Arrhenius law for  $k_{ter1}$ ,  $k_{ter2}$  constants given by Equation 22 and Equation 23. Figure III-14 (a) and Figure III-14 (b) show the activation energy  $E_a$  of each kinetic constant  $k_{ter1}$  and  $k_{ter2}$  versus  $\ln(A)$ . For both constants, we can draw a linear relationship between activation energy and reaction frequency factor  $A$  as shown in Equation 24.

$$k_{ter1} = A_{ter1} \cdot \exp\left(\frac{-E_{a_{ter1}}}{RT}\right) \quad \text{Equation 22}$$

$$k_{ter2} = A_{ter2} \cdot \exp\left(\frac{-E_{a_{ter2}}}{RT}\right) \quad \text{Equation 23}$$

$$E_{a_i} = b \cdot \ln A_i + c \quad \text{Equation 24}$$

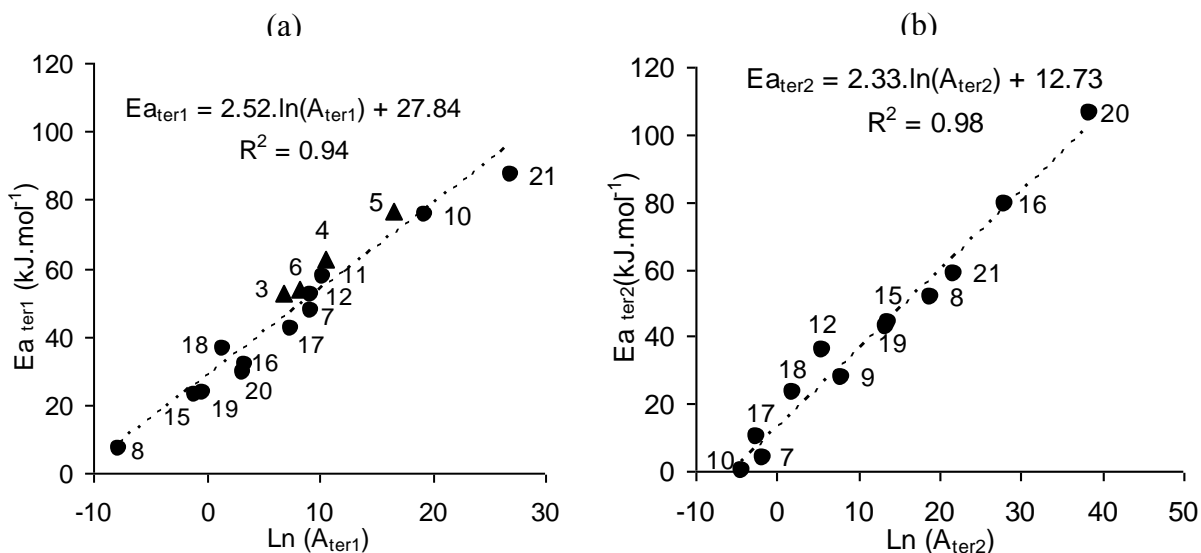


Figure III-14. Relation between Arrhenius parameters for  $k_{ter1}$  (a) and for  $k_{ter2}$  (b).

This correlation has been described in the literature as a compensation effect. According to Liu and Guo (2001) this effect has been observed in several fields of chemistry (adsorption, chromatography, substitution reaction, proton transfer, ...) and can have two sources.

#### 4.1 Statistical compensation

In the temperature range of the stopped-flow experiments, the neperian logarithm of the kinetic constant ( $\ln(k_{ter1})$  and  $\ln(k_{ter2})$ ) and the value of  $1/T$  have a limited variation which can account for uncertainty on the independent determination of pre-exponential factor and energy of activation. This indetermination can be a first explanation for the apparent compensation effect generally called the statistical compensation effect. This phenomenon is well described by Barrie (2012).

We determine for each molecule the confidence ellipse area in order to evaluate the impact of statistical compensation effect on our parameters (Draper and Smith, 1998). The expression of the confidence ellipse area is given by Equation 25 where  $\mathbf{b}$  is the vector of parameters ( $\ln(A)$ ;  $E_a$ ),  $\hat{\beta}$  is the estimation of ( $\ln(A)$ ;  $E_a$ ) represented by the center of the ellipse,  $\mathbf{C}$  is the covariance matrix between parameters,  $(p+1) = 2$  is the number of parameters,  $s^2$  is the residual variance,  $F_{\alpha; p; (n-p-1)}$  corresponds to the F-distribution value with a confidence level of  $(1-\alpha)\%$  and  $n$  is the number of data points used to estimate  $\hat{\beta}$ .

$$(\mathbf{b} - \hat{\beta})' \mathbf{C} (\mathbf{b} - \hat{\beta}) \leq (p+1) \cdot s^2 \cdot F_{\alpha; p; (n-p-1)} \quad \text{Equation 25}$$

#### 4. Effect of temperature

We represent in Figure III-15 the activation energy  $E_a$  versus  $\ln(A)$  for kinetic constant  $k_{ter1}$ . Indeed, this first order kinetic constant has the greatest sensitivity on  $k_0$  for most of the molecules which are generally close to  $n = 1$ . We limit our representation to molecules which are less impacted by statistical indetermination. We also indicate the confidence ellipse area. The plot has been realized with the function ellipse of the R software with a 95 % confidence level.

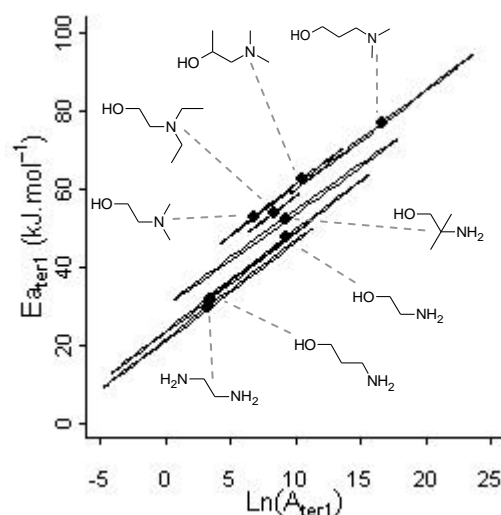


Figure III-15. Relation between Arrhenius parameters for  $k_{ter1}$  with confidence ellipse area.

Figure III-15 confirms a correlation between activation energy and reaction pre-exponential factor  $A$  even with ellipse confidence area. Moreover the position of the molecule on this figure is clearly dependent on the reactivity of the molecule characterized by the degree of substitution and steric hindrance of the amine function. In fact, ethylenediamine which is the most reactive molecule has the lowest value of activation energy and pre-exponential factor. On the other side, a tertiary amine (3-dimethylaminopropanolamine) has the highest value of activation energy and pre-exponential factor.

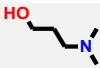
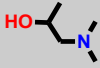
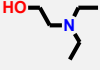
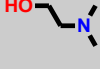
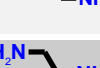
#### 4.2 Physico-chemical compensation

The statistical analysis shows that a part of the observed compensation effect may have a physical explanation. According to the transition state theory, activation energy can be related with activation enthalpy and pre-exponential factor with activation entropy according to Equation 26 and Equation 27 (Scacchi *et al.*, 1996), where  $\Delta^\ddagger H$  is the activation enthalpy,  $R$  is the gas constant,  $T$  the temperature (here we set at 298.15 K),  $k_B$  is the Boltzmann constant,  $h$  is the Planck constant,  $\Delta^\ddagger S$  is the activation entropy and  $c_0^{\Delta n^\ddagger}$  is the unitary concentration ( $1,000 \text{ mol.m}^{-3}$ ) with  $(1-\Delta n^\ddagger)$  which is the molecularity of the process (which is 3). Values of activation enthalpy and entropy are given in Table III-6.

$$E_a = \Delta^\ddagger H + RT \quad \text{Equation 26}$$

$$A = \exp(1) \times \frac{k_B T}{h} \times \exp\left(\frac{\Delta^\ddagger S}{R}\right) \times c_0^{\Delta n^\ddagger} \quad \text{Equation 27}$$

Table III-6. Corresponding number, structure, value of activation enthalpy and activation entropy determined according to transition state theory for amines of Figure III-15.

Number	Structure	$\Delta^\ddagger H$ (kJ.mol <sup>-1</sup> )	$\Delta^\ddagger S$ (J.mol <sup>-1</sup> .K <sup>-1</sup> )
4		74	-18
5		60	-68
6		51	-87
3		50	-99
12		50	-79
7		45	-78
16		29	-128
20		27	-128

For all molecules, values of activation entropy are negative. This variation of entropy, which reflects a reduction of molecular disorder, is due to the formation of a reaction intermediate from three molecules (amine, water and carbon dioxide) in the transition state. We notice that for linear primary amines n°20 and 16, the reduction of molecular disorder is more important than for tertiary amines n°4 and 5. At the same time the enthalpy of activation is less important for primary amines than for tertiary amines.

In fact primary amines have a higher reactivity with carbon dioxide in agreement with the lowest values of enthalpy. This higher reactivity is correlated with a larger reduction of entropy associated with reaction intermediate formation. A smaller reduction of entropy in the case of tertiary amine, especially for molecule n°4 may also come from a smaller association of the reactant molecules in the transient state. In fact, hydrogen bonding between the water molecule associated to the amine function and the hydroxyl group of the amine should be weaker in the case of molecule n°4 (propanolamine) than for ethanolamines.

## 5. Conclusion and scope of this work

In summary, a low activation enthalpy tends to be compensated by a large negative activation entropy. This physico-chemical compensation phenomenon has been observed between activation energy and pre-exponential factor of  $k_1$  which has an order of 1 according to amine.

### *5 Conclusion and scope of this work*

We have realized an in-depth study and interpretation of published kinetic data of the amine-CO<sub>2</sub> reaction obtained with the conductimetric stopped-flow technique.

This study has shown that it is impossible to determine with certainty the mechanism of the reaction, and then, to know the associated rate law. We have also demonstrated that it is impossible to determine the three kinetic constants associated with the zwitterion model. Although primary and secondary amines on the one hand and tertiary amines on the other hand are generally described by different mechanisms, we prefer the distinction between amines which form carbamates and amines which directly form carbonates. We also outline the importance of the basicity for amines which directly form carbonates and basicity and steric hindrance for amines which form carbamates. We also give some examples of the particular reactivity of multi-amines. Finally we observed a physical compensation effect between pre-exponential factor and activation energy of the second order kinetic constant  $k_{ter1}$  of the termolecular model.

These different observations help us to precise the objectives of our study. We will focus our work on three main targets in the progression of our work.

The first objective is to measure the kinetics of amine-CO<sub>2</sub> reaction for various structures of amines in diluted aqueous solutions at a temperature of 25 °C. As there is no consensus about the mechanisms we must propose a semi-empirical kinetic model adapted to our study and justify our choice. The molecules will be chosen among a large base of amines which can be considered as candidates for the post-combustion process. The molecules will also be chosen among families with large ranges of pKa and steric hindrance.

The second objective is to identify the different parameters affecting the kinetics of reaction such as basicity and steric hindrance. When it is possible, a relationship can be determined between the kinetic constants and the structural parameters. Moreover, even it is not possible to identify the mechanism which append, the results can be discussed in order to bring new elements on the reaction mechanism.

Finally, the ultimate objective of this work consists in establishing a Quantitative Structure-Property Relationship (QSPR) model. This model is expected to predict the kinetic constants of the amine-CO<sub>2</sub> reaction. To achieve this goal, we must select a method based on statistical modelling which appears to be the most adapted. For this method we can specially develop a parameter which describes a structural characteristic of each studied amines. Then we could compare the results obtained by the QSPR model and experiments and conclude about its ability to predict the kinetic properties of non-studied amines.

A summary of our approach is given in Figure III-16 which indicates the main content of the following chapters.

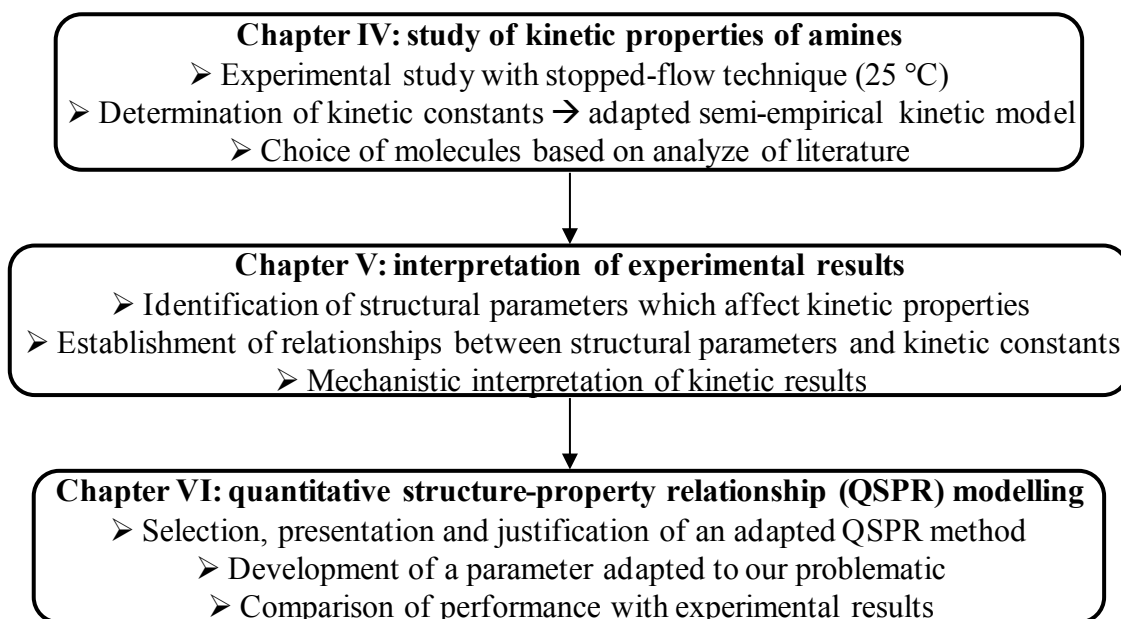


Figure III-16. Summary of our experimental and model approach to establish a quantitative structure-property relationship.

*«There is no single approach to study things. »*

Aristotle

## Chapter IV: METHODOLOGY

---

In this part we first describe the two experimental techniques used in this work: stopped-flow technique and acid-base titration. Then we present two complementary methods used to determine the apparent kinetic constant from the raw data of the stopped-flow measurements: the numerical method and the analytical method. For the analytical method, we will see that it has been necessary to develop experimental methods in order to respect the related assumptions. Thereafter, we present the method used to characterize kinetic properties of each amine from apparent kinetic constants with a semi-empirical model. We also use an original method to determine the uncertainty associated to each kinetic constant. Finally we present the studied molecules which have been chosen in order to cover the largest range of basicity and steric hindrance in different families of amines (alkanolamines, alkylamines, *etc.*).

### 1 Experimental techniques

In our study we used two main experimental techniques: the stopped-flow, used in order to obtain the kinetic constants of the amine-CO<sub>2</sub> reactions and acid-base titration, which gives complementary information about purity and thermodynamic constant of solutions. We present both of them in the next part.

#### 1.1 Stopped-flow technique

##### 1.1.1 Description

The stopped-flow technique is an analytical method which mixes two reagents (mixing time ranging between 1 and 5 ms) and measures the evolution of a physical signal (spectrometry, conductivity, *etc.*) of the solution after mixing. For our study we used the standard CSA-20 model manufactured by Hi-Tech Scientific, Ltd. (U.K.). This apparatus is equipped with a conductivity detector which monitors the ion formation as a function of time. This equipment can determine apparent kinetic constants between 0 and 500 s<sup>-1</sup> for a mixing time of 2 ms. It consists of four major parts:

- syringes, flexible tubing, the different valves and a pneumatic drive which are used to inject in the mixing cell reagents and to evacuate the product of the reaction. Two upstream syringes (drive syringes) are used to push the reagents in the mixing cell and one downstream syringe (stop syringe) is stopped on a stop block equipped with a microswitch. We used two upstream syringes of 2 mL and one downstream syringe of 1 mL.
- a cell composed of a mixing chamber and a conductivity cell. The conductivity cell, which has a cell constant announced by the manufacturer of 2.36 mm is connected to the conductivity control box. The conductivity change is measured by a circuit as described by Knipe *et al.*, (1974) which gives an output voltage directly proportional to the conductivity.

## 1. Experimental techniques

- an analogue-to-digital converter and a computer to record and treat data. We used the standard Kinetic Studio software provided by the manufacturer.
- a thermostated bath in which the cell is immersed. This system can regulate the temperature to a setting value within  $\pm 0.1$  °C.

A picture of the equipment without the thermostated bath is given by Figure IV-1.

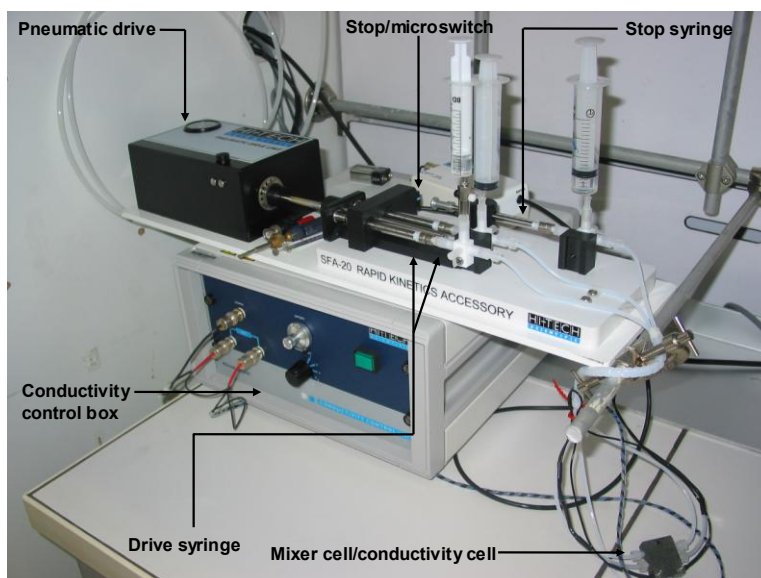


Figure IV-1. Stopped-flow CSA-20 equipment without thermostated bath.

### 1.1.2 Operating method

The thermostated bath and the conductivity control box are switched on at least one hour before starting to be sure that the temperature (25 °C) and the electric signal are stabilized. Then, three flushing cycles (three times 2 mL) are realized in order to put the system under operating conditions in term of reagent concentration. Thereafter, it is necessary to wait 3 minutes for the reagents to reach the temperature of the study. Meanwhile, we set the optimal conditions for the kinetic measurement. Then the air push button is pressed, the pneumatic plate pushes simultaneously the drive syringe piston and expels the same volume of reagents in the mixing cell. The solutions introduced in the cell displace the content left from the previous run or flush. The displaced volume drives the stop syringe until it hits the stop block, the flow stops and freshly mixed reagents in the mixing cell react. It corresponds to time  $t=0$  of the measurement of the conductance. If necessary, the conditions of measurements are adjusted in function of the result. At least three repetitions are realized for each condition of concentration of reagents. A chart represents the principle of the equipment on Figure IV-2.

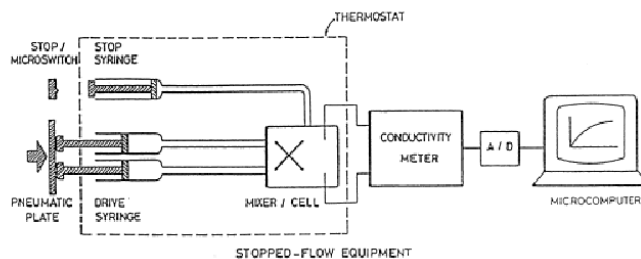


Figure IV-2. Stopped-flow apparatus chart (Ali *et al.*, 2000).

We perform stopped-flow measurements at least at six different concentrations of amine over at least one decade for each studied molecule.

### 1.1.3 Preparation of solutions

Aqueous solution of CO<sub>2</sub> and amine are prepared separately with special attention to avoid uncontrolled solubilisation of gaseous compounds, notably CO<sub>2</sub>. Therefore, water and amines were degassed separately with vacuum filling under agitation before dilutions or controlled saturation with CO<sub>2</sub>.

It is important to note that during the stopped-flow measurement, each reagent is mixed with an equal volume of the other solution. Reagents are then diluted by a factor 2 during the mixing process in comparison with their initial concentration.

#### 1.1.3.1 Amine

When water and pure solution of amine are degassed, a mother solution is prepared by sample weighting. Other solutions are prepared from this mother solution always by sample weighting. In this case, it is necessary to know the purity, the molecular mass and the density in order to determine the molar concentration of amine. Purity is known thanks to provider analysis certificate or determined by acid-base titration. Molecular mass is easy to determine and density is measured at each prepared concentration at 25 °C with a density meter DMA 4100 manufactured by Anton Paar.

#### 1.1.3.2 Carbon dioxide

Aqueous solutions of carbon dioxide are prepared by bubbling, using the principle of physical solubility. This principle is in accordance with the Henry law (Atkins and de Paula, 2006) which stipulates that "at a constant temperature, the amount of a given gas that dissolves in a given type and volume of liquid is directly proportional to the partial pressure of that gas in equilibrium with that liquid". It is thus possible to prepare an aqueous solution of carbon dioxide at a given concentration in equilibrium with a partial pressure of CO<sub>2</sub> according to Equation 28. In this equation,  $p_{CO_2}$  is the partial pressure of CO<sub>2</sub> (Pa),  $H_{CO_2}$  is the Henry's constant of the CO<sub>2</sub> in water ( $H_{CO_2} = 2,913 \text{ Pa}\cdot\text{m}^3\cdot\text{mol}^{-1}$  at T=25 °C (Harvey, 1996)) and  $[CO_2]$  is the concentration of CO<sub>2</sub> in the solution ( $\text{mol}\cdot\text{m}^{-3}$ ).

## 1. Experimental techniques

$$p_{CO_2} = H_{CO_2} \times [CO_2] \quad \text{Equation 28}$$

The partial pressure of CO<sub>2</sub> has been set with a mixture of dinitrogen and carbon dioxide flow rate delivered at atmospheric pressure by two Bronkhorst flow-meters. The dinitrogen flow-meter ranges between 0 to 100 NL/h and carbon dioxide flow-meter ranges between 0 to 20 NL/h. The mix of gases is introduced in a washing bottle which contains deionized water. This water is heated to 25 °C with a hot plate with magnetic stirrer to control the temperature and optimize the diffusion of CO<sub>2</sub> in the solution. The experimental set-up is represented by Figure IV-3.

With this method it is possible to prepare CO<sub>2</sub> solutions in the range of 1 to 35 mol.m<sup>-3</sup> with a relative uncertainty below 10 %. However to avoid any phenomenon of cavitation in the stopped-flow apparatus we choose to limit the concentration range between 1 and 20 mol.m<sup>-3</sup> for this study. Lower concentrations of CO<sub>2</sub> have been obtained by dilution with deionized water.

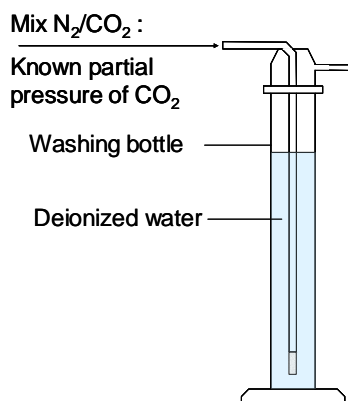


Figure IV-3. Experimental set-up for preparation of saturated CO<sub>2</sub> solutions.

### 1.2 Acid-base titration

In our case, acid-base titration consists in neutralising a basic compound with an acidic compound (here hydrochloric acid). This reaction is considered as total. The pH of the solution is measured as a function of the added volume of the strong acid. Titrations are performed to determine the unknown purity of an amine sample, the dissociation constant of the amines at 25°C and occasionally to check the concentration of CO<sub>2</sub> and amines on studied solutions. Those different analyses are realized thanks to the equipment 751 GPD titrino manufactured by Metrohm.

In the case of an amine solution or a carbon dioxide solution, the titration is realized at ambient temperature with an automatic sample changer 814 USB sample processor manufactured by Metrohm. In the case of the determination of the dissociation constant which depends on the temperature, the titration is performed in a thermostated vessel to control the temperature at 25.0 ± 0.5 °C.

### 1.2.1 Amine titration

From a given sample, it is possible to determine the concentration of amine functions. In the case of mono-amines, there is only one equivalent point EP1 which corresponds to the maximum of the derivate of the pH metric curve as indicated in Figure IV-4. It corresponds to the volume of hydrochloric acid needed to neutralize all amine functions in solution. In the case of multi-amines, we consider that all amine functions are neutralized at the latest equivalent point. The total quantity of amine present in solution is then given by Equation 29.

$$n_{Am}^{tot} = \frac{C_{HCl} \times V_{EP}}{N} \quad \text{Equation 29}$$

In this equation  $n_{Am}^{tot}$  corresponds to the total quantity of amine (mol),  $C_{HCl}$  is the concentration of HCl (generally  $0.1 \text{ mol.dm}^{-3}$ ),  $V_{EP}$  is the volume of the latest equivalent point ( $\text{m}^3$ ) and  $N$  is the number of amine function in the molecule.

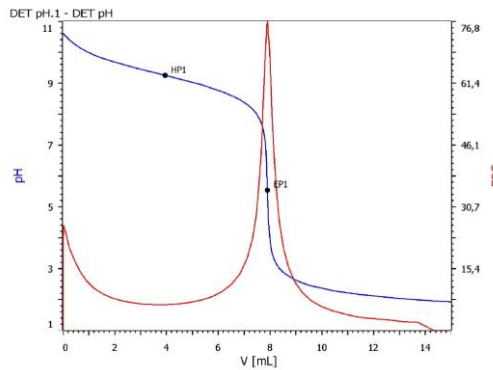


Figure IV-4. pH metric curve (blue line) and derivate (red line) obtained by titration of dimethylmonoethanolamine with hydrochlorid acid at  $0.1 \text{ mol.m}^{-3}$ .

### 1.2.2 Carbon dioxide titration

We develop an experimental method based on back titration in order to verify that  $\text{CO}_2$  bubbling achieves predicted concentration of  $\text{CO}_2$  in water according to Henry's law (Atkins and de Paula, 2006). This method is particularly adapted to low concentration of  $\text{CO}_2$  ( $1$  to  $40 \text{ mol.m}^{-3}$ ).

A sample of  $\text{CO}_2$  solution is neutralized by addition of a slight excess of sodium hydroxide. Carbonates and remaining sodium hydroxide are then titrated with an HCl solution. According to this method we assume that initial quantity of  $\text{CO}_2$  before addition of hydroxide sodium corresponds to the quantity of titrated  $\text{HCO}_3^-$  as indicated in Figure IV-5. The amount of  $\text{CO}_2$  initially present in solution is given by Equation 30. In this equation  $n_{\text{CO}_2}^i$  is the initial quantity of  $\text{CO}_2$  (mol),  $C_{HCl}$  is the concentration of hydrochloric acid ( $\text{mol.m}^{-3}$ ),  $V_{EP3}$  is the volume of the latest equivalent point ( $\text{m}^3$ ),  $V_{EP2}$  is the volume of the second-last equivalent point ( $\text{m}^3$ ). Further explanations are given in Chapter IX .3.1.

## 1. Experimental techniques

$$n_{CO_2}^i = C_{HCl} \cdot (V_{EP3} - V_{EP2}) \quad \text{Equation 30}$$

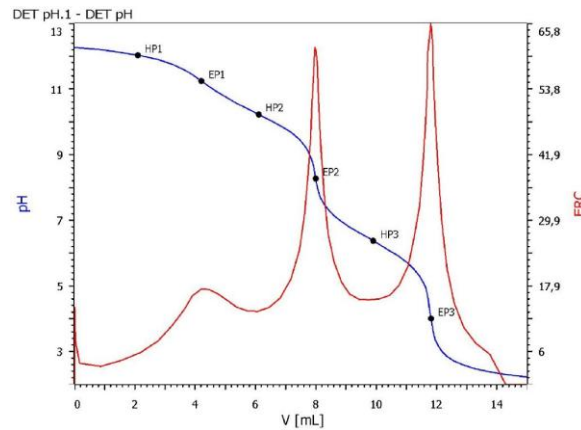


Figure IV-5. pH metric curves (blue lines) and derivatives (red lines). Titration of a mix of 27 g of  $[CO_2] = 30 \text{ mol.m}^{-3}$  neutralized with 12 g of  $[NaOH] = 100 \text{ mol.m}^{-3}$  by  $[HCl] = 100 \text{ mol.m}^{-3}$ .

The titration of carbon dioxide solutions confirms that the saturation method prepare aqueous solution of  $CO_2$  at the expected concentration. Indeed, for five different concentrations of  $CO_2$  (1, 5, 10, 20 and  $34 \text{ mol.m}^{-3}$ ) we observe that they follow the parity plot between experimental results and theoretical values as indicated in Figure IV-6. We also indicate the corresponding error bars. The average relative deviation between theoretical  $CO_2$  concentration and experimental  $CO_2$  concentration is around 7 %. This result validates the preparation method of  $CO_2$  solutions.

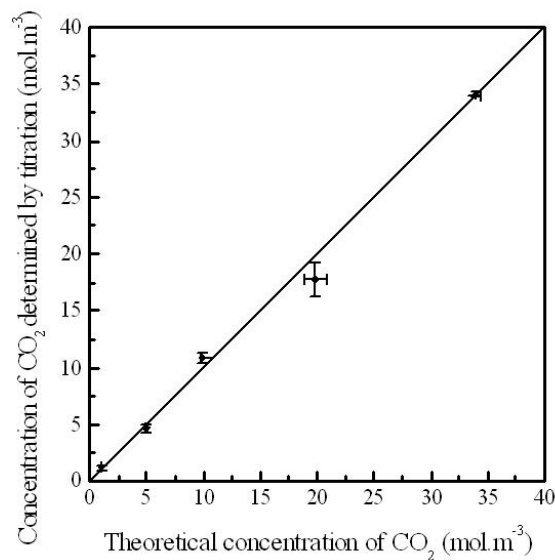


Figure IV-6. Parity plot between the concentrations of  $CO_2$  determined by titration of the theoretical concentrations of  $CO_2$  according to Henry's law.

### 1.2.3 Determination of the pKa

The pKa is defined as indicated in Equation 31 where  $K_a$  corresponds to the dissociation constant of the Reaction 11 (Chapter II .4.2) of an acid/base function (A). The expression of this constant is indicated in Equation 32 where  $a_{H_3O^+}$  is the hydronium ion activity,  $a_{A^-}$  is the activity of the basic form of A,  $a_{HA}$  is the activity of the acidic form of A and  $a_{H_2O}$  is the water activity.

$$pKa = -\log_{10}(K_a) \quad \text{Equation 31}$$

$$K_a = \frac{a_{H_3O^+} \times a_{A^-}}{a_{HA} \times a_{H_2O}} \quad \text{Equation 32}$$

When the titration is realised in diluted conditions (generally for concentration lower than  $0.1 \text{ mol.dm}^{-3}$ ) we assume that the activity of species are equal to their concentration ( $\text{mol.dm}^{-3}$ ) and that the water activity, which is the solvent, is equal to 1. In this condition the pH of the solution of a monoprotic acid/base function is indicated in Equation 33.

$$pH = pKa + \log_{10}\left(\frac{[A^-]}{[HA]}\right) \quad \text{Equation 33}$$

#### 1.2.3.1 Monoamines

When the amine is diluted and titrated by a strong acid, the value of the pKa is given by the value of the pH which corresponds to the half equivalent volume needed to neutralize entirely the amine. At this point, the amine concentration is equal to the ammonium ion concentration. In the Figure IV-4, pKa is given by the ordinate of the point HP1 (Half equivalent Point 1).

#### 1.2.3.2 Diamines

For diamines we distinguish two cases according to the difference of pKa between the first amine function ( $pKa_1$ ) and the second amine function ( $pKa_2$ ), with  $\Delta pKa$  which corresponds to the difference between  $pKa_1$  and  $pKa_2$ .

- $\Delta pKa > 1$ . The titration curve gives two inflection points. We assume that the ordinate of each half equivalent point indicates the value of pKa corresponding to each amine function of the molecule as indicated in Figure IV-7 (a).
- $\Delta pKa < 1$ . The titration curve gives only one inflection point as indicated in Figure IV-7 (b). In this case we use the CurTiPlot freeware (Curtiplot, 2013) in order to determine values of pKa by fitting the curve.

## 2. Characterisation of apparent kinetic constants

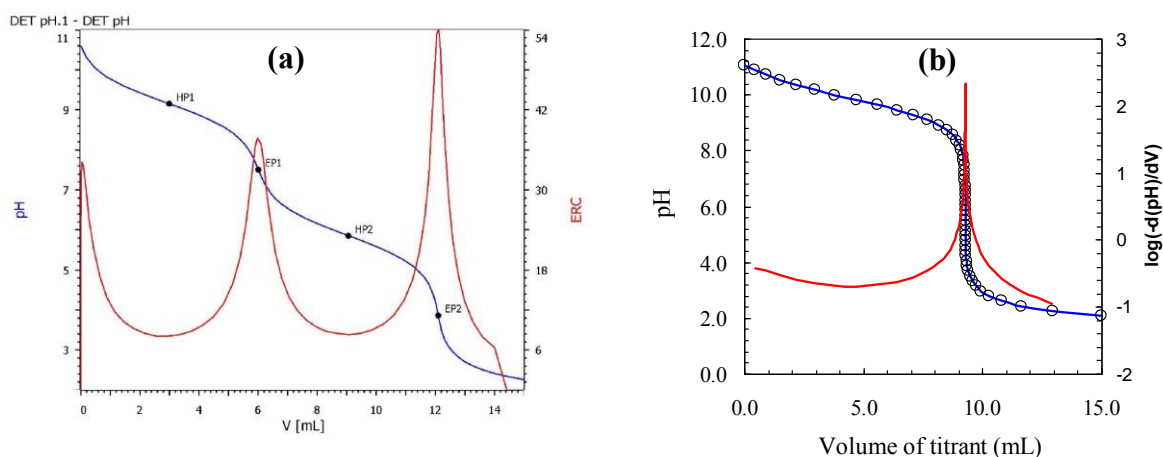


Figure IV-7. pH metric curves (blue lines) and derivates (red lines) obtained by titration of (a) N,N,N',N'-tetramethylethylenediamine (b) and N,N,N',N'-tetramethylhexanediamine experimental data (black circles), and fit with CurTiPlot (Curtiplot, 2013).

## 2 Characterisation of apparent kinetic constants

The stopped-flow technique with conductivity detector provides signals as indicated in Figure IV-8. Each experiment consists in three parts.

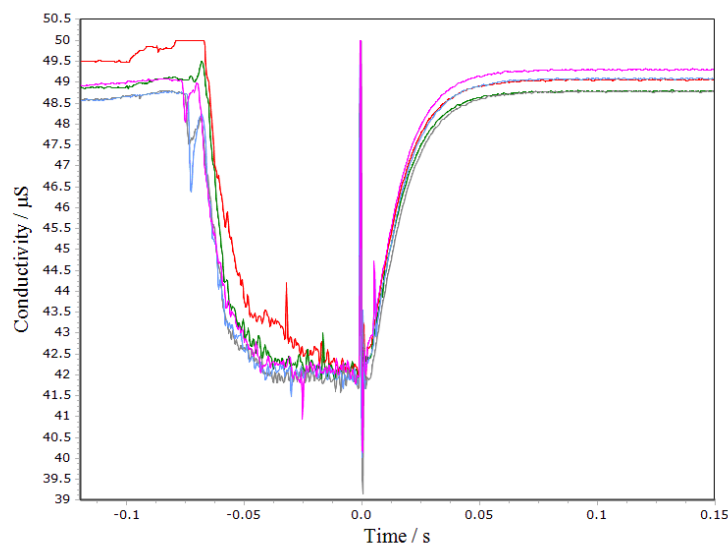


Figure IV-8. Example of conductivity curve as a function of time obtained by stopped-flow technique.  $[\text{Monoethanolamine}] = 40 \text{ mol.m}^{-3}$  and  $[\text{CO}_2] = 4 \text{ mol.m}^{-3}$  before mixing.

First between  $-\infty$  and around -0.1 s the conductivity remains almost constant, corresponding to the equilibrium state reached after the previous injection. The concentrations of all constituents stay constant. Then, a new injection takes place between around -0.1 and 0 s, the conductivity cell is flushed with freshly mixed solution of amine and  $\text{CO}_2$  which have not yet reacted. In this example, the conductivity decreases because reagents ( $\text{CO}_2$  and free

amine) are non ionic compounds and replace the ions formed by the previous reaction. Finally, between 0 and  $\infty$ , the flow is stopped and the conductivity cell measures the evolution of the conductance as a function of time. This evolution is representative of the extent of reaction. From this latter part, it is possible to extract the kinetic constant.

As we have seen in Chapter II .6 there are two different ways to determine the apparent kinetic constant from raw data: numerical method and analytical method. Both methods are presented in the next part.

## 2.1 Numerical method

A numerical method has been developed in order to determine kinetic constants from the conductimetric signal. This model can also be used to simulate a variation of conductance from a given set of amine kinetic constants and experimental conditions. It is also used to calculate the amine concentrations at initial conditions ( $t = 0$ ) and final conditions (equilibrium at the final state) of a stopped flow run. We present in this part the associated model only for monoamines, with the input and output data.

### 2.1.1 Description

The goal of the numerical method is to simulate or fit the variation of the conductance which takes place during the reaction of amine with  $\text{CO}_2$  with the kinetic constants and order of the reaction as the principal parameters which can be set for a simulation or determined by fitting. The method is based on the input data, the model of reaction and the output data. The input data are experimental parameters which characterize the amine solution and the operating conditions. The model consists in algebraic and differential equations corresponding to the physical and chemical phenomena that we take into account to represent the variation of the conductance as a function of time. We present it with further details in the following part. Finally we get several output data related to the optimal values of the kinetic constants, the resulting concentrations of all species as a function of time and the corresponding signal of conductance.

### 2.1.2 Input data

We must fill six input data as parameters of the model:  $\rho_i$  the density of the studied solution of amine after mixing ( $\text{kg.m}^{-3}$ ),  $M_i$  the molecular weight of the amine ( $\text{g.mol}^{-1}$ ),  $w_i$  the weight fraction of the amine,  $\alpha$  the loading of the solution defined in Equation 34,  $\alpha_{\text{HCl}}$  the loading of hydrochloric acid,  $\alpha_{\text{HCO}_2\text{H}}$  the loading of formic acid,  $K_a$  the dissociation constant of the amine and  $K_c$  the constant of carbamate stability. In Equation 34,  $n_{\text{CO}_2}^{\text{tot}}$  is the quantity of total carbon dioxide (mol) in its different species ( $\text{CO}_2$ ,  $\text{H}_2\text{CO}_3$ ,  $\text{HCO}_3^-$ ,  $\text{CO}_3^{2-}$  and  $\text{AmCOO}^-$ ) and  $n_{\text{Am}}^{\text{tot}}$  is the quantity of amine (mol) in its different species ( $\text{Am}$ ,  $\text{AmH}^+$  and  $\text{AmCOO}^-$ ). In Equation 35,  $n_{\text{HCl}}^{\text{tot}}$  is the quantity of total hydrochloric acid (mol) in its different species ( $\text{HCl}$  and  $\text{Cl}^-$ ). In Equation 36,  $n_{\text{HCO}_2\text{H}}^{\text{tot}}$  is the quantity of total formic acid (mol) in its

## 2. Characterisation of apparent kinetic constants

different species ( $\text{HCO}_2\text{H}$  and  $\text{HCOO}^-$ ). The integration of hydrochloric and formic acid will be justified in Chapter IV .2.3.

$$\alpha = \frac{n_{\text{CO}_2}^{\text{tot}}}{n_{\text{Am}}^{\text{tot}}} \quad \text{Equation 34}$$

$$\alpha_{\text{HCl}} = \frac{n_{\text{HCl}}^{\text{tot}}}{n_{\text{Am}}^{\text{tot}}} \quad \text{Equation 35}$$

$$\alpha_{\text{HCO}_2\text{H}} = \frac{n_{\text{HCO}_2\text{H}}^{\text{tot}}}{n_{\text{Am}}^{\text{tot}}} \quad \text{Equation 36}$$

The measured densities of injected amine solutions before mixing with  $\text{CO}_2$  are used to estimate the density of the studied solutions of amine after dilution with the aqueous solution of  $\text{CO}_2$ . As we have verified that the density of each  $\text{CO}_2$  solutions have the same density as water at 25 °C ( $997.1 \text{ g}\cdot\text{dm}^{-3}$ ) it is possible to estimate the value of the density of each reactive system from the fitting of experimental data (density of amine solutions before mixing) with an empirical second degree polynomial function as indicated in Figure IV-9. This method gives an estimation of the density of solution after mixing with a discrepancy smaller than  $0.1 \text{ kg}\cdot\text{m}^{-3}$ .

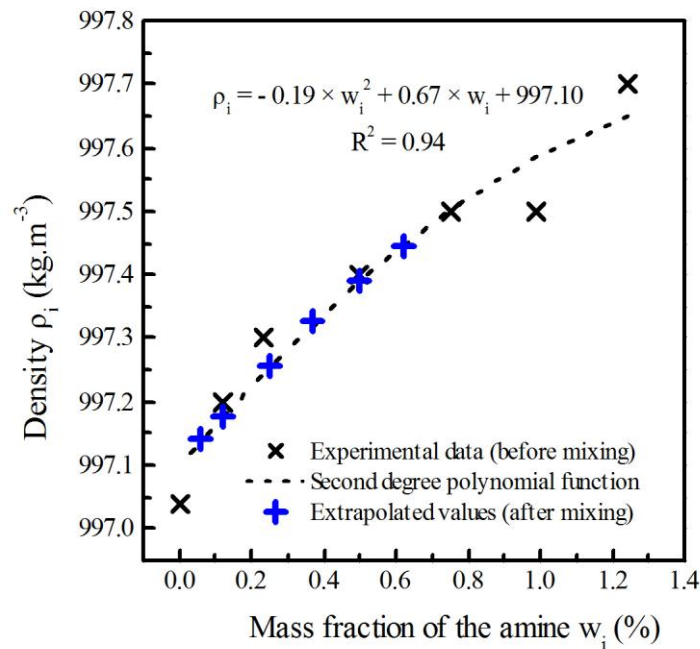


Figure IV-9. Density of monoethanolamine as a function of mass fraction.

### 2.1.3 Model

#### 2.1.3.1 Activity of chemical species

The description of chemical reactions and equilibria is written in terms of activities of the different species. We consider water as the only solvent of all other species which are considered as the solutes. The activity of water is given by its molar fraction as indicated by Equation 37.

$$a_{H_2O} = \frac{1}{1 + M_{H_2O} \times (1 + \alpha) \times \frac{w_i}{M_i \times (100 - w_i)}} \quad \text{Equation 37}$$

In this equation  $a_{H_2O}$  is the activity of the water,  $M_{H_2O}$  is the molecular mass of water ( $\text{kg}\cdot\text{mol}^{-1}$ ),  $\alpha$  is the loading of the solution,  $w_i$  is the weight fraction of the amine  $i$  (percents),  $M_i$  is the molecular mass of the amine  $i$  ( $\text{kg}\cdot\text{mol}^{-1}$ ).

The activities of the different species are calculated according to the extended Debye-Hückel's law (Guggenheim, 1935). The activity of each solute  $a_i$  is linked to the activity coefficient  $\gamma_i$  (in this case,  $i$  is a natural number different from zero which correspond to the charge number of the considered ionic species  $i$ ), to the molality of the solute  $m_i$  ( $\text{mol}\cdot\text{kg}^{-1}$ ) and to the molality at the standard state  $m^\circ$  ( $1 \text{ mol}\cdot\text{kg}^{-1}$ ) as indicated in Equation 38.

$$a_i = \gamma_i \times \frac{m_i}{m^\circ} \quad \text{Equation 38}$$

The coefficient of activity is equal to 1 for non ionic species. For ionic species,  $\gamma_i \leq 1$  and its value is determined thanks to relation indicated by Equation 39. In this relation  $A = 5.11 \times 10^{-1}$  (at 25 °C),  $B = 3.29 \times 10^9$  (at 25 °C),  $C = 2.80 \times 10^{-2}$ ,  $r = 2.99 \times 10^{-10}$  (Guggenheim, 1935),  $z_i$  is the charge number of the ion species  $i$ , and  $I_m$  is the ionic strength defined in Equation 40.

$$\log \gamma_i = \frac{-A \times z_i^2 \times \sqrt{I_m}}{1 + B \times r \times \sqrt{I_m}} + C \times \sqrt{I_m} \quad \text{Equation 39}$$

$$I_m = \frac{1}{2} \times \sum_i z_i^2 \times m_i \quad \text{Equation 40}$$

As indicated by Equation 41, the conversion between the molarity of species  $i$   $[i]$  ( $\text{mol}\cdot\text{m}^{-3}$ ) and the molality  $m_i$  ( $\text{mol}\cdot\text{kg}^{-1}$ ) is realized with the factor of conversion  $K_s$  ( $\text{kg}\cdot\text{m}^{-3}$ ) which corresponds to the ratio between the mass of solvent (water) and the volume of the

## 2. Characterisation of apparent kinetic constants

solution indicated in Equation 42 where  $\rho_i$  is the density of the solution ( $\text{kg.m}^{-3}$ ) and  $M_{CO_2}$  corresponds to the molecular mass of the  $CO_2$  ( $\text{kg.mol}^{-1}$ ).

$$[i] = K_S \times m_i \quad \text{Equation 41}$$

$$K_S = \frac{\rho_i}{1 + \frac{w_i}{100 - w_i} \times (1 + \alpha \frac{M_{CO_2}}{M_i})} \quad \text{Equation 42}$$

### 2.1.3.2 Mass balances and equilibria

We calculate the molalities of 11 or 12 solutes as a function of time: Am,  $AmH^+$ ,  $CO_2$ ,  $H_2CO_3$ ,  $HCO_3^-$ ,  $CO_3^{2-}$ ,  $HO^-$  and  $H^+$ ,  $Cl^-$ ,  $HCO_2H$ ,  $HCO_2^-$  in the case which do not form carbamate (tertiary and sterically hindered amines) and we add  $R_2NCO_2^-$  in the case of primary or secondary amines forming carbamates. For given conditions of total amine concentration and loading ( $\alpha$ ,  $\alpha_{HCl}$  and  $\alpha_{HCO_2H}$ ), the molalities of all species at equilibrium are determined by the resolution of a system of 11 equations (12 with carbamates). These equations are presented below.

First, there are five acid-base equilibria. The definition of equilibrium constants (mass action laws) gives the five equations presented in Table IV-1.

Table IV-1. Reactions considered in the numerical model and expression of the thermodynamic constant. Correlations for the thermodynamic constants are given in Chapter IX .4.1.

Reaction	Thermodynamic constant
$H_2O \xrightleftharpoons{K_w} H^+ + HO^-$	$K_w = \frac{a_{H^+} \times a_{HO^-}}{a_{H_2O}}$
$HCO_3^- \xrightleftharpoons{K_{CO_3^{2-}}} CO_3^{2-} + H^+$	$K_{CO_3^{2-}} = \frac{a_{H^+} \times a_{CO_3^{2-}}}{a_{HCO_3^-}}$
$H_2CO_3 \xrightleftharpoons{K_{HCO_3^-}} HCO_3^- + H^+$	$K_{HCO_3^-} = \frac{a_{H^+} \times a_{HCO_3^-}}{a_{H_2CO_3}}$
$Am + H_2O \xrightleftharpoons{K_b} AmH^+ + HO^-$	$K_b = \frac{a_{AmH^+} \times a_{HO^-}}{a_{Am} \times a_{H_2O}} = \frac{K_w}{K_a}$
$HCO_2H + H_2O \xrightleftharpoons{K_{HCO_2H}} HCO_2^- + H^+$	$K_{HCO_2^-} = \frac{a_{H^+} \times a_{HCO_2^-}}{a_{HCO_2H}}$

Then we determine the mass balance of the carbon dioxide as indicated by Equation 43. In this equation R is the sum of all rates of reaction with CO<sub>2</sub> which are kinetically limited. The contribution of each reaction to R is positive when the CO<sub>2</sub> is a reactant (forward reactions) and negative when the CO<sub>2</sub> is a product (inverse reactions). The reaction forming carbamate is considered as irreversible. Since we observe the kinetics on short time scale, we do not consider the reaction of carbamate hydrolysis. For all these reactions, the rate law is written according to the activity of the reagents. We suppose that all reversible reactions are one-step reactions and that the forward kinetic constant  $k_i^m$  is related to chemical equilibrium  $K_i$  and to reverse kinetic constant  $k_{-i}^m$  as indicated by Equation 44 according to the Brønsted-Bjerrum's law (Scacchi *et al.*, 1996).

$$-\frac{dm_{CO_2}}{dt} = R \quad \text{Equation 43}$$

$$K_i = \frac{k_i^m}{k_{-i}^m} \quad \text{Equation 44}$$

Among the reactions indicated in Table IV-2, the kinetic constants of the first two reactions are known.

Table IV-2. Reaction kinetically limited considered in the numerical model and expression of associated rate law. Correlations for the available constants are given in appendix.

Reaction	Reaction rate (mol.kg <sup>-1</sup> .s <sup>-1</sup> )
$CO_2 + H_2O \xrightleftharpoons[k_{H_2O}^m, -k_{H_2O}^m]{} H_2CO_3$	$r_{H_2O} = k_{H_2O}^m \times a_{H_2O} \times a_{CO_2}$ $r_{-H_2O} = k_{-H_2O}^m \times K_{H_2CO_3} \times a_{H_2CO_3}$
$CO_2 + HO^- \xrightleftharpoons[k_{HO^-}^m, -k_{HO^-}^m]{} HCO_3^-$	$r_{HO} = k_{HO}^m \times a_{HO^-} \times a_{CO_2}$ $r_{-HO} = k_{-HO}^m \times \frac{K_{H_2CO_3} \times K_w}{K_{HCO_3^-}} \times a_{HCO_3^-}$
$CO_2 + R_3N + H_2O \xrightleftharpoons[k_{R_3N}^m, -k_{R_3N}^m]{} HCO_3^- + R_3NH^+$	$r_{R_3N} = k_{R_3N}^m \times a_{R_3N} \times a_{CO_2} \times a_{H_2O}$ $r_{-R_3N} = k_{-R_3N}^m \times \frac{K_{H_2CO_3} \times K_{HCO_3^-} \times K_b}{K_w} \times a_{R_3NH^+} \times a_{HCO_3^-}$
$CO_2 + 2R_2NH \xrightarrow{k_{R_2NH}^m} R_2NCOO^- + R_2NH_2^+$	$r_{R_2NH} = k_{R_2NH}^m \times a_{R_2NH}^n \times a_{CO_2}$

## 2. Characterisation of apparent kinetic constants

The fitting of the conductimetric signals yields to the kinetic constant relative to the amine:  $k_{R3N}^m$  for tertiary amines or sterically hindered amines which do not form carbamate,  $k_{R2NH}^m$  and order n for amines which form carbamate. This latter reaction is considered that the reaction is irreversible at the short time scale where it is observed.

Then, we express the mass balances of amine species, carbonated species, carbamate, hydrochloric acid and formic acid species respectively in Equation 45, Equation 46, Equation 47, Equation 48 and Equation 49.

$$m_{Am}^{tot} = \frac{w_i}{100 - w_i} \times \frac{1000}{M_i} = m_{Am} + m_{AmH^+} + m_{R_2NCO_2^-} \quad \text{Equation 45}$$

$$\alpha_{CO_2} \times m_{Am}^{tot} = m_{CO_2} + m_{H_2CO_3} + m_{HCO_3^-} + m_{CO_3^{2-}} + m_{R_2NCO_2^-} \quad \text{Equation 46}$$

$$\frac{dm_{R_2NCO_2^-}}{dt} = r_{R_2NH} \quad \text{Equation 47}$$

$$\alpha_{HCl} \times m_{Am}^{tot} = m_{Cl^-} \quad \text{Equation 48}$$

$$\alpha_{HCO_2H} \times m_{Am}^{tot} = m_{HCO_2H} + m_{HCO_2^-} \quad \text{Equation 49}$$

Finally we express the electroneutrality of the system according to Equation 50.

$$m_{AmH^+} + m_{H^+} = m_{R_2NCO_2^-} + m_{HO^-} + m_{HCO_3^-} + 2 \times m_{CO_3^{2-}} + m_{Cl^-} + m_{HCO_2^-} \quad \text{Equation 50}$$

### 2.1.3.3 Initial state

Since the mixing of reagents studied in the conductimetric cell is not instantaneous, the extent of reaction is not equal to zero when the flow stops. In order to calculate the initial conditions, we consider the cell as a continuous-stirred tank reactor (CSTR) flushed by the perfectly mixed solution just before the flow stops. The assumption of steady state is confirmed by the stabilization of the conductimetric signal at the end of the injection (Figure IV-8). In these conditions the initial molalities of the species *i* in the conductance cell concentration in the cell ( $m_{i,0}$  expressed in mol.kg<sup>-1</sup>) are related to the equilibrium concentrations of this species reached in the syringes and entering the reactor  $m_{i,1}$  for the syringe containing the amine and  $m_{i,2}$  for the syringe containing the CO<sub>2</sub>. The time of exposure  $\tau$  is determined experimentally as in as the ratio of the cell volume  $V_{Cell}$  ( $2.1 \times 10^{-8}$  m<sup>3</sup>) and the volumic flow rate  $Q$  ( $4.7 \times 10^{-6}$  m<sup>3</sup>.s<sup>-1</sup>) and estimated at 4.5 ms.

We replace the differential equations by algebraic equations in the above system. We express the mass balance on CO<sub>2</sub> according to Equation 51. In this equation, if we consider that  $K_{S,2} = \rho_{\text{water}}$ , we get expression indicated in Equation 52. The molality  $m_{\text{CO}_2,2}$  is calculated by resolution of the system of equilibrium equations of CO<sub>2</sub> in water at 25 °C as indicated in Equation 53. Concerning carbamate, the mass balance is expressed as indicated in Equation 54.

$$\frac{Q}{2} \times m_{\text{CO}_2,2} \times K_{S,2} - R \times V_{\text{cell}} \times K_S = Q \times m_{\text{CO}_2,0} \times K_S \quad \text{Equation 51}$$

$$m_{\text{CO}_2,0} = \frac{m_{\text{CO}_2,2}}{2} \times \frac{\rho_{\text{water}}}{K_S} - R \times \tau \quad \text{Equation 52}$$

$$m_{\text{CO}_2,2} + m_{\text{H}_2\text{CO}_3,2} + m_{\text{HCO}_3,2} + m_{\text{CO}_3,2} = 2\alpha_{\text{CO}_2} \times \frac{\rho_{\text{water}}}{K_S} \times m_{\text{Am}}^{\text{tot}} \quad \text{Equation 53}$$

$$m_{\text{R}_2\text{NCOO}^-,0} = r_{\text{R}_2\text{NH}} \times \tau \quad \text{Equation 54}$$

This model still implies that the reactants enter in the conductimetric cell without upstream mixing and reaction. This is not exactly the case since the two streams join in a tiny T-mixer just upstream of the conductimetric chamber. To compensate this approximation, we introduce an offset parameter on the observed time  $t_0$ . In other words, the origin of the observed conductimetric signal  $t = 0$  corresponds to  $t = t_0$  since the initial state of the model.

#### 2.1.3.4 Conductivity modelling

For a given kinetic constant of the amine-CO<sub>2</sub> reaction, it is possible to determine the concentration of all species as a function of the time. We use the Kohlrausch additivity relationship (Equation 55) to model the conductance (Atkins and de Paula, 2006).

$$G(t) = G_0 \times \sum_0^n (\lambda_i^\infty \times [i](t)) \quad \text{Equation 55}$$

In this equation  $G(t)$  is the conductance (S),  $G_0$  is a fitting parameter which can be compared to the cell constant (m),  $\lambda_i^\infty$  is the limiting molar conductivity of the ionic species  $i$  (S.m<sup>2</sup>.mol<sup>-1</sup>) and  $[i](t)$  is the molar concentration of the species  $i$  (mol.m<sup>-3</sup>) as a function of time.

Values of ionic conductivity at infinite dilution are well known for HO<sup>-</sup>, H<sup>+</sup>, HCO<sub>3</sub><sup>-</sup> and CO<sub>3</sub><sup>2-</sup>. For other species we have drawn a correlation based on data of conductivity at infinite dilution of alkylammonium ions of different molecular mass. These data are indicated in Chapter IX .4.3.

## 2. Characterisation of apparent kinetic constants

The wedge parameter  $G_0$  is used to fit the value of the conductance at the chemical equilibrium of the final state in order to compensate residual errors in amine concentration or in estimation of ionic conductivity at infinite dilution and application of the Kohlrausch law which is valid only for dilute solution of strong electrolytes. The deviation from this theory can be observed by the ratio between  $G_0$  and the cell constant ( $2.36 \times 10^{-3}$  m).

### 2.1.3.5 Resolution of the numerical model

For a given value of fitting parameters,  $t_0$  and  $G_0$ , the resolution of the numerical model is realized according to the method described here. The system of equations of the stopped-flow model is composed of algebraic and differential equations as indicated respectively in Equation 56 and Equation 57. We also consider  $x(t_0) = x_0$ . In these equation  $x$  is the vector of molality of  $\text{CO}_2$  and carbamates which are driven by kinetically limited reactions (differential equation) and  $y$  is the vector of the molalities of all other species which are considered at the equilibrium at each moment (algebraic equation).

$$0 = g(x, y) \quad \text{Equation 56}$$

$$\frac{dx}{dt} = f(x, y) \quad \text{Equation 57}$$

This system is solved in a FORTRAN program. The algebraic equations are solved for  $y$  ( $x$  is given) by the HYBRD routine of the Minpack package (More *et al.*, 1980; Netlib, 2013b). The differential-algebraic system is formally rewritten as a purely differential system of equations, which is solved with the routine LSODE (Hindmarsh, 1983; Netlib, 2013a; Radhakrishnan and Hindmarsh, 1993). Let us denote  $y = h(x)$  the solution of the algebraic equations:  $0 = g(x, h(x))$ . The differential equations can then be rewritten as indicated in Equation 58. LSODE requires the user to supply a subroutine computing  $L$  for a value of  $x$ . For this,  $h(x)$  must be calculated, which means solving the algebraic equations. This is done as explained above by calling the HYBRD routine.

$$\frac{dx}{dt} = f(x, h(x)) = L(x) \quad \text{Equation 58}$$

An attempt has been made to solve the differential-algebraic system with a dedicated routine (DASPK) (Brenan *et al.*, 1989; Petzold, 1983). When it worked, it was much faster than LSODE+HYBRD. Unfortunately, it was not robust enough: there were many cases where DASPK stopped shortly after the initial time (the error test was not satisfied).

### 2.1.4 Output data

The fitting of the conductimetric signal by the numerical model yields to the estimation of the kinetic constant and the variation of the concentration of all species as a function of time. As an example, Figure IV-10 (a) shows the variation of the conductimetric signal corresponding to the first experiment shown in Figure IV-8. Kinetic constants for the fit are  $k_{R_2NH}^m$  and  $n$  (respectively  $5.40 \text{ kg}^n \cdot \text{mol}^{-n} \cdot \text{s}^{-1}$  and 1) which correspond to an apparent pseudo first order constant of  $k_0 = 76.7 \text{ s}^{-1}$ . The resulting variation of concentration of the main species as a function of time is given in Figure IV-10 (b).

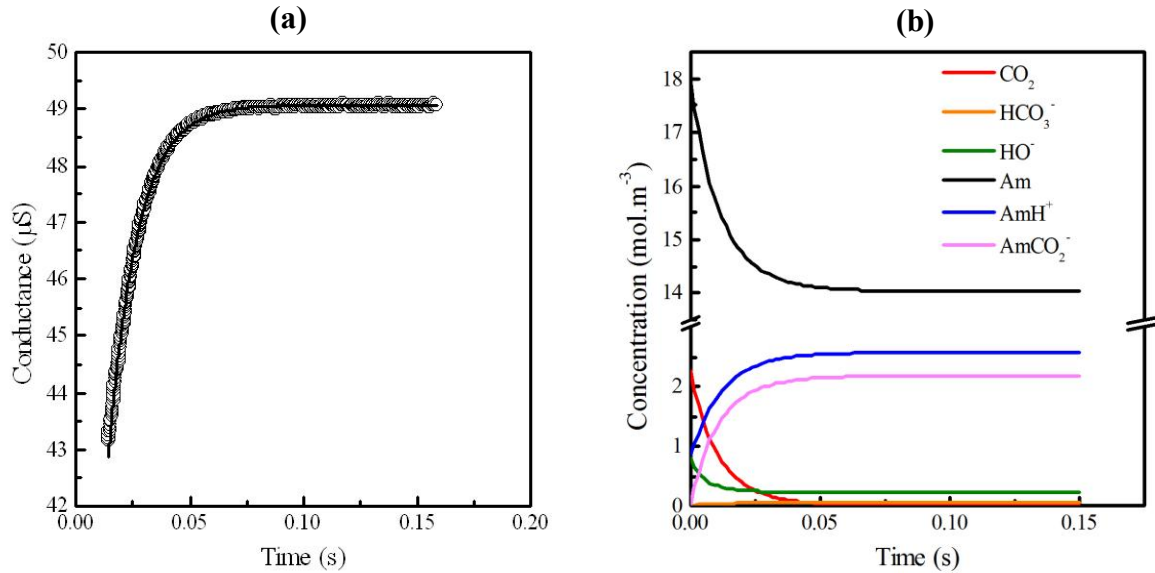


Figure IV-10. [Monoethanolamine] =  $40 \text{ mol} \cdot \text{m}^{-3}$  and  $[\text{CO}_2] = 4 \text{ mol} \cdot \text{m}^{-3}$  before mixing. (a) Conductance as function of time (circle) experimental and (line) modelled.  $G_0 = 2 \times 10^{-3} \text{ m}$ ,  $t_0 = 3 \text{ ms}$  and  $k_0 = 76.7 \text{ s}^{-1}$  ( $k_{R_2NH}^m = 5.40 \text{ kg}^n \cdot \text{mol}^{-n} \cdot \text{s}^{-1}$  and  $n = 1$ ). (b) Evolution of the different concentrations as function of the time.

The calculation of the apparent kinetic constant  $k_0$  with data of the numerical model is only realized for primary and secondary amines according to the expression given in Equation 59 **Erreur ! Source du renvoi introuvable.** Parameters  $k_{R_2NH}^m$  and  $n$  are determined by fitting with the numerical model.

$$k_0 = k_{R_2NH}^m \times [Am]^n = \frac{k_{R_2NH}^m}{(\rho_{H_2O})^n} \times [Am]^n \quad \text{Equation 59}$$

### 2.1.5 Strengths and weaknesses

Numerical method brings several information related to the reaction between amine and  $\text{CO}_2$ . Indeed, it can be used in order to determine the concentration of each species at the

## 2. Characterisation of apparent kinetic constants

beginning and at the end of the reaction, independently on the kinetics. Before to carry an experiment, it gives an estimation of variation of the conductance as a function of time. By fitting of data at different concentrations, the numerical method determines the kinetic constant and order of the amine-CO<sub>2</sub> reaction taking into account inverse and parallel reactions and the variation of all species involved in the reaction model.

However this method needs several fitting parameters to set which can have an impact on the estimation of the kinetic constant. Moreover it assumes that the ionic conductivity at infinite dilution of a carbamate is equal to the conductivity of an alkylammonium of equivalent molecular weight, which is given from a correlation established on available data. These hypotheses on the estimation of conductivities and their additivity are a supplementary source of error.

### 2.2 Analytical method

#### 2.2.1 Description

It is possible to determine an analytical expression for the variation of conductance if we consider three assumptions. Firstly, the molar conductivity of each species is assumed constant during the reaction. Secondly, the concentration of amine is considered as constant during the reaction. This hypothesis is accepted when the concentration of amine is at least 10 times higher than the concentration of carbon dioxide. Finally we consider a single reaction of amine with CO<sub>2</sub> which is kinetically limited and the irreversible reaction. The latter condition is met as we always keep a loading inferior to 0.1 mol CO<sub>2</sub> per mol of amine during the reaction. Parallel reactions of CO<sub>2</sub> with HO<sup>-</sup> and H<sub>2</sub>O are also considered irreversible and first order. According to these assumptions we demonstrate in appendix that it is possible to fit the variation of conductance by a monoexponential law with a pseudo first order kinetic constant  $k_0$  (s<sup>-1</sup>) as indicated in Equation 60. The demonstration of this equation is indicated in Chapter IX. 5. It is then possible to determine the apparent kinetic constant of each conductance curve by fitting as indicated in Figure IV-11 shows a conductance curve fitted by the analytical model yielding to a kinetic constant  $k_0$  of 78.0 s<sup>-1</sup>.

$$\frac{1}{R(t)} = G(t) = -A \times \exp(-k_0 \times t) + C \quad \text{Equation 60}$$

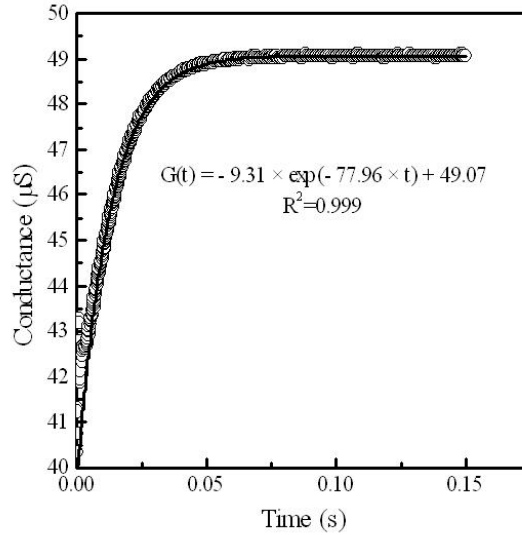


Figure IV-11. Conductivity curve as function of time: experimental (circle) and fit with analytical model (continuous line). [Monoethanolamine] = 40 mol.m<sup>-3</sup> and [CO<sub>2</sub>] = 4 mol.m<sup>-3</sup> before mixing.

This apparent kinetic constant is related with the concentration of amine and hydroxide ions by Equation 61 for amines which form carbamates and by Equation 62 for amines which form carbonates. Apparent kinetic constants are given here as a function of molar concentration. This approach is consistent with the activity model in diluted solution and in agreement with literature data.

$$k_0 = k_{R_2NH} \times [R_2NH]^n + k_{HO^-} \times [HO^-] + k'_{H_2O} \quad \text{Equation 61}$$

$$k_0 = k'_{R_3N} \times [R_3N] + k_{HO^-} \times [HO^-] + k'_{H_2O} \quad \text{Equation 62}$$

The question can be raised of the determination of the free amine concentration in Equation 61 and Equation 62. Indeed, even if we operate with an excess of amine, the concentration of free amine is not completely constant as indicated in Figure IV-10.

In order to determine the amine concentration we compare results between the numerical and analytical methods as described as follows. For monoethanolamine, we set values of  $k_{Am}$  and  $n$  equal respectively to 2.6 m<sup>3n</sup>.mol<sup>-n</sup>.s<sup>-1</sup> and 1.16. Those values are directly taken from the literature (Ali *et al.*, 2002). The evolution of the apparent kinetic constant as a function of the amine concentration determined from those parameters according to the power law model is considered as the reference and indicated in Figure IV-12 by the black line. Then, thanks to the numerical model we simulate the conductivity curves at six different total amine concentrations with those parameters. We consider a total concentration of CO<sub>2</sub> ten times lower than the corresponding total amine concentration. We determine the apparent kinetic constant of the six modelled curves by fitting them with the analytical model. Moreover we determine the initial and final amine concentration with the numerical model.

## 2. Characterisation of apparent kinetic constants

The results obtained at both concentrations for the corresponding value of apparent kinetic constant are then represented in Figure IV-12.

According to this result, the discrepancy between the reference and the analytical method at the initial state is more important (average relative error of 22.0 %) than for final state (average relative error of 4.8 %). It clearly shows that the apparent kinetic constant determined with the analytical method should be associated to the final concentration of amine. Usually, the first part of the conductivity curve (0 to some milliseconds) can not be exploited because it corresponds to the area of transition between flow and stopped-flow. It is also the period where concentration of the different species has the most important evolution. For this reasons we always associate the final concentration of amine of the reaction determined with the numerical method to the apparent kinetic constant determined with the analytical method.

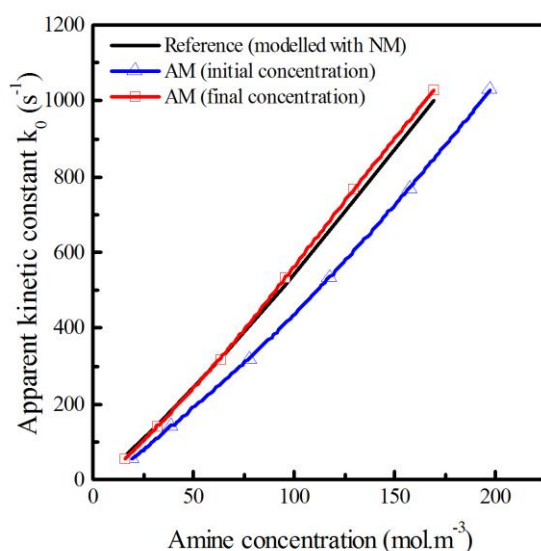


Figure IV-12. Apparent kinetic constant modelled of monoethanolamine with numerical method (NM) (black line), and determined with analytical method (AM) at the initial conditions (blue triangles) and at the final conditions (red squares).

### 2.2.2 Strength and weakness

The analytical method consists in a straightforward analysis of the conductimetric signal. Each run is analysed with the KineticStudio® developed by TgK according to simple first order kinetics which can be easily compared with other studies of the literature (Ali *et al.*, 2000). This method does not require fitting parameters and hypotheses on the conductivity on each species.

However the analytical method requires low CO<sub>2</sub> concentration over amine concentration ratio which has a limiting effect on the amplitude of the conductimetric signal. Another limitation on the amplitude of the signal is the amine concentration in order to keep the first order kinetic constant in the experimental range defined by the mixing time of the reagents.

## 2.3 Experimental optimization

Even if the numerical method is more exhaustive and a priori adapted to analyse data in a large range of experimental conditions such as amine concentration and CO<sub>2</sub> loading, the determination of kinetic constant can be affected by the uncertainty on each parameter (thermodynamic constants, kinetic constants of parallel and inverse reactions, ionic conductivities, fitting parameters). In most cases, the conductimetric signal is optimized to use the analytical model which directly determines the apparent kinetic constant. In order to respect the hypotheses and limitations of this method we set up several experimental methods.

### 2.3.1 Contribution of the reaction with hydroxide ions

In the case of tertiary amines and for some slow primary and secondary amines the kinetic contribution of the reaction between carbon dioxide and hydroxide ions can not be neglected as we have already shown in Chapter III. 3.2.3. In order to determine the kinetic constant with the analytical method we set up an experimental method which keeps this contribution under control. This method consists in adding hydrochloric acid in the tertiary amine solutions and formic acid in primary and secondary amine solutions in order to reduce the concentration of hydroxide ions and its relative variation during the reaction with CO<sub>2</sub>.

Indeed, in the case of tertiary amines which have generally a relatively important amplitude of the conductance signal, it is possible to use a strong acid with a conjugated base which has an important limiting molar conductivity ( $7.6 \times 10^{-3} \text{ S.m}^2.\text{mol}^{-1}$  (Lide, 1994)). The noise brought by chloride ions does not affect the measurement. However, in the case of primary and secondary amines, they have a relatively low amplitude of the conductance signal. For this kind of amine we select formic acid because its conjugated base has a lowest value of limiting molar conductivity than chloride ions ( $5.5 \times 10^{-3} \text{ S.m}^2.\text{mol}^{-1}$  (Lide, 1994)) and then introduce less of noise on the conductance signal. Moreover, the choice of this acid is also linked to its use for another experimental method that we detail in the next part.

We illustrate the experimental method which keep the contribution of hydroxide ions under control we the particular case of methyldiethanolamine. The Figure IV-13 shows the decrease of the pH, which is directly linked to the concentration of hydroxide ions, with the CO<sub>2</sub> loading range of the stopped-flow run for different rates of neutralization of the methyldiethanolamine with hydrochloric acid. The initial concentration of hydroxide ions for the different solutions is  $5.99 \times 10^{-4} \text{ mol.dm}^{-3}$  (no HCl),  $3.26 \times 10^{-5} \text{ mol.dm}^{-3}$  (10 % HCl) and  $1.09 \times 10^{-5} \text{ mol.dm}^{-3}$  (25 % HCl). Moreover, for the maximum range of loading fixed in this study (between 0 and 0.1), the addition of HCl decreases the relative variation of hydroxide concentration between initial and final loading. Indeed, there is a factor 39 between initial and final concentration for amine solutions without acid, a factor 4 with 10 % of HCl and a factor 2 with 25 % of HCl.

## 2. Characterisation of apparent kinetic constants

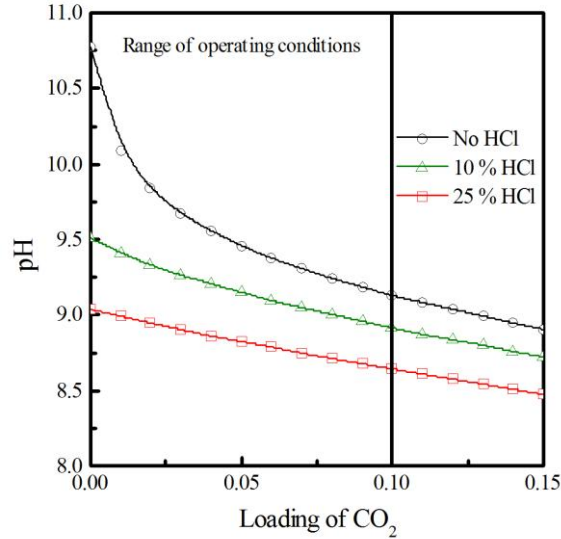


Figure IV-13. Titration of a solution of [methyldiethanolamine] = 100 mol.m<sup>-3</sup> with [CO<sub>2</sub>] = 100 mol.m<sup>-3</sup>. pH of the solution as function of the loading in carbon dioxide. Simulation realized using CurTiPlot.

Thanks to this method, it is possible to reduce significantly the kinetic contribution of the reaction between carbon dioxide and hydroxide ions. For methyldiethanolamine, the apparent kinetic and the contribution of the reaction between CO<sub>2</sub> and hydroxide ions on apparent kinetic constant (Equation 63) have been determined without hydrochloric acid and with 20 % of HCl. Thanks to the numerical model we determine the ratio of the Equation 63 for initial concentration of hydroxide ions, which is the most important, and final concentration of hydroxide ions, which is the less important. The area between the initial and the final concentration of hydroxide ions indicates the extremum area of the contribution of the kinetics of hydroxide ions on apparent kinetic constants. Then we indicate in Figure IV-14 (a) the extremum of the ratio between kinetic contribution of hydroxide ions and apparent kinetic constant as a function of the concentration of amine and (b) the corresponding results for the apparent kinetic constant as a function of the concentration of amine.

$$Ratio = \frac{k_{HO^-} \times [HO^-]}{k_0} \quad \text{Equation 63}$$

The Figure IV-14 (a) shows clearly that when the amine is not neutralized, there is an important variation of the contribution of hydroxide ions (ratio of 3.5 to 0.2 for weakest concentration of amine and 1.5 to 0.2 for strongest concentration of amine). At the same time, when solutions are neutralized with 20 % of HCl, the ratio varies from 0.30 to 0.28 for lowest concentration of amine and from 0.07 to 0.06 for strongest concentration of amine. As we have previously shown, the neutralization diminishes the kinetic contribution of hydroxide ions in such a way that it can be considered as insignificant and/or constant.

The Figure IV-14 (b) proves that the contribution of hydroxide ions has a non negligible effect on the value of the apparent kinetic constants. Indeed, there is a clear difference between apparent kinetic constants obtained without HCl and with 20 % of neutralisation of HCl. However for results obtained with 20 % of neutralisation, it remains a non negligible part of the kinetic contribution of hydroxide ions, (ratio  $\geq 0.1$ ) for a concentration of amine lower than  $400 \text{ mol.m}^{-3}$ . Nevertheless, even if this contribution is non negligible, it does not vary between the beginning and the end of the reaction and then it can be subtracted to the apparent kinetic constant.

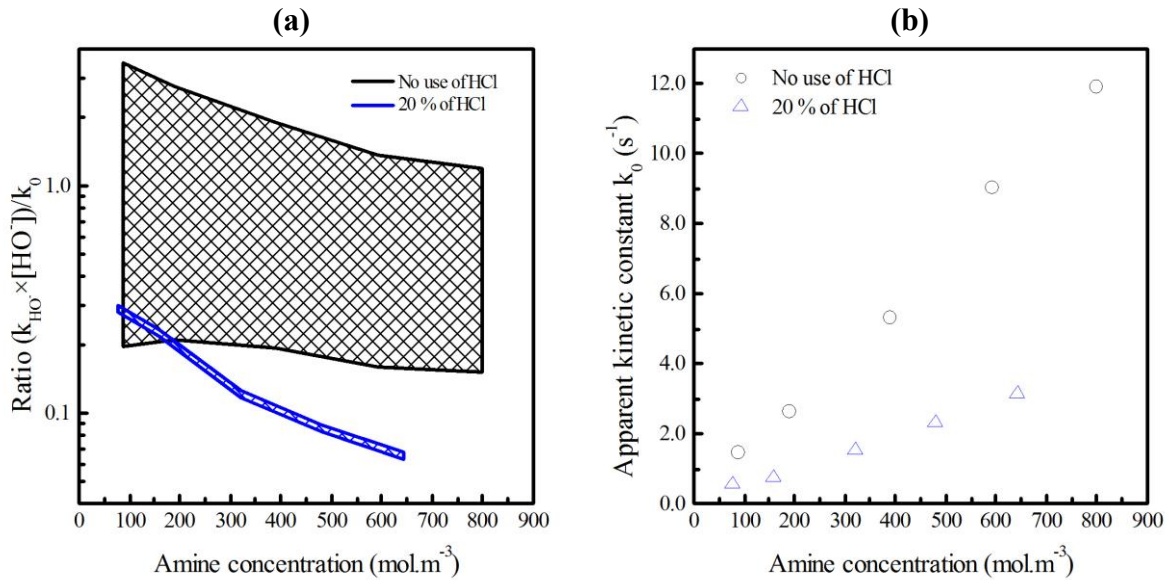


Figure IV-14. Methyldiethanolamine. (a) Extremum of the ratio of the kinetic contribution of hydroxide ions on the apparent kinetic constant as a function of the concentration of amine. (b) Apparent first order kinetic constants  $k_0$  as function of the amine concentration.

In summary, the partial neutralization of the amine with HCl or  $\text{HCO}_2\text{H}$  yields to make the contribution  $R_k$  of hydroxide ions and hydration to the reaction rate (which is extremely weak) (Equation 64) less than 10% and/or to make vary the concentration in hydroxide ions by less than 10% during the reaction (Equation 65). In those cases, it is possible to subtract the kinetic contribution of hydroxide ions and hydration. The choice of HCl to neutralize the tertiary amine results from an experimental study detailed in appendix in Chapter IX .3.2.1.

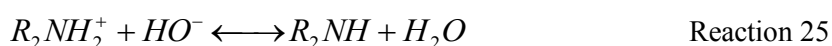
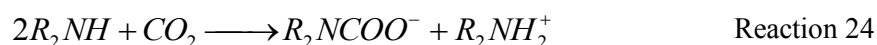
$$100 \times \frac{(k_0 - k_{HO^-} \times [HO^-]^f - k'_{H_2O})}{k_0} = R_k \leq 10\% \quad \text{Equation 64}$$

$$\frac{[HO^-]^i}{[HO^-]^f} = R_{HO^-} \leq 1.1 \quad \text{Equation 65}$$

## 2. Characterisation of apparent kinetic constants

### 2.3.2 Contribution to conductance signal of hydroxide ions

Amines which form carbamates react with CO<sub>2</sub> according to Reaction 24. This reaction, which is kinetically limited, tends to increase the conductivity of the solution by the formation of ionic species. In this reaction, amine is transformed into its acidic form. The equilibrium between the amine and its conjugated acid is displaced due to the addition of an acidic compound (CO<sub>2</sub>) which decreases the pH and then, the concentration of hydroxide ions. Hydroxide ions react instantaneously with ammonium ions according to Reaction 25 which tends to decrease the conductivity at the same rate of the limiting Reaction 24.



Because of the opposite contributions of those reactions to the variation of conductance, it is possible to obtain a very low amplitude or a negative amplitude of the signal depending on the studied amine. A negative amplitude is notably observed for strongly basic amines at high dilution where the increase of conductance due to the carbamate is less important than the decrease of conductance due to the consumption of highly conductive hydroxyde. In order to optimize the conductimetric signal, we developed two methods: the first one to attenuate the contribution of the Reaction 25 and the second one to enhance this contribution.

#### 2.3.2.1 Diminution of the contribution of hydroxide ions

For primary or secondary amine showing increased conductance while reacting with CO<sub>2</sub>, the amplitude of the signal is maximized if the negative contribution of Reaction 25 is decreased. Therefore we have developed a specific method of partial neutralization of the amine solutions. The chosen acid needs to be strong enough to react quantitatively with the amine, it has preferably a high molecular mass to limit the conductivity of the salt resulting from its neutralisation by the amine. In fact the addition of a salt tends to increase the baseline of the signal and the signal over noise ratio for a given variation due to the carbamate. A last, the salt needs to be soluble in the conditions of the experimental run and shall not affect the value of the apparent kinetic constant  $k_0$ . After a preliminary study described in appendix in Chapter IX .3.2.2, we have identified the formic acid as the best molecule. Indeed this acid has a relatively low pKa (3.75), the ionic conductivity at infinite dilution of the formiate ions is relatively low ( $5.5 \times 10^{-3} \text{ S.m}^2.\text{mol}^{-1}$  (Lide, 1994)) in comparison with chlorides ion, it is soluble and it does not disturb the measurement of the apparent kinetic constant  $k_0$ .

As indicated in Figure IV-15 (a), in the case of monoethanolamine, especially for low values of concentration of carbon dioxide, the partial neutralization of the amine with formic acid achieves a significant increase of the amplitude. For higher carbon dioxide and amine concentration, the contribution of hydroxide ions becomes relatively less important and the effect of amine neutralization has a more limited impact. Figure IV-15 (b) shows the good

agreement between apparent kinetic constant obtained with and without addition of formic acid. Indeed, the average relative deviation with the non neutralized data is 9.6 % with 5 % of formic acid and 19.5 % with 10 % of formic acid. The most important part of the deviation is brought by highest values of apparent kinetic constant which corresponds to the kinetic limit of the stopped-flow equipment.

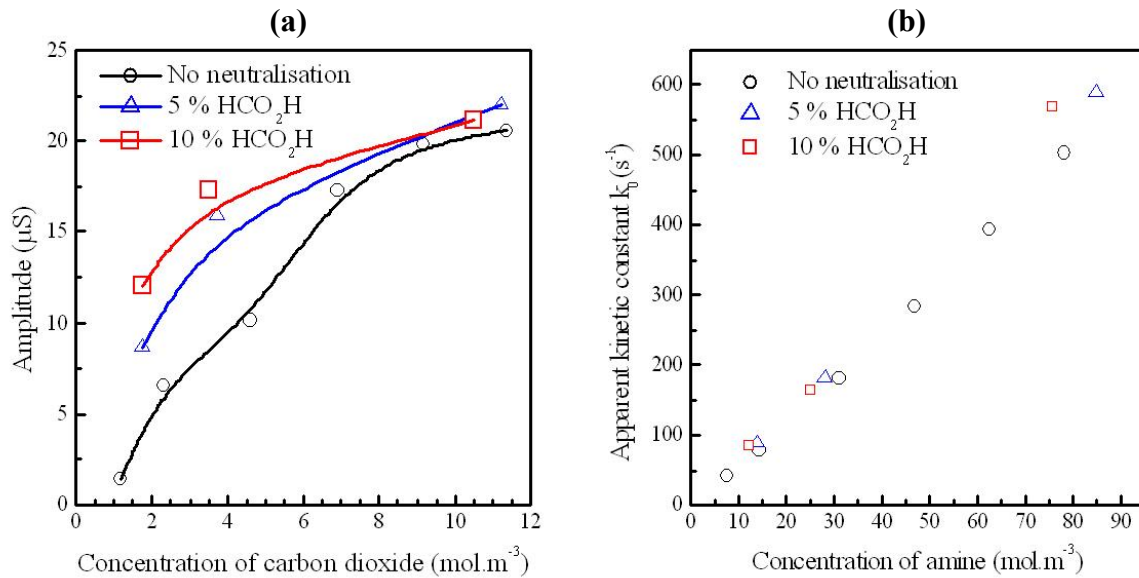


Figure IV-15. (a) Amplitude of the conductivity curve of monoethanolamine as function of the concentration of carbon dioxide. (b) Apparent kinetic constant as function of the concentration of amine.

### 2.3.2.2 *Enhancement of the contribution of hydroxide ions*

In some cases the amplitude of the conductivity is negative as indicated in Figure IV-16. In those cases it is difficult to add enough acid in order to diminish significantly the contribution of hydroxide ions while keeping a sufficiently low noise over signal. Then we choose to optimize the conductivity contribution of hydroxide ions as long as the kinetic contribution of hydroxide ions remains negligible and/or constant. This is possible by decreasing the concentration range of amine, by increasing the ratio between concentration of amine and concentration of carbon dioxide and by decreasing the ratio of neutralisation.

## 2. Characterisation of apparent kinetic constants

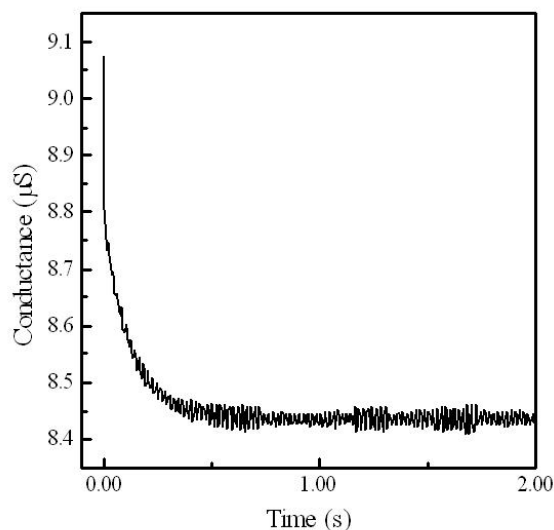


Figure IV-16. Conductance of [piperazine] =  $1.2 \text{ mol.m}^{-3}$  with  $[\text{CO}_2] = 0.09 \text{ mol.m}^{-3}$  before mixing as a function of the time.

### 2.3.3 Conclusion

In order to respect the hypotheses of the analytical method, which is preferred in this study, we optimize the experimental conditions. For amines which have a moderate rate of reaction with  $\text{CO}_2$ , the contribution of hydroxide ions to the reaction with carbon dioxide has to be reduced to less than 10% and/or set constant. For primary and secondary amines which form carbamate, the amplitude of the conductrimetric signal needs to be optimized, either by a reduction or by an amplification of the negative contribution due to the consumption of hydroxide ions during the reaction.

Therefore, experimental conditions have been defined for each studied amine: choice of amine concentrations, molar ratio between amine and  $\text{CO}_2$ , and neutralization of the amine by hydrochloric or formic acid. This optimization requires a preliminary test to have a first insight on the kinetic constant and the amplitude of the signal to set the operating conditions of the study according the logical flow-sheet indicated in Figure IV-17.

The preliminary test is realized in conditions of concentrations and neutralization based on the expected range of magnitude for  $k_0$  and measured  $\text{pK}_a$  of the amine at  $25^\circ\text{C}$ . These conditions are set by a simulation of the corresponding variation of conductance with the numerical method or based on the experience acquired with the previous studies. The experimental variation of conductance obtained from the pre-test can be increasing as Figure IV-8 or decreasing as Figure IV-16.

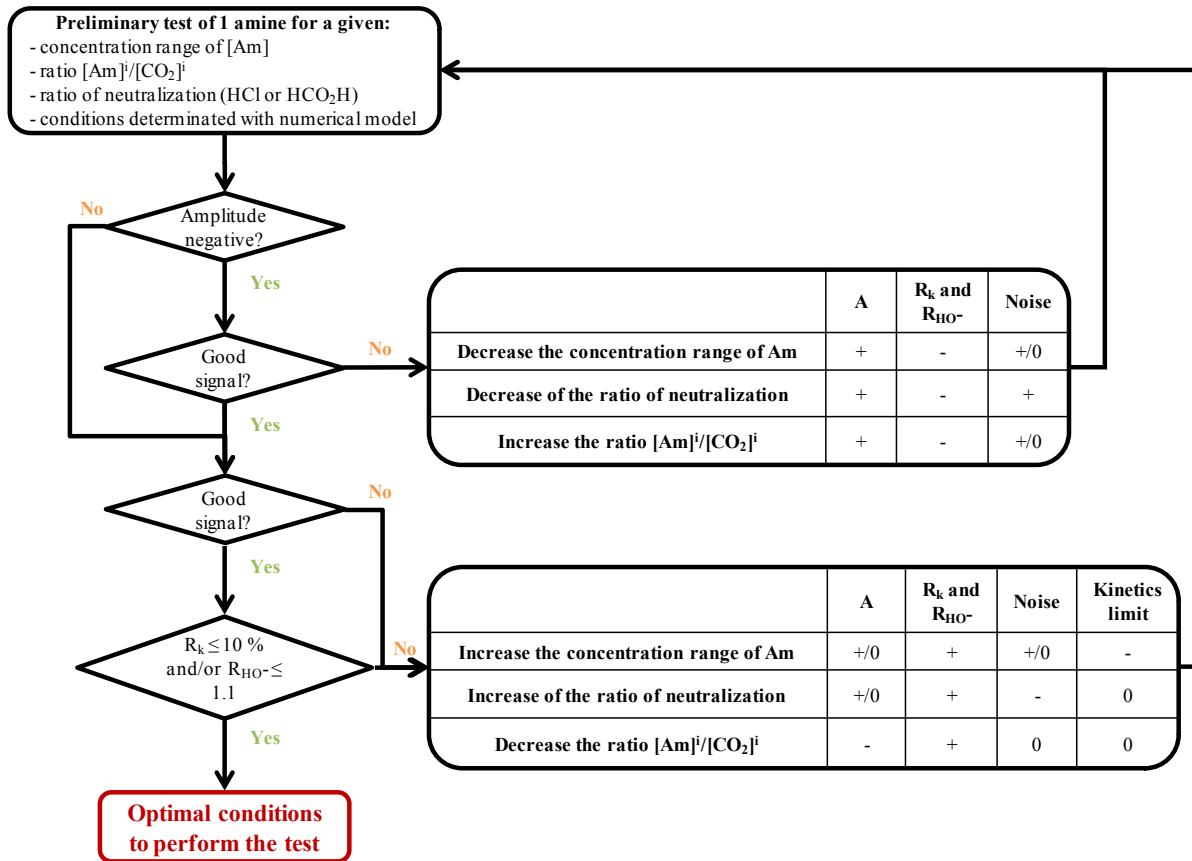


Figure IV-17. Flowsheet of the experimental optimization to determine the apparent kinetic constant of the amine-CO<sub>2</sub> reaction. A stands for the amplitude. Symbols +/-/- respectively indicate a positive effect, no effect or a negative effect of the actions on the signal and kinetic ratios.

For decreasing signals, the amplitude and the signal over noise ratio can be improved by decreasing the concentration range of amine and/or decreasing the ratio of neutralization and/or increasing the ratio amine over CO<sub>2</sub>. The drawback of these actions is to increase the kinetic contribution of hydroxide ions.

For increasing signals, the amplitude and the signal over noise ratio can be improved by two possible actions. On the one hand, we can increase the concentration range of amine. This action tends to improve the amplitude of the signal due to the increase of the concentration of carbon dioxide for a given ratio  $[Am]^i/[CO_2]^i$ . It also reduces the kinetic contribution of hydroxide ions, but also increases the value of the apparent kinetic constant measured and then approaches the limit of the equipment. On the other hand we can increase the ratio of neutralization. This action improves the amplitude of the signal, it diminishes the kinetic contribution of hydroxide ions, however it increases the noise of the signal due to the presence of spectator ions and there is no risk to exceed the kinetic limit with this method.

Finally, when increasing and decreasing conductivity curves have a good signal which can be fitted, if we do not verify that the contribution of hydroxide ions remains constant ( $R_k \leq 10\%$ ) and/or negligible ( $R_{HO^-} \leq 1.1$ ), we can increase the concentration range of amine,

## 2. Characterisation of apparent kinetic constants

increase the ratio of neutralisation and/or decrease the ratio  $[Am]^i/[CO_2]^i$  to respect these assumptions.

### 2.4 Method of data treatment

The selection of the method used to determine the apparent kinetic constant is illustrated by the Figure IV-18. The first condition to select the analytical method is the large excess of amine  $[Am]^i/[CO_2]^i \geq 10$ . If it is not the case we determine the apparent kinetic constant with the numerical method. Then we verify if the concentration of hydroxide ions is constant ( $R_{HO^-} \leq 1.1$ ). If it is the case, we can determine the apparent kinetic constant with the analytical method. In the other case, we should verify that the contribution of hydroxide ions is lower than 10 % ( $R_k \leq 10\%$ ). If it is the case, data can be treated with the analytical method. In the other case, data should be treated with the numerical method.

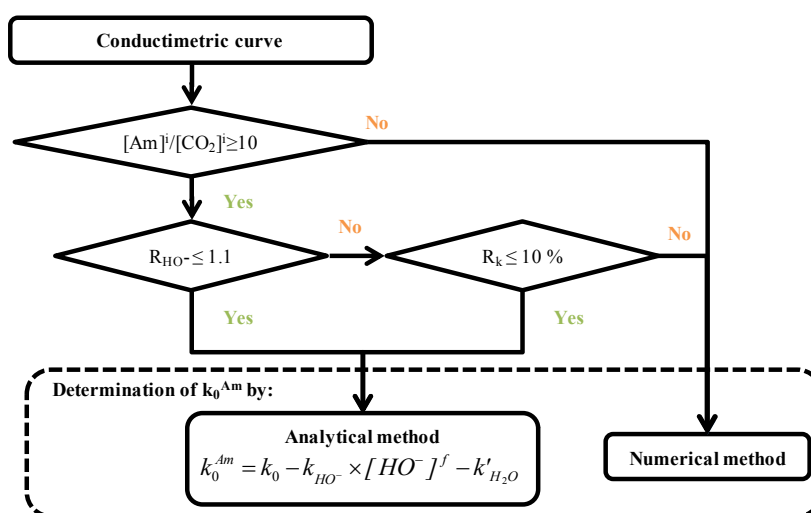


Figure IV-18. Flowsheet which indicates the method followed to treat conductivity curves.

In the case of the analytical method we directly determine from the conductivity curve the apparent kinetic constant  $k_0$ . However it remains in this constant a residual contribution of the reaction between hydroxide ions and carbon dioxide and also a contribution of carbon dioxide hydration for the slowest molecules. In order to remove this residual contribution we determine the apparent first order kinetic constant  $k_0^{Am}$  of the amine- $CO_2$  reaction according to Equation 66. The estimation of  $k_0^{Am}$  depends on the concentration of hydroxide ions at the plateau of conductance:  $[HO^-]^f$  which is determined by the calculation of the thermodynamic equilibrium with the numerical method ( $t \rightarrow \infty$ ). The kinetic constant  $k_{HO^-}$  is taken from Pinsent *et al.* (1956) and the kinetic constant  $k'_{H_2O}$  from Soli and Byrne (2002). The numerical method can determine directly the apparent kinetic constants  $k_0^{Am}$ . In the following sections, we focus on this apparent kinetic constant  $k_0^{Am}$ .

$$k_0^{Am} = k_0 - k_{HO^-} \times [HO^-]^f - k'_{H_2O} \quad \text{Equation 66}$$

## 2.5 Uncertainty of the apparent kinetic constant

The previous section describes how to get the apparent first order kinetic constant  $k_0^{Am}$  from a conductance curve. For each amine concentration studied, we measure between 5 and 10 curves. Each curve yields to an estimation of the apparent kinetic constant  $k_0^{Am}$ . The estimations of  $k_0^{Am}$  corresponding to the different curves are distributed according to the normal distribution if the pvalue is greater or equal than 0.05 (Saporta, 1990). The normality can also be checked by a normal probability plot for a visual verification (Figure IV-19). If the obtained pvalue is lower than 0.05, we remove data which does not respect the normal distribution using the normal probability plot as indicated in Figure IV-19. In this figure, the slope of the indicated equation (1.1) corresponds to the standard deviation and the intercept (75.9) is the experimental average of  $k_0^{Am}$ . After verification that data follows the normal distribution we determine for each concentration of amine (level) the average of the apparent kinetic constant and the associated standard deviation.

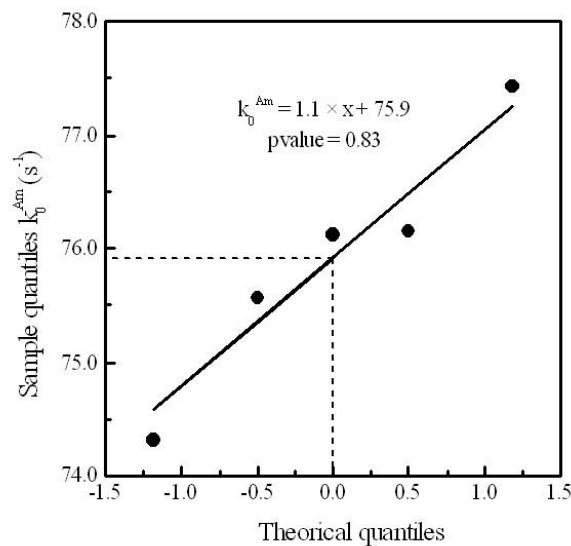


Figure IV-19. Normal probability plot of data. [Monoethanolamine] = 40 mol.m<sup>-3</sup> and [CO<sub>2</sub>] = 4 mol.m<sup>-3</sup> before mixing.

## 3 Characterisation of the constants of the kinetic model

As we previously saw, there is no consensus about the mechanism of reaction. However in kinetics, the last objective of the identification of the mechanism is to determine the associated rate law. In the next part we present the kinetic model we use in order to determine kinetic constants.

### 3. Characterisation of the constants of the kinetic model

#### 3.1 *Semi-empirical model*

##### 3.1.1 *Presentation*

We have not found a clear evidence in favour of one particular mechanism in our review of the literature. Since we noticed that the reaction between amine and carbon dioxide has an apparent partial order between 1 and 2 with respect to the amine, the simplest way to explain the experimental data consists in considering  $k_0^{Am}$  as the sum of two contributions: the first one ( $k_1$ ) is first order with respect to amine and water, the second one ( $k_2$ ) is second order with respect to amine. This semi-empirical model corresponds to Equation 67. The third order kinetic constants  $k_1$  and  $k_2$  are expressed in the same unit:  $m^6 \cdot mol^{-2} \cdot s^{-1}$ .

$$k_0^{Am} = k_1 \cdot [Am] \cdot [H_2O] + k_2 \cdot [Am]^2 \quad \text{Equation 67}$$

The fit of the kinetic data of  $k_0^{Am}$  versus  $[Am]$  yields to a value of  $k_1$  and  $k_2$  which are characteristic of the studied amine. Moreover, this model is more sensitive than the  $k_{Am, n}$  model described in the precedent chapter. Indeed, for data of the literature presented in Table III-1, in the model ( $k_{Am, n}$ ) parameters vary between  $1.7 \times 10^{-3} m^{3n} \cdot mol^{-n} \cdot s^{-1} < k_{Am} < 6.0 \times 10^0 m^{3n} \cdot mol^{-n} \cdot s^{-1}$  and  $1 < n < 2$  when we observe that they vary between  $6.7 \times 10^{-8} m^6 \cdot mol^{-2} \cdot s^{-1} < k_1 < 2.5 \times 10^{-4} m^6 \cdot mol^{-2} \cdot s^{-1}$  and  $1.2 \times 10^{-5} m^6 \cdot mol^{-2} \cdot s^{-1} < k_2 < 3.4 \times 10^{-1} m^6 \cdot mol^{-2} \cdot s^{-1}$  for the model ( $k_1, k_2$ ). Values of  $k_1$  and  $k_2$  of literature data have been indicated in Chapter IX .1.3.

In the case of amines which directly form carbonates we use the relation indicated by Equation 68. Since all these amines are first order, there is no need to determine the constant  $k_2$ . Moreover, in this equation the  $\varepsilon$  value corresponds to a residual error due to the uncertainty on the kinetic contribution of hydroxide ions.

$$k_0^{Am} = k_1 \cdot [Am] \cdot [H_2O] + \varepsilon \quad \text{Equation 68}$$

We use two methods to fit the variation of  $k_0^{Am}$  with the concentration of free amine: least square regression and weighted least square regression. In the latter method, we use as weight the sum of the standard deviation of the apparent kinetic constant and of the standard error of estimate between experimental conductivity curve and the fit of the analytical method. We select the method which gives the best fit using the value of the coefficient of determination.

In Figure IV-20 we represent the average apparent kinetic constant of the monoethanolamine as a function of the concentration of this unprotonated amine. We also indicate the result of the fit with the least square regression (red dash line) and the weighted least square regression (blue dot line). For this molecule we select the least square regression which has a better determination coefficient. Both least square regressions have been realised using the `lm` function (linear model) of the R software.

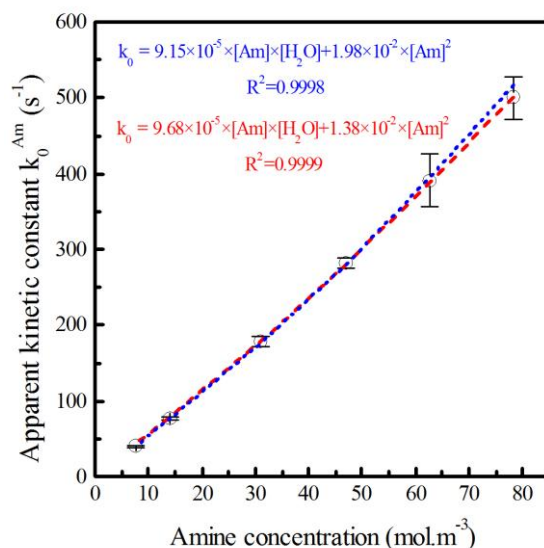


Figure IV-20. Average apparent kinetic constant as function of the amine concentration. Fit realized by least square regression (red dash line) and weighted least square regression (blue dot line).

### 3.1.2 Validation of the model

From literature data of  $k_0^{Am}$  for molecules indicated in Table III-1, we determine the third order kinetic constants  $k_1$  and  $k_2$ . The parity plot of Figure IV-21 compares the experimental values of  $k_0^{Am}$  with the model of Equation 25. This plot shows that the model indicated in Equation 67 represents experimental data with an average relation deviation of 8.1 %.

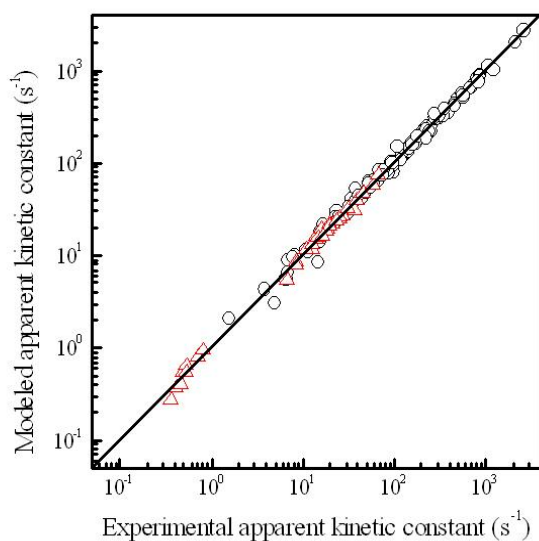


Figure IV-21. Parity plot between the apparent kinetic constant  $k_0^{Am}$  calculated from the  $k_1$ ,  $k_2$  model vs. experimental apparent kinetic constant of  $k_0^{Am}$ . Molecules of the Table III-1. Tertiary amines (red triangles). Primary and secondary amines (black circles).

### 3. Characterisation of the constants of the kinetic model

#### 3.2 Uncertainty of the constants of the kinetic model

Generally, when parameters are fully independent, the uncertainty of each parameter is characterized by the normal distribution and then, the confidence interval of each independent parameter is determined by using the Student distribution value. In our case, as parameters  $k_1$  and  $k_2$  are dependent, the uncertainty is characterized by an ellipse of confidence (Draper and Smith, 1998).

The general equation of this ellipse of confidence is indicated in Equation 69. In this equation  $b$  is the vector of parameters ( $k_1; k_2$ ),  $\beta$  is the estimation of ( $k_1; k_2$ ) as indicated by Equation 70,  $C$  is the covariance matrix between parameters as indicated by Equation 71,  $(p+1)=2$  is the number of parameters,  $s^2$  is the residual variance,  $F_{\alpha; p; (n-p-1)}$  corresponds to the F-distribution value with a confidence level of  $(1-\alpha)$  % and  $n$  is the number of data points used to estimate  $\beta$  (number of different concentration also called number of levels). In the covariance matrix,  $\sigma_{k_1}^2$  and  $\sigma_{k_2}^2$  correspond respectively to the variance on kinetic constants  $k_1$  and  $k_2$ , and  $\sigma_{k_1}\sigma_{k_2}$  corresponds to the covariance between kinetic constants  $k_1$  and  $k_2$ . In the case of an amine which directly form carbonates, we follow the same method. The only difference is the vector of kinetic parameters  $k_1$  and  $\varepsilon$  instead of  $k_1$  and  $k_2$ .

$$(b - \beta)' C (b - \beta) \leq (p + 1) \cdot s^2 \cdot F_{\alpha; p; (n-p-1)} \quad \text{Equation 69}$$

$$\beta = \begin{pmatrix} k_1 \\ k_2 \end{pmatrix} \quad \text{Equation 70}$$

$$C = \begin{pmatrix} \sigma_{k_1}^2 & \sigma_{k_1}\sigma_{k_2} \\ \sigma_{k_1}\sigma_{k_2} & \sigma_{k_2}^2 \end{pmatrix} \quad \text{Equation 71}$$

The interval of confidence of the kinetic constant  $k_i$  ( $CI_i$ ) can be calculated according to Equation 72. In this relation  $t_{\alpha, n-2}$  correspond to the value of the student's t-distribution with a significance level  $\alpha$  and a degree of freedom equal to  $n-2$  and  $\sigma_{k_i}^2$  is the variance of the kinetic constant  $k_i$ .

$$CI_{k_i} = t_{\alpha, n-2} \times \sqrt{\sigma_{k_i}^2} \quad \text{Equation 72}$$

For each amine we determine the area of confidence and the intervals of confidence of kinetic constants with a confidence level of 95 %. We represent this ellipse (or area) of confidence with the function ellipse of the ellipse library using the software R as shown by Figure IV-22 for monoethanolamine where the intervals of confidence are also represented. This following figure clearly shows that the area of the ellipse of confidence is different from the area delimited by the confidence interval of each kinetic constant. This justifies the choice to characterize the uncertainty with the ellipse of confidence.

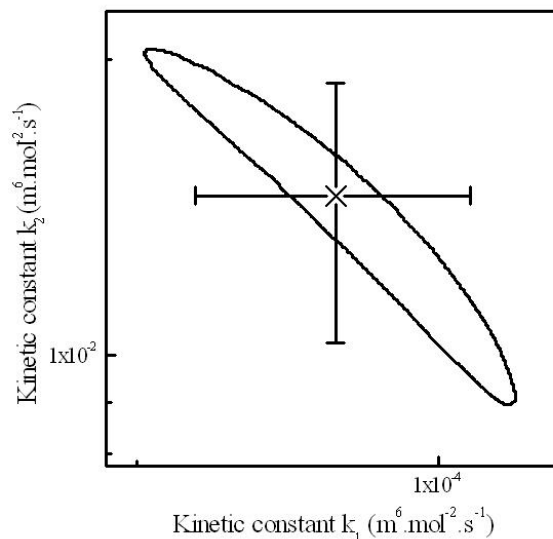


Figure IV-22. Optimal value and area of confidence for the kinetic constants  $k_1$  and  $k_2$  for monoethanolamine. The area of confidence is limited by the ellipse. The interval of confidence calculated on each parameter is indicated by error bars.

We have presented the different methods to apply in order to determine the kinetic constants of amine- $\text{CO}_2$  reaction for all kinds of amine. The selection of the molecules which have been studied on structural considerations is presented in the next section.

## 4 Design of experiments

### 4.1 General features

In our study we have identified a candidate base of around 300 amines that could be considered for the amine scrubbing post-combustion process. This number does not take into account some new molecules which could be synthesized. We have selected a limited number of amines with chemical structures which are representative of the 300 amines candidate base. We also needed to choose enough molecules in order to build a QSPR model.

We have selected molecules in different classes characterized by the nature of substituting group on the amine function. Those substituents bring additional chemical functions to the molecule which can change the reactivity of the amine function or the interactions with water and thereby have a specific effect on the kinetics of reaction with  $\text{CO}_2$ . For example, other things being equal, the addition of an alcohol group reduces the pKa but increases the solubility of the amine in water. Inside each class, we have selected the molecules in order to get the largest range of pKa and steric hindrance of the nitrogen lone electron pair. The cost of the molecule and its availability was also a practical criterion of selection. In the next section, we list by class the molecules that have been studied in the present work. We identify all the studied molecules with a 4-digit number. The first digit indicates the number of amine function in the molecule, the second digit gives the degree of substitution of the molecule (primary = 1, secondary = 2, tertiary = 3) in case of a monoamine and the smaller degree of substitution in case of a multiamine, the third digit identifies a

#### 4. Design of experiments

specific class of the molecule (alkylamines, alkanolamines, *etc*) and the fourth and last digit is the specific to the molecule in a given class.

##### 4.2 Tertiary amines

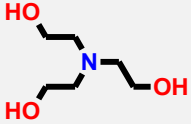
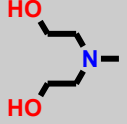
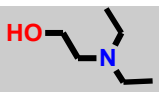
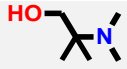
First we choose some alkylamines indicated in Table IV-3. For these molecules we were limited by their solubility in water. Indeed, for mono-alkylamines with more than six atoms of carbon, the solubility in water begin to be lower than  $1,000 \text{ mol.m}^{-3}$  (Chemspider, 2013). Moreover their basic properties do not differ from a lot.

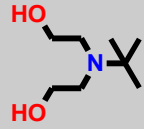
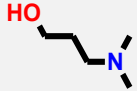
Table IV-3. Studied tertiary alkylamines.

Number	Name	CAS	Chemical structure
1300	Trimethylamine	75-50-3	
1301	N,N-Dimethylpropane-1-amine	923-63-6	
1302	Diethylmethylamine	616-39-7	

We study the alkanolamines presented in Table IV-4. Molecules 1310 to 1313 have already been studied in the literature and can be used as standards. Other molecules are chosen to see the effect of the steric hindrance (1314 and 1315) and the distance between the amino group and the alcohol group (3 carbons instead of 2 for 1316).

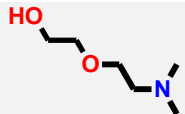
Table IV-4. Studied tertiary alkanolamines.

Number	Name	CAS	Chemical structure
1310	Triethanolamine	102-71-6	
1311	Methyldiethanolamine	105-59-9	
1312	Dimethylaminoethanol	108-01-0	
1313	Diethylethanolamine	100-37-8	
1314	2-Dimethylamino-2-methylpropanol	7005-47-2	

Number	Name	CAS	Chemical structure
1315	tert-Butylaminodiethanol	2160-93-2	
1316	3-Dimethylamino-1-propanol	3179-63-3	

We also select molecule 1320 and 1321 which have other functional groups as indicated in Table IV-5.

Table IV-5. Studied other acyclic tertiary amines.

Number	Name	CAS	Chemical structure
1320	2-[2-(Dimethylamino)ethoxy]ethanol	1704-62-7	
1321	3-Dimethylaminopropionitrile	1738-25-6	

We also study two cyclic tertiary alkylamines which do not contain other functional groups as indicated in Table IV-6.

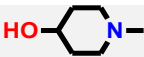
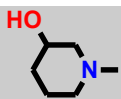
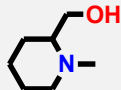
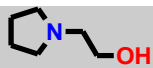
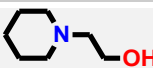
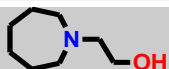
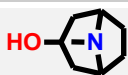
Table IV-6. Studied cyclic tertiary alkylamines.

Number	Name	CAS	Chemical structure
1330	1-Methylpiperidine	626-67-5	
1331	1-Methylpyrrolidine	120-94-5	

Table IV-7 presents cyclic tertiary alkanolamines. Molecules 1340 to 1342 have been chosen to study the effect of the position of a functional group on the cycle. Molecules 1343 to 1345 have been studied to learn about the effect of the number of atom which constitutes the cycle. In molecule 1346, the nitrogen is included in two heterocycles.

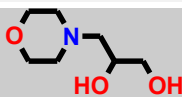
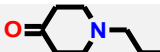
#### 4. Design of experiments

Table IV-7. Studied cyclic tertiary alkanolamines.

Number	Name	CAS	Chemical structure
1340	4-Hydroxy-N-methylpiperidine	106-52-5	
1341	1-Methyl-3-hydroxypiperidine	3554-74-3	
1342	1-Methyl-2-hydroxymethylpiperidine	20845-34-5	
1343	1-Pyrrolidineethanol	2955-88-6	
1344	1-Piperidineethanol	3040-44-6	
1345	1-Azepaneethanol	20603-00-3	
1346	Tropine	120-29-6	

Finally, four other cyclic tertiary amines have been chosen as indicated in Table IV-8. Molecules 1350 and 1351 are derivate from morpholine. Molecule 1352 is the one which have a ketone function and molecule 1353 have a nitrile function.

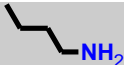
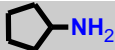
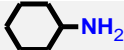
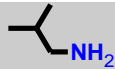
Table IV-8. Studied other cyclic tertiary amines.

Number	Name	CAS	Chemical structure
1350	N-Methylmorpholine	109-02-4	
1351	3-Morpholino-1,2-propanediol	6425-32-7	
1352	1-Propyl-4-piperidone	23133-37-1	
1353	1-Piperidinepropionitrile	3088-41-3	

#### 4.3 Primary and secondary amines

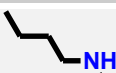
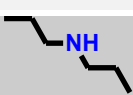
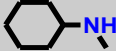
We chose molecules 1100 to 1106 which are primary alkylamines molecule with a progressive increase of steric hindrance as indicated in Table IV-9.

Table IV-9. Studied primary alkylamines.

Number	Name	CAS	Chemical structure
1100	Methylamine	74-89-5	
1101	n-Butylamine	109-73-9	
1102	Isopropylamine	75-31-0	
1103	Cyclopentylamine	1003-03-8	
1104	Cyclohexylamine	108-91-8	
1105	Isobutylamine	78-81-9	
1106	tert-Butylamine	75-64-9	

The tested secondary alkylamines are presented in Table IV-10. We choose again molecules with different degrees of steric hindrance. For all alkylamines, we are limited by the solubility in water.

Table IV-10. Studied secondary alkylamines.

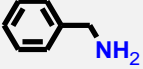
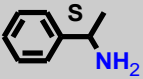
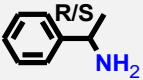
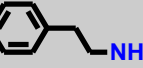
Number	Name	CAS	Chemical structure
1200	Dimethylamine	124-40-3	
1201	N-Methyl-1-propylamine	627-35-0	
1202	N-Methyl-1-butylamine	110-68-9	
1203	Di-n-propylamine	142-84-7	
1204	N-Isopropylmethylamine	4747-21-1	
1205	N-Methylcyclohexylamine	100-60-7	

The tested primary benzylamines are indicated in Table IV-11. Molecule 1110 is the simplest primary benzylamine. Molecules 1111 and 1112 have been chosen to study the effect

#### 4. Design of experiments

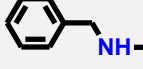
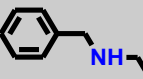
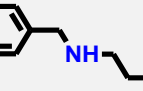
of a steric hindrance in the  $\alpha$  position and the effect of the enantiomeric purity. Molecule 1113 presents one additional carbon between the amino group and benzyl group.

Table IV-11. Studied primary benzylamines.

Number	Name	CAS	Chemical structure
1110	Benzylamine	100-46-9	
1111	S- $\alpha$ -Methylbenzylamine	2627-86-3	
1112	$\alpha$ -Methylbenzylamine	618-36-0	
1113	Phenethylamine	64-04-0	

We study the effect of steric hindrance (molecules 1210 and 1211) of secondary benzylamines as indicated in Table IV-12. We also choose molecule 1212 to study the impact of a third functional group.

Table IV-12. Studied secondary benzylamines.

Number	Name	CAS	Chemical structure
1210	Methylbenzylamine	103-67-3	
1211	Ethylbenzylamine	14321-27-8	
1212	2-Benzylaminoethanol	104-63-2	

The tested alkanolamines are indicated in Table IV-13. Molecule 1120 is the molecule of reference for primary and for secondary amines with respect to the effect of substituents. We study the effect of the length of the main chain with molecules 1121 to 1123. Molecules 1124 to 1127 have been chosen for their different degrees of steric hindrance. Molecules 1127 to 1129 are all derivatives of the tert-Butylamine but with different basicities due to the number of hydroxyl functions. The amine and hydroxyl function are separated by a 6-carbon cycle for molecule 1130.

Table IV-13. Studied primary alkanolamines.

Number	Name	CAS	Chemical structure
1120	Monoethanolamine	141-43-5	
1121	3-Amino-1-propanol	156-87-6	
1122	4-Amino-1-butanol	13325-10-5	
1123	6-Amino-1-hexanol	4048-33-3	
1124	1-Amino-2-propanol	78-96-6	
1125	2-Amino-1-propanol	6168-72-5	
1126	2-Aminobutane-1-ol	96-20-8	
1127	2-Amino-2-methyl-1-propanol	124-68-5	
1128	2-Amino-2-methyl-1,3-propanediol	115-69-5	
1129	2-Amino-2-(hydroxymethyl)-1,3-propanediol	77-86-1	
1130	Trans-4-aminocyclohexanol	27489-62-9	

Molecules indicated in Table IV-14 are the studied secondary alkanolamines. Molecules 1220 to 1226 show a progressive increase of steric hindrance. The dialkanolamine 1228 differs from 1227 by the steric hindrance in the  $\alpha$  position with respect to the hydroxyl functions and in the  $\beta$  and the  $\beta'$  positions with respect to the amine function.

Table IV-14. Studied secondary alkanolamines.

Number	Name	CAS	Chemical structure
1220	2-Methylaminoethanol	109-83-1	

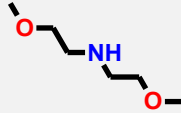
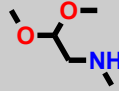
#### 4. Design of experiments

Number	Name	CAS	Chemical structure
1221	2-(ethylamino)-ethanol	110-73-6	
1222	2-(Propylamino)ethanol	16369-21-4	
1223	n-Butylaminoethanol	111-75-1	
1224	2-(Isopropylamino)ethanol	109-56-8	
1225	N-Cyclohexylaminoethanol	2842-38-8	
1226	tert-Butylaminoethanol	4620-70-6	
1227	Diethanolamine	111-42-2	
1228	Diisopropanolamine	110-97-4	

Molecules listed in Table IV-15 are primary and secondary amino-ethers. Molecules 1131 and 1132 are respectively a primary amino-ethers and a primary amino-hydroxyether. Molecule 1230 is a derivate of molecule 1227 where the two hydrogens of the hydroxyl functions have been substituted with methyl groups and molecule 1231 has two ether functions.

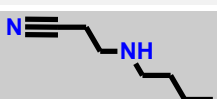
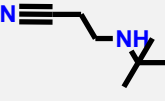
Table IV-15. Studied primary and secondary amino-ethers.

Number	Name	CAS	Chemical structure
1131	2-Methoxyethanamine	109-85-3	
1132	2-(2-Aminoethoxy)ethanol	929-06-6	

Number	Name	CAS	Chemical structure
1230	Bis(2-methoxyethyl)amine	111-95-5	
1231	2,2-Dimethoxy-N-methylethanamine	122-07-6	

Molecules indicated in Table IV-16 are the studied primary and secondary nitrilamines. Molecule 1140 is the only primary nitrilamines. Molecules 1240 to 1243 show an increasing degree of steric hindrance.

Table IV-16. Studied primary and secondary nitrilamines.

Number	Name	CAS	Chemical structure
1140	3-Aminopropionitrile	151-18-8	
1240	3-(Methylamino)propionitrile	693-05-0	
1241	Ethylaminopropionitrile	21539-47-9	
1242	3-(n-Butylamino)propionitrile	693-51-6	
1243	3-(tert-Butylamino)propionitrile	21539-53-7	

The tested cyclic alkylamines are presented in Table IV-17.

Table IV-17. Studied cyclic secondary alkylamines.

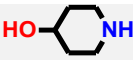
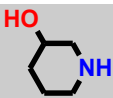
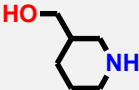
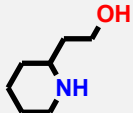
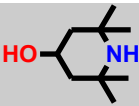
Number	Name	CAS	Chemical structure
1250	Pyrrolidine	123-75-1	
1251	Piperidine	110-89-4	

We also test the cyclic secondary alkanolamines indicated in Table IV-18. We study the effect of the position of the alcohol group on the cycle with molecules 1260 to 1264. For

#### 4. Design of experiments

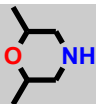
these molecules we also change the length of the hydroxyalkyl chain. We choose molecule 1265 for its particular steric hindrance.

Table IV-18. Studied cyclic secondary alkanolamines.

Number	Name	CAS	Chemical structure
1260	4-Hydroxypiperidine	5382-16-1	
1261	3-Hydroxypiperidine	6859-99-0	
1262	3-Piperidinemethanol	4606-65-9	
1263	2-Piperidinemethanol	3433-37-2	
1264	2-Piperidineethanol	1484-84-0	
1265	2,2,6,6-Tetramethyl-4-piperidinol	2403-88-5	

Finally we study the morpholine and one derivate as indicated in Table IV-19.

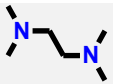
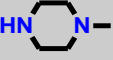
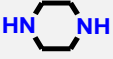
Table IV-19. Studied amines derivatives from morpholine.

Number	Name	CAS	Chemical structure
1270	Morpholine	110-91-8	
1271	2,6-Dimethylmorpholine	141-91-3	

#### 4.4 Multi-amines

Results on three different multi-amines indicated in Table IV-20 are presented in this work.

Table IV-20. Studied multi-amines.

Number	Name	CAS	Chemical structure
2300	N,N,N',N'- Tetramethylethylenediamine	110-18-9	
2200	1-Methylpiperazine	109-01-3	
2201	Piperazine	110-85-0	

## 5 Conclusion

The stopped-flow technique and acid-base titrations have been used to characterize the kinetics of reaction of CO<sub>2</sub> with different kind of amines at 25°C. Complementary numerical method and analytical method have been developed to determine the apparent kinetic constants  $k_0^{Am}$ . The analytical method is mostly preferred and valid to derive directly the apparent first order kinetic constant from the exponential variation of the conductance with time. Two new experimental methods have been found to optimize the conductimetric signal. The first one consists in partial neutralization of amine solutions with hydrochloric acid in order to anneal or control the contribution of hydroxide ions to the apparent kinetics of reaction. The second one is used to study the kinetics of carbamate formation from primary and secondary amines and consists in partial neutralization of amine solutions with formic acid. This neutralization decreases the effect on the hydroxide ions on the variation of conductance and enhances the amplitude of the signal due to the carbamate formation. A semi-empirical kinetic model with two third order kinetic constants is used to characterize the kinetics of reaction with CO<sub>2</sub> for each amine molecule. The optimal value of  $k_1$  and/or  $k_2$  is determined from the variation of  $k_0^{Am}$  with free amine concentration. Each parameter is determined with its interval of confidence and associated area of confidence in a ( $k_1$ ;  $k_2$ ) plot. 87 molecules have been selected in different classes of amine and tested in order to identify the influent structural parameters on the kinetics and establish a structure-property relationship.

In the next chapter, we present and discuss about experimental results of each molecules. First we discuss about mono-amines which do not form carbamates, then we discuss about results obtained by primary, acyclic secondary and cyclic secondary amines. Finally we present results of multi-amines.

*«The only source of knowledge is experience. Everything else is just information. »*

Albert EINSTEIN

## *Chapter V: INTERPRETATION OF EXPERIMENTAL RESULTS*

---

### **1 Overview**

All the experimental results obtained according to the methodology presented in the previous chapter as been indicated in appendicies. We indicate values of apparent kinetic constants in Chapter IX .7 and kinetic constant  $k_1$  and  $k_2$  in Chapter IX .8.

#### **1.1 Definitions**

Due to the number of data, we choose to separate results in five sections: tertiary amines, primary amines, acyclic secondary amines, cyclic secondary amines and multi-amines. Among these five sections there are two kinds of molecules. On the one hand molecules of the class A which form carbonates and correspond to all tertiary amines and some other sterically hindered amines. On the other hand molecules of the class B which form carbamates and correspond to all other molecules. In the case of multi-amines, we only take an interest in the most reactive function and then consider the class of the corresponding function even if the nature of the second function is taking into account in the discussion.

In the section corresponding to tertiary amines, all the molecules form carbonates and then correspond to molecules of the class A. We compare results of each kind of molecules family by family. At the end of this section, we justify that three sterically hindered amines correspond to the definition of amines of the class A and compare their results with other tertiary amines. In the section corresponding to primary amines, all the molecules form carbamates and then correspond to molecules of the class B. For this section we choose to study the effect of the pKa and the steric hindrance on the kinetics. We also study the effect of enantiomerism. In the section corresponding to acyclic secondary amines the major part of the molecules corresponds to the class B. In this part we first show the evolution of kinetic properties between primary and secondary amines. Then we point out the effect of the pKa and of the steric hindrance. We also represent molecules of the class A to show the evolution of the kinetic properties between both classes. In the section corresponding to cyclic secondary amines we follow the same logic as secondary amines. We choose to separate these sections because the two series do not have the same behavior. Finally, we present the result of multi-amines molecule by molecule and compare them with corresponding series of mono-amines.

From this moment, for practical reasons we write  $k_0^{\text{Am}}$  the apparent kinetic constant specific to the amine – carbone dioxide reaction  $k_0$  for this chapter.

The way to represent results has a great importance in order to compare and discuss the data. As there are two class of molecules (class A and class B), we choose an adapted method for each case. We present these methods in the next part.

## 1. Overview

### 1.2 Amines of the class A

As we previously show in Chapter III .3.2.4, many authors indicate that the first order kinetic constant according to the amine is correlated to the basicity of the corresponding amine. Then we choose to represent the kinetic constant  $k_1$  as a function of the pKa as indicated in Figure V-1. This representation uncouple the effect of the basicity which is already know with the kinetic constant and let appears others effects we present later. As indicated in Figure V-1, we study molecule with value of pKa ranged between 6.78 and 10.35 when kinetic constant vary between around  $2 \times 10^{-9}$  to  $1 \times 10^{-6}$  mol<sup>6</sup>.mol<sup>-2</sup>.s<sup>-1</sup>. This representation will be used to represent data of amines of the class A, mainly represented by tertiary amines.

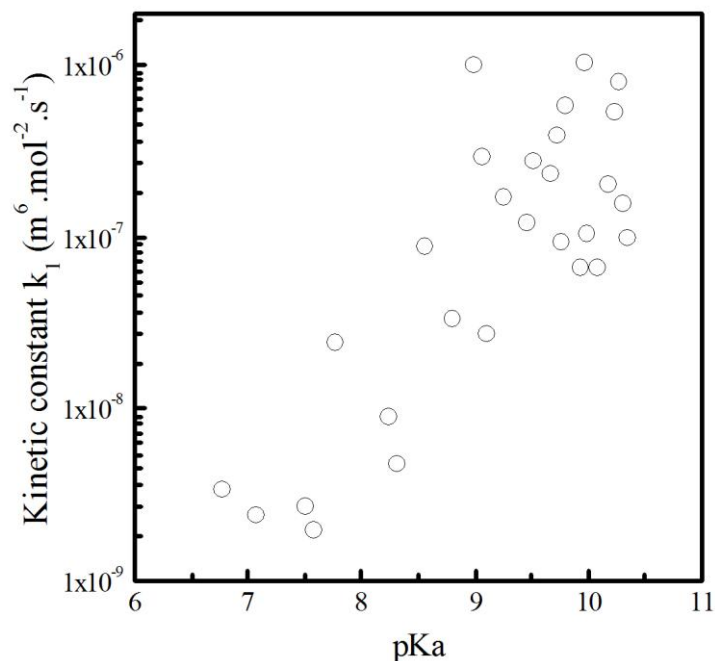


Figure V-1. Kinetic constant  $k_1$  as a function of the pKa for amines of the class A (black circles).

### 1.3 Amines of the class B

In the case of amines of the class B, kinetic constants  $k_1$  and  $k_2$  characterize the kinetic properties of the amine. For this reason we simply represent value of the kinetic constant  $k_2$  as a function of the kinetic constant  $k_1$  as indicated in Figure V-2.

With this representation, it is possible to indicate results got for amines of the class B (black circles) and also results got for secondary amines of the class A (red triangles) where the value of  $k_2$  have been arbitrary fixed to  $1 \times 10^{-7}$  mol<sup>6</sup>.mol<sup>-2</sup>.s<sup>-1</sup>. This value is low enough to do not impact the modeling of apparent kinetic constants. This representation will be used for primary and secondary amines which are mainly amines of the class B.

In order to compare results we also indicate iso- $k_0$  lines calculated for an amine concentration of 50 mol.m<sup>-3</sup> and a water concentration of 55,000 mol.m<sup>-3</sup>. For this

concentration, all molecules which are represented on this line have an apparent kinetic constant specific to the amine-CO<sub>2</sub> reaction which corresponds to the value indicated in the legend. It indicates that for a concentration of amine of 50 mol.m<sup>-3</sup> there is a factor of around 1,000,000 between the slowest and the fastest molecule. These lines are just marks determined with the “average” amine concentration used and do not correspond to experimental values of apparent kinetic constants.

Moreover we indicate iso-order lines to feed into the discussion concerning mechanism. To determine these lines we first model the apparent kinetic constant for several values of  $k_{Am}$  and  $n$  for an amine concentration ranged from 10 to 100 mol.m<sup>-3</sup> according to Equation 15. For all sets of  $k_{Am}$  and  $n$  we determine the corresponding value of  $k_1$  and  $k_2$  by fitting modelled apparent kinetic constants. Then, we plot on the  $k_1, k_2$  graph the line which links the values of  $k_1$  and  $k_2$  corresponding to several values of  $k_{Am}$  with the same value of  $n$ . According to these lines, the order of molecules of the class B mainly ranges between around 1.1 and 1.9 with respect to the amine. A value of the apparent order  $n$  near from 2 reveals an important contribution of the amine in the deprotonation step of the zwitterion mechanism (Reaction 19) or the involvement of two molecules of amine in the termolecular mechanism (Reaction 22) as indicated in Chapter III .3.3.2. In both cases a first molecule of amine is used to react with the carbon dioxide, and a second is used in the deprotonation step.

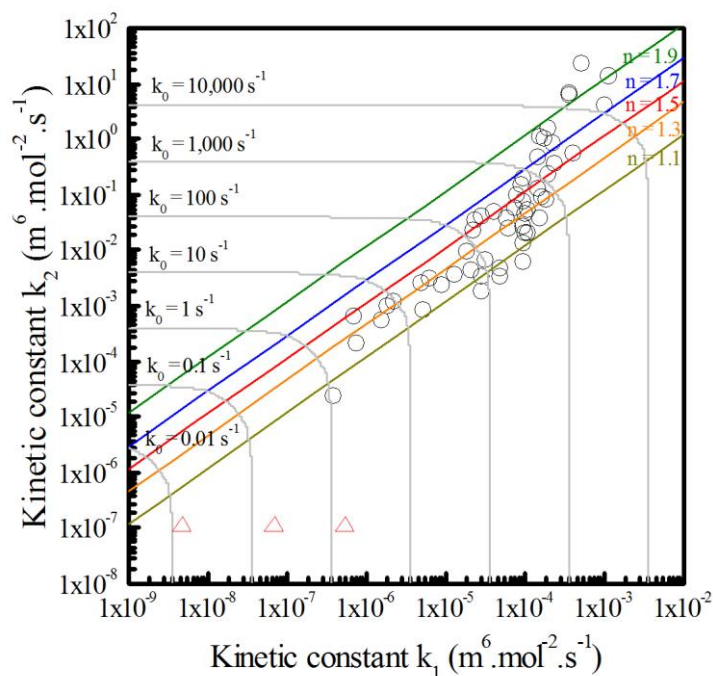


Figure V-2. Kinetic constant  $k_2$  as a function of the kinetic constant  $k_1$ . Amines of the class A (red triangles), of the class B (black circle), iso- $k_0$  lines (grey lines) and iso-order lines (colored lines).

## 2 Tertiary and sterically hindered secondary amines

### 2.1 Comparison with results from literature

In the case of tertiary amines it is possible to compare our results for triethanolamine (1310), methyldiethanolamine (1311), dimethylaminoethanol (1312) and diethylethanolamine (1313) with those obtained in the literature. We indicate this comparison in the Figure V-3 and in the Table V-1. The error bar indicated in the Figure V-3 corresponds to the projection of the confidence ellipse on the  $k_1$  axe. This representation of  $k_1$  is used below throughout this section.

For molecule 1310 and 1311, studied by (Crooks and Donnellan, 1990) which take into account the kinetic contribution of hydroxide ions, the relative deviation is below 40 %. However in the case of molecule 1312 and 1313 studied respectively by Henni *et al.*, (2008) and Li *et al.*, (2007) which do not withdraw the kinetic contribution of hydroxide ions, they always overestimate the kinetic constant  $k_1$  by more than 130 % in comparison with our results. Moreover they always overestimate the value of the kinetic constant due to this second parallel reaction. This confirms that the contribution of this parallel reaction can not be neglected a priori in the study of the tertiary amines.

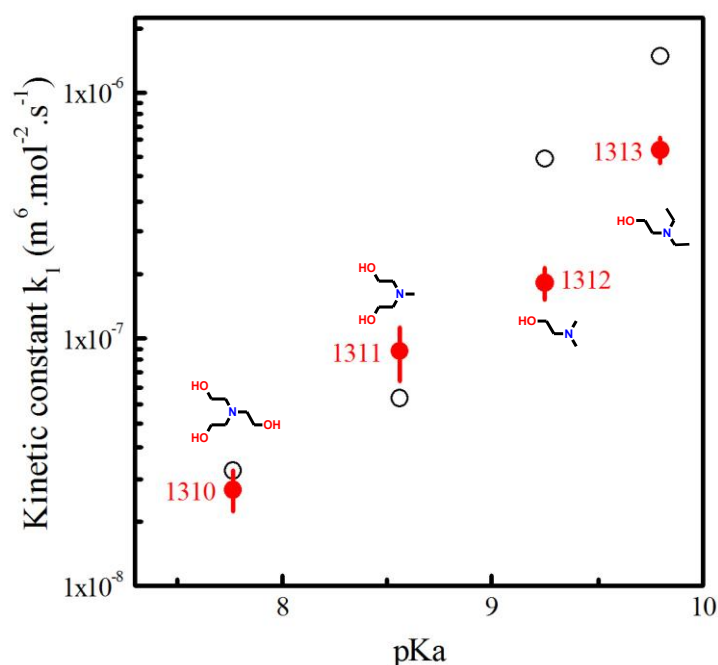


Figure V-3. Kinetic constant  $k_1$  as a function of the pKa for molecule studied in the literature (black circles) and our results (red circles).

Table V-1. Kinetic constant  $k_1$  for molecule 1310, 1311, 1312 and 1313. Comparison with the literature, relative deviation and references.

N°	$k_1$ our work ( $\text{m}^6 \cdot \text{mol}^{-2} \cdot \text{s}^{-1}$ )	$k_1$ other works ( $\text{m}^6 \cdot \text{mol}^{-2} \cdot \text{s}^{-1}$ )	Relative deviation	References
1310	$2.47 \times 10^{-8}$	$2.96 \times 10^{-8}$	19 %	(Crooks and Donnellan, 1990)
1311	$8.92 \times 10^{-8}$	$5.75 \times 10^{-8}$	36 %	(Crooks and Donnellan, 1990)
1312	$1.70 \times 10^{-7}$	$5.33 \times 10^{-7}$	214 %	(Henni <i>et al.</i> , 2008)
1313	$5.86 \times 10^{-7}$	$1.39 \times 10^{-6}$	137 %	(Li <i>et al.</i> , 2007)

## 2.2 Alkanolamines

### 2.2.1 Acyclic alkanolamines

We indicate in Figure V-4 results obtain for tertiary acyclic alkanolamines with the projection of the confidence ellipse. We represent triethanolamine (1310) which has three ethanol groups, methyldiethanolamine (1311) and tert-butylaminodiethanol (1315) which have two ethanol groups, dimethylaminoethanol (1312), diethylaminoethanol (1313) and 2-dimethylamino-2-methylpropanol (1314) which has one ethanol group and 3-dimethylamino-1-propanol (1316) which has one propanol group.

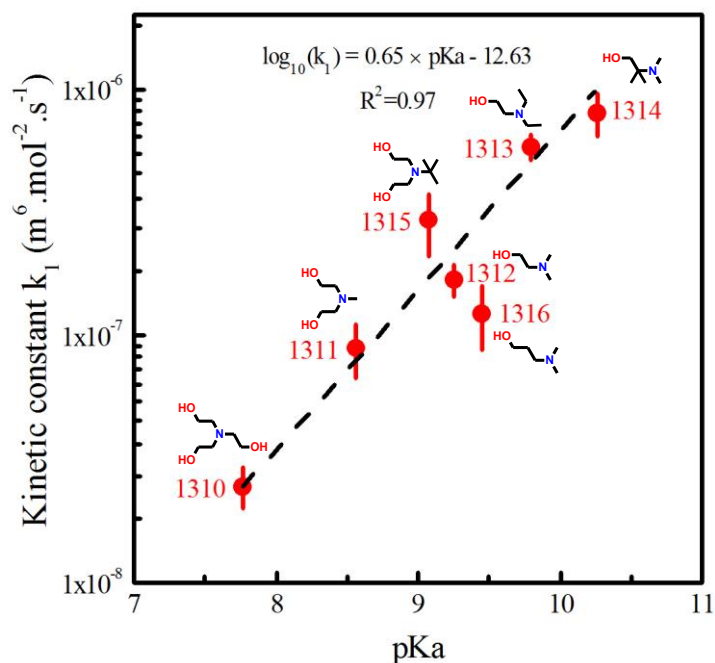


Figure V-4. Kinetic constant  $k_1$  as a function of the pKa for studied acyclic alkanolamines (red circles). Linear estimation realized with molecules 1310, 1311, 1312 and 1313.

## 2. Tertiary and sterically hindered secondary amines

We notice that the value of the pKa increases with a decreasing number of alcohol group due to the removal of an electron-withdrawing inductive effect group (-I). At the same time the value of the kinetic constant increases almost linearly with the basicity even when the kinetic contribution of hydroxide ions is taken into account. This Brønsted relationship has already been observed in the literature. We determine the coefficient of the linear model between the decimal logarithm of the kinetic constant  $k_1$  as a function of the pKa for molecules 1310, 1311, 1312 and 1313. We choose these molecules because they are the "simplest" alkanolamines with ethanol group on the larger range of pKa.

We take an interest in the series 1315, 1312 and 1316. For this series of molecules, even if the basicity increases the kinetic constant  $k_1$  decreases significantly by comparison with the uncertainty. We can first compare molecule 1312 and 1316. When the distance between the amino function and alcohol function increases, the influence of the electron-withdrawing group diminishes but the kinetic constant also decreases. Then we can compare results obtained for molecules 1312 and 1315. For approximately the same value of pKa (respectively 9.25 and 9.07), when an ethanol function is removed, the kinetic constant decreases. These two observations seem to show that all things being equal the proximity and the accessibility to alcohol groups has a major role on the kinetic properties. This specific role can be explained by the interactions of the alcohol functions with water. In fact, a water molecule is required in the reaction of a tertiary amine with CO<sub>2</sub> to form a carbonate. The presence of alcohol groups in the molecule can promote weak interactions with water by hydrogen bonding which can facilitate the reaction with CO<sub>2</sub>.

Another effect can also be discussed with molecule 1315 which has a tert-butyl substituent. In spite of the steric hindrance of this group on the nitrogen atom, molecule 1315 shows a higher value of  $k_1$  than the predicted value by the Brønsted relationship based on the less hindered molecules 1310 – 1314. From this example, the steric hindrance of the nitrogen atom does not seem to play a preponderant role on the reactivity of tertiary amines. However, a tert-butyl is known to have an important +I inductive donor effect (Taft, 1976). On the scale of polar substituent constants  $\sigma^*$  which indicates the +I inductive donor effect in the Taft equation (Chapter IX .2), the value for a methyl substituent is 0.0 and the value for the tert-butyl substituent is 3.0. The resulting negative charge on the nitrogen atom tends to increase the nucleophilicity for molecule 1315 which is more reactive than others alkanolamines with the same value of pKa.

### 2.2.2 Cyclic alkanolamines

We compare the results of 7 cyclic alkanolamines with 4 acyclic alkanolamines (1310, 1311, 1312 and 1313) in Figure V-5. Among cyclic alkanolamines, there are 4-hydroxy-N-methylpiperidine (1340) and tropine (1346) which have the alcohol group at the para position, 1-methyl-3-hydroxypiperidine (1341) which has the alcohol group in meta position, 1-methyl-2-hydroxymethylpiperidine (1342) which has a methoxy group at the ortho position and 1-pyrrolidinoethanol (1343), 1-piperidinoethanol (1344) and 1-azepanoethanol (1345) which have an ethanol group directly linked to the nitrogen atom.

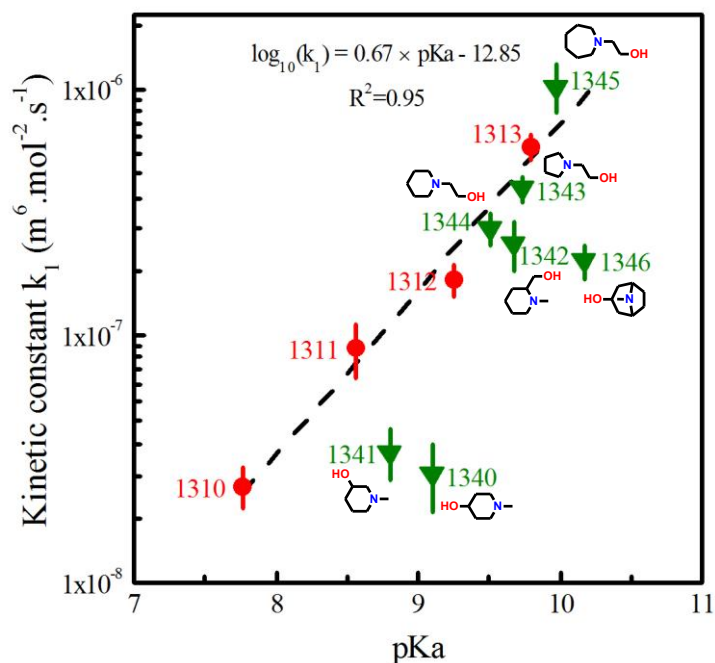


Figure V-5. Kinetic constant  $k_1$  as a function of the pKa for studied cyclic alkanolamines (green triangles) in comparison with acyclic alkanolamines (red circles). Linear estimation realized with molecules 1310, 1311, 1312, 1313, 1344, 1343 and 1345.

First we notice that molecule 1343, 1344 and 1345, which contain an ethanol function, follow the Brønsted relationship obtained for alkanolamines. This result shows that the cyclic structure formed by the two alkyl substituents of the cycle does not affect the reactivity of the amine function as long as it does not hinder the mobility of the alcohol group. We extend the Brønsted relationship established for acyclic ethanolamines between  $\log_{10}(k_1)$  and the pKa to cyclic ethanolamines 1343, 1344 and 1345.

We observe that molecule 1342 is slightly slower than 1344 (factor 0.86) although it has a slightly higher value of pKa value (respectively 9.67 and 9.51). This molecule has an alcohol group in  $\beta$  position of the nitrogen which is also in ortho position of the cycle. This can reduce the mobility of the alcohol group and its capacity to form hydrogen bond compared to molecule 1344 and then explains the difference between each kinetic constant.

Molecule 1341 has also an alcohol group on the  $\beta$  carbon with respect to the amine function, which is in meta position in the cycle. In this configuration, the accessibility of the alcohol group is reduced in comparison with molecules 1342 as same as its capacity to form hydrogen bonds with water close to the nitrogen atom.

Molecules 1340 and 1346 have one alcohol group linked to the  $\gamma$  carbon with respect to the amine function, which is in para position of the cycle. In this position the alcohol group is not able to form an hydrogen bond with water close to the nitrogen atom. In the case of the molecule 1341, a water molecule bound to the alcohol group may still interact with the

## 2. Tertiary and sterically hindered secondary amines

nitrogen atom. In the case of 1340 and 1346, this interaction is not possible and the alcohol function can not play any specific role to facilitate the reaction with CO<sub>2</sub>.

For the series amines 1340, 1341, 1342 and 1346, the comparison of  $k_1$  with its predicted value by the Brønsted relationship can be explained by the mobility of the alcohol function: in fact, the ratio between experimental value of  $k_1$  and Brønsted correlation is 0.83 for molecule 1344 (alcohol group in  $\beta$  position of the nitrogen not in the cycle). It gets down to 0.56 for 1342 (alcohol group in  $\beta$  and ortho position of the nitrogen) and 0.30 for 1341 (alcohol group in  $\beta$  and meta position of the nitrogen). Finally it decreases to 0.16 for molecule 1340 and 0.22 for molecule 1346 (alcohol group in  $\gamma$  and para position of the nitrogen). This ratio diminishes with the accessibility of the alcohol group.

In conclusion, the observations on cyclic alkanolamines confirm the effects observed on acyclic alkanolamines. Basicity (pKa) and the interactions between the alcohol function, the water bound molecule and the nitrogen atom seem to be the main factors to facilitate the reaction of alkanolamines with CO<sub>2</sub>.

## 2.3 Alkylamines

### 2.3.1 Acyclic

Three alkylamines have been studied: trimethylamine (1300), dimethylpropane-1-amine (1301) and diethylmethylamine (1302). They have been represented in Figure V-6 with some alkanolamines. Contrary to alkanolamines, alkylamines do not have alcohol group.

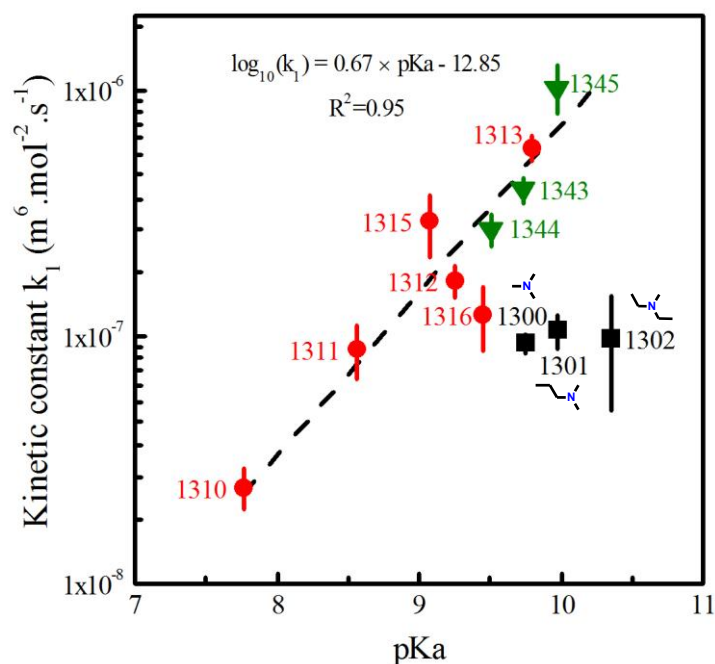


Figure V-6. Kinetic constant  $k_1$  as a function of the pKa for studied acyclic alkylamines (black squares) in comparison with acyclic alkanolamines (red circles) and cyclic alkanolamines (green triangles). Linear estimation realized with molecules 1310, 1311, 1312, 1313, 1344, 1343 and 1345.

With molecule 1300, we observe the continuation of the trend observed with molecules 1315, 1312 and 1316 where the kinetic constant is decreasing while the pKa is increasing. In fact the ratio with the Brønsted relationship is 1.74 for 1315 which is a diethanolamine, 0.76 for 1312 which is a monoethanolamine, 0.41 with 1312 which is propanolamine and 0.20 for 1300 which does not have any alcohol function. This value is very close to the ratio that we obtain for the cyclic alkanolamine 1346, where the alcohol function can not any role to facilitate the reaction with water and CO<sub>2</sub>.

When the length of the alkyle substituents is increased from 1300 to 1302, the +I electron-supplying effect increases the pKa but the kinetic constant does not change significantly with respect to experimental uncertainty. The ratio with Brønsted relationship is still decreasing from 0.2 with molecule 1300 to 0.15 with 1301 and 0.08 with 1302. This may be explained by the increasing hydrophobicity of the substituents: the hydrogen bounding of water with the amine (based-catalyzed hydration mechanism indicated by Reaction 15) or an intermediate zwitterion (zwitterion mechanism indicated by Reaction 16 and Reaction 17) in the mechanism of reaction with CO<sub>2</sub> gets more difficult for 1302 with two ethyle groups than for 1301 with two methyle groups and 1300 with one methyle groups.

### 2.3.2 Cyclic

Two cyclic alkylamines have been studied: 1-methylpiperidine (1330) and 1-methylpyrrolidine (1331). Their results have been compared to acyclic alkylamines in Figure V-7.

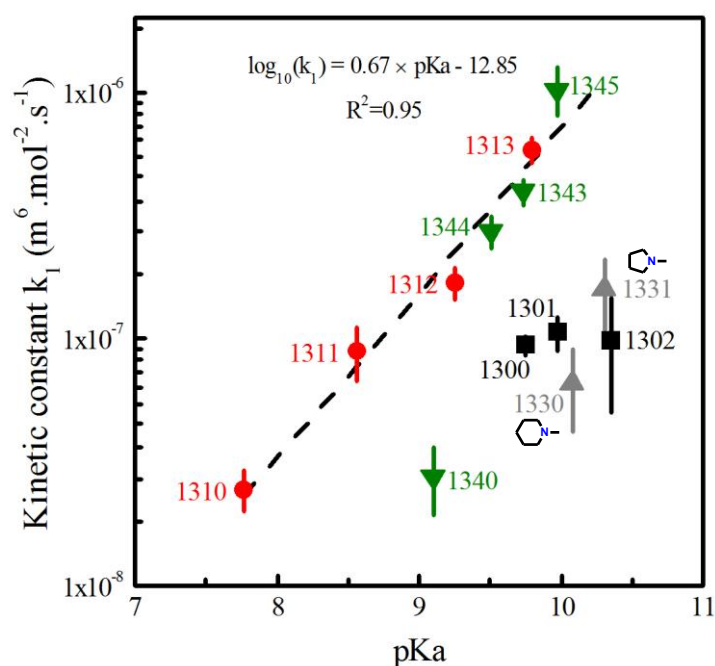


Figure V-7. Kinetic constant  $k_1$  as a function of the pKa for studied cyclic alkylamines (grey triangles) in comparison with acyclic alkylamines (black squares). Linear estimation realized with molecules 1310, 1311, 1312, 1313, 1344, 1343 and 1345.

## 2. Tertiary and sterically hindered secondary amines

Within the large experimental uncertainties, the values of  $k_1$  for these molecules are very close to acyclic tertiary alkylamines 1301 and 1302 which have respectively the same  $pK_a$  than 1330 and 1331. For these four molecules the ratio with the Brønsted relationship is between 0.08 and 0.15 which is very comparable to the cyclic molecule 1340 (0.16) for which the alcohol function is inactive in the reaction with  $CO_2$  and water.

### 2.4 Other tertiary amines

#### 2.4.1 Acyclic

We also study molecules with other functional groups: 3-dimethylaminopropionitrile (1321) and 2-[2-(dimethylamino)ethoxy]ethanol (1320) as indicated in Figure V-8.

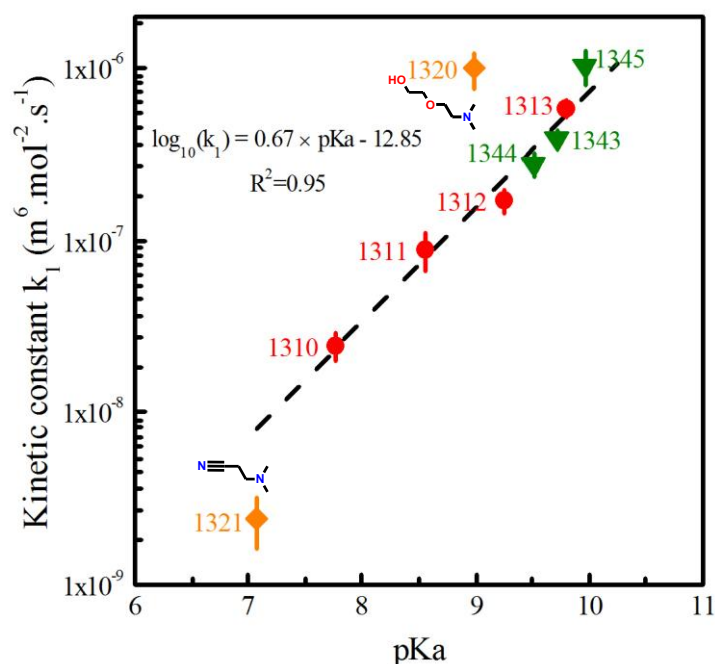


Figure V-8. Kinetic constant  $k_1$  as a function of the  $pK_a$  for studied other acyclic amines (orange diamonds). Linear estimation realized with molecules 1310, 1311, 1312, 1313, 1344, 1343 and 1345.

Molecule 1321 which has a nitrile group reacts more slowly than the alkanolamines and close to the alkylamines if we consider the ratio of  $k_1$  with the Brønsted relationship (0.30) and the experimental uncertainty. For this molecule, the nitrogen of the nitrile function can not directly form an hydrogen bond. The nitrogen of the nitrile function is H-bonded to a water molecule, which is too far to play a significant role on the kinetics.

On the contrary, molecule 1320 shows a surprisingly fast kinetics of reaction with  $CO_2$  compared to alkanolamines with a deviation corresponding to a ratio of 6.7 with the Brønsted relationship. A conjugated action of the ether group on the  $\beta$  carbon of the amino group with the alcohol group in the  $\beta$  carbon of the ether group may explain a particular conformation of the molecule which is particularly favorable to the reaction with water and  $CO_2$ .

## 2.4.2 Cyclic

We study four other cyclic tertiary amines: N-methylmorpholine (1350), 3-morpholino-1,2-propanediol (1351), 1-propyl-4-piperidone (1352) and 1-piperidinepropionitrile (1353). These molecules are indicated in Figure V-9.

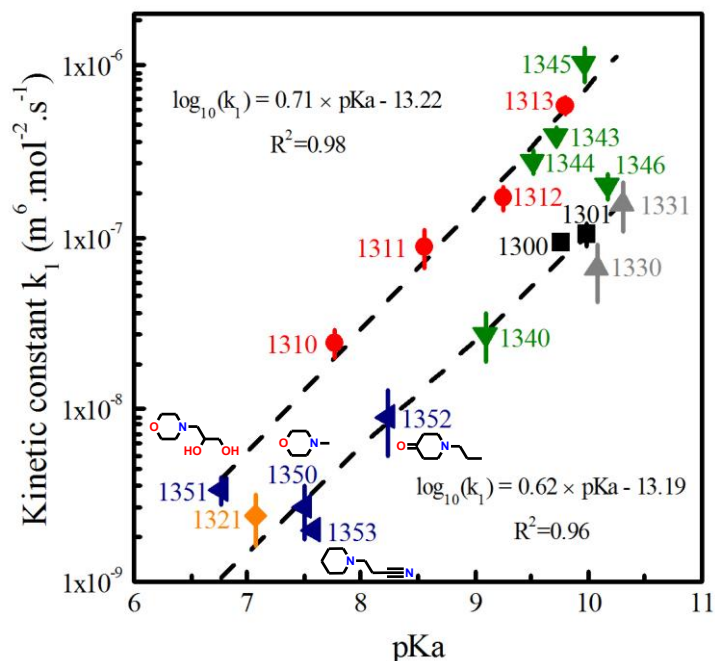


Figure V-9. Kinetic constant  $k_1$  as a function of the  $pK_a$  for studied other cyclic amines (blue triangles). Linear estimation realized with molecules 1310, 1311, 1312, 1313, 1344, 1343, 1345 and 1351. Second linear estimation realized with molecules 1300, 1301, 1321, 1330, 1331, 1340, 1346, 1350, 1352 and 1353.

Molecule 1351 has an ethanol group directly linked to the nitrogen of the amine as same as molecules 1343, 1344 and 1345. Therefore we extend the Brønsted relationship by taking into account this molecule which extends the  $pK_a$  range of ethanolamines down to 6.78.

Molecules 1350, 1352 and 1353 can be compared with alkylamines with a ratio between 0.14 (1353) and 0.21 (1350 and 1352) with respect to the new Brønsted relationship of ethanolamines. Therefore we can draw a second Brønsted relationship. This relationship has been realized with molecule 1300, 1301, 1321, 1330, 1331, 1340, 1346, 1350, 1352 and 1353. For these 10 molecules, chemical function different from amine does not play any role on the kinetics. We exclude molecule 1302 due to its important experimental error.

## 2. Tertiary and sterically hindered secondary amines

### 2.5 Secondary amines

We study three secondary amines with an important steric hindrance: tert-butylaminoethanol (1226), tert-butylaminopropionitrile (1243) and 2,2,6,6-tetramethyl-4-piperidinol (1265) as indicated in Figure V-10.

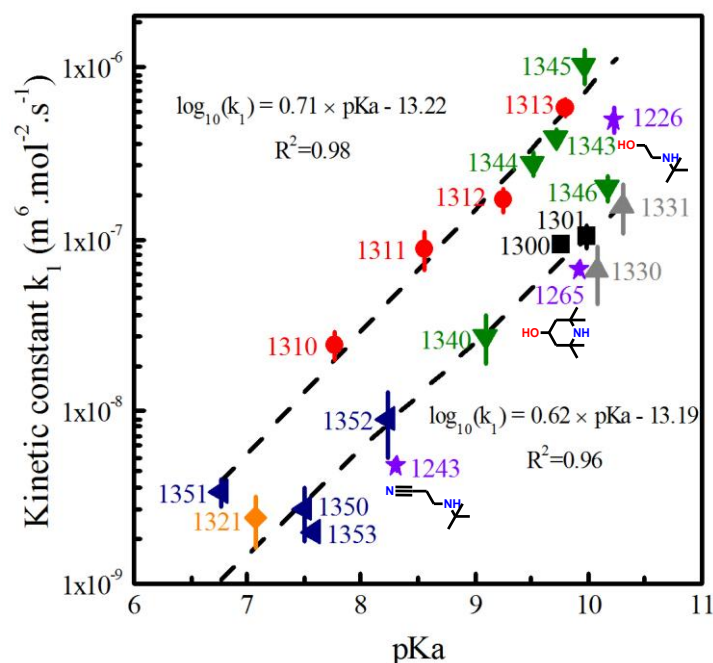


Figure V-10. Kinetic constant  $k_1$  as a function of the pKa for studied secondary amines of the class A (purple stars). Linear estimation realized with molecules 1310, 1311, 1312, 1313, 1344, 1343, 1345 and 1351. Second linear estimation realized with molecules 1300, 1301, 1321, 1330, 1331, 1340, 1346, 1350, 1352 and 1353.

We assume that these molecules do not form carbamates and react according to the same mechanism than tertiary amines (molecules of the class A). We base our assumption on the proximity of the kinetic properties of these molecules with kinetic properties of tertiary amines that we do not encounter for all other studied primary and secondary amines. Moreover, the important steric hindrance of the nitrogen atom is another argument for these three molecules. Indeed, stability of carbamate species depends on the steric hindrance of the nitrogen atom of the amine function (Chapter III .3.3.4.2).

In overall sterically secondary amines seem to react slightly slower than corresponding tertiary amines having the same value of pKa. First we take an interest in molecule 1226 and 1243 which have the same structure  $((\text{CH}_3)_3\text{C}-\text{NH}-\text{CH}_2-\text{CH}_2-\text{R})$  with R which corresponds respectively to OH and CN. We notice that the ratio between their experimental value of  $k_1$  and corresponding estimation by Brønsted relationship (obtained with ethanol tertiary amines for molecule 1226 and the second relationship for molecule 1243) is equal to 0.5 in both cases. This result can be explained by the missing alkyl group in the  $\alpha$  position of the amine

function. As we saw previously, all things being equal, alkyl groups increase the reactivity of amines by electron releasing effect on the nitrogen lone pair (+I effect).

As molecule 1265 has two tertiary carbons in  $\alpha$  position of the amine function, the compensation of the missing alkyl to obtain a tertiary amine is more important. This explains why for molecule 1265 the ratio between experimental value of  $k_1$  and corresponding value obtained with the second Brønsted relationship is 0.7 and then above the ratio of molecules 1226 and 1243 which is 0.5.

## 2.6 Conclusion

We represent in Figure V-11 a synthesis of data concerning tertiary and sterically hindered secondary amines. In the previous section we identify three parameters linked to the structure of molecules of the class A which drive the value of the kinetic constant  $k_1$ .

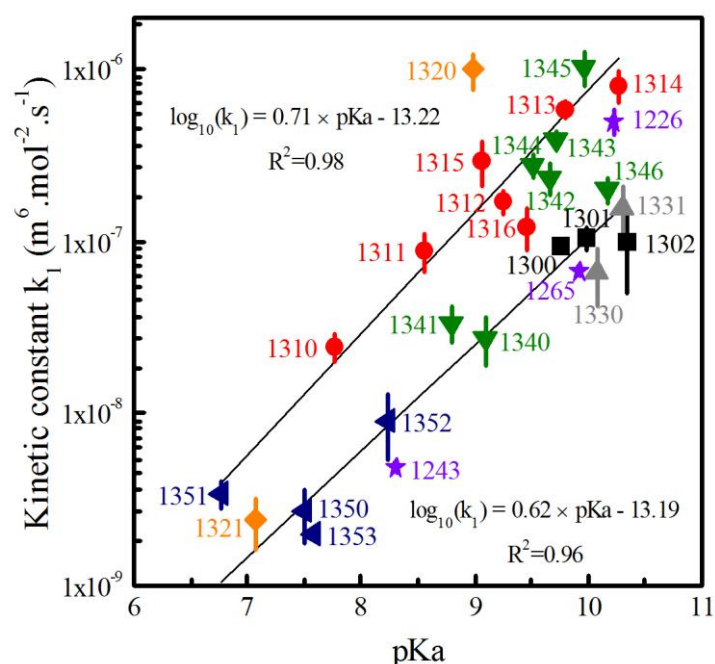


Figure V-11. Kinetic constant  $k_1$  as a function of the pKa for studied amines of the class A. Linear estimation realized with molecules 1310, 1311, 1312, 1313, 1344, 1343, 1345 and 1351. Second linear estimation realized with molecules 1300, 1301, 1321, 1330, 1331, 1340, 1346, 1350, 1352 and 1353.

The basicity, indicated by the value of the pKa is the parameter which mainly explains the evolution of the kinetic constant for tertiary and sterically hindered secondary amines. Other things being equal, when the pKa increases, the nucleophilicity also increases which promotes reaction with  $\text{CO}_2$  and water to form ammonium ion and  $\text{HCO}_3^-$ .

In this study we point out the importance of the contribution of alcohol groups to explain the kinetic constant  $k_1$ . Indeed we show that when a molecule consists of alcohol

### 3. Primary amines

groups the kinetic properties are improved other things being equal. This improvement depends on the distance of the alcohol group to the nitrogen and the accessibility of the alcohol group. This effect can be explained by the contribution of water in the reaction. Indeed alcohol groups are known for their affinity with water. The presence of alcohol groups close to the nitrogen atom can then favor the reaction. There are three kinds of behavior concerning the influence of alcohol groups:

- molecules which contain accessible alcohol groups (molecules 1310, 1311, 1312, 1313, 1344, 1343, 1345 and 1351) which corresponds to molecules used to estimate the first Brønsted relationship in Figure V-11;
- molecules which do not contain alcohol groups (molecules 1300, 1301, 1321, 1330, 1331, 1340, 1346, 1350, 1352 and 1353) which corresponds to molecules used to estimate the second Brønsted relationship in Figure V-11;
- other molecules which have an intermediate effect of the contribution of alcohol groups (especially molecules 1316, 1341 and 1342).

The inductive effect on the nitrogen atom of the amino group has also been observed in particular for molecule 1315 and in the case of all sterically hindered amines. Indeed, depending on the group linked to the nitrogen atom (or of the missing group in the case of secondary amines in comparison with tertiary amines) the kinetic constant can be improved or diminished by respectively +I or -I inductive effect. Indeed a group with an electron-releasing character (+I) improves the lone pair electron reactivity whereas it is the opposite for a group with an electron-withdrawing character (-I).

## 3 Primary amines

As we have shown in Chapter III .3.3.4, there are two main effects which drive kinetic properties of primary amines: basicity and steric hindrance. In this section we present the evolution of the kinetic constant  $k_1$  and  $k_2$  as a function of these two parameters. We also show the result of two enantiomers.

### 3.1 Effect of the basicity

In order to compare the effect of the basicity on the kinetic constants  $k_1$  and  $k_2$ , it is important to consider amines which have approximately the same steric hindrance. Therefore we identify two series of amines which can be considered as having the same steric hindrance with various values of pKa: linear primary amines and derivatives from tert-butylamines. These series are quite interesting because linear amines are the less sterically hindered amines that it is possible to consider and derivatives from tert-butylamines are the most sterically hindered primary amines that it is possible to study.

### 3.1.1 Linear amines

We represent on Figure V-12 the kinetic constant  $k_2$  as a function of the kinetic constant  $k_1$  for the series of linear primary amines. This series is composed of 3-aminopropionitrile (1140), 2-methoxyethanamine (1131), monoethanolamine (1120), benzylamine (1110), phenethylamine (1113), 3-amino-1-propanol (1121), 4-amino-1-butanol (1122), 6-amino-1-hexanol (1123), n-butylamine (1101) and methylamine (1100). We consider that this series have approximately the same steric hindrance with various values of pKa.

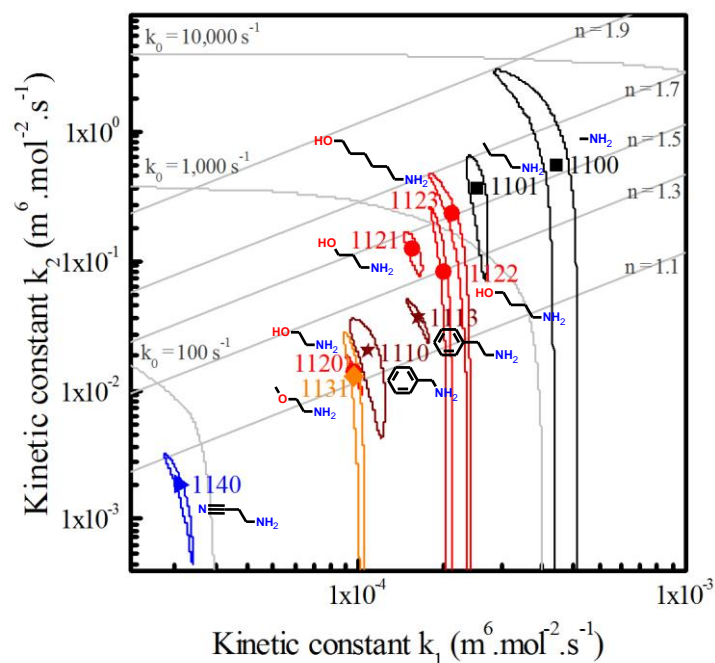


Figure V-12. Kinetic constant  $k_2$  as a function of the kinetic constant  $k_1$  for a series of linear primary amines. Alkylamines (black squares), alkanolamines (red circles), benzylamines (brown stars), etheramine (orange diamond) nitrilamine (blue triangle).

First, we notice that when the pKa of the amine increases the kinetic constants  $k_1$  and  $k_2$  increase. In fact  $k_1$  and  $k_2$  increase continuously from  $2.82 \times 10^{-5}$  for  $k_1$  with molecule 1140 (pKa = 7.74) up to  $1.81 \times 10^{-3}$   $\text{m}^6 \cdot \text{mol}^{-2} \cdot \text{s}^{-1}$  for molecule 1100 (pKa = 10.70) and  $4.03 \times 10^{-4}$  to  $5.46 \times 10^{-1}$   $\text{m}^6 \cdot \text{mol}^{-2} \cdot \text{s}^{-1}$  for the same molecules. We also notice that when the pKa increases the order of reaction with respect to amine also increases. It starts at around 1.1 for a value of pKa of 7.74 and increases almost linearly until around 1.6 to a value of pKa of around 10.70. In a mechanical point of view, the increase of the order corresponds to the predominance of the deprotonation by the amine which becomes more and more important. Indeed, for this series of amines, the nucleophilicity increase with the pKa and then it favors the ability of the amine to act in the deprotonation step.

Then we plot kinetic constant  $k_1$  and  $k_2$  as a function of the pKa value of the amine, fit the decimal logarithm of each kinetic constant as a function of the pKa for the series except

### 3. Primary amines

for molecule 1100 and represent the projection of each confidence ellipse as indicated in Figure V-13 (a) and (b). These values have been indicated in the Table V-2. For kinetic constants  $k_1$  and  $k_2$ , we notice that the series follows a linear trend except for molecule 1100 which seems to react faster than the trend. This difference can be explained by the difference of steric hindrance between molecule 1100, which is the methylamine, with all other molecules of the series, which are longer linear amines. It shows that we cannot compare the steric hindrance of methylamine with the steric hindrance of other molecules of the series.

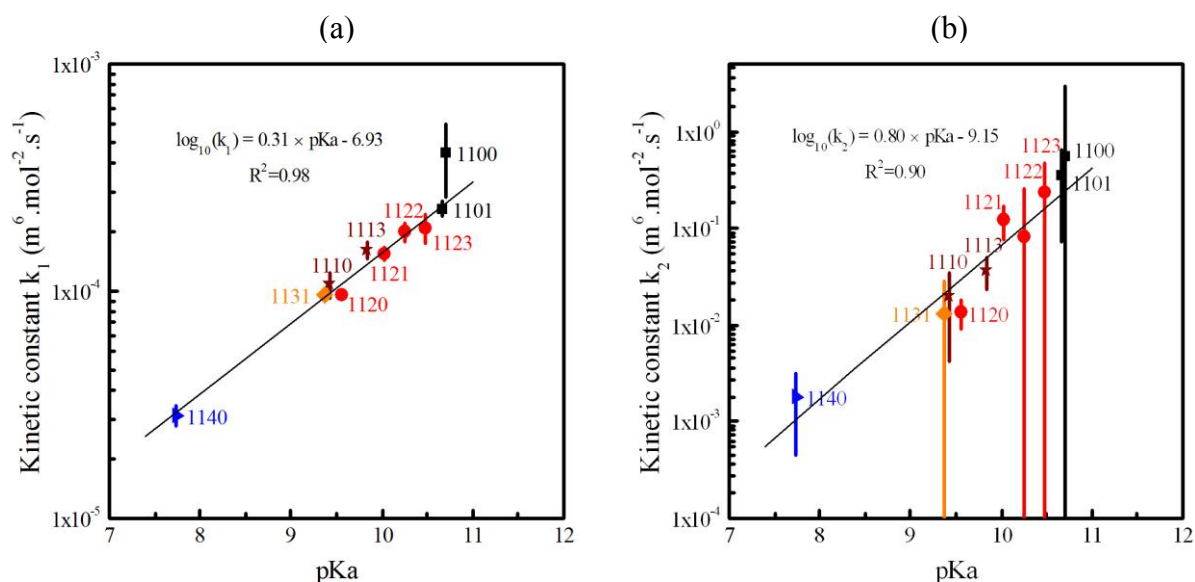


Figure V-13. Evolution of kinetic constant  $k_1$  (a) and  $k_2$  (b) as a function of the pKa of a series of linear primary amines. Alkylamines (black squares), alkanolamines (red circles), benzylamines (brown stars), etheramine (orange diamond) nitrilamine (blue triangle). Regression has been realized without molecule 1100.

Table V-2. Values of pKa and kinetic constant  $k_1$  and  $k_2$  for the series of linear primary amines.

Number	pKa	$k_1$ ( $\text{m}^6 \cdot \text{mol}^{-2} \cdot \text{s}^{-1}$ )	$k_2$ ( $\text{m}^6 \cdot \text{mol}^{-2} \cdot \text{s}^{-1}$ )
1140	7.74	$2.82 \times 10^{-5}$	$1.81 \times 10^{-3}$
1131	9.37	$9.67 \times 10^{-5}$	$1.29 \times 10^{-2}$
1110	9.43	$1.07 \times 10^{-4}$	$1.99 \times 10^{-2}$
1120	9.55	$9.68 \times 10^{-5}$	$1.38 \times 10^{-2}$
1113	9.84	$1.52 \times 10^{-4}$	$3.69 \times 10^{-2}$
1121	10.03	$1.46 \times 10^{-4}$	$1.23 \times 10^{-1}$
1122	10.25	$1.82 \times 10^{-4}$	$8.08 \times 10^{-2}$
1123	10.47	$1.91 \times 10^{-4}$	$2.32 \times 10^{-1}$
1101	10.66	$2.30 \times 10^{-4}$	$3.61 \times 10^{-1}$
1100	10.7	$4.03 \times 10^{-4}$	$5.46 \times 10^{-1}$

### 3.1.2 Derivate from tert-butylamine

We represent on Figure V-14 the kinetic constant  $k_2$  as a function of the kinetic constant  $k_1$  for the series of primary amines derivate from tert-butylamine. This series is composed of tert-butylamine (1106), 2-amino-2-methyl-1-propanol (1127), 2-amino-2-methyl-1,3-propanediol (1128) and 2-amino-2-hydroxymethyl-1,2-propanediol (1129).

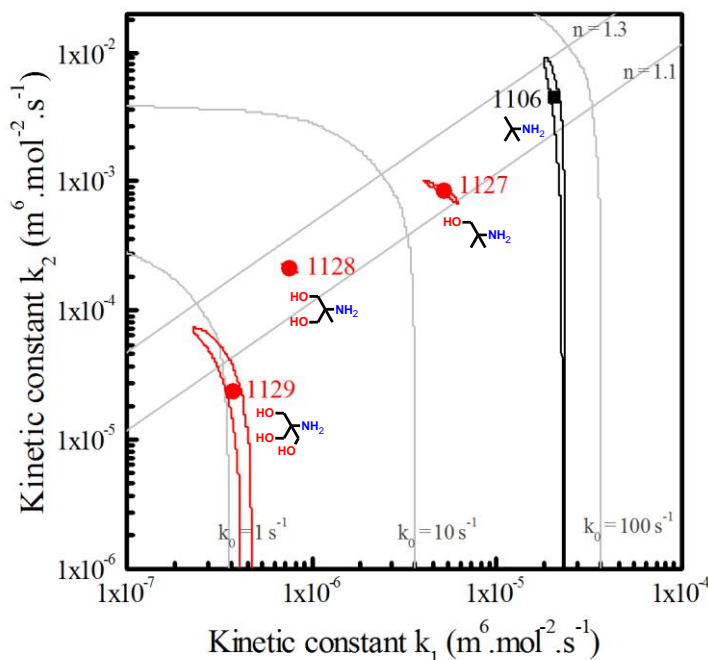


Figure V-14. Kinetic constant  $k_2$  as a function of the kinetic constant  $k_1$  for a series of derivates from tert-butylamine. Alkylamine (black square) and alkanolamines (red circles).

As same as previously we notice that when the pKa increases the kinetic constants  $k_1$  and  $k_2$  increase. It starts at respectively  $3.78 \times 10^{-7}$  and  $2.40 \times 10^{-5} \text{ m}^6 \cdot \text{mol}^{-2} \cdot \text{s}^{-1}$  with molecule 1129 for a value of pKa of 8.04 and increases almost linearly until molecule 1106 which has a pKa of 10.67 at  $2.07 \times 10^{-5}$  and  $4.51 \times 10^{-3} \text{ m}^6 \cdot \text{mol}^{-2} \cdot \text{s}^{-1}$ . We also note that contrary to the previous series, for approximately the same range of pKa, the order of reaction stays almost constant. Indeed it varies between almost 1.1 according to the uncertainty for lowest values of pKa and increase to 1.2 for highest value of pKa. It shows that for a series of sterically hindered primary amines the contribution of the deprotonation is less important than for linear primary amines.

Then, we observe the variation of  $k_1$  and  $k_2$  with pKa for these different molecules which present a similar steric hindrance. Values of  $k_1$ ,  $k_2$  and pKa have been indicated in Table V-3. Figure V-15 (a) and (b) present the variation of  $k_1$  and  $k_2$  as a function of the pKa value of each amine with the projection of the experimental ellipse of confidence.

### 3. Primary amines

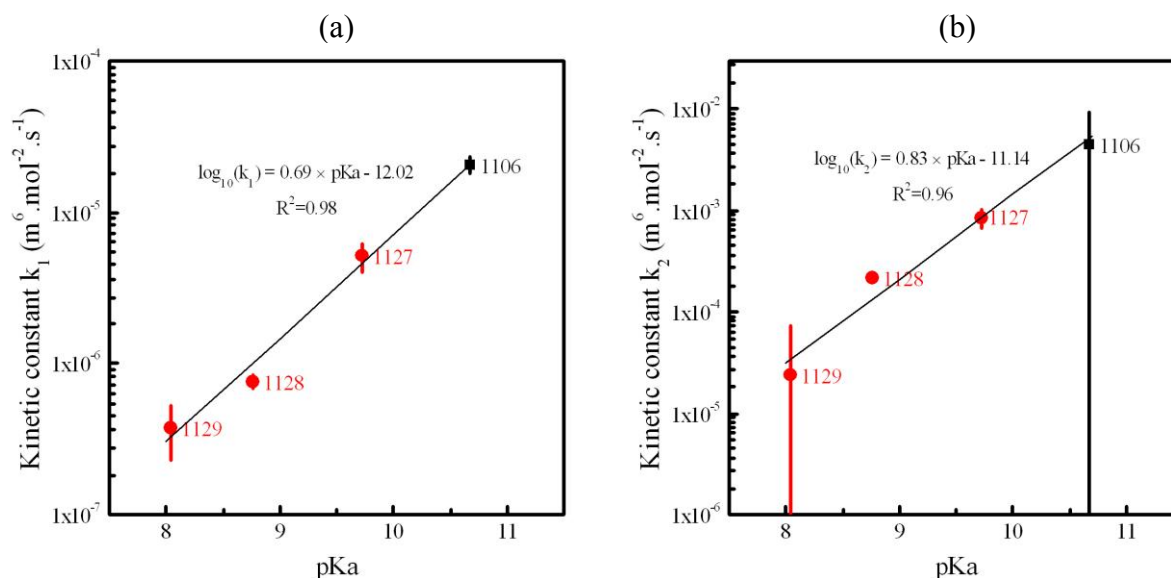


Figure V-15. Evolution of kinetic constant  $k_1$  (a) and  $k_2$  (b) as a function of the pKa for a series of derivatives of tert-butylamines. Alkylamine (black square) and alkanolamines (red circles).

The linear regressions show that variation  $k_1$  with pKa is more important for sterically hindered primary amines (slope of 0.69) than for linear primary amines (slope of 0.31). However, the average value for  $k_1$  for the derivatives of tert-butylamine is around 30 fold lower than the series of linear amines. For  $k_2$ , the variation is similar between the two series of amines (slope of 0.83 for the derivatives of tert-butylamine instead of 0.80 for linear primary amines) with a difference of two order of magnitude. We can conclude that the derivatives of tert-butylamine are less nucleophilic than linear amines which have higher values of  $k_1$  and  $k_2$  due to their most important steric hindrance.

Table V-3. Values of pKa and kinetic constant  $k_1$  and  $k_2$  of the series of derivatives from tert-butylamine.

Number	pKa	$k_1$ ( $\text{m}^6 \cdot \text{mol}^{-2} \cdot \text{s}^{-1}$ )	$k_2$ ( $\text{m}^6 \cdot \text{mol}^{-2} \cdot \text{s}^{-1}$ )
1129	8.04	$3.78 \times 10^{-7}$	$2.40 \times 10^{-5}$
1128	8.76	$7.61 \times 10^{-7}$	$2.14 \times 10^{-4}$
1127	9.72	$5.14 \times 10^{-6}$	$8.45 \times 10^{-4}$
1106	10.67	$2.07 \times 10^{-5}$	$4.51 \times 10^{-3}$

#### 3.2 Effect of the steric hindrance

In order to compare the effect of the steric hindrance on the different kinetic constant it is important to consider series of amines which have approximately the same value of pKa. In this condition we identify two series of amines which can be considered as having the same

pKa with various value of steric hindrance: alkylamines and derivate from monoethanolamine and benzylamine which are sterically hindered in  $\alpha$  and  $\beta$  position.

### 3.2.1 Derivate from methylamine

We represent on Figure V-16 the kinetic constant  $k_2$  as a function of the kinetic constant  $k_1$  for a series of primary alkylamines with various steric hindrance. This series is composed of methylamine (1100), n-butylamine (1101), isopropylamine (1102), cyclopentylamine (1103), cyclohexylamine (1104), isobutylamine (1105) and tert-butylamine (1106). The pKa of this series is approximately constant, it varies between 10.37 (molecule 1105) and 10.70 (molecule 1100).

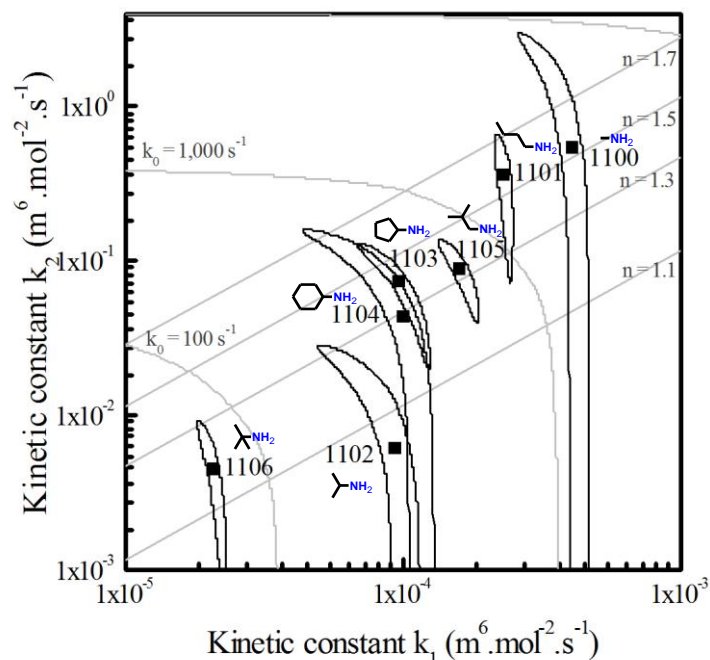


Figure V-16. Kinetic constant  $k_2$  as a function of the kinetic constant  $k_1$  for a series of alkylamines (black squares).

For this series of molecule we notice that the order of reactivity according to steric hindrance is tert-butyl < isopropyl < cyclohexyl < cyclopentyl < isobutyl < n-butyl < methyl. The hindrance of the amine function seems to be mainly controlled by the length of the substituent (n-butyl versus methyl) and the degree of substitution of the  $\alpha$  carbon. tert-butylamine with a tertiary carbon in  $\alpha$  is less reactive than amines with a secondary  $\alpha$  carbon (1102, 1103, 1104) which in turn are less reactive than the amines with a primary  $\alpha$  carbon (1100, 1101). The degree of substitution of the  $\beta$  has a lesser impact on the hindrance of the amine function. Amines with cyclic substituents (1103 and 1104) react faster than isopropylamine (1102) due to the particular structure of the cycle which limits the rotation around the secondary  $\alpha$  carbon.

Both kinetic constants  $k_1$  and  $k_2$  decrease as the steric hindrance increases and reduces the nucleophilicity of the amine. During the diminution of the steric hindrance the value of the

### 3. Primary amines

order vary between around 1.1 for slowest molecules to around 1.6 for faster amines. The increase of the steric hindrance diminishes the nucleophilicity of the amine and then its capacity to act during the deprotonation step.

Values of kinetic constants and pKa have been indicated in Table V-4. The Taft constant associated with each substituent is also given as a usual descriptor of steric hindrance. Figure V-17 (a) and (b) presents the variation of  $k_1$  and  $k_2$  as a function of the Taft constant for each amine with the projection of the experimental ellipse of confidence.

Table V-4. Value of Taft, pKa and constant and kinetic constant  $k_1$  and  $k_2$  of the series of alkylamines.

Number	Substituent	Es	pKa	$k_1$ ( $\text{m}^6 \cdot \text{mol}^{-2} \cdot \text{s}^{-1}$ )	$k_2$ ( $\text{m}^6 \cdot \text{mol}^{-2} \cdot \text{s}^{-1}$ )
1100	Methyl	-1.24	10.70	$4.03 \times 10^{-4}$	$5.46 \times 10^{-1}$
1101	n-Butyl	-1.63	10.66	$2.30 \times 10^{-4}$	$3.61 \times 10^{-1}$
1102	Isopropyl	-1.71	10.72	$9.38 \times 10^{-5}$	$6.20 \times 10^{-3}$
1103	Cyclopentyl	-1.75	10.67	$9.64 \times 10^{-5}$	$7.48 \times 10^{-2}$
1104	Cyclohexyl	-2.03	10.60	$9.92 \times 10^{-5}$	$4.38 \times 10^{-2}$
1105	Isobutyl	-2.17	10.37	$1.61 \times 10^{-4}$	$8.86 \times 10^{-2}$
1106	Tert-butyl	-2.78	10.67	$2.07 \times 10^{-5}$	$4.51 \times 10^{-3}$

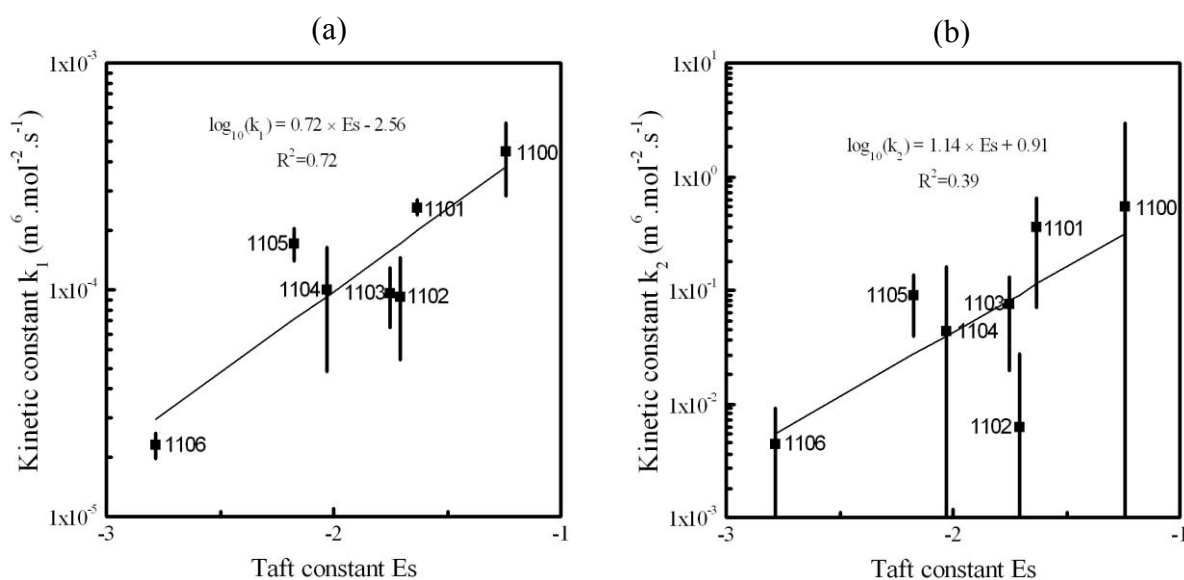


Figure V-17. Evolution of kinetic constant  $k_1$  (a) and  $k_2$  (b) as a function of the Taft constant of a series of alkylamines (black squares).

Apart from 1102 and 1105, the fits of  $\log_{10}(k_1)$  and  $\log_{10}(k_2)$  as a function of  $E_s$  illustrate the variation of  $k_1$  and  $k_2$  with steric hindrance. However, the Taft constant does not appear to be the best descriptor of steric hindrance for amines, as it predicts a larger hindrance for isobutyl ( $E_s = -2.17$ ) than for isopropyl ( $E_s = -1.71$ ).

### 3.2.2 Hindrance in $\alpha$ and $\beta$

We represent on Figure V-18 the kinetic constant  $k_2$  as a function of the kinetic constant  $k_1$  for a series of primary amines hindered in  $\alpha$  and  $\beta$ . This series is composed of benzylamines: benzylamine (1110) and  $\alpha$ -methylbenzylamine (1112) and alkanolamines: monoethanolamine (1120), 1-amino-2-propanol (1124), 2-amino-1-propanol (1125), 2-aminobutane-1-ol (1126) and 2-amino-2-methyl-1,3-propanol (1127). These series have a value of pKa which vary between 9.32 (molecule 1112) and 9.72 (molecule 1127).

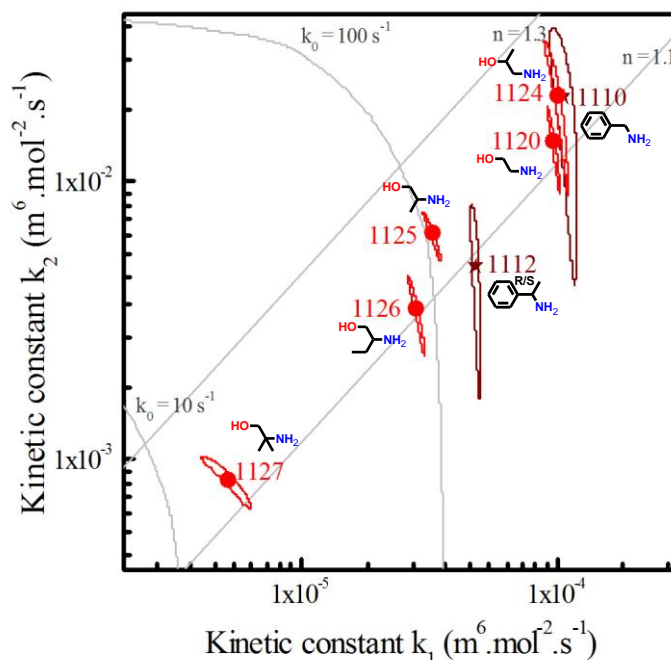


Figure V-18. Kinetic constant  $k_2$  as a function of the kinetic constant  $k_1$  for primary amines. Effect of  $\alpha$  and  $\beta$  hindrance. Alkanolamines (red circles) and benzylamines (brown stars).

According to the uncertainty, molecule 1120, 1124 and 1110 have approximately the same kinetic constants. They have a relative deviation lower than 10 % on  $k_1$  and lower than 50 % on  $k_2$ . In this area where order is lower than 1.2, kinetic constant  $k_1$  is clearly predominant. Molecules 1120 and 1110 have around the same pKa and if we consider that they have the same steric hindrance it shows that two molecules which have different structures but close physico-chemical properties in terms of basicity and steric hindrance have the same kinetic properties. Result of molecule 1124 indicates that a limited steric hindrance in  $\beta$  (methyl group) has no impact on kinetic properties.

Concerning steric hindrance in  $\alpha$  we first consider molecules 1112 and 1125 in comparison with respectively molecules 1110 and 1124. The results indicate that branching a methyl substituent on the  $\alpha$  carbon decreases the kinetic constants significantly (factor 2 to 3 on  $k_1$  and 2 to 4 on  $k_2$ ). This effect is stronger with an ethyl substituent on the  $\alpha$  carbon (molecule 1126). The effect is even more dramatic with a tertiary  $\alpha$  carbon as observed with

### 3. Primary amines

molecule 1127. These observations confirm the results obtained at higher pKa on the alkyl derivatives of methylamine.

Instead of alkylamines which have a value of pKa of around 10.50, steric hindrance on alkanolamines and benzylamines has a limited impact on the order. We then see two conditions for an amine to have a significant contribution of  $k_2$ : strong basicity and moderate hindrance of the nitrogen can favor the amine to be the preponderant base in the mechanism of reaction with  $\text{CO}_2$ .

#### 3.3 Enantiomerism

We compare the results of the two enantiomers: S- $\alpha$ -methylbenzylamine (1111) and racemic mixture of  $\alpha$ -methylbenzylamine (1112). As indicated in Figure V-19, we show that enantiomerism has no influence on kinetic properties.

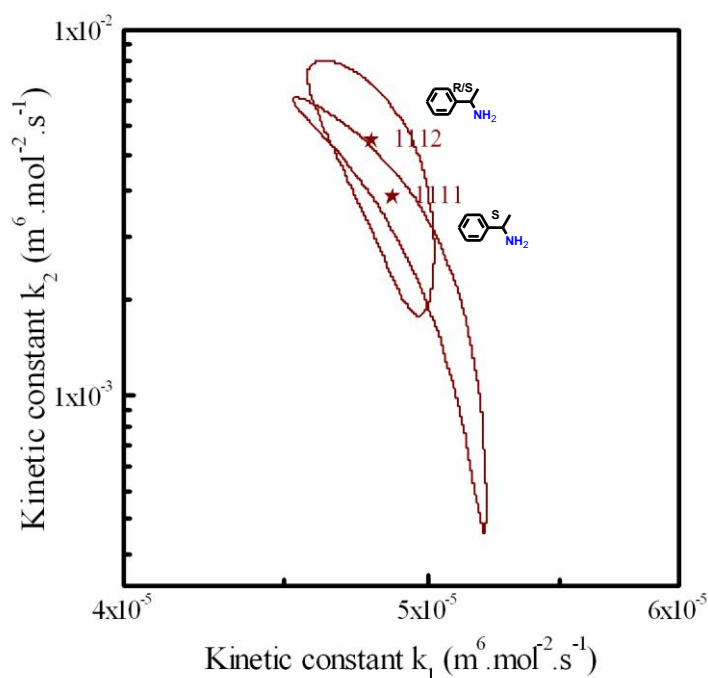


Figure V-19. Kinetic constant  $k_2$  as a function of the kinetic constant  $k_1$  of two stereoisomerisms.

#### 3.4 Conclusion

In this section we show that kinetic properties of primary amines are led by two major factors: basicity of the molecule and steric hindrance. In Figure V-20 we represent in black circles all primary amines we study. First of all we show for a series of linear primary amines that when the basicity increases, kinetic constants  $k_1$  and  $k_2$  also increase linearly with the basicity (around one order of magnitude for a pKa which vary between 7.74 and 10.66). This increase (indicated by a red line) is accompanied by an increase of the order of reaction (around 1.1 to around 1.6). Indeed increase of basicity induce in the series an increase of the nucleophilicity and then it favor the amine to participate to the deprotonation step. Then we show for a series of molecules derivate from tert-butylamine and then highly sterically

primary amines, that when the pKa increase kinetic constants  $k_1$  and  $k_2$  also increase linearly as indicated by violet line (around two orders of magnitude for a pKa which vary between 8.04 and 10.67). However we show that this increase happens with a less important variation of the order of reaction than in the case of linear primary amines (around 1.1 to around 1.2).

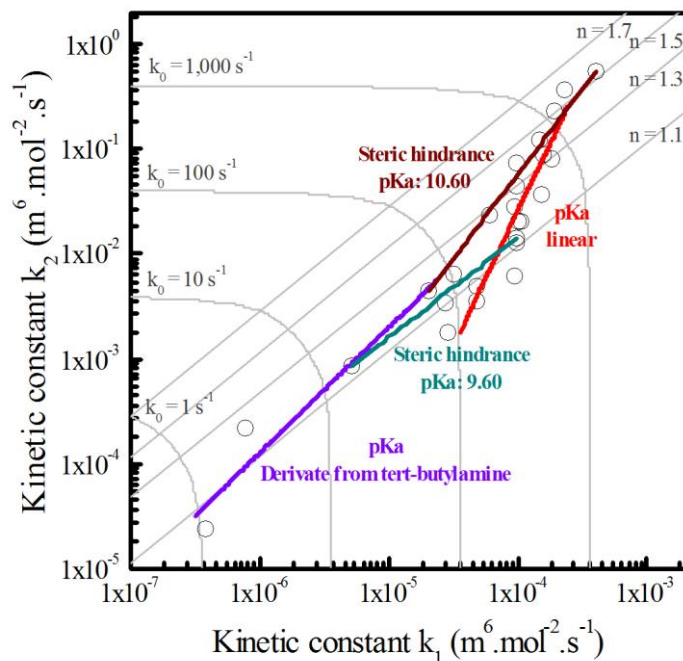


Figure V-20. Kinetic constant  $k_2$  as a function of the kinetic constant  $k_1$  for primary amines.

We also show for two series the influence of the steric hindrance. For the first series (alkylamines), we show as indicated by brown line that when the steric hindrance increases, the kinetic properties decrease (around one and a half order of magnitude between methyl and tert-butyl group). This reduction of kinetic properties is also accompanied of a reduction of the order of reaction (around 1.6 to 1.2). In the case of the series of alkanolamines, for which it has been possible to quantify steric hindrance, increase of this parameter also diminishes the kinetic properties as indicated by green line (around one order of magnitude). However this diminution is not accompanied by a change of the order of reaction.

We also show that stereoisomerism has no effect on kinetic properties.

We notice that series of benzylamines and alkanolamines which have different structures have approximately the same behavior. If we assume that benzyl group has the same steric hindrance as ethanol group, as benzylamine and alkanolamines have around the same value of pKa their kinetic constants are very close. This shows that the kinetic properties are led by physico-chemical parameters resulting from the structure. Two molecules with close structures but various values of steric hindrance and basicity will have different kinetic properties. However two molecules with very dissimilar structure but close basicity and steric hindrance will have close kinetic properties.

## 4. Acyclic secondary amines

### 4 Acyclic secondary amines

As same as primary amines there are two main effects which drive kinetic properties of acyclic secondary amines: basicity and steric hindrance. In this section we first present the evolution of the kinetic constant  $k_1$  and  $k_2$  during the change of degree of substitution primary to secondary amines. Then we study the effect of pKa and steric hindrance on kinetic properties.

#### 4.1 Change of degree of substitution

We represent on Figure V-21 the kinetic constant  $k_2$  as a function of the kinetic constant  $k_1$  for five couples of molecules. These couples correspond to a primary amine and its corresponding secondary amine with a methyl group. These molecules are methylamine (1100), dimethylamine (1200), n-butylamine (1101), N-methyl-1-butylamine (1202), benzylamine (1110), methylbenzylamine (1210), monoethanolamine (1120), 2-methylaminoethanol (1220), 3-aminopropionitrile (1140) and 3-methylaminopropionitrile (1240).

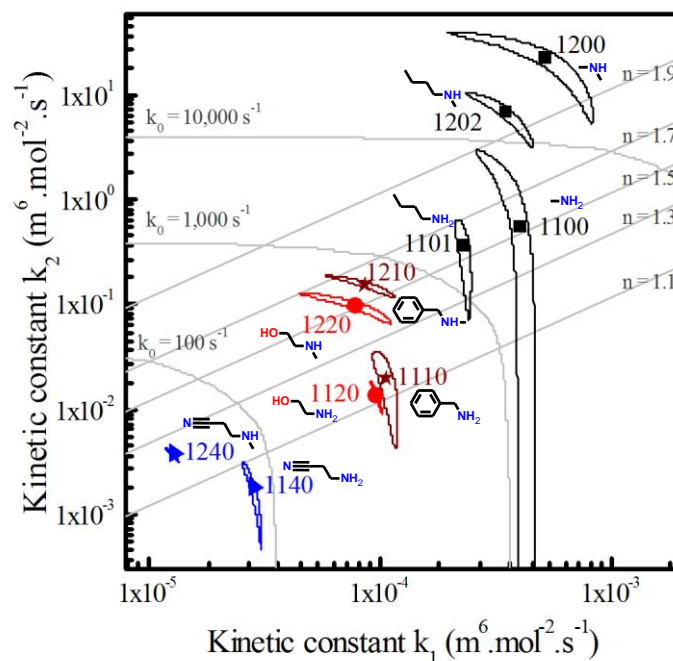


Figure V-21. Kinetic constant  $k_2$  as a function of the kinetic constant  $k_1$  for five series of amines.

Alkylamines (black squares), alkanolamines (red circles), benzylamines (brown stars) and nitrilamines (blue triangles).

For alkylamines, with a strong basicity, we notice that the acyclic secondary amines are more reactive than corresponding primary alkylamines. Comparison between 1100 and 1200 shows a 40 fold increase for  $k_2$  and a 1.3 fold increase for  $k_1$  while comparison between 1101 and 1202 shows a 19 fold increase for  $k_2$  and a 1.5 fold increase for  $k_1$ . In both cases, the apparent order of reaction increases from 1.6 to above 1.9 which corresponds to a most

important participation of the amine to the deprotonation step which become preponderant. The change of degree between primary amine and corresponding secondary methylamine increases the apparent pseudo first order constant  $k_0$  by one order of magnitude.

For alkanolamines and benzylamines, which have a moderate basicity, we notice that the change of degree of substitution leads to a less important increase of the kinetic constant  $k_2$  than alkylamines (factor of around 7.7 for 1210 and around 7.1 for 1220) and a diminution of the kinetic constant  $k_1$  (factor of around 0.82 for 1210 and around 0.81). The order of reaction increases from around 1.1 to around 1.6 which indicates a most important participation of the amine to the deprotonation step. For these two couples of amines which have a value of  $pK_a$  of around 9.60, the change of degree between primary amine and corresponding secondary with an additionnal methyl group leads to an improvement of kinetic properties close to a factor 1.7 according to values of  $k_0$ .

Finally for weakly basic nitrilamines, we still observe a moderate increase of  $k_2$  (2 fold between 1140 and 1240) compensated by a clear decrease of  $k_1$  (factor 0.45 between 1140 and 1240). The apparent order is then increased from 1.1 to 1.2. The apparent first order kinetic constant is decreased by a factor 2.

The addition of a methyl group on a nitrogen atom of a primary amine increases its charge by a +I inductive effect but also increase its steric hindrance. There is then a competition between the +I inductive effect which tends to increase the nucleophilicity of the amine group and the steric hindrance which diminishes it.

According to the previous observation, it seems that in the case of very basic amines (alkylamines) the contribution of the inductive effect widely predominate on the effect of steric hindrance which increases the nucleophilic behavior of the corresponding secondary amine. In these conditions, the secondary amine has a most important participation to the deprotonation step and then increases the order of reaction by the increase of the kinetic constant  $k_2$ . For amines with an intermediate value of  $pK_a$  (alkanolamines and benzylamines), the change of degree of substitution, the ratio inductive effect on the effect of the steric hindrance seems to diminish in comparison with amines with higher value of  $pK_a$ . Consequently, the improvement of the kinetic properties is less important than in the latest case. Finally in the case of nitrilamines which have a low value of  $pK_a$  (nitrilamines), the contribution of the steric hindrance predominates on the inductive effect which explains the diminution of kinetic properties.

## 4.2 Effect of the basicity

For secondary amines we indentify one series of amines for which we assume that the steric hindrance is almost the same. Molecules of this series are represented in Figure V-22. This series is composed of dimethylamine (1200), N-methyl-1-butylamine (1202), methylbenzylamine (1210), 2-methylaminoethanol (1220) and 3-methylaminopropionitrile (1240).

#### 4. Acyclic secondary amines

Kinetic constants and pKa are indicated in Table V-5. Figure V-23 (a) and (b) present the variation of  $k_1$  and  $k_2$  with the pKa of each amine with the projection of the experimental ellipse of confidence.

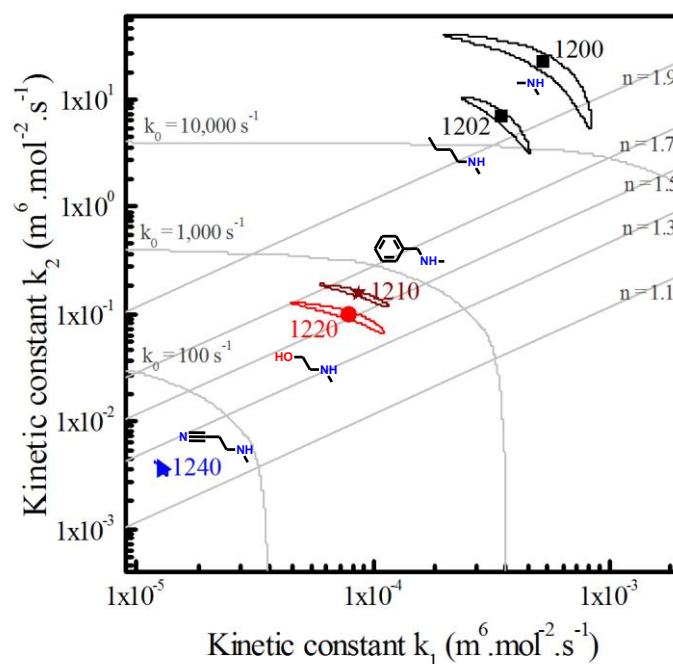


Figure V-22. Kinetic constant  $k_2$  as a function of the kinetic constant  $k_1$  for a series secondary amines. Alkylamines (black squares), alkanolamines (red circles), benzylamine (brown star) and nitrilamine (blue triangle).

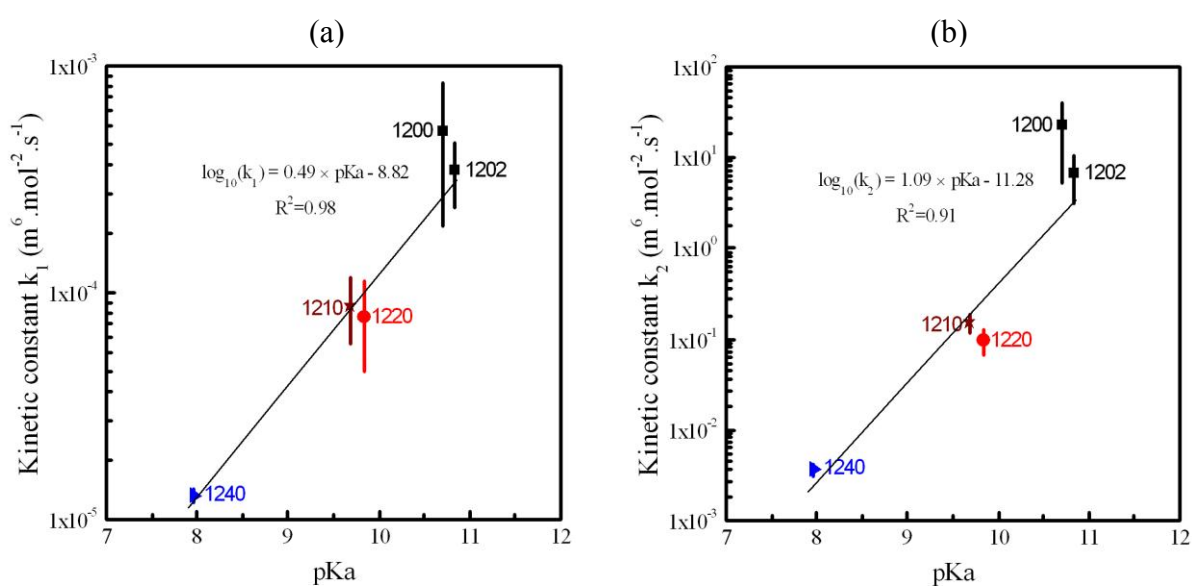


Figure V-23. Evolution of kinetic constant  $k_1$  (a) and  $k_2$  (b) as a function of the pKa for a series of secondary amines. Alkylamines (black squares), alkanolamines (red circles), benzylamine (brown star) and nitrilamine (blue triangle). Regression has been realized without molecule 1200.

First, we notice that the kinetic constants  $k_1$  and  $k_2$  increase with the pKa. Except for (dimethylamine) 1200 which is significantly less hindered than the others and then exclude from the fit, the kinetic constants of secondary methylamines are well fitted by a linear regression with the pKa.

From the slopes of the linear fits we also observe than the influence of the pKa on both constants is stronger from this series of secondary methylamines than for linear primary amines seen in section 3.1.1. In fact the slope of the fit are respectively 0.49 for  $k_1$  and 1.09 for  $k_2$  instead of respectively 0.31 and 0.80 for primary amines.

This result confirms the precedent comparison of methylamines with corresponding primary amines. For a given pKa,  $k_2$  of a secondary methylamine is always higher than a primary amine having the same pKa and degree of hindrance. According to the slopes of the fits which cross at pKa value of 10.5,  $k_1$  of a secondary methylamine is higher than a primary amine having the same pKa above 10.5 and lower below 10.5. Consequently the apparent order of the reaction related to the ratio  $k_2/k_1$  is systematically higher for a moderately hindered secondary methylamine than for a linear primary amines at the same pKa. The increase of the apparent order with the pKa is also sharper for secondary amines.

Table V-5. Value of pKa and kinetic constant  $k_1$  and  $k_2$  of the series of secondary amines.

Number	pKa	$k_1$ ( $\text{m}^6 \cdot \text{mol}^{-2} \cdot \text{s}^{-1}$ )	$k_2$ ( $\text{m}^6 \cdot \text{mol}^{-2} \cdot \text{s}^{-1}$ )
1240	7.96	$1.28 \times 10^{-5}$	$3.66 \times 10^{-3}$
1210	9.69	$8.77 \times 10^{-5}$	$1.54 \times 10^{-1}$
1220	9.84	$7.88 \times 10^{-5}$	$9.75 \times 10^{-2}$
1200	10.71	$5.18 \times 10^{-4}$	$2.28 \times 10^1$
1202	10.83	$3.48 \times 10^{-4}$	$6.86 \times 10^0$

### 4.3 Effect of the steric hindrance

In order to study the effect of the steric hindrance on the different kinetic constants we consider series of amines which have approximately the same value of pKa. In this condition we identify two effects that it is interesting to point out. On the one hand effect of steric hindrance on four series of molecule with different values of pKa and on the other hand effect of steric hindrance in  $\beta$  position.

#### 4.3.1 Derivate of four series

In this part, we consider four different series of secondary amines that we represent in three different figures. Each molecule of the same series has approximately the same pKa value and a various range of steric hindrance. The first series is composed of alkylamines: dimethylamine (1200), N-methyl-1-propylamine (1201), N-methyl-1-butylamine (12002), di-n-propylamine (1203), N-isopropylmethylamine (1204) and N-methylcyclohexylamine (1205). Molecules of this series have a pKa of around 10.80. We represent the kinetic

#### 4. Acyclic secondary amines

constant  $k_2$  as a function of the kinetic constant  $k_1$  of each molecules of this series in Figure V-24.

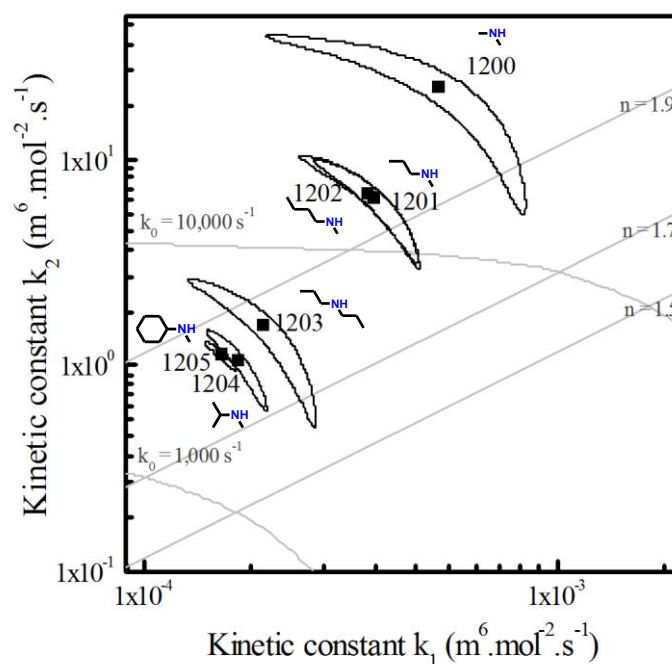


Figure V-24. Kinetic constant  $k_2$  as a function of the kinetic constant  $k_1$  for series of secondary alkylamines (black squares).

The second series is composed of benzylamines: methylbenzylamine (1210) and ethylbenzylamine (1211). Molecules of this series have a pKa of around 9.75. The third series is composed of alkanolamines: 2-methylaminoethanol (1220), 2-ethylaminoethanol (1221), 2-propylaminoethanol (1222), n-butylaminoethanol (1223), 2-isopropylaminoethanol (1224), N-cyclohexylaminoethanol (1225) and tert-butylaminoethanol (1226). Molecules of this series have a pKa of around 9.95. We represent the kinetic constant  $k_2$  as a function of the kinetic constant  $k_1$  of each molecules of these series in Figure V-25. In this figure we also indicate the trend obtained for alkylamines.

Finally, the fourth series is composed of nitrilamines: 3-methylaminopropionitrile (1240), 3-ethylaminopropionitrile (1241), 3-n-butylaminopropionitrile (1242) and tert-butylaminopropionitrile (1243). Molecules of this series have a pKa of around 8.10. We represent the kinetic constant  $k_2$  as a function of the kinetic constant  $k_1$  of each molecules of these series in Figure V-26. In this figure we also indicate the trend obtained for alkylamines, alkanolamines and benzylamines.

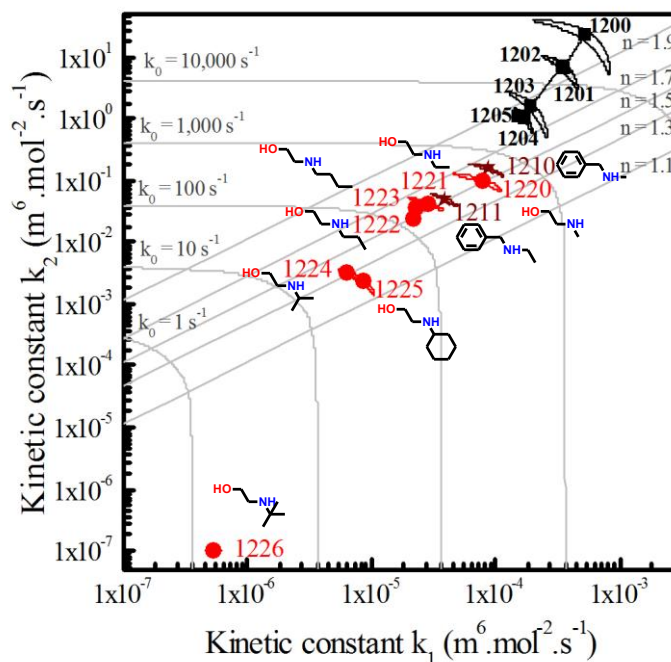


Figure V-25. Kinetic constant  $k_2$  as a function of the kinetic constant  $k_1$  for series of secondary benzylamines (brown stars) and alkanolamines (red circles). Trend obtained for alkylamines (black).

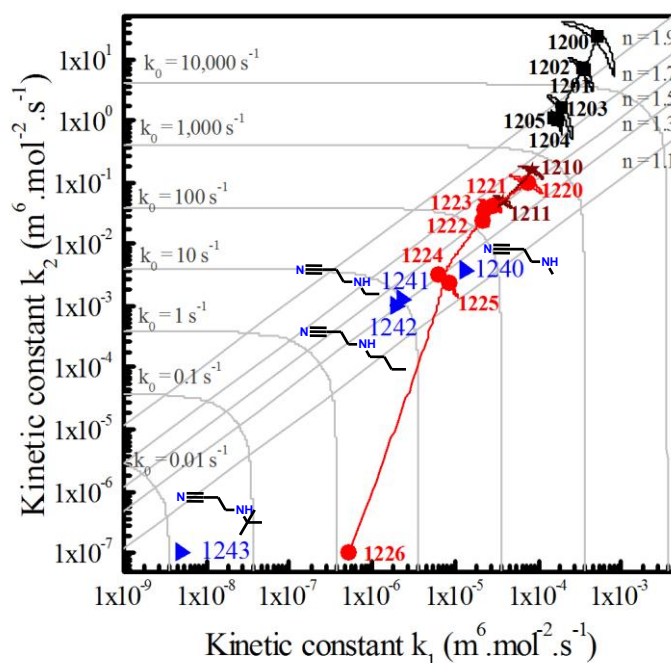


Figure V-26. Kinetic constant  $k_2$  as a function of the kinetic constant  $k_1$  for series of secondary nitrilamines (blue triangles). Trend obtained for alkylamines (black), benzylamines (brown) and alkanolamines (red).

For these four series we notice that the order of reactivity according to steric hindrance is tert-butyl  $\ll$  cyclohexyl  $\approx$  isopropyl  $<$  n-propyl  $\approx$  n-butyl  $\approx$  n-ethyl  $<$  methyl. This result

#### 4. Acyclic secondary amines

looks like result obtain for primary amines which was tert-butyl < isopropyl < cyclohexyl < cyclopentyl < isobutyl < n-butyl < methyl. However we notice that the difference between tert-butyl and other molecules of each series is more important than in the case of primary amines. Results of the four series are synthetized in Figure V-27 (a) and (b). For all series, values of kinetic constants and pKa have been indicated in Table V-6 to Table V-9 with the Taft constant which characterizes the steric hindrance contribution of the alkyle substituent.

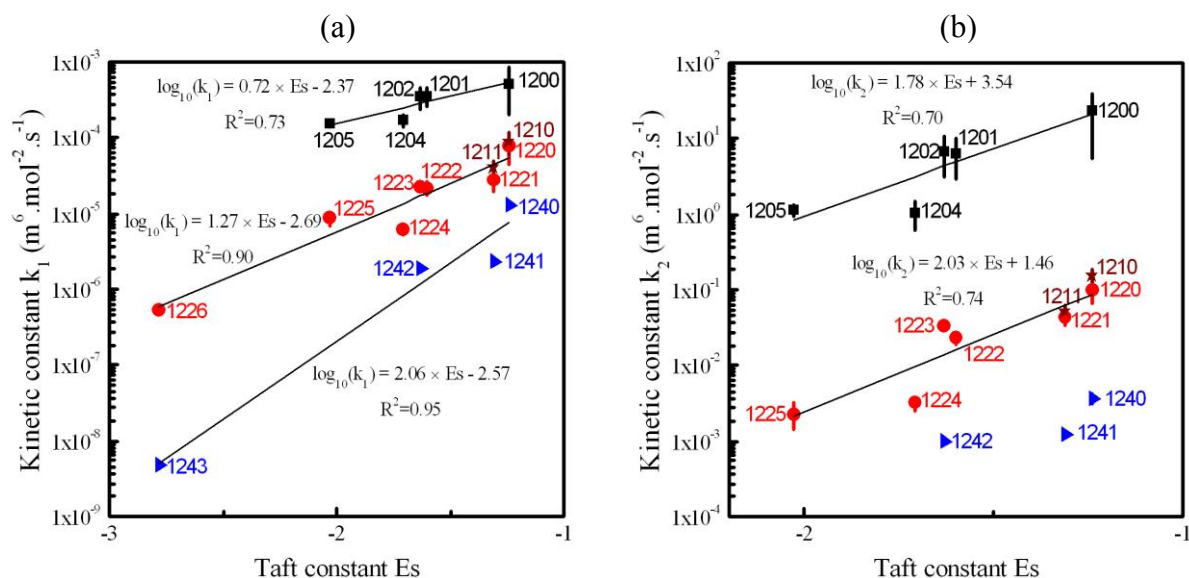


Figure V-27. Evolution of kinetic constant  $k_1$  (a) and  $k_2$  (b) as a function of the Taft constant of four series of secondary amines. Alkylamines (black squares), alkanolamines (red circles), benzylamines (brown stars) and nitrilamines (blue triangles).

As for primary amines, the hindrance of the amine function for each series of secondary amines seems to be mainly controled by the length of the alkyle substituent (n-ethyl to n-butyl versus methyl) and the degree of substitution of the  $\alpha$  carbon. Tert-butylamine with a tertiary carbon in  $\alpha$  is less reactive than amines with a secondary  $\alpha$  carbon which in turn are less reactive than the amines with a primary  $\alpha$  carbon.

The linear fit of  $k_1$  as a function of Taft constant gives almost the same regression than for primary alkylamines (Chapter V .3.2.1) with the same slope of 0.72. For this series of alkylamines with an average pKa of 10.8, the linear regression as a function of  $E_s$  confirms that secondary amines have systematically a higher value of  $k_2$  than corresponding primary amines (Chapter V .4.2). The sensitivity of  $E_s$  on  $k_2$  is also higher in the case of secondary amine with a slope of 1.78 for secondary alkylamines instead of 1.14 for primary alkylamines.

As for primary amines, if we exclude tert-butyl group which has a specific steric hindrance, the increase of  $E_s$  tends to decrease the order of reaction from 1.9 to 1.8 for secondary alkylamines, from 1.6 to 1.3 for alkanolamines. For nitrilamines which have a lower value of the pKa the order of reaction is around 1.3 whatever the steric hindrance is.

It is interesting to notice that tert-butylamines 1226 and 1243 which react as tertiary amines also follow the linear fit of secondary amines for amine. This result could support a continuity between the mechanism of reaction of tertiary amines and secondary amines.

Table V-6. Value of Taft constant, pKa and kinetic constant  $k_1$  and  $k_2$  for the series of secondary alkylamines.

Number	Substituent	Es	pKa	$k_1$ ( $\text{m}^6 \cdot \text{mol}^{-2} \cdot \text{s}^{-1}$ )	$k_2$ ( $\text{m}^6 \cdot \text{mol}^{-2} \cdot \text{s}^{-1}$ )
1200	Methyl	-1.24	10.71	$5.18 \times 10^{-4}$	$2.28 \times 10^1$
1201	n-Propyl	-1.6	10.78	$3.61 \times 10^{-4}$	$6.48 \times 10^0$
1202	n-Butyl	-1.63	10.83	$3.48 \times 10^{-4}$	$6.86 \times 10^0$
1204	Isopropyl	-1.71	10.94	$1.70 \times 10^{-4}$	$1.05 \times 10^0$
1205	Cyclohexyl	-2.03	10.90	$1.53 \times 10^{-4}$	$1.13 \times 10^0$

Table V-7. Value of Taft constant, pKa and kinetic constant  $k_1$  and  $k_2$  for the series of secondary benzylamines.

Number	Substituent	Es	pKa	$k_1$ ( $\text{m}^6 \cdot \text{mol}^{-2} \cdot \text{s}^{-1}$ )	$k_2$ ( $\text{m}^6 \cdot \text{mol}^{-2} \cdot \text{s}^{-1}$ )
1210	Methyl	-1.24	9.69	$8.77 \times 10^{-5}$	$1.54 \times 10^{-1}$
1211	Ethyl	-1.31	9.78	$3.95 \times 10^{-5}$	$5.01 \times 10^{-2}$

Table V-8. Value of Taft constant, pKa and kinetic constant  $k_1$  and  $k_2$  for the series of secondary alkanolamines.

Number	Substituent	Es	pKa	$k_1$ ( $\text{m}^6 \cdot \text{mol}^{-2} \cdot \text{s}^{-1}$ )	$k_2$ ( $\text{m}^6 \cdot \text{mol}^{-2} \cdot \text{s}^{-1}$ )
1220	Methyl	-1.24	9.84	$7.88 \times 10^{-5}$	$9.75 \times 10^{-2}$
1221	Ethyl	-1.31	9.86	$2.83 \times 10^{-5}$	$4.30 \times 10^{-2}$
1222	n-Propyl	-1.6	9.86	$2.18 \times 10^{-5}$	$2.33 \times 10^{-2}$
1223	n-Butyl	-1.63	9.99	$2.31 \times 10^{-5}$	$3.44 \times 10^{-2}$
1224	Isopropyl	-1.71	10.01	$6.31 \times 10^{-6}$	$3.16 \times 10^{-3}$
1225	Cyclohexyl	-2.03	9.91	$8.67 \times 10^{-6}$	$2.30 \times 10^{-3}$
1226	tert-Butyl	-2.78	10.23	$5.37 \times 10^{-7}$	$1.00 \times 10^{-7}$

Table V-9. Value of Taft constant, pKa and kinetic constant  $k_1$  and  $k_2$  for the series of secondary nitrilamines.

Number	Substituent	Es	pKa	$k_1$ ( $\text{m}^6 \cdot \text{mol}^{-2} \cdot \text{s}^{-1}$ )	$k_2$ ( $\text{m}^6 \cdot \text{mol}^{-2} \cdot \text{s}^{-1}$ )
1240	Methyl	-1.24	7.96	$1.28 \times 10^{-5}$	$3.66 \times 10^{-3}$
1241	Ethyl	-1.31	8.10	$2.26 \times 10^{-6}$	$1.24 \times 10^{-3}$
1242	n-Butyl	-1.63	8.05	$1.84 \times 10^{-6}$	$9.96 \times 10^{-4}$
1243	tert-Butyl	-2.78	8.31	$4.79 \times 10^{-9}$	$1.00 \times 10^{-7}$

## 4. Acyclic secondary amines

### 4.3.2 Hindrance in $\beta$

We represent on Figure V-28 the kinetic constant  $k_2$  as a function of the kinetic constant  $k_1$  of two amines: diethanolamine (1227) and diisopropanolamine (1228). The goal is to compare the influence of the two methyl groups in  $\beta$  position. These two molecules have approximately the same value of pKa 8.86. They both have an order of around 1.4. There is a factor 2.6 on  $k_1$  and 1.6 on  $k_2$ . This result shows that a double steric hindrance in  $\beta$  position decreases slightly the kinetic properties.

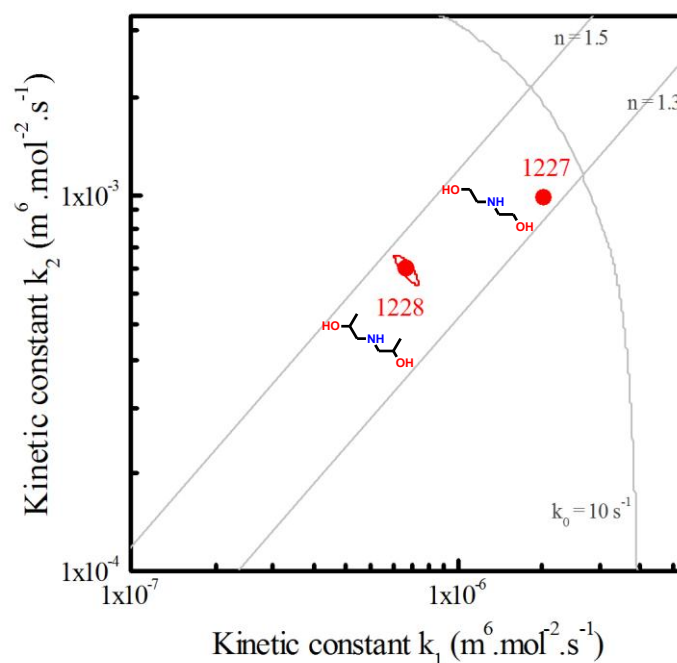


Figure V-28. Kinetic constant  $k_2$  as a function of the kinetic constant  $k_1$  for two secondary amines. Alkanolamines (red circles).

## 4.4 Conclusion

As same as for primary amines, we show in this section that behavior of secondary amines is mainly linked to their basicity and steric hindrance. In Figure V-29 we represent with black circles all acyclic secondary amines studied. First of all we show that the change of degree of substitution (primary amine to the corresponding secondary amines with a methyl substituant) introduce an important difference of behavior which is exalted by the basicity of the molecule. Indeed for amines with high value pKa (around 10.70) the kinetic properties increase by a factor of around 10. This increase is due to the positive electronic effect of the methyl group which is more important than the effect of associated steric hindrance. For amines with a low value of pKa (7.80) it is the opposite. The electronic effect cannot compensate the steric hindrance of the methyl group and then kinetics decrease by a factor of around 0.5.

Then we take an interest in a series with an assumed identical steric hindrance but different value of pKa ranged between 7.96 and 10.71. For this series we made the same

observation as in the case of primary amines. The kinetic constant can be linearly related to the value of the pKa since the molecules of the series have the same steric hindrance. This series has been indicated by the red lines on the following figure.

Then we show the effect of steric hindrance on secondary amines with series which have specific value of pKa. In overall, as same as for primary amines, we first show that kinetic constants decrease when the steric hindrance increase. However we point out the fact than the effect of the steric hindrance also depend on the basicity of each series for kinetic constant  $k_1$  but not kinetic constant  $k_2$ . Indeed, for the same difference of steric hindrance (methyl to butyl) the diminution of the kinetic constant  $k_1$  is less important for alkylamines (black line) than for alcanolamines (dark cyan line) and than for nitrilamines (green line). Nevertheless this diminution is approximately identical on kinetic constant  $k_2$ . This result shows once again than basicity and steric hindrance have a dependant effect to explain kinetic constants.

Finally we notice that when the steric hindrance is very important secondary amines behave as tertiary amines with a first order reaction with respect to amine and comparable values of  $k_1$ . This behavior has been observed for tert-butylaminoethanol and 3-tert-butylaminopropionitrile. For each of these amines, one of the substituent is a linear chain and the other is tert-butyl group with a tertiary  $\alpha$  carbon. These molecules are included in the definition of a severely hindered secondary amines (Savage *et al.*, 1982). However, we notice that these molecules also fit the trend obtained between kinetic constant  $k_1$  and  $E_s$ . This results seems to indicate that there is a continuity of mechanism between amines which form carbamates (class B) and amines which from carbonates (class A).

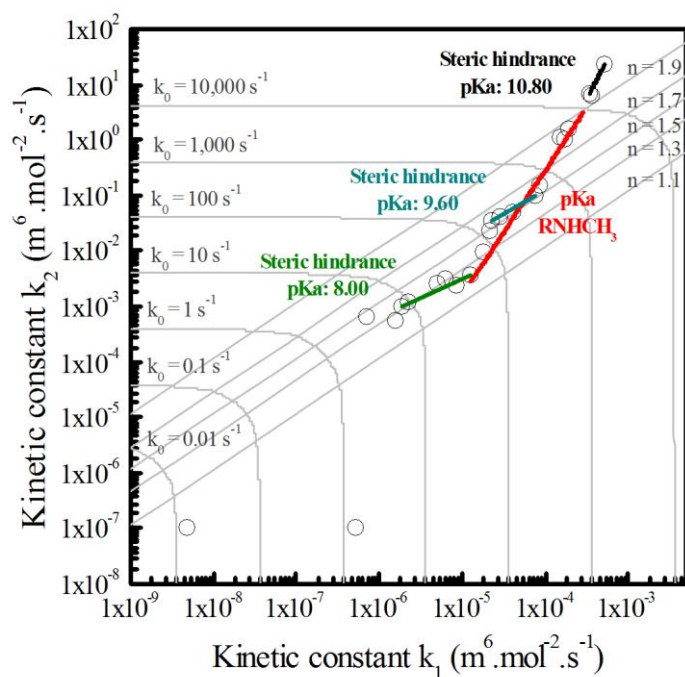


Figure V-29. Kinetic constant  $k_2$  as a function of the kinetic constant  $k_1$  for acyclic secondary amines.

## 5 Cyclic secondary amines

For secondary cyclic amines we point out the effects of basicity and steric hindrance. We first present effect of basicity on non-hindered cyclic amines, then we illustrate the effect of the steric hindrance of cyclic nitrogen and of the relative position of hydroxyle function with different hydroxypiperidines.

### 5.1 Effect of the basicity

We consider four secondary cyclic amines where the two substituents are connected to form a 5 atom or 6 atom heterocycle: pyrrolidine (1250), piperidine (1251), 4-hydroxypiperidine (1260) and morpholine (1270). Those molecules have a very low degree of hindrance of the nitrogen doublet since the two  $\alpha$  carbons and two  $\beta$  carbons are each bound to two atoms of hydrogen.

Results are presented on Figure V-30. Kinetic constants and pKa have been indicated in Table V-10. Figure V-31 (a) and (b) presents the variation of  $k_1$  and  $k_2$  with the pKa for these four amines with the projection of the experimental ellipse of confidence.

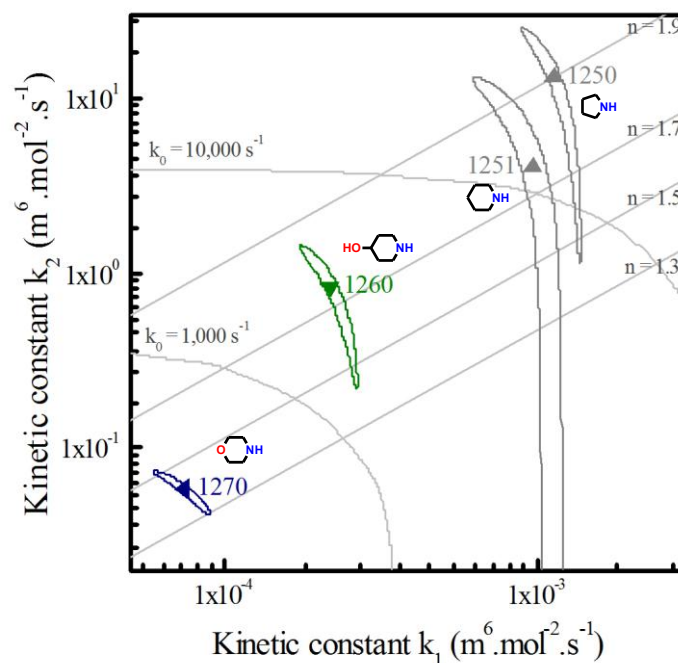


Figure V-30. Kinetic constant  $k_2$  as a function of the kinetic constant  $k_1$  for a series of cyclic secondary amines. Alkyl secondary cyclic amines (grey triangles), 4-hydroxypiperidine (green triangle) and morpholine (blue triangle).

First, we notice that the kinetic constants  $k_1$  and  $k_2$  increase with the pKa. The decimal logarithm of the kinetic constants of these four non hindered cyclic secondary methylamines are well fitted by a linear regression with the pKa.

(a)

(b)

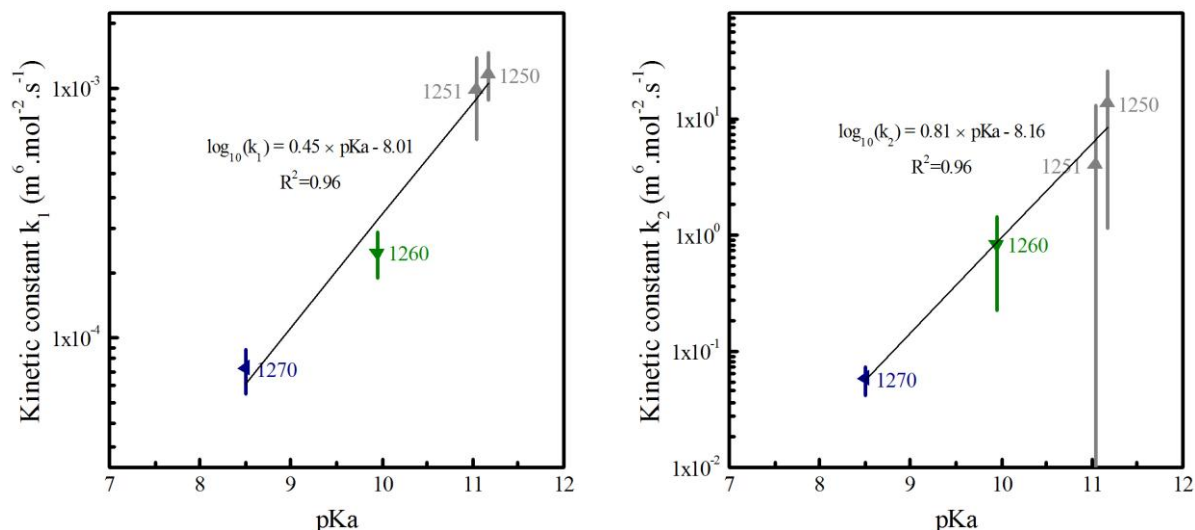


Figure V-31. Evolution of kinetic constant  $k_1$  (a) and  $k_2$  (b) as a function of the  $pK_a$  for a series of secondary cyclic amines. Alkyl secondary cyclic amines (grey triangles), 4-hydroxypiperidine (green triangle) and morpholine (blue triangle).

Table V-10. Value of  $pK_a$  and kinetic constant  $k_1$  and  $k_2$  of the series of cyclic secondary amines.

Number	$pK_a$	$k_1$ ( $m^6 \cdot mol^{-2} \cdot s^{-1}$ )	$k_2$ ( $m^6 \cdot mol^{-2} \cdot s^{-1}$ )
1270	8.5	$7.44 \times 10^{-5}$	$5.81 \times 10^{-2}$
1260	9.96	$2.20 \times 10^{-4}$	$8.31 \times 10^{-1}$
1251	11.04	$9.80 \times 10^{-4}$	$3.98 \times 10^0$
1250	11.17	$1.14 \times 10^{-3}$	$1.33 \times 10^1$

From the slopes of the linear fits we also observe that the influence of the  $pK_a$  on both constants is comparable with the series of acyclic secondary methylamines than for linear seen in Chapter V .4.2. In fact the slope of the fit are respectively 0.45 for  $k_1$  and 1.09 for  $k_2$  instead of respectively 0.49 and 0.81 for acyclic secondary methylamines. Similarly, the apparent order increases with the  $pK_a$  from 1.2 for a value of  $pK_a$  of 8.50 to 1.9 for a value of  $pK_a$  of 11.17. This indicates that relative contribution of the amine to the deprotonation step is quite comparable between acyclic and cyclic secondary amines at a given value of  $pK_a$  with an increasing contribution of the amine in the deprotonation step in both cases while the  $pK_a$  increases.

According to these fits, the kinetics constants are significantly increased between acyclic and cyclic amines. The increase is 3 fold for  $k_1$  at  $pK_a = 8.5$  and 2.3 fold at  $pK_a = 11$ . The increase is 5.5 fold for  $k_2$  at  $pK_a = 8.5$  and 1.1 fold at  $pK_a = 11$ . This increase of reactivity for both constants at a given value of  $pK_a$  indicates the strong increase of the nucleophilic character of cyclic amines due to the favorable position of the lone electron pair

## 5. Cyclic secondary amines

of the nitrogen. Indeed, it is not hindered by the rotation of substituents around the  $\alpha$  carbon as it is the case for acyclic amines.

### 5.2 Effect of the steric hindrance

We represent on Figure V-32 the kinetic constant  $k_2$  as a function of the kinetic constant  $k_1$  for a series of molecules derivates from 4-hydroxypiperidine. This series is composed of 4-hydroxypiperidine (1260), 3-hydroxypiperidine (1261), 3-piperidinemethanol (1262), 2-piperidinemethanol (1263), 2-piperidineethanol and 2,2,6,6-tetramethyl-4-piperidinol (1265). For this series of molecule the pKa is ranged between 9.67 for molecule 1261 and 10.41 for molecule 1264. Contrary to previous series there is an important variation due to the influence of hindering group on the cycle which is stronger than for acyclic molecules. Even it is difficult to make the difference between both effects we choose to analyze data carefully.

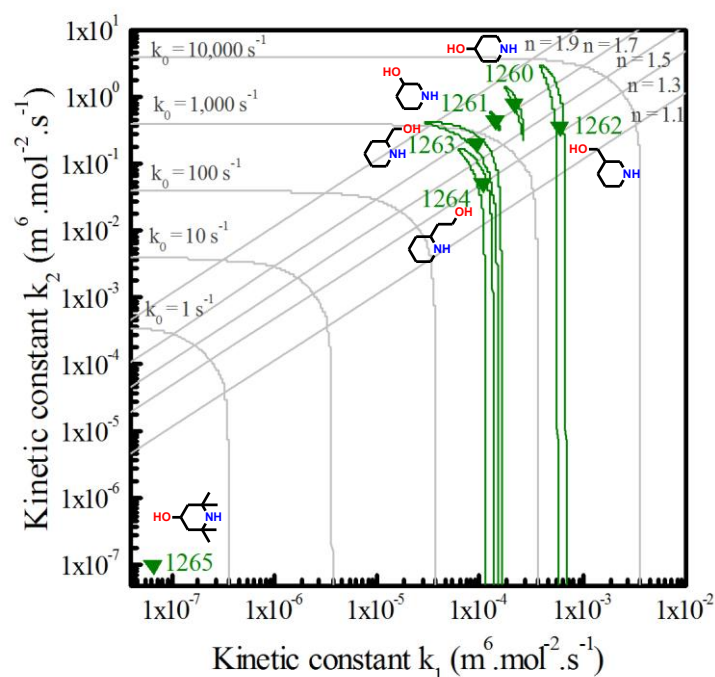


Figure V-32. Kinetic constant  $k_2$  as a function of the kinetic constant  $k_1$  for a series of secondary cyclic amines. Derivate of 4-hydroxypiperidine (Green triangles).

In a first time we compare results obtain between molecule 1260 and derivates with steric hindrance in meta position (1261 and 1262). While we add an hydroxyl group to molecule 1260 in meta position, there are a factor 0.64 on  $k_1$  and 0.56 on  $k_2$ . While the group is changed into methanol, the kinetic properties increase due to the increase of the pKa (9.96 for molecule 1260 and 10.37 for molecule 1262). For this case, the increase of the pKa has a stronger effect than steric hindrance.

Then we compare results obtain between molecule 1260 and derivates with steric hindrance in ortho position (1263 and 1264). When we add a methanol group to molecule

1260 in ortho position, there are a factor 0.43 on  $k_1$  and 0.25 on  $k_2$ . In the case of an ethanol group in ortho position (molecule 1264), the kinetic properties still decrease by comparison with molecule 1260 even if the value of the  $pK_a$  increase to 10.37. In this precise case the steric hindrance effect predominates the basicity effect. This shows that steric hindrance in ortho position have a greater effect than steric hindrance in meta position due to the proximity with the nitrogen atom.

Finally, when we have four methyl groups in ortho position (molecule 1265) the molecule behaves as tertiary amine due to the severe hindrance on both  $\alpha$  carbons.

### 5.3 Conclusion

In this section we show the effect of basicity and steric hindrance on cyclic secondary amines. In Figure V-33 we represent with black circles all studied cyclic secondary amines. In a first time we notice that the kinetic constant  $k_1$  and  $k_2$  follow linearly the  $pK_a$  of a series of non sterically hindered amines indicated in the figure by the red line. Then we show that steric hindrance decreases kinetic constant. However, because of the miss of descriptor for this case and because it have not been possible to identify large series with various steric hindrance for the same  $pK_a$  value we only present qualitatively this effect. As same as for acyclic secondary amines we notice that when the steric hindrance of a molecule is particularly important cyclic secondary amines can behave as tertiary amines.

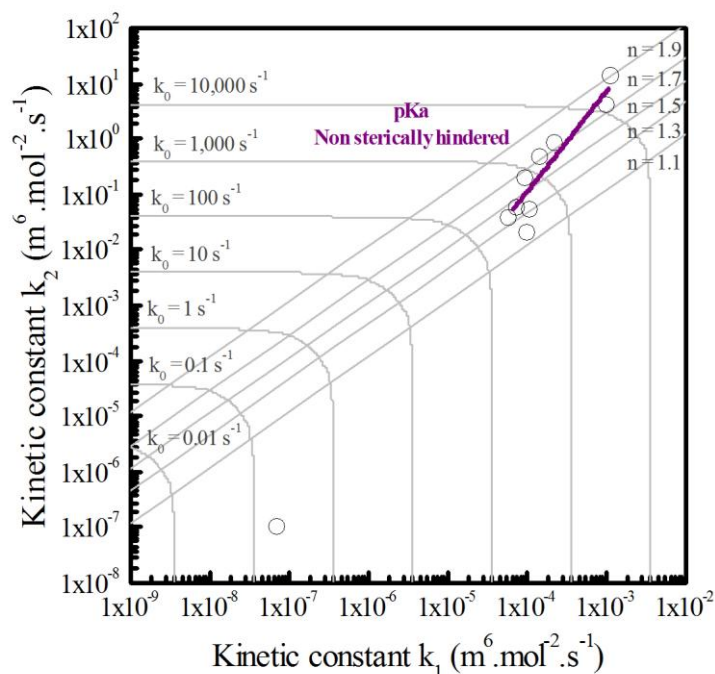


Figure V-33. Kinetic constant  $k_2$  as a function of the kinetic constant  $k_1$  for all studied secondary cyclic amines.

## 6 Multi-amines

We compare results of the three diamines with mono-amines results. We compare the reactivity of the diamine with equivalent monoamine based on the most reactive function of the diamine.

### 6.1 *N,N,N',N'*-Tetramethylethylenediamine

*N,N,N',N'*-tetramethylethylenediamine (molecule 2300), is a diamine which has two tertiary amine functions: the first one of unprotonated amine which has a higher pKa than CO<sub>2</sub> (9.19) and the second one of monoprotated amine which has a lower pKa than CO<sub>2</sub> (5.87). In this work we assume that the reactivity with the second amine function is so slow that it does not impact the kinetics of the most acid function. In summary, we consider that with multi-amine behave as a mono tertiary amine. We represent this molecule with the trend of mono tertiary amines which do not contain accessible alcohol groups as indicated in Figure V-34.

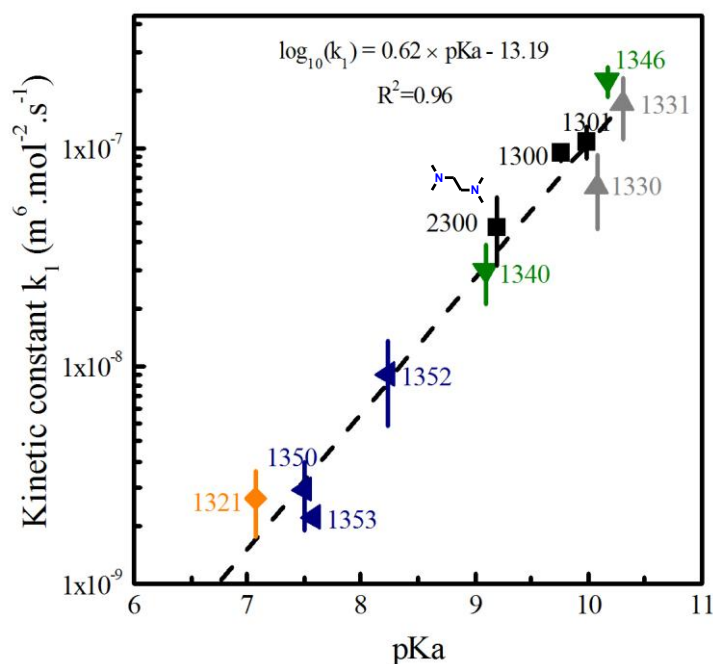


Figure V-34. Kinetic constant  $k_1$  as a function of the pKa for mono- tertiary amines which do not contain accessible alcohol groups and *N,N,N',N'*-tetramethylethylenediamine.

This figure shows that molecule 2300 follows the trend of molecules which do not have accessible alcohol groups. There is a factor 1.3 between the experimental value of  $k_1$  of molecule 2300 and the estimated value by the mono-amine fit. With the experimental and fit uncertainties, it is not possible to be certain that the factor 1.3 is due to the second amine function. It is likely that an entropic effect contributes to increase the kinetics of a diamine compared to a monoamine of the same pKa. Indeed, contrary to mono-amines, there are two equivalent reactive groups before the amine reacts. In other words, for a same amine

concentration there are twice more chances for a diamine molecule to react with a molecule of  $\text{CO}_2$  than for a mono-amine of equivalent  $\text{pK}_a$ .

## 6.2 1-Methylpiperazine

1-methylpiperazine (molecule 2201) is a diamine with one secondary amine function which form carbamates and a tertiary amine function both in the same cycle. The secondary amine protonates first ( $\text{pK}_a$  of 9.10 against 4.67 for the tertiary amine with the protonated secondary function). Moreover we show that formation of carbamates is by far faster than carbonates formation. For this reason we assume that this molecule behaves as a non sterically hindered mono cyclic amines and represent it in Figure V-35.

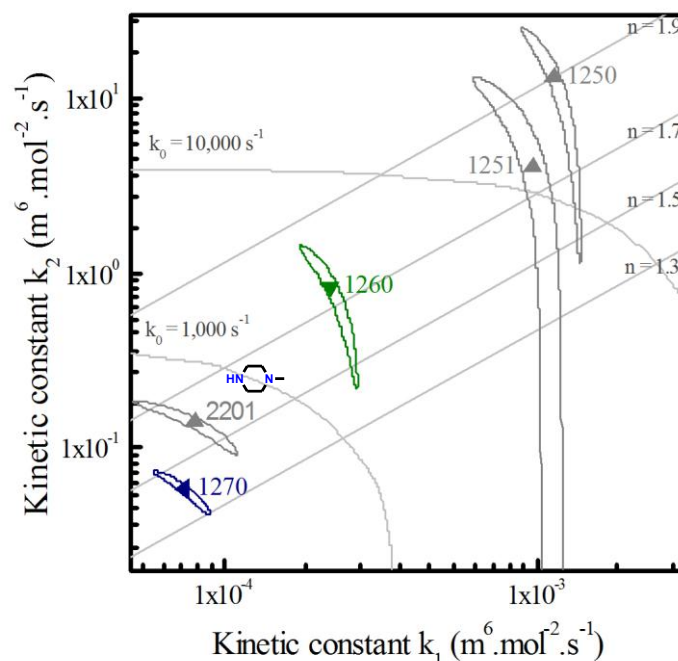


Figure V-35. Kinetic constant  $k_2$  as a function of the kinetic constant  $k_1$  for a series of secondary cyclic mono-amines and 1-methylpiperazine. Alkyl cyclic amines (grey triangles), 4-hydroxypiperidine (green triangle) and morpholine (blue triangle).

This molecule has an order of around 1.6 and seems to follow the trend of a non sterically hindered mono cyclic amines. We compare result of each kinetic constant as a function of the  $\text{pK}_a$  to the trend previously obtained as indicated in Figure V-36. We observe that the monoamine fit represents quite well the experimental values of  $k_1$  and  $k_2$ , which indicates that 1-methylpiperazine behaves as a cyclic secondary mono-amine.

## 6. Multi-amines

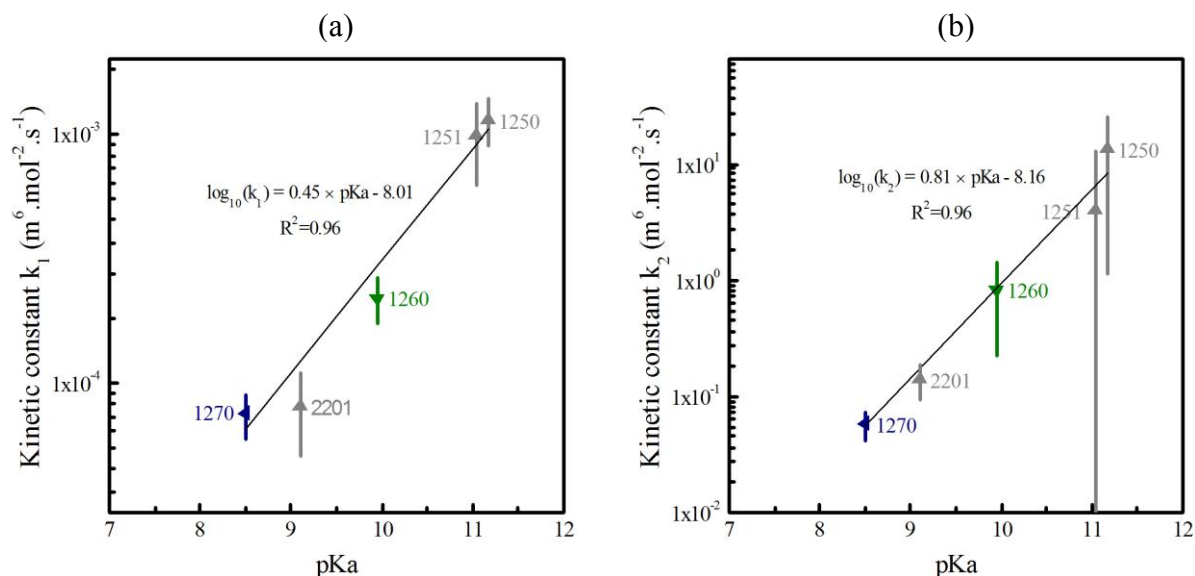


Figure V-36. Evolution of kinetic constant  $k_1$  (a) and  $k_2$  (b) as a function of the pKa for a series of secondary cyclic amines and 1-methylpiperazine. Alkyl cyclic amines (grey triangles), 4-hydroxypiperidine (green triangle) and morpholine (blue triangle).

### 6.3 Piperazine

Finally we also study piperazine (molecule 2200) which is a multi-amine with two secondary amine functions both in the same cycle. The first pKa of the molecule is 9.60 and the pKa of the second function is 5.48. We assume that the reactivity of the less reactive function is negligible in front of the most reactive. Then we represent on Figure V-37, the result obtained for this molecule in comparison with the series of mono-secondary cyclic amines. We also represent the result of molecule 2201.

This molecule presents an apparent order of around 1.7 and seems to follow the trend of non sterically hindered mono cyclic amines. We compare result of each kinetic constant as a function of the pKa to the trend previously obtained as indicated in Figure V-38. For the kinetic constant  $k_1$ , we observe a 1.6 fold increase with respect to the prediction of the mono-amine fit and a 2.0 fold increase for  $k_2$ . These results indicate that the behavior of this molecule seems to be faster than the trend. As same as molecule 2300 we assume that this effect is mainly due to the symmetric structure of the molecule. Indeed, before molecule 2200 reacts, there are two equivalent amine functions in comparison with equivalent mono-amine. Then there are twice more chances to find the good configuration and then for entropic reasons, we explain that this molecule will react twice faster than the observed trend for mono-amines.

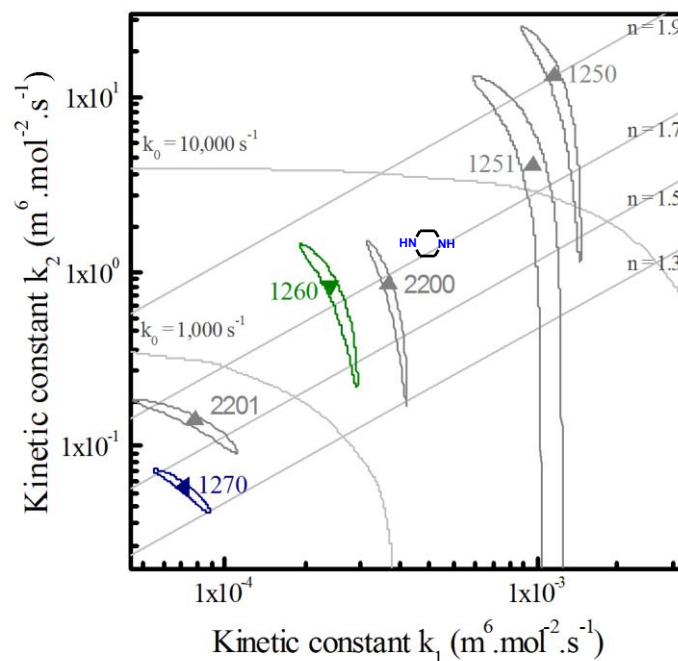


Figure V-37. Kinetic constant  $k_2$  as a function of the kinetic constant  $k_1$  for a series of secondary cyclic mono-amines, 1-methylpiperazine and piperazine. Alkyl cyclic amines (grey triangles), 4-hydroxypiperidine (green triangle) and morpholine (blue triangle).

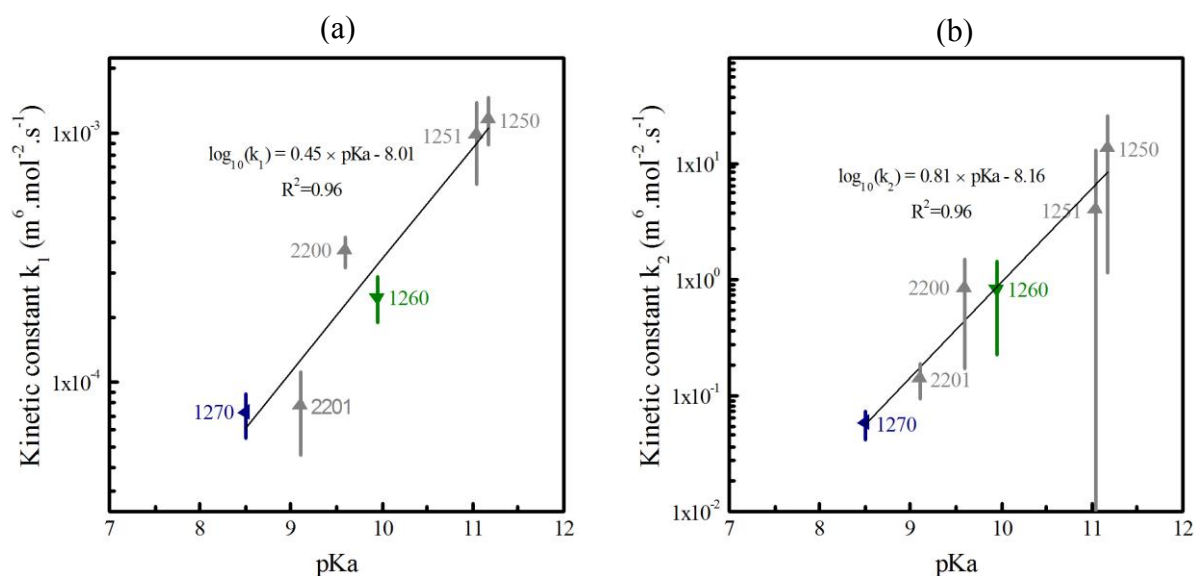


Figure V-38. Evolution of kinetic constant  $k_1$  (a) and  $k_2$  (b) as a function of the pKa for a series of secondary cyclic amines, 1-methylpiperazine and piperazine. Alkyl cyclic amines (grey triangles), 4-hydroxypiperidine (green triangle) and morpholine (blue triangle).

## 6.4 Conclusion

In this part we study three different multi-amines. We can class them into two kinds of multi-amines: on the one hand N,N,N',N'-tetramethylethylenediamine and piperazine which are symmetric amines and on the other hand 1-methylpiperazine which is asymmetric. In the case of asymmetric multi-amines we notice that they seem to behave as mono-amine with corresponding value of hindrance and basicity. However, in the case of symmetric multi-amines they seem to react twice faster than equivalent mono-amines on the basis of our preliminary results. We assume in this case that there is a positive entropic effect on the kinetic constants. Indeed, because of the symmetry of the amine, there are two equivalent amine functions for a di-amine before it reacts. Then a symmetric diamine has twice more chances to react with CO<sub>2</sub> than a monoamine with equivalent mono-amine function in terms of basicity and steric hindrance.

## 7 Discussion

Figure V-39 synthesizes the results obtained for the different classes of amines. The apparent first order kinetic constants  $k_0$  of the reaction between amine and carbon dioxide varies over 8 orders of magnitude with an apparent order between 1 for the slowest amines and almost 2 for the fastest.

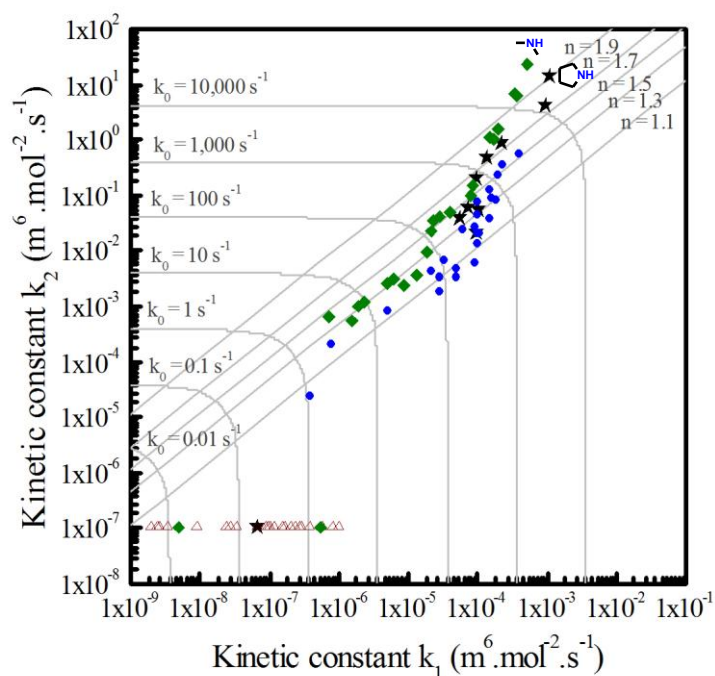


Figure V-39. Kinetic constant  $k_2$  as a function of the kinetic constant  $k_1$  for all mono-amines studied. Tertiary amines (red triangles), primary amines (blue circles), acyclic secondary amines (green diamonds), cyclic secondary amines (black stars).

Amines of class A, which consists of tertiary amines and three severely sterically hindered secondary amines, react with CO<sub>2</sub> to form carbonates. This reaction is first order

with respect to amine. For the sake of 2D representation, we set the value of  $k_2$  at  $1.0 \times 10^{-7} \text{ m}^6 \cdot \text{mol}^{-2} \cdot \text{s}^{-1}$ . Most of these amines are less reactive than primary and secondary amines which form carbonates. We notice that other things being equal, their kinetic constant  $k_1$  increase when the basicity of the amine increase. In this work we show that presence and the ability of alcohol group to interact with water in the reaction mechanism also impact the kinetic properties. Inductive effects of tertiary amines also drive the value of the kinetic constant.

We represent in Figure V-40 both reaction mechanisms proposed for tertiary amines. In the case of based-catalyzed mechanism (Figure V-40 (a)) which is one-step protonation of the amine and reaction between hydroxyde ion and carbon dioxide. In the case of the zwitterion mechanism (Figure V-40 (a)), the amine first reacts with the carbon dioxide to form a zwitterion which is then hydrolyzed by water. From an enthalpic point of view, the amine can react with two acidic compounds: carbon dioxide or water. Among both, carbon dioxide is the strongest acid. From the entropic point of view, other things being equal, each reaction need to bring the three molecules to happen. If we assume that both mechanisms happen in the same entropic conditions, enthalpy is in favour of a first nucleophilic addition of the amine on the carbon dioxide. This assumption is consistent with experimental observations concerning the continuity of kinetic constant  $k_1$  for acyclic secondary amines with increasing steric hindrance until to reach severely hindered secondary amines which behaves as tertiary amines (Chapter V .4.3.1). Considering this new argument, we propose in the case of the based-catalysed hydration mechanism that the amine reacts on the carbon dioxide which reacts on water in a one step mechanism. In this case, based-catalysed hydration mechanism is in the continuity of the termolecular mechanism proposed for primary and secondary amines in the case of a one step mechanism. Zwitterion mechanism is already consistent to explain continuity between amines which form carbamates and amines which form carbonates in the case of a two steps mechanism. For each mechanism the kinetic constant can be improved by hydrogen bonding of groups  $R_1$ ,  $R_2$  and/or  $R_3$  with water.

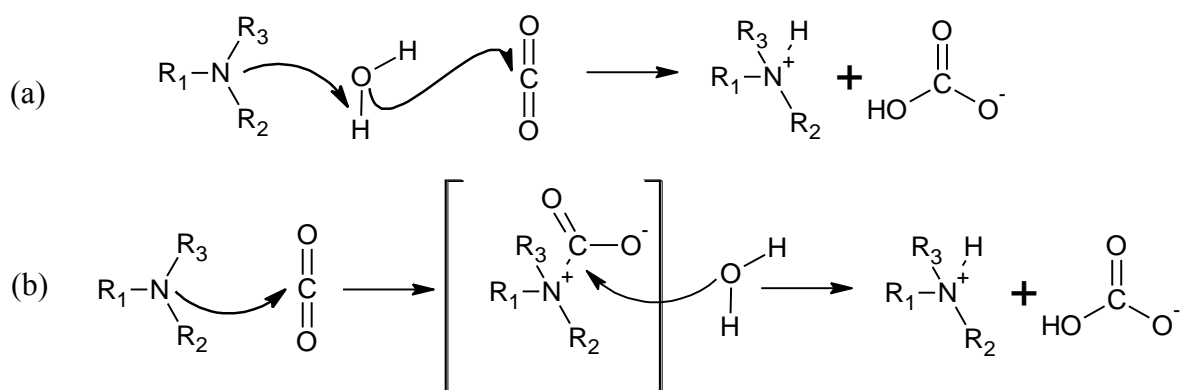


Figure V-40. (a) Based-catalyzed hydration mechanism. (b) Zwitterion mechanism for tertiary amines.

All studied primary amines form carbamates. The kinetic constants  $k_1$  and  $k_2$  are mainly driven by the basicity and the steric hindrance of the molecule. We evidence in this

## 7. Discussion

work that the sensitivity of each of these two parameters on the kinetics is also dependent of the other.

Most of acyclic secondary amines react with  $\text{CO}_2$  to form carbamates. A tert-butyl substituent defines a severe hindrance which leads the amine to react as tertiary amine and to form carbonates. This effect is observed on two amines of different values of pKa which shows that steric hindrance is the predominant factor to determine if an amine form carbonates or carbamates whatever its degree of substitution. It seems quite logical that the order of steric hindrance, other things being equal is primary amines < secondary amines < tertiary amines. As the steric hindrance of secondary amines is closer of steric hindrance of tertiary amines than primary amines, it is normal than the most sterically secondary can have the same steric hindrance than tertiary amines. We also observe the interdependency of both electronic and steric effects, just as for primary amines. During the change of degree of substitution between primary and corresponding secondary amine with a methyl group linked to the nitrogen, there is a competition between the additional +I inductive effect which improves kinetic properties and the steric hindrance which reduce them. The predominance of inductive effect on steric hindrance depends on the pKa of the molecule.

In the case of cyclic secondary amines the kinetic constants  $k_1$  and  $k_2$  are also mainly driven by the basicity and the steric hindrance of the molecule. As same as acyclic secondary amines, for cyclic secondary amines, a huge steric hindrance can lead the amine to react as tertiary amine and then to form carbonates.

Finally we study three diamines. The asymmetric diamine N-methylpiperazine with one tertiary function and one secondary amine function reacts as a mono-amine of equivalent pKa and steric hindrance. Both symmetric amines either with two tertiary or two secondary functions react faster than corresponding mono-amines. We assume that this difference can be explained by an entropic effect linked the increased probability of reaction with  $\text{CO}_2$ .

We compare the reactivity of tertiary amines with non sterically hindered linear primary amines, acyclic secondary amines and cyclic secondary amines. We represent in Figure V-41 the corresponding series of non sterically hindered amines as a function of the pKa for kinetic constant  $k_1$  (a) and  $k_2$  (b). We observe that tertiary amines are by far the less reactive in comparison with all the others confirming previous observations. Most of the time linear primary amines are slower than secondary amines. However, for lower pKa value, the inductive effect of the second group of acyclic secondary amines is not enough to counterbalance the effect of its steric hindrance and then in this condition primary amines can have better kinetic properties. We also observe that cyclic secondary amines are the most nucleophilic amines. Indeed, they benefit from inductive effect of two groups and are generally less sterically hindered than acyclic secondary amines.

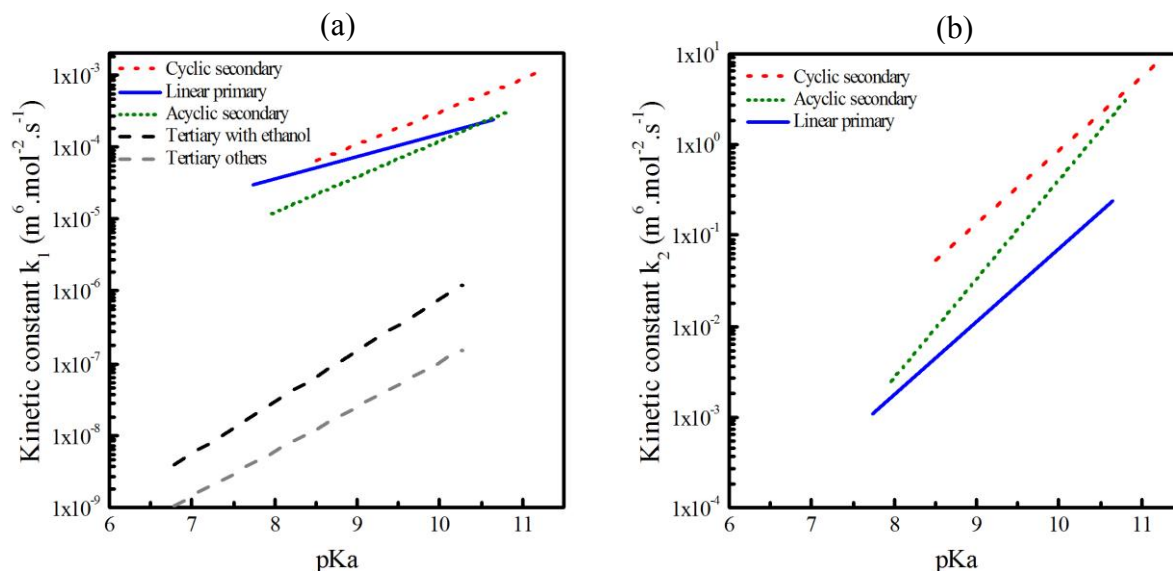


Figure V-41. Evolution of kinetic constant  $k_1$  (a) and  $k_2$  (b) as a function of the pKa for the series of tertiary amines and non sterically hindered primary and secondary amines studied.

We saw that it is not obvious to observe the effect of the steric hindrance on kinetic constants for two main reasons. On the one hand, it is impossible for a series of molecule to change only one parameter. Indeed the change of a group affect electronic and geometry of the molecule even if the effect can be more important for one of these parameters. On the over hand it does not exist universal descriptor of the steric hindrance. It is thus difficult to quantify this effect, even relatively.

On the basis of our observations the secondary amines with low steric hindrance are the faster molecules. Among the mono-amines studied, dimethylamine and pyrrolidine are the fastest molecules with the lowest possible steric hindrance for secondary amines. To increase further the kinetics of reaction with  $\text{CO}_2$ , it is necessary to increase the nucleophilicity by addition of inductive donor group. Nevertheless addition of donor group implies to increase the steric hindrance which has a negative effect on the kinetics which counterbalances the effect of the increased electronic density. Therefore we have not found faster mono-amines and assume that there is no mono-amines which reacts faster than dimethylamine and pyrrolidine with  $\text{CO}_2$ .

The choice of fast amine or activator in a post combustion process shall also be driven by other criteria. That is why it is important to be able to predict kinetic properties of each molecule to find the best candidate which should optimize all parameters affecting the efficiency and the costs of the process (thermodynamic, chemical stability, solubility, viscosity, price of the amine, volatility, *etc*) and to answer to the safety requirements (toxicity, corrosivity, *etc*).

## 8 *Conclusion*

We have presented the experimental results obtained for 25 primary, 34 secondary, 25 tertiary amines and 3 multi-amines.

In addition to the influence of the basicity which has been shown in the literature, we point out the specific role of alcohol functions and inductive effects in the case of amines which form carbonates. In the case of molecules which form carbamates, we show that there is an interdependent effect of basicity and steric hindrance to explain the variations of kinetic constants  $k_1$  and  $k_2$ . A positive entropic effect explains the positive effect on the kinetics of symmetric diamines.

After identifying the main effects which drive the kinetic properties and their complex interactions, we present in the next chapter the statistical approach which leads to the establishment of quantitative structure-property relationship based on molecular descriptors of the amines.

«. »

A Ddd

## Chapter VI: QSPR MODELLING

---

### 1 General points

In the previous chapter, we identified two kinds of amines with respect to their reaction with CO<sub>2</sub>, the former giving carbonates and the latter giving carbamates. In the first case, we have determined one third order kinetic constant  $k_1$ . In the second case, we have determined two kinetic constants  $k_1$  and  $k_2$ . These constants determine the rate of reaction of a given amine with CO<sub>2</sub> at 25 °C, in the studied range of concentration as indicated in Equation 67 in Chapter IV .3.1.1.

On the basis of these two sets of data, we build two distinct structure-property models which should be able to predict the kinetic constants of any mono-amine. The three studied multi-amines have not been included in the construction of the model. The first set of data consists in 25 tertiary amines and 3 sterically hindered secondary amines which form carbonates. The second set of data consists in 25 primary and 34 secondary amines, including the three sterically hindered secondary amines. By keeping these three molecules in both datasets, we expect to test the ability of both models to predict the behaviour of this kind of amines. The Quantitative Structure-Property Relationship models which are presented in this part are derived from a methodology known as Quantitative Structure-Activity Relationship (QSAR)(Todeschini *et al.*, 2009).

QSPR modelling consists in setting up a model which quantitatively predicts a given set of properties of a group of species in the framework of a specific study. There are two major difficulties to set up this model. The first difficulty consists in choosing a method to transcribe the molecule under a mathematical form (vector, polynomial function, etc) which describes correctly the structure. Then the second difficulty consists in choosing the degree of complexity of the model in order to obtain a balance between the accuracy of the prediction and the complexity of its implementation (Todeschini *et al.*, 2009).

In this study, each amine is characterized by means of molecular descriptors, which corresponds to electronic or structural parameters of molecules mainly calculated by molecular modelling. These descriptors are then linked to the kinetic constants  $k_1$  and  $k_2$  through a partial least square (PLS) model. Indeed, this kind of model has already been used to predict the chemical stability of amines properties in conditions of high temperature and partial pressures of carbon dioxide (Martin *et al.*, 2012). We call this method the QSPR descriptor modelling. Equation 73 represents the form of a QSPR descriptor model. It relates the kinetic constant, which is the property to be predicted, to molecular descriptors through a polynomial function determined by statistical method of regression.

$$k_i = f(\text{descriptors}) + \text{residual}$$

$$f \rightarrow \text{polynomial function}$$
Equation 73

## 2. QSPR descriptor model

In the following sections we first describe the different descriptors, statistical tools and the process followed to set up the QSPR model. Then we present the results obtained with this method and attempt to provide a physico-chemical explanation. Finally we conclude concerning the QSPR modelling.

## 2 QSPR descriptor model

In this section we first present the different identified descriptors together with the theory/methodology how to calculate them. Then we describe the QSPR model, its input data and the process of optimization leading to the best result.

### 2.1 Descriptors

Generally, most of the properties of molecules results from different contributions of electronic and geometric parameters which are contained in molecular descriptors as indicate some examples in Table VI-1 (Todeschini *et al.*, 2009).

Table VI-1. Examples of some electronic and geometric descriptors.

Electronic descriptors	Geometric descriptors
Charge of the nitrogen atom	Volume, surface
Basicity (pKa)	Number of bonds and hydrogen bonds
Energetic levels of orbitals	Flexibility

Since theoretical molecular descriptors are generally calculated for a single molecule in gas phase (*i.e.* no collective effects are considered), it is important to remark that the value of the descriptors will depend on the conformation of the molecule. Consequently it seems quite obvious to consider the most stable (*i.e.* more probable) conformation. That is the conformation exhibiting the lowest value of internal energy (sum of potential and kinetic energy). As a consequence, a previous step of geometrical optimization becomes necessary before calculating the descriptors. In this way different wide-known algorithms are available in the literature based on the calculation of the total energy of the system. In order to determine this energy two main groups of modelling methods to determine theoretical molecular descriptors: quantum chemistry methods and molecular mechanics (based on the use of force fields). In the next, both methodologies are briefly described (Leach, 2001).

Quantum chemistry methods consist in solving the Schrödinger equation with different levels of approximation depending on the formalism used. Despite it is impossible to eliminate all approximations, and residual error inevitably remains, this group of methods allows to determine with a high level of accuracy the optimal conformation of the molecule.

When considering larger systems or needing significantly lower computational efforts, molecular mechanics methods allow to obtain the optimized structures avoiding the use of

quantum chemistry. This group of methods relies on the use of simple classical expressions to describe the energy of the system (for example the harmonic oscillator to describe the vibration energy of a given bond). This group of simple expressions constitutes the force field. The parameterization of the force field (*i.e.* determining the constants appearing in the different expressions) is realized beforehand from experimental data or quantum calculations. Different force fields are readily available in the literature or implemented into the different software packages.

In this study we used three kinds of descriptors: standard theoretical descriptors which are proposed in common molecular modelling softwares, specific theoretical descriptors that we develop to evaluate the steric hindrance and experimental descriptors. In the next sections, we describe the optimisation and calculation method and bring a short description of the calculated descriptors.

### 2.1.1 Standard theoretical descriptors

#### 2.1.1.1 Geometrical optimisation

Prior to the calculation of generic descriptors, Density Functional Theory (DFT) calculations at the level of B3LYP/cc-pVTZ(-F)++//B3LYP/6-311G(d,p) were performed with Jaguar version 7.9 (Schrödinger, LCC, 2012) (Jaguar, 2013) to optimize the geometry in both the gas and aqueous phase. When optimization concerned aqueous phase, we used the Poisson-Boltzmann continuum solvation model with the following standard parameters for water: dielectric constant of 80.37, molecular mass of 18.02 g.mol<sup>-1</sup>, a density of 0.998 g.mL<sup>-1</sup> and a probe radius of 1.40 Å. For more clarity, in the following we class the descriptors in different categories. When nothing is specified, the descriptors have been calculated only in the gas phase.

#### 2.1.1.2 Presentation of descriptors

There are two kinds of standard theoretical descriptors: on the one hand those that need quantum calculation and on the other hand those that can be calculated with molecular mechanics methods. Descriptors of the class n° 1 to 3 have been obtained by quantum calculation using the Jaguar 7.9 software (Jaguar, 2013) and descriptors of the class n° 5 to 17, which only need molecular mechanics methods, have been calculated using the Material Studio's QSAR module (Material Studio, 2013). In what follows, we succinctly describe the different calculated descriptors.

Class n°1: energetic levels and dipole moment. The energetic levels of Highest Occupied Molecular Orbital (HOMO) and Lowest Unoccupied Molecular Orbital (LUMO) were determined from quantum calculations. In the same way the difference between HOMO and LUMO (HOMO-LUMO) and the total dipole magnitude (Dipole) were extracted from the same calculation. HOMO level gives information about the reactivity of the electrons shared to form a bond with another reagent and accepted in LUMO. Calculations have been realized in aqueous and gaseous phase.

## 2. QSPR descriptor model

Class n°2: polarisability and hyperpolarisability. Polarisability ( $\alpha$ ) and hyperpolarisability ( $\beta$ ) reflect the degree of potential disturbance of an electron cloud by an electric field. Both parameters are defined in Equation 74 where  $\mu$  is the permanent dipole of the molecule,  $\mu'$  is the induced dipole of the molecule and E is the external electric field.

$$\mu' = \mu + \alpha E + \frac{1}{2} \beta E^2 + \dots \quad \text{Equation 74}$$

Class n°3: solvation energy. Solvation energy ( $E_{\text{solv}}$ ) corresponds to the variation of energy when the molecule is transferred from the gas phase into aqueous phase. The more the polarity of the molecule is important, the more this transfer is favourable and the more this energy is negative.

Class n°4: basicity of the molecule. The basicity has been determined thanks to value of the pKa obtained from the Chemicalize online calculation tool website (Chemicalize, 2013). This value is calculated from relation indicated by Equation 75. In this equation, Q corresponds to the partial charge increment, P is the polarizability increment, S corresponds to the sum of the structure specific increments and a, b, c and d are regression coefficients specific to the ionization site. Values of these parameters are specific to the software. According to (Szegezdi and Csizmadia, 2007) the standard deviation of the regression obtained from 269 molecules is 0.75.

$$pKa = a \times Q + b \times P + c \times S + d \quad \text{Equation 75}$$

Class n°5: structural descriptors. Four structural descriptors have been calculated: Chiral centers which is the number of chiral centers (R or S) in a molecule, Rotatable bonds which corresponds to the number of rotatable bonds, Hydrogen bond acceptor which is the number of hydrogen-bond acceptors and Hydrogen bond donor which is the number of hydrogen-bond donors.

Class n°6: thermodynamic descriptors. Two variants of the decimal logarithm of the partition coefficient between octanol and water have been determined: Alog P and Alog P98 along with the molar refractivity. LogP is related to the hydrophobic character of the molecule. The molecular refractivity index of a component is a combined measure of its size and polarizability (Ghose and Crippen, 1986).

Class n°7: topologic descriptors. Balaban's descriptors (JX and JY) (Balaban, 1982; Balaban and Ivanciuc, 1989), Kier & Hall's descriptors (Kappa and Chi) (Kier and Hall, 1976; Kier and Hall, 1985; Kier and Hall, 1990), index of Wiener (Wiener, 1947) and Zagreb (Bonchev, 1983) and molecular flexibility (Hall, 1991). They differentiate molecules as a function of their size, number of atoms, cyclic structure, degree of branching, flexibility and general form.

Class n°8: multigraph information content descriptors. To determine information-content descriptors, molecules are viewed as structures that can be partitioned into subsets of elements that are in some sense equivalent. The notion of equivalence depends on the particular descriptor. Four descriptors of this class have been calculated: information content (IC), bonding information content (BIC), structural information content (SIC) and complementary information content (CIC) (Bonchev *et al.*, 1981; Bonchev, 1983; Katritzky and Gordeeva, 1993; Rohrbaugh and Jurs, 1987).

Class n°9: electrotopological descriptors. Electro-topological state keys are numerical values, computed for each atom in a molecule, which encode information about both the topological environment of that atom and the electronic interactions due to all other atoms in the molecule (Hall and Kier, 1995). The topological part of the relationship is based on the distances between each atom and all other atoms in the molecule. The electronic part is based on an intrinsic state value, plus perturbation due to the differences of intrinsic state between atoms in the molecule. The descriptor calculated E-state keys (sums): S<sub>ssCH2</sub> corresponds to the sum of the electro-topological state keys.

Class n°10: Van der Waals surface and Van der Waals volume. These two descriptors describe the surface and volume which envelop the molecule (Figure VI-1). It corresponds to the surface which intersects with the Van der Waals radii of the atoms in the structure (equivalent of the surface of the solvent with a probe radius equal to 0 Å). The molecular Van der Waals surface determines the extent to which a molecule exposes itself to the external environment. This descriptor is related to binding, transport, and solubility properties. Molecular volume is only related to binding and transport.

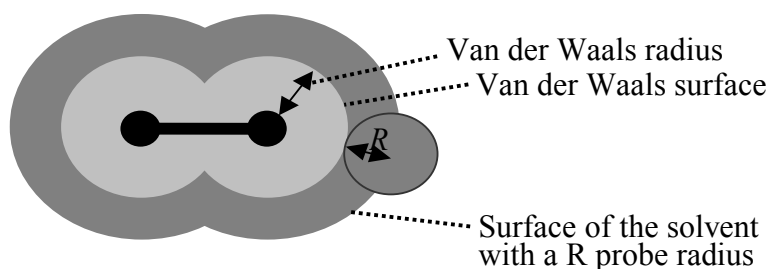


Figure VI-1. Van der Waals surface.

Class n°11: molecular density. Molecular density is defined as the ratio between the molecular weight and the molecular volume, expressed in  $\text{g}\cdot\text{ml}^{-1}$ . The molecular density reflects the types of atoms and how tightly they are packed in a molecule. It can be related to transport and melting behavior.

Class n°12: moments of inertia. The moments of inertia (magnitude, or its projections on the X, Y or Z axis) are determined by means of Equation 76 where  $m_i$  is the mass of the molecule and  $d_i$  is the perpendicular distance from each atom to the axis (Hill, 1960).

## 2. QSPR descriptor model

$$I = \sum_i m_i \times d_i^2 \quad \text{Equation 76}$$

Class n°13: radius of gyration. The radius of gyration is a structural descriptor calculated according to the expression indicated in Equation 77 where N is the number of atoms and x, y, and z are the atomic coordinates relative to the center of mass.

$$R_g = \sqrt{\frac{\sum (x_i^2 + y_i^2 + z_i^2)}{N}} \quad \text{Equation 77}$$

Class n°14: ellipsoidal volume. The ellipsoidal volume describes the volume of the ellipsoid of inertia derived from the inertia tensor of the system. This has axes proportional to the inverse of the square root of the principal moments of inertia, aligned along the principal axes.

Class n°15: molecular shadow indexes: distance, surface and volume. The shape of a molecule can be described by its projection over the different planes of a three-dimensional space (XY, XZ and YZ) as indicated in Figure VI-2. Since this calculation depends on the conformation and of the orientation of the molecule, the molecule is aligned with the main axis of the moment of inertia (Rohrbaugh and Jurs, 1987). Nine descriptors can be calculated:

- 3 lengths: lengths of the shadows projected over the X, Y and Z direction;
- 3 surfaces: surfaces of the shadows projected about the XY, XZ and YZ planes;
- 3 fractions: surface of the molecular shadow / surface of the enveloping rectangle.

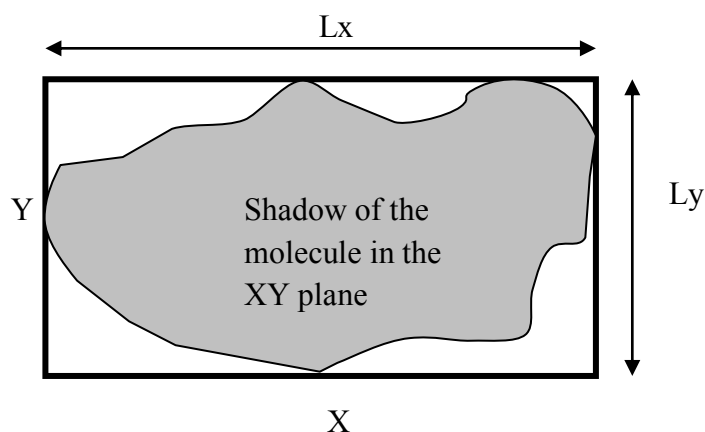


Figure VI-2. Projection of the molecule in the z direction.

Class n°16: dipole moments descriptors. These descriptors characterize the molecular dipole moments from partial charges (contrary to the dipole moments determined from quantum calculations in the first group of descriptors) defined on the atoms of the molecule. Partial charges of each atom are CHarges from Electrostatic Potentials using a Grid based method (CHELPG) calculated from a fit of the electrostatic potential (Breneman and Wiberg, 1990). Charges have been calculated from the Jaguar software and then imported in Material Studio. We determine the dipole moment magnitude as well as the X, Y and Z components.

Class n°17: jurs descriptors. This set of 30 descriptors combines shape and electronic information to characterize molecules. The set is based on the work by (Stanton and Jurs, 1990). The descriptors are calculated by mapping atomic partial charges onto solvent-accessible surface areas of individual atoms.

### 2.1.1.3 Selection of descriptors

A classification needs to be applied on the 110 descriptors, on the basis of their values calculated on 87 amines. This classification aims to select the descriptors which are the less correlated with each other. If it exists various statistical methods of classification of individuals (Cordon, 1999), there are many fewer for the classification of variables (Vigneau and Qannari, 2003). In order to classify descriptors we use the method called "clustering of variables around latent components". This technique combines by successive integration the descriptors in classes which are each represented by a latent component. A latent component of a class corresponds to a linear combination of descriptors which compose the class. This classification is a first step to identify descriptors which are strongly correlated by regrouping them in different classes. This classification is represented by the dendrogram in Figure VI-3.

The interruption of the dendrogram to a given level indicates a partition of descriptors for the same number of classes as there are branches at the corresponding level. Each of this class can be represented with a latent variable. The initial partition corresponds to step zero of the treatment. This partition corresponds to the case where each descriptor corresponds to a class. When the number of classes diminishes, the most correlated descriptors combine inside a class around latent variables. After, each latent variable in turn combines to form a series of interlocked partitions. When the information is classified, the number of variables (descriptors) diminishes and there is a loss of information. The variance of data which corresponds to a partition is called explicated inertia. Even if there are no formal rules to determine the optimal partition, this choice must bring to a reasonable number of classes with a significant explicated inertia (generally around 80 %). In this work we consider that the partition giving 12 classes with 77.0 % percent of explicated inertia is the optimal. In Figure VI-3, each class is represented with a specific color and the number of each descriptor is also indicated.

## 2. QSPR descriptor model

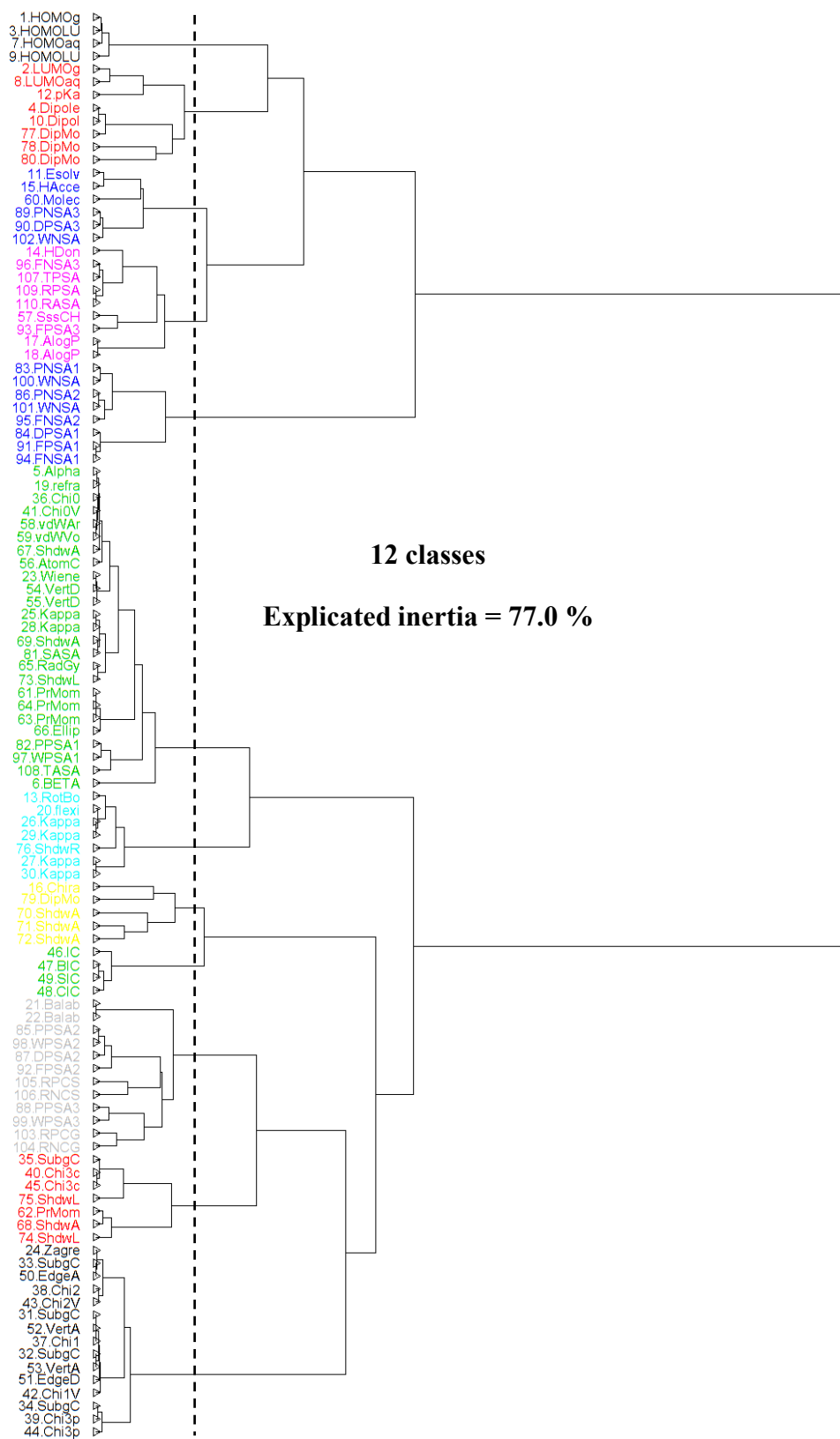


Figure VI-3. Dendrogram of the 110 generic theoretical descriptors. Dashed line indicates a partition of descriptors into 12 classes which correspond to an explicated inertia of 77.0 %.

Inside each class of the dendrogram, we represent the scatter plots of the different descriptors of the corresponding class. Each plot represents the values of one descriptor calculated for the 87 amines as a function of the values of another descriptor. In Figure VI-4 we represent the scatter plot of the descriptors of the class 1. For each class we retain the descriptors which appear visually to be the less correlated. For example in the class 1, we only retain HOMOg and HOMOLUMOaq.

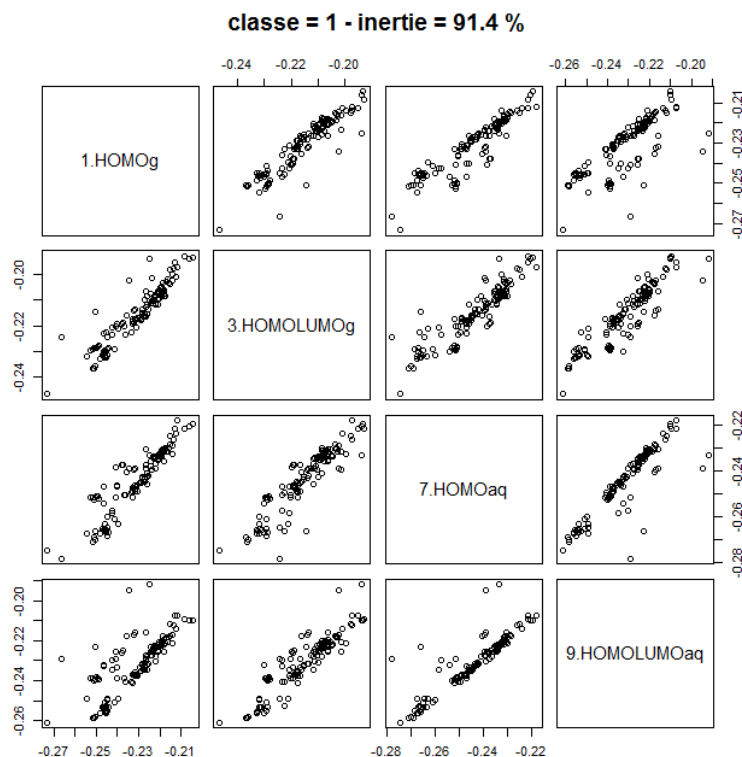


Figure VI-4. Scatter plot of variables of the class 1. Inertia of the class = 91.4 %. Variables are HOMOg, HOMOLUMOg, HOMOaq, HOMOLUMOaq.

From the 110 initial descriptors, and thanks to the dendrogram and the observation of each scatter plot, we select the 66 less correlated variables. They are indicated in bold in the Table IX-20 in Chapter IX .9. In the next part we present the specific theoretical descriptor and the experimental descriptor we add to the 66 retained standard theoretical descriptors.

### 2.1.2 Specific theoretical descriptor of the steric hindrance

Class n°18: steric hindrance. We have seen previously that steric hindrance of the nitrogen is a key factor on the rate of the amine-CO<sub>2</sub> reaction. Parameters such as the Taft constant are available to describe the steric hindrance owing to the presence of a given substituent in a series of similar-structured amine molecules (*i.e.* the effect relative to a reference molecule). Nevertheless, this descriptor is not able to provide a universal and absolute value for the totality of the considered molecules. Consequently, using this type of descriptors is not adequate for a QSPR approach. For this reason we have developed a molecular descriptor that we name the Nitrogen Accessible Surface which is directly inspired

## 2. QSPR descriptor model

from calculation of accessible area of solids as MOF and zeolites (Düren *et al.*, 2007; Düren, 2013). This descriptor consists in determining the contribution of the nitrogen of the amine group to the total Van der Waals surface. In other words we calculate the surface area of the nitrogen atom of the amine function which is not shared with the Van der Waals surface of any other atom of the molecule. This surface is illustrated by the blue points of the Figure VI-5. We expect the value of this surface to be correlated with the accessibility for the CO<sub>2</sub> molecule to the amine group. In other words, as lower the value of the nitrogen accessible surface is, the higher the steric hindrance will be. This seems to be quite intuitive if we consider two completely different scenarios. On one hand, if we consider primary amines we expect to obtain the higher values for the Nitrogen Accessible Surface. On the other hand when considering tertiary amines, the nitrogen atom is almost buried into the accessible molecular surface and then the lower values for the proposed descriptor are expected.

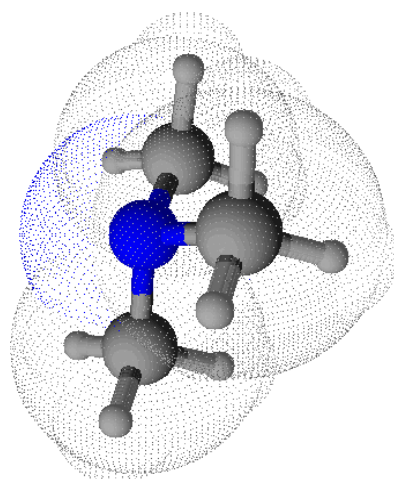


Figure VI-5. Illustration of the nitrogen accessible surface for the case of trimethylamine.

We set up this descriptor in order to describe as much accurately as possible the effect of steric hindrance which is observed on the kinetics of reaction of amines with CO<sub>2</sub>. Since our goal is to obtain a purely geometric descriptor able to determine the steric hindrance independently from electronic effects, we decided to calculate the optimal geometry by reducing the intermolecular potential to the Lennard-Jones contribution accounting for the dispersion-repulsion interactions between uncharged atoms. This operation was performed with the Conformers module of Material Studio Software with the Dreiding forcefield setting the values of the atomic punctual charges to zero (Mayo *et al.*, 1990). This fact implies that for the case of this descriptor classical molecular mechanics calculations were performed instead of the previously described quantum calculations. We precise that the selection of the Conformers module to optimize the geometries was done in order to avoid problems with local energy minima blocking. In this way the optimization is done by exploring the totality of the conformational space. This is done by systematically varying a few crucial torsion angles by a set amount. This systematic grid searching allows to obtain the global minimum.

Fianlly a homemade Monte Carlo integration code (Chapter IX .10.1) was used to determine the nitrogen accessible surface of the different molecules. The methodology used

consists in randomly generating a huge number of points  $nb_{total}$  on the Van der Waals nitrogen surface  $S_{VDW}^N$  ( $\text{\AA}^2$ ). Then we determine the number of these points outside the Van der Waals volume of other atoms  $nb_{out}$ , in other words which are only on the Van der Waals nitrogen surface. The ratio between the number of point  $nb_{out}$  and  $nb_{total}$  indicates the probability  $P_{out}$  to obtain a point of the Van der Waals nitrogen surface not belonging to the Van der Waals volume of any other atom. As indicated in Equation 78, the nitrogen accessible surface  $S_A^N$  ( $\text{\AA}^2$ ) corresponds to the product between the probability  $P_{out}$  and the Van der Waals nitrogen surface  $S_{VDW}^N$  ( $\text{\AA}^2$ ). It is worth mentioning that a necessary condition is to generate a sufficient number of random points in order to obtain reliable values for  $S_A^N$ . The parameters (Rappe *et al.*, 1992) used in the calculations are indicated in Table VI-2.

$$S_A^N = P_{out} \times S_{VDW}^N = \frac{nb_{out}}{nb_{total}} \times S_{VDW}^N \quad \text{Equation 78}$$

Table VI-2. Van der Waals parameters used to calculate the accessible surface (Rappe *et al.*, 1992).

Atom	C	H	O	N
Van der Waals radius ( $\text{\AA}$ )	3.47	2.85	3.03	3.30

Two verifications comfort us in the suitability of this descriptor. We first notice, as indicated in Figure VI-6 (a), that primary amines present in average higher values of  $S_A^N$  than secondary and tertiary amines. This result confirms that the accessibility of the nitrogen atom decreases when the degree of substitution of the amine increases. The nature of the substituents is also very sensitive as we see for secondary amines, where  $S_A^N$  varies between  $4.36 \text{ \AA}^2$  and  $8.01 \text{ \AA}^2$ . The higher values of  $S_A^N$  for secondary amines overlap the range of  $S_A^N$  covered by primary amines ( $7.44 - 8.91 \text{ \AA}^2$ ). The inferior part of this scale corresponds to sterically hindered amines and overlaps the range of  $S_A^N$  covered by tertiary amines ( $2.08 - 5.71 \text{ \AA}^2$ ). Therefore it is possible to delimit the frontier (indicated by the vertical black line) which separates the primary and secondary amines forming carbamates ( $S_A^N > 5.7 \text{ \AA}^2$ ) from amines forming carbonates ( $S_A^N \leq 5.7 \text{ \AA}^2$ ) which consists of tertiary amines and sterically hindered secondary amines. For the first time, we show a quantitative evidence of the continuity of steric hindrance between severely hindered secondary amine which do not form stable carbamates and tertiary amines (Sartori and Savage, 1983). Finally, as indicated in Figure VI-6 (b), for the series of studied alcanolamines there is a good correlation between accessible surface and the Taft constant which is an experimental descriptor of the steric hindrance (Taft, 1976). Calculated values of the nitrogen accessible surface have been indicated in Chapter IX .10.2.

## 2. QSPR descriptor model

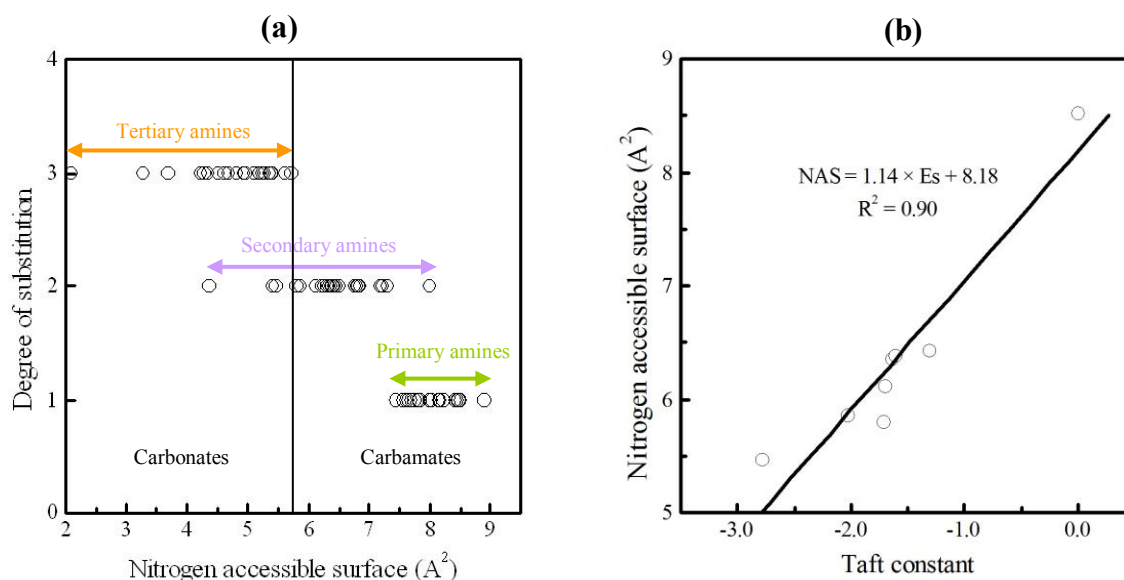


Figure VI-6. (a) Degree of substitution vs. accessible surface for the molecules studied in this work. (b) Relation between accessible surface and Taft constant for alkanolamines.

### 2.1.3 Experimental descriptor

The basicity of the amines (4) has been finally described by the value of the experimental pKa. Indeed, we show previously that the value of the pKa is strongly correlated to the kinetic properties. For this reason it is important to give the most precise description of the basicity which corresponds to the experimental value of the pKa. This descriptor is fastly determined by acid-base titration, as we have seen in chapter IV.

### 2.1.4 Conclusion

In Table VI-3 we indicate a summary of the nature of the 112 descriptors we calculate. We detail in Chapter IX .9 the precise name of each calculated descriptors. The calculation of the generic descriptors has been realized for each amines studied in this work. We calculate the value of the 110 generic descriptors for the 87 molecules. We determine the nitrogen accessible surface of all mono-amines studied in this work and we get the value of the experimental pKa for all molecules (mono and multi-amines) studied here. The value of the nitrogen accessible surface has been indicated in Chapter IX .10.

Table VI-3. List of descriptors and obtaining method.

Input	Class	Descriptors	Geometric optimization	Software	Module
1-4	1	HOMO, LUMO, HOMO-LUMO and dipole (gas phase)	B3LYP	Jaguar	B3LYP
5-6	2	Polarisability and hyperpolarisability	B3LYP	Jaguar	B3LYP
7-10	1	HOMO, LUMO, HOMO-LUMO and dipole (aqueous phase)	B3LYP	Jaguar	B3LYP
11	3	Solvation energy	B3LYP	Jaguar	B3LYP
12	4	pKa	-	<a href="http://www.chemicalize.org/">http://www.chemicalize.org/</a>	-
13-16	5	Structural descriptors	B3LYP	Material Studio	Fast descriptors
17-19	6	Thermodynamics descriptors	B3LYP	Material Studio	Fast descriptors
20	7	Molecular flexibility	B3LYP	Material Studio	Fast descriptors
21-24	7	Balaban, Wiener, Zagreb descriptors	B3LYP	Material Studio	Fast descriptors
25-30	7	Topological descriptors (Kappa)	B3LYP	Material Studio	Fast descriptors
31-35	7	Topological descriptors (Subgraph)	B3LYP	Material Studio	Fast descriptors
36-45	7	Topological descriptors (Chi)	B3LYP	Material Studio	Fast descriptors
46-56	8	IC, BIC and SIC descriptors	B3LYP	Material Studio	Fast descriptors
57	9	Electrotopological descriptor	B3LYP	Material Studio	Fast descriptors
58-59	10	Van der Waals volume and Van der Waals surface	B3LYP	Material Studio	Spatial descriptors
60	11	Molecular density	B3LYP	Material Studio	Spatial descriptors
61-64	12	Moments of inertia	B3LYP	Material Studio	Spatial descriptors
65	13	Radius of gyration	B3LYP	Material Studio	Spatial descriptors
66	14	Ellipsoidal volume	B3LYP	Material Studio	Spatial descriptors
67-76	15	Molecular shadow indices	B3LYP	Material Studio	Spatial descriptors
77-80	16	Dipole moments	B3LYP	Jaguar + Material Studio	Spatial descriptors
81-110	17	Jurs descriptors	B3LYP	Material Studio	Jurs descriptors
111	4	Experimental pKa	-	(experimental)	-
112	18	Nitrogen accessible surface	Dreiding	Material Studio	Conformers + Fortran program

## 2. QSPR descriptor model

### 2.2 QSPR model

In this section we first define the input data of the QSPR model. Then present the model and the process followed to realize the prediction of the kinetic constants. Finally, we show the different parameters fixed or to set up in order to improve the performance of the QSPR model.

#### 2.2.1 Input data

In the QSPR for each individual (amines), there are two kinds of variables. On the one hand variables used in order to build the model (descriptors) and on the other hand variables that we must predict (kinetic constant). From this point, to be clearer, we call descriptors "variables" and kinetic constant "property".

The property must be homogeneously distributed in order to be correctly predicted. We represent in Figure VI-7 the histogram of the property of tertiary amines when we directly consider the kinetic constant  $k_1$  (a), and when we consider the decimal logarithm of this constant (b). In the linear scale the bin used is  $1 \times 10^{-7} \text{ m}^6 \cdot \text{mol}^{-2} \cdot \text{s}^{-1}$  and in the logarithm scale the bin used is 0.5. In both cases we get 7 different classes. These figures clearly indicate that we obtain a better distribution with the logarithm scale than with the linear scale. This is due to the order of magnitude of the kinetic constant which varies on around 3 decades in the case of tertiary amines. This variation is over more than 5 decades for  $k_1$  and 6 decades for  $k_2$  for primary and secondary amines. The property to model and predict is thus  $y = \log_{10}(k)$ .

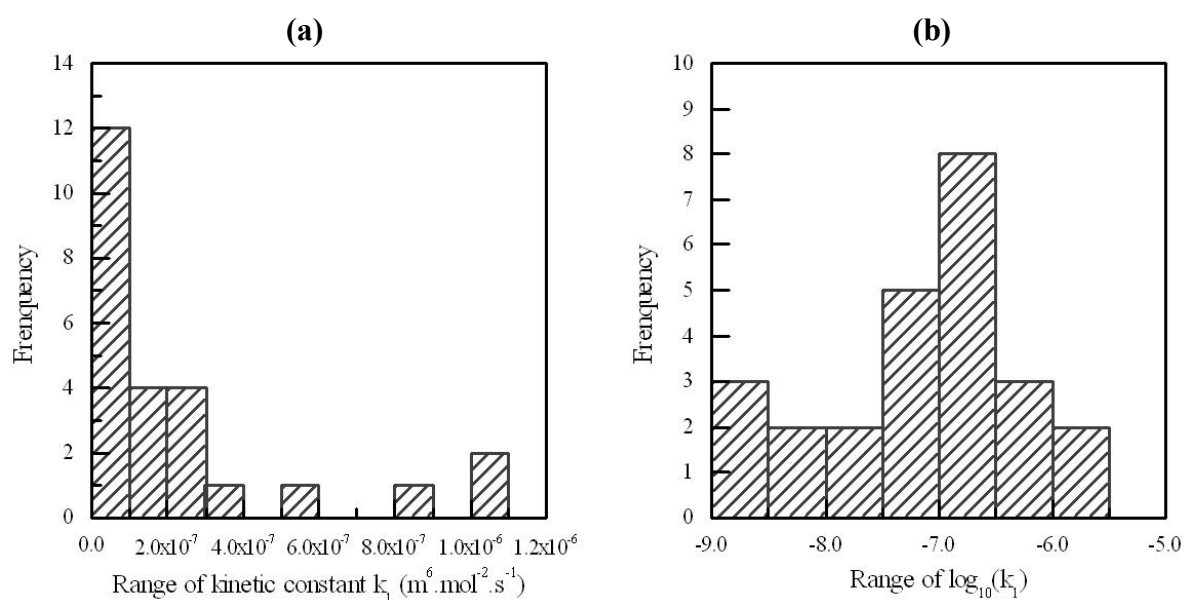


Figure VI-7. Histogram of tertiary amines data for (a) kinetic constant  $k_1$  and for (b) the decimal logarithm of kinetic constant  $k_1$ .

We define the matrix  $X$  which corresponds to the value of the variables (for  $N$  individuals (amines) and  $J$  variables (descriptors)) as indicated in Equation 79 and the vector  $Y$  which corresponds to the property for  $N$  individuals as indicated in the Equation 80.

$$X_{N,J} = \begin{pmatrix} x_1^1 & \cdots & x_1^J \\ \vdots & \ddots & \vdots \\ x_N^1 & \cdots & x_N^J \end{pmatrix} \quad \text{Equation 79}$$

$$Y_{N,1} = \begin{pmatrix} y_1 \\ \vdots \\ y_N \end{pmatrix} \quad \text{Equation 80}$$

## 2.2.2 QSPR model

In what follows, we first select the most adapted linear regression method and present its main characteristics. Then we describe the process followed to obtain the QSPR model used for prediction. Finally we present parameters which could optimize the performance of the QSPR model.

### 2.2.2.1 Description of the regression method

There are two kinds of linear methods used to link variables to the property: partial least squares (PLS) and multiple linear regression (MLR). Unlike the multiple linear regression which are optimized by least square regression, the partial least square can be used when the number of variables is more important than the number of individuals and when those variables are correlated. As in our case, variables are correlated and more numerous than individuals (68 descriptors for 59 molecules primary and secondary amines on one hand and 28 tertiary and severely hindered secondary amines on the other hand) we choose to realize the regression using partial least square.

The PLS consists in calculating by successive iterations linear combinations  $t$ , defined in Equation 81, of variables in order to optimize the prediction of the property by minimization of the square of the covariance between the property and the linear combinations ( $\text{cov}^2(Y, t)$ ). In Equation 81  $t$  corresponds to the matrix of the PLS components (which are linear combinations) and  $W$  corresponds to the matrix of coefficients composed of  $J$  lines and  $H$  columns. The number  $H$  corresponds to the number of iterations of the algorithm and then to the number of PLS components. In the case of the nonlinear iterative partial least square (NIPALS) algorithm which is one of the most common, each variable  $x_j$  and properties  $y$  are projected on the first PLS component at the first iteration. Then, for the next iteration, the algorithm is applied to the residues of the successive projections by a succession of simple linear regression of variables and properties on the PLS components. The number of PLS components is generally determined by cross validation which indicates the termination criteria for the algorithm (Tenenhaus, 1998).

$$t_{N,H} = X_{N,J} W_{J,H} \quad \text{Equation 81}$$

## 2. QSPR descriptor model

In our case we choose to use the PLS generalised linear regression (PLS-GLR) proposed by (Bastien *et al.*, 2005). It corresponds to a modified version of the NIPALS algorithm. It operates like NIPALS algorithm, iteratively. However it also uses the Student's t-test associated to the linear regression to select at each iteration, during the construction of PLS components, variables  $x_j$  which are correlated to the modelled property  $y$  with a statistical significance of 0.05. It attributes the value of 0 to the coefficients of variables which are not significantly correlated to the property. While for a given iteration none variables  $x_j$  are significantly correlated, the process stops. The number of PLS components is then directly determined by the algorithm without the help of cross validation. Moreover, this algorithm is used in order to determine each PLS components only with descriptors which explain the final property and then to reduce the number of descriptors in the final model.

The initial variables  $x_1, x_2, x_j, \dots, x_J$  and corresponding property  $y$  are first standardized in  $x_1^{(0)}, x_2^{(0)}, x_j^{(0)}, \dots, x_J^{(0)}$  and  $y^{(0)}$  which then are used in the first iteration. The final model can be expressed as indicated in the Equation 82. During the construction, the PLS components  $t_h$  indicated in the Equation 83 must be orthogonal. From this model (Bastien *et al.*, 2005) consider that parameters  $c_h$  and  $w_{hj}$  must be estimated. In those equations  $c_h$  are the coefficients of the regression of  $y^{(0)}$  on the component  $t_h$  and  $w_{hj}$  is the coefficient of the component  $t_h$  on the variables  $x_j^{(0)}$ .

$$y^{(0)} = \sum_h c_h \left( \sum_j w_{hj} x_j^{(0)} \right) + \text{residue} \quad \text{Equation 82}$$

$$t_h = \sum_j w_{hj} x_j^{(0)} \quad \text{Equation 83}$$

The value of the normalized predicted property  $\hat{y}_H^{(0)}$  can then be expressed as indicated in Equation 84. To this value are associated H PLS components. From the previous relation, it is possible to determine the "normal" predicted property  $\hat{y}_H$  as indicated in Equation 85. In this relation  $b_0$  corresponds to the intercept and the vector B which contain J lines, is the vector of coefficients of the property  $\hat{y}_H$  on the corresponding variables  $x_j$  for one individual. It is those coefficients we can use to directly calculate the kinetic constant.

$$\hat{y}_H^{(0)} = \sum_h c_h \left( \sum_j w_{hj} x_j^{(0)} \right) = \left( \sum_j \sum_h c_h w_{hj} \right) x_j^{(0)} \quad \text{Equation 84}$$

$$\hat{y}_H = b_0 + \sum_{j=1}^J b_j x_j = b_0 + X_{1,J} B_{J,1} \quad \text{Equation 85}$$

Those parameters are determined thanks to Equation 86 for  $b_0$  and Equation 87 for each coefficient  $b_j$  of the vector  $B$ . In these relations  $\bar{y}$  is the average of the property,  $\sigma_y$  is the standard deviation of the property,  $\bar{x}_j$  is the average of variables,  $\sigma_{x_j}$  is the standard deviation of variables,  $\bar{X}_{J,J}$  is the diagonal matrix of the average of the variables and  $\Sigma_{X_{J,J}}^{-2}$  is the diagonal matrix of the standard deviation of the variables.

$$b_0 = \bar{y} - \sigma_y \sum_{j,h} \frac{\bar{x}_j}{\sigma_{x_j}} w_{jh} c_h = \bar{y} - \sigma_y \bar{X}_{J,J} \Sigma_{X_{J,J}}^{-2} W_{J,H} C_{H,1} \quad \text{Equation 86}$$

$$b_j = \sigma_y \sum_h c_h \frac{w_{hj}}{\sigma_{x_j}} = \sigma_y \Sigma_{X_{J,J}}^{-2} W_{J,H} C_{H,1} \quad \text{Equation 87}$$

### 2.2.2.2 Description of the process

The determination of the QSPR model is realized in two steps. First we generate  $M$  models and then we determine the QSPR model from those models.

#### 2.2.2.2.1 Generation of the $M$ models

Generally a PLS regression is realized using two set of data: a training set, and a prediction set. The training set, which contains a part of variables and corresponding property for a given number of individuals, is used by the PLS algorithm in order to determine the coefficients  $b_j$  of the optimal model. The prediction set, which contain the remaining data, characterize the performance of the model. Each set of data is determined at the beginning and remains constant for all the study. However, the determination of the model by PLS regression depends on the nature and the number of data used to build the model. For a given number of data, this means that if we change the nature of individuals which composed the training set, the result will be different.

In this work, in order to avoid this effect, we first select molecules of the prediction set, and then, from the remaining molecules, we randomly generate  $M$  models composed each of two set of data: a training set and a validation set. For each model, all the remaining molecules are distributed among the two sets. Moreover, each molecule must be at least one time in each set as indicated in Figure VI-8.

The training set is used in order to determine the optimal coefficients  $b_j$  for each model. It is also used to determine the coefficient of the QSPR model determined from a method we detail at a later time. The validation set is used to estimate the performance obtained from the training set of the corresponding model. Moreover, the optimization of the modelling is realized by using the validation set. Finally, the prediction set estimates the performance of the optimized QSPR model.

## 2. QSPR descriptor model

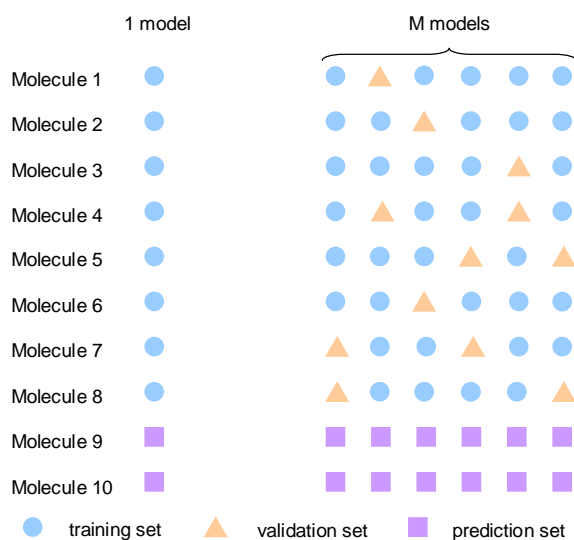


Figure VI-8. On left, one model with 80 % of the molecules in the training set and 20 % in a prediction set. On right, M different models composed each of 60 % of the molecules in the training set, 20 % in the validation set and 20 % in the prediction set.

We choose to generate  $M = 500$  models according to results detailed in Chapter IX .11.2. Moreover, we determine the proportion of each set as indicated in Table VI-4. In overall we choose around 75 % of molecules in the training set, around 15 % in the validation set and 10 % in the prediction set. For each modelling ( $k_1$  of amines III,  $k_1$  of amines I/II and  $k_2$  of amines I/II) we use the same 500 training and validation set for the complete study. The molecules of each prediction set are indicated in Table VI-5. We choose the same molecules for the modelling of  $k_1$  and  $k_2$  of primary and secondary amines in order to compare the predicted result with experimental data in the  $k_1$ ,  $k_2$  graph with ellipse of confidence. The justification of the proportion of molecules in each set and the nature of molecules of the prediction set is justified in Chapter IX .11.1.

Table VI-4. Number of amines and proportion of data in each set for each modelling.

	$k_1$ / amines III	$k_1$ / amines I/II	$k_2$ / amines I/II
Training set	21 (75 %)	46 (78 %)	43 (77 %)
Validation set	4 (14 %)	8 (14 %)	8 (14%)
Prediction set	3 (11 %)	5 (8 %)	5 (9 %)
Total	28	59	56

Table VI-5. Molecules of each prediction set.

Prediction set $k_1$ / amine III	Prediction set $k_1$ & $k_2$ / amine I/II
tert-Butylaminodiethanol (1315)	Cyclopentylamine (1103)
1-Pyrrolidineethanol (1343)	2-Amino-2-(hydroxymethyl)-1,3-propanediol (1129)
N-Methylmorpholine (1350)	N-Methyl-1-butylamine (1202)
	2-(Propylamino)ethanol (1222)
	3-(Methylamino)propanenitrile (1240)

First, we determine the coefficient of the PLS-GLR model ( $b_0$  and  $b_j$  of the Equation 85) of each of the 500 models. From each of these models, we predict the property of the amines of the corresponding validation set. We determine for each validation set the error of prediction between predicted values and experimental values with the root mean square error of prediction (RMSEP). The expression of the RMSEP is indicated in Equation 88. In this equation  $n$  is the number of amines in the validation set. The values of the RMSEP of each validation set are sorted by decreasing order and plot as indicated in the Figure VI-9.

$$RMSEP = \sqrt{\frac{1}{n} \sum_{i=1}^n (y_i - \hat{y}_i)^2} \quad \text{Equation 88}$$

The global quality of the prediction of the 500 models can be described by the average of the value of the RMSEP of the 500 validation set and interval from the 2.5 % quantile ( $Q_{2.5}$ ) to the 97.5 % quantile ( $Q_{97.5}$ ). The average and the interval are represented in Figure VI-9. During the process of selection of the QSPR model that we describe in Chapter VI .2.2.3, we use the average of the RMSEP of the 500 RMSEP of the validation set as a criterion of comparison of performance of the modelling. The value of the quantiles also gives an idea of the distribution of the RMSEP values. Indeed, this criterion takes into account of coefficients of 500 models determined with the same number of training sets and a performance evaluated with molecules of validation sets which have not been used to determine the coefficients.

## 2. QSPR descriptor model

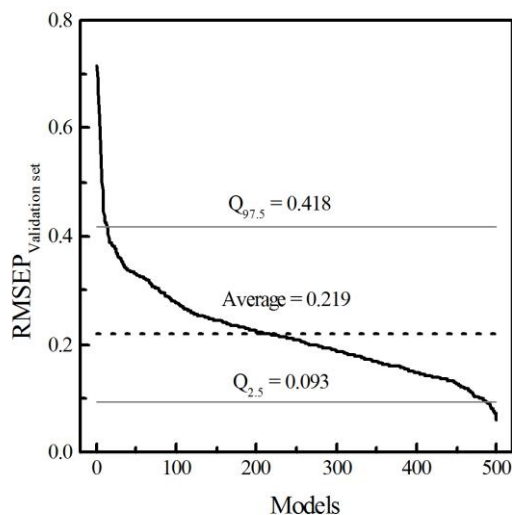


Figure VI-9. Example of distribution of RMSEP of validation for modelling of  $\log_{10}(k_1)$  of amines which form carbamates with 68 descriptors.

### 2.2.2.2 Determination of the QSPR model

The QSPR model, expressed in Equation 89, is determined from the 500 previous models. Indeed, the intercept and the coefficient of the QSPR model are the average of the corresponding intercept and coefficient of the 500 models as indicated in Equation 90. This method has been selected in order to give robustness to the QSPR model. In the same way the coefficient of the standardized variables can be determined from Equation 84. They can be used to determine the weight of each variable which corresponds to the contribution of each variable to explain the property. The expression of the weight of the variable  $j$  is indicated in Equation 91 where  $\bar{b}_j^{(0)}$  is the coefficient of the standardized variable  $j$  of the QSPR model.

$$\hat{y}_H^{pred} = \bar{b}_0 + X_{1,j} \bar{B}_{j,1} \quad \text{Equation 89}$$

$$\bar{b}_0 = \frac{\sum_{m=0}^M b_0}{M} ; \bar{B}_{j,1} = \frac{\sum_{m=0}^M B_{j,1}}{M} ; M = 500 \quad \text{Equation 90}$$

$$\text{weight of } j = 100 \times \frac{|\bar{b}_j^{(0)}|}{\sum_{j=0}^J |\bar{b}_j^{(0)}|} \quad \text{Equation 91}$$

We evaluate the performance of the QSPR model by calculating the value of the property of this model  $\hat{y}_H^{pred}$  for each molecule of the prediction set. Then we determine the RMSEP between all the predicted values of the property and the corresponding experimental values. Moreover, we determine the average relative deviation (ARD) between the kinetic constant determined from the prediction and the experimental kinetic constant as indicated in

Equation 92. In this equation  $n$  is the number of amines in the prediction set. The advantage of the ARD is that it is determined from the kinetic constants.

$$ARD = 100 \times \frac{\sum_{i=1}^n \frac{|10^{y_i^{exp}} - 10^{\bar{y}_{Hi}^{pred}}|}{10^{y_i}}}{n} \quad \text{Equation 92}$$

### 2.2.3 Selection of the QSPR model

The selection of the model consists in choosing the appropriate number of descriptors and the appropriate order of these terms to obtain the best QSPR model. We define a term as a variable (descriptor) or the product of several variables, identical or not. We also remind that we use the average of the RMSEP of the 500 models to compare the performance of several modelling as indicated in Chapter VI .2.2.2.1. In the next parts we first present the method to increase the order of descriptors, then the methods to determine the appropriate number of terms and finally the process followed to select the QSPR model which gives the best performance.

#### 2.2.3.1 Order of terms

As shown in the Chapter V, if a major part of the kinetic properties of amines which form carbonates can be explained by the pKa, the kinetic properties of amines which form carbamates are explained at least by a dependant combination of the pKa and the steric hindrance. In this case, first order descriptors may be insufficient to explain kinetic constants. In order to bring complexity to the model, from first order terms we generate second order terms (square and rectangle terms). Those terms (first and second order) are then introduced as variables in the modelling process. We notice that when the order of all terms is equal to 1, the number of variables (descriptors) corresponds to the number of terms. For the section Chapter VI .2.2.3.3 we call this method: OoT.

#### 2.2.3.2 Number of terms

As indicated in Chapter VI .2.2.2.1, when a variable is not significantly correlated to the property the value of 0 is attributed to its coefficient. We consider that a variable does not bring a significant information when its coefficient is equal to 0 for more than 95 % of the 500 models. In other words, a term is considered as significant when the value of its coefficient is different from 0 for more than 25 over 500 models. In Chapter VI .2.2.3.3 we call this method: NoT1.

Another method consists to select terms which explain to given part of the information. To realize this selection, we first sort by descending order the values of the parameters of each standardized variables of the QSPR model. Then, we determine the weight of each coefficient of standardized variables as indicated in Chapter VI.2.2.2.2. Finally we select the terms which explain a given level of cumulative weight. Thanks to this method we only conserve terms which have the most important coefficient. We use method in too cases.

## 2. QSPR descriptor model

First, when they are too many terms (more than 34 first order terms which corresponds to the half of the first order terms). We use this method to exclude coarsely the less correlated terms which represent 5 % of the cumulative weight (method NoT2). We also use this method to refine the optimal number of terms. We start by selecting the terms which explain 80 % of the cumulative weight. Then we set up several QSPR model by removing one by one the less correlated terms until to reach the best performance (method NoT3).

### 2.2.3.3 Process of selection

We choose to determine to determine two optimal QSPR models, the first one which is the best first order model that we call “the first order QSPR model” and the second one which is the best second order model that we call “the second order QSPR model”. In what follows we describe the method followed to obtain these two models. The entire process to achieve the first order QSPR model is described in Figure VI-10.

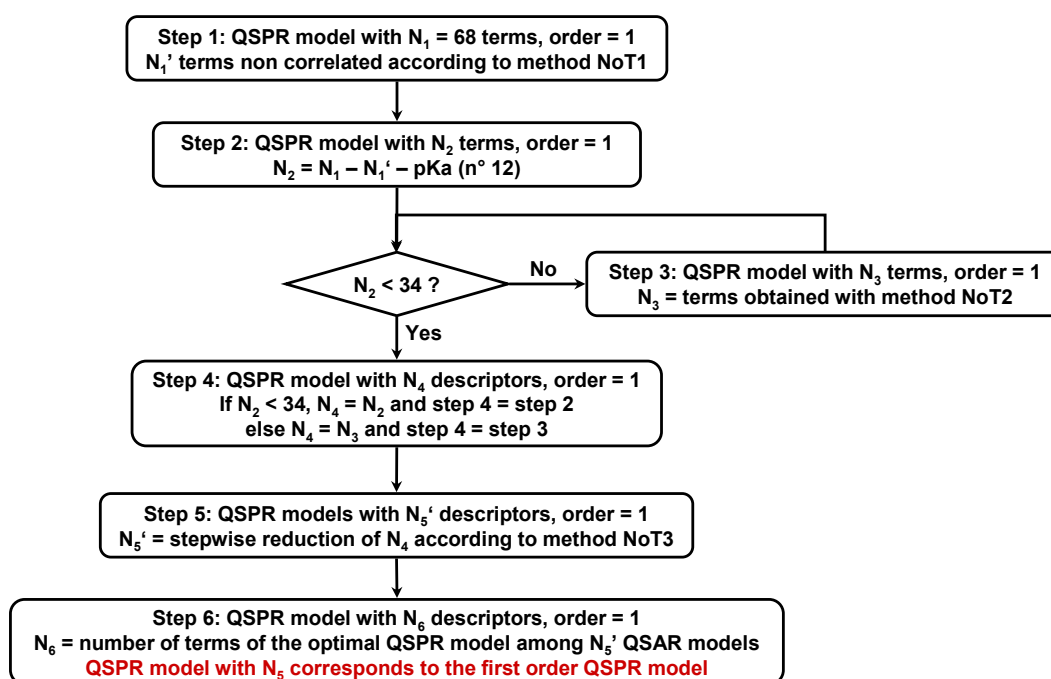


Figure VI-10. Flowchart of the obtaining method of the QSPR first order model.

It starts with step 1 which corresponds to the QSPR model of the 68 descriptors, considered here as terms. At the end of this modelling, there are  $N_1'$  descriptors which are not significantly correlated to the property according to the method NoT1. For step 2 we only retain terms correlated to the property of the previous modelling except for the theoretical value of the pKa (provided by chemicalize) that we remove. Indeed, this descriptor was initially selected as an alternative to the experimental pKa. As the performance of this descriptor is not comparable to the experimental value we choose to only conserve the experimental value of the pKa for the next. At the end of the step 2, if the number of terms is higher or equal to 34 it

is necessary to realize the step 3 in order to reduce the number of terms. This step consists to determine the number of terms to retain with the method NoT2.

The step 4 corresponds to the end of the step 2 if the number of terms  $N_2$  is lower than 34 or to the end of the step 3 if it is not the case. From this step we use the method NoT3 to reduce stepwise the number of terms in order to find the optimal in the step 5. Finally we consider that the optimal QSPR model among the  $N_5'$  terms obtained with the method NoT3 corresponds to the step 6. We consider that the first order QSPR model corresponds to the QSPR model with  $N_6$  terms. Indeed, this model brings the best performance with the lowest number of first order terms.

The entire process which describes how to achieve the second order QSPR model in indicated in Figure VI-12. First it starts with step 7 which consists in determining the QSPR model with the first and second order terms of terms determined in the step 4 ( $N_4$ ) with the OoT method. The QSPR model which corresponds to this step is the most complete second order model. At the end of the step, there are  $N_7'$  terms which are not correlated to the property according to the method NoT1. In the step 8 we determine the QSPR model only with descriptors which are correlated to the property according in the step 7. We also determine in step 9 the QSPR model with the first and second order terms of terms determined in the step 6 ( $N_6$ ) with the OoT method. This step only considers descriptors of the first order QSPR model and their cross interactions. At the end of the step 9, there are  $N_9'$  terms which are not correlated to the property according to the method NoT1. In the step 10 we determine the QSPR model only with descriptors which are correlated to the property according in the step 9. Finally step 11 consists in comparing the performance obtained between step 8 and step 10. The second order QSPR model corresponds to the most performant QSPR model between step 8 and 10.

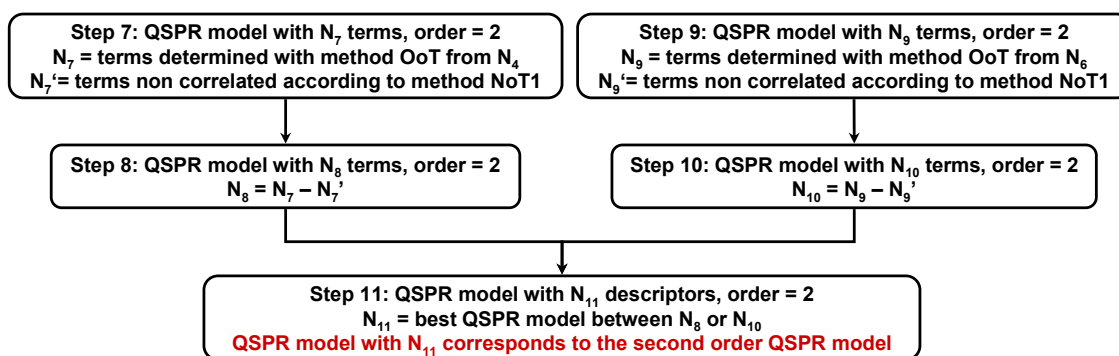


Figure VI-11. Flowchart of the obtaining method of the QSPR second order model.

### 2.3 Conclusion

In this work, we choose to predict the kinetic properties of the amine – carbone dioxide reaction thanks to a method that we call QSPR descriptors. This method consists in describing the molecule as a vector of molecular descriptors which are generic, specific (nitrogen accessible surface) or experimental (pKa) and to link this vector to the property with

### 3. Results

a PLS model. First we show that from 110 different generic descriptors we select the 66 less correlated descriptors with a clustering of variables around latent components method in addition to the nitrogen accessible surface and the experimental pKa which are specific to this study.

Then we present the input data and show that we must predict the decimal logarithm of each kinetic constant to obtain an optimal distribution of data. We justify to use partial least square regression and explain the functioning of this method. Among the different PLS we indicate that we use the PLS-GLR method which presents some advantages in comparison with the NIPALS algorithm. Then we explain how we set up several PLS-GLR models and the need to use a training set, a validation set and a prediction set. We use 500 models and around 75 % of data in the training set, 15 % in validation set and 10 % in prediction set. We also indicate that the QSPR model is determined by the average of the coefficients of the 500 PLS-GLR models. We present the method to follow in order to optimize the QSPR model by selecting the most significant variables or by complicating the model with square and rectangle terms. We justify comparing the performance of the different modelling with the average RMSEP of the 500 validation set and to estimate the performance of the corresponding QSPR model with the ARD.

In the next section, we present the results obtained for the modelling. In a first step, we present the results obtained for kinetic constant  $k_1$  of tertiary and sterically amines (molecules which form directly carbonates). Then we consider results obtained for primary and secondary amines. In this part, we start with all primary and secondary amines which all have a kinetic constant  $k_1$  and we continue with only molecules which form carbamates and modelled kinetic constant  $k_2$ .

## 3 Results

### 3.1 Modelling of tertiary and sterically hindered amines

We follow the process indicated previously to optimize the results of the modelling of the kinetic constant  $k_1$  of tertiary and sterically hindered amines. The results of this process are indicated in Figure VI-12 (a) and Figure VI-12 (b). They represent the distribution of the RMSEP of the validation set as a function of the number of terms of the corresponding QSPR models. For each modelling we attribute a number indicated on these figures. We report in Table VI-6 the results of the different modelling and specify the corresponding step of the process.

We start with the 68 descriptors (step 1) to obtain a first order modelling n° 1. In the corresponding 500 models, 13 descriptors are not correlated to the property according to the PLS-GLR. If we remove these 13 descriptors along with the theoretical pKa (descriptor number 12) we get to the modelling n° 2 (step 2) with 54 descriptors. This correlation slightly reduces the average of the RMSEP which is in agreement with the fact that it only remains descriptors correlated to the property according to PLS-GLR. There are still too many descriptors to introduce second order terms in the QSP correlation. For this reason we use the step 3 of the Figure VI-10. This step leads to select the 24 descriptors which explain 95 % of

the cumulated information (modelling  $n^{\circ}3$ ). It improves the performance of the model in terms of average value of RMSEP and dispersion.

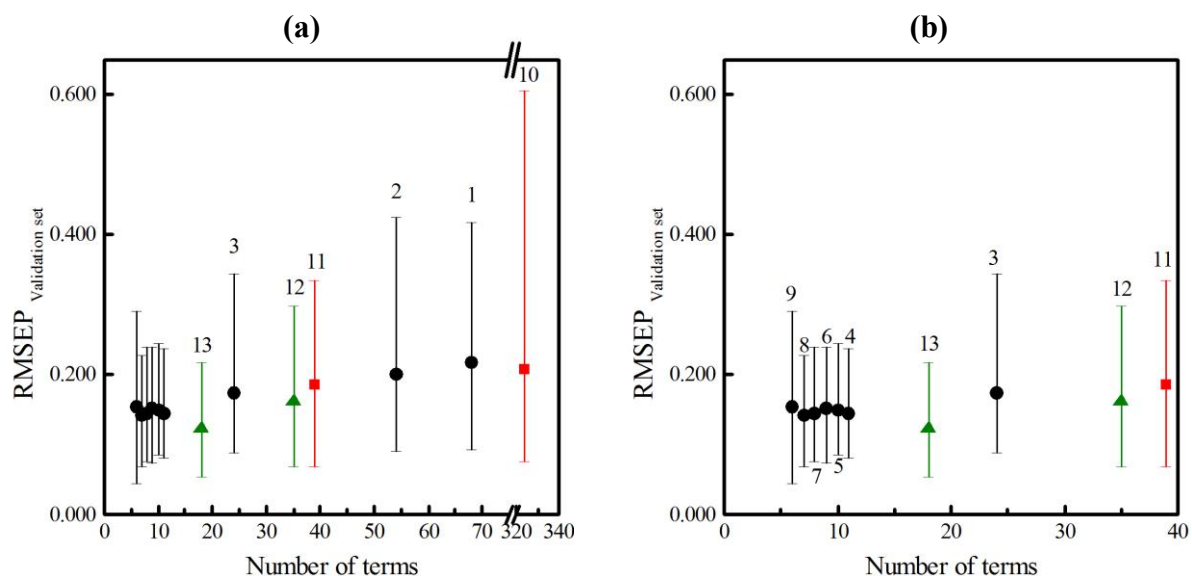


Figure VI-12. Distribution of the RMSEP of the prediction sets of  $k_1$  of tertiary and sterically hindered amines (average,  $Q_{2.5}$  and  $Q_{97.5}$ ) as a function of the number of terms used in the corresponding QSPR model. (a) All results. (b) Zoom between 0 and 40 terms. First order results (black circles), second order results with 24 descriptors (red squares) and second order results with 7 descriptors (green triangles). The number of the modelling is also indicated.

Table VI-6. Results of modelling of tertiary and sterically hindered secondary amines.

N <sup>o</sup>	Step	Number of terms	Order	Number of descriptors	Average RMSEP	$Q_{97.5}$	$Q_{2.5}$
1	1	68	1	68	0.219	0.418	0.093
2	2	54	1	54	0.201	0.425	0.091
3	3-4	24	1	24	0.174	0.344	0.087
4	5	11	1	11	0.145	0.237	0.080
5	5	10	1	10	0.149	0.244	0.086
6	5	9	1	9	0.151	0.240	0.074
7	5	8	1	8	0.143	0.239	0.076
<b>8</b>	<b>5-6</b>	<b>7</b>	<b>1</b>	<b>7</b>	<b>0.141</b>	<b>0.227</b>	<b>0.068</b>
9	5	6	1	6	0.153	0.290	0.044
10	7	324	2	24	0.208	0.606	0.075
11	8	39	2	24	0.185	0.335	0.068
12	9	35	2	7	0.162	0.298	0.069
<b>13</b>	<b>10-11</b>	<b>18</b>	<b>2</b>	<b>7</b>	<b>0.122</b>	<b>0.217</b>	<b>0.053</b>

### 3. Results

According to the method of the step 5 describe previously we select the 11 descriptors which explain more than 80 % of the information. Those descriptors are indicated in bold in the Table VI-7.

Table VI-7. Normalized coefficients of the modelling n° 3. Descriptors which explain more than 80 % of the information are indicated in bold.

<b>Descriptor</b>	<b>Weight (%)</b>	<b>Cumulative weight (%)</b>
<b>pka_exp</b>	19.38	19.38
<b>Dipoleaq</b>	18.71	38.09
<b>HOMOg</b>	17.15	55.24
<b>BETA</b>	9.55	64.79
<b>PNSA2</b>	2.65	67.44
<b>RotBonds</b>	2.65	70.09
<b>WNSA1</b>	2.64	72.73
<b>RPCG</b>	2.60	75.33
<b>DPSA1</b>	2.39	77.72
<b>flexibility</b>	2.37	80.09
<b>Kappa3</b>	2.15	82.24
EllipsVolume	2.12	84.36
PrMomInY	1.96	86.32
Kappa1	1.91	88.23
Surf_acces	1.81	90.04
PrMomInX	1.39	91.42
EdgeDistMagn	1.23	92.66
HOMOLUMOaq	1.21	93.86
ShdwR	1.16	95.02
SubgCnts3path	1.06	96.08
HAccept	1.06	97.14
BalabanJX	1.02	98.17
Esolv	0.99	99.16
AtomComp	0.84	100.00

We then progressively realize modelling by reducing the number of the descriptors from 11 to 6 (modelling n° 4 to 9) and compare results obtained (step 5). The best results are obtained when 7 descriptors are used (modelling n° 8). Indeed models with 6, 8 or more descriptors have a largest value of the average RMSEP and a larger dispersion of the value of the quantiles. The coefficients and the coefficients of the normalized variables of this model are indicated in Table VI-8. We consider that this model corresponds to the first order QSPR model (step 6) for  $k_1$  of the tertiary and sterically hindered amines. We notice that the

experimental pKa is the descriptor which is the most correlated to the kinetic constant as observed in the previous chapter.

Table VI-8. Coefficients of the first order QSPR model for the kinetic constant  $k_1$  of tertiary and sterically hindered amines.

Descriptor	Coefficients	Coefficients of standardized variables	Weight (%)	Cumulative weight (%)
Intercept	$-3.35 \times 10^0$	-	-	-
pka_exp	$2.95 \times 10^{-1}$	$3.87 \times 10^{-1}$	22.83	22.83
Dipoleaq	$-1.91 \times 10^{-1}$	$-3.61 \times 10^{-1}$	21.30	44.12
HOMOg	$2.94 \times 10^1$	$3.29 \times 10^{-1}$	19.38	63.51
WNSA1	$1.24 \times 10^{-2}$	$2.26 \times 10^{-1}$	13.31	76.82
RotBonds	$7.71 \times 10^{-2}$	$2.11 \times 10^{-1}$	12.46	89.28
BETA	$-8.81 \times 10^{-4}$	$-1.58 \times 10^{-1}$	9.32	98.60
RPCG	$3.30 \times 10^{-1}$	$2.38 \times 10^{-2}$	1.40	100.00

We then introduce second order terms according to step 7 (modelling n° 10), 8 (modelling n° 11), 9 (modelling n° 12) and 10 (modelling n° 13). According to the results obtained the modelling n° 13 has the best performance. For this reason we consider it as the second order QSPR model for  $k_1$  of tertiary and sterically hindered amines.

According to results indicated in Table VI-9 the second order QSPR model is more efficient in term of interpolation (training and validation set) and extrapolation (prediction set) than the first order QSPR model. For a closer analysis, we represent the parity plot of the first and second order QSPR models respectively in Figure VI-13 (a) and in Figure VI-13 (b). We notice that for each model the discrepancy around the parity line has the same order of magnitude between molecules of the training and validation set and molecules of the prediction set except for one molecule of the prediction set of the second order QSPR model. Moreover, we notice for the first order QSPR model that molecules of the prediction set that they are at the extremum of the distribution of molecules of the training and validation set which explain the important error of prediction (around 108 %).

Table VI-9. Average relative deviation and standard deviation of the relative deviation between experimental and modelled value of  $k_1$  of tertiary and sterically hindered secondary amines for training and validation set and prediction set of the first and second order QSPR models.

$k_1$	First order QSPR model	Second order QSPR model
Training and validation set	$44.8 \pm 27.4 \%$	$32.8 \pm 27.4 \%$
Prediction set	$107.5 \pm 76.7 \%$	$73.1 \pm 81.9 \%$

### 3. Results

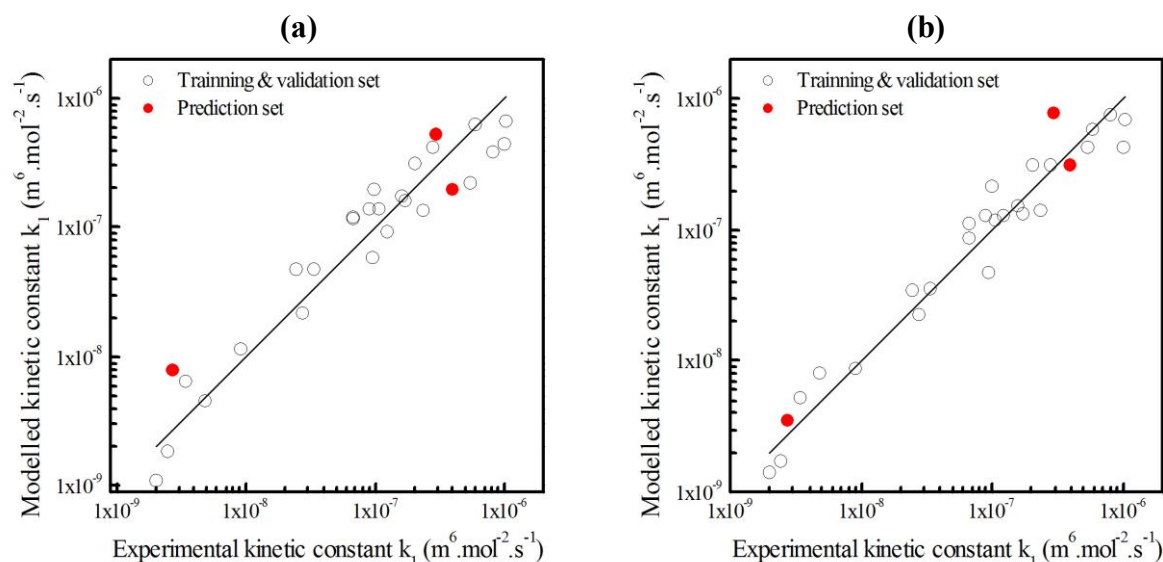


Figure VI-13. Parity plot between modelled kinetic constant  $k_1$  and experimental kinetic constant of tertiary and sterically hindered amines. (a) First order QSPR model. (b) Second order QSPR model.

When we analyse the prediction set of each model, we notice that one molecule highly increases the value of the ARD as shown in Table VI-10. We notice that this molecule is not the same depending on the model. By taking only the two others the ARD is 64 % for the first order QSPR model and 26 % for the second order QSPR model which is more representative of the ARD of the training and validation set. We see here that the value of the ARD, which represent the error of prediction of each model, is highly impacted by the weak number of amines in the prediction set. It will be interesting to predict the kinetic constant  $k_1$  to supplementary in order to obtain a value of the ARD with a representative number of individuals.

Table VI-10. Relative deviation of the molecules of the prediction set of tertiary and sterically hindered amines for the first and second order QSPR models.

Molecule	First order QSPR model	Second order QSPR model
N-Methylmorpholine (1350)	194.5 %	29.7 %
tert-Butylaminodiethanol (1315)	78.4 %	167.6 %
1-Pyrrolidineethanol (1343)	49.6 %	22.1 %
Average $\pm$ standard deviation	107.5 $\pm$ 76.7 %	73.1 $\pm$ 81.9 %

We represent the kinetic constant of each molecule of the prediction set as a function of the  $pK_a$  for the first order QSPR model in Figure VI-14 (a) and for the second order QSPR model in Figure VI-14 (b). We observe that in the case of the first order QSPR model, the estimation of the kinetic constant never fit the experimental value of  $k_1$  defined within its experimental uncertainty. In the case of the QSPR second order model, the kinetic constant of the molecule 1350 is estimated within the projection of the confidence ellipse of experimental

$k_1$  and molecule 1343 is well predicted (relative deviation lower than 23 %). Molecule 1315 is widely overestimated (around 168 %).

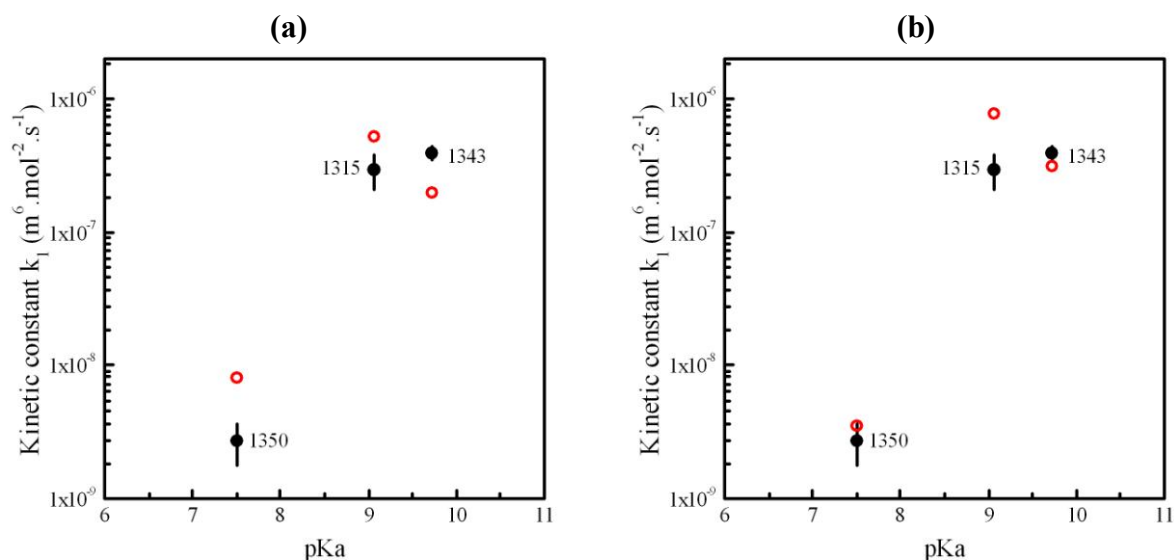


Figure VI-14. Kinetic constant  $k_1$  of molecules of the prediction set of tertiary amines as a function of the pKa. (a) First order QSPR model. (b) Second order QSPR model. Experimental values (black circles) and predicted values (red open circles). The error bar corresponds to the projections of the confidence ellipse on the experimental kinetic constant  $k_1$ .

Finally for both models we calculate the apparent kinetic constant for molecules of the training and validation set and the prediction set. The calculation has been realized by using the values of the amine and water concentrations of the experimental tests performed. We also introduce the value of  $\varepsilon$  to be representative to experimental values according to the Equation 68. We determine the average relative deviation and the standard deviation of the relative deviation between experimental and modelled values for each model and each set of data and indicate results in Table VI-11. The trends observed in Table VI-9 are respected even if values are generally lower except for the prediction set of the second order QSPR model. This result seems obvious because in the case of tertiary and sterically hindered secondary amines, the apparent kinetic constant is directly linked to the kinetic constant  $k_1$  for a given value of amine and water concentration.

Table VI-11. Average relative deviation and standard deviation of the relative deviation between experimental and modelled value of  $k_0^{\text{Am}}$  of tertiary and sterically hindered secondary amines for training and validation set and prediction set of the first and second order QSPR models.

$k_0^{\text{Am}}$	First order QSPR model	Second order QSPR model
Training and validation set	$35.6 \pm 25.8 \%$	$25.7 \pm 19.6 \%$
Prediction set	$99.2 \pm 58.6 \%$	$75.1 \pm 83.9 \%$

### 3. Results

Then we compare results obtained with experimental values in the parity plot indicated in Figure VI-15 (a) for the first order QSPR model and in Figure VI-15 (b) for the second order QSPR model. These figures show visually that the dispersion of the different sets is less important in the case of the second order QSPR model than in the case of the first order QSPR model.

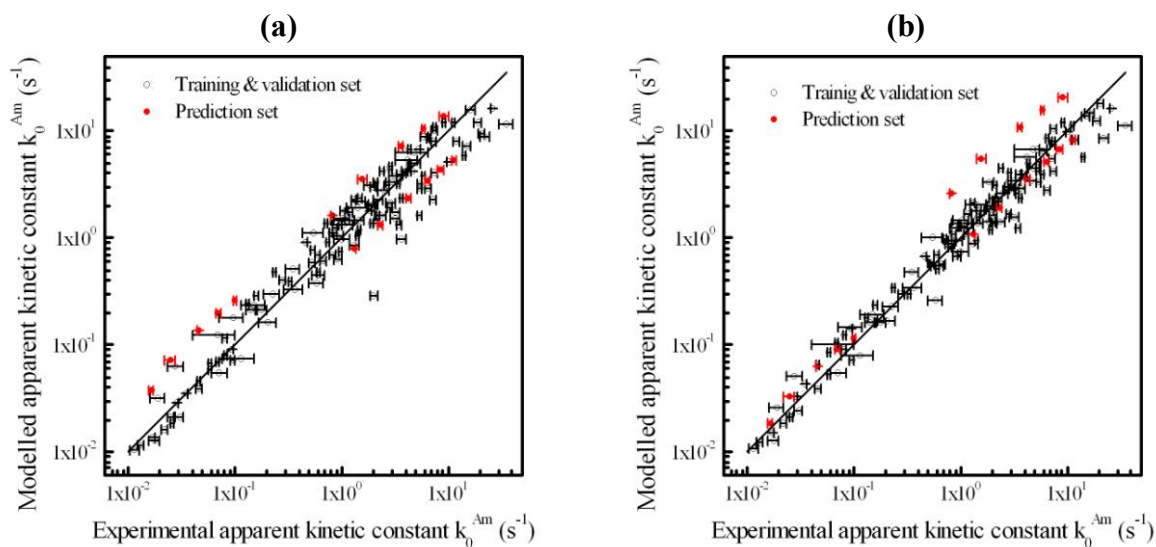


Figure VI-15. Parity plot between modelled and experimental apparent kinetic constant of tertiary and sterically hindered amines. (a) First order QSPR model. (b) Second order QSPR model. Error bars correspond to the experimental confidence interval.

The average of the relative confidence interval (which is the ratio between the confidence interval and the corresponding value of apparent kinetic constant as indicated in Equation 93) is around 8 % for tertiary and sterically hindered secondary amines. This value is lower than the ARD of the different values of different set and the different models. However the value of the ARD of  $k_1$  and  $k_0^{Am}$  are comparable (if we exclude the only molecule of each prediction set which increase the ARD) to the difference observed between our results and other authors which. Indeed, this value is lower than 40 % as indicated in Chapter V .2.1. Moreover, even if the first order QSPR model is less efficient than the second order QSPR model, it also needs less information and then is faster to implement. This observation show the interest to use both QSPR models set up in this work.

$$\frac{CI_{k_0^{Am}}}{k_0^{Am}}$$

Equation 93

## 3.2 Modelling of primary and secondary amines

### 3.2.1 Kinetic constant $k_1$

We follow the same process to establish the optimal QSPR for the third order kinetic constant  $k_1$  of primary and secondary amines forming carbamates. This process is summarized in Figure VI-16 (a) and Figure VI-16 (b) which represent distribution of the RMSEP of validation set for each QSPR model identified by a number (1-11) as a function of the number of terms. Each correlation is described in Table VI-12.

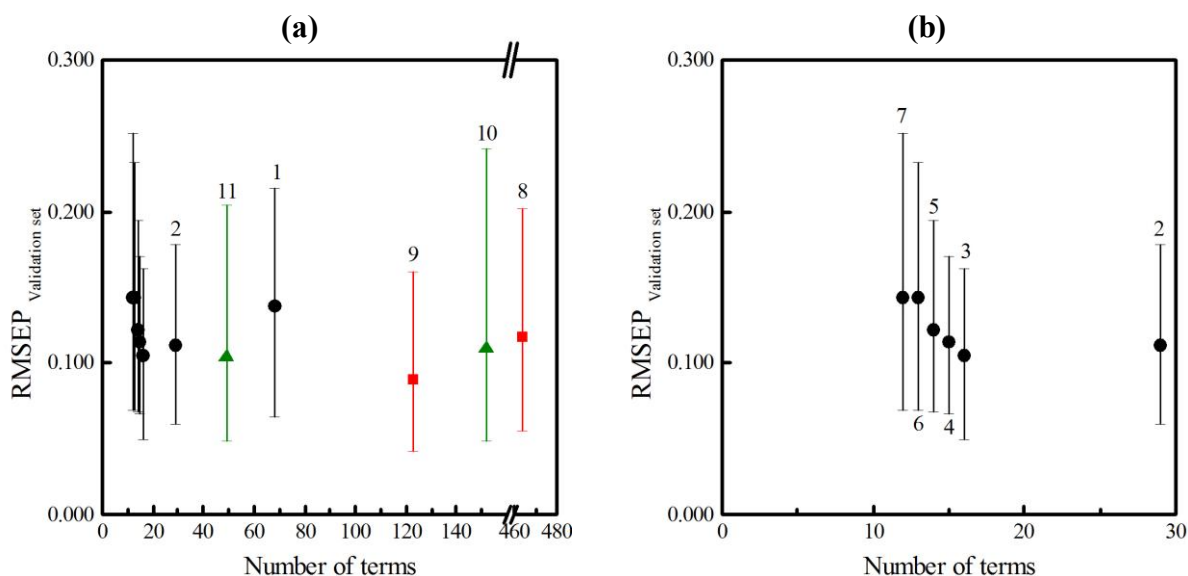


Figure VI-16. Modelling of kinetic constant  $k_1$  of primary and secondary amines. Average RMSEP and quartiles as a function of the number of terms. (a) All results. (b) Zoom between 0 and 30 terms. First order results (black circles), second order results with 29 descriptors (red squares) and second order results with 16 descriptors (green triangles). The number of the modelling is also indicated.

We start with the 68 descriptors to obtain a first order QSPR model (modelling n° 1). At the end of the step 1, 38 descriptors are not correlated to the property. If we remove these 38 descriptors along with the calculated pKa (descriptor number 12), we get to the modelling n° 2 with 29 descriptors (step 2). This slightly reduces the average of the RMSEP and the dispersion of the quantiles values. The descriptors of the modelling n° 2 are indicated in Table VI-13. As the number of descriptor is low enough we directly pass to the step 5. These descriptors are indicated in bold in Table VI-13. Among the five modelling of this step (modelling n° 3 to 7) the modelling n° 3 has the best efficiency. It corresponds to the first order QSPR model for kinetic constant  $k_1$  of the primary and secondary amines.

### 3. Results

Table VI-12. Results of the modelling of the kinetic constant  $k_1$  of primary and secondary amines.

N°	Step	Number of terms	Order	Number of descriptors	Average RMSEP	Q <sub>97.5</sub>	Q <sub>2.5</sub>
1	1	68	1	68	0.137	0.215	0.064
2	2-4	29	1	29	0.111	0.178	0.060
<b>3</b>	<b>5-6</b>	<b>16</b>	<b>1</b>	<b>16</b>	<b>0.105</b>	<b>0.163</b>	<b>0.050</b>
4	5	15	1	15	0.114	0.171	0.067
5	5	14	1	14	0.121	0.194	0.067
6	5	13	1	13	0.144	0.232	0.068
7	5	12	1	12	0.143	0.252	0.069
8	7	464	2	29	0.117	0.201	0.055
<b>9</b>	<b>8-11</b>	<b>123</b>	<b>2</b>	<b>29</b>	<b>0.089</b>	<b>0.160</b>	<b>0.042</b>
10	9	152	2	16	0.109	0.242	0.048
11	10	49	2	16	0.104	0.204	0.048

Table VI-13. Normalized coefficients of the modelling n° 2. Descriptors which explain more than 80 % of the information are indicated in bold.

Descriptor	Weight (%)	Cumulative weight (%)
Surf_acces	8.20	8.20
<b>pka_exp</b>	7.68	15.88
Dipoleaq	7.61	23.49
<b>Chi3cluster</b>	5.55	29.04
<b>HOMOLUMOaq</b>	5.19	34.23
<b>SssCH2</b>	5.11	39.34
<b>DPSA2</b>	4.99	44.33
<b>ShdwLenLZ</b>	4.94	49.26
<b>RNCG</b>	4.83	54.09
<b>ChiralCenter</b>	4.56	58.66
<b>WPSA2</b>	4.35	63.01
<b>SubgCnts0cluster</b>	4.31	67.31
<b>RPCG</b>	4.10	71.41
<b>RotBonds</b>	3.85	75.26
<b>DipMomX</b>	3.75	79.00
<b>PNSA2</b>	3.48	82.48
HAccept	3.34	85.83
ShdwAreaFrZXplane	2.56	88.39
EllipsVolume	2.54	90.93

RPCS	2.32	93.25
Kappa1	1.72	94.97
FPSA3	1.51	96.48
DPSA1	1.49	97.97
DipMomY	0.88	98.85
ShdwAreaFrYZ	0.42	99.27
Chi2ValModif	0.37	99.64
ShdwAreaFrXY	0.21	99.85
LUMOaq	0.12	99.96
BETA	0.04	100.00

The coefficients, coefficients of the standardized variables weight and cumulative weight of the modelling n° 3 are indicated in Table VI-14. We notice that the experimental pKa and the nitrogen accessible surface are the descriptors which are the most correlated to the kinetic constant as observed in the previous chapter.

Table VI-14. Coefficients of the first order QSPR model for the kinetic constant  $k_1$  of primary and secondary amines.

Descriptor	Coefficients	Coefficients of standardized variables	Weight (%)	Cumulative weight (%)
Intercept	$-3.69 \times 10^0$	-	-	-
pka_exp	$3.52 \times 10^{-1}$	$2.87 \times 10^{-1}$	12.22	12.22
Surf_acces	$2.68 \times 10^{-1}$	$2.71 \times 10^{-1}$	11.50	23.72
DPSA2	$-7.52 \times 10^{-4}$	$-1.73 \times 10^{-1}$	7.37	31.10
Dipoleaq	$-1.43 \times 10^{-1}$	$-1.66 \times 10^{-1}$	7.06	38.16
ChiralCenter	$2.95 \times 10^{-1}$	$1.45 \times 10^{-1}$	6.18	44.34
HOMOLUMOaq	$1.26 \times 10^1$	$1.45 \times 10^{-1}$	6.15	50.49
Chi3cluster	$-2.69 \times 10^{-1}$	$-1.44 \times 10^{-1}$	6.14	56.62
SubgCnts0cluster	$-9.41 \times 10^{-2}$	$-1.42 \times 10^{-1}$	6.04	62.67
ShdwLenLZ	$-2.06 \times 10^{-1}$	$-1.28 \times 10^{-1}$	5.46	68.12
RotBonds	$-6.89 \times 10^{-2}$	$-1.27 \times 10^{-1}$	5.39	73.51
DipMomX	$-9.45 \times 10^{-2}$	$-1.23 \times 10^{-1}$	5.23	78.74
PNSA2	$8.30 \times 10^{-4}$	$1.20 \times 10^{-1}$	5.09	83.83
WPSA2	$-1.77 \times 10^{-3}$	$-1.12 \times 10^{-1}$	4.77	88.61
RNCG	$-6.52 \times 10^{-1}$	$-9.58 \times 10^{-2}$	4.07	92.68
SssCH2	$4.13 \times 10^{-2}$	$8.75 \times 10^{-2}$	3.72	96.40
RPCG	$-1.37 \times 10^0$	$-8.46 \times 10^{-2}$	3.60	100.00

### 3. Results

Then, we introduce second order terms according to step 7 (modelling n° 8), 8 (modelling n° 9), 9 (modelling n° 10) and 10 (modelling n° 11). According to the results obtained the modelling n° 9 has the best performance. We consider this model as the second order QSPR model for  $k_1$  of primary and secondary amines.

According to results indicated in Table VI-15 the second order QSPR model is more efficient in term of interpolation (training and validation set) but the first order QSPR model is more efficient in term of extrapolation (prediction set). For a closer analysis, we represent the parity plot of the first and second order QSPR models respectively in Figure VI-17 (a) and in Figure VI-17 (b). We notice that for each model the discrepancy around the parity line has the same order of magnitude between molecules of the training and validation set and molecules of the prediction set except for one molecule of the prediction set of the second order QSPR model. Moreover, we notice for the first order QSPR model that molecules are generally more dispersed than molecules of the second order QSPR model. It explains why the ARD of the training and validation set is better for the second order QSPR model and why it is not the case for the prediction set.

Table VI-15. Average relative deviation and standard deviation of the relative deviation between experimental and modelled value of  $k_1$  of primary and secondary amines for training and validation set and prediction set of the first and second order QSPR models.

$k_1$	QSPR first order model	QSPR second order model
Training and validation set	$41.7 \pm 38.6 \%$	$23.1 \pm 20.3 \%$
Prediction set	$30.8 \pm 27.8 \%$	$37.5 \pm 42.2 \%$

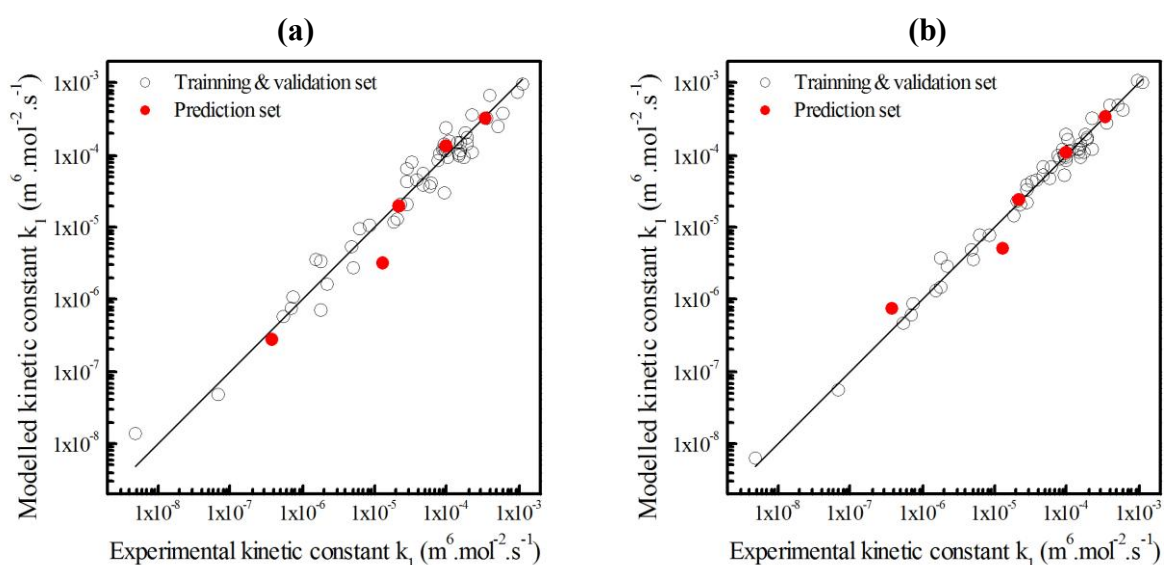


Figure VI-17. Parity plot between modelled kinetic constant  $k_1$  and experimental kinetic constant of primary and secondary amines. (a) First order QSPR model. (b) Second order QSPR model.

As we analyse the results of the prediction set indicated in Table VI-16, we notice as previously that the discrepancy around the average value is relatively important (standard deviation of the relative deviation of the molecules 28 % for the first order QSPR model and 42 % for the second order QSPR model). As previously, this is due to the weak number of molecules and to the important error of prediction of one amine in the prediction set for both models which increase the value of the ARD.

Table VI-16. Relative deviation of the molecules of the prediction set of primary and secondary amines for the first and second order QSPR model.

Molecule	QSPR first order model	QSPR second order model
2-Amino-2-(hydroxymethyl)-1,3-propanediol (1129)	26.1 %	101.6 %
Cyclopentylamine (1103)	37.0 %	10.7 %
2-(Propylamino)ethanol (1222)	9.3 %	12.8 %
3-(Methylamino)propanenitrile (1240)	75.2 %	59.3 %
N-Methyl-1-butylamine (1202)	6.4 %	2.9 %
Average $\pm$ standard deviation	30.8 $\pm$ 27.8 %	37.5 $\pm$ 42.2 %

### 3.2.2 Kinetic constant $k_2$

As for  $k_1$ , we establish the optimal QSPR for  $k_2$ . The optimization process is summarized on Figure VI-18 (a) and Figure VI-18 (b) which represent the distribution of the RMSEP of the validation set for each QSPR identified by a number (1-10) as a function of the number of terms. Each correlation is described in Table VI-17.

We start with the 68 descriptors to obtain a first order QSPR model (modelling n° 1). At the end of the step 1, 37 descriptors are not correlated to the property. Surprisingly the nitrogen accessible surface is one of these 37 descriptors and seems not to be correlated to the property according to the PLS-GLR algorithm. If we remove these 38 descriptors along with the calculated pKa (descriptor number 12), we get to the modelling n° 2 with 30 descriptors (step 2). This slightly reduces the average of the RMSEP and the dispersion of the quantiles values. The descriptors of the modelling n° 2 are indicated in Table VI-18. As the number of descriptor is low enough we directly pass to the step 5. These descriptors are indicated in bold in Table VI-18. Among the five modelling of this step (modelling n° 3 to 6) the modelling n° 4 has the best performance with the smaller number of terms. It corresponds to the first order QSPR model for kinetic constant  $k_2$  of the primary and secondary amines.

### 3. Results

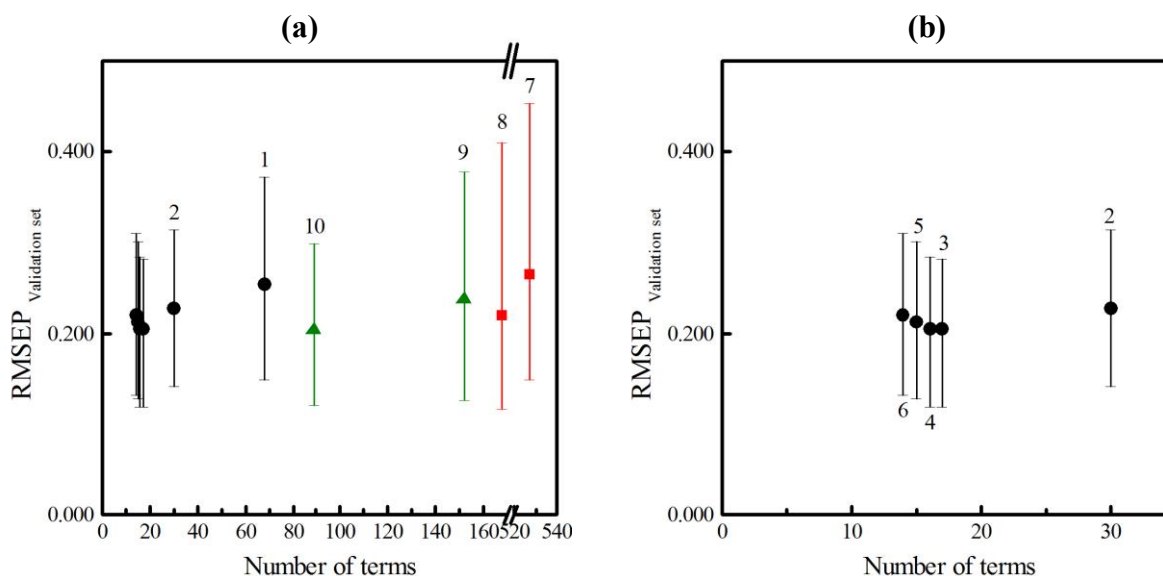


Figure VI-18. Modelling of kinetic constant  $k_2$  of primary and secondary amines. Average RMSEP and quartiles as a function of the number of terms. (a) All results. (b) Zoom between 0 and 35 terms. First order results (black circles), second order results with 31 descriptors (red squares) and second order results with 16 descriptors (green triangles). The number of the modelling is also indicated.

Table VI-17. Results of the modelling of the kinetic constant  $k_2$  of primary and secondary amines.

N°	Step	Number of terms	Order	Number of descriptors	Average RMSEP	Q <sub>97.5</sub>	Q <sub>2.5</sub>
1	1	68	1	68	0.255	0.372	0.148
2	2-4	30	1	30	0.227	0.314	0.141
3	5	17	1	17	0.205	0.281	0.118
4	5-6	16	1	16	<b>0.204</b>	<b>0.283</b>	<b>0.118</b>
5	5	15	1	15	0.212	0.300	0.127
6	5	14	1	14	0.220	0.311	0.131
7	7*	527	2	31*	0.264	0.452	0.148
8	8*	168	2	31*	0.219	0.410	0.116
9	9	152	2	16	0.237	0.378	0.126
10	10-11	89	2	16	<b>0.203</b>	<b>0.299</b>	<b>0.121</b>

\* The nitrogen accessible surface has been added to descriptors of modelling n° 2 based on observation realized in Chapter V.

Table VI-18. Normalized coefficients of the modelling n° 2. Descriptors which explain more than 80 % of the information are indicated in bold.

<b>Descriptor</b>	<b>Weight (%)</b>	<b>Cumulative weight (%)</b>
<b>pka_exp</b>	7.50	7.50
<b>DPSA2</b>	6.33	13.83
<b>HOMOLUMOaq</b>	6.01	19.84
<b>HOMOg</b>	5.92	25.75
<b>DipMomZ</b>	5.33	31.08
<b>BalabanJX</b>	5.23	36.31
<b>HAccept</b>	4.99	41.30
<b>LUMOg</b>	4.84	46.14
<b>Kappa1</b>	4.83	50.97
<b>RPCS</b>	4.77	55.74
<b>MolecDensity</b>	4.07	59.81
<b>Dipoleaq</b>	3.95	63.76
<b>FPSA2</b>	3.84	67.60
<b>EllipsVolume</b>	3.72	71.32
<b>SubgCnts0cluster</b>	3.52	74.84
<b>Chi3cluster</b>	3.44	78.28
<b>SubgCnts3path</b>	3.14	81.42
<b>ShdwAreaFrZXplane</b>	3.04	84.46
<b>PrMomInX</b>	2.58	87.04
<b>ShdwAreaYZ</b>	2.50	89.53
<b>ShdwAreaFrYZ</b>	2.11	91.64
<b>WPSA2</b>	2.09	93.73
<b>DipMomY</b>	1.98	95.71
<b>LUMOaq</b>	1.35	97.07
<b>ShdwLenLY</b>	0.98	98.05
<b>BETA</b>	0.66	98.71
<b>DPSA1</b>	0.51	99.22
<b>ChiralCenter</b>	0.36	99.58
<b>ShdwLenLZ</b>	0.22	99.80
<b>ShdwAreaFrXY</b>	0.20	100.00

The coefficients, coefficients of the standardized variables weight and cumulative weight of the modelling n° 4 are indicated in Table VI-19. We notice that the experimental pKa is the second most correlated descriptor to the kinetic constant unlike the nitrogen accessible surface which have been removed by the PLS-GLR algorithm.

### 3. Results

Table VI-19. Coefficients of the first order QSPR model for the kinetic constant  $k_2$  of primary and secondary amines.

Descriptor	Coefficients	Coefficients of standardized variables	Weight (%)	Cumulative weight (%)
Intercept	$1.01 \times 10^1$	-	-	-
HOMOLUMOaq	$2.18 \times 10^1$	$2.12 \times 10^{-1}$	11.78	11.78
pka_exp	$2.26 \times 10^{-1}$	$1.58 \times 10^{-1}$	8.79	20.58
DipMomZ	$-1.88 \times 10^{-1}$	$-1.32 \times 10^{-1}$	7.33	27.90
DPSA2	$-7.91 \times 10^{-4}$	$-1.30 \times 10^{-1}$	7.20	35.10
HOMOG	$1.47 \times 10^1$	$1.29 \times 10^{-1}$	7.19	42.29
LUMOG	$4.04 \times 10^1$	$1.24 \times 10^{-1}$	6.87	49.16
BalabanJX	$-3.50 \times 10^{-1}$	$-1.14 \times 10^{-1}$	6.34	55.50
HAccept	$-1.90 \times 10^{-1}$	$-1.04 \times 10^{-1}$	5.80	61.30
Kappa1	$-7.70 \times 10^{-2}$	$-1.03 \times 10^{-1}$	5.73	67.03
RPCS	$3.55 \times 10^{-2}$	$1.03 \times 10^{-1}$	5.71	72.74
Dipoleaq	$-9.14 \times 10^{-2}$	$-8.81 \times 10^{-2}$	4.89	77.63
MolecDensity	$-1.82 \times 10^0$	$-8.64 \times 10^{-2}$	4.80	82.43
FPSA2	$-2.57 \times 10^{-1}$	$-8.43 \times 10^{-2}$	4.68	87.11
EllipsVolume	$-7.20 \times 10^{-4}$	$-7.89 \times 10^{-2}$	4.38	91.49
SubgCnts0cluster	$-8.91 \times 10^{-2}$	$-7.70 \times 10^{-2}$	4.27	95.76
Chi3cluster	$-2.31 \times 10^{-1}$	$-7.64 \times 10^{-2}$	4.24	100.00

Then we introduce second order terms according to step 7 (modelling n° 7), 8 (modelling n° 8), 9 (modelling n° 9) and 10 (modelling n° 10). However in step 7 we also add the nitrogen accessible surface in which explain why there are 31 descriptors while there are 30 in the step 4. We justify this choice by observation realized in Chapter V were we observed even for kinetic constant  $k_2$  cross effects between the basicity and the steric hindrance. Nonetheless, we do not add the nitrogen accessible surface in the step 9 and 10 (modelling n° 9 and 10). According to the results obtained the modelling n° 10 has the best performance among the second order models. We notice that it does not improve significantly results by comparison with modelling n° 4. However, we consider this model as the second order QSPR model for  $k_2$  of primary and secondary amines.

According to results indicated in Table VI-20 the second order QSPR model is more efficient in term of interpolation (training and validation set) and extrapolation (prediction set). We also notice for both models the important error of interpolation in comparison with extrapolation. For a closer analysis, we represent the parity plot of the first and second order QSPR models respectively in Figure VI-19 (a) and in Figure VI-19 (b). We notice that for each model the discrepancy around the parity line is more important for molecules of the training and the validation set in comparison with the prediction set. This observation confirms results of the Table VI-20. This result could be linked to the nature of the amines of the prediction set. Indeed we choose “simple” amines to keep others in order to build the QSPR models. It could be interesting to predict the property of more “complex” amines and to verify the performance of the prediction the first and second order QSPR models.

Table VI-20. Average relative deviation and standard deviation of the relative deviation between experimental and modelled value of  $k_2$  of primary and secondary amines for training and validation set and prediction set of the first and second order QSPR models.

$k_2$	First order QSPR model	Second order QSPR model
Training and validation set	$129.5 \pm 172.5 \%$	$117.7 \pm 145.3 \%$
Prediction set	$42.9 \pm 47.9 \%$	$23.3 \pm 22.1 \%$

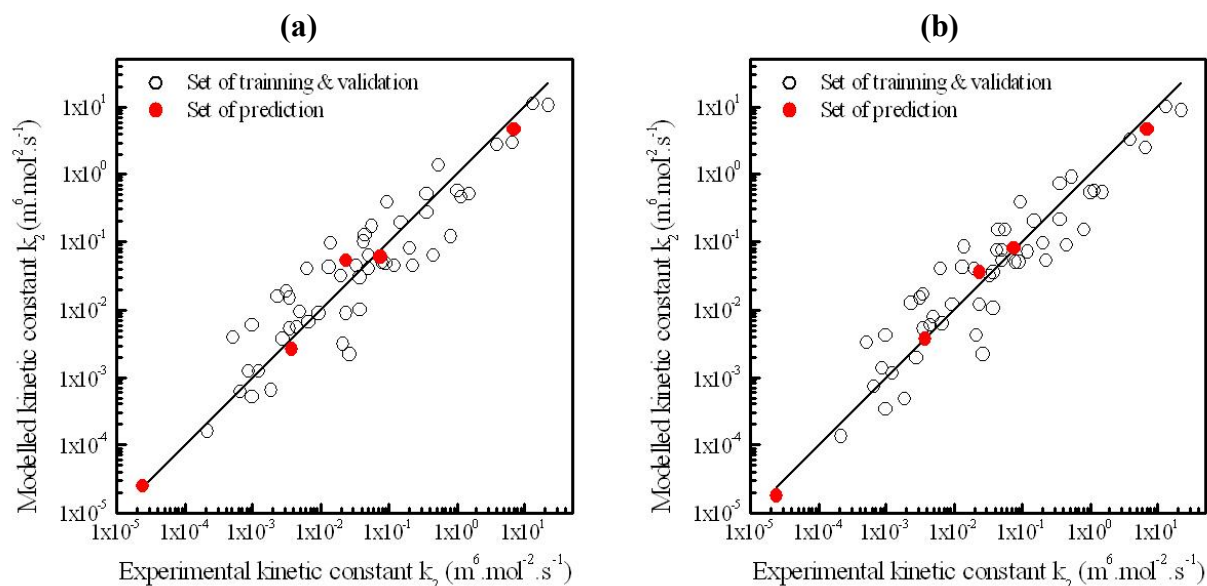


Figure VI-19. Parity plot between modelled kinetic constant  $k_2$  and experimental kinetic constant of primary and secondary amines. (a) First order QSPR model. (b) Second order QSPR model.

In Table VI-21, we notice as previously that the dispersion of relative deviations around the average value is relatively important (standard deviation of 48 % for the first order QSPR model and 22 % for the second order QSPR model). Once again, it will be interesting to enhance the prediction set to be more representative.

Table VI-21. Relative deviation of the molecules of the prediction set of primary and secondary amines for the first and second order QSPR model.

Molecule	First order QSPR model	Second order QSPR model
2-Amino-2-(hydroxymethyl)-1,3-propanediol (1129)	7.5 %	25.0 %
Cyclopentylamine (1103)	18.9 %	4.3 %
2-(Propylamino)ethanol (1222)	126.8 %	55.6 %
3-(Methylamino)propanenitrile (1240)	27.3 %	1.2 %
N-Methyl-1-butylamine (1202)	34.2 %	30.6 %
Average $\pm$ standard deviation	$42.9 \pm 47.9 \%$	$23.3 \pm 22.1 \%$

### 3. Results

#### 3.2.3 Gathering of kinetic constant $k_1$ and $k_2$

We represent both third order kinetic constant  $k_1$  and  $k_2$  of each molecule of the prediction set in Figure VI-20 (a) for the first order QSPR models and in Figure VI-20 (b) for the second order QSPR models. With the first order QSPR models, the estimations of the kinetic constants for molecules 1129, 1103 and 1202 are close to the experimental determination represented by their ellipse of confidence. Estimations of the first order QSPR models show an important discrepancy on  $k_1$  for molecule 1240 and  $k_2$  for molecule 1222. With the second order QSPR models, the kinetic constant of the molecule 1103 is estimated inside the ellipse of confidence. For molecules 1202 and 1222, the estimations remain close to the experimental value. Molecules 1129 and 1240 are not well predicted due to error on  $k_1$  (respectively 102 and 60 % of deviation). As for tertiary and sterically hindered amines it would be interesting to apply these models in comparison with experimental data on new molecules to precise their performance.

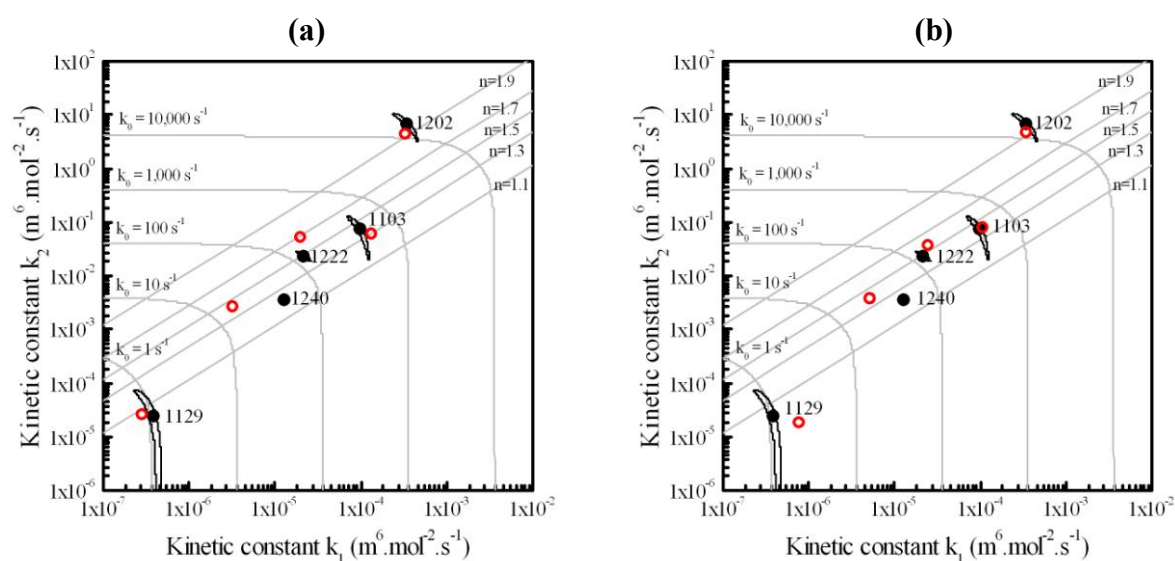


Figure VI-20. Kinetic constant  $k_2$  of molecules of the prediction set of tertiary amines as a function of the kinetic constant  $k_1$ . (a) First order QSPR model. (b) Second order QSPR model. Experimental values (black circles) and predicted values (red open circles). The confidence ellipses are represented.

Finally for both models we calculate the apparent kinetic constant for molecules of the training and validation set and the prediction set according to Equation 67. For the calculation we use the values of the amine and water concentrations of the experimental tests performed. We determine the average relative deviation and the standard deviation of the relative deviation between experimental and modelled values for each model and each set of data and indicate results in Table VI-22. It shows that second order QSPR models are more accurate in terms of interpolation and extrapolation. Even if the difference of accuracy in extrapolation is not very important, the standard deviation, more important for second order QSPR models indicates that the first order QSPR models are more precise than the second order QSPR models.

Table VI-22. Average relative deviation and standard deviation of the relative deviation between experimental and modelled value of  $k_0^{Am}$  of primary and secondary amines for training and validation set and prediction set of the first and second order QSPR models.

$k_0^{Am}$	First order QSPR model	Second order QSPR model
Training and validation set	$57.7 \pm 67.2 \%$	$39.2 \pm 45.7 \%$
Prediction set	$40.5 \pm 23.7 \%$	$39.9 \pm 28.4 \%$

Then we compare results obtained with experimental values in the parity plot indicated in Figure VI-21 (a) for the first order QSPR model and in Figure VI-21 (b) for the second order QSPR model. These figures show visually that the dispersion of the different sets is less important in the case of the second order QSPR model than in the case of the first order QSPR model.

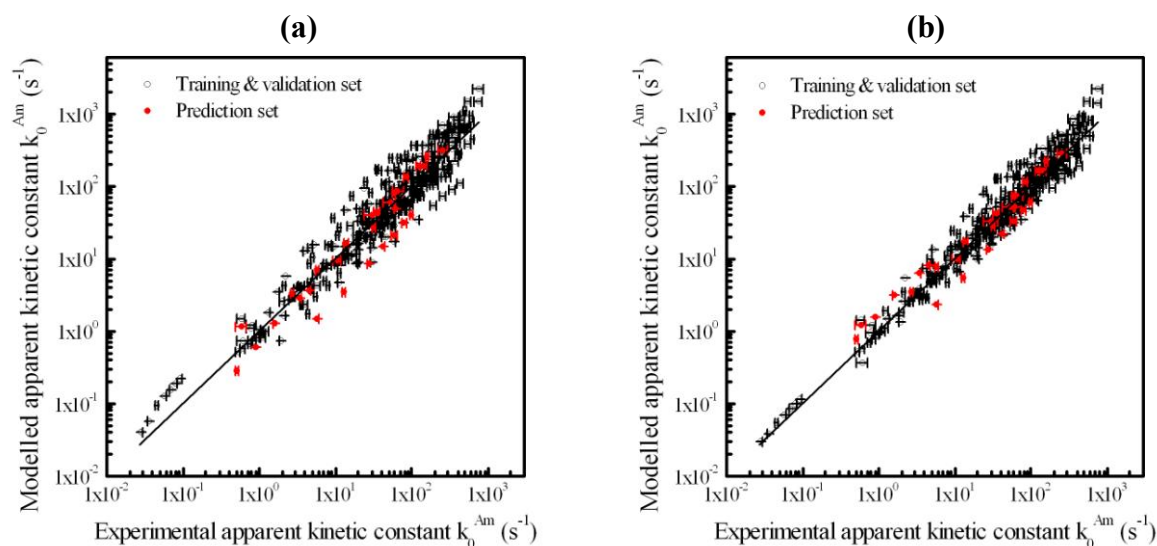


Figure VI-21. Parity plot between modelled and experimental apparent kinetic constant of primary and secondary. (a) First order QSPR model. (b) Second order QSPR model. Error bars correspond to the experimental confidence interval.

The average of the relative confidence interval (indicated in Equation 93) is around 7 % for primary and secondary amines. This value is lower than the ARD of the different values of different set and the different models. However the value of the ARD of  $k_1$ ,  $k_2$  and  $k_0^{Am}$  have the same order of magnitude (coarsely around 40 %) than the difference observed between different authors. Indeed, we show in Chapter II .5.1 that for diethanolamine a dispersion of around 50 % is observed between different authors in the same concentration range. In other words, the prediction error of our QSAR models has the same order of magnitude than the reproducibility error between different authors. Moreover, even if the first order QSPR models are less efficient than the second order QSPR models, they also need less information and then are faster to implement. This observation shows the interest to use both QSPR models set up in this work.

## 4 Discussion

Due to the huge number of terms in all second order QSPR models it is not possible to attempt to give a physico-chemical explanation. However, in this section we try to analyze the particular effects of the main descriptors which explain the most part of the information in the prediction of constants  $k_1$  and  $k_2$  according to the first order QSPR models previously presented.

### 4.1 Tertiary and sterically hindered amines

In the first order QSPR model of tertiary and sterically hindered secondary amines, the experimental pKa, the value of the dipole calculated in aqueous solution and the value of the HOMO in gas phase explain 60 % of the information. Those three descriptors each explain more than 15 % of the information. We do not take an interest in other descriptors which have a smaller impact on  $k_1$ . In the Chapter V, we have already discussed the correlation between the kinetic constant  $k_1$  and the pKa. Therefore we focus here on the effect of dipole aq and HOMO g. We represent the kinetic data by classes of amines as indicated in Table VI-23.

Table VI-23. Classes for tertiary and sterically hindered amines.

Class	Nature
1	Acyclic alkylamines
2	Acyclic alkanolamines
3	Others acyclic amines
4	Cyclic alkylamines
5	Cyclic alkanolamines
6	Others cyclic amines
7	Sterically hindered secondary amines

In the following, we represent the experimental kinetic constant  $k_1$  as a function of the dipole aq in Figure VI-22 (a) and the class of the amine as a function of the dipole aq in Figure VI-22 (b). Then we represent the experimental kinetic constant  $k_1$  as a function of the HOMO g in Figure VI-23 (a) and the class of the amine as a function of the HOMO g in Figure VI-23 (b). For Figure VI-22 (a) and Figure VI-23 (a) we have indicated the formula of different the acyclic tertiary alkanolamines. For Figure VI-22 (b) and Figure VI-23 (b) we indicate for each class, the structure of the amines which have the highest and the lowest value of the corresponding descriptor.

In the case of the Dipole aq, we observe a correlation between the kinetic constant  $k_1$  and the value of the Dipole aq. As indicated by the negative coefficient in the first order QSPR model,  $k_1$  tends to decrease when Dipole aq increases. We also notice that acyclic and cyclic alkylamines present the lower values of Dipole aq (close to 1 D). At the opposite, nitrilamines present the higher values of Dipole aq (around 5.5 D). Other amines present intermediate values of Dipole aq between 1.6 and 4.6 D. In some ways this descriptor gives a part of the information concerning the accessibility of the alcohol groups. We notice that the

series of dialkanolamines have higher values than monoalkanolamines. This is due to the calculation of the dipole  $aq$  which takes into account of the position and the electrostatic charges of atoms. With heteroatoms, the value of the dipole can increase. However the presence of heteroatoms also decreases the value of the  $pK_a$  and then decreases the kinetic constant. As long there are correlation between descriptors we only could assume of the nature of the contribution of each descriptor.

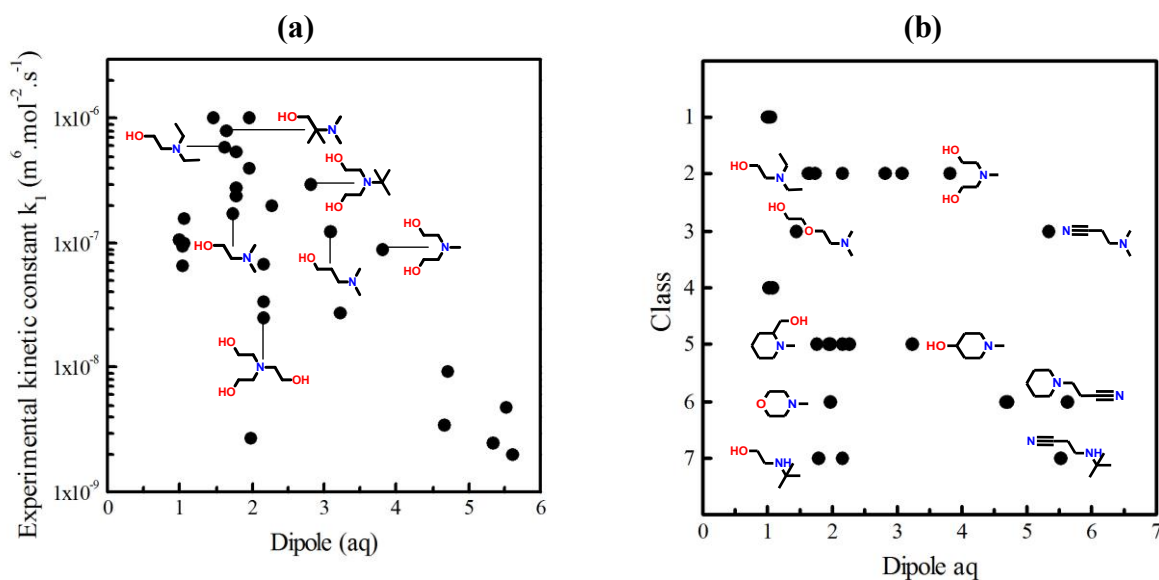


Figure VI-22. (a) Experimental kinetic constant  $k_1$  and (b) class of tertiary and sterically hindered amines as a function of the value of the dipole  $aq$ .

We also observe a correlation between the kinetic constant  $k_1$  and HOMO  $g$ . The HOMO (Highest Occupied Molecular Orbital) is linked to the reactivity of the lone electron pair and then to the nucleophilic character of the amine. In overall the kinetic constant  $k_1$  increases with the value of the HOMO  $g$  as same as the experimental  $pK_a$ . Molecules which have the lowest value of HOMO  $g$  are nitrilamines and triethanolamine (HOMO  $g$  below  $-0.235$  Ha) and molecules which have the strongest value of HOMO  $g$  are 1-azepaneethanol for cyclic and 2-dimethylamino-2-methylpropanol for acyclic (HOMO  $g$  above  $-0.215$  Ha).

For acyclic tertiary alkanolamines, we notice that the value of HOMO  $g$  is increased with the +I donor effect of alkyle groups on the amine. Among monoalkanolamines, the dimethylaminoethanol has the lowest value of the HOMO  $g$ . When the distance between the atom of nitrogen and oxygen increases (3-dimethylamino-1-propanol), the influence of the alcohol group is less important and the value of the HOMO  $g$  increases. For diethylethanolamine, there is the influence of two ethyl groups which increase the reactivity of the lone electron pair. The +I effect is maximal for 2-dimethylamino-2-methylpropanol, the nitrogen atom is surrounded by a tertiary carbon and two methyl groups. Even if HOMO  $g$  seems to be correlated to the  $pK_a$ , it also seems to bring complementary information especially concerning the electronic supply to the nitrogen atom by inductive effect (exemple of tert-butylaminodiethanol in comparison with methyl-diethanolamine).

## 4. Discussion

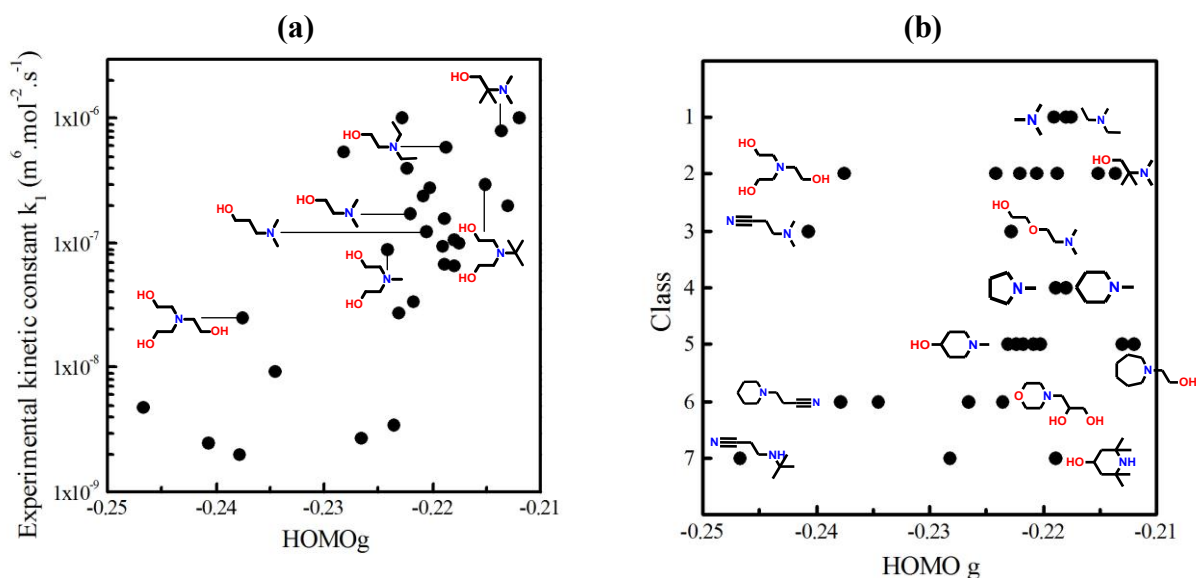


Figure VI-23. (a) Experimental kinetic constant  $k_1$  and (b) class of tertiary and sterically hindered amines as a function of the value of the HOMO g.

In all first order QSPR models we notice that among the 7 descriptors of the tertiary and sterically hindered amines model, we find again 4 descriptors (pKa, Dipole aq, Rotbonds and RPCG) in the model of kinetic constant  $k_1$  for primary and secondary amines which explains 28.27 % of the variability of  $k_1$  and 3 descriptors (pKa, dipole aq, HOMO g) in the model of kinetic constant  $k_2$  for primary and secondary amines which explains 20.87 % of the variability of  $k_2$ . If we assume that there is a high correlation in the modelling between kinetic constant  $k_1$  and  $k_2$  of primary and secondary amines, it shows that there is a non negligible part of the information of the model of primary and secondary amines which explain the result of tertiary amines. This observation may be another clue about the continuity of reactivity between primary/secondary amines and tertiary/sterically hindered amines. It should be interesting to predict the kinetic constant  $k_1$  of primary, secondary and tertiary amines at the same time and to compare its performance with models obtained in this work.

### 4.2 Primary and secondary amines

After the observations of the Chapter V, we expected to obtain the pKa and the nitrogen accessible surface highly correlated to the kinetic constants  $k_1$  and  $k_2$ . If it is the case for the kinetic constant  $k_1$ , it is not the case for kinetic constant  $k_2$ , even in the second order QSPR model. In this part we focus on the nitrogen accessible surface. Indeed, we do not take an interest in other descriptors which bring less information and then which are more difficult to explain because they are not correlated enough to the property to model. As previously, we represent the kinetic data by classes of amines as indicated in Table VI-24. Then for each class of amines, we represent the value of the nitrogen accessible surface as indicated in Figure VI-24. We indicate on this figure and for each class, the amines which have the highest and the lowest value of nitrogen accessible surface.

Table VI-24. Classes of primary and secondary amines.

Class	Nature
1	Primary acyclic alkylamines
2	Secondary acyclic alkylamines
3	Primary benzylamines
4	Secondary benzylamines
5	Primary acyclic alkanolamines
6	Secondary acyclic alkanolamines
7	Primary acyclic ether-amines
8	Secondary acyclic ether-amines
9	Primary acyclic nitrilamines
10	Secondary acyclic nitrilamines
11	Secondary cyclic alkylamines
12	Secondary cyclic alkanolamines
13	Derivates of morpholine

In overall we observe that primary amines are more accessible and then less sterically hindered than secondary amines. We notice that most of secondary cyclic amines are more accessible than secondary acyclic amines. This result, which confirms our previous assumptions (Chapter V .5 and Chapter V .7) is due to the particular structure of secondary cyclic amines. The three amines which do not form carbamates have a nitrogen accessible surface below  $5.5 \text{ \AA}^2$ . We also confirm that series of molecules with different pKa but with similar substituents have approximately the same steric hindrance. Indeed the series of linear primary amines have an average value of  $8.46 \text{ \AA}^2$  and a standard deviation of  $0.09 \text{ \AA}^2$ , series of derivates from tert-butyl have an average value of  $7.69 \text{ \AA}^2$  and a standard deviation of  $0.12 \text{ \AA}^2$  and series of linear secondary amines have an average value of  $6.72 \text{ \AA}^2$  and a standard deviation of  $0.13 \text{ \AA}^2$ . It also confirms that methyl group brings far less hindrance than others alkyl groups. Indeed, methylamine which has a nitrogen accessible surface of  $8.91 \text{ \AA}^2$  is significantly different of others molecules of the series of linear primary amines (average of  $8.46 \text{ \AA}^2$  and standard deviation of  $0.09 \text{ \AA}^2$ ). The same observation can be realized for dimethylamine which have a nitrogen accessible surface of  $7.21 \text{ \AA}^2$  with linear secondary amines (average of  $6.72 \text{ \AA}^2$  and a standard deviation of  $0.13 \text{ \AA}^2$ ).

## 4. Discussion

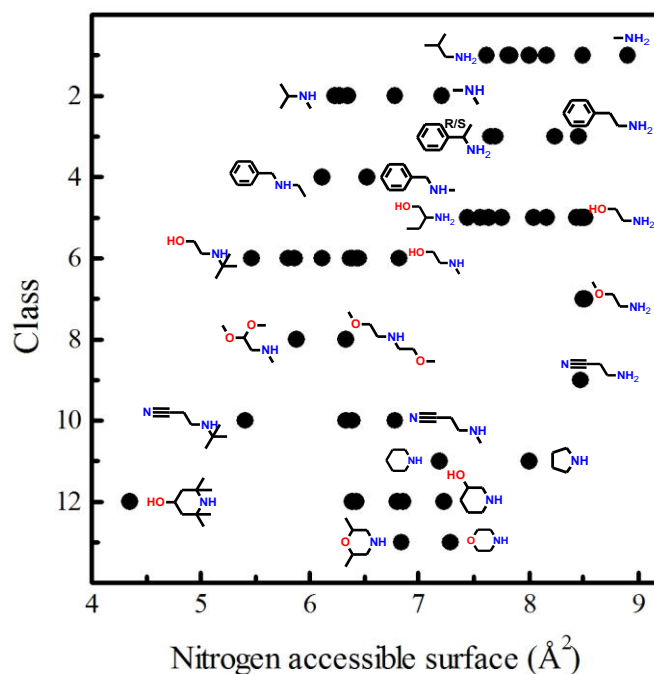


Figure VI-24. Value of the nitrogen accessible surface as a function of the class of primary and secondary amines.

However we notice, especially for primary amines which contain a secondary or a tertiary carbon linked to the amine function, some illogical values of nitrogen accessible surface. We choose to illustrate this effect with the series of acyclic primary alkylamines.

In Figure VI-25 (a) and (b) we respectively represent the kinetic constant  $k_1$  and  $k_2$  as a function of a series of acyclic primary alkylamines. In overall, we notice that the trend followed by methylamine, n-butylamine, cyclohexylamine and cyclopentylamine is almost linear. Isopropylamine fit correctly the trend for kinetic constant  $k_1$  but not for kinetic constant  $k_2$ . This comes from the experimental observation realised in Chapter V. Finally, it remains isobutylamine and tert-butylamine. In the case isobutylamine, value of nitrogen accessible surface is always overestimated to fit the correlation whereas it is the contrary for tert-butylamine.

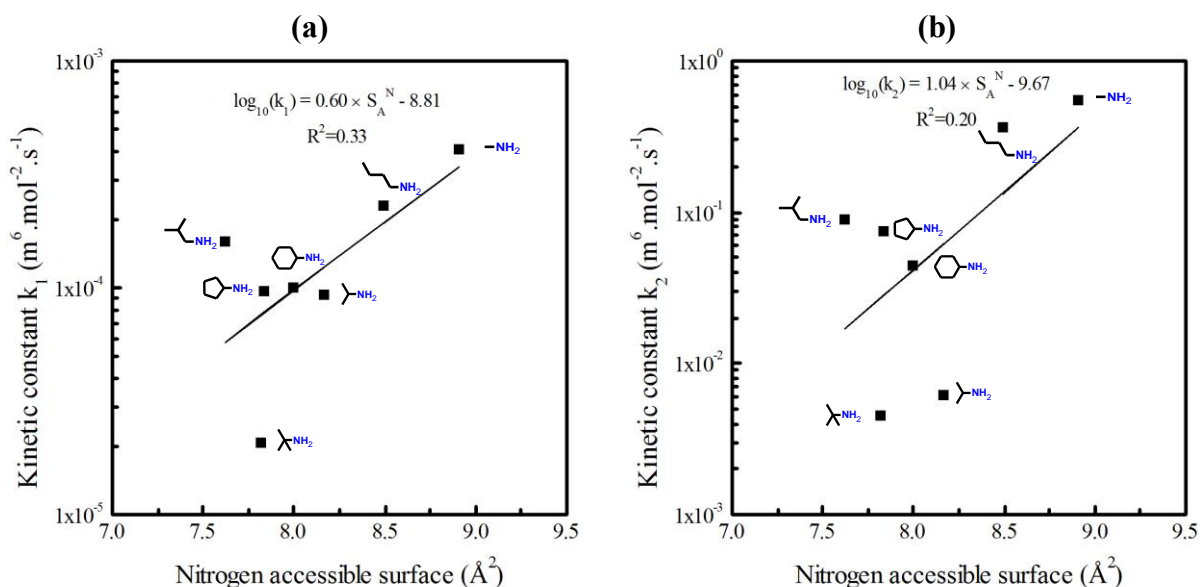


Figure VI-25. Kinetic constant (a)  $k_1$  and (b)  $k_2$  as a function of the nitrogen accessible surface for a series of primary acyclic alkylamines.

These results can be explained by the process of determination of the optimal structure. The conformer module optimizes the structure of a given molecule from different initial configurations. Then we obtain as many optimised structures as there are initial configurations of the molecule. Each optimised structure can be characterized by the value of its energy. A structure with a lower energy will be more stable than a structure with an higher energy. The interest of this method is to avoid falling in a local minimum as indicated in the Figure VI-26 with black continuous curve and red dotted curve where the energy is represented as a function of the conformation. Generally, in molecular modelling we consider a temperature of 0 K which means that only the lowest energy state exists. However, raising the temperature excites some molecules into higher energy states, and more and more states become accessible. The conformation of these energy states are distributed according to the Boltzmann distribution indicated in Equation 94 (Atkins and de Paula, 2006). In this equation,  $N_i$  corresponds to the number of conformation in the state  $i$  which has an energy state  $E_i$ ,  $N$  corresponds to the total number of conformation,  $k_B$  is the Boltzmann constant and  $T$  the temperature.

$$N_i = \frac{N \times \exp\left(-\frac{E_i}{k_B \times T}\right)}{\sum_i \exp\left(-\frac{E_i}{k_B \times T}\right)} \quad \text{Equation 94}$$

#### 4. Discussion

By analysing the energy of each optimized structure as a function of the initial configuration, we notice that we obtain three kinds of results schematised in Figure VI-26.

First, result indicated by the blue dashed curve which corresponds to a molecule where whatever the initial conformation we always find approximately the same optimized structure. It is the case of methylamine and tert-butylamine. In this case, the value of the accessible surface is the same because all optimized structures are the same.

Then, result indicated by the black continuous curve which corresponds to a molecule with important difference of energy between each optimized structure and then several local minimums. If the difference between the energy of the optimal conformation and the second optimal conformation is higher than  $k_B \times T$ , then the probability to find the second optimised structure is very low. Here we assume the product  $k_B \times T$  corresponds to the energy needed to increase the entropy of the system (Atkins and de Paula, 2006). In this case, as the energy of other conformations is not accessible, we can consider the value of the nitrogen accessible surface of the optimal conformation indicated by a black cross. This case concerns n-butylamine and isopropylamine.

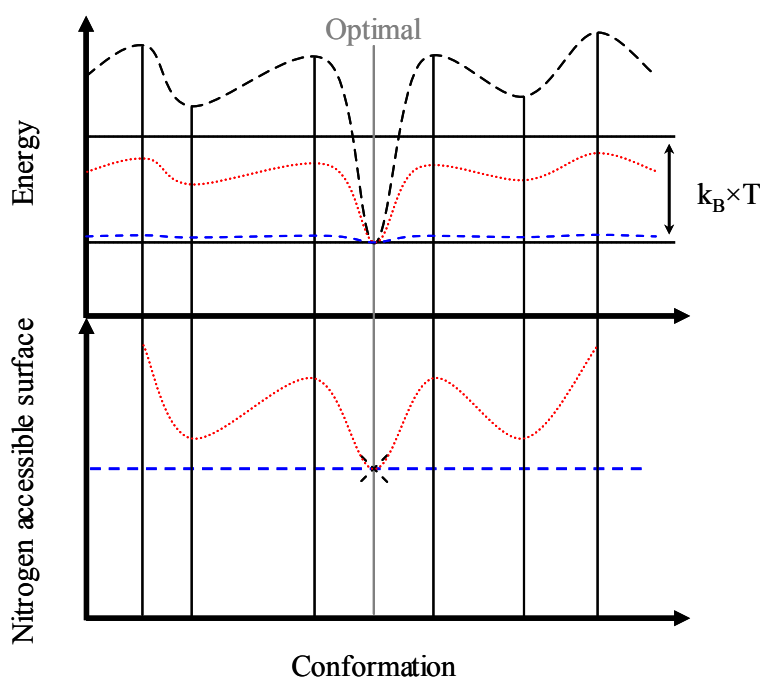


Figure VI-26. Scheme of the different configuration of the conformers results.

In the last case, represented by the red dotted curve, we obtain an optimal conformation and several local minimum conformations where their difference of energy are inferior to the product  $k_B \times T$  with the energy of the optimal configuration. In this case, even if these conformations are not predominant they exist and should be taking into account. Each of these conformations has a different value of nitrogen accessible surface than the optimal. This case concern cyclohexylamine, cyclopentylamine and isobutylamine. In the case of

cyclohexylamine and cyclopentylamine this difference of conformation leads to a maximum difference of nitrogen accessible surface of  $0.39 \text{ \AA}^2$ . In the case of isobutylamine this difference is higher than  $1.06 \text{ \AA}^2$ . Indeed we find out, for some optimal conformations of this molecule, value of nitrogen accessible surface of  $8.68 \text{ \AA}^2$ . This value will be closer to the trends obtained in Figure VI-25 (a) and (b) than the value of the optimal conformation. This weakness could explain why the nitrogen accessible surface have been removed by the PLS-GLR algorithm to model the kinetic constant  $k_2$  even if we outlined clear correlation of the steric hindrance of the amine and this kinetic constant in the Chapter V.

It shows that the descriptor of the nitrogen accessible surface could be improved by considering the value of less stable conformations. To realize this improvement, we propose to determine, always in gas phase, a huge number of different structures by using dynamic molecular modelling and by determining the average of the nitrogen accessible surface of these structures which should be representatives of the proportion we could find in the interval of the product  $k_B \times T$ .

However, nitrogen accessible surface has also non negligible strength that we illustrate from now. We first represent the kinetic constant  $k_1$  (Figure VI-27 (a)) and  $k_2$  (Figure VI-27 (b)) as a function of the nitrogen accessible surface for a series a acyclic secondary alkylamines. We first notice that in this case there is a good agreement between kinetic constants and the steric hindrance descriptor and moreover, contrary to Taft constant, we are able to give a value of the steric hindrance of the di-n-propylamine.

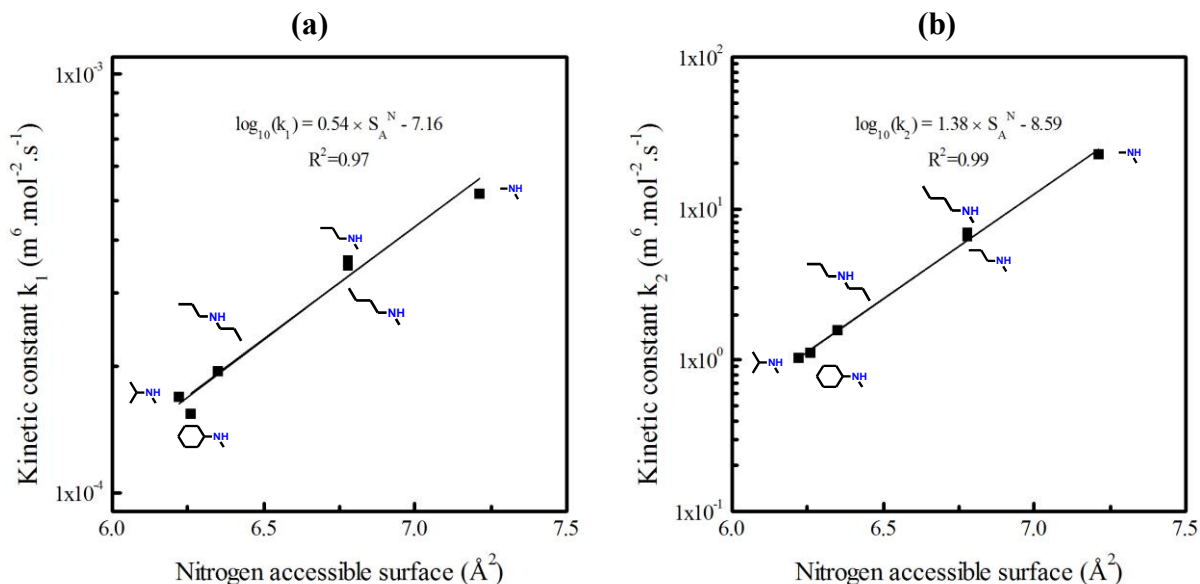


Figure VI-27. Kinetic constant (a)  $k_1$  and (b)  $k_2$  as a function of the nitrogen accessible surface for a series of secondary acyclic alkylamines.

If we now represent kinetic constant  $k_1$  (Figure VI-28 (a)) and  $k_2$  (Figure VI-28 (b)) as a function of nitrogen accessible surface of the series of acyclic secondary amines, which has the most numerous derivatives, we also find a good correlation between kinetic constants and

## 5. Conclusion

the descriptor of steric hindrance. The quality of this correlation is comparable or even better than when the Taft constant is used to describe the relative steric hindrance.

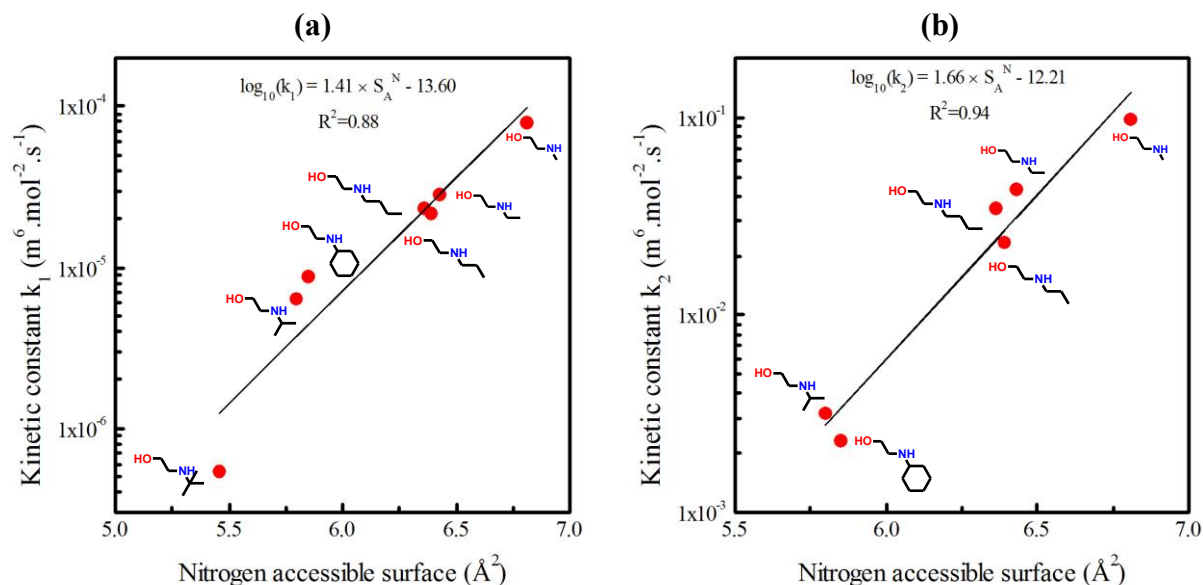


Figure VI-28. Kinetic constant (a)  $k_1$  and (b)  $k_2$  as a function of the nitrogen accessible surface for a series of secondary acyclic alkanolamines.

The loss of sensibility in the determination of  $k_2$  can also explain why nitrogen accessible surface has not been found as correlated to this kinetic constant. Indeed, as observed in Chapter V ellipse of confidence are more extended on the  $k_2$  axis than on the  $k_1$  axis. This indicates that the uncertainty on  $k_2$  is more important. In this condition, it is more difficult to the PLS-GLR algorithm to find a correlation between  $k_2$  and nitrogen accessible surface even if we know that it makes sense in a physico-chemical point of view.

We also notice that pKa, DPSA2, dipole aq, HOMOLUMO, Chi3Cluster and SubgCnts0Cluster are descriptors common to the first order QSPR model of kinetic constants  $k_1$  and  $k_2$  of primary and secondary amines. They explain together 45% of the variability for  $k_1$  it represents and 42 % of the variability on  $k_2$ . This statistical result tends to confirm the observation of Chapter V where we saw that an increase of kinetic constant  $k_1$  is often accompanied of an increase of kinetic constant  $k_2$ .

## 5 Conclusion

We have developed a method to realize QSPR models for the kinetic constant  $k_1$  of tertiary and sterically hindered secondary amines on the one hand and for kinetic constants  $k_1$  and  $k_2$  of primary and secondary amines forming carbamates on the other hand. This method is based on molecular descriptors and the PLS-GLR algorithm. We use three kinds of descriptors: 108 generic theoretical descriptors, 1 specific theoretical descriptor and 1 experimental descriptor in order to describe the parameters of each molecule. The generic theoretical descriptors have been determined with the Jaguar<sup>®</sup> the Material Studio<sup>®</sup> molecular

modelling softwares. We have used a hierarchical clustering method to select only 66 generic theoretical descriptors which are the less correlated between each other. We also calculate the nitrogen accessible surface as a new descriptor of the steric hindrance and introduce the experimental pKa as a descriptor of the amine basicity.

For each kinetic constant we determine two models through an optimization process based on a PLS-GLR regression: a first order QSPR model which is first order model with a limited number of descriptors and a second order QSPR model, more efficient but also more complicated due to its degree (2) and to the number of terms. In the case of the modelling of kinetic constant  $k_1$ , we obtain a first order QSPR model with 7 descriptors with an average relative deviation of prediction equal to 107 % and a second order QSPR model with 18 terms of the second order composed of 7 descriptors with an average relative deviation of prediction of 73 %. We expect that this important average relative deviation could be reduced with additional molecules in the prediction set. In the case of primary and secondary amines, the first order QSPR models have an average relative deviation of prediction equal to 31 % on  $k_1$  (16 descriptors) and 43 % on  $k_2$  (16 descriptors). The second order QSPR models have an average relative deviation of prediction equal to 37 % on  $k_1$  (123 second order terms of 29 descriptors) and of 23 % on  $k_2$  (89 second order terms of 16 descriptors). The modelled set of kinetic constants ( $k_1$ ;  $k_2$ ) determined by each independent model approach most of time the experimental ellipse of confidence even if the second order QSPR models have a slightly better performance than the first order QSPR models. We have shown that each QSPR model for tertiary and sterically hindered amines or primary and secondary amines can predict the value of kinetic constant  $k_1$ ,  $k_2$  and  $k_0^{Am}$  with a performance comparable to reproducibility error which is around 50 %.

For tertiary and sterically hindered amines, the calculated descriptors dipole  $aq$  and HOMO  $g$  explains an important variability on  $k_1$  and shed some light on the specific effects of the alcohol functions and inductive effects on the amine reactivity. For primary and secondary amines we confirm the important effect of steric hindrance described by the nitrogen accessible surface. However we point out some weakness in this descriptor which comes from the possibility to have others relatively stable conformations with a value of nitrogen accessible surface significantly different than the value of the optimal conformation. We propose a method to develop this descriptor by using dynamic molecular modelling. We assume that this effect could explain why kinetic constant  $k_2$  is not correlated to nitrogen accessible surface according to the PLS-GLR algorithm. However we also show that it concern particular cases and that in overall nitrogen accessible surface have non negligible strength.



## *Chapter VII: GENERAL CONCLUSION AND PERSPECTIVES*

---

In Chapter II we saw that the post-combustion process using amine scrubbing is the most mature method to remove carbon dioxide from flue gases. However it still suffers from important cost penalties. To reduce these costs, it is necessary to optimize three parameters: thermodynamics, kinetics and chemical stability of the solvent. In this study, we take an interest in the kinetic properties which are the second item of expenditure. The different reactions and kinetic laws associated have been presented. We show there are for primary/secondary amines and tertiary amine several mechanisms proposed to explain the kinetic properties. Then we present the different experimental methods to study the kinetics of reaction between amine and carbon dioxide. We justify using stopped-flow technique which is the most adapted to our study. We also present the numerical and the analytical method used to extract kinetic data from the different stopped-flow signals.

Thanks to an in-depth study of literature data obtained by stopped-flow equipment with conductivity detection and determined with analytical method, we obtain numerous information indicated in Chapter III. First we verify that primary/secondary amines generally react faster than tertiary amines. Then, with a power law relation, we show that tertiary amines have an order of 1 with respect to the amine while primary and secondary amines have an order undertaken between 1 and 2. Except for carbamic acid mechanism, all mechanisms proposed in the literature explain the observed experimental results. However, in the case of the zwitterion mechanism, we outline a mathematical indetermination. We also argue that it will be more consistent to consider in one side amines which form carbamates and on this other side amines which directly form carbonates rather than primary/secondary amines and tertiary amines. Indeed, tert-butylethanolamine, which is a sterically hindered secondary amine, behaves as a tertiary amine. The basicity of amines which directly form carbonates is directly linked to kinetic properties. When amines form carbamates, the kinetic properties are linked to the basicity and the steric hindrance of the molecule. We find out a compensation phenomena between the activation energy of the first order kinetic constant according to the amine of the termolecular model and the corresponding pre-exponential factor. It seems to indicate that the enthalpy and the entropy of the transition state are correlated. Thanks to this study of literature data, we precise the objectives of our work. Indeed, the two main objectives of this work are on the one hand to study the kinetic properties of amines in order to have a better understanding of the CO<sub>2</sub>-amine rate of reaction as a function of the structure and on the other hand to set up a predictive QSPR model.

In Chapter IV, we precise the different methods used in this study to characterise the kinetic properties, the associated uncertainty and the design of experiments. We first present the two experimental techniques used: stopped-flow with conductivity detection to study the kinetic properties and acid-base titration to quantify amine, CO<sub>2</sub> and to determine dissociation constant of amines. We set up two methods to extract kinetic data: an analytical and a numerical. If we justify to use the analytical method to determine the apparent kinetic constants. We also show that we can not do without the numerical model which is useful for

determining the speciation or to simulate conductance curves and to prepare operating conditions of experiments. We set up two experimental methods to respect the assumptions of the analytical method. Then we indicate that we measure the apparent kinetic constant at least at six different concentrations with five repetitions in order to determine the average apparent kinetic constant and the associated uncertainty. We present the semi-empirical model we use to determine the kinetic constants. It consists in two kinetic constant: one first order kinetic constant according to the amine and on second order kinetic constant according to the amine. We also show that for this kinetic model the uncertainty is characterised by a confidence ellipse. We finally present the design of experiment which corresponds to amines we identify as the most representative of our field of study.

In Chapter V, we analyse results obtained by degree of substitution. We first take an interest in tertiary amines. For this kind of molecules, we show that the basicity of the amine is the parameter which mostly drives the kinetic properties. We also indicate that the accessibility to alcohol group to the atom of nitrogen of the amine function favour the kinetic properties. We assume that this effect comes from the intervention of the water in the reaction. Then, concerning primary amines, we indicate for several series the influence of the basicity and the steric hindrance. At this point, we noticed it does not exist exhaustive descriptor of steric hindrance. We also noticed that there is a cross effect between basicity and steric hindrance of the molecule. The same observation have been realised for acyclic secondary amines. We showed that there is a clear difference of behaviour between primary and acyclic secondary amines. In the case of cyclic secondary amines, we show that basicity and steric hindrance impact kinetic properties but it a limited area in comparison with acyclic secondary amines. Among the three studied di-amines, we class them into two different groups: symmetric and asymmetric. In the case of symmetric amines, we notice that they always react faster (around 2 times) than corresponding mono-amines. We assume this observation comes from an entropic effect. However we do not have enough data to prove it. In the case of asymmetric di-amines, we show that it behaves as mono-amine because one of the two functions reacts much slowly than the other.

In Chapter VI we first present the method used and finally the results of the QSPR modelling. First we present the method used to calculate 110 molecular descriptors and then how we retain only the 68 less correlated of them. Among those descriptors we set up especially a new descriptor called nitrogen accessible surface. It corresponds to a descriptor of the steric hindrance. Contrary to most of others descriptors of steric hindrance, this one could be applied to any molecules. The 68 descriptors were used to reflect the physico-chemical parameters of each studied amine. We link those descriptors to the kinetic properties using a PLS-GLR algorithm which is the most adapted to our study. Moreover, we show that the use a training set, a validation set and a prediction set with several models is necessary to build the "best model". We justify to optimize this "best model" by determining the degree and the number of terms. For each class of amine we determine a physico-chemical model, which is a little bit less efficient but with a limited complexity and a statistical model, a little bit more efficient but more complicated. In the case of tertiary amines we show that we are able to predict data with a limited performance (ARD of 107 % for physico-chemical model and 73

% for statistic model). We assume that this important relatively important relative average relative deviation comes from the weak number of molecules in the prediction set (3 amines). In the case of primary and secondary we predict kinetic constants  $k_1$  with an ARD of 31 % for physico-chemical model and 37 % with statistical model and  $k_2$  with an ARD of 43 % for physico-chemical model and 23 % with statistical model. We discuss about the effect of the 3 most correlated descriptors of the physico-chemical model of amines which directly form carbonates. In the case of primary and secondary amines we discuss about the strengths and the weaknesses of the nitrogen accessible surface.

In future works, it will be interesting to study other multi-amines in order to conclude about the entropic effect observed. Moreover, study of multi-amines will show if this latest kind of molecules behaves as several mono-amines sites with corresponding basicity and steric hindrance or if there is an activation phenomenon due to the presence of several amine functions in the same molecule. It would also be interesting to study some others mono-amines in order to apply the QSPR model and then to verify its predictive capacity, especially for tertiary amines. A complete study of nitrogen accessible surface will be useful to improve it. This descriptor could be then use in other field as a "universal" descriptor of the steric hindrance. After the improvement of the nitrogen accessible surface, it would be interesting to set up a new QSPR model with the same descriptors used in order to verify if the improvement of the nitrogen accessible surface improve the prediction of the QSPR model. Finally it would be interesting to apply this methodology to the two others most important fields of the amine scrubbing process (thermodynamics and chemical stability), to predict the properties of all existing amines and then to cross results of the kinetics with the two others in order to identify amines which have the best performance. It will be a method to ensure that the selected system confers the best performance to the process.



## Chapter VIII: BIBLIOGRAPHIC REFERENCES

---

- Ali S.H., Merchant S.Q. and Fahim M.A., (2000), "Kinetic study of reactive absorption of some primary amines with carbon dioxide in ethanol solution", *Separation and Purification Technology*, **Volume 18**, Issue 3, Pages 163-175.
- Ali S.H., Merchant S.Q. and Fahim M.A., (2002), "Reaction kinetics of some secondary alkanolamines with carbon dioxide in aqueous solutions by stopped flow technique", *Separation and Purification Technology*, **Volume 27**, Issue 2, Pages 121-136.
- Ali S.H., (2004), "Kinetic study of the reaction of diethanolamine with carbon dioxide in aqueous and mixed solvent systems--application to acid gas cleaning", *Separation and Purification Technology*, **Volume 38**, Issue 3, Pages 281-296.
- Ali S.H., (2005), "Kinetics of the reaction of carbon dioxide with blends of amines in aqueous media using the stopped-flow technique", *International Journal of Chemical Kinetics*, **Volume 37**, Issue 7, Pages 391-405.
- Ali S.H., Al-Rashed O. and Merchant S.Q., (2010), "Opportunities for faster carbon dioxide removal: A kinetic study on the blending of methyl monoethanolamine and morpholine with 2-amino-2-methyl-1-propanol", *Separation and Purification Technology*, **Volume 74**, Issue 1, Pages 64-72.
- Alper E., (1990a), "Kinetics of Reactions of Carbon-Dioxide with Diglycolamine and Morpholine", *Chemical Engineering Journal and the Biochemical Engineering Journal*, **Volume 44**, Issue 2, Pages 107-111.
- Alper E., (1990b), "Reaction mechanism and kinetics of aqueous solutions of 2-amino-2-methyl-1-propanol and carbon dioxide", *Industrial & Engineering Chemistry Research*, **Volume 29**, Issue 8, Pages 1725-1728.
- Anheden M., Yan J. and De Smedt G., (2005), "Denitrogenation (or Oxyfuel Concepts)", *Oil & Gas Science and Technology - Rev.IFP*, **Volume 60**, Issue 3, Pages 485-495.
- Astarita G., Savage D.W. and Bisio A., (1983), *Gas Treating with Chemical Solvents*, John Wiley & Sons Inc (ed(s)/éd.), New York.
- Atkins P. and de Paula J., (2006), *Physical Chemistry 8th Edition*, Oxford University Press (ed(s)/éd.), Oxford.
- Balaban A.T., (1982), "Highly discriminating distance-based topological index", *Chemical Physics Letters*, **Volume 89**, Issue 5, Pages 399-404.
- Balaban, A.T. and Ivanciuc, O., (1989), "FORTRAN 77 Computer Program for Calculating the Topological Index J for Molecules Containing Heteroatoms", in *MATH/CHEM/COMP*, Graovac, A. (éd.), Elsevier, Amsterdam.
- Barrie P.J., (2012), "The mathematical origins of the kinetic compensation effect: 1. the effect of random experimental errors", *Physical Chemistry Chemical Physics*, **Volume 14**, Issue 1, Pages 318-326.

- Barth D., Tondre C., Lappai G. and Delpuech J.J., (1981), "Kinetic study of carbon dioxide reaction with tertiary amines in aqueous solutions", *The Journal of Physical Chemistry*, **Volume 85**, Issue 24, Pages 3660-3667.
- Barth D., Tondre C. and Delpuech J.J., (1983), "Stopped-flow determination of carbon dioxide-diethanolamine reaction mechanism: Kinetics of carbamate formation", *International Journal of Chemical Kinetics*, **Volume 15**, Issue 11, Pages 1147-1160.
- Barth D., Tondre C. and Delpuech J.J., (1984), "Kinetics and mechanisms of the reactions of carbon dioxide with alkanolamines: a discussion concerning the cases of MDEA and DEA", *Chemical Engineering Science*, **Volume 39**, Issue 12, Pages 1753-1757.
- Barth D., (1984), "Mécanismes des réactions du gaz carbonique avec des amino-alcools en solutions aqueuses : étude cinétique et thermodynamique", PhD Thesis, Université de Nancy I.
- Barth D., Tondre C. and Delpuech J.-J., (1986), "Stopped-flow investigations of the reaction kinetics of carbon dioxide with some primary and secondary alkanolamines in aqueous solutions", *International Journal of Chemical Kinetics*, **Volume 18**, Issue 4, Pages 445-457.
- Bastien P., Vinzi V.E. and Tenenhaus M., (2005), "PLS generalised linear regression", *Computational Statistics & Data Analysis*, **Volume 48**, Issue 1, Pages 17-46.
- Bonchev D., (1983), *Information Theoretic Indices for Characterization of Chemical Structures*, Research Studies Press (ed(s)/éd.), New York.
- Bonchev D., Mekenyan O.V. and Trinajstić N., (1981), "Isomer discrimination by topological information approach", *Journal of Computational Chemistry*, **Volume 2**, Issue 2, Pages 127-148.
- Bouhamra W., Bavbek O. and Alper E., (1999), "Reaction mechanism and kinetics of aqueous solutions of 2-amino-2-methyl-1,3-propanediol and carbon dioxide", *Chemical Engineering Journal*, **Volume 73**, Issue 1, Pages 67-70.
- Brenan K.E., Campbell S.L. and Petzold L.R., (1989), *Numerical Solution of Initial-Value Problems in Differential-Algebraic Equations*, New York.
- Breneman C.M. and Wiberg K.B., (1990), "Determining atom-centered monopoles from molecular electrostatic potentials. The need for high sampling density in formamide conformational analysis", *Journal of Computational Chemistry*, **Volume 11**, Issue 3, Pages 361-373.
- Caplow M., (1968), "Kinetics of carbamate formation and breakdown", *Journal of the American Chemical Society*, **Volume 90**, Issue 24, Pages 6795-6803.
- Capture Ready, (2013) ;  
<http://www.captureready.com/en/Channels/Research/showDetail2.asp?objID=298>
- Charpentier, J.C. (1981) Mass-Transfer Rates in Gas-Liquid Absorbers and Reactors, in *Advances in Chemical Engineering*, Thomas, B.D. (éd.), Academic Press.

- Chemicalize, (2012a) ;  
<http://www.chemicalize.org/structure/#!mol=CCCCNCCO&source=calculate>
- Chemicalize, (2012b) ;  
<http://www.chemicalize.org/structure/#!mol=CCCCNCCO&source=calculate>
- Chemicalize, (2012c) ;  
<http://www.chemicalize.org/structure/#!mol=CCNCCO&source=calculate>
- Chemicalize, (2012d) ;  
<http://www.chemicalize.org/structure/#!mol=CCCCNCCO&source=calculate>
- Chemicalize, (2013) ; <http://www.chemicalize.org/>
- Chemspider, (2013) ; <http://www.chemspider.com/>
- CLC, (2013) ; [http://www.chemical-looping.at/Upload/image/CLC\\_Concept\\_Tobi.JPG](http://www.chemical-looping.at/Upload/image/CLC_Concept_Tobi.JPG)
- Commission européenne (2009) *Le système communautaire d'échange de quotas d'émission (SCEQE): L'action de l'UE pour lutter contre le changement climatique*, Office des publications officielles des Communautés européennes, Luxembourg.
- Committee on Climate Change (2008) *Building a low-carbon economy – The UK's contribution to tackling climate change*.
- Contribution of Working Groups I, II and III to the Fourth Assessment Report of the Intergovernmental Panel on Climate Change, Pachauri R.K., Reisinger A., (2008) *Climate Change 2007: Synthesis Report, IPCC*, Geneva, Switzerland.
- Conway W., Wang X., Fernandes D., Burns R., Lawrance G., Puxty G. and Maeder M., (2011), "Comprehensive kinetic and thermodynamic study of the reactions of CO<sub>2</sub>(aq) and HCO<sub>3</sub><sup>-</sup> with monoethanolamine (MEA) in aqueous solution", *Journal of Physical Chemistry A*, **Volume 115**, Issue 50, Pages 14340-14349.
- Conway W., Wang X., Fernandes D., Burns R., Lawrance G., Puxty G. and Maeder M., (2012a), "Toward Rational Design of Amine Solutions for PCC Applications: The Kinetics of the Reaction of CO<sub>2</sub>(aq) with Cyclic and Secondary Amines in Aqueous Solution", *Environmental Science & Technology*, **Volume 46**, Issue 13, Pages 7422-7429.
- Conway W.O., Maeder M., Burns R., Wang X., Lawrance G.A., Puxty G. and Fernandes D., (2012b), "Towards the Understanding of Chemical Absorption Processes for Post Combustion Capture of Carbon Dioxide: Electronic and Steric Considerations from the Kinetics of Reactions of CO<sub>2</sub>(aq) with Sterically-hindered Amines", *Environmental Science & Technology*, **Volume 47**, Issue 2, Pages 1163-1169.
- Conway W., Fernandes D., Beyad Y., Burns R., Lawrance G., Puxty G. and Maeder M., (2013), "Reactions of CO<sub>2</sub> with Aqueous Piperazine Solutions: Formation and Decomposition of Mono- and Dicarbamic Acids/Carbamates of Piperazine at 25.0°C", *The Journal of Physical Chemistry A*, **Volume 117**, Issue 5, Pages 806-813.
- Cordon A.D. (1999) *Classification, 2nd ed*, Chapman and Hall (ed(s)/éd.).

- Crooks J.E. and Donnellan J.P., (1989), "Kinetics and mechanism of the reaction between carbon dioxide and amines in aqueous solution", *Journal of the Chemical Society, Perkin Transactions 2*, Issue 4, Pages 331-333.
- Crooks J.E. and Donnellan J.P., (1990), "Kinetics of the reaction between carbon dioxide and tertiary amines", *Journal of Organic Chemistry*, **Volume 55**, Issue 4, Pages 1372-1374.
- Curtiplot, (2013) ; <http://www2.iq.usp.br/docente/gutz/Curtipot.html>
- da Silva E.F. and Svendsen H.F., (2004), "Ab Initio Study of the Reaction of Carbamate Formation from CO<sub>2</sub> and Alkanolamines", *Industrial & Engineering Chemistry Research*, **Volume 43**, Issue 13, Pages 3413-3418.
- da Silva E.F. and Svendsen H.F., (2005), "Study of the Carbamate Stability of Amines Using ab Initio Methods and Free-Energy Perturbations", *Industrial & Engineering Chemistry Research*, **Volume 45**, Issue 8, Pages 2497-2504.
- da Silva E.F. and Svendsen H.F., (2007), "Computational chemistry study of reactions, equilibrium and kinetics of chemical CO<sub>2</sub> absorption", *International Journal of Greenhouse Gas Control*, **Volume 1**, Issue 2, Pages 151-157.
- Danckwerts P.V., (1970), *Gas liquid reactions*, McGraw-Hill Book Company (ed(s)/éd.), London.
- Danckwerts P.V., (1979), "The reaction of CO<sub>2</sub> with ethanolamines", *Chemical Engineering Science*, **Volume 34**, Issue 4, Pages 443-446.
- Donaldson T.L. and Nguyen Y.N., (1980), "Carbon Dioxide Reaction Kinetics and Transport in Aqueous Amine Membranes", *Industrial & Engineering Chemistry Fundamentals*, **Volume 19**, Issue 3, Pages 260-266.
- Draper N.R. and Smith H., (1998), *Applied Regression Analysis, 3rd Edition*, Wiley (ed(s)/éd.).
- Düren T., Millange F., Férey G., Walton K.S. and Snurr R.Q., (2007), "Calculating Geometric Surface Areas as a Characterization Tool for Metal–Organic Frameworks", *The Journal of Physical Chemistry C*, **Volume 111**, Issue 42, Pages 15350-15356.
- Düren T., (2013) ; [http://www.see.ed.ac.uk/~tduren/research/surface\\_area/](http://www.see.ed.ac.uk/~tduren/research/surface_area/)
- Edwards T.J., Maurer G., Newman J. and Prausnitz J.M., (1978), "Vapor-liquid equilibria in multicomponent aqueous solutions of volatile weak electrolytes", *AIChE Journal*, **Volume 24**, Issue 6, Pages 966-976.
- Eide L.I. and Bailey D.W., (2005), "Precombustion Decarbonisation Processes", *Oil & Gas Science and Technology - Rev.IFP*, **Volume 60**, Issue 3, Pages 475-484.
- Eide L.I., Anheden M., Lyngfelt A., Abanades C., Younes M., Clodic D., Bill A.A., Feron P.H.M., Rojey A. and Giroudière F., (2005), "Novel Capture Process", *Oil & Gas Science and Technology - Rev.IFP*, **Volume 60**, Issue 3, Pages 497-508.

- Ellerman A.D. and Buchner B.K., (2007), "The European Union Emissions Trading Scheme: Origins, Allocation, and Early Results", *Review of Environmental Economics and Policy*, **Volume 1**, Issue 1, Pages 66-87.
- Ellerman D. and Buchner B., (2008), "Over-Allocation or Abatement? A Preliminary Analysis of the EU ETS Based on the 2005-06 Emissions Data", *Environmental and Resource Economics*, **Volume 41**, Pages 267-287.
- Feron P.H.M. and Hendriks C.A., (2005), "CO<sub>2</sub> Capture Principles and Costs", *Oil & Gas Science and Technology - Rev.IFP*, **Volume 60**, Issue 3, Pages 451-459.
- Ghose A.K. and Crippen G.M., (1986), "Atomic Physicochemical Parameters for Three-Dimensional Structure-Directed Quantitative Structure-Activity Relationships I. Partition Coefficients as a Measure of Hydrophobicity", *Journal of Computational Chemistry*, **Volume 7**, Issue 4, Pages 565-577.
- Gordesli F.P. and Alper E., (2011), "The kinetics of carbon dioxide capture by solutions of piperazine and N-methyl piperazine", *International Journal of Global Warming*, **Volume 3**, Issue 1, Pages 67-76.
- Guggenheim E.A., (1935), "The specific thermodynamic properties of aqueous solutions of strong electrolytes", *Philosophical Magazine Series 7*, **Volume 19**, Issue 127, Pages 588-643.
- Hall, L.H., (1991), The molecular connectivity Chi indexes and Kappa shape indexes in structure-property modelling, in *Reviews in Computational Chemistry*.
- Hall L.H. and Kier L.B., (1995), Electrotopological State Indices for Atom Types: A Novel Combination of Electronic, Topological, and Valence State Information, *Journal of Chemical Information and Computer Sciences*, **Volume 35**, Issue 6, Pages 1039-1045.
- Hamborg E.S. and Versteeg G.F., (2009), "Dissociation Constants and Thermodynamic Properties of Amines and Alkanolamines from (293 to 353) K", *Journal of Chemical & Engineering Data*, **Volume 54**, Issue 4, Pages 1318-1328.
- Harned H.S. and Owen B.B., (1958), *The Physical Chemistry of Electrolyte Solutions*, Reinhold (ed(s)/éd.), New York.
- Härtel G., Rompf F. and Püschel T., (1996), "Separation of a CO<sub>2</sub>/H<sub>2</sub> gas mixture under high pressure with polyethylene terephthalate membranes", *Journal of Membrane Science*, **Volume 113**, Pages 115-120.
- Harvey A.H., (1996), "Semiempirical correlation for Henry's constants over large temperature ranges", *AIChE Journal*, **Volume 42**, Issue 5, Pages 1491-1494.
- Henni A., Li J. and Tontiwachwuthikul P., (2008), "Reaction Kinetics of CO<sub>2</sub> in Aqueous 1-Amino-2-Propanol, 3-Amino-1-Propanol, and Dimethylmonoethanolamine Solutions in the Temperature Range of 298–313 K Using the Stopped-Flow Technique", *Industrial & Engineering Chemistry Research*, **Volume 47**, Issue 7, Pages 2213-2220.
- Hill T.L., (1960), *Introduction to statistical thermodynamics*, Addison-Wesley (ed(s)/éd.).

- Hindmarsh, A.C., (1983), ODEPACK, A systematized Collection of ODE Solvers, in *IMACS Transactions on Scientific Computation*, Stepleman, R.S. (éd.), Amsterdam.
- IFP Energies nouvelles, (2013) ; <http://www.ifpenergiesnouvelles.fr/espace-decouverte/les-cles-pour-comprendre/les-sources-d-energie/le-gaz-naturel>
- Iida K. and Sato H., (2012), "Proton Transfer Step in the Carbon Dioxide Capture by Monoethanol Amine: A Theoretical Study at the Molecular Level", *The Journal of Physical Chemistry B*, **Volume 116**, Issue 7, Pages 2244-2248.
- International Energy Agency, (2008), *Energy technology perspectives*, OECD Publishing, Paris.
- International Energy Agency, (2011), *CO<sub>2</sub> emissions from fuel combustion 2011*, OECD Publishing, Paris.
- Jaguar, (2013) ; <http://www.schrodinger.com/productpage/14/7/>
- Kadiwala S., Rayer A.V. and Henni A., (2012), "Kinetics of carbon dioxide (CO<sub>2</sub>) with ethylenediamine, 3-amino-1-propanol in methanol and ethanol, and with 1-dimethylamino-2-propanol and 3-dimethylamino-1-propanol in water using stopped-flow technique", *Chemical Engineering Journal*, **Volume 179**, Issue 0, Pages 262-271.
- Katritzky A.R. and Gordeeva E.V., (1993), "Traditional topological indexes vs electronic, geometrical, and combined molecular descriptors in QSAR/QSPR research", *Journal of Chemical Information and Computer Sciences*, **Volume 33**, Issue 6, Pages 835-857.
- Kier, L.B. and Hall, L.H., (1976), Molecular connectivity indices in chemistry and drug research, in *Medicinal Chemistry*, Stevens, G. (éd.), Academic Press, New York.
- Kier L.B. and Hall L.H., (1985), *Molecular connectivity in Structure-activity Analysis*, Research Studies Press (ed(s)/éd.), New York.
- Kier L.B. and Hall L.H., (1990), "An Electrotopological-State Index for Atoms in Molecules", *Pharm Res*, **Volume 7**, Issue 8, Pages 801-807.
- Knipe A.C., McLean D. and Tranter R.L., (1974), "A fast response conductivity amplifier for chemical kinetics", *Journal of Physics E: Scientific Instruments*, **Volume 7**, Issue 7, Pages 586.
- Kumar P.S., Hogendoorn J.A., Versteeg G.F. and Feron P.H.M., (2003), "Kinetics of the reaction of CO<sub>2</sub> with aqueous potassium salt of taurine and glycine", *AIChE Journal*, **Volume 49**, Issue 1, Pages 203-213.
- Laurent A. and Charpentier J.C., (1974), "Aires interfaciales et coefficients de transfert de matière dans les divers types d'absorbants et de réacteurs gaz--liquide", *The Chemical Engineering Journal*, **Volume 8**, Issue 2, Pages 85-101.

- Laurent A., Prost C. and Charpentier J.-C., (1975), "Détermination par méthode chimique des aires interfaciales et des coefficients de transfert de matière dans les divers types d'absorbants et de réacteurs gaz-liquide.", *Journal de Chimie Physique*, **Volume 72**, Issue 2, Pages 236-244.
- Leach A., (2001), *Molecular Modelling: Principles and Applications*, Pearson Education EMA (ed(s)/éd.).
- Lecomte F. *et al.*, (2010), *Le captage du CO<sub>2</sub>, des technologies pour réduire les émissions de gaz à effet de serre*, Technip (ed(s)/éd.), Paris.
- Li J., Henni A. and Tontiwachwuthikul P., (2007), "Reaction Kinetics of CO<sub>2</sub> in Aqueous Ethylenediamine, Ethyl Ethanolamine, and Diethyl Monoethanolamine Solutions in the Temperature Range of 298–313 K, Using the Stopped-Flow Technique", *Industrial & Engineering Chemistry Research*, **Volume 46**, Issue 13, Pages 4426-4434.
- Lide D.R., (1994), *CRC Handbook of Chemistry and Physics, 75th edition*, CRC Press (ed(s)/éd.), London.
- Littel R.J., Swaaij van W.P.M. and Versteeg G.F., (1990a), "Kinetics of Carbon Dioxide with tertiary Amines in aqueous solution", *AIChE Journal*, **Volume 36**, Issue 11, Pages 1633-1640.
- Littel R.J., Bos M. and Knoop G.J., (1990b), "Dissociation constants of some alkanolamines at 293, 303, 318, and 333 K", *Journal of Chemical & Engineering Data*, **Volume 35**, Issue 3, Pages 276-277.
- Liu L. and Guo Q.X., (2001), "Isokinetic relationship, isoequilibrium relationship, and enthalpy-entropy compensation", *Chemical reviews*, **Volume 101**, Issue 3, Pages 673-695.
- Martin S., Lepaumier H., Picq D., Kittel J., de Bruin T., Faraj A. and Carrette P.L., (2012), "New Amines for CO<sub>2</sub> Capture. IV. Degradation, Corrosion, and Quantitative Structure Property Relationship Model", *Industrial & Engineering Chemistry Research*, **Volume 51**, Issue 18, Pages 6283-6289.
- Material Studio, (2013) ; <http://accelrys.com/products/materials-studio/>
- Mayo S.L., Olafson B.D. and Goddard W.A., (1990), "DREIDING: a generic force field for molecular simulations", *The Journal of Physical Chemistry*, **Volume 94**, Issue 26, Pages 8897-8909.
- McCann N., Phan D., Wang X., Conway W., Burns R., Attalla M., Puxty G. and Maeder M., (2009), "Kinetics and Mechanism of Carbamate Formation from CO<sub>2</sub>(aq), Carbonate Species, and Monoethanolamine in Aqueous Solution", *The Journal of Physical Chemistry A*, **Volume 113**, Issue 17, Pages 5022-5029.
- More J.J., Garbow B.S. and Hillstrom K.E., (1980), *User Guide for MINPACK-1, technical report ANL-80-74*, Argonne National Laboratory.
- Netlib, (2013a) ; <http://www.netlib.org/minpack/>

Netlib, (2013b) ; <http://www.netlib.org/odepack/index.html>

Olofsson G. and Hepler L., (1975), "Thermodynamics of ionization of water over wide ranges of temperature and pressure", *J Solution Chem*, **Volume 4**, Issue 2, Pages 127-143.

Peiper J.C. and Pitzer K.S., (1982), "Thermodynamics of aqueous carbonate solutions including mixtures of sodium carbonate, bicarbonate, and chloride", *The Journal of Chemical Thermodynamics*, **Volume 14**, Issue 7, Pages 613-638.

Petzold L.R., (1983), A description of DASSL: A differential/algebraic system solver, *Scientific computing* 65-68.

Pinsent B.R.W., Pearson L. and Roughton F.J.W., (1956), "The kinetics of combination of carbon dioxide with hydroxide ions", *Transactions of the Faraday Society*, **Volume 52**, Pages 1512-1520.

Porcheron F., Gibert A., Jacquin M., Mougin P., Faraj A., Goulon A., Bouillon P.A., Delfort B., Le Pennec D. and Raynal L., (2011), "High throughput screening of amine thermodynamic properties applied to post-combustion CO<sub>2</sub> capture process evaluation", *Energy Procedia*, **Volume 4**, Pages 15-22.

Puxty G., Rowland R. and Attalla M., (2010), "Comparison of the rate of CO<sub>2</sub> absorption into aqueous ammonia and monoethanolamine", *Chemical Engineering Science*, **Volume 65**, Issue 2, Pages 915-922.

Radhakrishnan K. and Hindmarsh A.C. (1993) *Description and Use of LSODE, the Livermore Solver for Ordinary Differential Equations*.

Rappe A.K., Casewit C.J., Colwell K.S., Goddard W.A. and Skiff W.M., (1992), "UFF, a full periodic table force field for molecular mechanics and molecular dynamics simulations", *Journal of the American Chemical Society*, **Volume 114**, Issue 25, Pages 10024-10035.

Rayer A.V., Sumon K.Z., Henni A. and Tontiwachwuthikul P., (2011), "Kinetics of the reaction of carbon dioxide (CO<sub>2</sub>) with cyclic amines using the stopped-flow technique", *Energy Procedia*, **Volume 4**, Pages 140-147.

Rinker E.B., Ashour S.S. and Sandall O.C., (1996), "Kinetics and Modeling of Carbon Dioxide Absorption into Aqueous Solutions of Diethanolamine", *Industrial & Engineering Chemistry Research*, **Volume 35**, Issue 4, Pages 1107-1114.

Rohrbaugh R.H. and Jurs P.C., (1987), Descriptions of molecular shape applied in studies of structure/activity and structure/property relationships, *Analytica Chimica Acta*, **Volume 199**, Issue 0, Pages 99-109.

Saporta G., (1990), *Probabilités analyse des données et statistique*, Technip (ed(s)/éd.), Paris.

Sartori G. and Savage D.W., (1983), "Sterically hindered amines for carbon dioxide removal from gases", *Industrial & Engineering Chemistry Fundamentals*, **Volume 22**, Issue 2, Pages 239-249.

- Savage D. W., Sartori G. and Stogryn E. L., (1982), "Process for the selective removal of hydrogen sulfide from gaseous mixtures with several sterically hindered secondary amino compounds", Patent n° US4405581 A.
- Scacchi G., Bouchy M., Faucaut J.F. and Zahraa O., (1996), *Cinétique et catalyse*.
- Soli A.L. and Byrne R.H., (2002), "CO<sub>2</sub> system hydration and dehydration kinetics and the equilibrium CO<sub>2</sub>/H<sub>2</sub>CO<sub>3</sub> ratio in aqueous NaCl solution", *Marine Chemistry*, **Volume 78**, Issue 2-3, Pages 65-73.
- Stanton D.T. and Jurs P.C. (1990) Development and use of charged partial surface area structural descriptors in computer-assisted quantitative structure-property relationship studies, *Analytical Chemistry*, **Volume 62**, Issue 21, Pages 2323-2329.
- Szegezdi J. and Csizmadia F., (2007), *American Chemical Society Spring meeting*, 3/25/2007.
- Taft R.W., (1976), *Progress in physical organic chemistry*.
- Tenehaus M., (1998), *La régression PLS - Théorie et pratique*, Technip (ed(s)/éd.), Paris.
- Todeschini, R., Consonni, V., and Gramatica, P., (2009), Chemometrics in QSAR, in *Comprehensive Chemometrics*, Brown, S., Tauler, R., et Walczak, R. (eds), Oxford.
- Total, (2013) ; [http://www.total.com/MEDIAS/MEDIAS\\_INFOS/2173/FR/captage.gif](http://www.total.com/MEDIAS/MEDIAS_INFOS/2173/FR/captage.gif)
- Ume C.S. and Alper E., (2012), "Reaction kinetics of carbon dioxide with 2-amino-2-hydroxymethyl-1,3-propanediol in aqueous solution obtained from the stopped flow method", *Turkish Journal of Chemistry*, **Volume 36**, Issue 3, Pages 427-435.
- Ume C.S., Ozturk M.C. and Alper E., (2012), "Kinetics of CO<sub>2</sub> Absorption by a Blended Aqueous Amine Solution", *Chemical Engineering & Technology*, **Volume 35**, Issue 3, Pages 464-468.
- Vaidya P.D. and Kenig E.Y., (2007), "CO<sub>2</sub>-alkanolamine reaction kinetics: A review of recent studies", *Chemical Engineering & Technology*, **Volume 30**, Issue 11, Pages 1467-1474.
- Vattenfall, (2013a) ; <http://www.vattenfall.com/en/ccs/oxfuel-combustion.htm>
- Vattenfall, (2013b) ; <http://www.vattenfall.com/en/ccs/precombustion.htm>
- Versteeg G.F. and Vanswaaij W.P.M., (1988), "On the Kinetics Between CO<sub>2</sub> and Alkanolamines Both in Aqueous and Non-Aqueous Solutions .1. Primary and Secondary-Amines", *Chemical Engineering Science*, **Volume 43**, Issue 3, Pages 573-585.
- Versteeg G.F. and Van Swaaij W.P.M., (1988), "On the kinetics between CO<sub>2</sub> and alkanolamines both in aqueous and non-aqueous solutions. 2. Tertiary amines", *Chemical Engineering Science*, **Volume 43**, Issue 3, Pages 587-591.

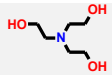
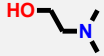
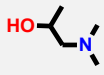
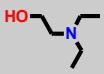
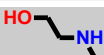
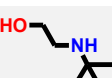
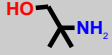
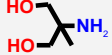
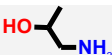
- Vigneau E. and Qannari E.M., (2003), "Clustering of Variables Around Latent Components", *Communications in Statistics - Simulation and Computation*, **Volume 32**, Issue 4, Pages 1131-1150.
- Vitelli A., (2013), "EU Carbon Permits Pare Early Losses, Tracking German 2014 Power", *Bloomberg*,
- Wang X., Conway W., Fernandes D., Lawrance G., Burns R., Puxty G. and Maeder M., (2011), "Kinetics of the Reversible Reaction of CO<sub>2</sub> (aq) with Ammonia in Aqueous Solution", *The Journal of Physical Chemistry A*, **Volume 115**, Issue 24, Pages 6405-6412.
- Wiener H., (1947), Structural Determination of Paraffin Boiling Points, *Journal of the American Chemical Society*, **Volume 69**, Issue 1, Pages 17-20.
- Xiang Q., Fang M., Yu H. and Maeder M., (2012), "Kinetics of the Reversible Reaction of CO<sub>2</sub>(aq) and HCO<sub>3</sub><sup>-</sup> with Sarcosine Salt in Aqueous Solution", *The Journal of Physical Chemistry A*, **Volume 116**, Issue 42, Pages 10276-10284.
- Yu W.C., Astarita G. and Savage D.W., (1985), "Kinetics of carbon dioxide absorption in solutions of methyldiethanolamine", *Chemical Engineering Science*, **Volume 40**, Issue 8, Pages 1585-1590.
- Zero (2013) ; <http://www.zeroco2.no/capture/capture-technology/post-combustion>

## Chapter IX: APPENDICES

### 1 Bibliography

#### 1.1 Kinetic constants and orders at 25°C

Table IX-1. Chemical structure, number, values of  $k_{Am}$  and  $n$  for selected data with average relative deviation between model and experimental first order constant  $k_0$  on concentration range specified in Table III-1.

Chemical structure	Number	$k_{Am}$ ( $m^3n \cdot mol^{-n} \cdot s^{-1}$ )	$n$	Average relative deviation on $k_0$ (%)
	1	$1.66 \times 10^{-3}$	0.99	0.4
	2	$3.20 \times 10^{-3}$	0.99	3.3
	3	$2.64 \times 10^{-2}$	1.01	2.4
	4	$3.29 \times 10^{-2}$	0.99	12.1
	5	$1.06 \times 10^{-1}$	0.76	3.6
	5'	$2.17 \times 10^{-2}$	1.00	7.3
	6	$1.58 \times 10^{-1}$	0.89	3.3
	6'	$7.58 \times 10^{-2}$	1.00	5.9
	7	$2.42 \times 10^0$	1.16	5.4
	8	$6.54 \times 10^{-1}$	1.71	3.6
	9	$4.76 \times 10^{-2}$	1.95	7.9
	10	$3.17 \times 10^{-1}$	1.43	3.3
	11	$9.54 \times 10^{-1}$	0.57	12.6
	11'	$1.83 \times 10^{-1}$	1.00	20.6
	12	$1.84 \times 10^{-1}$	1.15	5.9
	13	$3.31 \times 10^{-2}$	1.21	8.3
	14	$7.54 \times 10^{-3}$	1.22	5.0
	15	$9.29 \times 10^{-1}$	1.31	3.7

## 1. Bibliography

Chemical structure	Number	$k_{Am}$ ( $m^{3n} \cdot mol^{-n} \cdot s^{-1}$ )	n	Average relative deviation on $k_0$ (%)
	16	$2.15 \times 10^0$	1.18	2.1
	17	$2.25 \times 10^0$	1.14	7.6
	18	$8.96 \times 10^{-3}$	1.62	2.9
	19	$2.78 \times 10^0$	1.14	7.7
	20	$5.95 \times 10^0$	1.14	5.5
	21	$4.30 \times 10^0$	1.41	7.2
	22	$2.84 \times 10^0$	1.41	30.9

## 1.2 Bibliography: variation of $k_{ter1}$ and $k_{ter2}$ with temperature

Table IX-2. Second order kinetic constants  $k_{ter1}$  and  $k_{ter2}$  and average relative deviation between termolecular model and experimental values of  $k_0$  from literature data specified in Table III-1.

Number	Temperature (°C)	$k_{ter1}$ ( $m^6 \cdot mol^{-2} \cdot s^{-1}$ )	$k_{ter2}$ ( $m^6 \cdot mol^{-2} \cdot s^{-1}$ )	Average relative deviation on $k_0$ (%)
3	25	$5.27 \times 10^{-7}$	-	2.5
	30	$7.49 \times 10^{-7}$	-	2.2
	35	$1.03 \times 10^{-6}$	-	3.7
	40	$1.47 \times 10^{-6}$	-	3.7
4	25	$6.01 \times 10^{-7}$	-	12.0
	30	$1.06 \times 10^{-6}$	-	11.3
	35	$1.74 \times 10^{-6}$	-	6.1
	40	$2.64 \times 10^{-6}$	-	7.6
5	25	$4.22 \times 10^{-7}$	-	5.8
	30	$6.19 \times 10^{-7}$	-	7.6
	35	$9.54 \times 10^{-7}$	-	4.7
	40	$1.40 \times 10^{-6}$	-	5.6
6	25	$1.48 \times 10^{-6}$	-	3.7
	30	$2.10 \times 10^{-6}$	-	6.1
	35	$3.03 \times 10^{-6}$	-	5.8
	40	$4.17 \times 10^{-6}$	-	5.6
7	25	$5.31 \times 10^{-5}$	$3.60 \times 10^{-2}$	4.6
	30	$6.92 \times 10^{-5}$	$4.09 \times 10^{-2}$	1.3
	35	$9.39 \times 10^{-5}$	$4.22 \times 10^{-2}$	3.9
	40	$1.33 \times 10^{-4}$	$3.86 \times 10^{-2}$	3.2
8	10	$2.33 \times 10^{-5}$	$5.11 \times 10^{-2}$	18.5
	15	$2.99 \times 10^{-5}$	$7.26 \times 10^{-2}$	11.9
	25	$2.40 \times 10^{-5}$	$1.98 \times 10^{-1}$	3.1
	35	$3.36 \times 10^{-5}$	$2.74 \times 10^{-1}$	5.5
9	25	-	$3.75 \times 10^{-2}$	7.3
	30	-	$4.43 \times 10^{-2}$	6.0
	35	-	$5.35 \times 10^{-2}$	3.5
	40	-	$6.40 \times 10^{-2}$	2.5

## 1. Bibliography

Number	Temperature (°C)	$k_{ter1}$ ( $m^6 \cdot mol^{-2} \cdot s^{-1}$ )	$k_{ter2}$ ( $m^6 \cdot mol^{-2} \cdot s^{-1}$ )	Average relative deviation on $k_0$ (%)
10	10	$2.49 \times 10^{-6}$	$1.18 \times 10^{-2}$	9.7
	15	$5.13 \times 10^{-6}$	$1.58 \times 10^{-2}$	3.6
	25	$1.93 \times 10^{-5}$	$1.28 \times 10^{-2}$	6.8
	35	$3.20 \times 10^{-5}$	$1.32 \times 10^{-2}$	4.2
11	5	$6.73 \times 10^{-7}$	-	17.8
	15	$1.19 \times 10^{-6}$	-	17.5
	25	$3.31 \times 10^{-6}$	-	22.3
	35	$6.99 \times 10^{-6}$	-	22.6
12	5	$1.59 \times 10^{-6}$	$5.29 \times 10^{-5}$	7.9
	15	$3.56 \times 10^{-6}$	$1.04 \times 10^{-4}$	12.4
	25	$7.22 \times 10^{-6}$	$1.48 \times 10^{-4}$	10.1
14	15	$1.63 \times 10^{-7}$	$1.00 \times 10^{-5}$	13.8
	25	$4.37 \times 10^{-7}$	$1.15 \times 10^{-5}$	7.3
	30	$5.29 \times 10^{-7}$	$1.44 \times 10^{-5}$	4.1
15	25	$3.73 \times 10^{-5}$	$2.10 \times 10^{-2}$	3.3
	30	$4.61 \times 10^{-5}$	$2.56 \times 10^{-2}$	2.7
	35	$5.50 \times 10^{-5}$	$3.38 \times 10^{-2}$	3.2
	40	$5.72 \times 10^{-5}$	$4.92 \times 10^{-2}$	4.2
16	25	$7.35 \times 10^{-5}$	$2.17 \times 10^{-2}$	2.0
	30	$9.69 \times 10^{-5}$	$3.27 \times 10^{-2}$	2.1
	35	$1.09 \times 10^{-4}$	$6.78 \times 10^{-2}$	2.0
	40	$1.40 \times 10^{-4}$	$9.26 \times 10^{-2}$	2.5
17	5	$2.28 \times 10^{-5}$	$7.93 \times 10^{-4}$	7.5
	15	$4.00 \times 10^{-5}$	$3.08 \times 10^{-3}$	10.9
	25	$7.79 \times 10^{-5}$	$1.03 \times 10^{-3}$	9.1
18	25	$1.89 \times 10^{-6}$	$6.72 \times 10^{-4}$	6.7
	30	$2.89 \times 10^{-6}$	$7.77 \times 10^{-4}$	7.3
	35	$2.62 \times 10^{-6}$	$1.01 \times 10^{-3}$	6.7
	40	$4.27 \times 10^{-6}$	$1.01 \times 10^{-3}$	6.3
19	5	$2.97 \times 10^{-5}$	$7.23 \times 10^{-3}$	7.6
	10	$4.13 \times 10^{-5}$	$7.03 \times 10^{-3}$	4.7

Number	Temperature (°C)	$k_{ter1}$ ( $m^6 \cdot mol^{-2} \cdot s^{-1}$ )	$k_{ter2}$ ( $m^6 \cdot mol^{-2} \cdot s^{-1}$ )	Average relative deviation on $k_0$ (%)
	15	$3.79 \times 10^{-5}$	$2.05 \times 10^{-2}$	21.5
	25	$6.23 \times 10^{-5}$	$2.09 \times 10^{-2}$	3.5
20	5	$2.06 \times 10^{-5}$	$2.55 \times 10^{-2}$	5.2
	15	$1.52 \times 10^{-4}$	$7.15 \times 10^{-2}$	3.1
	25	$2.53 \times 10^{-4}$	$1.39 \times 10^{-1}$	14.8
21	25	$1.70 \times 10^{-4}$	$1.62 \times 10^{-2}$	6.5
	30	$2.24 \times 10^{-4}$	$1.56 \times 10^{-2}$	5.5
	35	$2.64 \times 10^{-4}$	$4.19 \times 10^{-2}$	3.7
	40	$3.03 \times 10^{-4}$	$1.16 \times 10^{-1}$	2.9

## 1. Bibliography

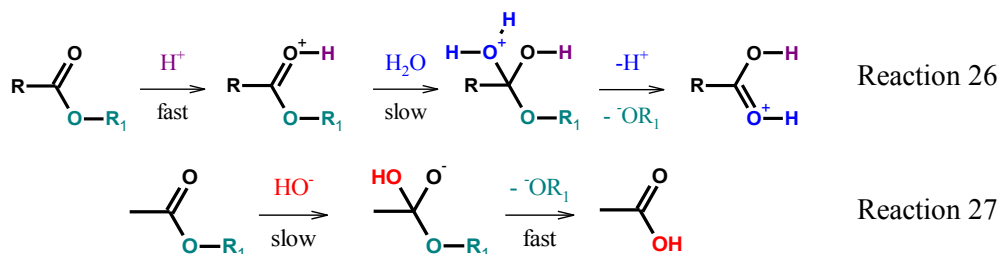
### 1.3 Bibliography: kinetic constants $k_1$ and $k_2$

Table IX-3. Number, value of  $k_1$  and  $k_2$  and average relative of literature data specified in Table III-1.

Number	Temperature (°C)	$k_1$ ( $\text{m}^6 \cdot \text{mol}^{-2} \cdot \text{s}^{-1}$ )	$k_2$ ( $\text{m}^6 \cdot \text{mol}^{-2} \cdot \text{s}^{-1}$ )	Average relative error (%)
1	25	$6.76 \times 10^{-8}$	-	16.3
2	25	$9.73 \times 10^{-8}$	-	9.7
3	25	$5.27 \times 10^{-7}$	-	2.5
4	25	$6.01 \times 10^{-7}$	-	12.0
5	25	$4.22 \times 10^{-7}$	-	5.8
6	25	$1.48 \times 10^{-6}$	-	3.7
7	25	$5.31 \times 10^{-5}$	$3.60 \times 10^{-2}$	4.6
8	25	$2.40 \times 10^{-5}$	$1.98 \times 10^{-1}$	3.1
9	25	-	$3.75 \times 10^{-2}$	7.3
10	25	$1.93 \times 10^{-5}$	$1.28 \times 10^{-2}$	6.8
11	25	$3.31 \times 10^{-6}$	-	22.3
12	25	$7.22 \times 10^{-6}$	$1.48 \times 10^{-4}$	10.1
13	25	$1.48 \times 10^{-6}$	$6.61 \times 10^{-5}$	8.1
14	25	$4.37 \times 10^{-7}$	$1.15 \times 10^{-5}$	7.3
15	25	$3.73 \times 10^{-5}$	$2.10 \times 10^{-2}$	3.3
16	25	$7.35 \times 10^{-5}$	$2.17 \times 10^{-2}$	2.0
17	25	$7.79 \times 10^{-5}$	$1.03 \times 10^{-3}$	9.1
18	25	$1.89 \times 10^{-6}$	$6.72 \times 10^{-4}$	6.7
19	25	$6.23 \times 10^{-5}$	$2.09 \times 10^{-2}$	3.5
20	25	$2.53 \times 10^{-4}$	$1.39 \times 10^{-1}$	14.8
21	25	$1.70 \times 10^{-4}$	$1.62 \times 10^{-2}$	6.5
22	25	$4.67 \times 10^{-5}$	$3.37 \times 10^{-1}$	21.7

## 2 Taft constant

It is generally admitted that the rate of chemical reactions results mainly from steric and electronic effects. Some works on the hydrolysis of aromatic esters have shown that electronic effects of substituent R are weak in acidic conditions (Reaction 26), while there are important under basic conditions (Reaction 27).



Taft postulated (Taft, 1976) that this difference of influence of electronic effects could be used to determinate the contribution of steric hindrance and electronic effect of several substituents. He studies the reaction rate of hydrolysis of  $\text{CH}_3\text{COOR}_1$  with different substituents  $\text{R}_1$ . He defines a reference (hydrogen or methyl depending on tables) and determines the Taft equation indicated by Equation 95.

In this equation  $k_{R_1}$  is the rate constant of the ester with the substituent  $\text{R}_1$ ,  $k_{R_{\text{Ref}}}$  in the rate constant of the ester with the reference substituent,  $\rho^*$  is the sensitivity factor to polar effects,  $\sigma^*$  is the polar substituent constant that describes the field and inductive effects,  $\delta$  is the sensitivity to steric effects and  $E_s$  is the steric substituent constant.

$$\log\left(\frac{k_{R_1}}{k_{R_{\text{Ref}}}}\right) = \rho^* \sigma^* + \delta E_s \quad \text{Equation 95}$$

Taft assume that the kinetic constant under basic conditions is linked to steric, polar and resonance effects while in acidic conditions there is just the contribution of steric effects. He also assumed that steric and resonance contributions to acidic and basic hydrolysis would be equivalent and that the difference of reactivity between basic and acidic conditions would be attributed to polar effects.

Finally he defined the steric and polar parameters respectively as indicated in Equation 96 and Equation 97.

$$E_s = \frac{1}{\delta} \log\left(\frac{k_{R_1}}{k_{R_{\text{Ref}}}}\right)_{\text{Acidic}} \quad \text{Equation 96}$$

$$\sigma^* = \left(\frac{1}{2.48 \times \rho^*}\right) \left[ \log\left(\frac{k_{R_1}}{k_{R_{\text{Ref}}}}\right)_{\text{Basic}} - \log\left(\frac{k_{R_1}}{k_{R_{\text{Ref}}}}\right)_{\text{Acidic}} \right] \quad \text{Equation 97}$$

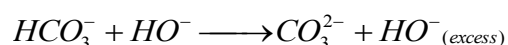
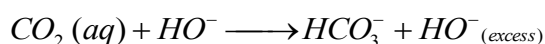
### 3. Experimental method

## 3 Experimental method

### 3.1 Determination of CO<sub>2</sub> concentration in aqueous solutions

When CO<sub>2</sub> is dissolved in water it exists mostly under its two acidic forms (area 1) as indicated in Figure IX-1 (a). Then there are two steps in the determination of the concentration of CO<sub>2</sub> in aqueous solutions.

First we add a slight excess of hydroxide sodium to transform all derivate of CO<sub>2</sub> species (CO<sub>2</sub>, H<sub>2</sub>CO<sub>3</sub> and eventually HCO<sub>3</sub><sup>-</sup>) into CO<sub>3</sub><sup>2-</sup> and HCO<sub>3</sub><sup>-</sup>. The pH of the solution with addition of soda must be at least higher than 8.4. Indeed, according to the pKa values of the equilibrium between H<sub>2</sub>CO<sub>3</sub> and HCO<sub>3</sub><sup>-</sup> (which is around 6.4) the predominant species to the pH of 8.4 is HCO<sub>3</sub><sup>-</sup>.



Then we realize a back titration of this solution using hydrochloric acid. The goal is to determine the quantity of HCO<sub>3</sub><sup>-</sup> in the solution which corresponds to the initial concentration of CO<sub>2</sub> in solution.

In some cases, if the excess of hydroxide ions is very important (initial pH>12.3), it appears a first equivalent point with a value of pH to the half equivalent point higher than 10.3. This area (area 2) corresponds to the titration of the excess of hydroxide ions as indicated in Figure IX-1 (a) and (b).



Then another equivalent point appears which correspond to the titration of CO<sub>3</sub><sup>2-</sup> species. This reaction appear if the pH of the solution is higher than 8.4. The goal of the reaction is to transform all derivate of CO<sub>2</sub> into HCO<sub>3</sub><sup>-</sup> species in order to titrate them. The half equivalent point of this reaction is around 10.3. This area (area 3) as been indicated in Figure IX-1 (a) and (b).



Finally we titrate all HCO<sub>3</sub><sup>-</sup> species which are representative of the initial quantity of CO<sub>2</sub>. This titration is indicated by a half equivalent point around 6.4. This part corresponds to the area 4 indicated in Figure IX-1 (a) and (b).

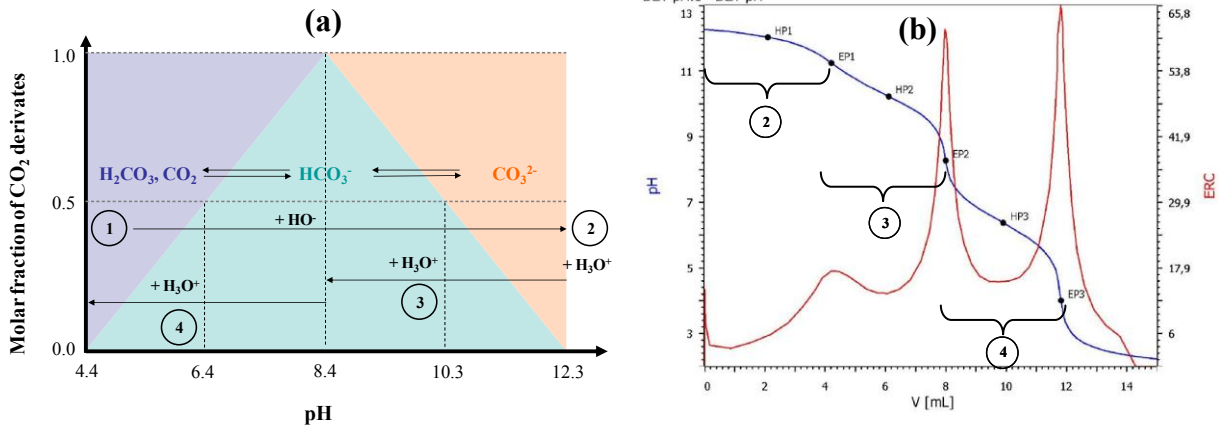
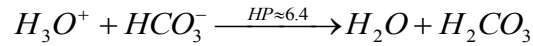


Figure IX-1. (a) Scheme of the molar fraction vs. the pH of the solution for the different step of the titration (1, 2, 3 and 4). (b) Titration of a mix of 27 g of [CO<sub>2</sub>]=30 mol.m<sup>-3</sup> neutralized with 12 g of [NaOH]=100 mol.m<sup>-3</sup> by [HCl]=100 mol.m<sup>-3</sup>. pH metric curves (blue line) and derivatives (red line). Corresponding step 2, 3 and 4 are also indicated.

This quantity corresponds to the amount of hydrochloric acid used to titrate HCO<sub>3</sub><sup>-</sup> ions. Then it corresponds to the difference to the quantity used between the latest equivalent point and the second-last equivalent point as indicated in the following equation.

$$n_{CO_2}^i = n_{HCO_3^-} = C_{HCl} \cdot V_{HCO_3^-} = C_{HCl} \cdot (V_{EP3} - V_{EP2})$$

In this equation  $n_{CO_2}^i$  is the initial quantity of CO<sub>2</sub> (mol),  $n_{HCO_3^-}$  is the quantity of HCO<sub>3</sub><sup>-</sup> at the end of the step 3 (mol),  $C_{HCl}$  is the concentration of hydrochloric acid (mol.m<sup>-3</sup>),  $V$  is the volume of hydrochloric acid used during step 4 (m<sup>3</sup>),  $V_{EP3}$  is the volume of the latest equivalent point (m<sup>3</sup>),  $V_{EP2}$  is the volume of the second-last equivalent point (m<sup>3</sup>).

### 3. Experimental method

#### 3.2 Experimental optimization

##### 3.2.1 Contribution of the reaction with hydroxide ions

We have tested two different methods to anneal and/or control the contribution of hydroxide ions to the reaction with CO<sub>2</sub>. In the first case, the amine solutions are neutralized with carbon dioxide. In the second case, the amine solutions are neutralized with hydrochloric acid. Table IX-4 presents the advantages and drawbacks of both methods.

Table IX-4. Neutralization of amine solutions with carbon dioxide or hydrochloric acid to neutralize the hydroxide ions contribution.

	<b>Carbon dioxide</b>	<b>Hydrochloric acid</b>
Reversibility of the reaction	Possible contribution	No contribution
Ratio signal/noise	Small negative effect	Other thing being equal, the negative effect is more important than with carbon dioxide
Additional ionic species	Carbonates	Introduction of the a new specie (chloride ions)
Strength of the acid	Weak acid	Strong acid

We have determined the kinetic constant  $k'_{R_3N}$  of several tertiary amines using neutralization with carbon dioxide and hydrochloric acid and compared our results with the literature (Table IX-5). The relative deviation between the two methods is lower than 15 % except for molecule 1351 and 1321 where the kinetic constant determined with precarbonated amine solution is nearly half of the value obtained on amine solutions which were neutralized with hydrochloric acid are the less reactive and which have a relative deviation around 50 %.

We verify the contribution of the reverse reaction thanks to the relation indicated in the Equation 98. We determine the constant of the backward reaction thanks to the relation indicated by the Equation 99 from the thermodynamic constant and the kinetic constant previously determined. For that we assume that we are diluted enough to assimile the activity of species as equal to their concentration (mol.dm<sup>-3</sup>).

We notice that the contribution of the backward reaction is lower than 15 % except for molecule 1351 and 1321 and diminish when the pKa increase. In the case of molecule 1351 and 1321 the contribution of the backward reaction is respectively 30 % and 50 %. This contribution could explain the earlier deviation observed between use of hydrochloric acid and CO<sub>2</sub>. In order to avoid as far as possible any contribution which disturb the determination of the kinetic constant we choose to realize the neutralisation using the hydrochloric acid. Moreover hydrochloric acid is a strong acid which can efficiently neutralize kinetics contribution of hydroxide ions.

$$r_{CO_2}^{t=0} = \underbrace{k'_{R_3N} \cdot [R_3N]^i \cdot [CO_2]^i}_{\text{forwardreaction}} + k_{HO^-} \cdot [HO^-]^i \cdot [CO_2]^i + k'_{H_2O} \cdot [CO_2]^i - \underbrace{k'_{-R_3N} \cdot [HCO_3^-]^i \cdot [R_3NH^+]^i}_{\text{backwardreaction}}$$

Equation  
98

$$K_{R_3N} = \frac{K_{HCO_3^-}}{K_a} = \frac{k'_{R_3N}}{k'_{-R_3N}}$$

Equation  
99

Table IX-5 also shows that the relative deviation between our results and the results obtained by Crooks and Barth, who take into account the contribution of hydroxide ions, is lower than 35 %. At the same time, the relative deviation with the results of Henni and Li who do not consider this contribution are respectively 96 and 190 %.

Table IX-5. First order kinetic constant determined for some tertiary amines with neutralization with hydrochloric acid and carbon dioxide in comparison with literature results.

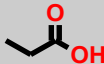
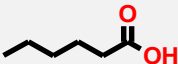
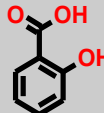
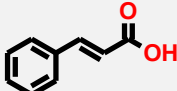
Molecule	$k'_{R_3N} \text{ (HCl)}$ ( $\text{m}^3 \cdot \text{mol}^{-1} \cdot \text{s}^{-1}$ )	$k'_{R_3N} \text{ (CO}_2\text{)}$ ( $\text{m}^3 \cdot \text{mol}^{-1} \cdot \text{s}^{-1}$ )	$k'_{R_3N} \text{ (literature)}$ ( $\text{m}^3 \cdot \text{mol}^{-1} \cdot \text{s}^{-1}$ )	References
1351	$1.23 \times 10^{-4}$	$5.71 \times 10^{-5}$	-	-
1321	$1.49 \times 10^{-4}$	$7.00 \times 10^{-5}$	-	-
1310	$1.50 \times 10^{-3}$	$1.40 \times 10^{-3}$	$1.61 \times 10^{-3}$	(Crooks and Donnellan, 1990)
1352	$5.81 \times 10^{-3}$	$5.05 \times 10^{-3}$	-	-
1311	$5.20 \times 10^{-3}$	$4.50 \times 10^{-3}$	$3.50 \times 10^{-3}$	(Crooks and Donnellan, 1990)
			$3.20 \times 10^{-3}$	(Barth <i>et al.</i> , 1984)
1340	$1.90 \times 10^{-3}$	$1.90 \times 10^{-3}$	-	-
1312	$9.60 \times 10^{-3}$	$8.50 \times 10^{-3}$	$2.74 \times 10^{-2}$	(Henni <i>et al.</i> , 2008)
1313	$3.79 \times 10^{-2}$	$3.29 \times 10^{-2}$	$7.98 \times 10^{-2}$	(Li <i>et al.</i> , 2007)
1314	$6.22 \times 10^{-2}$	$6.25 \times 10^{-2}$	-	-

### 3. Experimental method

#### 3.2.2 Contribution of hydroxide ions to the conductance

We study the effect of amine neutralization of six different acids (five weak acids and one strong acid) in order to maximize the amplitude of the variation of conductance associated with the formation of a carbamate salt. The main properties of these acids are indicated in the Table IX-6. The best candidate should be soluble in our experimental conditions, react quantitatively with free amine, and present a limited contribution to the conductance to keep a good signal over noise ratio.

Table IX-6. Properties of acids used to maximize the variations of conductance in carbamate forming reaction. CRC Handbook of chemistry and physics, 75<sup>th</sup> Edition; CRC Press, 1995 (Lide, 1994).

Name	Chemical structure	pKa at 25 °C	Solubility in water at 25 °C (g.dm <sup>-3</sup> )	Limiting molar conductivity of the conjugated base (S.m <sup>2</sup> .mol <sup>-1</sup> )
Formic acid		3.75	Soluble	54.6×10 <sup>-4</sup>
Propionic acid		4.86	Soluble	35.8×10 <sup>-4</sup>
Hexanoic acid		4.85	9.6	32.4×10 <sup>-4</sup>
Salicylic acid		2.97	2.2	36.0×10 <sup>-4</sup>
E-cinnamic acid		4.44	1.0	-
Hydrochloric acid	HCl	0 in water	451.0	76.3×10 <sup>-4</sup>

The hydrochloric acid was not chosen to study carbamate forming reactions because the resulting conductance due to chloride ions is too high compared to the observed variation of conductance due to formation of the carbamate salt. We then realized a pre-study with monoethanolamine (MEA) at three different rates of neutralization (5, 10 and 15 %) for each acid and verify that the increased ionic strength associated with the corresponding salt does not impact significantly the apparent kinetic constant (less than 20 %) as indicated in Table IX-7 The formic acid appears to be the best candidate to optimize the signal.

Table IX-7. Results of the pre-study realized to optimize the amplitude.

Acid	Rate of neutralization (%)	$C^{\circ}_{MEA}$ (mol.m <sup>-3</sup> )	$k_0$ (s <sup>-1</sup> )	$k_0$ ref (s <sup>-1</sup> )	RD	ARD	Amplitude (μS)
Formic acid	15	17	-	-	-	-	-
		34	-	-	-		-
		102	-	-	-		-
	10	12	86	68	28%	19%	12.0
		25	163	145	12%		17.3
		76	569	480	19%		21.1
	5	14	87	79	11%	10%	8.6
		28	180	165	9%		15.9
		85	588	542	8%		22.0
Propionic acid	15	17	84	81	4%	6%	8.7
		34	173	170	2%		17.0
		102	491	554	11%		18.0
	10	18	85	91	7%	17%	9.0
		36	174	192	9%		16.0
		108	417	627	34%		18.0
	5	19	85	102	17%	17%	8.7
		38	183	216	15%		14.0
		114	567	705	20%		19.5
Hexanoic acid	15	17	81	81	0%	10%	9.0
		34	157	170	8%		18.5
		102	435	554	21%		20.0
	10	18	83	91	9%	24%	10.0
		36	-	-	-		16.5
		108	386	627	39%		20.5
	5	19	85	102	17%	19%	9.0
		38	169	216	22%		15.0
		114	-	-	-		20.0
E-cinnamic acid	15	17	-	-	-	-	13.5
		34	-	-	-		16.0
		102	-	-	-		18.0
	10	18	-	-	-	15%	11.5
		36	163	192	15%		18.0
		108	-	-	-		19.0
	5	19	80	102	22%	22%	10.0
		38	-	-	-		15.5
		114	-	-	-		17.0
Salicylic acid	15	17	80	81	1%	2%	9.0
		34	166	170	2%		15.0
		102	570	554	3%		16.0
	10	18	88	91	3%	8%	10.0
		36	169	192	12%		17.5
		108	572	627	9%		17.0
	5	19	86	102	16%	13%	8.7
		38	192	216	11%		15.0
		114	614	705	13%		18.0

#### 4. Additional information concerning the numerical model

### 4 Additional information concerning the numerical model

#### 4.1 Thermodynamic parameters

Table IX-8. Equilibrium constants. Temperatures T are expressed in K.

Thermodynamic constant	Value	Reference
$K_w$	$-\log(K_w) = -8,909.483$ $+ \frac{142,613.6}{T}$ $+ 4,229.195 \times \log(T)$ $- 9.7384 \times T$ $+ 0.0129638 \times T^2$ $- 1.15068 \times 10^{-5} \times T^3$ $+ 4.602 \times 10^{-9} \times T^4$	(Olofsson and Hepler, 1975)
$K_{H_2CO_3}$	$1/K_{H_2CO_3} = 1523.9 - 3.825 \times T$	(Harned and Owen, 1958)
$K_{H_2CO_3} \times K_{HCO_3^-}$	$\ln(K_{H_2CO_3} \times K_{HCO_3^-}) = 235.482$ $- \frac{12,092.1}{T}$ $- 36.7816 \times \ln(T)$	(Edwards <i>et al.</i> , 1978)
$K_{CO_3^{2-}}$	$\ln(K_{CO_3^{2-}}) = -23.802$ $+ 1,768 \times \left( \frac{1}{298.15} - \frac{1}{T} \right)$ $- 31.25 \left( \frac{298.15}{T} - 1 + \ln \left( \frac{T}{298.15} \right) \right)$	(Peiper and Pitzer, 1982)
$K_{HCO_2H}$	$K_{HCO_2H} = 10^{-3.75} (25 \text{ }^\circ\text{C})$	(Lide, 1994)

## 4.2 Kinetic parameters

Table IX-9. Kinetic constants. Temperatures T are expressed in K.

Kinetics constant	Value	Reference
$k_{H_2O}^m$	$k_{H_2CO_3}^m = \frac{k'_{H_2CO_3}}{a_{H_2O}}$ $\log(k'_{H_2CO_3}) = 329.85$ $- 110.541 \times \log(T)$ $- \frac{17,265.4}{T}$ $k'_{H_2CO_3} (s^{-1})$	(Pinsent <i>et al.</i> , 1956)
$k_{HO^-}^m$	$k_{HO^-}^m = k_{HO^-} \times \frac{K_S}{\gamma_1}$ $\log(k_{HO^-}) = 10.635 - \frac{2,895}{T}$ $k_{HO^-} (dm^3 \cdot mol^{-1} \cdot s^{-1})$	(Pinsent <i>et al.</i> , 1956)
$k_{R_3N}^m$	$k_{R_3N}^m = k'_{R_3N} \times \frac{K_S}{a_{H_2O}}$	-
$k_{R_2NH}^m$	$k_{R_2NH}^m = k_{R_2NH} \times K_S^n$	-

#### 4. Additional information concerning the numerical model

##### 4.3 Conductivity parameters

Table IX-10. Limiting molar conductivity at 25 °C. Data available in CRC Handbook of chemistry and physics, 75<sup>th</sup> Edition; CRC Press, 1995 (Lide, 1994).

Ion	$\lambda_i^\infty$ (S.m <sup>2</sup> .mol <sup>-1</sup> )
H <sub>3</sub> O <sup>+</sup>	34.97×10 <sup>-3</sup>
HO <sup>-</sup>	19.80×10 <sup>-3</sup>
CO <sub>3</sub> <sup>2-</sup>	13.86×10 <sup>-3</sup>
HCO <sub>3</sub> <sup>-</sup>	4.45×10 <sup>-3</sup>
Cl <sup>-</sup>	7.63×10 <sup>-3</sup>
HCO <sub>2</sub> <sup>-</sup>	5.46×10 <sup>-3</sup>

Table IX-11. Limiting molar conductivity at 25 °C of some alkylammonium at 25 °C. Data available in CRC Handbook of chemistry and physics, 75<sup>th</sup> Edition; CRC Press, 1995 (Lide, 1994).

Name	Molecular weight (g.mol <sup>-1</sup> )	$\lambda_i^\infty$ (S.m <sup>2</sup> .mol <sup>-1</sup> )
ethylammonium	46	4.72×10 <sup>-3</sup>
trimethylammonium	60	4.72×10 <sup>-3</sup>
tetramethylammonium	74	4.49×10 <sup>-3</sup>
ethanolammonium	76	4.22×10 <sup>-3</sup>
piperidinium	86	3.72×10 <sup>-3</sup>
pentylammonium	88	3.70×10 <sup>-3</sup>
ethyltrimethylammonium	89	4.05×10 <sup>-3</sup>
triethylammonium	102	3.43×10 <sup>-3</sup>
tetraethylammonium	130	3.26×10 <sup>-3</sup>
hexyltrimethylammonium	144	2.96×10 <sup>-3</sup>
octyltrimethylammonium	172	2.65×10 <sup>-3</sup>
tetrapropylammonium	186	2.34×10 <sup>-3</sup>
tetrabutylammonium	186	1.95×10 <sup>-3</sup>
octadecyltrimethylammonium	256	1.99×10 <sup>-3</sup>
tetradecyltrimethylammonium	256	2.15×10 <sup>-3</sup>
hexadecyltrimethylammonium	284	2.09×10 <sup>-3</sup>
tetraisopentylammonium	298	1.79×10 <sup>-3</sup>
tetrapentylammonium	298	1.75×10 <sup>-3</sup>
octadecyltripropylammonium	298	1.72×10 <sup>-3</sup>
octadecyltriethylammonium	345	1.79×10 <sup>-3</sup>
octadecyltributylammonium	495	1.66×10 <sup>-3</sup>

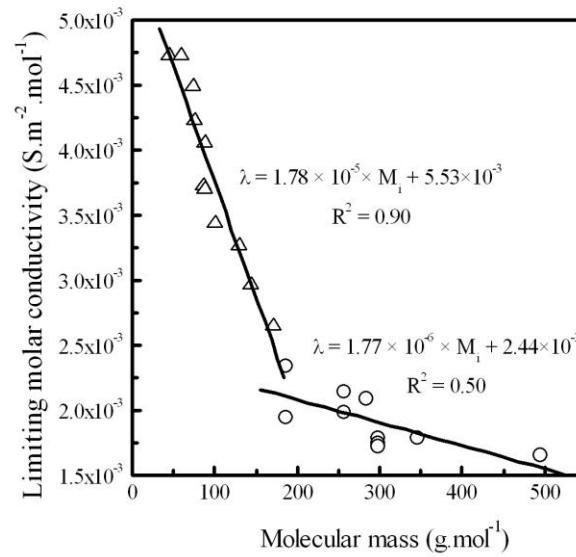


Figure IX-2. Limiting molar conductivity vs. molecular mass of alkylammonium of the Table IX-11.

From this graphic we obtain 2 relations.

For  $M_i \leq 186 \text{ g.mol}^{-1}$ ,  $\lambda_i^\infty = 1.78 \times 10^{-5} \times M_i + 5.53 \times 10^{-3}$ .

For  $M_i \geq 186 \text{ g.mol}^{-1}$ ,  $\lambda_i^\infty = 1.77 \times 10^{-6} \times M_i + 2.44 \times 10^{-3}$ .

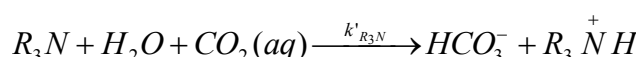
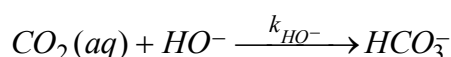
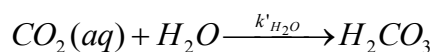
## 5. Additional information concerning the analytical model

### 5 Additional information concerning the analytical model

For the homogeneity with the thermodynamic constants, the molar concentrations have to be expressed in mol.dm<sup>-3</sup> in the following equations.

#### 5.1 Tertiary amines

We consider three kinetically limited reactions: hydration of CO<sub>2</sub>, reaction between CO<sub>2</sub> and HO<sup>-</sup> and reaction between CO<sub>2</sub>, amine and water.



In stopped-flow regime, the global rate of CO<sub>2</sub> consumption followed in the conductance cell is indicated by the differential equation below where  $\xi$  is the extent of reaction.

$$\frac{d\xi}{dt} = (k'_{R_3N} \times [R_3N] + k_{HO^-} \times [HO^-] + k'_{H_2O}) \times ([CO_2]^i - \xi)$$

From this equation we assume that we work in such conditions that the concentrations of amine and hydroxide ions are fairly constant ( $[R_3N] \approx [R_3N]^f$  and  $[HO^-] \approx [HO^-]^f$ ).

$$\frac{d\xi}{dt} = (k'_{R_3N} \times [R_3N]^f + k_{HO^-} \times [HO^-]^f + k'_{H_2O}) \times ([CO_2]^i - \xi)$$

From this expression we define the apparent kinetic constant  $k_0$  as it follows.

$$k_0 = k'_{R_3N} \times [R_3N]^f + k_{HO^-} \times [HO^-]^f + k'_{H_2O}$$

The solution of the differential equation of reaction rate is indicated as it follows.

$$\xi = [CO_2]^i \times (1 - \exp(-k_0 t))$$

Mass balance on carbon dioxide gives the equation below.

$$C_{CO_2}^{tot} = [CO_2]^i + [HCO_3^-]^i + [CO_3^{2-}]^i = \underbrace{[CO_2]^i}_{[CO_2]} - \xi + [HCO_3^-]^i + [CO_3^{2-}]^i$$

If we write,  $\beta^i = [HCO_3^-]^i + [CO_3^{2-}]^i$  we obtain the following equation.

$$[HCO_3^-]^i + [CO_3^{2-}]^i = \xi + \beta^i$$

Taking into account the mass action laws, we do the approximation that solutions are infinitely diluted in water so that the molality in  $\text{mol.kg}^{-1}$  of the species is taken equal to the molar concentrations in  $\text{mol.dm}^{-3}$ .

The equilibrium between  $\text{HO}^-$ ,  $\text{HCO}_3^-$  and  $\text{CO}_3^{2-}$  yields to the following expression.

$$[\text{HCO}_3^-] = \frac{K_w \times [\text{CO}_3^{2-}]}{[\text{HO}^-]^f \times K_{\text{CO}_3^{2-}}} = \frac{K_w \times ([\text{HCO}_3^-] + \beta^i + \xi)}{[\text{HO}^-]^f \times K_{\text{CO}_3^{2-}}}$$

$$[\text{HCO}_3^-] = \frac{K_w \times (\beta^i + \xi)}{K_w + K_{\text{CO}_3^{2-}} \times [\text{HO}^-]^f} = C_1 \times (\beta^i + \xi)$$

$$[\text{CO}_3^{2-}] = \frac{K_{\text{CO}_3^{2-}} \times K_w \times (\beta^i + \xi)}{K_w + K_{\text{CO}_3^{2-}} \times [\text{HO}^-]^f} = C_2 \times (\beta^i + \xi)$$

The electroneutrality of the solution yields to the equation below.

$$[\text{R}_3\text{NH}^+] = [\text{HCO}_3^-] + 2 \times [\text{CO}_3^{2-}] + [\text{HO}^-]^f$$

The evolution of the conductance is given by the Kohlrausch additivity law as follows.

$$G(t) = K_{\text{cell}} \times (\lambda_{\text{HCO}_3^-} \times [\text{HCO}_3^-] + \lambda_{\text{CO}_3^{2-}} \times [\text{CO}_3^{2-}] + \lambda_{\text{R}_3\text{NH}^+} \times [\text{R}_3\text{NH}^+] + \lambda_{\text{HO}^-} \times [\text{HO}^-]^f)$$

$$G(t) = K_{\text{cell}} \times \left\{ (\lambda_{\text{R}_3\text{NH}^+} + \lambda_{\text{HO}^-}) \times [\text{HO}^-]^f + \left[ (\lambda_{\text{R}_3\text{NH}^+} + \lambda_{\text{HCO}_3^-}) \times C_1 + (2\lambda_{\text{R}_3\text{NH}^+} + \lambda_{\text{CO}_3^{2-}}) \times C_2 \right] \times (\beta^i + \xi) \right\}$$

With the monoexponential variation of  $\xi$  with time, we get the following expression.

$$G(t) = -A \times \exp(-k_0 \times t) + C$$

In this expression we define A and C as follows.

$$A = K_{\text{cell}} \times \left[ (\lambda_{\text{R}_3\text{NH}^+} + \lambda_{\text{HCO}_3^-}) \times C_1 + (2\lambda_{\text{R}_3\text{NH}^+} + \lambda_{\text{CO}_3^{2-}}) \times C_2 \right] \times [\text{CO}_2]^i$$

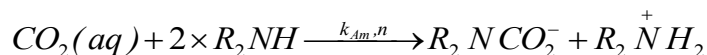
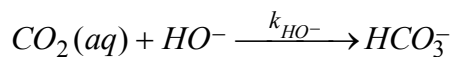
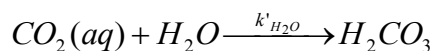
$$C = K_{\text{cell}} \times \left\{ (\lambda_{\text{R}_3\text{NH}^+} + \lambda_{\text{HO}^-}) \times [\text{HO}^-]^f + \left[ (\lambda_{\text{R}_3\text{NH}^+} + \lambda_{\text{HCO}_3^-}) \times C_1 + (2\lambda_{\text{R}_3\text{NH}^+} + \lambda_{\text{CO}_3^{2-}}) \times C_2 \right] \times ([\text{CO}_2]^i + \beta^i) \right\}$$

The variation of the conductance can then be fitted by a monoexponential law, where  $k_0$  is the apparent overall kinetic constant, the amplitude A of the variation is proportional to the concentration of  $\text{CO}_2$  which has not reacted during the mixing time and is converted during the acquisition of the signal. The plateau of conductance C is proportional to the concentration of hydroxide ions and the total concentration of  $\text{CO}_2$ .

## 5. Additional information concerning the analytical model

### 5.2 Primary and secondary amines

We consider three kinetically limited reactions: hydration of CO<sub>2</sub>, reaction between CO<sub>2</sub> and HO<sup>-</sup> and reaction between CO<sub>2</sub> and amine.



In stopped-flow regime, the global rate of CO<sub>2</sub> consumption followed in the conductance cell is indicated by the differential equation below where  $\xi$  is the extent of reaction.

$$\frac{d\xi}{dt} = (k_{R_2NH} \times ([R_2NH])^n + k_{HO^-} \times [HO^-] + k'_{H_2O}) \times ([CO_2]^i - \xi)$$

In conditions where  $R_{HO^-} \leq 1.1$  and/or  $R_k \leq 10\%$ , the contribution of the hydroxide ions to the apparent constant is taken equal to the contribution of this reaction at  $t = \infty$  ( $k_{HO^-} \times [HO^-] \approx k_{HO^-} \times [HO^-]^f$ ). Since amine is in large excess, we consider the concentration of unprotonated amine as fairly constant ( $[R_2NH] \approx [R_2NH]^f$ ).

We then define the apparent kinetic constant  $k_0$  as indicated below by considering these new elements.

$$k_0 = k'_{R_2N} \times [R_2NH]^f + k_{HO^-} \times [HO^-]^f + k'_{H_2O}$$

The solution of the differential equation of reaction rate is given as follows.

$$\xi = [CO_2]^i \times (1 - \exp(-k_0 t))$$

Mass balance on carbon dioxide gives the following equation.

$$C_{CO_2}^{tot} = [CO_2]^i + [HCO_3^-]^i + [CO_3^{2-}]^i + [R_2NCO_2^-]^i = \underbrace{[CO_2]^i}_{[CO_2]} - \xi + [R_2NCO_2^-] + [HCO_3^-] + [CO_3^{2-}]$$

In conditions where  $R_{HO^-} \leq 1.1$  and/or  $R_k \leq 10\%$ , we consider that the sum of the concentration of HCO<sub>3</sub><sup>-</sup> and CO<sub>3</sub><sup>2-</sup> is equal to ( $[HCO_3^-] + [CO_3^{2-}] = [HCO_3^-]^i + [CO_3^{2-}]^i$ ). Then we can simplify as follows.

$$[R_2NCO_2^-] = \xi + [R_2NCO_2^-]^i$$

The total concentration of amine species  $C_{R_2NH}^{tot}$  is constant and indicated as follows.

$$C_{R_2NH}^{tot} = [R_2NH] + [R_2NH_2^+] + [R_2NCO_2^-]$$

The electroneutrality of the solution yields to the following expressions.

$$[R_2NH_2^+] = [R_2NCO_2^-] + [HO^-] + [HCO_3^-] + 2 \times [CO_3^{2-}]$$

$$[R_2NH_2^+] = \xi + [HO^-] + \beta^i$$

We define  $\beta^i$  as equal to  $[HCO_3^-]^i + 2 \times [CO_3^{2-}]^i + [R_2NCO_2^-]^i$ .

The concentration of free amine is also related to the concentration of hydroxide ions by the mass action law.

$$[R_2NH] = \frac{[R_2NH_2^+][HO^-]}{K_b} = \frac{[HO^-]^2}{K_b} + \frac{[HO^-] \times (\xi + \beta^i)}{K_b}$$

The mass balance on amine species yields to a second order equation with respect to the hydroxide concentration as indicated below.

$$\frac{[HO^-]^2}{K_b} + \frac{[HO^-] \times (\xi + \beta^i + K_b)}{K_b} + (2 \times \xi + \beta^i + [R_2NCO_2^-]^i) = C_{R_2NH}^{tot}$$

$$[HO^-]^2 + (\xi + \beta^i + K_b) \times [HO^-] + K_b \times (2 \times \xi - \delta^i) = 0$$

In this equation we define  $\delta^i$  as  $\delta^i = C_{R_2NH}^{tot} - \beta^i - [R_2NCO_2^-]^i \approx C_{R_2NH}^{tot}$ .

The discriminant of the previous equation can be expressed as follows.

$$\Delta = (\xi + \beta^i + K_b)^2 + 4 \times (\delta^i - 2 \times \xi) K_b$$

The concentration of hydroxide ions is then expressed according to the equation below.

$$[HO^-] = \frac{-(\xi + \beta^i + K_b) + \sqrt{\Delta}}{2}$$

It is possible to consider two limit cases.

## 5. Additional information concerning the analytical model

First, for amine which are not very basic ( $pK_a < 10$ ), the concentration of hydroxide ions is very weak. In this case, their contribution of the conductance can be neglected. In this situation we consider that in the discriminant, the first term is preponderant as indicated below.

$$(\xi + \beta^i + K_b)^2 \gg 4 \times (\delta^i - 2 \times \xi) K_b$$

In this case, the evolution of the conductance is given by the Kohlrausch additivity law as indicated below.

$$G(t) = K_{cell} \times (\lambda_{HCO_3^-} \times [HCO_3^-] + \lambda_{CO_3^{2-}} \times [CO_3^{2-}] + \lambda_{R_3NH^+} \times [R_3NH^+] + \lambda_{R_2NCO_2^-} \times [R_2NCO_2^-])$$

$$G(t) = K_{cell} \times \left\{ (\lambda_{R_3NH^+} + \lambda_{HCO_3^-}) \times [HCO_3^-]^i + (2\lambda_{R_3NH^+} + \lambda_{CO_3^{2-}}) \times [CO_3^{2-}]^i + (\lambda_{R_3NH^+} + \lambda_{R_2NCO_2^-}) \times (\xi + [R_2NCO_2^-]^i) \right\}$$

This expression can be identified to the monoexponential variation of  $\xi$  with time as indicated in the following equation.

$$G(t) = -A \times \exp(-k_0 \times t) + C$$

In this particular case the value of A and C are defined as it follows.

$$A = K_{cell} \times [\lambda_{R_3NH^+} + \lambda_{R_2NCO_2^-}] \times [CO_2]^i$$

$$C = K_{cell} \times \left\{ (\lambda_{R_3NH^+} + \lambda_{HCO_3^-}) \times [HCO_3^-]^i + (2\lambda_{R_3NH^+} + \lambda_{CO_3^{2-}}) \times [CO_3^{2-}]^i + (\lambda_{R_3NH^+} + \lambda_{R_2NCO_2^-}) \times ([CO_2]^i + [R_2NCO_2^-]^i) \right\}$$

The variation of the conductance can then be fitted by a monoexponential law, where  $k_0$  is the apparent overall kinetic constant, the amplitude A of the increasing variation is proportional to the concentration of  $CO_2$  which has not reacted during the mixing time and is converted during the acquisition of the signal. The plateau of conductance C is proportional to the total concentration of  $CO_2$ .

Then, for amine which are very basic ( $pK_a > 10$ ) the second term of the discriminant is preponderant as indicated below.

$$(\xi + \beta^i + K_b)^2 \ll 4 \times (\delta^i - 2 \times \xi) K_b$$

In this case, the concentration of hydroxide ions is expressed as indicated in the following equation.

$$[HO^-] \approx \sqrt{K_b \delta^i} \times \sqrt{\left(1 - \frac{2 \times \xi}{\delta^i}\right)}$$

$$\text{As } \frac{2x}{\delta^i} \rightarrow 0, [HO^-] \rightarrow \sqrt{K_b \delta^i} \times \left(1 - \frac{\xi}{\delta^i}\right).$$

In this case, the evolution of the conductance is given by the Kohlrausch additivity law as indicated below.

$$G(t) = K_{cell} \times \left\{ \begin{aligned} &(\lambda_{R_3NH^+} + \lambda_{HCO_3^-}) \times [HCO_3^-]^i + (2\lambda_{R_3NH^+} + \lambda_{CO_3^{2-}}) \times [CO_3^{2-}]^i + (\lambda_{R_3NH^+} + \lambda_{HO^-}) \times [HO^-] \\ &+ (\lambda_{R_3NH^+} + \lambda_{R_2NCO_2^-}) \times (\xi + [R_2NCO_2^-]^i) \end{aligned} \right\}$$

With This expression can be identified to the monoexponential variation of  $\xi$  with time as indicated in the following equation.

$$G(t) = -A \times \exp(-k_0 \times t) + C$$

In this particular case the value of A and C are defined as it follows.

$$A = K_{cell} \times \left\{ \left[ \lambda_{R_3NH^+} + \lambda_{R_2NCO_2^-} \right] - \sqrt{\frac{K_b}{\delta^i}} \times \left[ \lambda_{R_3NH^+} + \lambda_{HO^-} \right] \right\} \times [CO_2]^i$$

$$C = K_{cell} \times \left\{ \begin{aligned} &(\lambda_{R_3NH^+} + \lambda_{HCO_3^-}) \times [HCO_3^-]^i + (2\lambda_{R_3NH^+} + \lambda_{CO_3^{2-}}) \times [CO_3^{2-}]^i + (\lambda_{R_3NH^+} + \lambda_{R_2NCO_2^-}) \times ([CO_2]^i + [R_2NCO_2^-]^i) \\ &+ (\lambda_{R_3NH^+} + \lambda_{HO^-}) \times \left( \sqrt{K_b \delta^i} - \sqrt{\frac{K_b}{\delta^i}} [CO_2]^i \right) \end{aligned} \right\}$$

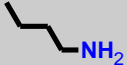
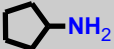
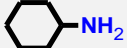
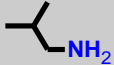
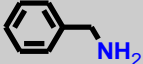
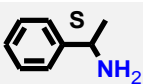
The variation of conductance is still fitted by a monexponential law. The amplitude of the signal is either positive (increasing variation) or negative (decreasing variation). A negative amplitude  $A < 0$  corresponds to the case of very dilute solutions indicate by the following relation.

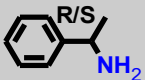
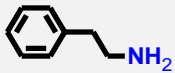
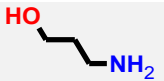
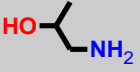
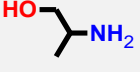
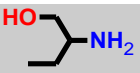
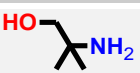
$$\sqrt{\frac{K_b}{\delta^i}} \times \left[ \lambda_{R_3NH^+} + \lambda_{HO^-} \right] > \lambda_{R_3NH^+} + \lambda_{R_2NCO_2^-}$$

## 6. List of studied molecules

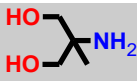
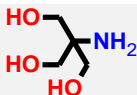
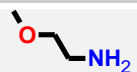
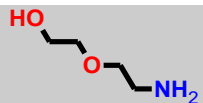
### 6 List of studied molecules

#### 6.1 Primary amines

Number	Name	CAS	Chemical structure	Suppliers	References	Purity
1100	Methylamine	74-89-5		Alfa Aesar	L00894	39.6 % <sup>1,w</sup>
1101	n-Butylamine	109-73-9		Fluka	19480	99.9 % <sup>2</sup>
1102	Isopropylamine	75-31-0		Sigma-Aldrich	471291	99.9 % <sup>2</sup>
1103	Cyclopentylamine	1003-03-8		Alfa Aesar	L01966	99.9 % <sup>2</sup>
1104	Cyclohexylamine	108-91-8		Alfa Aesar	A15851	99.0 % <sup>2</sup>
1105	Isobutylamine	78-81-9		Alfa Aesar	A11017	99.9 % <sup>2</sup>
1106	tert-Butylamine	75-64-9		Sigma-Aldrich	A111	99.8 % <sup>2</sup>
1110	Benzylamine	100-46-9		Sigma-Aldrich	185701	99.6 % <sup>2</sup>
1111	S- $\alpha$ -Methylbenzylamine	2627-86-3		Fluka	77870	99.8 % <sup>2</sup>

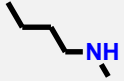
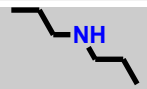
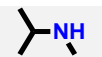
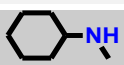
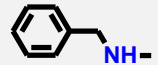
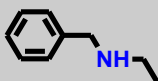
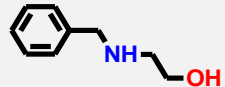
Number	Name	CAS	Chemical structure	Suppliers	References	Purity
1112	$\alpha$ -Methylbenzylamine	618-36-0		Sigma-Aldrich	M31104	99.7 % <sup>2</sup>
1113	Phenethylamine	64-04-0		Sigma-Aldrich	241008	99.9 % <sup>2</sup>
1120	Monoethanolamine	141-43-5		Sigma-Aldrich	411000	99.8 % <sup>2</sup>
1121	3-Amino-1-propanol	156-87-6		Sigma-Aldrich	A76400	99.9 % <sup>2</sup>
1122	4-Amino-1-butanol	13325-10-5		Sigma-Aldrich	178330	97.5 % <sup>2</sup>
1123	6-Amino-1-hexanol	4048-33-3		Sigma-Aldrich	A56353	98.4 % <sup>2</sup>
1124	1-Amino-2-propanol	78-96-6		Sigma-Aldrich	110248	94.4 % <sup>2</sup>
1125	2-Amino-1-propanol	6168-72-5		Sigma-Aldrich	192171	99.3 % <sup>2</sup>
1126	2-Aminobutane-1-ol	96-20-8		Sigma-Aldrich	A43804	99.8 % <sup>2</sup>
1127	2-Amino-2-methyl-1-propanol	124-68-5		Merck	8014651000	93.4 % <sup>2</sup>

## 6. List of studied molecules

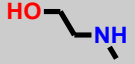
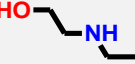
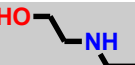
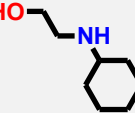
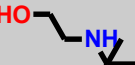
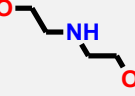
Number	Name	CAS	Chemical structure	Suppliers	References	Purity
1128	2-Amino-2-methyl-1,3-propanediol	115-69-5		Sigma-Aldrich	A9754	100.0 % <sup>1</sup>
1129	2-Amino-2-(hydroxymethyl)-1,3-propanediol	77-86-1		Sigma-Aldrich	T1378	100.0 % <sup>1</sup>
1130	Trans-4-aminocyclohexanol	27489-62-9		Alfa Aesar	B22365	98.1 % <sup>1</sup>
1131	2-Methoxyethanamine	109-85-3		Sigma-Aldrich	241077	99.4 % <sup>2</sup>
1132	2-(2-Aminoethoxy)ethanol	929-06-6		Sigma-Aldrich	A54059	98.7 % <sup>2</sup>
1140	3-Aminopropionitrile	151-18-8		Alfa Aesar	A13043	99.7 % <sup>2</sup>

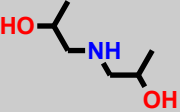
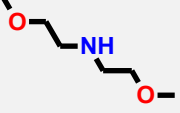
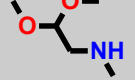
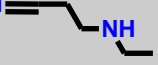
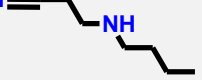
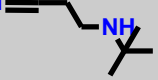
<sup>1</sup> Purity determined by titration / <sup>2</sup> Purity determined by gas chromatography / <sup>w</sup> Commercial solution diluted in water

## 6.2 Secondary amines

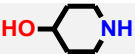
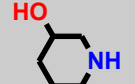
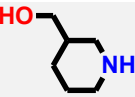
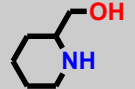
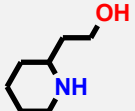
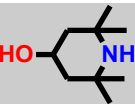
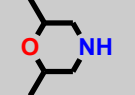
Number	Name	CAS	Chemical structure	Suppliers	References	Purity
1200	Dimethylamine	124-40-3		Alfa Aesar	31458	40.2 % <sup>1,w</sup>
1201	N-Methyl-1-propylamine	627-35-0		Alfa Aesar	A16903	97.1 % <sup>2</sup>
1202	N-Methyl-1-butylamine	110-68-9		Alfa Aesar	B23032	99.0 % <sup>2</sup>
1203	Di-n-propylamine	142-84-7		Alfa Aesar	L15808	99.9 % <sup>2</sup>
1204	N-Isopropylmethylamine	4747-21-1		Sigma-Aldrich	359378	99.9 % <sup>2</sup>
1205	N-Methylcyclohexylamine	100-60-7		Sigma-Aldrich	103322	98.9 % <sup>2</sup>
1210	Methylbenzylamine	103-67-3		Fluka	13565	99.5 % <sup>2</sup>
1211	Ethylbenzylamine	14321-27-8		Sigma-Aldrich	126993	97.5 % <sup>2</sup>
1212	2-Benzylaminoethanol	104-63-2		Sigma-Aldrich	B22003	98.4 % <sup>2</sup>

## 6. List of studied molecules

Number	Name	CAS	Chemical structure	Suppliers	References	Purity
1220	2-Methylaminoethanol	109-83-1		Sigma-Aldrich	471445	99.5 % <sup>2</sup>
1221	2-(ethylamino)-ethanol	110-73-6		Sigma-Aldrich	471461	99.3 % <sup>2</sup>
1222	2-(Propylamino)ethanol	16369-21-4		Sigma-Aldrich	470201	99.9 % <sup>2</sup>
1223	n-Butylaminoethanol	111-75-1		Sigma-Aldrich	471496	99.5 % <sup>2</sup>
1224	2-(Isopropylamino)ethanol	109-56-8		ABCR	AB137468	99.0 % <sup>2</sup>
1225	N-Cyclohexylaminoethanol	2842-38-8		Alfa Aesar	L10821	99.5 % <sup>2</sup>
1226	tert-Butylaminoethanol	4620-70-6		Sigma-Aldrich	471518	99.6 % <sup>2</sup>
1227	Diethanolamine	111-42-2		Sigma-Aldrich	D83303	99.8 % <sup>2</sup>

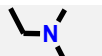
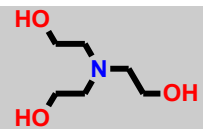
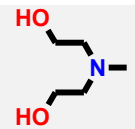
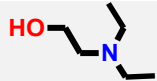
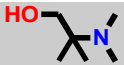
Number	Name	CAS	Chemical structure	Suppliers	References	Purity
1228	Diisopropanolamine	110-97-4		Alfa Aesar	A18451	98.8 % <sup>2</sup>
1230	Bis(2-methoxyethyl)amine	111-95-5		Sigma-Aldrich	B48207	99.4 % <sup>2</sup>
1231	2,2-Dimethoxy-N-methylethanamine	122-07-6		Fluka	65610	99.5 % <sup>2</sup>
1240	3-(Methylamino)propionitrile	693-05-0		Sigma-Aldrich	M27603	99.6 % <sup>2</sup>
1241	Ethylaminopropionitrile	21539-47-9		Acrôs organics	302490250	97.5 % <sup>2</sup>
1242	3-(n-Butylamino)propionitrile	693-51-6		Matrix Scientific	4510	99.3 % <sup>2</sup>
1243	3-(tert-Butylamino)propionitrile	21539-53-7		Matrix Scientific	6515	99.7 % <sup>2</sup>
1250	Pyrrolidine	123-75-1		Sigma-Aldrich	394238	99.9 % <sup>2</sup>
1251	Piperidine	110-89-4		Sigma-Aldrich	411027	99.8 % <sup>2</sup>

## 6. List of studied molecules

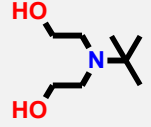
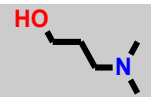
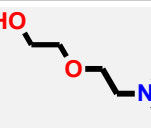
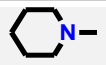
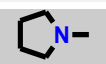
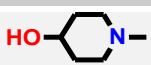
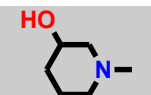
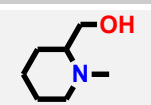
Number	Name	CAS	Chemical structure	Suppliers	References	Purity
1260	4-Hydroxypiperidine	5382-16-1		Fluka	56220	99.9 % <sup>1</sup>
1261	3-Hydroxypiperidine	6859-99-0		Fluka	56210	99.4 % <sup>1</sup>
1262	3-Piperidinemethanol	4606-65-9		Sigma-Aldrich	155233	98.8 % <sup>2</sup>
1263	2-Piperidinemethanol	3433-37-2		TCI	P1017	98.5 % <sup>2</sup>
1264	2-Piperidineethanol	1484-84-0		Acrôs organics	157611000	98.8 % <sup>2</sup>
1265	2,2,6,6-Tetramethyl-4-piperidinol	2403-88-5		Sigma-Aldrich	115746	99.9 % <sup>2</sup>
1270	Morpholine	110-91-8		Merck	8.06127.0100	96.0 % <sup>1</sup>
1271	2,6-Dimethylmorpholine	141-91-3		Sigma-Aldrich	126527	97.1 % <sup>2</sup>

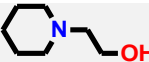
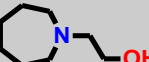
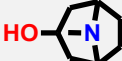
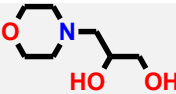
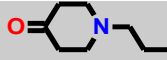
<sup>1</sup> Purity determined by titration / <sup>2</sup> Purity determined by gas chromatography / <sup>w</sup> Commercial solution diluted in water

## 6.3 Tertiary amines

Number	Name	CAS	Chemical structure	Suppliers	References	Purity
1300	Trimethylamine	75-50-3		Sigma-Aldrich	92262	43.3 % <sup>1,w</sup>
1301	N,N-Dimethylpropane-1-amine	923-63-6		Pfaltz & Bauer	D44480	97.0% <sup>2</sup>
1302	Diethylmethylamine	616-39-7		Fluka	32441	98.5 % <sup>2</sup>
1310	Triethanolamine	102-71-6		Sigma-Aldrich	T58300	98.0 % <sup>2</sup>
1311	Methyldiethanolamine	105-59-9		Sigma-Aldrich	471828	99.9 % <sup>2</sup>
1312	Dimethylaminoethanol	108-01-0		Sigma-Aldrich	471453	100.0 % <sup>2</sup>
1313	Diethylethanolamine	100-37-8		Sigma-Aldrich	471321	100.0 % <sup>2</sup>
1314	2-Dimethylamino-2-methylpropanol	7005-47-2		Sigma-Aldrich	423041	79.8 % <sup>1,w</sup>

## 6. List of studied molecules

Number	Name	CAS	Chemical structure	Suppliers	References	Purity
1315	tert-Butylaminodiethanol	2160-93-2		Sigma-Aldrich	455709	98.2 % <sup>2</sup>
1316	3-Dimethylamino-1-propanol	3179-63-3		Sigma-Aldrich	D144401	99.3 % <sup>2</sup>
1320	2-[2-(Dimethylamino)ethoxy]ethanol	1704-62-7		Sigma-Aldrich	424552	99.8 % <sup>2</sup>
1321	3-Dimethylaminopropionitrile	1738-25-6		Sigma-Aldrich	218480	96.4 % <sup>2</sup>
1330	1-Methylpiperidine	626-67-5		Alfa Aesar	L03398	99.8 % <sup>2</sup>
1331	1-Methylpyrrolidine	120-94-5		Alfa Aesar	B23799	99.9 % <sup>2</sup>
1340	4-Hydroxy-N-methylpiperidine	106-52-5		Alfa Aesar	L06415	99.3 % <sup>2</sup>
1341	1-Methyl-3-hydroxypiperidine	3554-74-3		Sigma-Aldrich	H42001	99.9 % <sup>2</sup>
1342	1-Methyl-2-hydroxymethylpiperidine	20845-34-5		Alfa Aesar	B22187	99.1 % <sup>2</sup>

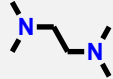
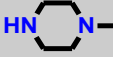
Number	Name	CAS	Chemical structure	Suppliers	References	Purity
1343	1-Pyrrolidineethanol	2955-88-6		Sigma-Aldrich	H29404	99.0 % <sup>2</sup>
1344	1-Piperidineethanol	3040-44-6		Alfa Aesar	B23816	99.8 % <sup>2</sup>
1345	1-Azepaneethanol	20603-00-3		Synthesis	-	99.0 % <sup>1</sup>
1346	Tropine	120-29-6		Sigma-Aldrich	93550	97.7 % <sup>2</sup>
1350	N-Methylmorpholine	109-02-4		Merck	8.05894.0250	99.7 % <sup>2</sup>
1351	3-Morpholino-1,2-propanediol	6425-32-7		Sigma-Aldrich	218480	96.4 % <sup>2</sup>
1352	1-Propyl-4-piperidone	23133-37-1		Alfa Aesar	B25477	98.9 % <sup>2</sup>
1353	1-Piperidinepropionitrile	3088-41-3		Alfa Aesar	L01469	99.9 % <sup>2</sup>

<sup>1</sup> Purity determined by titration / <sup>2</sup> Purity determined by gas chromatography / <sup>w</sup> Commercial solution diluted in water

Molecule number 1345 has been synthesized. It has been obtained by reaction between azepane (CAS: 111-49-9) and ethylene oxide (CAS: 75-21-8).

## 6. List of studied molecules

### 6.4 Multi-amines

Number	Name	CAS	Chemical structure	Suppliers	References	Purity
2300	N,N,N',N'- Tetramethylethylenediamine	110-18-9		Sigma-Aldrich	13001	99.9 % <sup>1</sup>
2200	1-Methylpiperazine	109-01-3		Sigma-Aldrich	411019	100.0 % <sup>1</sup>
2201	Piperazine	110-85-0		Sigma-Aldrich	P45907	100 % <sup>1</sup>

<sup>1</sup> Purity determined by gas chromatography

### 6.5 Acidic solutions

Hydrochloric acid (37 %) provided by Carlo Erba (reference: 524525).

Formic acid provided by Alfa Aesar (reference: A13285).

### 6.6 Gas

Carbon dioxide provided by Air Liquide. Purity : 99.9 %.

Dinitrogen provided by Air Liquide.

## 7 Kinetic results of each studied amine for each concentration

In this part we indicate for each molecule the total concentration after mixing of amine ( $C_{Am}$ ) and carbon dioxide ( $C_{CO_2}$ ). Each concentration is expressed in  $\text{mol.m}^{-3}$ . We also indicate if we use an acid and the rate of neutralization. We write the final concentration of amine  $[Am]^f$  determined by the numerical model (Chapter IV .2.1) and the final concentration of water  $[H_2O]^f$ . For all systems studied with the analytical method we indicate the average values of the amplitude A ( $\mu\text{S}$ ), the value of the conductance at the equilibrium C ( $\mu\text{S}$ ) and the apparent kinetic constant  $k_0$ . Then we write down values of the ratio R between initial concentration of amine and carbon dioxide, the evolution of the concentration of hydroxide ions and the kinetic contribution of other reactions than amine- $\text{CO}_2$  in order to verify assumption of the analytical method.

$$R = \frac{[Am]^i}{[CO_2]^i} \quad \text{Equation 100}$$

$$\text{Evolution } HO^- = \frac{[HO^-]^i}{[HO^-]^f} \quad \text{Equation 101}$$

$$\text{Contribution } HO^- = 100 \times \frac{k_{HO^-} \times [HO^-]^f + k'_{H_2O}}{k_0} = 100 \times \frac{k_0 - k_0^{Am}}{k_0} \quad \text{Equation 102}$$

After that we indicate if we use numerical or analytical to determine the kinetic constant. Finally we show the value of the apparent kinetic constant which is specific to the amine- $\text{CO}_2$  reaction  $k_0^{Am}$  and the associated standard deviation. For questions of readability we separate data by degree of substitution.

## 7. Kinetic results of each studied amine for each concentration

Table IX-12. Experimental results of primary amines.

N°	C <sub>Am</sub>	C <sub>CO<sub>2</sub></sub>	Acid	Neutra	[Am] <sup>f</sup>	[H <sub>2</sub> O] <sup>f</sup>	A	C	k <sub>0</sub>	R	Evolution HO <sup>-</sup>	Contribution HO <sup>-</sup>	Model used	k <sub>0</sub> <sup>Am</sup>	σ (k <sub>0</sub> <sup>Am</sup> )
1100	6.05×10 <sup>0</sup>	6.19×10 <sup>-1</sup>	No	0.0%	3.7	55381.4	-	-	-	7	1.36	9.7%	Numerical	8.90×10 <sup>1</sup>	2.64×10 <sup>0</sup>
	4.03×10 <sup>0</sup>	4.13×10 <sup>-1</sup>	No	0.0%	2.3	55385.6	-	-	-	7	1.32	12.3%	Numerical	5.52×10 <sup>1</sup>	2.17×10 <sup>0</sup>
	2.05×10 <sup>0</sup>	2.06×10 <sup>-1</sup>	No	0.0%	1.0	55389.7	-	-	-	6	1.27	19.5%	Numerical	2.19×10 <sup>0</sup>	3.23×10 <sup>-1</sup>
	1.03×10 <sup>0</sup>	1.03×10 <sup>-1</sup>	No	0.0%	0.4	55391.8	-	-	-	5	1.24	29.7%	Numerical	8.21×10 <sup>0</sup>	3.97×10 <sup>-1</sup>
1101	1.21×10 <sup>1</sup>	1.21×10 <sup>0</sup>	No	0.0%	8.2	55339.1	-	-	-	8	1.46	9.2%	Numerical	1.25×10 <sup>2</sup>	3.53×10 <sup>0</sup>
	9.13×10 <sup>0</sup>	9.09×10 <sup>-1</sup>	No	0.0%	6.0	55353.9	-	-	-	8	1.41	10.8%	Numerical	9.25×10 <sup>1</sup>	3.90×10 <sup>0</sup>
	6.07×10 <sup>0</sup>	6.06×10 <sup>-1</sup>	No	0.0%	3.8	55369.0	-	-	-	8	1.36	14.3%	Numerical	5.49×10 <sup>1</sup>	1.44×10 <sup>0</sup>
	3.08×10 <sup>0</sup>	3.03×10 <sup>-1</sup>	No	0.0%	1.7	55383.7	-	-	-	7	1.29	21.8%	Numerical	2.32×10 <sup>1</sup>	7.97×10 <sup>-1</sup>
	1.56×10 <sup>0</sup>	1.52×10 <sup>-1</sup>	No	0.0%	0.7	55391.2	-	-	-	6	1.25	31.6%	Numerical	9.49×10 <sup>0</sup>	1.38×10 <sup>-1</sup>
1102	1.82×10 <sup>2</sup>	1.30×10 <sup>1</sup>	HCO <sub>2</sub> H	14.8%	126.6	54631.5	68.3	754	7.71×10 <sup>2</sup>	12	1.57	2.5%	Analytical	7.52×10 <sup>2</sup>	4.71×10 <sup>1</sup>
	1.22×10 <sup>2</sup>	9.90×10 <sup>0</sup>	HCO <sub>2</sub> H	14.7%	82.1	54890.7	31.0	559	4.69×10 <sup>2</sup>	10	1.64	3.6%	Analytical	4.52×10 <sup>2</sup>	2.27×10 <sup>1</sup>
	6.11×10 <sup>1</sup>	4.77×10 <sup>0</sup>	HCO <sub>2</sub> H	14.7%	40.7	55152.5	15.3	333	2.58×10 <sup>2</sup>	10	1.55	5.7%	Analytical	2.43×10 <sup>2</sup>	1.27×10 <sup>1</sup>
	3.04×10 <sup>1</sup>	2.27×10 <sup>0</sup>	HCO <sub>2</sub> H	14.6%	19.9	55285.0	3.4	205	9.61×10 <sup>1</sup>	11	1.45	13.2%	Analytical	8.34×10 <sup>1</sup>	1.06×10 <sup>1</sup>
	1.02×10 <sup>1</sup>	7.60×10 <sup>-1</sup>	HCO <sub>2</sub> H	14.7%	6.1	55371.9	-2.9	101	6.36×10 <sup>1</sup>	10	1.33	14.2%	Analytical	5.46×10 <sup>1</sup>	2.92×10 <sup>0</sup>
1103	6.04×10 <sup>1</sup>	4.04×10 <sup>0</sup>	HCO <sub>2</sub> H	30.4%	33.1	55076.4	16.9	430	2.66×10 <sup>2</sup>	10	1.43	2.8%	Analytical	2.59×10 <sup>2</sup>	1.95×10 <sup>1</sup>
	4.02×10 <sup>1</sup>	2.79×10 <sup>0</sup>	HCO <sub>2</sub> H	30.4%	21.6	55185.1	10.6	309	1.52×10 <sup>2</sup>	10	1.43	4.5%	Analytical	1.45×10 <sup>2</sup>	6.87×10 <sup>0</sup>
	2.01×10 <sup>1</sup>	1.27×10 <sup>0</sup>	HCO <sub>2</sub> H	30.4%	10.7	55293.3	4.0	180	7.20×10 <sup>1</sup>	10	1.36	8.7%	Analytical	6.58×10 <sup>1</sup>	5.33×10 <sup>0</sup>
	1.52×10 <sup>1</sup>	1.02×10 <sup>0</sup>	HCO <sub>2</sub> H	30.4%	7.8	55320.1	2.7	145	5.81×10 <sup>1</sup>	10	1.37	9.9%	Analytical	5.23×10 <sup>1</sup>	4.73×10 <sup>0</sup>

Nº	C <sub>Am</sub>	C <sub>CO<sub>2</sub></sub>	Acid	Neutra	[Am] <sup>f</sup>	[H <sub>2</sub> O] <sup>f</sup>	A	C	k <sub>0</sub>	R	Evolution HO <sup>-</sup>	Contribution HO <sup>-</sup>	Model used	k <sub>0</sub> <sup>Am</sup>	σ (k <sub>0</sub> <sup>Am</sup> )
	1.01×10 <sup>1</sup>	5.09×10 <sup>-1</sup>	HCO <sub>2</sub> H	30.4%	5.3	55347.6	0.7	107	3.60×10 <sup>1</sup>	12	1.25	15.7%	Analytical	3.03×10 <sup>1</sup>	3.31×10 <sup>0</sup>
1104	5.24×10 <sup>1</sup>	3.80×10 <sup>0</sup>	HCO <sub>2</sub> H	25.4%	30.6	55071.3	15.6	342	2.17×10 <sup>2</sup>	10	1.48	3.4%	Analytical	2.10×10 <sup>2</sup>	8.65×10 <sup>0</sup>
	3.91×10 <sup>1</sup>	2.79×10 <sup>0</sup>	HCO <sub>2</sub> H	25.4%	22.8	55152.7	10.5	272	1.51×10 <sup>2</sup>	10	1.46	4.7%	Analytical	1.44×10 <sup>2</sup>	1.14×10 <sup>1</sup>
	2.61×10 <sup>1</sup>	1.79×10 <sup>0</sup>	HCO <sub>2</sub> H	25.4%	15.1	55232.6	5.4	201	9.98×10 <sup>1</sup>	10	1.41	6.7%	Analytical	9.32×10 <sup>1</sup>	9.20×10 <sup>0</sup>
	6.54×10 <sup>0</sup>	5.40×10 <sup>-1</sup>	HCO <sub>2</sub> H	25.4%	3.3	55352.7	-1.7	76	2.84×10 <sup>1</sup>	8	1.41	15.7%	Analytical	2.39×10 <sup>1</sup>	1.53×10 <sup>0</sup>
	7.75×10 <sup>1</sup>	6.08×10 <sup>0</sup>	HCO <sub>2</sub> H	25.1%	45.3	55006.9	34.1	469	5.55×10 <sup>2</sup>	9	1.56	0.8%	Analytical	5.50×10 <sup>2</sup>	2.68×10 <sup>1</sup>
1105	6.03×10 <sup>1</sup>	4.57×10 <sup>0</sup>	HCO <sub>2</sub> H	25.1%	35.4	55095.2	25.3	379	4.36×10 <sup>2</sup>	10	1.53	1.0%	Analytical	4.31×10 <sup>2</sup>	9.42×10 <sup>0</sup>
	3.99×10 <sup>1</sup>	3.06×10 <sup>0</sup>	HCO <sub>2</sub> H	25.1%	23.3	55198.7	15.0	269	2.81×10 <sup>2</sup>	10	1.53	1.5%	Analytical	2.76×10 <sup>2</sup>	2.91×10 <sup>1</sup>
	2.01×10 <sup>1</sup>	1.53×10 <sup>0</sup>	HCO <sub>2</sub> H	25.1%	11.6	55298.9	5.5	155	1.16×10 <sup>2</sup>	9	1.49	3.3%	Analytical	1.12×10 <sup>2</sup>	4.77×10 <sup>0</sup>
	1.51×10 <sup>1</sup>	1.02×10 <sup>0</sup>	HCO <sub>2</sub> H	25.1%	8.8	55324.2	3.6	123	9.31×10 <sup>1</sup>	11	1.41	4.1%	Analytical	8.93×10 <sup>1</sup>	7.49×10 <sup>0</sup>
	1.01×10 <sup>1</sup>	7.69×10 <sup>-1</sup>	HCO <sub>2</sub> H	25.1%	5.6	55349.6	1.4	90	5.42×10 <sup>1</sup>	9	1.45	6.3%	Analytical	5.08×10 <sup>1</sup>	4.17×10 <sup>0</sup>
1106	1.90×10 <sup>2</sup>	8.02×10 <sup>0</sup>	HCO <sub>2</sub> H	25.1%	124.1	54386.0	45.9	960	1.99×10 <sup>2</sup>	18	1.27	6.5%	Analytical	1.86×10 <sup>2</sup>	1.94×10 <sup>1</sup>
	1.49×10 <sup>2</sup>	6.31×10 <sup>0</sup>	HCO <sub>2</sub> H	25.1%	97.3	54601.3	45.6	771	1.62×10 <sup>2</sup>	18	1.26	7.7%	Analytical	1.50×10 <sup>2</sup>	1.27×10 <sup>1</sup>
	1.14×10 <sup>2</sup>	4.78×10 <sup>0</sup>	HCO <sub>2</sub> H	25.1%	74.3	54787.8	34.8	627	1.18×10 <sup>2</sup>	18	1.26	10.1%	Analytical	1.06×10 <sup>2</sup>	3.91×10 <sup>0</sup>
	7.61×10 <sup>1</sup>	3.02×10 <sup>0</sup>	HCO <sub>2</sub> H	25.1%	49.6	54989.3	22.7	460	8.10×10 <sup>1</sup>	19	1.24	13.8%	Analytical	6.98×10 <sup>1</sup>	1.78×10 <sup>0</sup>
	3.82×10 <sup>1</sup>	1.53×10 <sup>0</sup>	HCO <sub>2</sub> H	25.1%	24.4	55191.1	11.5	276	4.03×10 <sup>1</sup>	18	1.23	24.1%	Analytical	3.06×10 <sup>1</sup>	1.11×10 <sup>-1</sup>
	1.91×10 <sup>1</sup>	5.37×10 <sup>-1</sup>	HCO <sub>2</sub> H	25.1%	12.2	55293.0	3.1	167	2.16×10 <sup>1</sup>	25	1.14	40.9%	Analytical	1.27×10 <sup>1</sup>	5.41×10 <sup>-1</sup>
1110	1.20×10 <sup>2</sup>	9.84×10 <sup>0</sup>	HCO <sub>2</sub> H	15.3%	81.6	54692.4	48.2	431	6.05×10 <sup>2</sup>	10	1.78	0.2%	Analytical	6.05×10 <sup>2</sup>	1.26×10 <sup>1</sup>

## 7. Kinetic results of each studied amine for each concentration

N°	C <sub>Am</sub>	C <sub>CO<sub>2</sub></sub>	Acid	Neutra	[Am] <sup>f</sup>	[H <sub>2</sub> O] <sup>f</sup>	A	C	k <sub>0</sub>	R	Evolution HO <sup>-</sup>	Contribution HO <sup>-</sup>	Model used	k <sub>0</sub> <sup>Am</sup>	σ (k <sub>0</sub> <sup>Am</sup> )
	7.87×10 <sup>1</sup>	6.69×10 <sup>0</sup>	HCO <sub>2</sub> H	15.3%	53.2	54934.8	34.8	302	3.86×10 <sup>2</sup>	10	1.82	0.2%	Analytical	3.85×10 <sup>2</sup>	2.17×10 <sup>1</sup>
	4.00×10 <sup>1</sup>	3.26×10 <sup>0</sup>	HCO <sub>2</sub> H	15.3%	27.3	55163.0	20.0	164	1.80×10 <sup>2</sup>	10	1.78	0.5%	Analytical	1.79×10 <sup>2</sup>	5.10×10 <sup>0</sup>
	2.01×10 <sup>1</sup>	1.51×10 <sup>0</sup>	HCO <sub>2</sub> H	15.3%	13.9	55280.1	16.6	95	8.60×10 <sup>1</sup>	11	1.69	0.9%	Analytical	8.52×10 <sup>1</sup>	1.64×10 <sup>0</sup>
1111	1.00×10 <sup>2</sup>	9.01×10 <sup>0</sup>	HCO <sub>2</sub> H	10.6%	71.6	54725.1	47.0	294	2.09×10 <sup>2</sup>	10	2.11	0.5%	Analytical	2.08×10 <sup>2</sup>	5.30×10 <sup>0</sup>
	9.02×10 <sup>1</sup>	8.04×10 <sup>0</sup>	HCO <sub>2</sub> H	10.6%	64.5	54793.7	44.2	259	1.90×10 <sup>2</sup>	10	2.10	0.5%	Analytical	1.89×10 <sup>2</sup>	4.70×10 <sup>0</sup>
	8.03×10 <sup>1</sup>	7.02×10 <sup>0</sup>	HCO <sub>2</sub> H	10.6%	57.6	54860.9	40.6	234	1.65×10 <sup>2</sup>	10	2.08	0.6%	Analytical	1.64×10 <sup>2</sup>	3.17×10 <sup>0</sup>
	6.02×10 <sup>1</sup>	5.29×10 <sup>0</sup>	HCO <sub>2</sub> H	10.6%	43.1	54996.2	34.0	182	1.24×10 <sup>2</sup>	10	2.08	0.7%	Analytical	1.23×10 <sup>2</sup>	1.77×10 <sup>0</sup>
	3.99×10 <sup>1</sup>	3.55×10 <sup>0</sup>	HCO <sub>2</sub> H	10.6%	28.4	55132.5	25.3	128	8.01×10 <sup>1</sup>	10	2.09	1.1%	Analytical	7.93×10 <sup>1</sup>	1.08×10 <sup>0</sup>
	2.00×10 <sup>1</sup>	1.78×10 <sup>0</sup>	HCO <sub>2</sub> H	10.6%	14.3	55265.2	13.6	71	3.95×10 <sup>1</sup>	10	2.05	2.0%	Analytical	3.87×10 <sup>1</sup>	5.11×10 <sup>-1</sup>
	1.00×10 <sup>1</sup>	7.67×10 <sup>-1</sup>	HCO <sub>2</sub> H	10.6%	7.4	55331.9	4.7	37	1.98×10 <sup>1</sup>	12	1.80	4.2%	Analytical	1.90×10 <sup>1</sup>	2.62×10 <sup>-1</sup>
1112	1.76×10 <sup>2</sup>	8.06×10 <sup>0</sup>	HCO <sub>2</sub> H	10.0%	141.9	54212.5	43.1	382	4.57×10 <sup>2</sup>	20	1.53	0.3%	Analytical	4.56×10 <sup>2</sup>	2.59×10 <sup>1</sup>
	1.41×10 <sup>2</sup>	7.08×10 <sup>0</sup>	HCO <sub>2</sub> H	10.0%	112.4	54449.6	37.9	320	3.69×10 <sup>2</sup>	18	1.59	0.3%	Analytical	3.68×10 <sup>2</sup>	3.31×10 <sup>1</sup>
	1.06×10 <sup>2</sup>	6.09×10 <sup>0</sup>	HCO <sub>2</sub> H	10.0%	82.8	54686.4	31.3	255	2.62×10 <sup>2</sup>	16	1.69	0.4%	Analytical	2.61×10 <sup>2</sup>	1.30×10 <sup>1</sup>
	7.03×10 <sup>1</sup>	4.04×10 <sup>0</sup>	HCO <sub>2</sub> H	10.0%	55.1	54924.4	22.0	179	1.56×10 <sup>2</sup>	16	1.69	0.7%	Analytical	1.55×10 <sup>2</sup>	6.19×10 <sup>0</sup>
	3.52×10 <sup>1</sup>	2.54×10 <sup>0</sup>	HCO <sub>2</sub> H	10.0%	26.5	55160.1	16.4	102	7.52×10 <sup>1</sup>	13	1.88	1.2%	Analytical	7.43×10 <sup>1</sup>	1.04×10 <sup>0</sup>
	1.77×10 <sup>1</sup>	1.29×10 <sup>0</sup>	HCO <sub>2</sub> H	10.0%	13.2	55277.4	8.3	57	3.65×10 <sup>1</sup>	12	1.85	2.3%	Analytical	3.57×10 <sup>1</sup>	5.67×10 <sup>-1</sup>
1113	9.00×10 <sup>1</sup>	7.64×10 <sup>0</sup>	HCO <sub>2</sub> H	15.7%	60.4	54777.0	44.2	358	6.35×10 <sup>2</sup>	10	1.78	0.3%	Analytical	6.33×10 <sup>2</sup>	1.26×10 <sup>1</sup>
	6.02×10 <sup>1</sup>	5.09×10 <sup>0</sup>	HCO <sub>2</sub> H	15.7%	40.3	54981.5	25.1	251	4.04×10 <sup>2</sup>	10	1.78	0.5%	Analytical	4.02×10 <sup>2</sup>	1.16×10 <sup>1</sup>

N°	C <sub>Am</sub>	C <sub>CO<sub>2</sub></sub>	Acid	Neutra	[Am] <sup>f</sup>	[H <sub>2</sub> O] <sup>f</sup>	A	C	k <sub>0</sub>	R	Evolution HO <sup>-</sup>	Contribution HO <sup>-</sup>	Model used	k <sub>0</sub> <sup>Am</sup>	σ (k <sub>0</sub> <sup>Am</sup> )
	4.50×10 <sup>1</sup>	3.82×10 <sup>0</sup>	HCO <sub>2</sub> H	15.7%	30.1	55085.0	18.5	199	2.86×10 <sup>2</sup>	10	1.77	0.7%	Analytical	2.85×10 <sup>2</sup>	1.78×10 <sup>1</sup>
	3.01×10 <sup>1</sup>	2.56×10 <sup>0</sup>	HCO <sub>2</sub> H	15.7%	20.1	55186.9	12.4	140	1.80×10 <sup>2</sup>	10	1.76	1.0%	Analytical	1.78×10 <sup>2</sup>	1.48×10 <sup>1</sup>
	1.51×10 <sup>1</sup>	1.30×10 <sup>0</sup>	HCO <sub>2</sub> H	15.7%	10.0	55289.7	5.7	77	8.79×10 <sup>1</sup>	10	1.72	2.0%	Analytical	8.61×10 <sup>1</sup>	3.64×10 <sup>0</sup>
	7.52×10 <sup>0</sup>	5.44×10 <sup>-1</sup>	HCO <sub>2</sub> H	15.7%	5.1	55341.8	1.5	45	4.35×10 <sup>1</sup>	11	1.51	3.9%	Analytical	4.18×10 <sup>1</sup>	1.38×10 <sup>0</sup>
1120	1.01×10 <sup>2</sup>	1.14×10 <sup>1</sup>	No	0.0%	78.2	55070.3	56.2	163	5.02×10 <sup>2</sup>	9	6.41	0.5%	Analytical	5.00×10 <sup>2</sup>	1.42×10 <sup>1</sup>
	8.12×10 <sup>1</sup>	9.16×10 <sup>0</sup>	No	0.0%	62.7	55135.0	45.0	138	3.93×10 <sup>2</sup>	9	5.91	0.6%	Analytical	3.91×10 <sup>2</sup>	1.77×10 <sup>1</sup>
	6.09×10 <sup>1</sup>	6.89×10 <sup>0</sup>	No	0.0%	46.8	55200.5	34.5	110	2.85×10 <sup>2</sup>	9	5.30	0.8%	Analytical	2.82×10 <sup>2</sup>	3.64×10 <sup>0</sup>
	4.05×10 <sup>1</sup>	4.60×10 <sup>0</sup>	No	0.0%	31.0	55265.8	22.8	82	1.81×10 <sup>2</sup>	9	4.54	1.2%	Analytical	1.79×10 <sup>2</sup>	3.28×10 <sup>0</sup>
	1.90×10 <sup>1</sup>	2.32×10 <sup>0</sup>	No	0.0%	14.2	55334.2	9.7	49	7.78×10 <sup>1</sup>	8	3.66	2.4%	Analytical	7.59×10 <sup>1</sup>	1.13×10 <sup>0</sup>
	1.02×10 <sup>1</sup>	1.16×10 <sup>0</sup>	No	0.0%	7.6	55362.2	2.7	32	4.13×10 <sup>1</sup>	8	2.74	4.4%	Analytical	3.95×10 <sup>1</sup>	5.28×10 <sup>-1</sup>
1121	4.55×10 <sup>1</sup>	3.82×10 <sup>0</sup>	HCO <sub>2</sub> H	14.5%	30.9	55198.8	22.2	219	3.67×10 <sup>2</sup>	10	1.76	0.9%	Analytical	3.64×10 <sup>2</sup>	2.62×10 <sup>1</sup>
	3.03×10 <sup>1</sup>	2.55×10 <sup>0</sup>	HCO <sub>2</sub> H	14.5%	20.5	55263.3	13.2	157	2.28×10 <sup>2</sup>	10	1.73	1.3%	Analytical	2.25×10 <sup>2</sup>	2.56×10 <sup>1</sup>
	1.52×10 <sup>1</sup>	1.30×10 <sup>0</sup>	HCO <sub>2</sub> H	14.5%	10.1	55327.4	5.1	89	9.67×10 <sup>1</sup>	10	1.67	2.8%	Analytical	9.40×10 <sup>1</sup>	5.38×10 <sup>0</sup>
	7.65×10 <sup>0</sup>	5.43×10 <sup>-1</sup>	HCO <sub>2</sub> H	14.5%	5.1	55359.4	1.3	56	4.75×10 <sup>1</sup>	11	1.45	5.5%	Analytical	4.49×10 <sup>1</sup>	1.48×10 <sup>0</sup>
1122	8.22×10 <sup>0</sup>	8.18×10 <sup>-1</sup>	No	0.0%	6.0	55353.7	-	-	-	9	1.75	8.0%	Numerical	6.34×10 <sup>1</sup>	1.12×10 <sup>0</sup>
	6.13×10 <sup>0</sup>	6.14×10 <sup>-1</sup>	No	0.0%	4.4	55364.1	-	-	-	9	1.67	9.6%	Numerical	4.62×10 <sup>1</sup>	7.92×10 <sup>-1</sup>
	4.10×10 <sup>0</sup>	4.09×10 <sup>-1</sup>	No	0.0%	2.9	55374.1	-	-	-	8	1.56	12.5%	Numerical	2.95×10 <sup>1</sup>	8.37×10 <sup>-1</sup>
	2.08×10 <sup>0</sup>	2.05×10 <sup>-1</sup>	No	0.0%	1.3	55384.2	-	-	-	8	1.41	19.0%	Numerical	1.34×10 <sup>1</sup>	4.10×10 <sup>-1</sup>

## 7. Kinetic results of each studied amine for each concentration

N°	C <sub>Am</sub>	C <sub>CO<sub>2</sub></sub>	Acid	Neutra	[Am] <sup>f</sup>	[H <sub>2</sub> O] <sup>f</sup>	A	C	k <sub>0</sub>	R	Evolution HO <sup>-</sup>	Contribution HO <sup>-</sup>	Model used	k <sub>0</sub> <sup>Am</sup>	σ (k <sub>0</sub> <sup>Am</sup> )
	1.07×10 <sup>0</sup>	1.02×10 <sup>-1</sup>	No	0.0%	0.6	55389.1	-	-	-	7	1.30	28.7%	Numerical	5.76×10 <sup>0</sup>	1.51×10 <sup>-1</sup>
1123	1.03×10 <sup>1</sup>	1.03×10 <sup>0</sup>	No	0.0%	7.4	55327.6	-	-	-	9	1.69	8.2%	Numerical	9.13×10 <sup>1</sup>	3.33×10 <sup>0</sup>
	8.21×10 <sup>0</sup>	8.23×10 <sup>-1</sup>	No	0.0%	5.8	55341.1	-	-	-	8	1.63	10.0%	Numerical	6.73×10 <sup>1</sup>	3.04×10 <sup>0</sup>
	6.19×10 <sup>0</sup>	6.17×10 <sup>-1</sup>	No	0.0%	4.2	55354.3	-	-	-	8	1.56	12.0%	Numerical	4.86×10 <sup>1</sup>	9.00×10 <sup>-1</sup>
	4.12×10 <sup>0</sup>	4.11×10 <sup>-1</sup>	No	0.0%	2.7	55367.7	-	-	-	8	1.48	15.1%	Numerical	3.14×10 <sup>1</sup>	5.72×10 <sup>-1</sup>
	2.09×10 <sup>0</sup>	2.06×10 <sup>-1</sup>	No	0.0%	1.2	55380.9	-	-	-	7	1.36	22.3%	Numerical	1.42×10 <sup>1</sup>	4.10×10 <sup>-1</sup>
	1.05×10 <sup>0</sup>	1.03×10 <sup>-1</sup>	No	0.0%	0.5	55387.7	-	-	-	6	1.27	33.0%	Numerical	5.77×10 <sup>0</sup>	2.29×10 <sup>-1</sup>
1124	9.09×10 <sup>1</sup>	7.62×10 <sup>0</sup>	HCO <sub>2</sub> H	15.1%	61.8	54997.4	51.3	372	4.14×10 <sup>2</sup>	10	1.81	0.2%	Analytical	4.13×10 <sup>2</sup>	1.18×10 <sup>1</sup>
	7.58×10 <sup>1</sup>	6.37×10 <sup>0</sup>	HCO <sub>2</sub> H	15.1%	51.5	55062.5	43.2	313	3.47×10 <sup>2</sup>	10	1.82	0.3%	Analytical	3.46×10 <sup>2</sup>	2.69×10 <sup>1</sup>
	5.84×10 <sup>1</sup>	5.08×10 <sup>0</sup>	HCO <sub>2</sub> H	15.1%	39.3	55137.6	37.9	252	2.47×10 <sup>2</sup>	10	1.85	0.3%	Analytical	2.46×10 <sup>2</sup>	1.40×10 <sup>1</sup>
	4.55×10 <sup>1</sup>	3.81×10 <sup>0</sup>	HCO <sub>2</sub> H	15.1%	30.9	55193.0	29.8	201	1.89×10 <sup>2</sup>	10	1.82	0.4%	Analytical	1.88×10 <sup>2</sup>	3.53×10 <sup>0</sup>
	3.03×10 <sup>1</sup>	2.55×10 <sup>0</sup>	HCO <sub>2</sub> H	15.1%	20.6	55257.9	21.0	138	1.23×10 <sup>2</sup>	10	1.81	0.6%	Analytical	1.22×10 <sup>2</sup>	1.96×10 <sup>0</sup>
	1.52×10 <sup>1</sup>	1.30×10 <sup>0</sup>	HCO <sub>2</sub> H	15.1%	10.2	55322.7	9.8	73	5.86×10 <sup>1</sup>	10	1.81	1.3%	Analytical	5.79×10 <sup>1</sup>	1.83×10 <sup>0</sup>
1125	7.64×10 <sup>0</sup>	5.43×10 <sup>-1</sup>	HCO <sub>2</sub> H	15.1%	5.3	55354.7	4.0	41	2.98×10 <sup>1</sup>	12	1.60	2.6%	Analytical	2.91×10 <sup>1</sup>	4.18×10 <sup>-1</sup>
	1.51×10 <sup>2</sup>	7.13×10 <sup>0</sup>	HCO <sub>2</sub> H	5.1%	128.4	54755.3	46.8	265	3.38×10 <sup>2</sup>	20	1.88	0.8%	Analytical	3.35×10 <sup>2</sup>	1.31×10 <sup>1</sup>
	1.21×10 <sup>2</sup>	5.88×10 <sup>0</sup>	HCO <sub>2</sub> H	5.1%	102.3	54882.6	36.3	215	2.49×10 <sup>2</sup>	20	1.90	1.1%	Analytical	2.47×10 <sup>2</sup>	1.16×10 <sup>1</sup>
	9.06×10 <sup>1</sup>	4.34×10 <sup>0</sup>	HCO <sub>2</sub> H	5.1%	76.9	55009.6	28.4	171	1.79×10 <sup>2</sup>	20	1.86	1.5%	Analytical	1.76×10 <sup>2</sup>	4.42×10 <sup>0</sup>
	6.04×10 <sup>1</sup>	2.81×10 <sup>0</sup>	HCO <sub>2</sub> H	5.1%	51.4	55137.2	17.3	122	1.13×10 <sup>2</sup>	20	1.79	2.2%	Analytical	1.10×10 <sup>2</sup>	2.04×10 <sup>0</sup>

Nº	C <sub>Am</sub>	C <sub>CO<sub>2</sub></sub>	Acid	Neutra	[Am] <sup>f</sup>	[H <sub>2</sub> O] <sup>f</sup>	A	C	k <sub>0</sub>	R	Evolution HO <sup>-</sup>	Contribution HO <sup>-</sup>	Model used	k <sub>0</sub> <sup>Am</sup>	σ (k <sub>0</sub> <sup>Am</sup> )
	3.03×10 <sup>1</sup>	1.30×10 <sup>0</sup>	HCO <sub>2</sub> H	5.1%	25.8	55264.7	6.8	71	5.19×10 <sup>1</sup>	22	1.64	4.6%	Analytical	4.95×10 <sup>1</sup>	8.60×10 <sup>-1</sup>
	1.51×10 <sup>1</sup>	7.95×10 <sup>-1</sup>	HCO <sub>2</sub> H	5.1%	12.5	55329.1	3.4	45	2.58×10 <sup>1</sup>	18	1.67	7.6%	Analytical	2.38×10 <sup>1</sup>	3.87×10 <sup>-1</sup>
1126	1.61×10 <sup>2</sup>	7.63×10 <sup>0</sup>	HCO <sub>2</sub> H	10.5%	128.3	54567.1	46.1	394	2.56×10 <sup>2</sup>	19	1.53	0.8%	Analytical	2.54×10 <sup>2</sup>	1.73×10 <sup>1</sup>
	1.29×10 <sup>2</sup>	6.13×10 <sup>0</sup>	HCO <sub>2</sub> H	10.5%	102.6	54731.6	39.9	323	1.94×10 <sup>2</sup>	19	1.53	1.0%	Analytical	1.92×10 <sup>2</sup>	9.34×10 <sup>0</sup>
	9.65×10 <sup>1</sup>	4.59×10 <sup>0</sup>	HCO <sub>2</sub> H	10.5%	77.0	54896.5	32.4	254	1.43×10 <sup>2</sup>	19	1.53	1.3%	Analytical	1.41×10 <sup>2</sup>	3.16×10 <sup>0</sup>
	6.44×10 <sup>1</sup>	3.05×10 <sup>0</sup>	HCO <sub>2</sub> H	10.5%	51.3	55061.4	21.0	177	8.99×10 <sup>1</sup>	19	1.52	2.0%	Analytical	8.81×10 <sup>1</sup>	1.96×10 <sup>0</sup>
	3.23×10 <sup>1</sup>	1.55×10 <sup>0</sup>	HCO <sub>2</sub> H	10.5%	25.6	55226.5	11.8	100	4.30×10 <sup>1</sup>	19	1.51	3.9%	Analytical	4.13×10 <sup>1</sup>	9.38×10 <sup>-1</sup>
	1.61×10 <sup>1</sup>	7.94×10 <sup>-1</sup>	HCO <sub>2</sub> H	10.5%	12.7	55309.7	5.4	56	2.09×10 <sup>1</sup>	18	1.48	7.3%	Analytical	1.93×10 <sup>1</sup>	3.15×10 <sup>-1</sup>
1127	5.02×10 <sup>2</sup>	1.01×10 <sup>1</sup>	HCO <sub>2</sub> H	15.2%	403.7	52766.2	49.0	1195	2.52×10 <sup>2</sup>	42	1.16	1.3%	Analytical	2.49×10 <sup>2</sup>	2.28×10 <sup>1</sup>
	4.02×10 <sup>2</sup>	8.09×10 <sup>0</sup>	HCO <sub>2</sub> H	15.2%	323.2	53287.9	35.9	1007	1.77×10 <sup>2</sup>	42	1.16	1.8%	Analytical	1.74×10 <sup>2</sup>	1.34×10 <sup>1</sup>
	3.01×10 <sup>2</sup>	6.11×10 <sup>0</sup>	HCO <sub>2</sub> H	15.2%	242.3	53811.5	34.6	807	1.20×10 <sup>2</sup>	42	1.16	2.6%	Analytical	1.16×10 <sup>2</sup>	6.14×10 <sup>0</sup>
	2.01×10 <sup>2</sup>	4.05×10 <sup>0</sup>	HCO <sub>2</sub> H	15.2%	161.9	54334.5	27.4	579	7.37×10 <sup>1</sup>	42	1.16	3.9%	Analytical	7.09×10 <sup>1</sup>	3.44×10 <sup>0</sup>
	1.00×10 <sup>2</sup>	2.04×10 <sup>0</sup>	HCO <sub>2</sub> H	15.2%	80.6	54863.4	17.2	318	2.97×10 <sup>1</sup>	42	1.17	8.9%	Analytical	2.71×10 <sup>1</sup>	8.28×10 <sup>-1</sup>
	5.03×10 <sup>1</sup>	1.04×10 <sup>0</sup>	HCO <sub>2</sub> H	15.2%	40.3	55126.7	10.9	180	1.36×10 <sup>1</sup>	41	1.17	17.8%	Analytical	1.11×10 <sup>1</sup>	1.27×10 <sup>-1</sup>
1128	3.54×10 <sup>2</sup>	7.59×10 <sup>0</sup>	HCO <sub>2</sub> H	15.0%	285.1	53544.2	43.7	862	2.93×10 <sup>1</sup>	40	1.17	1.3%	Analytical	2.89×10 <sup>1</sup>	7.69×10 <sup>-1</sup>
	2.83×10 <sup>2</sup>	6.10×10 <sup>0</sup>	HCO <sub>2</sub> H	15.0%	227.9	53914.5	39.6	722	2.10×10 <sup>1</sup>	40	1.18	1.7%	Analytical	2.06×10 <sup>1</sup>	3.61×10 <sup>-1</sup>
	2.12×10 <sup>2</sup>	4.57×10 <sup>0</sup>	HCO <sub>2</sub> H	15.0%	170.5	54286.6	31.9	572	1.37×10 <sup>1</sup>	40	1.18	2.5%	Analytical	1.34×10 <sup>1</sup>	1.54×10 <sup>-1</sup>
	1.41×10 <sup>2</sup>	3.04×10 <sup>0</sup>	HCO <sub>2</sub> H	15.0%	113.4	54656.5	23.9	402	7.70×10 <sup>0</sup>	40	1.18	4.3%	Analytical	7.37×10 <sup>0</sup>	1.00×10 <sup>-1</sup>

## 7. Kinetic results of each studied amine for each concentration

N°	C <sub>Am</sub>	C <sub>CO<sub>2</sub></sub>	Acid	Neutra	[Am] <sup>f</sup>	[H <sub>2</sub> O] <sup>f</sup>	A	C	k <sub>0</sub>	R	Evolution HO <sup>-</sup>	Contribution HO <sup>-</sup>	Model used	k <sub>0</sub> <sup>Am</sup>	σ (k <sub>0</sub> <sup>Am</sup> )
	7.02×10 <sup>1</sup>	1.54×10 <sup>0</sup>	HCO <sub>2</sub> H	15.0%	56.6	55024.9	14.5	218	3.25×10 <sup>0</sup>	39	1.19	9.6%	Analytical	2.94×10 <sup>0</sup>	3.28×10 <sup>-2</sup>
	3.51×10 <sup>1</sup>	7.90×10 <sup>-1</sup>	HCO <sub>2</sub> H	15.0%	28.2	55208.8	9.6	118	1.62×10 <sup>0</sup>	38	1.19	18.0%	Analytical	1.33×10 <sup>0</sup>	1.75×10 <sup>-2</sup>
1129	2.45×10 <sup>2</sup>	5.04×10 <sup>0</sup>	HCO <sub>2</sub> H	20.6%	183.9	54118.6	29.6	802	4.70×10 <sup>0</sup>	39	1.14	1.6%	Analytical	4.62×10 <sup>0</sup>	5.18×10 <sup>-2</sup>
	1.95×10 <sup>2</sup>	4.03×10 <sup>0</sup>	HCO <sub>2</sub> H	20.6%	146.6	54379.3	24.4	663	3.54×10 <sup>0</sup>	39	1.14	2.1%	Analytical	3.46×10 <sup>0</sup>	3.86×10 <sup>-2</sup>
	9.73×10 <sup>1</sup>	2.03×10 <sup>0</sup>	HCO <sub>2</sub> H	20.6%	73.1	54886.9	13.5	362	1.64×10 <sup>0</sup>	38	1.15	4.3%	Analytical	1.57×10 <sup>0</sup>	1.61×10 <sup>-2</sup>
	4.85×10 <sup>1</sup>	1.04×10 <sup>0</sup>	HCO <sub>2</sub> H	20.6%	36.4	55137.2	6.2	190	9.68×10 <sup>-1</sup>	38	1.15	7.0%	Analytical	9.00×10 <sup>-1</sup>	8.32×10 <sup>-3</sup>
	2.43×10 <sup>1</sup>	5.39×10 <sup>-1</sup>	HCO <sub>2</sub> H	20.6%	18.2	55260.9	3.5	100	5.70×10 <sup>-1</sup>	37	1.16	11.5%	Analytical	5.04×10 <sup>-1</sup>	1.19×10 <sup>-2</sup>
1130	9.03×10 <sup>1</sup>	7.65×10 <sup>0</sup>	HCO <sub>2</sub> H	15.8%	60.3	54836.2	40.5	380	2.92×10 <sup>2</sup>	10	1.76	1.1%	Analytical	2.88×10 <sup>2</sup>	1.13×10 <sup>1</sup>
	7.48×10 <sup>1</sup>	6.40×10 <sup>0</sup>	HCO <sub>2</sub> H	15.8%	49.8	54931.7	33.2	320	2.23×10 <sup>2</sup>	10	1.77	1.4%	Analytical	2.20×10 <sup>2</sup>	1.37×10 <sup>1</sup>
	6.02×10 <sup>1</sup>	5.10×10 <sup>0</sup>	HCO <sub>2</sub> H	15.8%	40.1	55021.6	26.6	267	1.79×10 <sup>2</sup>	10	1.75	1.8%	Analytical	1.75×10 <sup>2</sup>	7.19×10 <sup>0</sup>
	4.49×10 <sup>1</sup>	3.83×10 <sup>0</sup>	HCO <sub>2</sub> H	15.8%	29.8	55116.1	19.9	202	1.21×10 <sup>2</sup>	10	1.75	2.5%	Analytical	1.18×10 <sup>2</sup>	5.06×10 <sup>0</sup>
	2.99×10 <sup>1</sup>	2.56×10 <sup>0</sup>	HCO <sub>2</sub> H	15.8%	19.7	55208.6	12.4	146	8.00×10 <sup>1</sup>	10	1.72	3.6%	Analytical	7.71×10 <sup>1</sup>	4.83×10 <sup>0</sup>
	7.55×10 <sup>0</sup>	5.45×10 <sup>-1</sup>	HCO <sub>2</sub> H	15.8%	5.0	55345.8	1.1	52	1.97×10 <sup>1</sup>	11	1.46	12.6%	Analytical	1.72×10 <sup>1</sup>	3.47×10 <sup>-2</sup>
1131	1.01×10 <sup>2</sup>	8.09×10 <sup>0</sup>	HCO <sub>2</sub> H	15.3%	69.0	54934.7	56.2	407	4.48×10 <sup>2</sup>	11	1.76	0.2%	Analytical	4.47×10 <sup>2</sup>	3.44×10 <sup>1</sup>
	8.06×10 <sup>1</sup>	6.62×10 <sup>0</sup>	HCO <sub>2</sub> H	15.3%	54.9	55026.9	45.3	336	3.35×10 <sup>2</sup>	10	1.79	0.2%	Analytical	3.34×10 <sup>2</sup>	4.01×10 <sup>1</sup>
	6.04×10 <sup>1</sup>	4.83×10 <sup>0</sup>	HCO <sub>2</sub> H	15.3%	41.4	55119.1	36.7	258	2.60×10 <sup>2</sup>	11	1.76	0.3%	Analytical	2.59×10 <sup>2</sup>	1.82×10 <sup>1</sup>
	4.03×10 <sup>1</sup>	3.05×10 <sup>0</sup>	HCO <sub>2</sub> H	15.3%	27.9	55211.1	24.5	176	1.58×10 <sup>2</sup>	11	1.72	0.5%	Analytical	1.58×10 <sup>2</sup>	2.28×10 <sup>0</sup>
	2.02×10 <sup>1</sup>	1.55×10 <sup>0</sup>	HCO <sub>2</sub> H	15.3%	13.9	55302.7	13.4	95	7.88×10 <sup>1</sup>	11	1.72	0.9%	Analytical	7.81×10 <sup>1</sup>	1.98×10 <sup>0</sup>

N°	C <sub>Am</sub>	C <sub>CO<sub>2</sub></sub>	Acid	Neutra	[Am] <sup>f</sup>	[H <sub>2</sub> O] <sup>f</sup>	A	C	k <sub>0</sub>	R	Evolution HO <sup>-</sup>	Contribution HO <sup>-</sup>	Model used	k <sub>0</sub> <sup>Am</sup>	σ (k <sub>0</sub> <sup>Am</sup> )
	1.01×10 <sup>1</sup>	7.92×10 <sup>-1</sup>	HCO <sub>2</sub> H	15.3%	6.9	55348.6	7.3	52	3.84×10 <sup>1</sup>	11	1.71	1.7%	Analytical	3.77×10 <sup>1</sup>	1.18×10 <sup>0</sup>
1132	9.10×10 <sup>1</sup>	7.59×10 <sup>0</sup>	HCO <sub>2</sub> H	15.1%	61.9	54893.5	52.6	353	4.30×10 <sup>2</sup>	10	1.80	0.2%	Analytical	4.29×10 <sup>2</sup>	2.02×10 <sup>1</sup>
	7.59×10 <sup>1</sup>	6.35×10 <sup>0</sup>	HCO <sub>2</sub> H	15.1%	51.6	54976.3	45.0	303	3.42×10 <sup>2</sup>	10	1.81	0.3%	Analytical	3.41×10 <sup>2</sup>	1.78×10 <sup>1</sup>
	6.08×10 <sup>1</sup>	5.06×10 <sup>0</sup>	HCO <sub>2</sub> H	15.1%	41.4	55059.4	35.3	247	2.53×10 <sup>2</sup>	10	1.81	0.4%	Analytical	2.52×10 <sup>2</sup>	1.23×10 <sup>1</sup>
	4.55×10 <sup>1</sup>	3.80×10 <sup>0</sup>	HCO <sub>2</sub> H	15.1%	31.0	55142.9	26.7	190	1.93×10 <sup>2</sup>	10	1.81	0.5%	Analytical	1.92×10 <sup>2</sup>	1.00×10 <sup>1</sup>
	3.03×10 <sup>1</sup>	2.54×10 <sup>0</sup>	HCO <sub>2</sub> H	15.1%	20.6	55226.6	18.0	131	1.22×10 <sup>2</sup>	10	1.81	0.7%	Analytical	1.21×10 <sup>2</sup>	1.09×10 <sup>0</sup>
	1.53×10 <sup>1</sup>	1.29×10 <sup>0</sup>	HCO <sub>2</sub> H	15.1%	10.3	55309.3	8.9	69	6.06×10 <sup>1</sup>	10	1.79	1.3%	Analytical	5.98×10 <sup>1</sup>	6.87×10 <sup>-1</sup>
	7.68×10 <sup>0</sup>	5.40×10 <sup>-1</sup>	HCO <sub>2</sub> H	15.1%	5.3	55351.1	3.7	39	3.06×10 <sup>1</sup>	12	1.59	2.7%	Analytical	2.98×10 <sup>1</sup>	4.28×10 <sup>-1</sup>
1140	1.81×10 <sup>2</sup>	7.53×10 <sup>0</sup>	HCO <sub>2</sub> H	14.9%	138.7	54682.6	61.2	650	2.51×10 <sup>2</sup>	21	1.36	0.0%	Analytical	2.51×10 <sup>2</sup>	2.12×10 <sup>1</sup>
	1.51×10 <sup>2</sup>	6.30×10 <sup>0</sup>	HCO <sub>2</sub> H	14.9%	115.7	54800.3	55.1	547	2.02×10 <sup>2</sup>	21	1.37	0.0%	Analytical	2.02×10 <sup>2</sup>	1.23×10 <sup>1</sup>
	1.21×10 <sup>2</sup>	4.01×10 <sup>0</sup>	HCO <sub>2</sub> H	14.9%	94.7	54918.6	35.8	437	1.59×10 <sup>2</sup>	26	1.29	0.0%	Analytical	1.59×10 <sup>2</sup>	6.68×10 <sup>0</sup>
	9.04×10 <sup>1</sup>	2.52×10 <sup>0</sup>	HCO <sub>2</sub> H	14.9%	71.9	55038.1	25.6	329	1.24×10 <sup>2</sup>	31	1.24	0.0%	Analytical	1.24×10 <sup>2</sup>	4.13×10 <sup>0</sup>
	6.04×10 <sup>1</sup>	1.53×10 <sup>0</sup>	HCO <sub>2</sub> H	14.9%	48.3	55156.1	16.2	224	7.92×10 <sup>1</sup>	34	1.22	0.1%	Analytical	7.92×10 <sup>1</sup>	1.27×10 <sup>0</sup>
	3.02×10 <sup>1</sup>	5.36×10 <sup>-1</sup>	HCO <sub>2</sub> H	14.9%	24.6	55274.5	7.3	114	4.09×10 <sup>1</sup>	49	1.15	0.1%	Analytical	4.09×10 <sup>1</sup>	5.27×10 <sup>-1</sup>
	1.50×10 <sup>1</sup>	5.36×10 <sup>-1</sup>	HCO <sub>2</sub> H	14.9%	11.7	55334.1	6.9	62	1.99×10 <sup>1</sup>	24	1.33	0.3%	Analytical	1.99×10 <sup>1</sup>	1.76×10 <sup>-1</sup>

## 7. Kinetic results of each studied amine for each concentration

Table IX-13. Experimental results of secondary amines.

N°	C <sub>Am</sub>	C <sub>CO2</sub>	Acid	Neutra	[Am] <sup>f</sup>	[H <sub>2</sub> O] <sup>f</sup>	A	C	k <sub>0</sub>	R	Evolution HO <sup>-</sup>	Contribution HO <sup>-</sup>	Model used	k <sub>0</sub> <sup>Am</sup>	σ (k <sub>0</sub> <sup>Am</sup> )
1200	2.05×10 <sup>0</sup>	1.56×10 <sup>-1</sup>	No	0.0%	1.1	55389.3	-2.0	48	6.52×10 <sup>1</sup>	8	1.23	8.5%	Analytical	5.97×10 <sup>1</sup>	1.67×10 <sup>0</sup>
	1.03×10 <sup>0</sup>	4.16×10 <sup>-2</sup>	No	0.0%	0.5	55391.9	-0.7	31	2.36×10 <sup>1</sup>	13	1.09	16.9%	Analytical	1.96×10 <sup>1</sup>	4.84×10 <sup>-1</sup>
	5.22×10 <sup>-1</sup>	1.87×10 <sup>-2</sup>	No	0.0%	0.2	55393.1	-0.5	18	8.04×10 <sup>0</sup>	12	1.06	31.8%	Analytical	5.49×10 <sup>0</sup>	1.51×10 <sup>-1</sup>
	2.64×10 <sup>-1</sup>	6.25×10 <sup>-3</sup>	No	0.0%	0.1	55393.8	-0.5	10	2.80×10 <sup>0</sup>	14	1.03	56.3%	Analytical	1.22×10 <sup>0</sup>	4.23×10 <sup>-2</sup>
1201	3.11×10 <sup>0</sup>	1.58×10 <sup>-1</sup>	No	0.0%	1.8	55381.4	-1.8	66	6.66×10 <sup>1</sup>	13	1.16	12.2%	Analytical	5.85×10 <sup>1</sup>	1.75×10 <sup>0</sup>
	2.08×10 <sup>0</sup>	1.05×10 <sup>-1</sup>	No	0.0%	1.1	55386.0	-1.3	51	3.76×10 <sup>1</sup>	12	1.14	17.1%	Analytical	3.12×10 <sup>1</sup>	4.19×10 <sup>-1</sup>
	1.04×10 <sup>0</sup>	4.20×10 <sup>-2</sup>	No	0.0%	0.5	55390.5	-0.8	32	1.44×10 <sup>1</sup>	12	1.09	29.6%	Analytical	1.01×10 <sup>1</sup>	2.35×10 <sup>-1</sup>
	5.03×10 <sup>-1</sup>	1.47×10 <sup>-2</sup>	No	0.0%	0.2	55392.8	-0.4	19	5.36×10 <sup>0</sup>	13	1.05	49.0%	Analytical	2.74×10 <sup>0</sup>	7.53×10 <sup>-2</sup>
	2.65×10 <sup>-1</sup>	4.20×10 <sup>-3</sup>	No	0.0%	0.1	55393.9	-0.3	11	2.42×10 <sup>0</sup>	19	1.02	68.4%	Analytical	7.66×10 <sup>-1</sup>	3.98×10 <sup>-2</sup>
1202	3.27×10 <sup>0</sup>	1.88×10 <sup>-1</sup>	No	0.0%	1.9	55377.3	-2.2	66	6.91×10 <sup>1</sup>	11	1.18	12.4%	Analytical	6.05×10 <sup>1</sup>	1.11×10 <sup>0</sup>
	2.17×10 <sup>0</sup>	1.05×10 <sup>-1</sup>	No	0.0%	1.2	55383.4	-1.5	51	3.89×10 <sup>1</sup>	12	1.13	17.8%	Analytical	3.20×10 <sup>1</sup>	8.61×10 <sup>-1</sup>
	1.09×10 <sup>0</sup>	4.19×10 <sup>-2</sup>	No	0.0%	0.5	55389.5	-0.8	32	1.50×10 <sup>1</sup>	13	1.08	30.6%	Analytical	1.04×10 <sup>1</sup>	5.78×10 <sup>-1</sup>
	5.49×10 <sup>-1</sup>	1.47×10 <sup>-2</sup>	No	0.0%	0.2	55392.5	-0.5	19	5.62×10 <sup>0</sup>	14	1.05	51.6%	Analytical	2.72×10 <sup>0</sup>	6.38×10 <sup>-2</sup>
	2.79×10 <sup>-1</sup>	4.19×10 <sup>-3</sup>	No	0.0%	0.1	55394.0	-0.3	10	2.35×10 <sup>0</sup>	20	1.02	75.1%	Analytical	5.84×10 <sup>-1</sup>	5.43×10 <sup>-2</sup>
1203	6.29×10 <sup>0</sup>	4.19×10 <sup>-1</sup>	No	0.0%	3.9	55357.0	-3.7	96	7.88×10 <sup>1</sup>	11	1.25	16.7%	Analytical	6.56×10 <sup>1</sup>	1.97×10 <sup>0</sup>
	4.20×10 <sup>0</sup>	2.52×10 <sup>-1</sup>	No	0.0%	2.4	55369.8	-2.7	76	4.67×10 <sup>1</sup>	11	1.19	23.1%	Analytical	3.59×10 <sup>1</sup>	9.34×10 <sup>-1</sup>
	2.10×10 <sup>0</sup>	1.05×10 <sup>-1</sup>	No	0.0%	1.0	55382.5	-1.2	49	2.03×10 <sup>1</sup>	11	1.13	36.1%	Analytical	1.29×10 <sup>1</sup>	2.18×10 <sup>-1</sup>
	1.05×10 <sup>0</sup>	4.19×10 <sup>-2</sup>	No	0.0%	0.4	55388.8	-0.7	30	8.21×10 <sup>0</sup>	11	1.08	57.9%	Analytical	3.46×10 <sup>0</sup>	6.14×10 <sup>-2</sup>

N°	C <sub>Am</sub>	C <sub>CO2</sub>	Acid	Neutra	[Am] <sup>f</sup>	[H <sub>2</sub> O] <sup>f</sup>	A	C	k <sub>0</sub>	R	Evolution HO <sup>-</sup>	Contribution HO <sup>-</sup>	Model used	k <sub>0</sub> <sup>Am</sup>	σ (k <sub>0</sub> <sup>Am</sup> )
	5.32×10 <sup>-1</sup>	1.47×10 <sup>-2</sup>	No	0.0%	0.2	55391.9	-0.4	17	3.56×10 <sup>0</sup>	12	1.05	83.7%	Analytical	5.80×10 <sup>-1</sup>	3.59×10 <sup>-2</sup>
1204	6.44×10 <sup>0</sup>	4.20×10 <sup>-1</sup>	No	0.0%	4.0	55364.4	-3.7	110	6.78×10 <sup>1</sup>	11	1.24	20.3%	Analytical	5.41×10 <sup>1</sup>	3.14×10 <sup>0</sup>
	4.29×10 <sup>0</sup>	2.52×10 <sup>-1</sup>	No	0.0%	2.5	55375.0	-2.3	83	4.10×10 <sup>1</sup>	11	1.19	27.3%	Analytical	2.98×10 <sup>1</sup>	5.63×10 <sup>-1</sup>
	2.15×10 <sup>0</sup>	1.05×10 <sup>-1</sup>	No	0.0%	1.1	55385.5	-1.0	55	1.88×10 <sup>1</sup>	11	1.12	40.3%	Analytical	1.12×10 <sup>1</sup>	2.63×10 <sup>-1</sup>
	1.08×10 <sup>0</sup>	3.15×10 <sup>-2</sup>	No	0.0%	0.4	55390.8	-0.5	35	8.57×10 <sup>0</sup>	15	1.06	58.5%	Analytical	3.55×10 <sup>0</sup>	8.88×10 <sup>-2</sup>
	5.43×10 <sup>-1</sup>	1.47×10 <sup>-2</sup>	No	0.0%	0.2	55393.4	-0.4	21	4.17×10 <sup>0</sup>	12	1.04	73.4%	Analytical	1.11×10 <sup>0</sup>	4.70×10 <sup>-2</sup>
1205	7.71×10 <sup>0</sup>	5.41×10 <sup>-1</sup>	No	0.0%	5.0	55345.9	-5.7	121	8.43×10 <sup>1</sup>	10	1.29	16.8%	Analytical	7.01×10 <sup>1</sup>	5.09×10 <sup>0</sup>
	5.14×10 <sup>0</sup>	3.33×10 <sup>-1</sup>	No	0.0%	3.1	55362.1	-3.2	92	4.89×10 <sup>1</sup>	11	1.23	23.8%	Analytical	3.73×10 <sup>1</sup>	6.43×10 <sup>-1</sup>
	3.86×10 <sup>0</sup>	2.29×10 <sup>-1</sup>	No	0.0%	2.2	55370.2	-2.4	78	3.48×10 <sup>1</sup>	11	1.19	29.0%	Analytical	2.47×10 <sup>1</sup>	4.84×10 <sup>-1</sup>
	2.58×10 <sup>0</sup>	1.46×10 <sup>-1</sup>	No	0.0%	1.4	55378.2	-1.8	60	2.17×10 <sup>1</sup>	10	1.16	37.0%	Analytical	1.37×10 <sup>1</sup>	2.13×10 <sup>-1</sup>
	1.29×10 <sup>0</sup>	5.20×10 <sup>-2</sup>	No	0.0%	0.6	55386.3	-0.7	38	9.94×10 <sup>0</sup>	12	1.09	54.1%	Analytical	4.56×10 <sup>0</sup>	1.10×10 <sup>-1</sup>
	5.11×10 <sup>-1</sup>	1.46×10 <sup>-2</sup>	No	0.0%	0.1	55391.2	-0.4	19	3.66×10 <sup>0</sup>	12	1.05	78.0%	Analytical	8.04×10 <sup>-1</sup>	5.92×10 <sup>-2</sup>
1210	6.96×10 <sup>1</sup>	6.34×10 <sup>0</sup>	HCO <sub>2</sub> H	10.1%	49.6	54931.8	29.3	213	6.15×10 <sup>2</sup>	10	2.12	0.3%	Analytical	6.13×10 <sup>2</sup>	2.03×10 <sup>1</sup>
	5.96×10 <sup>1</sup>	5.32×10 <sup>0</sup>	HCO <sub>2</sub> H	10.1%	42.8	54999.0	24.8	187	4.93×10 <sup>2</sup>	10	2.08	0.4%	Analytical	4.91×10 <sup>2</sup>	2.49×10 <sup>1</sup>
	4.01×10 <sup>1</sup>	3.58×10 <sup>0</sup>	HCO <sub>2</sub> H	10.1%	28.7	55131.1	17.5	134	2.76×10 <sup>2</sup>	10	2.05	0.7%	Analytical	2.75×10 <sup>2</sup>	1.40×10 <sup>1</sup>
	2.00×10 <sup>1</sup>	1.79×10 <sup>0</sup>	HCO <sub>2</sub> H	10.1%	14.2	55265.7	8.6	76	9.73×10 <sup>1</sup>	10	1.97	1.7%	Analytical	9.57×10 <sup>1</sup>	2.80×10 <sup>0</sup>
	1.51×10 <sup>1</sup>	1.28×10 <sup>0</sup>	HCO <sub>2</sub> H	10.1%	10.8	55298.5	5.8	60	6.53×10 <sup>1</sup>	10	1.86	2.6%	Analytical	6.36×10 <sup>1</sup>	2.42×10 <sup>0</sup>
	1.01×10 <sup>1</sup>	7.71×10 <sup>-1</sup>	HCO <sub>2</sub> H	10.1%	7.3	55331.9	2.6	44	3.88×10 <sup>1</sup>	11	1.69	4.3%	Analytical	3.71×10 <sup>1</sup>	1.07×10 <sup>0</sup>

## 7. Kinetic results of each studied amine for each concentration

N°	C <sub>Am</sub>	C <sub>CO2</sub>	Acid	Neutra	[Am] <sup>f</sup>	[H <sub>2</sub> O] <sup>f</sup>	A	C	k <sub>0</sub>	R	Evolution HO <sup>-</sup>	Contribution HO <sup>-</sup>	Model used	k <sub>0</sub> <sup>Am</sup>	σ (k <sub>0</sub> <sup>Am</sup> )
1211	7.56×10 <sup>1</sup>	6.33×10 <sup>0</sup>	HCO <sub>2</sub> H	14.9%	51.4	54803.9	32.1	290	2.44×10 <sup>2</sup>	10	1.80	0.8%	Analytical	2.42×10 <sup>2</sup>	2.18×10 <sup>1</sup>
	6.04×10 <sup>1</sup>	5.04×10 <sup>0</sup>	HCO <sub>2</sub> H	14.9%	41.1	54921.9	27.0	230	1.76×10 <sup>2</sup>	10	1.79	1.1%	Analytical	1.74×10 <sup>2</sup>	1.53×10 <sup>1</sup>
	4.49×10 <sup>1</sup>	3.79×10 <sup>0</sup>	HCO <sub>2</sub> H	14.9%	30.4	55042.5	20.4	179	1.17×10 <sup>2</sup>	10	1.80	1.5%	Analytical	1.15×10 <sup>2</sup>	1.44×10 <sup>0</sup>
	3.02×10 <sup>1</sup>	2.53×10 <sup>0</sup>	HCO <sub>2</sub> H	14.9%	20.5	55156.4	13.9	129	6.76×10 <sup>1</sup>	10	1.77	2.5%	Analytical	6.59×10 <sup>1</sup>	1.61×10 <sup>0</sup>
	1.51×10 <sup>1</sup>	1.29×10 <sup>0</sup>	HCO <sub>2</sub> H	14.9%	10.1	55274.0	6.5	74	2.58×10 <sup>1</sup>	10	1.73	6.1%	Analytical	2.42×10 <sup>1</sup>	4.53×10 <sup>-1</sup>
	7.64×10 <sup>0</sup>	5.39×10 <sup>-1</sup>	HCO <sub>2</sub> H	14.9%	5.2	55332.6	2.2	43	1.06×10 <sup>1</sup>	12	1.52	14.9%	Analytical	9.01×10 <sup>0</sup>	1.95×10 <sup>-1</sup>
1212	1.51×10 <sup>2</sup>	1.42×10 <sup>1</sup>	HCO <sub>2</sub> H	5.0%	114.9	54238.2	77.4	252	6.67×10 <sup>1</sup>	10	3.08	0.6%	Analytical	6.62×10 <sup>1</sup>	1.11×10 <sup>0</sup>
	1.20×10 <sup>2</sup>	1.12×10 <sup>1</sup>	HCO <sub>2</sub> H	5.0%	91.7	54473.6	67.7	206	4.83×10 <sup>1</sup>	10	3.09	0.9%	Analytical	4.78×10 <sup>1</sup>	6.34×10 <sup>-1</sup>
	9.03×10 <sup>1</sup>	8.56×10 <sup>0</sup>	HCO <sub>2</sub> H	5.0%	68.6	54704.4	57.2	164	3.17×10 <sup>1</sup>	10	3.13	1.3%	Analytical	3.13×10 <sup>1</sup>	3.79×10 <sup>-1</sup>
	8.03×10 <sup>1</sup>	7.58×10 <sup>0</sup>	HCO <sub>2</sub> H	5.0%	61.1	54781.7	50.0	145	2.74×10 <sup>1</sup>	10	3.13	1.5%	Analytical	2.70×10 <sup>1</sup>	3.50×10 <sup>-1</sup>
	6.02×10 <sup>1</sup>	5.58×10 <sup>0</sup>	HCO <sub>2</sub> H	5.0%	46.0	54936.8	40.8	115	1.83×10 <sup>1</sup>	10	3.08	2.2%	Analytical	1.79×10 <sup>1</sup>	2.38×10 <sup>-1</sup>
	3.01×10 <sup>1</sup>	2.81×10 <sup>0</sup>	HCO <sub>2</sub> H	5.0%	23.0	55168.1	21.6	63	7.73×10 <sup>0</sup>	10	3.04	4.9%	Analytical	7.36×10 <sup>0</sup>	1.27×10 <sup>-1</sup>
	1.51×10 <sup>1</sup>	1.28×10 <sup>0</sup>	HCO <sub>2</sub> H	5.0%	11.7	55284.2	11.6	35	3.62×10 <sup>0</sup>	11	2.70	10.7%	Analytical	3.24×10 <sup>0</sup>	6.64×10 <sup>-2</sup>
1220	1.00×10 <sup>2</sup>	7.58×10 <sup>0</sup>	HCO <sub>2</sub> H	15.2%	69.7	54947.5	84.5	416	7.67×10 <sup>2</sup>	11	1.69	0.3%	Analytical	7.65×10 <sup>2</sup>	6.47×10 <sup>1</sup>
	8.04×10 <sup>1</sup>	6.09×10 <sup>0</sup>	HCO <sub>2</sub> H	15.2%	55.7	55036.2	50.7	334	5.59×10 <sup>2</sup>	11	1.69	0.4%	Analytical	5.56×10 <sup>2</sup>	2.82×10 <sup>1</sup>
	6.03×10 <sup>1</sup>	4.56×10 <sup>0</sup>	HCO <sub>2</sub> H	15.2%	41.8	55125.0	30.1	263	3.65×10 <sup>2</sup>	11	1.69	0.6%	Analytical	3.63×10 <sup>2</sup>	2.81×10 <sup>1</sup>
	4.02×10 <sup>1</sup>	3.03×10 <sup>0</sup>	HCO <sub>2</sub> H	15.2%	27.8	55213.9	19.7	186	1.89×10 <sup>2</sup>	11	1.68	1.1%	Analytical	1.87×10 <sup>2</sup>	9.11×10 <sup>0</sup>
	2.01×10 <sup>1</sup>	1.54×10 <sup>0</sup>	HCO <sub>2</sub> H	15.2%	13.8	55303.3	10.1	105	6.87×10 <sup>1</sup>	11	1.65	2.8%	Analytical	6.68×10 <sup>1</sup>	1.43×10 <sup>0</sup>

Nº	C <sub>Am</sub>	C <sub>CO2</sub>	Acid	Neutra	[Am] <sup>f</sup>	[H <sub>2</sub> O] <sup>f</sup>	A	C	k <sub>0</sub>	R	Evolution HO <sup>-</sup>	Contribution HO <sup>-</sup>	Model used	k <sub>0</sub> <sup>Am</sup>	σ (k <sub>0</sub> <sup>Am</sup> )
	1.01×10 <sup>1</sup>	7.89×10 <sup>-1</sup>	HCO <sub>2</sub> H	15.2%	6.8	55347.6	4.7	62	2.87×10 <sup>1</sup>	11	1.60	6.1%	Analytical	2.70×10 <sup>1</sup>	5.36×10 <sup>-1</sup>
1221	9.01×10 <sup>1</sup>	7.59×10 <sup>0</sup>	HCO <sub>2</sub> H	15.4%	60.7	54915.6	42.1	367	2.59×10 <sup>2</sup>	10	1.78	0.9%	Analytical	2.57×10 <sup>2</sup>	1.19×10 <sup>1</sup>
	7.51×10 <sup>1</sup>	6.35×10 <sup>0</sup>	HCO <sub>2</sub> H	15.4%	50.6	54994.8	36.5	307	1.85×10 <sup>2</sup>	10	1.79	1.2%	Analytical	1.83×10 <sup>2</sup>	7.03×10 <sup>0</sup>
	6.01×10 <sup>1</sup>	5.06×10 <sup>0</sup>	HCO <sub>2</sub> H	15.4%	40.4	55074.3	29.1	255	1.34×10 <sup>2</sup>	10	1.78	1.6%	Analytical	1.32×10 <sup>2</sup>	1.54×10 <sup>0</sup>
	4.50×10 <sup>1</sup>	3.80×10 <sup>0</sup>	HCO <sub>2</sub> H	15.4%	30.3	55153.7	23.7	201	9.11×10 <sup>1</sup>	10	1.77	2.3%	Analytical	8.90×10 <sup>1</sup>	2.47×10 <sup>0</sup>
	2.98×10 <sup>1</sup>	2.54×10 <sup>0</sup>	HCO <sub>2</sub> H	15.4%	19.9	55234.3	16.0	143	5.20×10 <sup>1</sup>	10	1.76	3.8%	Analytical	5.00×10 <sup>1</sup>	1.44×10 <sup>0</sup>
	1.50×10 <sup>1</sup>	1.29×10 <sup>0</sup>	HCO <sub>2</sub> H	15.4%	9.9	55312.3	8.0	84	2.23×10 <sup>1</sup>	10	1.72	8.1%	Analytical	2.05×10 <sup>1</sup>	3.24×10 <sup>-1</sup>
	7.54×10 <sup>0</sup>	5.41×10 <sup>-1</sup>	HCO <sub>2</sub> H	15.4%	5.1	55351.8	3.0	50	1.02×10 <sup>1</sup>	11	1.50	17.6%	Analytical	8.37×10 <sup>0</sup>	1.30×10 <sup>-1</sup>
1222	9.02×10 <sup>1</sup>	7.48×10 <sup>0</sup>	HCO <sub>2</sub> H	15.6%	60.9	54836.6	41.2	354	1.60×10 <sup>2</sup>	10	1.76	1.4%	Analytical	1.58×10 <sup>2</sup>	5.10×10 <sup>0</sup>
	7.53×10 <sup>1</sup>	6.26×10 <sup>0</sup>	HCO <sub>2</sub> H	15.6%	50.8	54928.6	34.5	300	1.26×10 <sup>2</sup>	10	1.77	1.8%	Analytical	1.23×10 <sup>2</sup>	4.30×10 <sup>0</sup>
	6.03×10 <sup>1</sup>	4.99×10 <sup>0</sup>	HCO <sub>2</sub> H	15.6%	40.7	55020.8	31.5	252	8.77×10 <sup>1</sup>	10	1.76	2.5%	Analytical	8.55×10 <sup>1</sup>	3.15×10 <sup>0</sup>
	4.52×10 <sup>1</sup>	3.74×10 <sup>0</sup>	HCO <sub>2</sub> H	15.6%	30.5	55113.9	25.0	197	6.06×10 <sup>1</sup>	10	1.75	3.5%	Analytical	5.85×10 <sup>1</sup>	1.22×10 <sup>0</sup>
	3.01×10 <sup>1</sup>	2.50×10 <sup>0</sup>	HCO <sub>2</sub> H	15.6%	20.2	55207.0	17.3	140	3.66×10 <sup>1</sup>	10	1.74	5.4%	Analytical	3.46×10 <sup>1</sup>	1.41×10 <sup>0</sup>
	1.51×10 <sup>1</sup>	1.27×10 <sup>0</sup>	HCO <sub>2</sub> H	15.6%	10.0	55299.5	10.4	79	1.55×10 <sup>1</sup>	10	1.70	11.7%	Analytical	1.37×10 <sup>1</sup>	4.86×10 <sup>-1</sup>
	7.53×10 <sup>0</sup>	5.33×10 <sup>-1</sup>	HCO <sub>2</sub> H	15.6%	5.1	55345.9	3.2	47	7.45×10 <sup>0</sup>	12	1.49	24.0%	Analytical	5.66×10 <sup>0</sup>	1.17×10 <sup>-1</sup>
1223	1.50×10 <sup>2</sup>	1.02×10 <sup>1</sup>	HCO <sub>2</sub> H	15.1%	106.6	54333.7	55.6	488	5.30×10 <sup>2</sup>	13	1.60	0.7%	Analytical	5.26×10 <sup>2</sup>	3.04×10 <sup>1</sup>
	1.20×10 <sup>2</sup>	1.02×10 <sup>1</sup>	HCO <sub>2</sub> H	15.1%	81.3	54543.9	46.7	410	3.32×10 <sup>2</sup>	10	1.78	1.0%	Analytical	3.29×10 <sup>2</sup>	2.14×10 <sup>1</sup>
	9.03×10 <sup>1</sup>	7.63×10 <sup>0</sup>	HCO <sub>2</sub> H	15.1%	61.0	54755.5	38.0	327	2.10×10 <sup>2</sup>	10	1.78	1.5%	Analytical	2.07×10 <sup>2</sup>	1.21×10 <sup>1</sup>

## 7. Kinetic results of each studied amine for each concentration

N°	C <sub>Am</sub>	C <sub>CO2</sub>	Acid	Neutra	[Am] <sup>f</sup>	[H <sub>2</sub> O] <sup>f</sup>	A	C	k <sub>0</sub>	R	Evolution HO <sup>-</sup>	Contribution HO <sup>-</sup>	Model used	k <sub>0</sub> <sup>Am</sup>	σ (k <sub>0</sub> <sup>Am</sup> )
	5.88×10 <sup>1</sup>	5.09×10 <sup>0</sup>	HCO <sub>2</sub> H	15.1%	39.3	54977.7	26.5	231	1.06×10 <sup>2</sup>	10	1.79	2.7%	Analytical	1.03×10 <sup>2</sup>	1.83×10 <sup>0</sup>
	3.01×10 <sup>1</sup>	2.55×10 <sup>0</sup>	HCO <sub>2</sub> H	15.1%	20.2	55179.5	14.3	134	4.28×10 <sup>1</sup>	10	1.74	6.2%	Analytical	4.02×10 <sup>1</sup>	1.26×10 <sup>0</sup>
	1.51×10 <sup>1</sup>	1.30×10 <sup>0</sup>	HCO <sub>2</sub> H	15.1%	9.9	55285.8	7.5	79	1.76×10 <sup>1</sup>	10	1.68	13.7%	Analytical	1.52×10 <sup>1</sup>	3.25×10 <sup>-1</sup>
1224	1.50×10 <sup>2</sup>	1.23×10 <sup>1</sup>	HCO <sub>2</sub> H	15.0%	102.2	54486.9	69.3	516	7.14×10 <sup>1</sup>	10	1.76	5.0%	Analytical	6.79×10 <sup>1</sup>	1.76×10 <sup>0</sup>
	1.21×10 <sup>2</sup>	9.90×10 <sup>0</sup>	HCO <sub>2</sub> H	14.8%	82.5	54666.6	60.5	431	5.37×10 <sup>1</sup>	10	1.76	6.5%	Analytical	5.02×10 <sup>1</sup>	8.74×10 <sup>-1</sup>
	8.02×10 <sup>1</sup>	6.73×10 <sup>0</sup>	HCO <sub>2</sub> H	15.0%	54.3	54912.3	49.0	312	3.19×10 <sup>1</sup>	10	1.77	10.0%	Analytical	2.87×10 <sup>1</sup>	6.51×10 <sup>-1</sup>
	4.01×10 <sup>1</sup>	3.28×10 <sup>0</sup>	HCO <sub>2</sub> H	14.9%	27.2	55155.9	30.1	184	1.42×10 <sup>1</sup>	10	1.72	20.9%	Analytical	1.13×10 <sup>1</sup>	2.96×10 <sup>-1</sup>
	2.01×10 <sup>1</sup>	1.52×10 <sup>0</sup>	HCO <sub>2</sub> H	14.7%	13.8	55277.1	15.0	104	7.83×10 <sup>0</sup>	11	1.61	36.5%	Analytical	4.98×10 <sup>0</sup>	1.29×10 <sup>-1</sup>
	1.01×10 <sup>1</sup>	7.60×10 <sup>-1</sup>	HCO <sub>2</sub> H	15.4%	6.7	55337.4	8.3	64	4.57×10 <sup>0</sup>	11	1.53	54.3%	Analytical	2.09×10 <sup>0</sup>	5.56×10 <sup>-2</sup>
1225	1.81×10 <sup>2</sup>	7.53×10 <sup>0</sup>	HCO <sub>2</sub> H	15.3%	137.5	53962.0	37.6	523	1.10×10 <sup>2</sup>	20	1.35	3.4%	Analytical	1.06×10 <sup>2</sup>	4.35×10 <sup>0</sup>
	1.51×10 <sup>2</sup>	6.30×10 <sup>0</sup>	HCO <sub>2</sub> H	15.3%	114.5	54200.1	33.6	455	8.95×10 <sup>1</sup>	20	1.35	4.0%	Analytical	8.59×10 <sup>1</sup>	1.95×10 <sup>0</sup>
	1.21×10 <sup>2</sup>	5.02×10 <sup>0</sup>	HCO <sub>2</sub> H	15.3%	91.6	54437.6	28.9	382	6.75×10 <sup>1</sup>	20	1.35	5.2%	Analytical	6.40×10 <sup>1</sup>	2.64×10 <sup>0</sup>
	9.03×10 <sup>1</sup>	3.77×10 <sup>0</sup>	HCO <sub>2</sub> H	15.3%	68.6	54676.3	23.8	302	4.66×10 <sup>1</sup>	20	1.35	7.3%	Analytical	4.32×10 <sup>1</sup>	1.15×10 <sup>0</sup>
	5.84×10 <sup>1</sup>	2.52×10 <sup>0</sup>	HCO <sub>2</sub> H	15.3%	44.1	54928.9	18.8	216	2.74×10 <sup>1</sup>	20	1.36	11.6%	Analytical	2.42×10 <sup>1</sup>	5.44×10 <sup>-1</sup>
	3.01×10 <sup>1</sup>	1.28×10 <sup>0</sup>	HCO <sub>2</sub> H	15.3%	22.6	55153.1	11.8	130	1.35×10 <sup>1</sup>	20	1.33	21.6%	Analytical	1.06×10 <sup>1</sup>	1.45×10 <sup>-1</sup>
	1.51×10 <sup>1</sup>	5.37×10 <sup>-1</sup>	HCO <sub>2</sub> H	15.3%	11.4	55272.1	6.3	78	7.33×10 <sup>0</sup>	24	1.25	37.9%	Analytical	4.55×10 <sup>0</sup>	1.03×10 <sup>-1</sup>
1226	4.43×10 <sup>2</sup>	4.45×10 <sup>0</sup>	HCO <sub>2</sub> H	39.9%	289.2	52160.2	24.6	2536	1.11×10 <sup>1</sup>	60	1.05	34.7%	Analytical	7.28×10 <sup>0</sup>	2.67×10 <sup>-1</sup>
	3.53×10 <sup>2</sup>	3.56×10 <sup>0</sup>	HCO <sub>2</sub> H	39.9%	231.0	52807.7	23.3	2152	9.07×10 <sup>0</sup>	60	1.05	40.9%	Analytical	5.35×10 <sup>0</sup>	1.48×10 <sup>-1</sup>

N°	C <sub>Am</sub>	C <sub>CO2</sub>	Acid	Neutra	[Am] <sup>f</sup>	[H <sub>2</sub> O] <sup>f</sup>	A	C	k <sub>0</sub>	R	Evolution HO <sup>-</sup>	Contribution HO <sup>-</sup>	Model used	k <sub>0</sub> <sup>Am</sup>	σ (k <sub>0</sub> <sup>Am</sup> )
	2.66×10 <sup>2</sup>	2.67×10 <sup>0</sup>	HCO <sub>2</sub> H	39.9%	174.0	53443.2	21.1	1740	7.16×10 <sup>0</sup>	60	1.05	49.3%	Analytical	3.63×10 <sup>0</sup>	1.83×10 <sup>-1</sup>
	1.76×10 <sup>2</sup>	1.79×10 <sup>0</sup>	HCO <sub>2</sub> H	39.9%	115.5	54094.9	17.0	1249	5.30×10 <sup>0</sup>	60	1.06	61.9%	Analytical	2.02×10 <sup>0</sup>	7.65×10 <sup>-2</sup>
	8.84×10 <sup>1</sup>	9.16×10 <sup>-1</sup>	HCO <sub>2</sub> H	39.9%	57.8	54740.2	11.7	696	3.53×10 <sup>0</sup>	59	1.06	82.6%	Analytical	6.14×10 <sup>-1</sup>	5.62×10 <sup>-2</sup>
	4.43×10 <sup>1</sup>	4.76×10 <sup>-1</sup>	HCO <sub>2</sub> H	39.9%	28.8	55065.4	6.9	373	2.63×10 <sup>0</sup>	57	1.06	100.1%	Analytical	-1.60×10 <sup>-3</sup>	5.77×10 <sup>-2</sup>
1227	2.22×10 <sup>2</sup>	5.05×10 <sup>0</sup>	HCO <sub>2</sub> H	10.6%	188.3	54217.0	37.6	466	5.44×10 <sup>1</sup>	40	1.24	1.1%	Analytical	5.38×10 <sup>1</sup>	1.66×10 <sup>0</sup>
	1.78×10 <sup>2</sup>	4.03×10 <sup>0</sup>	HCO <sub>2</sub> H	10.6%	150.5	54452.6	31.7	380	3.80×10 <sup>1</sup>	40	1.24	1.5%	Analytical	3.75×10 <sup>1</sup>	1.19×10 <sup>0</sup>
	1.33×10 <sup>2</sup>	3.03×10 <sup>0</sup>	HCO <sub>2</sub> H	10.6%	112.8	54687.5	26.0	297	2.44×10 <sup>1</sup>	40	1.25	2.2%	Analytical	2.39×10 <sup>1</sup>	2.03×10 <sup>-1</sup>
	8.87×10 <sup>1</sup>	2.03×10 <sup>0</sup>	HCO <sub>2</sub> H	10.6%	75.2	54922.4	18.7	206	1.38×10 <sup>1</sup>	39	1.25	3.8%	Analytical	1.32×10 <sup>1</sup>	2.68×10 <sup>-1</sup>
	4.44×10 <sup>1</sup>	1.04×10 <sup>0</sup>	HCO <sub>2</sub> H	10.6%	37.6	55156.7	10.3	111	5.70×10 <sup>0</sup>	39	1.26	8.6%	Analytical	5.21×10 <sup>0</sup>	5.84×10 <sup>-2</sup>
	2.22×10 <sup>1</sup>	5.39×10 <sup>-1</sup>	HCO <sub>2</sub> H	10.6%	18.7	55274.7	6.0	60	2.70×10 <sup>0</sup>	37	1.27	17.1%	Analytical	2.23×10 <sup>0</sup>	1.66×10 <sup>-2</sup>
1228	4.26×10 <sup>2</sup>	4.79×10 <sup>0</sup>	HCO <sub>2</sub> H	30.1%	243.1	52660.4	25.3	1668	4.90×10 <sup>1</sup>	85	1.05	0.5%	Analytical	4.87×10 <sup>1</sup>	3.44×10 <sup>0</sup>
	3.49×10 <sup>2</sup>	4.02×10 <sup>0</sup>	HCO <sub>2</sub> H	30.1%	202.1	53120.0	21.7	1444	3.30×10 <sup>1</sup>	88	1.05	0.8%	Analytical	3.28×10 <sup>1</sup>	2.92×10 <sup>0</sup>
	2.83×10 <sup>2</sup>	3.27×10 <sup>0</sup>	HCO <sub>2</sub> H	30.1%	161.8	53567.3	19.1	1233	2.25×10 <sup>1</sup>	80	1.05	1.1%	Analytical	2.22×10 <sup>1</sup>	6.07×10 <sup>-1</sup>
	2.11×10 <sup>2</sup>	2.28×10 <sup>0</sup>	HCO <sub>2</sub> H	30.1%	121.6	54020.8	13.3	938	1.42×10 <sup>1</sup>	83	1.05	1.7%	Analytical	1.39×10 <sup>1</sup>	6.18×10 <sup>-1</sup>
	1.41×10 <sup>2</sup>	1.53×10 <sup>0</sup>	HCO <sub>2</sub> H	30.1%	81.2	54477.0	10.0	678	7.56×10 <sup>0</sup>	91	1.04	3.0%	Analytical	7.33×10 <sup>0</sup>	4.74×10 <sup>-2</sup>
	7.04×10 <sup>1</sup>	7.86×10 <sup>-1</sup>	HCO <sub>2</sub> H	30.1%	40.3	54933.4	6.3	373	2.73×10 <sup>0</sup>	67	1.06	7.6%	Analytical	2.52×10 <sup>0</sup>	2.33×10 <sup>-2</sup>
	3.52×10 <sup>1</sup>	5.38×10 <sup>-1</sup>	HCO <sub>2</sub> H	30.1%	19.6	55161.5	5.1	201	1.20×10 <sup>0</sup>	33	1.13	15.5%	Analytical	1.01×10 <sup>0</sup>	1.08×10 <sup>-2</sup>
1230	2.21×10 <sup>2</sup>	5.06×10 <sup>0</sup>	HCO <sub>2</sub> H	10.2%	188.2	53722.4	35.1	429	3.48×10 <sup>1</sup>	40	1.25	1.0%	Analytical	3.44×10 <sup>1</sup>	8.10×10 <sup>-1</sup>

## 7. Kinetic results of each studied amine for each concentration

Nº	C <sub>Am</sub>	C <sub>CO2</sub>	Acid	Neutra	[Am] <sup>f</sup>	[H <sub>2</sub> O] <sup>f</sup>	A	C	k <sub>0</sub>	R	Evolution HO <sup>-</sup>	Contribution HO <sup>-</sup>	Model used	k <sub>0</sub> <sup>Am</sup>	σ (k <sub>0</sub> <sup>Am</sup> )
	1.77×10 <sup>2</sup>	4.05×10 <sup>0</sup>	HCO <sub>2</sub> H	10.2%	150.8	54053.7	29.5	354	2.52×10 <sup>1</sup>	40	1.25	1.3%	Analytical	2.48×10 <sup>1</sup>	5.63×10 <sup>-1</sup>
	1.33×10 <sup>2</sup>	3.04×10 <sup>0</sup>	HCO <sub>2</sub> H	10.2%	113.3	54386.2	25.0	278	1.67×10 <sup>1</sup>	40	1.25	1.9%	Analytical	1.64×10 <sup>1</sup>	3.56×10 <sup>-1</sup>
	8.87×10 <sup>1</sup>	2.04×10 <sup>0</sup>	HCO <sub>2</sub> H	10.2%	75.5	54720.9	18.6	195	9.64×10 <sup>0</sup>	40	1.26	3.2%	Analytical	9.33×10 <sup>0</sup>	1.69×10 <sup>-1</sup>
	4.42×10 <sup>1</sup>	1.04×10 <sup>0</sup>	HCO <sub>2</sub> H	10.2%	37.6	55057.1	10.4	104	4.15×10 <sup>0</sup>	39	1.27	7.0%	Analytical	3.86×10 <sup>0</sup>	3.52×10 <sup>-2</sup>
	1.66×10 <sup>1</sup>	5.41×10 <sup>-1</sup>	HCO <sub>2</sub> H	10.2%	13.8	55266.3	6.6	56	2.02×10 <sup>0</sup>	28	1.38	12.6%	Analytical	1.76×10 <sup>0</sup>	2.08×10 <sup>-2</sup>
1231	1.01×10 <sup>2</sup>	8.08×10 <sup>0</sup>	HCO <sub>2</sub> H	15.1%	69.3	54713.4	55.6	354	1.15×10 <sup>2</sup>	11	1.78	0.3%	Analytical	1.14×10 <sup>2</sup>	2.41×10 <sup>0</sup>
	8.06×10 <sup>1</sup>	6.61×10 <sup>0</sup>	HCO <sub>2</sub> H	15.1%	55.2	54849.1	49.3	291	8.62×10 <sup>1</sup>	10	1.80	0.4%	Analytical	8.59×10 <sup>1</sup>	2.11×10 <sup>0</sup>
	6.03×10 <sup>1</sup>	4.82×10 <sup>0</sup>	HCO <sub>2</sub> H	15.1%	41.6	54985.8	36.7	221	5.78×10 <sup>1</sup>	11	1.79	0.5%	Analytical	5.75×10 <sup>1</sup>	2.35×10 <sup>0</sup>
	4.03×10 <sup>1</sup>	3.04×10 <sup>0</sup>	HCO <sub>2</sub> H	15.1%	28.1	55121.0	24.9	152	3.60×10 <sup>1</sup>	11	1.74	0.8%	Analytical	3.57×10 <sup>1</sup>	6.55×10 <sup>-1</sup>
	2.01×10 <sup>1</sup>	1.54×10 <sup>0</sup>	HCO <sub>2</sub> H	15.1%	14.0	55257.5	14.5	81	1.61×10 <sup>1</sup>	11	1.76	1.8%	Analytical	1.59×10 <sup>1</sup>	3.23×10 <sup>-1</sup>
	1.01×10 <sup>1</sup>	7.91×10 <sup>-1</sup>	HCO <sub>2</sub> H	15.1%	7.0	55325.6	8.3	44	7.59×10 <sup>0</sup>	11	1.77	3.6%	Analytical	7.32×10 <sup>0</sup>	1.30×10 <sup>-1</sup>
1240	1.21×10 <sup>2</sup>	3.49×10 <sup>0</sup>	HCO <sub>2</sub> H	15.6%	95.2	54801.6	32.7	429	1.00×10 <sup>2</sup>	30	1.24	0.1%	Analytical	1.00×10 <sup>2</sup>	2.27×10 <sup>0</sup>
	1.01×10 <sup>2</sup>	2.50×10 <sup>0</sup>	HCO <sub>2</sub> H	15.6%	80.2	54899.7	27.1	360	7.92×10 <sup>1</sup>	35	1.21	0.1%	Analytical	7.91×10 <sup>1</sup>	2.55×10 <sup>0</sup>
	7.84×10 <sup>1</sup>	1.76×10 <sup>0</sup>	HCO <sub>2</sub> H	15.6%	62.6	55010.0	20.2	282	5.88×10 <sup>1</sup>	38	1.19	0.1%	Analytical	5.87×10 <sup>1</sup>	2.16×10 <sup>0</sup>
	6.06×10 <sup>1</sup>	1.27×10 <sup>0</sup>	HCO <sub>2</sub> H	15.6%	48.6	55096.6	14.6	221	4.27×10 <sup>1</sup>	41	1.18	0.2%	Analytical	4.26×10 <sup>1</sup>	6.90×10 <sup>-1</sup>
	4.05×10 <sup>1</sup>	7.77×10 <sup>-1</sup>	HCO <sub>2</sub> H	15.6%	32.6	55194.6	9.4	151	2.70×10 <sup>1</sup>	45	1.16	0.3%	Analytical	2.70×10 <sup>1</sup>	5.28×10 <sup>-1</sup>
	2.03×10 <sup>1</sup>	5.32×10 <sup>-1</sup>	HCO <sub>2</sub> H	15.6%	16.0	55292.8	11.2	79	1.28×10 <sup>1</sup>	33	1.23	0.5%	Analytical	1.28×10 <sup>1</sup>	3.73×10 <sup>-1</sup>
	1.01×10 <sup>1</sup>	5.32×10 <sup>-1</sup>	HCO <sub>2</sub> H	15.6%	7.5	55342.0	8.3	47	5.90×10 <sup>0</sup>	16	1.49	1.0%	Analytical	5.84×10 <sup>0</sup>	5.16×10 <sup>-2</sup>

Nº	C <sub>Am</sub>	C <sub>CO2</sub>	Acid	Neutra	[Am] <sup>f</sup>	[H <sub>2</sub> O] <sup>f</sup>	A	C	k <sub>0</sub>	R	Evolution HO <sup>-</sup>	Contribution HO <sup>-</sup>	Model used	k <sub>0</sub> <sup>Am</sup>	σ (k <sub>0</sub> <sup>Am</sup> )
1241	1.85×10 <sup>2</sup>	3.78×10 <sup>0</sup>	HCO <sub>2</sub> H	15.0%	149.5	54322.4	30.7	534	4.61×10 <sup>1</sup>	42	1.17	0.2%	Analytical	4.60×10 <sup>1</sup>	1.56×10 <sup>0</sup>
	1.48×10 <sup>2</sup>	3.02×10 <sup>0</sup>	HCO <sub>2</sub> H	15.0%	119.6	54535.6	25.4	439	3.24×10 <sup>1</sup>	42	1.17	0.3%	Analytical	3.23×10 <sup>1</sup>	8.05×10 <sup>-1</sup>
	1.05×10 <sup>2</sup>	2.28×10 <sup>0</sup>	HCO <sub>2</sub> H	15.0%	84.8	54783.2	20.9	325	1.96×10 <sup>1</sup>	40	1.18	0.5%	Analytical	1.95×10 <sup>1</sup>	2.51×10 <sup>-1</sup>
	7.42×10 <sup>1</sup>	1.53×10 <sup>0</sup>	HCO <sub>2</sub> H	15.0%	60.0	54962.4	14.6	236	1.20×10 <sup>1</sup>	42	1.18	0.8%	Analytical	1.19×10 <sup>1</sup>	1.57×10 <sup>-1</sup>
	3.70×10 <sup>1</sup>	7.86×10 <sup>-1</sup>	HCO <sub>2</sub> H	15.0%	29.8	55178.0	8.6	124	4.85×10 <sup>0</sup>	41	1.18	1.8%	Analytical	4.76×10 <sup>0</sup>	7.22×10 <sup>-2</sup>
	1.86×10 <sup>1</sup>	5.38×10 <sup>-1</sup>	HCO <sub>2</sub> H	15.0%	14.7	55284.5	6.7	67	2.25×10 <sup>0</sup>	30	1.26	3.7%	Analytical	2.16×10 <sup>0</sup>	2.20×10 <sup>-2</sup>
1242	2.41×10 <sup>2</sup>	5.12×10 <sup>0</sup>	HCO <sub>2</sub> H	15.1%	194.2	53574.3	31.9	617	5.70×10 <sup>1</sup>	40	1.17	0.2%	Analytical	5.69×10 <sup>1</sup>	1.98×10 <sup>0</sup>
	2.01×10 <sup>2</sup>	4.36×10 <sup>0</sup>	HCO <sub>2</sub> H	15.1%	161.8	53875.3	29.8	534	4.19×10 <sup>1</sup>	40	1.18	0.2%	Analytical	4.18×10 <sup>1</sup>	4.99×10 <sup>-1</sup>
	1.61×10 <sup>2</sup>	3.33×10 <sup>0</sup>	HCO <sub>2</sub> H	15.1%	129.9	54177.3	25.3	442	2.98×10 <sup>1</sup>	42	1.17	0.3%	Analytical	2.97×10 <sup>1</sup>	6.03×10 <sup>-1</sup>
	1.21×10 <sup>2</sup>	2.57×10 <sup>0</sup>	HCO <sub>2</sub> H	15.1%	97.4	54479.8	19.5	344	1.93×10 <sup>1</sup>	40	1.18	0.5%	Analytical	1.92×10 <sup>1</sup>	2.71×10 <sup>-1</sup>
	8.05×10 <sup>1</sup>	1.56×10 <sup>0</sup>	HCO <sub>2</sub> H	15.1%	65.2	54783.6	12.6	239	1.11×10 <sup>1</sup>	44	1.16	0.8%	Analytical	1.10×10 <sup>1</sup>	1.69×10 <sup>-1</sup>
	3.95×10 <sup>1</sup>	7.99×10 <sup>-1</sup>	HCO <sub>2</sub> H	15.1%	32.0	55092.6	7.9	125	4.39×10 <sup>0</sup>	43	1.17	1.9%	Analytical	4.31×10 <sup>0</sup>	6.90×10 <sup>-2</sup>
	1.97×10 <sup>1</sup>	5.47×10 <sup>-1</sup>	HCO <sub>2</sub> H	15.1%	15.7	55242.0	6.8	68	1.97×10 <sup>0</sup>	31	1.25	4.0%	Analytical	1.89×10 <sup>0</sup>	9.80×10 <sup>-3</sup>
1243	4.01×10 <sup>2</sup>	7.69×10 <sup>0</sup>	HCO <sub>2</sub> H	25.2%	283.1	52360.7	68.5	1458	2.00×10 <sup>-1</sup>	39	1.12	52.6%	Analytical	9.47×10 <sup>-2</sup>	6.12×10 <sup>-4</sup>
	3.34×10 <sup>2</sup>	6.43×10 <sup>0</sup>	HCO <sub>2</sub> H	25.2%	236.3	52860.8	59.4	1273	1.84×10 <sup>-1</sup>	39	1.12	55.9%	Analytical	8.12×10 <sup>-2</sup>	1.26×10 <sup>-3</sup>
	2.67×10 <sup>2</sup>	5.13×10 <sup>0</sup>	HCO <sub>2</sub> H	25.2%	189.2	53365.4	49.2	1068	1.70×10 <sup>-1</sup>	39	1.12	59.2%	Analytical	6.93×10 <sup>-2</sup>	1.01×10 <sup>-3</sup>
	2.00×10 <sup>2</sup>	3.85×10 <sup>0</sup>	HCO <sub>2</sub> H	25.2%	142.0	53870.9	34.5	813	1.56×10 <sup>-1</sup>	39	1.12	62.7%	Analytical	5.82×10 <sup>-2</sup>	6.24×10 <sup>-4</sup>
	1.34×10 <sup>2</sup>	2.57×10 <sup>0</sup>	HCO <sub>2</sub> H	25.2%	94.7	54376.7	28.2	581	1.40×10 <sup>-1</sup>	39	1.12	67.2%	Analytical	4.59×10 <sup>-2</sup>	7.95×10 <sup>-4</sup>

## 7. Kinetic results of each studied amine for each concentration

N°	C <sub>Am</sub>	C <sub>CO2</sub>	Acid	Neutra	[Am] <sup>f</sup>	[H <sub>2</sub> O] <sup>f</sup>	A	C	k <sub>0</sub>	R	Evolution HO <sup>-</sup>	Contribution HO <sup>-</sup>	Model used	k <sub>0</sub> <sup>Am</sup>	σ (k <sub>0</sub> <sup>Am</sup> )
	6.70×10 <sup>1</sup>	1.31×10 <sup>0</sup>	HCO <sub>2</sub> H	25.2%	47.5	54882.2	15.3	319	1.24×10 <sup>-1</sup>	39	1.12	71.4%	Analytical	3.55×10 <sup>-2</sup>	3.98×10 <sup>-4</sup>
	3.34×10 <sup>1</sup>	5.48×10 <sup>-1</sup>	HCO <sub>2</sub> H	25.2%	23.9	55137.6	6.6	166	1.15×10 <sup>-1</sup>	47	1.10	74.8%	Analytical	2.89×10 <sup>-2</sup>	3.84×10 <sup>-4</sup>
1250	3.26×10 <sup>0</sup>	3.42×10 <sup>-1</sup>	No	0.0%	1.3	55381.6	-	-	-	5	1.26	9.4%	Numerical	1.03×10 <sup>2</sup>	2.70×10 <sup>0</sup>
	2.47×10 <sup>0</sup>	2.56×10 <sup>-1</sup>	No	0.0%	0.9	55384.7	-	-	-	5	1.25	11.6%	Numerical	6.81×10 <sup>1</sup>	2.00×10 <sup>0</sup>
	1.63×10 <sup>0</sup>	1.71×10 <sup>-1</sup>	No	0.0%	0.5	55388.0	-	-	-	4	1.24	16.9%	Numerical	3.28×10 <sup>1</sup>	8.86×10 <sup>-1</sup>
	8.15×10 <sup>-1</sup>	8.55×10 <sup>-2</sup>	No	0.0%	0.2	55391.2	-	-	-	3	1.23	27.0%	Numerical	1.08×10 <sup>1</sup>	2.22×10 <sup>-1</sup>
	4.08×10 <sup>-1</sup>	4.27×10 <sup>-2</sup>	No	0.0%	0.1	55392.8	-	-	-	2	1.23	45.0%	Numerical	2.78×10 <sup>0</sup>	6.63×10 <sup>-2</sup>
1251	5.08×10 <sup>0</sup>	5.30×10 <sup>-1</sup>	No	0.0%	2.5	55370.4	-	-	-	6	1.29	7.3%	Numerical	1.59×10 <sup>2</sup>	1.14×10 <sup>1</sup>
	4.07×10 <sup>0</sup>	4.24×10 <sup>-1</sup>	No	0.0%	1.9	55375.2	-	-	-	6	1.28	8.0%	Numerical	1.26×10 <sup>2</sup>	4.89×10 <sup>0</sup>
	3.07×10 <sup>0</sup>	3.18×10 <sup>-1</sup>	No	0.0%	1.3	55379.9	-	-	-	5	1.26	11.0%	Numerical	7.50×10 <sup>1</sup>	1.78×10 <sup>0</sup>
	2.05×10 <sup>0</sup>	2.12×10 <sup>-1</sup>	No	0.0%	0.8	55384.8	-	-	-	5	1.25	14.0%	Numerical	4.39×10 <sup>1</sup>	8.60×10 <sup>-1</sup>
	1.03×10 <sup>0</sup>	1.06×10 <sup>-1</sup>	No	0.0%	0.3	55389.6	-	-	-	4	1.23	24.4%	Numerical	1.37×10 <sup>1</sup>	4.14×10 <sup>-1</sup>
	3.81×10 <sup>-1</sup>	5.30×10 <sup>-2</sup>	No	0.0%	0.1	55392.6	-	-	-	2	1.33	32.0%	Numerical	3.99×10 <sup>0</sup>	1.80×10 <sup>-1</sup>
1260	6.30×10 <sup>0</sup>	6.23×10 <sup>-1</sup>	No	0.0%	4.8	55362.5	-1.9	38	8.00×10 <sup>1</sup>	9	1.85	4.1%	Analytical	7.67×10 <sup>1</sup>	1.09×10 <sup>0</sup>
	4.20×10 <sup>0</sup>	4.15×10 <sup>-1</sup>	No	0.0%	3.1	55372.8	-1.7	30	4.91×10 <sup>1</sup>	9	1.70	5.8%	Analytical	4.62×10 <sup>1</sup>	4.93×10 <sup>-1</sup>
	2.09×10 <sup>0</sup>	2.08×10 <sup>-1</sup>	No	0.0%	1.5	55383.1	-1.2	21	2.21×10 <sup>1</sup>	8	1.51	10.0%	Analytical	1.99×10 <sup>1</sup>	2.79×10 <sup>-1</sup>
	1.05×10 <sup>0</sup>	1.04×10 <sup>-1</sup>	No	0.0%	0.7	55388.2	-0.7	14	9.65×10 <sup>0</sup>	8	1.37	17.2%	Analytical	8.00×10 <sup>0</sup>	1.80×10 <sup>-1</sup>
1261	8.45×10 <sup>0</sup>	8.38×10 <sup>-1</sup>	No	0.0%	6.6	55352.8	-1.5	32	7.41×10 <sup>1</sup>	9	2.28	3.0%	Analytical	7.19×10 <sup>1</sup>	2.42×10 <sup>0</sup>

N°	C <sub>Am</sub>	C <sub>CO2</sub>	Acid	Neutra	[Am] <sup>f</sup>	[H <sub>2</sub> O] <sup>f</sup>	A	C	k <sub>0</sub>	R	Evolution HO <sup>-</sup>	Contribution HO <sup>-</sup>	Model used	k <sub>0</sub> <sup>Am</sup>	σ (k <sub>0</sub> <sup>Am</sup> )
	6.34×10 <sup>0</sup>	6.29×10 <sup>-1</sup>	No	0.0%	4.9	55363.1	-1.4	28	5.14×10 <sup>1</sup>	9	2.11	4.1%	Analytical	4.93×10 <sup>1</sup>	1.54×10 <sup>0</sup>
	4.22×10 <sup>0</sup>	4.19×10 <sup>-1</sup>	No	0.0%	3.3	55373.2	-1.2	23	3.26×10 <sup>1</sup>	9	1.91	5.7%	Analytical	3.07×10 <sup>1</sup>	2.66×10 <sup>-1</sup>
	2.12×10 <sup>0</sup>	2.10×10 <sup>-1</sup>	No	0.0%	1.6	55383.0	-0.8	16	1.49×10 <sup>1</sup>	9	1.65	10.1%	Analytical	1.34×10 <sup>1</sup>	2.39×10 <sup>-1</sup>
	1.07×10 <sup>0</sup>	1.05×10 <sup>-1</sup>	No	0.0%	0.8	55387.9	-0.6	11	6.95×10 <sup>0</sup>	9	1.45	17.0%	Analytical	5.77×10 <sup>0</sup>	2.06×10 <sup>-1</sup>
1262	7.65×10 <sup>0</sup>	7.94×10 <sup>-1</sup>	No	0.0%	5.4	55351.9	-7.7	66	1.93×10 <sup>2</sup>	8	1.70	3.2%	Analytical	1.87×10 <sup>2</sup>	5.82×10 <sup>0</sup>
	6.12×10 <sup>0</sup>	6.35×10 <sup>-1</sup>	No	0.0%	4.3	55361.3	-5.1	59	1.55×10 <sup>2</sup>	8	1.63	3.7%	Analytical	1.49×10 <sup>2</sup>	4.79×10 <sup>0</sup>
	4.57×10 <sup>0</sup>	4.77×10 <sup>-1</sup>	No	0.0%	3.1	55370.8	-4.6	50	1.18×10 <sup>2</sup>	8	1.57	4.3%	Analytical	1.13×10 <sup>2</sup>	2.38×10 <sup>0</sup>
	3.07×10 <sup>0</sup>	3.18×10 <sup>-1</sup>	No	0.0%	2.0	55380.0	-3.2	40	6.84×10 <sup>1</sup>	7	1.47	6.2%	Analytical	6.42×10 <sup>1</sup>	2.36×10 <sup>0</sup>
	1.55×10 <sup>0</sup>	1.59×10 <sup>-1</sup>	No	0.0%	0.9	55389.3	-1.9	27	2.61×10 <sup>1</sup>	7	1.35	11.9%	Analytical	2.30×10 <sup>1</sup>	1.20×10 <sup>0</sup>
	7.82×10 <sup>-1</sup>	7.94×10 <sup>-2</sup>	No	0.0%	0.4	55394.1	-1.4	17	1.03×10 <sup>1</sup>	6	1.27	21.1%	Analytical	8.13×10 <sup>0</sup>	2.56×10 <sup>-1</sup>
1263	2.53×10 <sup>1</sup>	2.56×10 <sup>0</sup>	No	0.0%	19.7	55243.3	-7.9	88	1.83×10 <sup>2</sup>	9	2.49	3.1%	Analytical	1.77×10 <sup>2</sup>	6.64×10 <sup>0</sup>
	2.03×10 <sup>1</sup>	2.05×10 <sup>0</sup>	No	0.0%	15.7	55273.5	-7.8	79	1.48×10 <sup>2</sup>	9	2.36	3.6%	Analytical	1.42×10 <sup>2</sup>	8.91×10 <sup>0</sup>
	1.52×10 <sup>1</sup>	1.55×10 <sup>0</sup>	No	0.0%	11.7	55303.3	-5.5	67	9.59×10 <sup>1</sup>	9	2.20	5.1%	Analytical	9.10×10 <sup>1</sup>	2.80×10 <sup>0</sup>
	1.01×10 <sup>1</sup>	1.05×10 <sup>0</sup>	No	0.0%	7.7	55333.4	-4.1	56	5.39×10 <sup>1</sup>	9	2.02	8.0%	Analytical	4.96×10 <sup>1</sup>	2.89×10 <sup>0</sup>
	5.05×10 <sup>0</sup>	5.44×10 <sup>-1</sup>	No	0.0%	3.7	55363.5	-2.3	39	1.92×10 <sup>1</sup>	8	1.79	17.5%	Analytical	1.59×10 <sup>1</sup>	7.43×10 <sup>-1</sup>
	2.56×10 <sup>0</sup>	2.72×10 <sup>-1</sup>	No	0.0%	1.8	55378.2	-1.1	28	7.29×10 <sup>0</sup>	8	1.57	36.2%	Analytical	4.66×10 <sup>0</sup>	1.26×10 <sup>-1</sup>
1264	3.02×10 <sup>1</sup>	3.04×10 <sup>0</sup>	No	0.0%	23.0	55190.1	-13.9	141	1.70×10 <sup>2</sup>	9	2.13	6.4%	Analytical	1.59×10 <sup>2</sup>	1.05×10 <sup>1</sup>
	2.01×10 <sup>1</sup>	2.04×10 <sup>0</sup>	No	0.0%	15.0	55259.6	-12.7	116	1.11×10 <sup>2</sup>	9	1.97	8.5%	Analytical	1.02×10 <sup>2</sup>	3.77×10 <sup>0</sup>

## 7. Kinetic results of each studied amine for each concentration

Nº	C <sub>Am</sub>	C <sub>CO2</sub>	Acid	Neutra	[Am] <sup>f</sup>	[H <sub>2</sub> O] <sup>f</sup>	A	C	k <sub>0</sub>	R	Evolution HO <sup>-</sup>	Contribution HO <sup>-</sup>	Model used	k <sub>0</sub> <sup>Am</sup>	σ (k <sub>0</sub> <sup>Am</sup> )
	1.01×10 <sup>1</sup>	1.04×10 <sup>0</sup>	No	0.0%	7.2	55329.3	-8.3	81	5.01×10 <sup>1</sup>	8	1.75	14.5%	Analytical	4.28×10 <sup>1</sup>	1.53×10 <sup>0</sup>
	5.10×10 <sup>0</sup>	5.42×10 <sup>-1</sup>	No	0.0%	3.4	55363.6	-4.9	56	2.40×10 <sup>1</sup>	8	1.59	22.9%	Analytical	1.85×10 <sup>1</sup>	5.58×10 <sup>-1</sup>
1265	3.02×10 <sup>2</sup>	2.53×10 <sup>0</sup>	HCO <sub>2</sub> H	29.9%	204.9	52587.9	33.2	1229	3.78×10 <sup>0</sup>	84	1.05	68.4%	Analytical	1.19×10 <sup>0</sup>	5.07×10 <sup>-2</sup>
	2.51×10 <sup>2</sup>	2.03×10 <sup>0</sup>	HCO <sub>2</sub> H	29.9%	170.5	53060.1	29.7	1074	3.55×10 <sup>0</sup>	87	1.05	71.0%	Analytical	1.03×10 <sup>0</sup>	8.43×10 <sup>-2</sup>
	2.01×10 <sup>2</sup>	1.79×10 <sup>0</sup>	HCO <sub>2</sub> H	29.9%	136.6	53520.1	25.4	875	3.40×10 <sup>0</sup>	80	1.05	71.5%	Analytical	9.69×10 <sup>-1</sup>	1.70×10 <sup>-2</sup>
	1.51×10 <sup>2</sup>	1.29×10 <sup>0</sup>	HCO <sub>2</sub> H	29.9%	102.7	53987.0	20.1	701	3.19×10 <sup>0</sup>	83	1.05	73.1%	Analytical	8.58×10 <sup>-1</sup>	2.25×10 <sup>-2</sup>
	1.01×10 <sup>2</sup>	7.88×10 <sup>-1</sup>	HCO <sub>2</sub> H	29.9%	68.5	54457.1	13.6	499	2.95×10 <sup>0</sup>	91	1.04	74.8%	Analytical	7.43×10 <sup>-1</sup>	1.63×10 <sup>-2</sup>
	5.03×10 <sup>1</sup>	5.39×10 <sup>-1</sup>	HCO <sub>2</sub> H	29.9%	33.9	54927.7	10.8	283	2.59×10 <sup>0</sup>	66	1.06	76.6%	Analytical	6.05×10 <sup>-1</sup>	1.58×10 <sup>-2</sup>
	2.52×10 <sup>1</sup>	5.39×10 <sup>-1</sup>	HCO <sub>2</sub> H	29.9%	16.4	55163.1	11.9	162	2.26×10 <sup>0</sup>	33	1.12	76.5%	Analytical	5.30×10 <sup>-1</sup>	1.59×10 <sup>-2</sup>
1270	9.05×10 <sup>1</sup>	7.62×10 <sup>0</sup>	HCO <sub>2</sub> H	15.4%	61.3	54971.4	64.0	388	4.63×10 <sup>2</sup>	10	1.82	0.0%	Analytical	4.63×10 <sup>2</sup>	1.83×10 <sup>1</sup>
	7.54×10 <sup>1</sup>	6.37×10 <sup>0</sup>	HCO <sub>2</sub> H	15.4%	51.1	55041.8	50.1	326	3.72×10 <sup>2</sup>	10	1.83	0.0%	Analytical	3.71×10 <sup>2</sup>	2.60×10 <sup>1</sup>
	6.03×10 <sup>1</sup>	5.08×10 <sup>0</sup>	HCO <sub>2</sub> H	15.4%	40.9	55112.3	40.1	264	2.66×10 <sup>2</sup>	10	1.83	0.0%	Analytical	2.65×10 <sup>2</sup>	1.78×10 <sup>1</sup>
	4.53×10 <sup>1</sup>	3.81×10 <sup>0</sup>	HCO <sub>2</sub> H	15.4%	30.7	55182.4	33.8	206	1.75×10 <sup>2</sup>	10	1.84	0.1%	Analytical	1.75×10 <sup>2</sup>	4.22×10 <sup>0</sup>
	3.02×10 <sup>1</sup>	2.55×10 <sup>0</sup>	HCO <sub>2</sub> H	15.4%	20.5	55252.2	25.7	141	1.07×10 <sup>2</sup>	10	1.85	0.1%	Analytical	1.07×10 <sup>2</sup>	1.82×10 <sup>0</sup>
	1.51×10 <sup>1</sup>	1.30×10 <sup>0</sup>	HCO <sub>2</sub> H	15.4%	10.2	55322.1	13.7	72	4.94×10 <sup>1</sup>	10	1.87	0.2%	Analytical	4.92×10 <sup>1</sup>	1.22×10 <sup>0</sup>
	7.57×10 <sup>0</sup>	5.43×10 <sup>-1</sup>	HCO <sub>2</sub> H	15.4%	5.3	55356.8	7.2	38	2.41×10 <sup>1</sup>	12	1.70	0.5%	Analytical	2.40×10 <sup>1</sup>	3.89×10 <sup>-1</sup>
1271	7.64×10 <sup>1</sup>	6.32×10 <sup>0</sup>	HCO <sub>2</sub> H	14.8%	52.4	54893.4	38.3	277	2.73×10 <sup>2</sup>	10	1.83	0.0%	Analytical	2.73×10 <sup>2</sup>	2.42×10 <sup>1</sup>
	6.12×10 <sup>1</sup>	5.04×10 <sup>0</sup>	HCO <sub>2</sub> H	14.8%	42.0	54992.7	33.8	230	1.97×10 <sup>2</sup>	10	1.83	0.1%	Analytical	1.97×10 <sup>2</sup>	1.11×10 <sup>1</sup>

N°	$C_{Am}$	$C_{CO_2}$	Acid	Neutra	$[Am]^f$	$[H_2O]^f$	A	C	$k_0$	R	Evolution $HO^-$	Contribution $HO^-$	Model used	$k_0^{Am}$	$\sigma(k_0^{Am})$
	$4.59 \times 10^1$	$3.78 \times 10^0$	HCO <sub>2</sub> H	14.8%	31.6	55092.1	28.9	178	$1.37 \times 10^2$	10	1.84	0.1%	Analytical	$1.37 \times 10^2$	$2.74 \times 10^0$
	$3.06 \times 10^1$	$2.53 \times 10^0$	HCO <sub>2</sub> H	14.8%	21.1	55191.7	20.6	121	$8.47 \times 10^1$	10	1.85	0.1%	Analytical	$8.46 \times 10^1$	$1.24 \times 10^0$
	$1.53 \times 10^1$	$1.29 \times 10^0$	HCO <sub>2</sub> H	14.8%	10.5	55291.6	11.1	62	$4.04 \times 10^1$	10	1.87	0.3%	Analytical	$4.03 \times 10^1$	$1.14 \times 10^0$
	$7.71 \times 10^0$	$5.38 \times 10^{-1}$	HCO <sub>2</sub> H	14.8%	5.5	55341.4	5.4	33	$1.99 \times 10^1$	12	1.69	0.6%	Analytical	$1.98 \times 10^1$	$4.01 \times 10^{-1}$

## 7. Kinetic results of each studied amine for each concentration

Table IX-14. Experimental results of tertiary amines.

N°	C <sub>Am</sub>	C <sub>CO2</sub>	Acid	Neutra	[Am] <sup>f</sup>	[H <sub>2</sub> O] <sup>f</sup>	A	C	k <sub>0</sub>	R	Evolution HO <sup>-</sup>	Contribution HO <sup>-</sup>	Model used	k <sub>0</sub> <sup>Am</sup>	σ (k <sub>0</sub> <sup>Am</sup> )
1300	7.91×10 <sup>2</sup>	1.01×10 <sup>1</sup>	HCl	35.0%	496.3	51813.6	121.7	4942	4.55×10 <sup>0</sup>	51	1.08	37.0%	Analytical	2.87×10 <sup>0</sup>	7.46×10 <sup>-2</sup>
	6.34×10 <sup>2</sup>	1.01×10 <sup>1</sup>	HCl	35.0%	394.8	52519.6	130.4	4236	3.95×10 <sup>0</sup>	41	1.10	40.4%	Analytical	2.35×10 <sup>0</sup>	1.20×10 <sup>-1</sup>
	4.78×10 <sup>2</sup>	7.61×10 <sup>0</sup>	HCl	35.0%	297.6	53226.0	111.3	3424	3.46×10 <sup>0</sup>	41	1.09	43.8%	Analytical	1.94×10 <sup>0</sup>	3.40×10 <sup>-2</sup>
	3.16×10 <sup>2</sup>	5.07×10 <sup>0</sup>	HCl	35.0%	197.3	53955.8	83.0	2451	2.82×10 <sup>0</sup>	41	1.09	49.7%	Analytical	1.42×10 <sup>0</sup>	2.40×10 <sup>-2</sup>
	1.61×10 <sup>2</sup>	2.55×10 <sup>0</sup>	HCl	35.0%	100.3	54661.8	47.5	1371	2.23×10 <sup>0</sup>	41	1.09	56.0%	Analytical	9.82×10 <sup>-1</sup>	2.06×10 <sup>-2</sup>
	8.04×10 <sup>1</sup>	1.29×10 <sup>0</sup>	HCl	35.0%	50.2	55025.9	24.0	717	1.80×10 <sup>0</sup>	41	1.09	62.4%	Analytical	6.79×10 <sup>-1</sup>	2.33×10 <sup>-2</sup>
1301	5.42×10 <sup>2</sup>	1.01×10 <sup>1</sup>	HCl	46.6%	272.0	51937.9	60.0	4271	4.92×10 <sup>0</sup>	29	1.11	34.3%	Analytical	3.23×10 <sup>0</sup>	2.14×10 <sup>-1</sup>
	4.07×10 <sup>2</sup>	7.54×10 <sup>0</sup>	HCl	46.6%	204.5	52794.2	54.3	3478	4.58×10 <sup>0</sup>	29	1.11	35.1%	Analytical	2.97×10 <sup>0</sup>	1.70×10 <sup>-1</sup>
	2.72×10 <sup>2</sup>	5.03×10 <sup>0</sup>	HCl	46.6%	136.9	53652.9	43.2	2556	4.03×10 <sup>0</sup>	29	1.11	37.1%	Analytical	2.53×10 <sup>0</sup>	1.56×10 <sup>-1</sup>
	1.36×10 <sup>2</sup>	2.52×10 <sup>0</sup>	HCl	46.6%	68.9	54516.9	24.8	1446	3.51×10 <sup>0</sup>	29	1.10	37.7%	Analytical	2.19×10 <sup>0</sup>	1.14×10 <sup>-1</sup>
	6.87×10 <sup>1</sup>	1.28×10 <sup>0</sup>	HCl	46.6%	34.6	54951.1	14.6	788	3.16×10 <sup>0</sup>	29	1.10	37.7%	Analytical	1.97×10 <sup>0</sup>	1.01×10 <sup>-1</sup>
1302	9.84×10 <sup>2</sup>	9.81×10 <sup>0</sup>	HCl	40.0%	571.0	49441.8	92.8	5644	1.05×10 <sup>1</sup>	61	1.06	54.0%	Analytical	4.83×10 <sup>0</sup>	8.35×10 <sup>-1</sup>
	7.89×10 <sup>2</sup>	9.82×10 <sup>0</sup>	HCl	40.0%	454.5	50613.8	101.2	4809	9.58×10 <sup>0</sup>	49	1.08	56.5%	Analytical	4.17×10 <sup>0</sup>	4.85×10 <sup>-1</sup>
	5.94×10 <sup>2</sup>	7.42×10 <sup>0</sup>	HCl	40.0%	341.9	51794.3	87.7	4000	7.59×10 <sup>0</sup>	48	1.08	68.0%	Analytical	2.43×10 <sup>0</sup>	6.23×10 <sup>-2</sup>
	3.98×10 <sup>2</sup>	4.98×10 <sup>0</sup>	HCl	40.0%	228.9	52980.6	72.3	2982	6.64×10 <sup>0</sup>	48	1.08	72.2%	Analytical	1.84×10 <sup>0</sup>	1.06×10 <sup>-1</sup>
	1.99×10 <sup>2</sup>	2.51×10 <sup>0</sup>	HCl	40.0%	114.6	54182.3	46.0	1714	5.65×10 <sup>0</sup>	48	1.08	74.7%	Analytical	1.43×10 <sup>0</sup>	1.59×10 <sup>-1</sup>
	9.98×10 <sup>1</sup>	1.25×10 <sup>0</sup>	HCl	40.0%	57.2	54785.8	25.1	950	4.79×10 <sup>0</sup>	48	1.08	78.1%	Analytical	1.05×10 <sup>0</sup>	1.21×10 <sup>-1</sup>
1310	8.33×10 <sup>2</sup>	9.96×10 <sup>0</sup>	HCl	10.1%	738.0	49485.6	43.9	1278	1.16×10 <sup>0</sup>	76	1.11	7.8%	Analytical	1.07×10 <sup>0</sup>	4.36×10 <sup>-2</sup>

Nº	C <sub>Am</sub>	C <sub>CO2</sub>	Acid	Neutra	[Am] <sup>f</sup>	[H <sub>2</sub> O] <sup>f</sup>	A	C	k <sub>0</sub>	R	Evolution HO <sup>-</sup>	Contribution HO <sup>-</sup>	Model used	k <sub>0</sub> <sup>Am</sup>	σ (k <sub>0</sub> <sup>Am</sup> )
	6.18×10 <sup>2</sup>	7.52×10 <sup>0</sup>	HCl	10.1%	547.3	51012.7	38.4	1058	8.12×10 <sup>-1</sup>	74	1.12	10.9%	Analytical	7.24×10 <sup>-1</sup>	1.21×10 <sup>-2</sup>
	4.07×10 <sup>2</sup>	5.05×10 <sup>0</sup>	HCl	10.1%	360.8	52505.5	32.6	782	5.51×10 <sup>-1</sup>	73	1.12	15.5%	Analytical	4.65×10 <sup>-1</sup>	5.32×10 <sup>-3</sup>
	2.02×10 <sup>2</sup>	2.54×10 <sup>0</sup>	HCl	10.1%	178.7	53962.7	19.4	431	3.16×10 <sup>-1</sup>	72	1.13	25.6%	Analytical	2.35×10 <sup>-1</sup>	3.84×10 <sup>-3</sup>
	1.01×10 <sup>2</sup>	1.27×10 <sup>0</sup>	HCl	10.1%	89.2	54677.9	11.3	234	2.09×10 <sup>-1</sup>	72	1.13	37.1%	Analytical	1.32×10 <sup>-1</sup>	2.73×10 <sup>-3</sup>
1311	8.19×10 <sup>2</sup>	1.00×10 <sup>1</sup>	HCl	20.1%	642.3	50326.8	44.8	2531	3.15×10 <sup>0</sup>	66	1.07	7.3%	Analytical	2.92×10 <sup>0</sup>	4.88×10 <sup>-2</sup>
	6.11×10 <sup>2</sup>	7.57×10 <sup>0</sup>	HCl	20.1%	479.3	51612.9	38.4	2092	2.32×10 <sup>0</sup>	65	1.07	9.6%	Analytical	2.10×10 <sup>0</sup>	5.10×10 <sup>-2</sup>
	4.08×10 <sup>2</sup>	5.08×10 <sup>0</sup>	HCl	20.1%	319.9	52870.0	30.5	1539	1.53×10 <sup>0</sup>	65	1.07	13.8%	Analytical	1.32×10 <sup>0</sup>	3.46×10 <sup>-2</sup>
	2.01×10 <sup>2</sup>	2.56×10 <sup>0</sup>	HCl	20.1%	158.0	54146.0	18.4	857	7.43×10 <sup>-1</sup>	64	1.08	25.8%	Analytical	5.51×10 <sup>-1</sup>	6.20×10 <sup>-2</sup>
	1.00×10 <sup>2</sup>	1.28×10 <sup>0</sup>	HCl	20.1%	78.8	54770.2	10.9	457	5.33×10 <sup>-1</sup>	64	1.08	33.4%	Analytical	3.55×10 <sup>-1</sup>	2.69×10 <sup>-2</sup>
1312	8.01×10 <sup>2</sup>	9.97×10 <sup>0</sup>	HCl	30.0%	545.6	51083.1	64.1	4380	5.24×10 <sup>0</sup>	57	1.07	12.7%	Analytical	4.58×10 <sup>0</sup>	3.70×10 <sup>-2</sup>
	6.02×10 <sup>2</sup>	7.53×10 <sup>0</sup>	HCl	30.0%	410.3	52152.2	52.1	3680	4.05×10 <sup>0</sup>	56	1.07	15.7%	Analytical	3.41×10 <sup>0</sup>	4.99×10 <sup>-2</sup>
	3.46×10 <sup>2</sup>	5.06×10 <sup>0</sup>	HCl	30.0%	235.0	53529.4	45.2	2568	2.46×10 <sup>0</sup>	48	1.08	23.3%	Analytical	1.89×10 <sup>0</sup>	7.53×10 <sup>-3</sup>
	2.00×10 <sup>2</sup>	2.54×10 <sup>0</sup>	HCl	30.0%	136.6	54314.1	27.1	1813	1.55×10 <sup>0</sup>	56	1.07	34.1%	Analytical	1.02×10 <sup>0</sup>	8.99×10 <sup>-2</sup>
	1.00×10 <sup>2</sup>	1.27×10 <sup>0</sup>	HCl	30.0%	68.5	54851.1	17.6	1209	1.07×10 <sup>0</sup>	56	1.07	44.9%	Analytical	5.89×10 <sup>-1</sup>	4.49×10 <sup>-2</sup>
1313	8.04×10 <sup>2</sup>	1.01×10 <sup>1</sup>	HCl	35.0%	504.6	49743.4	43.5	4243	1.81×10 <sup>1</sup>	52	1.08	10.2%	Analytical	1.63×10 <sup>1</sup>	8.52×10 <sup>-1</sup>
	6.02×10 <sup>2</sup>	7.60×10 <sup>0</sup>	HCl	35.0%	377.9	51158.1	38.5	3643	1.30×10 <sup>1</sup>	52	1.08	13.5%	Analytical	1.13×10 <sup>1</sup>	1.78×10 <sup>-1</sup>
	3.90×10 <sup>2</sup>	5.11×10 <sup>0</sup>	HCl	35.0%	245.0	52643.5	33.1	2821	8.92×10 <sup>0</sup>	50	1.08	18.3%	Analytical	7.29×10 <sup>0</sup>	1.80×10 <sup>-1</sup>
	2.00×10 <sup>2</sup>	2.57×10 <sup>0</sup>	HCl	35.0%	126.0	53978.7	23.7	1875	5.37×10 <sup>0</sup>	51	1.07	27.3%	Analytical	3.91×10 <sup>0</sup>	1.44×10 <sup>-1</sup>

## 7. Kinetic results of each studied amine for each concentration

N°	C <sub>Am</sub>	C <sub>CO2</sub>	Acid	Neutra	[Am] <sup>f</sup>	[H <sub>2</sub> O] <sup>f</sup>	A	C	k <sub>0</sub>	R	Evolution HO <sup>-</sup>	Contribution HO <sup>-</sup>	Model used	k <sub>0</sub> <sup>Am</sup>	σ (k <sub>0</sub> <sup>Am</sup> )
	1.00×10 <sup>2</sup>	1.29×10 <sup>0</sup>	HCl	35.0%	63.2	54682.9	17.2	1262	3.30×10 <sup>0</sup>	51	1.07	39.9%	Analytical	1.98×10 <sup>0</sup>	8.97×10 <sup>-2</sup>
1314	8.01×10 <sup>2</sup>	9.95×10 <sup>0</sup>	HCl	40.0%	461.3	49842.3	54.8	4285	2.54×10 <sup>1</sup>	49	1.08	17.2%	Analytical	2.10×10 <sup>1</sup>	7.20×10 <sup>-1</sup>
	5.98×10 <sup>2</sup>	7.52×10 <sup>0</sup>	HCl	40.0%	344.3	51244.4	51.7	3609	1.93×10 <sup>1</sup>	48	1.08	21.7%	Analytical	1.51×10 <sup>1</sup>	5.94×10 <sup>-1</sup>
	3.97×10 <sup>2</sup>	5.05×10 <sup>0</sup>	HCl	40.0%	228.6	52633.3	44.4	2719	1.39×10 <sup>1</sup>	48	1.08	27.9%	Analytical	1.00×10 <sup>1</sup>	1.24×10 <sup>-1</sup>
	1.99×10 <sup>2</sup>	2.54×10 <sup>0</sup>	HCl	40.0%	114.3	54010.6	30.0	1591	8.87×10 <sup>0</sup>	47	1.08	38.6%	Analytical	5.45×10 <sup>0</sup>	1.40×10 <sup>-1</sup>
	9.90×10 <sup>1</sup>	1.27×10 <sup>0</sup>	HCl	40.0%	56.9	54702.3	22.9	883	6.25×10 <sup>0</sup>	47	1.08	48.7%	Analytical	3.20×10 <sup>0</sup>	1.56×10 <sup>-1</sup>
1315	8.06×10 <sup>2</sup>	9.80×10 <sup>0</sup>	HCl	30.0%	550.8	48429.7	24.2	2948	9.63×10 <sup>0</sup>	58	1.06	4.5%	Analytical	9.20×10 <sup>0</sup>	4.22×10 <sup>-1</sup>
	5.99×10 <sup>2</sup>	7.40×10 <sup>0</sup>	HCl	30.0%	409.7	50217.1	22.6	2500	6.38×10 <sup>0</sup>	57	1.06	6.6%	Analytical	5.95×10 <sup>0</sup>	1.01×10 <sup>-1</sup>
	3.97×10 <sup>2</sup>	4.97×10 <sup>0</sup>	HCl	30.0%	271.7	51963.4	18.0	1920	4.06×10 <sup>0</sup>	56	1.06	9.8%	Analytical	3.67×10 <sup>0</sup>	9.50×10 <sup>-2</sup>
	1.98×10 <sup>2</sup>	2.50×10 <sup>0</sup>	HCl	30.0%	135.2	53687.1	12.3	1123	1.93×10 <sup>0</sup>	56	1.06	18.6%	Analytical	1.57×10 <sup>0</sup>	7.49×10 <sup>-2</sup>
	9.85×10 <sup>1</sup>	1.25×10 <sup>0</sup>	HCl	30.0%	67.5	54541.3	8.6	616	1.14×10 <sup>0</sup>	56	1.06	28.7%	Analytical	8.13×10 <sup>-1</sup>	7.64×10 <sup>-3</sup>
1316	6.40×10 <sup>2</sup>	1.00×10 <sup>1</sup>	HCl	35.0%	400.6	51343.9	54.3	3636	3.74×10 <sup>0</sup>	42	1.09	21.6%	Analytical	2.93×10 <sup>0</sup>	1.48×10 <sup>-1</sup>
	4.80×10 <sup>2</sup>	7.52×10 <sup>0</sup>	HCl	35.0%	300.8	52351.2	51.8	2982	2.97×10 <sup>0</sup>	42	1.08	26.0%	Analytical	2.20×10 <sup>0</sup>	5.94×10 <sup>-2</sup>
	3.20×10 <sup>2</sup>	5.01×10 <sup>0</sup>	HCl	35.0%	200.6	53363.9	42.5	2189	2.19×10 <sup>0</sup>	42	1.08	33.0%	Analytical	1.47×10 <sup>0</sup>	3.19×10 <sup>-2</sup>
	1.61×10 <sup>2</sup>	2.52×10 <sup>0</sup>	HCl	35.0%	100.8	54373.0	26.6	1243	1.48×10 <sup>0</sup>	42	1.08	43.7%	Analytical	8.33×10 <sup>-1</sup>	2.66×10 <sup>-2</sup>
	8.00×10 <sup>1</sup>	1.28×10 <sup>0</sup>	HCl	35.0%	50.2	54883.9	17.7	653	1.20×10 <sup>0</sup>	41	1.08	48.8%	Analytical	6.13×10 <sup>-1</sup>	4.03×10 <sup>-2</sup>
1320	8.13×10 <sup>2</sup>	9.83×10 <sup>0</sup>	HCl	29.9%	556.0	49360.8	36.7	3354	3.60×10 <sup>1</sup>	58	1.06	1.0%	Analytical	3.56×10 <sup>1</sup>	2.66×10 <sup>0</sup>
	6.07×10 <sup>2</sup>	7.43×10 <sup>0</sup>	HCl	29.9%	415.8	50880.2	32.5	2797	2.27×10 <sup>1</sup>	58	1.06	1.6%	Analytical	2.23×10 <sup>1</sup>	1.28×10 <sup>0</sup>

Nº	C <sub>Am</sub>	C <sub>CO2</sub>	Acid	Neutra	[Am] <sup>f</sup>	[H <sub>2</sub> O] <sup>f</sup>	A	C	k <sub>0</sub>	R	Evolution HO <sup>-</sup>	Contribution HO <sup>-</sup>	Model used	k <sub>0</sub> <sup>Am</sup>	σ (k <sub>0</sub> <sup>Am</sup> )
	4.03×10 <sup>2</sup>	4.99×10 <sup>0</sup>	HCl	29.9%	276.1	52394.9	25.2	2088	1.44×10 <sup>1</sup>	57	1.06	2.4%	Analytical	1.41×10 <sup>1</sup>	2.62×10 <sup>-1</sup>
	2.01×10 <sup>2</sup>	2.51×10 <sup>0</sup>	HCl	29.9%	137.8	53896.0	15.3	1196	6.88×10 <sup>0</sup>	57	1.06	4.5%	Analytical	6.58×10 <sup>0</sup>	2.45×10 <sup>-1</sup>
	1.00×10 <sup>2</sup>	1.26×10 <sup>0</sup>	HCl	29.9%	68.9	54643.6	9.1	653	3.75×10 <sup>0</sup>	57	1.06	7.5%	Analytical	3.47×10 <sup>0</sup>	6.61×10 <sup>-2</sup>
1321	7.95×10 <sup>2</sup>	1.00×10 <sup>1</sup>	HCl	10.2%	703.7	50792.3	81.2	1489	1.39×10 <sup>-1</sup>	72	1.11	30.8%	Analytical	9.62×10 <sup>-2</sup>	2.31×10 <sup>-3</sup>
	5.98×10 <sup>2</sup>	7.57×10 <sup>0</sup>	HCl	10.2%	529.2	51933.8	68.2	1202	1.15×10 <sup>-1</sup>	71	1.11	36.9%	Analytical	7.25×10 <sup>-2</sup>	6.19×10 <sup>-3</sup>
	4.00×10 <sup>2</sup>	5.09×10 <sup>0</sup>	HCl	10.2%	353.7	53080.9	50.9	875	8.75×10 <sup>-2</sup>	71	1.12	47.7%	Analytical	4.57×10 <sup>-2</sup>	1.57×10 <sup>-3</sup>
	2.00×10 <sup>2</sup>	2.56×10 <sup>0</sup>	HCl	10.2%	176.9	54236.5	27.8	471	6.60×10 <sup>-2</sup>	71	1.12	61.9%	Analytical	2.51×10 <sup>-2</sup>	9.17×10 <sup>-4</sup>
	1.00×10 <sup>2</sup>	1.28×10 <sup>0</sup>	HCl	10.2%	88.7	54812.4	14.8	253	5.78×10 <sup>-2</sup>	71	1.12	69.5%	Analytical	1.76×10 <sup>-2</sup>	9.57×10 <sup>-4</sup>
1330	5.98×10 <sup>2</sup>	7.60×10 <sup>0</sup>	HCl	35.0%	374.6	51646.6	78.0	3433	5.30×10 <sup>0</sup>	52	1.08	62.9%	Analytical	1.97×10 <sup>0</sup>	6.88×10 <sup>-2</sup>
	3.99×10 <sup>2</sup>	5.07×10 <sup>0</sup>	HCl	35.0%	250.1	52892.4	66.1	2567	4.56×10 <sup>0</sup>	52	1.08	68.1%	Analytical	1.46×10 <sup>0</sup>	1.03×10 <sup>-1</sup>
	2.00×10 <sup>2</sup>	2.54×10 <sup>0</sup>	HCl	35.0%	125.4	54136.0	41.2	1477	3.80×10 <sup>0</sup>	52	1.08	72.3%	Analytical	1.06×10 <sup>0</sup>	1.34×10 <sup>-1</sup>
	1.00×10 <sup>2</sup>	1.29×10 <sup>0</sup>	HCl	35.0%	62.8	54759.4	26.1	812	3.36×10 <sup>0</sup>	51	1.08	73.1%	Analytical	9.03×10 <sup>-1</sup>	6.52×10 <sup>-2</sup>
1331	8.00×10 <sup>2</sup>	1.02×10 <sup>1</sup>	HCl	40.1%	459.8	50938.6	119.0	5241	9.83×10 <sup>0</sup>	48	1.08	50.4%	Analytical	4.87×10 <sup>0</sup>	2.91×10 <sup>-1</sup>
	6.00×10 <sup>2</sup>	7.61×10 <sup>0</sup>	HCl	40.1%	345.0	52046.8	94.1	4209	8.60×10 <sup>0</sup>	48	1.08	54.9%	Analytical	3.88×10 <sup>0</sup>	1.03×10 <sup>-1</sup>
	4.01×10 <sup>2</sup>	5.08×10 <sup>0</sup>	HCl	40.1%	230.4	53155.2	75.7	3106	7.05×10 <sup>0</sup>	48	1.08	62.2%	Analytical	2.66×10 <sup>0</sup>	8.60×10 <sup>-2</sup>
	2.01×10 <sup>2</sup>	2.55×10 <sup>0</sup>	HCl	40.1%	115.3	54271.6	44.9	1775	5.72×10 <sup>0</sup>	48	1.08	67.2%	Analytical	1.87×10 <sup>0</sup>	7.91×10 <sup>-2</sup>
	1.01×10 <sup>2</sup>	1.30×10 <sup>0</sup>	HCl	40.1%	57.7	54830.2	24.9	971	4.86×10 <sup>0</sup>	47	1.08	70.1%	Analytical	1.46×10 <sup>0</sup>	7.15×10 <sup>-2</sup>
1340	8.13×10 <sup>2</sup>	1.01×10 <sup>1</sup>	HCl	25.0%	595.3	50224.2	69.3	3450	1.50×10 <sup>0</sup>	61	1.07	38.5%	Analytical	9.19×10 <sup>-1</sup>	4.06×10 <sup>-2</sup>

## 7. Kinetic results of each studied amine for each concentration

N°	C <sub>Am</sub>	C <sub>CO2</sub>	Acid	Neutra	[Am] <sup>f</sup>	[H <sub>2</sub> O] <sup>f</sup>	A	C	k <sub>0</sub>	R	Evolution HO <sup>-</sup>	Contribution HO <sup>-</sup>	Model used	k <sub>0</sub> <sup>Am</sup>	σ (k <sub>0</sub> <sup>Am</sup> )
	6.07×10 <sup>2</sup>	7.62×10 <sup>0</sup>	HCl	25.0%	444.6	51527.6	60.3	2960	1.16×10 <sup>0</sup>	60	1.07	47.6%	Analytical	6.09×10 <sup>-1</sup>	1.36×10 <sup>-2</sup>
	4.03×10 <sup>2</sup>	5.12×10 <sup>0</sup>	HCl	25.0%	295.7	52819.2	46.9	2340	8.83×10 <sup>-1</sup>	60	1.07	58.8%	Analytical	3.64×10 <sup>-1</sup>	3.77×10 <sup>-2</sup>
	2.01×10 <sup>2</sup>	2.58×10 <sup>0</sup>	HCl	25.0%	147.3	54109.1	30.2	1553	6.75×10 <sup>-1</sup>	59	1.07	69.3%	Analytical	2.07×10 <sup>-1</sup>	1.96×10 <sup>-2</sup>
	1.00×10 <sup>2</sup>	1.29×10 <sup>0</sup>	HCl	25.0%	73.5	54751.1	17.7	1072	5.42×10 <sup>-1</sup>	59	1.07	78.9%	Analytical	1.15×10 <sup>-1</sup>	1.98×10 <sup>-2</sup>
1341	8.13×10 <sup>2</sup>	1.01×10 <sup>1</sup>	HCl	25.0%	596.5	50202.4	47.4	2839	1.45×10 <sup>0</sup>	61	1.07	21.6%	Analytical	1.13×10 <sup>0</sup>	3.27×10 <sup>-2</sup>
	6.07×10 <sup>2</sup>	7.60×10 <sup>0</sup>	HCl	25.0%	445.5	51509.3	44.4	2379	1.10×10 <sup>0</sup>	60	1.07	27.3%	Analytical	7.98×10 <sup>-1</sup>	1.53×10 <sup>-2</sup>
	4.03×10 <sup>2</sup>	5.07×10 <sup>0</sup>	HCl	25.0%	296.1	52807.5	10.4	539	8.20×10 <sup>-1</sup>	60	1.07	34.5%	Analytical	5.37×10 <sup>-1</sup>	1.16×10 <sup>-2</sup>
	2.01×10 <sup>2</sup>	2.54×10 <sup>0</sup>	HCl	25.0%	147.6	54101.5	25.1	1026	5.35×10 <sup>-1</sup>	60	1.07	48.0%	Analytical	2.78×10 <sup>-1</sup>	8.03×10 <sup>-3</sup>
	1.01×10 <sup>2</sup>	1.29×10 <sup>0</sup>	HCl	25.0%	74.0	54744.3	17.9	563	4.14×10 <sup>-1</sup>	59	1.07	56.9%	Analytical	1.78×10 <sup>-1</sup>	9.20×10 <sup>-3</sup>
1342	8.14×10 <sup>2</sup>	1.01×10 <sup>1</sup>	HCl	29.9%	553.3	49584.2	48.1	3110	9.20×10 <sup>0</sup>	57	1.08	18.0%	Analytical	7.54×10 <sup>0</sup>	2.46×10 <sup>-1</sup>
	6.08×10 <sup>2</sup>	7.60×10 <sup>0</sup>	HCl	29.9%	413.1	51051.4	46.3	2620	7.02×10 <sup>0</sup>	56	1.08	22.7%	Analytical	5.42×10 <sup>0</sup>	1.18×10 <sup>-1</sup>
	4.03×10 <sup>2</sup>	5.07×10 <sup>0</sup>	HCl	29.9%	274.0	52510.5	41.4	1999	5.14×10 <sup>0</sup>	56	1.08	29.0%	Analytical	3.65×10 <sup>0</sup>	5.71×10 <sup>-2</sup>
	2.01×10 <sup>2</sup>	2.54×10 <sup>0</sup>	HCl	29.9%	136.6	53954.0	29.8	1177	3.43×10 <sup>0</sup>	56	1.08	38.8%	Analytical	2.10×10 <sup>0</sup>	4.77×10 <sup>-2</sup>
	1.01×10 <sup>2</sup>	1.29×10 <sup>0</sup>	HCl	29.9%	68.6	54669.2	21.6	652	2.53×10 <sup>0</sup>	55	1.08	47.6%	Analytical	1.32×10 <sup>0</sup>	6.85×10 <sup>-2</sup>
1343	8.15×10 <sup>2</sup>	1.02×10 <sup>1</sup>	HCl	34.9%	512.7	50147.0	49.5	3909	1.29×10 <sup>1</sup>	53	1.07	12.4%	Analytical	1.13×10 <sup>1</sup>	3.00×10 <sup>-1</sup>
	6.51×10 <sup>2</sup>	1.02×10 <sup>1</sup>	HCl	34.9%	406.1	51199.5	57.6	3419	1.01×10 <sup>1</sup>	42	1.09	14.9%	Analytical	8.60×10 <sup>0</sup>	2.49×10 <sup>-1</sup>
	4.86×10 <sup>2</sup>	7.61×10 <sup>0</sup>	HCl	34.9%	303.3	52257.8	50.2	2816	7.87×10 <sup>0</sup>	42	1.09	18.3%	Analytical	6.43×10 <sup>0</sup>	1.80×10 <sup>-1</sup>
	3.23×10 <sup>2</sup>	5.08×10 <sup>0</sup>	HCl	34.9%	201.6	53307.2	40.0	2063	5.61×10 <sup>0</sup>	42	1.09	23.9%	Analytical	4.27×10 <sup>0</sup>	9.72×10 <sup>-2</sup>

Nº	C <sub>Am</sub>	C <sub>CO2</sub>	Acid	Neutra	[Am] <sup>f</sup>	[H <sub>2</sub> O] <sup>f</sup>	A	C	k <sub>0</sub>	R	Evolution HO <sup>-</sup>	Contribution HO <sup>-</sup>	Model used	k <sub>0</sub> <sup>Am</sup>	σ (k <sub>0</sub> <sup>Am</sup> )
	1.61×10 <sup>2</sup>	2.55×10 <sup>0</sup>	HCl	34.9%	100.6	54351.2	28.0	1173	3.52×10 <sup>0</sup>	41	1.09	34.0%	Analytical	2.32×10 <sup>0</sup>	6.14×10 <sup>-2</sup>
	8.02×10 <sup>1</sup>	1.30×10 <sup>0</sup>	HCl	34.9%	50.2	54872.2	16.8	625	2.42×10 <sup>0</sup>	41	1.09	44.5%	Analytical	1.35×10 <sup>0</sup>	2.16×10 <sup>-2</sup>
1344	8.15×10 <sup>2</sup>	1.02×10 <sup>1</sup>	HCl	35.0%	512.9	49536.7	42.4	3685	8.56×10 <sup>0</sup>	52	1.07	11.2%	Analytical	7.60×10 <sup>0</sup>	1.35×10 <sup>-1</sup>
	6.50×10 <sup>2</sup>	1.02×10 <sup>1</sup>	HCl	35.0%	406.2	50716.9	47.8	3244	6.88×10 <sup>0</sup>	42	1.09	13.3%	Analytical	5.96×10 <sup>0</sup>	2.30×10 <sup>-1</sup>
	4.84×10 <sup>2</sup>	7.61×10 <sup>0</sup>	HCl	35.0%	303.0	51903.2	43.1	2678	5.23×10 <sup>0</sup>	42	1.09	16.8%	Analytical	4.35×10 <sup>0</sup>	1.02×10 <sup>-1</sup>
	3.22×10 <sup>2</sup>	5.08×10 <sup>0</sup>	HCl	35.0%	201.7	53069.4	34.4	1991	3.69×10 <sup>0</sup>	42	1.08	22.3%	Analytical	2.86×10 <sup>0</sup>	5.31×10 <sup>-2</sup>
	1.60×10 <sup>2</sup>	2.55×10 <sup>0</sup>	HCl	35.0%	100.5	54234.0	24.2	1138	2.22×10 <sup>0</sup>	41	1.08	33.0%	Analytical	1.49×10 <sup>0</sup>	3.98×10 <sup>-2</sup>
	8.02×10 <sup>1</sup>	1.30×10 <sup>0</sup>	HCl	35.0%	50.3	54812.1	16.7	607	1.53×10 <sup>0</sup>	41	1.08	43.3%	Analytical	8.69×10 <sup>-1</sup>	1.70×10 <sup>-2</sup>
1345	8.16×10 <sup>2</sup>	1.01×10 <sup>1</sup>	HCl	35.0%	512.1	48913.0	29.9	3497	2.85×10 <sup>1</sup>	53	1.08	9.4%	Analytical	2.58×10 <sup>1</sup>	2.72×10 <sup>-1</sup>
	6.09×10 <sup>2</sup>	7.61×10 <sup>0</sup>	HCl	35.0%	382.4	50557.8	29.3	2966	2.19×10 <sup>1</sup>	52	1.08	11.7%	Analytical	1.93×10 <sup>1</sup>	8.28×10 <sup>-1</sup>
	4.05×10 <sup>2</sup>	5.07×10 <sup>0</sup>	HCl	35.0%	254.3	52180.7	26.0	2274	1.44×10 <sup>1</sup>	52	1.08	16.7%	Analytical	1.20×10 <sup>1</sup>	4.65×10 <sup>-1</sup>
	2.01×10 <sup>2</sup>	2.55×10 <sup>0</sup>	HCl	35.0%	126.4	53797.0	20.2	1336	8.04×10 <sup>0</sup>	52	1.08	26.6%	Analytical	5.90×10 <sup>0</sup>	8.08×10 <sup>-2</sup>
	1.01×10 <sup>2</sup>	1.29×10 <sup>0</sup>	HCl	35.0%	63.1	54594.1	14.7	746	5.13×10 <sup>0</sup>	51	1.08	37.4%	Analytical	3.21×10 <sup>0</sup>	1.75×10 <sup>-1</sup>
1346	1.05×10 <sup>3</sup>	1.00×10 <sup>1</sup>	HCl	40.8%	601.5	47692.6	88.9	4669	1.27×10 <sup>1</sup>	62	1.06	29.0%	Analytical	9.03×10 <sup>0</sup>	1.55×10 <sup>-1</sup>
	8.32×10 <sup>2</sup>	1.00×10 <sup>1</sup>	HCl	40.8%	472.9	49281.4	99.5	4226	1.11×10 <sup>1</sup>	49	1.08	32.0%	Analytical	7.53×10 <sup>0</sup>	2.24×10 <sup>-1</sup>
	6.18×10 <sup>2</sup>	7.57×10 <sup>0</sup>	HCl	40.8%	351.1	50847.2	94.7	3621	9.87×10 <sup>0</sup>	49	1.08	34.4%	Analytical	6.48×10 <sup>0</sup>	9.60×10 <sup>-2</sup>
	4.07×10 <sup>2</sup>	5.09×10 <sup>0</sup>	HCl	40.8%	231.4	52390.7	74.8	2758	8.56×10 <sup>0</sup>	48	1.08	36.9%	Analytical	5.41×10 <sup>0</sup>	2.67×10 <sup>-2</sup>
	2.01×10 <sup>2</sup>	2.56×10 <sup>0</sup>	HCl	40.8%	114.4	53905.3	49.5	1617	7.15×10 <sup>0</sup>	47	1.08	38.9%	Analytical	4.37×10 <sup>0</sup>	7.40×10 <sup>-2</sup>

## 7. Kinetic results of each studied amine for each concentration

N°	C <sub>Am</sub>	C <sub>CO2</sub>	Acid	Neutra	[Am] <sup>f</sup>	[H <sub>2</sub> O] <sup>f</sup>	A	C	k <sub>0</sub>	R	Evolution HO <sup>-</sup>	Contribution HO <sup>-</sup>	Model used	k <sub>0</sub> <sup>Am</sup>	σ (k <sub>0</sub> <sup>Am</sup> )
	1.01×10 <sup>2</sup>	1.28×10 <sup>0</sup>	HCl	40.8%	57.5	54643.7	33.0	917	6.00×10 <sup>0</sup>	47	1.08	41.3%	Analytical	3.53×10 <sup>0</sup>	1.26×10 <sup>-1</sup>
1350	8.09×10 <sup>2</sup>	1.01×10 <sup>1</sup>	HCl	19.9%	637.5	50816.9	64.9	2724	1.48×10 <sup>-1</sup>	65	1.06	32.7%	Analytical	9.96×10 <sup>-2</sup>	1.38×10 <sup>-3</sup>
	6.05×10 <sup>2</sup>	7.54×10 <sup>0</sup>	HCl	19.9%	476.5	51971.5	56.0	2222	1.17×10 <sup>-1</sup>	65	1.07	40.5%	Analytical	6.99×10 <sup>-2</sup>	1.58×10 <sup>-3</sup>
	4.01×10 <sup>2</sup>	5.03×10 <sup>0</sup>	HCl	19.9%	316.4	53120.1	43.5	1622	9.20×10 <sup>-2</sup>	65	1.07	50.5%	Analytical	4.55×10 <sup>-2</sup>	5.46×10 <sup>-4</sup>
	2.01×10 <sup>2</sup>	2.52×10 <sup>0</sup>	HCl	19.9%	158.4	54254.3	26.8	912	6.96×10 <sup>-2</sup>	65	1.07	64.5%	Analytical	2.47×10 <sup>-2</sup>	1.38×10 <sup>-3</sup>
	1.00×10 <sup>2</sup>	1.28×10 <sup>0</sup>	HCl	19.9%	78.9	54824.9	14.4	477	6.00×10 <sup>-2</sup>	63	1.07	72.7%	Analytical	1.63×10 <sup>-2</sup>	4.91×10 <sup>-4</sup>
1351	1.07×10 <sup>3</sup>	1.01×10 <sup>1</sup>	HCl	10.0%	952.4	47553.1	26.1	1844	1.94×10 <sup>-1</sup>	96	1.08	19.1%	Analytical	1.57×10 <sup>-1</sup>	4.39×10 <sup>-3</sup>
	8.45×10 <sup>2</sup>	1.01×10 <sup>1</sup>	HCl	10.0%	749.9	49208.6	27.7	1707	1.88×10 <sup>-1</sup>	76	1.11	19.5%	Analytical	1.52×10 <sup>-1</sup>	1.90×10 <sup>-2</sup>
	6.22×10 <sup>2</sup>	7.64×10 <sup>0</sup>	HCl	10.0%	552.0	50842.6	28.8	1512	1.32×10 <sup>-1</sup>	74	1.11	27.6%	Analytical	9.59×10 <sup>-2</sup>	1.25×10 <sup>-2</sup>
	4.12×10 <sup>2</sup>	5.12×10 <sup>0</sup>	HCl	10.0%	365.3	52383.4	25.8	1258	1.06×10 <sup>-1</sup>	73	1.11	34.2%	Analytical	6.99×10 <sup>-2</sup>	1.54×10 <sup>-2</sup>
	2.03×10 <sup>2</sup>	2.58×10 <sup>0</sup>	HCl	10.0%	180.2	53909.0	20.7	476	6.37×10 <sup>-2</sup>	72	1.12	56.2%	Analytical	2.79×10 <sup>-2</sup>	2.47×10 <sup>-3</sup>
	1.01×10 <sup>2</sup>	1.29×10 <sup>0</sup>	HCl	10.0%	89.7	54653.9	11.5	281	5.44×10 <sup>-2</sup>	72	1.12	65.2%	Analytical	1.89×10 <sup>-2</sup>	1.44×10 <sup>-3</sup>
1352	8.17×10 <sup>2</sup>	9.96×10 <sup>0</sup>	HCl	20.0%	642.7	49236.4	41.7	2576	4.50×10 <sup>-1</sup>	66	1.07	27.8%	Analytical	3.25×10 <sup>-1</sup>	6.11×10 <sup>-3</sup>
	6.09×10 <sup>2</sup>	7.52×10 <sup>0</sup>	HCl	20.0%	479.2	50802.0	44.8	2262	3.44×10 <sup>-1</sup>	65	1.07	35.3%	Analytical	2.23×10 <sup>-1</sup>	1.81×10 <sup>-2</sup>
	4.04×10 <sup>2</sup>	4.93×10 <sup>0</sup>	HCl	20.0%	317.6	52351.5	38.1	1844	2.58×10 <sup>-1</sup>	66	1.07	45.1%	Analytical	1.42×10 <sup>-1</sup>	8.12×10 <sup>-3</sup>
	2.01×10 <sup>2</sup>	2.54×10 <sup>0</sup>	HCl	20.0%	158.4	53875.5	24.7	1284	1.89×10 <sup>-1</sup>	64	1.07	57.1%	Analytical	8.13×10 <sup>-2</sup>	2.41×10 <sup>-3</sup>
	1.01×10 <sup>2</sup>	1.27×10 <sup>0</sup>	HCl	20.0%	79.2	54633.0	14.1	475	1.59×10 <sup>-1</sup>	64	1.07	63.8%	Analytical	5.77×10 <sup>-2</sup>	1.15×10 <sup>-3</sup>
1353	2.51×10 <sup>2</sup>	2.53×10 <sup>0</sup>	HCl	20.0%	198.0	53492.3	23.6	977	7.83×10 <sup>-2</sup>	80	1.05	61.2%	Analytical	3.03×10 <sup>-2</sup>	1.18×10 <sup>-3</sup>

N°	$C_{Am}$	$C_{CO_2}$	Acid	Neutra	$[Am]^f$	$[H_2O]^f$	A	C	$k_0$	R	Evolution $HO^*$	Contribution $HO^*$	Model used	$k_0^{Am}$	$\sigma(k_0^{Am})$
	$2.01 \times 10^2$	$2.03 \times 10^0$	HCl	20.0%	158.4	53874.1	20.2	815	$7.35 \times 10^{-2}$	80	1.05	64.5%	Analytical	$2.61 \times 10^{-2}$	$5.08 \times 10^{-4}$
	$1.50 \times 10^2$	$1.53 \times 10^0$	HCl	20.0%	118.8	54255.1	16.0	635	$6.84 \times 10^{-2}$	80	1.06	68.4%	Analytical	$2.16 \times 10^{-2}$	$7.57 \times 10^{-4}$
	$9.79 \times 10^1$	$1.04 \times 10^0$	HCl	20.0%	77.3	54654.2	11.1	427	$6.33 \times 10^{-2}$	77	1.06	72.5%	Analytical	$1.74 \times 10^{-2}$	$1.56 \times 10^{-4}$
	$5.01 \times 10^1$	$5.38 \times 10^{-1}$	HCl	20.0%	39.5	55017.5	6.5	233	$5.80 \times 10^{-2}$	76	1.06	77.3%	Analytical	$1.32 \times 10^{-2}$	$4.97 \times 10^{-4}$
	$2.51 \times 10^1$	$5.38 \times 10^{-1}$	HCl	20.0%	19.5	55207.6	6.7	124	$5.48 \times 10^{-2}$	38	1.12	79.1%	Analytical	$1.15 \times 10^{-2}$	$6.28 \times 10^{-4}$

## 7. Kinetic results of each studied amine for each concentration

Table IX-15. Experimental results of multi-amines.

N°	C <sub>Am</sub>	C <sub>CO2</sub>	Acid	Neutra	[Am] <sup>f</sup>	[H <sub>2</sub> O] <sup>f</sup>	A	C	k <sub>0</sub>	R	Evolution HO <sup>-</sup>	Contribution HO <sup>-</sup>	Model used	k <sub>0</sub> <sup>Am</sup>	σ (k <sub>0</sub> <sup>Am</sup> )
2200	6.14×10 <sup>0</sup>	5.49×10 <sup>-1</sup>	HCO <sub>2</sub> H	0.0%	4.9	55370.2	-1.2	29	1.12×10 <sup>2</sup>	11	2.02	1.8%		1.10×10 <sup>2</sup>	6.41×10 <sup>0</sup>
	4.91×10 <sup>0</sup>	4.27×10 <sup>-1</sup>	HCO <sub>2</sub> H	0.0%	3.9	55375.2	-1.2	26	8.79×10 <sup>1</sup>	11	1.89	2.2%		8.60×10 <sup>1</sup>	3.40×10 <sup>0</sup>
	3.69×10 <sup>0</sup>	3.05×10 <sup>-1</sup>	HCO <sub>2</sub> H	0.0%	2.9	55380.0	-1.1	23	6.42×10 <sup>1</sup>	11	1.72	2.8%		6.24×10 <sup>1</sup>	2.02×10 <sup>0</sup>
	2.46×10 <sup>0</sup>	2.14×10 <sup>-1</sup>	HCO <sub>2</sub> H	0.0%	1.9	55384.7	-0.9	18	3.99×10 <sup>1</sup>	10	1.63	3.8%		3.84×10 <sup>1</sup>	4.95×10 <sup>-1</sup>
	1.23×10 <sup>0</sup>	9.15×10 <sup>-2</sup>	HCO <sub>2</sub> H	0.0%	0.9	55389.3	-0.5	13	1.75×10 <sup>1</sup>	12	1.37	7.2%		1.63×10 <sup>1</sup>	4.23×10 <sup>-1</sup>
	6.16×10 <sup>-1</sup>	4.58×10 <sup>-2</sup>	HCO <sub>2</sub> H	0.0%	0.4	55391.6	-0.3	8	7.92×10 <sup>0</sup>	11	1.26	11.8%		6.98×10 <sup>0</sup>	1.40×10 <sup>-1</sup>
2201	5.03×10 <sup>1</sup>	4.76×10 <sup>0</sup>	No	0.0%	40.8	55115.4	26.7	67	4.14×10 <sup>2</sup>	10	6.46	0.2%		4.13×10 <sup>2</sup>	8.51×10 <sup>0</sup>
	4.02×10 <sup>1</sup>	3.76×10 <sup>0</sup>	No	0.0%	32.8	55170.9	20.4	51	2.98×10 <sup>2</sup>	11	5.82	0.3%		2.97×10 <sup>2</sup>	1.04×10 <sup>1</sup>
	3.02×10 <sup>1</sup>	2.76×10 <sup>0</sup>	No	0.0%	24.7	55226.2	12.6	42	1.92×10 <sup>2</sup>	11	5.07	0.5%		1.91×10 <sup>2</sup>	3.18×10 <sup>0</sup>
	2.01×10 <sup>1</sup>	1.77×10 <sup>0</sup>	No	0.0%	16.6	55281.7	6.8	30	1.10×10 <sup>2</sup>	11	4.16	0.9%		1.09×10 <sup>2</sup>	2.19×10 <sup>0</sup>
	1.01×10 <sup>1</sup>	9.75×10 <sup>-1</sup>	No	0.0%	8.2	55337.3	0.7	18	4.90×10 <sup>1</sup>	10	3.49	1.7%		4.81×10 <sup>1</sup>	2.19×10 <sup>0</sup>
	2.54×10 <sup>0</sup>	2.29×10 <sup>-1</sup>	No	0.0%	2.1	55379.2	-0.5	9	2.19×10 <sup>1</sup>	11	2.08	3.2%		2.12×10 <sup>1</sup>	5.63×10 <sup>-1</sup>
2300	7.89×10 <sup>2</sup>	1.00×10 <sup>1</sup>	HCl	15.0%	538.4	49477.5	62.2	3600	1.78×10 <sup>0</sup>	56	1.07	31.9%		1.21×10 <sup>0</sup>	3.97×10 <sup>-2</sup>
	5.94×10 <sup>2</sup>	7.58×10 <sup>0</sup>	HCl	15.0%	405.5	50929.9	60.4	3132	1.34×10 <sup>0</sup>	55	1.07	40.8%		7.94×10 <sup>-1</sup>	9.19×10 <sup>-3</sup>
	3.97×10 <sup>2</sup>	5.09×10 <sup>0</sup>	HCl	15.0%	271.2	52402.9	47.5	2512	9.39×10 <sup>-1</sup>	55	1.07	55.0%		4.22×10 <sup>-1</sup>	1.46×10 <sup>-2</sup>
	1.99×10 <sup>2</sup>	2.56×10 <sup>0</sup>	HCl	15.0%	136.4	53887.1	30.0	1674	6.64×10 <sup>-1</sup>	55	1.07	70.0%		1.99×10 <sup>-1</sup>	6.17×10 <sup>-3</sup>
	1.00×10 <sup>2</sup>	1.28×10 <sup>0</sup>	HCl	15.0%	68.5	54636.0	19.7	1152	5.20×10 <sup>-1</sup>	56	1.07	81.4%		9.67×10 <sup>-2</sup>	1.30×10 <sup>-2</sup>

## 8 *Thermodynamic and kinetic parameters of each molecule*

In this section for each molecule we indicate the value of the molar mass and the value of the pKa. We also write the nature of the regression used to determine kinetic parameters. We show kinetic constant  $k_1$  and  $k_2$  expressed in  $\text{m}^6.\text{mol}^{-2}.\text{s}^{-1}$  and the value of  $\varepsilon$  also expressed in  $\text{m}^6.\text{mol}^{-2}.\text{s}^{-1}$  (Chapter IV. 3.1). We also indicate the value of the parameters of the covariance matrix which are the variance of  $k_1$ , the variance of  $k_2$ , the variance of  $\varepsilon$ , the covariance between  $k_1$  and  $k_2$  and the covariance between  $k_1$  and  $\varepsilon$ . We write the value of the Fisher parameter which a confidence level of 95 %. We show the value of the determination coefficient of the fit of experimental data. Finally we indicate values of the confidence interval on kinetic constant  $k_1$  and  $k_2$  which are respectively  $\text{CI}k_1$  and  $\text{CI}k_2$ . Once again we divided the table by degree of substitution of each amine.

## 8. Thermodynamic and kinetic parameters of each molecule

Table IX-16. Physico-chemical parameters of primary amines.

N°	M	pKa	Regression	$k_1$	$k_2$	$\varepsilon$	$\sigma^2 k_1$	$\sigma^2 k_2$	$\sigma^2 \varepsilon$	COV( $k_1, k_2$ )	COV( $k_1, \varepsilon$ )	Fisher	R <sup>2</sup>	CIk <sub>1</sub>	CIk <sub>2</sub>
1100	31.6	10.70	Classical	$4.03 \times 10^{-4}$	$5.46 \times 10^{-1}$		$5.41 \times 10^{-10}$	$1.57 \times 10^{-1}$		$-8.92 \times 10^{-6}$		6.16	0.9996	$6.46 \times 10^{-5}$	$1.10 \times 10^0$
1101	73.14	10.66	Weighted	$2.30 \times 10^{-4}$	$3.61 \times 10^{-1}$		$1.72 \times 10^{-11}$	$4.38 \times 10^{-3}$		$-1.87 \times 10^{-7}$		4.37	0.9995	$1.15 \times 10^{-5}$	$1.84 \times 10^{-1}$
1102	59.11	10.72	Classical	$9.38 \times 10^{-5}$	$6.20 \times 10^{-3}$		$1.04 \times 10^{-10}$	$2.54 \times 10^{-5}$		$-4.96 \times 10^{-8}$		4.37	0.9980	$2.83 \times 10^{-5}$	$1.40 \times 10^{-2}$
1103	85.15	10.67	Classical	$9.64 \times 10^{-5}$	$7.48 \times 10^{-2}$		$4.25 \times 10^{-11}$	$1.59 \times 10^{-4}$		$-7.88 \times 10^{-8}$		4.37	0.9994	$1.81 \times 10^{-5}$	$3.51 \times 10^{-2}$
1104	99.18	10.60	Classical	$9.92 \times 10^{-5}$	$4.38 \times 10^{-2}$		$8.27 \times 10^{-11}$	$3.55 \times 10^{-4}$		$-1.67 \times 10^{-7}$		6.16	0.9994	$2.52 \times 10^{-5}$	$5.23 \times 10^{-2}$
1105	73.14	10.37	Weighted	$1.61 \times 10^{-4}$	$8.86 \times 10^{-2}$		$5.26 \times 10^{-11}$	$1.72 \times 10^{-4}$		$-8.56 \times 10^{-8}$		3.73	0.9991	$2.01 \times 10^{-5}$	$3.64 \times 10^{-2}$
1106	73.14	10.67	Weighted	$2.07 \times 10^{-5}$	$4.51 \times 10^{-3}$		$4.81 \times 10^{-13}$	$1.59 \times 10^{-6}$		$-7.96 \times 10^{-10}$		3.73	0.9994	$1.93 \times 10^{-6}$	$3.50 \times 10^{-3}$
1110	107.15	9.43	Weighted	$1.07 \times 10^{-4}$	$1.99 \times 10^{-2}$		$4.66 \times 10^{-12}$	$6.47 \times 10^{-6}$		$-4.30 \times 10^{-9}$		6.16	0.9998	$5.99 \times 10^{-6}$	$7.06 \times 10^{-3}$
1111	121.18	9.36	Classical	$4.87 \times 10^{-5}$	$3.48 \times 10^{-3}$		$1.02 \times 10^{-12}$	$8.08 \times 10^{-7}$		$-8.84 \times 10^{-10}$		3.40	0.9999	$2.80 \times 10^{-6}$	$2.50 \times 10^{-3}$
1112	121.18	9.32	Weighted	$4.80 \times 10^{-5}$	$4.94 \times 10^{-3}$		$3.52 \times 10^{-13}$	$7.83 \times 10^{-7}$		$-3.97 \times 10^{-10}$		3.73	0.9998	$1.65 \times 10^{-6}$	$2.46 \times 10^{-3}$
1113	121.18	9.84	Classical	$1.52 \times 10^{-4}$	$3.69 \times 10^{-2}$		$1.13 \times 10^{-11}$	$1.36 \times 10^{-5}$		$-1.18 \times 10^{-8}$		3.73	0.9999	$9.35 \times 10^{-6}$	$1.02 \times 10^{-2}$
1120	61.08	9.55	Classical	$9.68 \times 10^{-5}$	$1.38 \times 10^{-2}$		$2.32 \times 10^{-12}$	$1.62 \times 10^{-6}$		$-1.88 \times 10^{-9}$		3.73	1.0000	$4.23 \times 10^{-6}$	$3.53 \times 10^{-3}$
1121	75.11	10.03	Weighted	$1.46 \times 10^{-4}$	$1.23 \times 10^{-1}$		$2.39 \times 10^{-12}$	$5.65 \times 10^{-5}$		$-8.91 \times 10^{-9}$		6.16	0.9999	$4.29 \times 10^{-6}$	$2.09 \times 10^{-2}$
1122	89.14	10.25	Classical	$1.82 \times 10^{-4}$	$8.08 \times 10^{-2}$		$1.48 \times 10^{-11}$	$1.69 \times 10^{-3}$		$-1.53 \times 10^{-7}$		4.37	0.9999	$1.07 \times 10^{-5}$	$1.14 \times 10^{-1}$
1123	117.19	10.47	Classical	$1.91 \times 10^{-4}$	$2.32 \times 10^{-1}$		$5.55 \times 10^{-11}$	$4.41 \times 10^{-3}$		$-4.78 \times 10^{-7}$		3.73	0.9997	$2.07 \times 10^{-5}$	$1.84 \times 10^{-1}$
1124	75.11	9.43	Classical	$9.99 \times 10^{-5}$	$2.05 \times 10^{-2}$		$1.02 \times 10^{-11}$	$1.18 \times 10^{-5}$		$-1.06 \times 10^{-8}$		3.40	0.9998	$8.88 \times 10^{-6}$	$9.52 \times 10^{-3}$
1125	75.11	9.49	Classical	$3.23 \times 10^{-5}$	$6.46 \times 10^{-3}$		$4.59 \times 10^{-13}$	$1.18 \times 10^{-7}$		$-2.25 \times 10^{-10}$		3.73	0.9999	$1.88 \times 10^{-6}$	$9.55 \times 10^{-4}$
1126	89.14	9.53	Classical	$2.81 \times 10^{-5}$	$3.45 \times 10^{-3}$		$3.50 \times 10^{-13}$	$8.98 \times 10^{-8}$		$-1.71 \times 10^{-10}$		3.73	0.9999	$1.64 \times 10^{-6}$	$8.32 \times 10^{-4}$

N°	M	pKa	Regression	$k_1$	$k_2$	$\varepsilon$	$\sigma^2 k_1$	$\sigma^2 k_2$	$\sigma^2 \varepsilon$	COV( $k_1, k_2$ )	COV( $k_1, \varepsilon$ )	Fisher	R <sup>2</sup>	CIk <sub>1</sub>	CIk <sub>2</sub>
1127	89.14	9.72	Classical	$5.14 \times 10^{-6}$	$8.45 \times 10^{-4}$		$9.46 \times 10^{-14}$	$2.32 \times 10^{-9}$		$-1.43 \times 10^{-11}$		3.73	0.9998	$8.54 \times 10^{-7}$	$1.34 \times 10^{-4}$
1128	105.14	8.76	Classical	$7.61 \times 10^{-7}$	$2.14 \times 10^{-4}$		$4.58 \times 10^{-16}$	$2.31 \times 10^{-11}$		$-9.93 \times 10^{-14}$		3.73	1.0000	$5.94 \times 10^{-8}$	$1.33 \times 10^{-5}$
1129	121.14	8.04	Classical	$3.78 \times 10^{-7}$	$2.40 \times 10^{-5}$		$1.16 \times 10^{-15}$	$1.31 \times 10^{-10}$		$-3.78 \times 10^{-13}$		4.37	0.9990	$9.47 \times 10^{-8}$	$3.17 \times 10^{-5}$
1130	115.18	10.04	Classical	$6.06 \times 10^{-5}$	$2.37 \times 10^{-2}$		$6.84 \times 10^{-12}$	$8.14 \times 10^{-6}$		$-7.25 \times 10^{-9}$		3.73	0.9998	$7.26 \times 10^{-6}$	$7.92 \times 10^{-3}$
1131	75.11	9.37	Weighted	$9.67 \times 10^{-5}$	$1.29 \times 10^{-2}$		$3.71 \times 10^{-12}$	$1.71 \times 10^{-5}$		$-7.19 \times 10^{-9}$		3.73	0.9997	$5.34 \times 10^{-6}$	$1.15 \times 10^{-2}$
1132	105.14	9.46	Classical	$9.43 \times 10^{-5}$	$2.74 \times 10^{-2}$		$1.57 \times 10^{-11}$	$1.78 \times 10^{-5}$		$-1.62 \times 10^{-8}$		3.40	0.9997	$1.10 \times 10^{-5}$	$1.17 \times 10^{-2}$
1140	70.10	7.74	Classical	$2.82 \times 10^{-5}$	$1.81 \times 10^{-3}$		$7.11 \times 10^{-13}$	$1.61 \times 10^{-7}$		$-3.27 \times 10^{-10}$		3.40	0.9998	$2.34 \times 10^{-6}$	$1.11 \times 10^{-3}$

## 8. Thermodynamic and kinetic parameters of each molecule

Table IX-17. Physico-chemical parameters of secondary amines.

N°	M	pKa	Regression	$k_1$	$k_2$	$\varepsilon$	$\sigma^2 k_1$	$\sigma^2 k_2$	$\sigma^2 \varepsilon$	COV( $k_1, k_2$ )	COV( $k_1, \varepsilon$ )	Fisher	R <sup>2</sup>	CIk <sub>1</sub>	CIk <sub>2</sub>
1200	45.08	10.71	Classical	$5.18 \times 10^{-4}$	$2.28 \times 10^1$		$2.71 \times 10^{-9}$	$8.00 \times 10^0$		$-1.42 \times 10^{-4}$		6.16	0.9996	$1.45 \times 10^{-4}$	$7.85 \times 10^0$
1201	73.14	10.78	Classical	$3.61 \times 10^{-4}$	$6.48 \times 10^0$		$5.66 \times 10^{-10}$	$6.47 \times 10^{-1}$		$-1.85 \times 10^{-5}$		4.37	0.9996	$6.60 \times 10^{-5}$	$2.23 \times 10^0$
1202	87.16	10.83	Classical	$3.48 \times 10^{-4}$	$6.86 \times 10^0$		$6.56 \times 10^{-10}$	$7.17 \times 10^{-1}$		$-2.10 \times 10^{-5}$		4.37	0.9996	$7.11 \times 10^{-5}$	$2.35 \times 10^0$
1203	101.19	10.92	Classical	$1.94 \times 10^{-4}$	$1.56 \times 10^0$		$2.32 \times 10^{-10}$	$5.93 \times 10^{-2}$		$-3.59 \times 10^{-6}$		4.37	0.9995	$4.23 \times 10^{-5}$	$6.76 \times 10^{-1}$
1204	73.14	10.94	Classical	$1.70 \times 10^{-4}$	$1.05 \times 10^0$		$4.20 \times 10^{-11}$	$1.03 \times 10^{-2}$		$-6.37 \times 10^{-7}$		4.37	0.9999	$1.80 \times 10^{-5}$	$2.82 \times 10^{-1}$
1205	113.2	10.90	Classical	$1.53 \times 10^{-4}$	$1.13 \times 10^0$		$1.33 \times 10^{-11}$	$2.31 \times 10^{-3}$		$-1.68 \times 10^{-7}$		3.73	0.9999	$1.01 \times 10^{-5}$	$1.34 \times 10^{-1}$
1210	121.18	9.69	Classical	$8.77 \times 10^{-5}$	$1.54 \times 10^{-1}$		$5.88 \times 10^{-11}$	$9.62 \times 10^{-5}$		$-7.28 \times 10^{-8}$		3.73	0.9997	$2.13 \times 10^{-5}$	$2.72 \times 10^{-2}$
1211	135.21	9.78	Classical	$3.95 \times 10^{-5}$	$5.01 \times 10^{-2}$		$7.17 \times 10^{-12}$	$1.15 \times 10^{-5}$		$-8.79 \times 10^{-9}$		3.73	0.9997	$7.43 \times 10^{-6}$	$9.43 \times 10^{-3}$
1212	151.21	8.84	Classical	$4.95 \times 10^{-6}$	$2.70 \times 10^{-3}$		$1.86 \times 10^{-14}$	$6.35 \times 10^{-9}$		$-1.05 \times 10^{-11}$		3.40	0.9999	$3.79 \times 10^{-7}$	$2.21 \times 10^{-4}$
1220	75.11	9.84	Classical	$7.88 \times 10^{-5}$	$9.75 \times 10^{-2}$		$8.33 \times 10^{-11}$	$7.33 \times 10^{-5}$		$-7.56 \times 10^{-8}$		3.73	0.9994	$2.53 \times 10^{-5}$	$2.38 \times 10^{-2}$
1221	89.14	9.86	Classical	$2.83 \times 10^{-5}$	$4.30 \times 10^{-2}$		$6.89 \times 10^{-12}$	$8.15 \times 10^{-6}$		$-7.25 \times 10^{-9}$		3.40	0.9995	$7.29 \times 10^{-6}$	$7.93 \times 10^{-3}$
1222	103.16	9.86	Classical	$2.18 \times 10^{-5}$	$2.33 \times 10^{-2}$		$1.55 \times 10^{-12}$	$1.82 \times 10^{-6}$		$-1.63 \times 10^{-9}$		3.40	0.9997	$3.46 \times 10^{-6}$	$3.75 \times 10^{-3}$
1223	117.19	9.99	Classical	$2.31 \times 10^{-5}$	$3.44 \times 10^{-2}$		$3.71 \times 10^{-13}$	$1.38 \times 10^{-7}$		$-2.19 \times 10^{-10}$		3.73	1.0000	$1.69 \times 10^{-6}$	$1.03 \times 10^{-3}$
1224	103.16	10.01	Classical	$6.31 \times 10^{-6}$	$3.16 \times 10^{-3}$		$7.12 \times 10^{-14}$	$2.73 \times 10^{-8}$		$-4.28 \times 10^{-11}$		3.73	0.9999	$7.41 \times 10^{-7}$	$4.59 \times 10^{-4}$
1225	143.23	9.91	Classical	$8.67 \times 10^{-6}$	$2.30 \times 10^{-3}$		$3.10 \times 10^{-13}$	$6.96 \times 10^{-8}$		$-1.42 \times 10^{-10}$		3.40	0.9994	$1.55 \times 10^{-6}$	$7.33 \times 10^{-4}$
1226	117.19	10.23	Weighted	$5.37 \times 10^{-7}$		$-1.11 \times 10^0$	$4.92 \times 10^{-16}$		$4.22 \times 10^{-2}$		$-3.90 \times 10^{-9}$	3.73	0.9932	$6.16 \times 10^{-8}$	
1227	105.14	8.86	Classical	$1.85 \times 10^{-6}$	$9.86 \times 10^{-4}$		$1.23 \times 10^{-16}$	$1.45 \times 10^{-11}$		$-4.07 \times 10^{-14}$		3.73	1.0000	$3.08 \times 10^{-8}$	$1.06 \times 10^{-5}$
1228	133.19	8.87	Weighted	$7.00 \times 10^{-7}$	$6.35 \times 10^{-4}$		$2.88 \times 10^{-16}$	$2.87 \times 10^{-10}$		$-2.46 \times 10^{-13}$		3.40	0.9998	$4.71 \times 10^{-8}$	$4.70 \times 10^{-5}$

N°	M	pKa	Regression	k <sub>1</sub>	k <sub>2</sub>	ε	σ <sup>2</sup> k <sub>1</sub>	σ <sup>2</sup> k <sub>2</sub>	σ <sup>2</sup> ε	COV(k <sub>1</sub> ,k <sub>2</sub> )	COV(k <sub>1</sub> ,ε)	Fisher	R <sup>2</sup>	CIk <sub>1</sub>	CIk <sub>2</sub>
1230	133.19	8.60	Classical	1.56×10 <sup>-6</sup>	5.28×10 <sup>-4</sup>		4.46×10 <sup>-15</sup>	5.17×10 <sup>-10</sup>		-1.47×10 <sup>-12</sup>		3.73	0.9999	1.85×10 <sup>-7</sup>	6.31×10 <sup>-5</sup>
1231	119.16	8.94	Classical	1.83×10 <sup>-5</sup>	9.52×10 <sup>-3</sup>		4.25×10 <sup>-13</sup>	3.77×10 <sup>-7</sup>		-3.87×10 <sup>-10</sup>		3.73	0.9999	1.81×10 <sup>-6</sup>	1.70×10 <sup>-3</sup>
1240	84.12	7.96	Classical	1.28×10 <sup>-5</sup>	3.66×10 <sup>-3</sup>		5.66×10 <sup>-14</sup>	2.72×10 <sup>-8</sup>		-3.80×10 <sup>-11</sup>		3.40	0.9999	6.61×10 <sup>-7</sup>	4.58×10 <sup>-4</sup>
1241	98.08	8.10	Classical	2.26×10 <sup>-6</sup>	1.24×10 <sup>-3</sup>		1.50×10 <sup>-15</sup>	2.81×10 <sup>-10</sup>		-6.27×10 <sup>-13</sup>		3.73	1.0000	1.08×10 <sup>-7</sup>	4.66×10 <sup>-5</sup>
1242	126.20	8.05	Classical	1.84×10 <sup>-6</sup>	9.96×10 <sup>-4</sup>		2.33×10 <sup>-15</sup>	2.59×10 <sup>-10</sup>		-7.51×10 <sup>-13</sup>		3.40	1.0000	1.34×10 <sup>-7</sup>	4.47×10 <sup>-5</sup>
1243	126.20	8.31	Weighted	4.79×10 <sup>-9</sup>		2.25×10 <sup>-2</sup>	6.04×10 <sup>-21</sup>		2.88×10 <sup>-7</sup>		-3.09×10 <sup>-14</sup>	3.40	0.9987	2.16×10 <sup>-10</sup>	
1250	71.12	11.17	Classical	1.14×10 <sup>-3</sup>	1.33×10 <sup>1</sup>		3.21×10 <sup>-9</sup>	7.71×10 <sup>0</sup>		-1.52×10 <sup>-4</sup>		4.37	0.9997	1.57×10 <sup>-4</sup>	7.71×10 <sup>0</sup>
1251	85.15	11.04	Classical	9.80×10 <sup>-4</sup>	3.98×10 <sup>0</sup>		9.04×10 <sup>-9</sup>	6.01×10 <sup>0</sup>		-2.26×10 <sup>-4</sup>		3.73	0.9982	2.64×10 <sup>-4</sup>	6.81×10 <sup>0</sup>
1260	101.15	9.96	Classical	2.20×10 <sup>-4</sup>	8.31×10 <sup>-1</sup>		5.58×10 <sup>-11</sup>	9.78×10 <sup>-3</sup>		-7.15×10 <sup>-7</sup>		6.16	0.9999	2.07×10 <sup>-5</sup>	2.75×10 <sup>-1</sup>
1261	101.15	9.67	Classical	1.40×10 <sup>-4</sup>	4.67×10 <sup>-1</sup>		1.40×10 <sup>-11</sup>	1.33×10 <sup>-3</sup>		-1.32×10 <sup>-7</sup>		4.37	0.9999	1.04×10 <sup>-5</sup>	1.01×10 <sup>-1</sup>
1262	115.17	10.37	Classical	5.96×10 <sup>-4</sup>	3.63×10 <sup>-1</sup>		3.15×10 <sup>-9</sup>	4.61×10 <sup>-1</sup>		-3.69×10 <sup>-5</sup>		3.73	0.9980	1.56×10 <sup>-4</sup>	1.89×10 <sup>0</sup>
1263	115.17	10.06	Classical	9.50×10 <sup>-5</sup>	2.05×10 <sup>-1</sup>		3.16×10 <sup>-10</sup>	3.49×10 <sup>-3</sup>		-1.02×10 <sup>-6</sup>		3.73	0.9967	4.93×10 <sup>-5</sup>	1.64×10 <sup>-1</sup>
1264	129.20	10.41	Classical	1.05×10 <sup>-4</sup>	5.14×10 <sup>-2</sup>		5.00×10 <sup>-11</sup>	3.75×10 <sup>-4</sup>		-1.32×10 <sup>-7</sup>		6.16	0.9996	1.96×10 <sup>-5</sup>	5.38×10 <sup>-2</sup>
1265	157.26	9.93	Weighted	6.76×10 <sup>-8</sup>		4.78×10 <sup>-1</sup>	2.60×10 <sup>-18</sup>		5.46×10 <sup>-5</sup>		-9.84×10 <sup>-12</sup>	3.40	0.9972	4.48×10 <sup>-9</sup>	
1270	87.12	8.50	Classical	7.44×10 <sup>-5</sup>	5.81×10 <sup>-2</sup>		2.02×10 <sup>-11</sup>	2.35×10 <sup>-5</sup>		-2.11×10 <sup>-8</sup>		3.40	0.9996	1.25×10 <sup>-5</sup>	1.35×10 <sup>-2</sup>
1271	115.18	8.46	Classical	5.72×10 <sup>-5</sup>	3.87×10 <sup>-2</sup>		5.76×10 <sup>-12</sup>	8.94×10 <sup>-6</sup>		-6.94×10 <sup>-9</sup>		3.73	0.9998	6.66×10 <sup>-6</sup>	8.30×10 <sup>-3</sup>

## 8. Thermodynamic and kinetic parameters of each molecule

Table IX-18. Physico-chemical parameters of tertiary amines.

N°	M	pKa	Regression	k <sub>1</sub>	k <sub>2</sub>	E	σ <sup>2</sup> k <sub>1</sub>	σ <sup>2</sup> k <sub>2</sub>	σ <sup>2</sup> ε	COV(k <sub>1</sub> ,k <sub>2</sub> )	COV(k <sub>1</sub> ,ε)	Fisher	R <sup>2</sup>	CIk <sub>1</sub>	CIk <sub>2</sub>
1300	59.11	9.75	Weighted	9.44×10 <sup>-8</sup>		4.37×10 <sup>-1</sup>	4.24×10 <sup>-18</sup>		3.96×10 <sup>-4</sup>		-3.40×10 <sup>-11</sup>	3.73	0.9981	5.72×10 <sup>-9</sup>	
1301	87.16	9.98	Weighted	1.06×10 <sup>-7</sup>		1.78×10 <sup>0</sup>	1.46×10 <sup>-17</sup>		7.31×10 <sup>-4</sup>		-8.51×10 <sup>-11</sup>	4.37	0.9961	1.22×10 <sup>-9</sup>	
1302	87.16	10.35	Weighted	9.86×10 <sup>-8</sup>		7.11×10 <sup>-1</sup>	1.70×10 <sup>-16</sup>		3.72×10 <sup>-2</sup>		-2.33×10 <sup>-9</sup>	3.73	0.9346	3.62×10 <sup>-9</sup>	
1310	149.19	7.77	Weighted	2.47×10 <sup>-8</sup>		6.32×10 <sup>-3</sup>	1.21×10 <sup>-18</sup>		1.36×10 <sup>-4</sup>		-1.07×10 <sup>-11</sup>	4.37	0.9941	3.51×10 <sup>-9</sup>	
1311	119.16	8.56	Weighted	8.92×10 <sup>-8</sup>		-8.65×10 <sup>-2</sup>	2.48×10 <sup>-17</sup>		7.12×10 <sup>-3</sup>		-3.40×10 <sup>-10</sup>	4.37	0.9907	1.59×10 <sup>-8</sup>	
1312	89.14	9.25	Weighted	1.70×10 <sup>-7</sup>		-2.35×10 <sup>-1</sup>	3.60×10 <sup>-17</sup>		7.17×10 <sup>-3</sup>		-4.82×10 <sup>-10</sup>	4.37	0.9963	1.91×10 <sup>-8</sup>	
1313	117.19	9.80	Weighted	5.86×10 <sup>-7</sup>		-7.42×10 <sup>-2</sup>	2.27×10 <sup>-16</sup>		2.07×10 <sup>-2</sup>		-1.73×10 <sup>-9</sup>	4.37	0.9980	4.80×10 <sup>-8</sup>	
1314	117.19	10.26	Weighted	8.06×10 <sup>-7</sup>		5.22×10 <sup>-1</sup>	1.33×10 <sup>-15</sup>		1.10×10 <sup>-1</sup>		-1.06×10 <sup>-8</sup>	4.37	0.9939	1.16×10 <sup>-7</sup>	
1315	161.24	9.07	Weighted	2.93×10 <sup>-7</sup>		-2.75×10 <sup>-1</sup>	3.62×10 <sup>-16</sup>		7.82×10 <sup>-3</sup>		-1.49×10 <sup>-9</sup>	4.37	0.9875	6.06×10 <sup>-9</sup>	
1316	103.17	9.45	Weighted	1.23×10 <sup>-7</sup>		1.90×10 <sup>-1</sup>	6.38×10 <sup>-17</sup>		4.79×10 <sup>-3</sup>		-4.85×10 <sup>-10</sup>	4.37	0.9875	2.54×10 <sup>-9</sup>	
1320	133.19	8.99	Weighted	1.00×10 <sup>-6</sup>		-3.44×10 <sup>-1</sup>	3.11×10 <sup>-15</sup>		1.01×10 <sup>-1</sup>		-1.51×10 <sup>-8</sup>	4.37	0.9908	1.77×10 <sup>-7</sup>	
1321	98.15	7.08	Weighted	2.45×10 <sup>-9</sup>		3.33×10 <sup>-3</sup>	3.50×10 <sup>-20</sup>		6.48×10 <sup>-6</sup>		-3.83×10 <sup>-13</sup>	4.37	0.9829	5.96×10 <sup>-10</sup>	
1330	99.18	10.08	Weighted	6.66×10 <sup>-8</sup>		6.52×10 <sup>-1</sup>	1.63×10 <sup>-17</sup>		2.82×10 <sup>-3</sup>		-1.81×10 <sup>-10</sup>	6.16	0.9927	1.74×10 <sup>-8</sup>	
1331	85.15	10.31	Weighted	1.59×10 <sup>-7</sup>		8.88×10 <sup>-1</sup>	1.31×10 <sup>-16</sup>		1.45×10 <sup>-2</sup>		-1.17×10 <sup>-9</sup>	4.37	0.9847	3.65×10 <sup>-9</sup>	
1340	115.17	9.10	Weighted	2.77×10 <sup>-8</sup>		-1.29×10 <sup>-2</sup>	3.85×10 <sup>-18</sup>		1.21×10 <sup>-3</sup>		-5.94×10 <sup>-11</sup>	4.37	0.9851	6.25×10 <sup>-9</sup>	
1341	115.18	8.81	Weighted	3.40×10 <sup>-8</sup>		2.07×10 <sup>-2</sup>	3.33×10 <sup>-18</sup>		5.14×10 <sup>-4</sup>		-3.45×10 <sup>-11</sup>	4.37	0.9914	5.81×10 <sup>-9</sup>	
1342	129.20	9.67	Weighted	2.37×10 <sup>-7</sup>		3.52×10 <sup>-1</sup>	1.46×10 <sup>-16</sup>		1.92×10 <sup>-2</sup>		-1.47×10 <sup>-9</sup>	4.37	0.9923	3.85×10 <sup>-8</sup>	
1343	115.17	9.73	Weighted	3.95×10 <sup>-7</sup>		2.45×10 <sup>-1</sup>	1.74×10 <sup>-16</sup>		3.82×10 <sup>-3</sup>		-6.39×10 <sup>-10</sup>	3.73	0.9956	3.66×10 <sup>-8</sup>	

N°	M	pKa	Regression	$k_1$	$k_2$	E	$\sigma^2 k_1$	$\sigma^2 k_2$	$\sigma^2 \varepsilon$	COV( $k_1, k_2$ )	COV( $k_1, \varepsilon$ )	Fisher	R <sup>2</sup>	CI $k_1$	CI $k_2$
1344	129.20	9.51	Weighted	$2.75 \times 10^{-7}$		$8.63 \times 10^{-2}$	$1.27 \times 10^{-16}$		$4.00 \times 10^{-3}$		$-5.40 \times 10^{-10}$	3.73	0.9933	$3.12 \times 10^{-8}$	
1345	143.23	9.97	Weighted	$1.03 \times 10^{-6}$		$-7.97 \times 10^{-1}$	$2.76 \times 10^{-15}$		$1.93 \times 10^{-1}$		$-1.92 \times 10^{-8}$	4.37	0.9922	$1.67 \times 10^{-7}$	
1346	141.21	10.18	Weighted	$2.02 \times 10^{-7}$		$2.98 \times 10^0$	$7.85 \times 10^{-17}$		$1.32 \times 10^{-2}$		$-9.55 \times 10^{-10}$	3.73	0.9923	$2.46 \times 10^{-8}$	
1350	101.15	7.50	Weighted	$2.70 \times 10^{-9}$		$3.13 \times 10^{-3}$	$4.56 \times 10^{-20}$		$9.46 \times 10^{-6}$		$-5.38 \times 10^{-13}$	4.37	0.9816	$6.79 \times 10^{-10}$	
1351	161.20	6.78	Weighted	$3.43 \times 10^{-9}$		$3.48 \times 10^{-4}$	$2.89 \times 10^{-20}$		$5.57 \times 10^{-6}$		$-2.66 \times 10^{-13}$	3.73	0.9903	$4.72 \times 10^{-10}$	
1352	141.21	8.24	Weighted	$9.14 \times 10^{-9}$		$1.55 \times 10^{-2}$	$7.54 \times 10^{-19}$		$4.51 \times 10^{-5}$		$-4.54 \times 10^{-12}$	4.37	0.9736	$2.76 \times 10^{-9}$	
1353	138.21	7.57	Weighted	$2.00 \times 10^{-9}$		$8.98 \times 10^{-3}$	$9.23 \times 10^{-22}$		$2.03 \times 10^{-8}$		$-4.05 \times 10^{-15}$	3.73	0.9991	$8.43 \times 10^{-11}$	

## 8. Thermodynamic and kinetic parameters of each molecule

Table IX-19. Physico-chemical parameters of multi-amines.

N°	M	pKa	Regression	$k_1$	$k_2$	$\epsilon$	$\sigma^2 k_1$	$\sigma^2 k_2$	$\sigma^2 \epsilon$	COV( $k_1, k_2$ )	COV( $k_1, \epsilon$ )	Fisher	R <sup>2</sup>	CI $k_1$	CI $k_2$
2200	86.14	9.60-5.48	Classical	$3.35 \times 10^{-4}$	$8.30 \times 10^{-1}$		$1.74 \times 10^{-10}$	$3.12 \times 10^{-2}$		$-2.25 \times 10^{-6}$		3.73	0.9997	$3.66 \times 10^{-5}$	$4.91 \times 10^{-1}$
2201	100.17	9.10-4.67	Classical	$8.04 \times 10^{-5}$	$1.39 \times 10^{-1}$		$6.29 \times 10^{-11}$	$1.61 \times 10^{-4}$		$-9.77 \times 10^{-8}$		3.73	0.9994	$2.20 \times 10^{-5}$	$3.53 \times 10^{-2}$
2300	116.20	9.19-5.87	Weighted	$4.35 \times 10^{-8}$		$-1.15 \times 10^{-1}$	$1.17 \times 10^{-17}$		$1.91 \times 10^{-3}$		$-1.29 \times 10^{-10}$	4.37	0.9819	$1.09 \times 10^{-8}$	

## 9 Molecular descriptors

### 9.1 Complete list of molecular descriptors

Table IX-20. List of descriptors used for QSPR modelling. Descriptors in bold have been retained after a hierarchical clustering analysis.

Number	Descriptor	Class	Class (stat.)	Long name	Unit
<b>1</b>	<b>HOMO(g)</b>	<b>1</b>	<b>1</b>	<b>Highest occupied molecular orbital</b>	<b>Ha</b>
<b>2</b>	<b>LUMO(g)</b>	<b>1</b>	<b>2</b>	<b>Lowest unoccupied molecular orbital</b>	<b>Ha</b>
3	HOMO-LUMO(g)	1	1	-	Ha
4	Dipole(g)	1	2	-	D
<b>5</b>	<b>Alpha</b>	<b>2</b>	<b>6</b>	-	<b>e<sup>2</sup>.a<sub>0</sub><sup>2</sup>.Ha</b>
<b>6</b>	<b>Beta</b>	<b>2</b>	<b>6</b>	-	<b>e<sup>3</sup>.a<sub>0</sub><sup>3</sup>.Ha</b>
7	HOMO(aq)	1	1	Highest occupied molecular orbital	Ha
<b>8</b>	<b>LUMO(aq)</b>	<b>1</b>	<b>2</b>	<b>Lowest unoccupied molecular orbital</b>	<b>Ha</b>
9	HOMO-LUMO(aq)	1	1	-	Ha
10	Dipole(aq)	1	2	-	D
11	Esolv	3	3	Solvation energy	kcal.mol <sup>-1</sup>
12	pKa	4	2	-	-
13	Rotatable bonds	5	7	-	-
14	Hydrogen bond donor	5	4	-	-
15	Hydrogen bond acceptor	5	3	-	-
16	Chiral centers	5	8	-	-
17	AlogP	6	4	-	-
18	AlogP98	6	4	-	-
19	Molecular refractivity	6	6	-	-
20	<b>Molecular flexibility</b>	<b>7</b>	<b>7</b>	-	-
21	<b>Balaban index JX</b>	<b>7</b>	<b>10</b>	-	-
22	Balaban index JY	7	10	-	-
23	Wiener index	7	6	-	-
24	<b>Zagreb index</b>	<b>7</b>	<b>12</b>	-	-
25	<b>Kappa-1</b>	<b>7</b>	<b>6</b>	-	-
26	Kappa-2	7	7	-	-
27	<b>Kappa-3</b>	<b>7</b>	<b>7</b>	-	-
28	Kappa-1 (alphamodified)	7	6	-	-
29	Kappa-2 (alphamodified)	7	7	-	-
30	Kappa-3 (alpha modified)	7	7	-	-
31	Subgraph counts (0): path	7	12	-	-

## 9. Molecular descriptors

Number	Descriptor	Class	Class (stat.)	Long name	Unit
32	Subgraph counts (1): path	7	12	-	-
33	Subgraph counts (2): path	7	12	-	-
34	<b>Subgraph counts (3): path</b>	7	12	-	-
35	<b>Subgraph counts (3): cluster</b>	7	11	-	-
36	Chi (0)	7	6	-	-
37	<b>Chi (1)</b>	7	12	-	-
38	Chi (2)	7	12	-	-
39	Chi (3): path	7	12	-	-
40	<b>Chi (3): cluster</b>	7	11	-	-
41	Chi (0) (valence modified)	7	6	-	-
42	<b>Chi (1) (valence modified)</b>	7	12	-	-
43	<b>Chi (2) (valence modified)</b>	7	12	-	-
44	<b>Chi (3): path (valence modified)</b>	7	12	-	-
45	Chi (3): cluster (valence modified)	7	11	-	-
46	<b>Information content (IC)</b>	8	9	-	-
47	<b>Bond information content (BIC)</b>	8	9	-	-
48	<b>Complementary information content (CIC)</b>	8	9	-	-
49	Structural information content (SIC)	8	9	-	-
50	Edge adjacency/magnitude	8	12	-	-
51	<b>Edge distance/magnitude</b>	8	12	-	-
52	Vertex adjacency/equality	8	12	-	-
53	Vertex adjacency/magnitude	8	12	-	-
54	Vertex distance/equality	8	6	-	-
55	<b>Vertex distance/magnitude</b>	8	6	-	-
56	<b>Atomic composition (total)</b>	8	6	-	-
57	<b>E-state keys (sums): S<sub>ssCH2</sub></b>	9	4	-	-
58	Molecular area (vdW area)	10	6	Van der Waals area	Å <sup>2</sup>

Number	Descriptor	Class	Class (stat.)	Long name	Unit
59	Molecular volume (vdW volume)	10	6	Van der Waals volume	Å <sup>3</sup>
<b>60</b>	<b>Molecular density</b>	<b>11</b>	<b>3</b>	-	<b>g.cm<sup>-3</sup></b>
61	Principal moments of inertia (magnitude)	12	6	-	u.Å <sup>2</sup>
<b>62</b>	<b>Principal moment of inertia X</b>	<b>12</b>	<b>11</b>	-	<b>u.Å<sup>2</sup></b>
<b>63</b>	<b>Principal moment of inertia Y</b>	<b>12</b>	<b>6</b>	-	<b>u.Å<sup>2</sup></b>
64	Principal moment of inertia Z	12	6	-	u.Å <sup>2</sup>
65	Radius of gyration	13	6	-	-
<b>66</b>	<b>Ellipsoidal volume</b>	<b>14</b>	<b>6</b>	-	<b>Å<sup>3</sup></b>
67	Shadow area: XY plane	15	6	-	Å <sup>2</sup>
<b>68</b>	<b>Shadow area: YZ plane</b>	<b>15</b>	<b>11</b>	-	<b>Å<sup>2</sup></b>
69	Shadow area: ZX plane	15	6	-	Å <sup>2</sup>
<b>70</b>	<b>Shadow area fraction: XY plane</b>	<b>15</b>	<b>8</b>	-	<b>Å<sup>2</sup></b>
<b>71</b>	<b>Shadow area fraction: YZ plane</b>	<b>15</b>	<b>8</b>	-	<b>Å<sup>2</sup></b>
<b>72</b>	<b>Shadow area fraction: ZX plane</b>	<b>15</b>	<b>8</b>	-	<b>Å<sup>2</sup></b>
<b>73</b>	<b>Shadow length: LX</b>	<b>15</b>	<b>6</b>	-	<b>Å</b>
<b>74</b>	<b>Shadow length: LY</b>	<b>15</b>	<b>11</b>	-	<b>Å</b>
<b>75</b>	<b>Shadow length: LZ</b>	<b>15</b>	<b>11</b>	-	<b>Å</b>
<b>76</b>	<b>Shadow ratio</b>	<b>15</b>	<b>7</b>	-	<b>-</b>
77	Dipole moment (magnitude)	16	2	-	D
<b>78</b>	<b>Dipole moment X</b>	<b>16</b>	<b>2</b>	-	<b>D</b>
<b>79</b>	<b>Dipole moment Y</b>	<b>16</b>	<b>8</b>	-	<b>D</b>
<b>80</b>	<b>Dipole moment Z</b>	<b>16</b>	<b>2</b>	-	<b>D</b>
81	SASA	17	6	Total molecular solvent-accessible surface	Å <sup>2</sup>
82	PPSA1	17	6	Partial positive surface area	Å <sup>2</sup>
83	PNSA1	17	5	Partial negative surface area	Å <sup>2</sup>
<b>84</b>	<b>DPSA1</b>	<b>17</b>	<b>5</b>	<b>Difference in charged partial surface areas</b>	<b>Å<sup>2</sup></b>
85	PPSA2	17	10	Total charge-weighted positive surface area	Å <sup>2</sup>
<b>86</b>	<b>PNSA2</b>	<b>17</b>	<b>5</b>	<b>Total charge-weighted negative surface area</b>	<b>Å<sup>2</sup></b>

## 9. Molecular descriptors

Number	Descriptor	Class	Class (stat.)	Long name	Unit
87	DPSA2	17	10	Difference in total charge-weighted surface areas	Å <sup>2</sup>
88	PPSA3	17	10	Atomic charge-weighted positive surface area	Å <sup>2</sup>
89	PNSA3	17	3	Atomic charge-weighted negative surface area	Å <sup>2</sup>
90	DPSA3	17	3	Difference in atomic charge-weighted surface areas	Å <sup>2</sup>
91	FPSA1	17	5	Fractional partial positive surface area	Å <sup>2</sup>
92	FPSA2	17	10	Fractional charge-weighted positive surface area	Å <sup>2</sup>
93	FPSA3	17	4	Fractional atomic charge-weighted positive surface area	Å <sup>2</sup>
94	FNSA1	17	5	Fractional partial negative surface area	Å <sup>2</sup>
95	FNSA2	17	5	Fractional charge-weighted negative surface area	Å <sup>2</sup>
96	FNSA3	17	4	Fractional atomic charge-weighted negative surface area	Å <sup>2</sup>
97	WPSA1	17	6	Surface-weighted partial positive surface area	
98	WPSA2	17	10	Surface-weighted charge-weighted positive surface area	Å <sup>2</sup>
99	WPSA3	17	10	Surface-weighted atomic charge-weighted positive surface area	Å <sup>2</sup>
100	WNSA1	17	5	Surface-weighted partial negative surface area	Å <sup>2</sup>
101	WNSA2	17	5	Surface-weighted charge-weighted negative surface area	Å <sup>2</sup>
102	WNSA3	17	3	Surface-weighted atomic charge-weighted negative surface area	Å <sup>2</sup>
103	RPCG	17	10	Relative positive charge	-
104	RNCG	17	10	Relative negative charge	-
105	RPCS	17	10	Relative positive charge surface area	-
106	RNCS	17	10	Relative negative charge	-

Number	Descriptor	Class	Class (stat.)	Long name	Unit
				<b>surface area</b>	
107	TPSA	17	4	Total polar surface area	Å <sup>2</sup>
<b>108</b>	<b>TASA</b>	<b>17</b>	<b>6</b>	<b>Total apolar surface area</b>	<b>Å<sup>2</sup></b>
109	RPSA	17	4	Relative polar surface area	Å <sup>2</sup>
<b>110</b>	<b>RASA</b>	<b>17</b>	<b>4</b>	<b>Relative apolar surface area</b>	<b>Å<sup>2</sup></b>
<b>111</b>	<b>Experimental pKa</b>	<b>4</b>	-	-	-
<b>112</b>	<b>Nitrogen accessible surface</b>	<b>18</b>	-	-	<b>Å<sup>2</sup></b>

## 9. Molecular descriptors

### 9.2 Values of molecular descriptors for primary amines

Table IX-21. Values of the 68 retained descriptors for primary amines. The numbers of the left column indicate the number of the amine. The numbers of the top line indicate the number of the descriptor.

	1	2	5	6	8	9	10	11	12	13	14	15	16	18	20	21	24
1100	-0.2462	-0.0136	26.4	18.2	-0.0113	-0.2550	2.15	-4.26	10.08	0	2	1	0	-0.65	0.00	0.93	2
1101	-0.2452	-0.0126	63.8	0.3	-0.0103	-0.2557	2.24	-3.99	10.21	2	2	1	0	0.68	3.93	2.16	14
1102	-0.2463	-0.0152	51.4	-16.6	-0.0124	-0.2535	2.31	-4.16	10.43	0	2	1	0	0.08	1.28	2.27	12
1103	-0.2460	-0.0145	70.0	-12.9	-0.0116	-0.2535	2.25	-3.74	10.45	0	2	1	0	0.75	1.10	2.16	26
1104	-0.2413	-0.0120	82.3	2.7	-0.0103	-0.2508	2.31	-3.94	10.45	0	2	1	0	1.21	1.69	2.10	30
1105	-0.2450	-0.0132	63.2	19.6	-0.0106	-0.2496	2.10	-3.22	10.24	1	2	1	0	0.54	2.19	2.50	16
1106	-0.2458	-0.0164	63.4	35.4	-0.0141	-0.2509	2.21	-4.16	10.65	0	2	1	0	0.28	0.97	2.97	20
1110	-0.2427	-0.0194	93.1	13.7	-0.0273	-0.2300	2.14	-4.67	9.51	1	2	1	0	0.94	1.65	2.82	34
1111	-0.2424	-0.0216	105.7	82.8	-0.0238	-0.2346	2.37	-6.18	9.73	1	2	1	1	1.31	1.85	2.83	40
1112	-0.2408	-0.0206	105.7	67.3	-0.0223	-0.2291	1.56	-4.89	9.73	1	2	1	1	1.31	1.85	2.83	40
1113	-0.2466	-0.0164	106.4	-10.5	-0.0219	-0.2323	2.06	-5.48	9.79	2	2	1	0	1.26	2.28	2.60	38
1120	-0.2448	-0.0155	43.4	40.2	-0.0137	-0.2548	1.98	-9.97	9.55	2	3	2	0	-1.19	2.86	1.86	10
1121	-0.2483	-0.0152	56.0	40.1	-0.0113	-0.2561	4.16	-11.33	9.84	3	3	2	0	-1.12	3.86	2.10	14
1122	-0.2477	-0.0143	68.6	33.1	-0.0106	-0.2476	1.80	-10.82	9.90	4	3	2	0	-0.54	4.85	2.27	18
1123	-0.2462	-0.0142	94.1	34.9	-0.0109	-0.2465	1.85	-10.69	10.21	6	3	2	0	0.37	6.85	2.48	26
1124	-0.2602	-0.0195	55.7	69.8	-0.0122	-0.2534	3.34	-8.49	9.60	2	3	2	1	-0.81	2.14	2.43	16

	<b>1</b>	<b>2</b>	<b>5</b>	<b>6</b>	<b>8</b>	<b>9</b>	<b>10</b>	<b>11</b>	<b>12</b>	<b>13</b>	<b>14</b>	<b>15</b>	<b>16</b>	<b>18</b>	<b>20</b>	<b>21</b>	<b>24</b>
1125	-0.2507	-0.0150	55.6	17.4	-0.0119	-0.2583	1.64	-10.29	9.79	2	3	2	1	-0.81	2.14	2.43	16
1126	-0.2440	-0.0153	67.9	42.0	-0.0132	-0.2536	1.90	-9.17	9.84	3	3	2	1	-0.29	3.08	2.66	20
1127	-0.2448	-0.0205	67.4	64.1	-0.0155	-0.2493	3.99	-9.51	10.04	2	3	2	0	-0.60	1.56	3.06	24
1128	-0.2544	-0.0223	71.3	29.8	-0.0181	-0.2492	2.29	-13.71	9.48	4	4	3	0	-1.49	2.22	3.21	28
1129	-0.2455	-0.0230	75.8	98.2	-0.0140	-0.2526	3.80	-18.29	8.95	6	5	4	0	-2.38	2.93	3.39	32
1130	-0.2462	-0.0141	87.1	42.2	-0.0098	-0.2535	2.06	-11.15	10.15	1	3	2	0	-0.03	1.86	2.15	36
1131	-0.2512	-0.0146	55.9	18.6	-0.0102	-0.2588	1.81	-8.10	9.45	2	2	2	0	-0.78	3.86	2.02	14
1132	-0.2521	-0.0154	74.1	-36.6	-0.0117	-0.2508	2.25	-14.63	9.45	5	3	3	0	-1.32	5.78	2.27	22
1140	-0.2730	-0.0263	52.2	-32.5	-0.0135	-0.2611	5.17	-9.89	7.85	2	2	2	0	-0.67	3.07	2.41	14

## 9. Molecular descriptors

	<b>25</b>	<b>27</b>	<b>34</b>	<b>35</b>	<b>37</b>	<b>40</b>	<b>42</b>	<b>43</b>	<b>44</b>	<b>46</b>	<b>47</b>	<b>48</b>	<b>51</b>	<b>55</b>	<b>56</b>	<b>57</b>	<b>60</b>
1100	2.0	0.0	0	0	1.00	0.00	0.58	0.00	0.00	0.00	0.00	1.00	0.00	4.00	8.04	0.00	0.773
1101	5.0	4.0	2	0	2.41	0.00	2.12	1.14	0.56	1.52	0.76	0.80	55.14	103.66	17.95	3.23	0.809
1102	4.0	0.0	0	1	1.73	0.58	1.49	1.24	0.00	0.81	0.51	1.19	23.26	56.05	14.82	0.00	0.799
1103	4.2	1.0	7	1	2.89	0.29	2.65	2.04	1.40	1.92	0.74	0.67	172.93	172.66	19.82	5.25	0.878
1104	5.1	1.5	8	1	3.39	0.29	3.15	2.40	1.65	1.84	0.66	0.96	258.01	257.49	22.82	6.66	0.875
1105	5.0	4.0	2	1	2.27	0.41	1.97	1.63	0.47	1.92	0.96	0.40	56.00	104.93	17.95	0.81	0.808
1106	5.0	0.0	0	4	2.00	2.00	1.79	2.37	0.00	0.72	0.36	1.60	57.36	106.25	17.95	0.00	0.809
1110	6.1	1.8	10	1	3.93	0.20	2.67	1.69	1.08	2.16	0.62	0.84	362.46	361.11	21.31	0.64	0.956
1111	7.1	2.0	12	2	4.30	0.50	3.11	2.20	1.33	2.20	0.61	0.97	487.52	486.38	24.38	0.00	0.942
1112	7.1	2.0	12	2	4.30	0.50	3.11	2.20	1.33	2.20	0.61	0.97	487.52	486.38	24.38	0.00	0.940
1113	7.1	2.4	11	1	4.43	0.20	3.17	2.02	1.28	2.42	0.67	0.75	485.80	484.06	24.38	1.73	0.943
1120	4.0	4.0	1	0	1.91	0.00	1.22	0.51	0.13	1.00	0.63	1.00	22.50	55.14	16.40	0.47	0.934
1121	5.0	4.0	2	0	2.41	0.00	1.72	0.87	0.36	1.52	0.76	0.80	55.14	103.66	20.02	1.53	0.916
1122	6.0	5.3	3	0	2.91	0.00	2.22	1.22	0.61	1.58	0.68	1.00	103.66	169.35	23.43	2.75	0.899
1123	8.0	7.2	5	0	3.91	0.00	3.22	1.93	1.11	1.50	0.53	1.50	253.28	356.33	29.93	5.42	0.883
1124	5.0	4.0	2	1	2.27	0.41	1.65	1.08	0.34	1.92	0.96	0.40	56.00	104.93	20.02	0.36	0.921
1125	5.0	4.0	2	1	2.27	0.41	1.64	1.16	0.29	1.92	0.96	0.40	56.00	104.93	20.02	0.08	0.914

	<b>25</b>	<b>27</b>	<b>34</b>	<b>35</b>	<b>37</b>	<b>40</b>	<b>42</b>	<b>43</b>	<b>44</b>	<b>46</b>	<b>47</b>	<b>48</b>	<b>51</b>	<b>55</b>	<b>56</b>	<b>57</b>	<b>60</b>
1126	6.0	3.0	4	1	2.81	0.29	2.17	1.35	0.76	1.92	0.83	0.67	105.07	171.36	23.43	0.97	0.905
1127	6.0	5.3	3	4	2.56	1.56	1.96	2.15	0.41	1.79	0.77	0.79	105.97	172.72	23.43	0.05	0.906
1128	7.0	2.7	6	4	3.12	1.21	2.13	1.97	0.72	1.95	0.75	0.86	172.62	258.01	27.00	-0.35	0.983
1129	8.0	2.2	9	4	3.68	0.93	2.30	1.84	0.94	1.81	0.65	1.19	258.41	363.21	29.90	-1.21	1.059
1130	6.1	1.8	10	2	3.79	0.58	3.22	2.57	1.74	1.50	0.50	1.50	362.69	361.57	28.62	3.81	0.944
1131	5.0	4.0	2	0	2.41	0.00	1.61	0.78	0.32	1.52	0.76	0.80	55.14	103.66	20.02	1.29	0.910
1132	7.0	6.0	4	0	3.41	0.00	2.30	1.12	0.50	1.56	0.60	1.25	169.35	253.28	27.00	1.55	0.977
1140	5.0	4.0	2	0	2.41	0.00	1.49	0.70	0.26	2.32	0.90	0.00	55.14	103.66	15.79	0.95	0.942

## 9. Molecular descriptors

	<b>62</b>	<b>63</b>	<b>66</b>	<b>68</b>	<b>70</b>	<b>71</b>	<b>72</b>	<b>73</b>	<b>74</b>	<b>75</b>	<b>76</b>	<b>78</b>	<b>79</b>	<b>80</b>	<b>84</b>	<b>86</b>	<b>87</b>
1100	4.89	22.28	24.76	11.63	0.76	0.71	0.70	4.74	4.16	3.94	1.20	-0.42	-0.33	1.17	-38.71	-113.63	185.46
1101	27.96	259.68	127.97	15.06	0.70	0.77	0.75	9.16	4.61	4.23	2.17	-0.07	0.81	-0.95	60.90	-133.46	345.29
1102	60.67	63.78	41.23	18.27	0.66	0.60	0.63	6.73	6.02	5.07	1.33	-0.03	0.10	1.27	137.30	-86.84	420.06
1103	79.67	169.25	69.79	22.68	0.66	0.67	0.66	7.21	6.66	5.10	1.41	0.07	0.12	1.21	90.38	-111.99	338.34
1104	119.31	230.94	76.05	25.01	0.66	0.71	0.68	8.28	6.73	5.19	1.59	-1.11	-0.47	-0.45	121.73	-128.16	447.44
1105	67.99	147.78	76.14	21.14	0.64	0.65	0.66	7.82	6.25	5.20	1.50	-0.23	-1.13	0.53	138.62	-108.33	463.70
1106	110.46	111.08	45.30	23.42	0.66	0.64	0.67	6.73	6.12	6.01	1.12	-0.94	-0.33	-0.68	193.12	-69.47	589.28
1110	104.57	342.97	155.71	21.50	0.62	0.60	0.61	9.50	7.10	5.05	1.88	-0.55	-1.15	0.45	108.52	-144.46	456.58
1111	148.53	429.41	118.84	22.38	0.73	0.65	0.60	9.60	6.69	5.14	1.87	1.34	-0.13	0.32	117.27	-194.42	617.11
1112	147.79	469.55	177.45	26.17	0.65	0.58	0.56	9.49	6.95	6.44	1.47	-0.71	-0.65	-0.17	157.28	-159.69	633.20
1113	113.93	595.78	216.57	23.09	0.64	0.71	0.64	10.54	6.70	4.88	2.16	-0.08	-0.48	-1.12	96.44	-232.48	661.46
1120	33.50	93.72	57.58	16.34	0.66	0.59	0.59	6.93	5.32	5.20	1.33	-0.10	-0.94	-0.12	-9.15	-189.76	364.39
1121	25.39	253.91	139.62	15.05	0.68	0.77	0.70	8.89	4.61	4.26	2.09	-0.13	2.26	-0.81	33.54	-190.28	438.99
1122	30.39	444.25	207.31	16.11	0.68	0.79	0.73	10.14	4.81	4.23	2.40	0.20	0.77	-0.91	-9.13	-289.75	561.54
1123	42.85	1052.57	345.07	15.95	0.71	0.79	0.77	12.72	4.79	4.22	3.02	0.18	0.77	-0.95	-137.25	-505.86	726.29
1124	58.94	141.89	52.84	17.94	0.63	0.60	0.66	7.74	5.84	5.14	1.51	-2.12	2.17	0.11	75.40	-179.85	516.61
1125	64.40	140.86	74.59	20.65	0.64	0.65	0.61	7.57	6.12	5.22	1.45	0.11	-0.81	0.32	117.61	-127.33	487.61

	<b>62</b>	<b>63</b>	<b>66</b>	<b>68</b>	<b>70</b>	<b>71</b>	<b>72</b>	<b>73</b>	<b>74</b>	<b>75</b>	<b>76</b>	<b>78</b>	<b>79</b>	<b>80</b>	<b>84</b>	<b>86</b>	<b>87</b>
1126	67.46	264.54	111.27	18.72	0.64	0.60	0.66	9.01	6.13	5.09	1.77	-0.27	-0.91	0.44	75.33	-170.70	471.73
1127	111.86	192.01	79.29	23.75	0.67	0.63	0.65	7.33	6.17	6.08	1.21	-0.17	-0.84	-2.24	126.00	-181.91	695.74
1128	114.12	303.44	130.79	24.49	0.63	0.65	0.65	8.30	6.18	6.06	1.37	2.13	-1.00	-0.84	76.32	-255.16	705.77
1129	213.13	302.21	107.07	27.86	0.63	0.69	0.67	7.84	6.69	6.04	1.30	0.65	2.00	-1.20	100.50	-276.87	851.83
1130	119.49	381.46	118.26	25.31	0.66	0.71	0.67	9.02	6.72	5.27	1.71	-0.34	0.06	-1.14	95.95	-253.17	743.88
1131	34.16	212.80	108.76	17.75	0.64	0.61	0.63	8.44	5.60	5.21	1.62	-1.04	0.62	-0.04	62.57	-140.17	374.27
1132	33.02	640.46	260.95	15.69	0.69	0.78	0.74	11.11	4.71	4.25	2.61	0.34	1.34	0.83	-133.23	-598.54	836.19
1140	19.65	221.07	170.85	16.13	0.64	0.78	0.70	8.26	4.86	4.25	1.95	-2.99	2.87	-0.93	45.70	-150.65	371.93

## 9. Molecular descriptors

	<b>88</b>	<b>92</b>	<b>93</b>	<b>96</b>	<b>97</b>	<b>98</b>	<b>99</b>	<b>100</b>	<b>102</b>	<b>103</b>	<b>104</b>	<b>105</b>	<b>106</b>	<b>108</b>	<b>110</b>	<b>111</b>	<b>112</b>
1100	22.73	0.42	0.132	-0.135	11.43	12.34	3.90	18.08	-3.97	0.39	0.85	3.49	17.09	85.12	0.50	10.70	8.91
1101	21.14	0.79	0.079	-0.075	44.14	56.82	5.67	27.81	-5.39	0.30	0.74	0.36	11.85	196.70	0.73	10.66	8.49
1102	27.00	1.42	0.115	-0.087	43.47	78.01	6.32	11.33	-4.76	0.36	0.53	0.00	7.31	159.19	0.68	10.72	8.17
1103	18.59	0.85	0.070	-0.056	47.84	60.53	4.97	23.67	-3.99	0.40	0.79	0.00	9.50	205.28	0.77	10.67	7.84
1104	19.04	1.12	0.067	-0.061	57.95	90.99	5.43	23.26	-4.99	0.32	0.63	0.00	9.86	223.68	0.78	10.60	8.00
1105	27.75	1.37	0.107	-0.064	51.88	92.46	7.22	15.82	-4.36	0.21	0.49	0.00	5.06	180.94	0.70	10.37	7.62
1106	30.28	2.06	0.120	-0.081	56.33	131.35	7.65	7.53	-5.16	0.36	0.43	0.00	5.65	183.15	0.72	10.67	7.82
1110	30.57	1.06	0.103	-0.062	59.69	92.23	9.03	27.62	-5.41	0.20	0.53	5.83	5.61	217.62	0.74	9.43	8.24
1111	31.74	1.33	0.100	-0.060	68.83	133.99	10.06	31.66	-6.06	0.26	0.45	0.00	4.41	255.26	0.81	9.36	7.70
1112	32.43	1.49	0.102	-0.076	75.32	150.27	10.29	25.40	-7.68	0.19	0.46	0.00	6.99	245.38	0.77	9.32	7.65
1113	34.96	1.32	0.108	-0.083	68.34	139.25	11.35	37.03	-8.75	0.27	0.47	0.45	7.59	251.05	0.77	9.84	8.46
1120	29.21	0.79	0.133	-0.148	23.28	38.49	6.44	25.30	-7.21	0.23	0.56	6.82	9.47	97.35	0.44	9.55	8.52
1121	31.48	0.99	0.125	-0.149	35.99	62.69	7.94	27.54	-9.46	0.23	0.55	6.65	8.86	123.24	0.49	10.03	8.48
1122	31.01	0.95	0.109	-0.139	39.45	77.59	8.85	42.06	-11.29	0.24	0.49	0.29	7.65	155.33	0.54	10.25	8.48
1123	30.70	0.63	0.088	-0.120	37.02	76.99	10.72	84.95	-14.62	0.19	0.47	5.72	7.46	218.27	0.62	10.47	8.49
1124	32.83	1.36	0.132	-0.125	40.18	83.61	8.15	21.46	-7.70	0.23	0.42	0.00	3.31	130.48	0.53	9.43	8.44
1125	32.67	1.46	0.133	-0.130	44.77	88.69	8.04	15.82	-7.87	0.27	0.50	0.00	6.84	125.30	0.51	9.49	8.16

	<b>88</b>	<b>92</b>	<b>93</b>	<b>96</b>	<b>97</b>	<b>98</b>	<b>99</b>	<b>100</b>	<b>102</b>	<b>103</b>	<b>104</b>	<b>105</b>	<b>106</b>	<b>108</b>	<b>110</b>	<b>111</b>	<b>112</b>
1126	26.74	1.10	0.098	-0.105	47.44	82.07	7.29	26.90	-7.80	0.23	0.54	6.83	7.03	170.97	0.63	9.53	7.44
1127	33.80	1.95	0.128	-0.136	51.51	135.70	8.93	18.24	-9.50	0.25	0.36	0.00	4.86	153.08	0.58	9.72	7.75
1128	34.10	1.64	0.124	-0.152	48.49	124.18	9.40	27.45	-11.51	0.21	0.39	0.00	4.07	130.47	0.47	8.76	7.63
1129	43.41	2.00	0.151	-0.180	55.68	165.14	12.47	26.82	-14.84	0.16	0.33	0.00	4.16	106.22	0.37	8.04	7.55
1130	31.74	1.63	0.106	-0.121	59.56	147.45	9.54	30.73	-10.96	0.22	0.41	0.00	6.63	185.81	0.62	10.04	8.04
1131	24.95	0.94	0.100	-0.100	38.88	58.37	6.22	23.28	-6.22	0.24	0.66	6.91	9.85	156.69	0.63	9.37	8.52
1132	32.29	0.77	0.105	-0.157	27.09	73.37	9.97	68.22	-14.92	0.20	0.37	0.14	5.58	167.52	0.54	9.46	8.50
1140	28.90	0.92	0.120	-0.178	34.46	53.26	6.95	23.46	-10.30	0.26	0.61	0.32	9.66	91.25	0.38	7.74	8.47

## 9. Molecular descriptors

### 9.3 Values of molecular descriptors for secondary amines

Table IX-22. Values of the 68 retained descriptors for secondary amines. The numbers of the left column indicate the number of the amine. The numbers of the top line indicate the number of the descriptor.

	1	2	5	6	8	9	10	11	12	13	14	15	16	18	20	21	24
1200	-0.2290	-0.0111	39.3	95.1	-0.0101	-0.2349	1.67	-3.88	10.52	0	1	1	0	-0.22	1.93	1.52	6
1201	-0.2220	-0.0107	63.4	29.8	-0.0092	-0.2301	1.85	-3.84	10.59	2	1	1	0	0.66	3.93	2.12	14
1202	-0.2216	-0.0111	76.0	59.7	-0.0091	-0.2206	1.66	-3.76	10.21	3	1	1	0	1.11	4.93	2.28	18
1203	-0.2271	-0.0107	89.5	103.9	-0.0096	-0.2298	1.52	-2.76	10.77	4	1	1	0	1.53	5.93	2.38	22
1204	-0.2290	-0.0114	64.0	70.9	-0.0100	-0.2354	1.80	-3.76	10.59	1	1	1	0	0.51	2.19	2.45	16
1205	-0.2272	-0.0122	94.5	65.1	-0.0111	-0.2326	1.76	-3.15	10.70	1	1	1	0	1.64	2.34	2.09	34
1210	-0.2323	-0.0182	107.0	94.3	-0.0225	-0.2171	1.66	-3.33	9.70	2	1	1	0	1.37	2.28	2.58	38
1211	-0.2318	-0.0182	120.2	84.9	-0.0232	-0.2159	1.67	-3.00	9.78	3	1	1	0	1.72	2.97	2.40	42
1212	-0.2355	-0.0194	124.9	-9.4	-0.0231	-0.2177	1.73	-9.64	9.18	5	2	2	0	0.83	3.65	2.23	46
1220	-0.2329	-0.0138	56.4	-10.0	-0.0104	-0.2369	1.96	-10.53	9.81	3	2	2	0	-0.76	3.86	2.06	14
1221	-0.2323	-0.0137	69.3	13.2	-0.0105	-0.2371	1.86	-10.29	9.89	4	2	2	0	-0.41	4.85	2.22	18
1222	-0.2317	-0.0139	81.8	-4.7	-0.0109	-0.2369	1.96	-10.29	10.01	5	2	2	0	0.12	5.85	2.34	22
1223	-0.2314	-0.0137	94.6	19.7	-0.0107	-0.2358	1.93	-9.86	10.00	6	2	2	0	0.57	6.85	2.44	26
1224	-0.2283	-0.0131	81.0	50.7	-0.0106	-0.2324	1.60	-10.37	9.97	4	2	2	0	-0.03	4.04	2.57	24
1225	-0.2304	-0.0138	112.7	28.5	-0.0113	-0.2378	1.95	-10.09	10.18	4	2	2	0	1.10	3.76	1.97	42
1226	-0.2282	-0.0144	92.6	53.0	-0.0121	-0.2313	1.78	-10.16	10.06	4	2	2	0	0.18	3.02	3.00	32

	<b>1</b>	<b>2</b>	<b>5</b>	<b>6</b>	<b>8</b>	<b>9</b>	<b>10</b>	<b>11</b>	<b>12</b>	<b>13</b>	<b>14</b>	<b>15</b>	<b>16</b>	<b>18</b>	<b>20</b>	<b>21</b>	<b>24</b>
1227	-0.2365	-0.0162	73.8	31.6	-0.0116	-0.2388	3.85	-17.03	9.26	6	3	3	0	-1.29	5.78	2.30	22
1228	-0.2400	-0.0206	99.1	167.5	-0.0126	-0.2335	6.59	-14.32	9.55	6	3	3	2	-0.54	4.67	2.78	34
1230	-0.2359	-0.0128	101.1	154.6	-0.0100	-0.2337	3.22	-10.26	9.08	6	1	3	0	-0.48	7.77	2.41	30
1231	-0.2309	-0.0102	86.0	5.2	-0.0092	-0.2377	2.18	-8.89	8.93	4	1	3	0	-0.28	4.95	2.81	28
1240	-0.2525	-0.0229	65.4	-49.3	-0.0126	-0.2389	5.35	-9.18	7.95	3	1	2	0	-0.24	4.04	2.45	18
1241	-0.2513	-0.0221	78.5	-43.5	-0.0124	-0.2390	5.40	-8.91	8.04	4	1	2	0	0.11	5.02	2.51	22
1242	-0.2501	-0.0217	104.2	-79.9	-0.0124	-0.2384	5.46	-8.42	8.20	6	1	2	0	1.09	6.99	2.62	30
1243	-0.2466	-0.0234	102.0	-37.0	-0.0144	-0.2325	5.53	-8.72	8.22	4	1	2	0	0.69	3.26	3.12	36
1250	-0.2292	-0.0124	58.0	98.4	-0.0116	-0.2336	1.80	-3.55	11.40	0	1	1	0	0.25	0.89	2.03	20
1251	-0.2278	-0.0116	70.2	91.0	-0.0106	-0.2344	1.66	-3.54	10.40	0	1	1	0	0.70	1.51	1.96	24
1260	-0.2265	-0.0137	74.3	21.5	-0.0115	-0.2274	2.28	-9.78	9.73	1	2	2	0	-0.78	1.65	2.05	30
1261	-0.2271	-0.0173	74.1	90.7	-0.0120	-0.2307	3.64	-10.91	9.75	1	2	2	1	-0.27	1.65	2.05	30
1262	-0.2203	-0.0141	86.7	14.5	-0.0120	-0.2188	1.32	-10.31	9.97	2	2	2	1	-0.20	2.30	2.07	34
1263	-0.2313	-0.0142	87.3	2.6	-0.0104	-0.2310	1.40	-10.02	8.30	2	2	2	1	0.19	2.30	2.06	34
1264	-0.2293	-0.0144	100.2	115.0	-0.0099	-0.2317	3.33	-10.24	10.06	3	2	2	1	0.25	3.01	2.02	38
1265	-0.2189	-0.0159	123.4	85.4	-0.0134	-0.2174	2.17	-9.27	10.09	1	2	2	0	0.38	2.01	2.60	58
1270	-0.2360	-0.0124	62.8	19.4	-0.0095	-0.2409	2.27	-7.72	8.51	0	1	2	0	-0.53	1.47	1.87	24
1271	-0.2332	-0.0108	88.1	9.0	-0.0087	-0.2407	1.98	-7.67	8.76	0	1	2	2	0.23	1.86	2.12	36

## 9. Molecular descriptors

	<b>25</b>	<b>27</b>	<b>34</b>	<b>35</b>	<b>37</b>	<b>40</b>	<b>42</b>	<b>43</b>	<b>44</b>	<b>46</b>	<b>47</b>	<b>48</b>	<b>51</b>	<b>55</b>	<b>56</b>	<b>57</b>	<b>60</b>
1200	3.0	0.0	0	0	1.41	0.00	1.00	0.50	0.00	0.92	0.92	0.67	4.00	22.50	11.57	0.00	0.790
1201	5.0	4.0	2	0	2.41	0.00	2.06	1.10	0.50	1.52	0.76	0.80	55.14	103.66	17.95	2.37	0.807
1202	6.0	5.3	3	0	2.91	0.00	2.56	1.46	0.78	1.58	0.68	1.00	103.66	169.35	21.00	3.76	0.809
1203	7.0	6.0	4	0	3.41	0.00	3.12	1.75	0.85	1.56	0.60	1.25	169.35	253.28	23.99	4.85	0.811
1204	5.0	4.0	2	1	2.27	0.41	1.94	1.44	0.58	1.92	0.96	0.40	56.00	104.93	17.95	0.00	0.805
1205	6.1	1.8	10	1	3.93	0.20	3.61	2.62	2.01	2.16	0.72	0.84	362.46	361.11	25.79	7.13	0.868
1210	7.1	2.4	11	1	4.43	0.20	3.12	2.02	1.22	2.42	0.67	0.75	485.80	484.06	24.38	0.96	0.937
1211	8.1	3.1	12	1	4.93	0.20	3.68	2.27	1.42	2.65	0.72	0.68	629.07	627.32	27.41	2.02	0.927
1212	9.1	3.8	13	1	5.43	0.20	3.79	2.39	1.46	2.66	0.70	0.80	793.22	791.62	33.40	1.70	0.980
1220	5.0	4.0	2	0	2.41	0.00	1.67	0.83	0.36	1.52	0.76	0.80	55.14	103.66	20.02	0.93	0.915
1221	6.0	5.3	3	0	2.91	0.00	2.23	1.08	0.54	1.58	0.68	1.00	103.66	169.35	23.43	1.91	0.897
1222	7.0	6.0	4	0	3.41	0.00	2.73	1.47	0.72	1.56	0.60	1.25	169.35	253.28	26.72	3.13	0.889
1223	8.0	7.2	5	0	3.91	0.00	3.23	1.83	1.00	1.50	0.53	1.50	253.28	356.33	29.93	4.46	0.880
1224	7.0	6.0	4	1	3.27	0.41	2.61	1.83	0.66	2.52	0.98	0.29	169.91	254.60	26.72	0.94	0.888
1225	8.1	3.1	12	1	4.93	0.20	4.27	3.01	2.15	2.05	0.62	1.28	629.07	627.32	34.90	7.78	0.920
1226	8.0	7.2	5	4	3.56	1.56	2.92	2.90	0.77	2.41	0.86	0.59	254.47	359.69	29.93	0.90	0.884
1227	7.0	6.0	4	0	3.41	0.00	2.34	1.20	0.58	1.56	0.60	1.25	169.35	253.28	27.00	1.42	0.976

	<b>25</b>	<b>27</b>	<b>34</b>	<b>35</b>	<b>37</b>	<b>40</b>	<b>42</b>	<b>43</b>	<b>44</b>	<b>46</b>	<b>47</b>	<b>48</b>	<b>51</b>	<b>55</b>	<b>56</b>	<b>57</b>	<b>60</b>
1228	9.0	8.0	6	2	4.13	0.82	3.19	2.36	0.88	1.84	0.61	1.33	357.35	481.89	33.93	1.09	0.944
1230	9.0	8.0	6	0	4.41	0.00	3.10	1.74	0.97	1.44	0.48	1.73	356.33	479.27	33.93	3.34	0.939
1231	8.0	3.7	7	1	3.85	0.20	2.55	1.46	0.90	2.16	0.77	0.84	256.63	360.65	30.52	0.73	0.954
1240	6.0	5.3	3	0	2.91	0.00	1.93	1.01	0.49	2.58	0.92	0.00	103.66	169.35	19.30	1.41	0.919
1241	7.0	6.0	4	0	3.41	0.00	2.49	1.26	0.66	2.52	0.84	0.29	169.35	253.28	22.66	2.41	0.906
1242	9.0	8.0	6	0	4.41	0.00	3.49	2.01	1.12	2.28	0.69	0.89	356.33	479.27	29.09	4.96	0.889
1243	9.0	8.0	6	4	4.06	1.56	3.18	3.08	0.89	2.42	0.73	0.75	357.03	482.38	29.09	1.39	0.888
1250	3.2	0.6	5	0	2.50	0.00	2.21	1.46	0.96	0.00	0.00	2.32	106.01	106.01	16.77	5.28	0.880
1251	4.2	1.3	6	0	3.00	0.00	2.71	1.81	1.21	0.00	0.00	2.58	172.16	172.16	19.82	6.72	0.880
1260	5.1	1.5	8	1	3.39	0.29	2.78	1.98	1.31	1.84	0.66	0.96	258.01	257.49	25.40	3.84	0.966
1261	5.1	1.5	8	1	3.39	0.29	2.78	2.00	1.27	1.84	0.66	0.96	258.01	257.49	25.40	3.98	0.960
1262	6.1	1.8	10	1	3.93	0.20	3.25	2.39	1.66	2.16	0.72	0.84	362.46	361.11	28.62	4.93	0.946
1263	6.1	1.8	10	1	3.93	0.20	3.27	2.33	1.63	2.16	0.72	0.84	362.46	361.11	28.62	5.09	0.945
1264	7.1	2.4	11	1	4.43	0.20	3.77	2.66	1.89	2.11	0.67	1.06	485.80	484.06	31.78	6.29	0.933
1265	9.1	2.5	16	9	4.81	2.70	4.28	4.95	2.17	2.37	0.68	1.09	805.05	804.18	37.97	1.72	0.915
1270	4.2	1.3	6	0	3.00	0.00	2.28	1.36	0.85	0.00	0.00	2.58	172.16	172.16	22.07	3.83	0.985
1271	6.1	1.8	10	2	3.79	0.58	3.15	2.42	1.33	2.25	0.75	0.75	363.53	362.48	28.62	2.01	0.945

## 9. Molecular descriptors

	<b>62</b>	<b>63</b>	<b>66</b>	<b>68</b>	<b>70</b>	<b>71</b>	<b>72</b>	<b>73</b>	<b>74</b>	<b>75</b>	<b>76</b>	<b>78</b>	<b>79</b>	<b>80</b>	<b>84</b>	<b>86</b>	<b>87</b>
1200	14.56	54.61	42.09	13.24	0.66	0.69	0.70	6.58	4.58	4.17	1.58	0.31	0.02	0.93	180.67	-8.20	137.32
1201	39.31	219.21	101.95	18.84	0.65	0.64	0.68	8.65	5.66	5.19	1.67	-0.77	0.63	0.29	108.82	-95.89	324.16
1202	52.83	378.48	169.54	19.73	0.63	0.65	0.70	9.92	5.94	5.12	1.94	-0.78	0.57	0.20	140.00	-72.40	276.77
1203	61.63	582.50	244.92	20.67	0.67	0.66	0.69	10.89	6.02	5.17	2.11	0.03	-0.02	0.81	94.38	-170.04	477.37
1204	67.65	140.83	72.77	20.57	0.65	0.64	0.67	7.79	6.39	5.03	1.55	0.19	0.14	-0.93	141.49	-103.22	455.04
1205	134.64	376.37	136.07	26.07	0.66	0.70	0.64	9.62	6.65	5.61	1.71	0.17	-0.07	0.87	37.09	-165.21	374.91
1210	108.45	577.06	273.62	21.82	0.63	0.60	0.64	10.53	7.11	5.14	2.05	-0.40	-0.77	-0.51	175.21	-92.70	397.34
1211	129.32	865.91	408.92	23.61	0.62	0.60	0.62	11.86	7.20	5.49	2.16	-0.47	-0.75	-0.48	135.37	-196.70	632.22
1212	130.41	1304.79	645.23	23.41	0.61	0.60	0.62	12.75	7.23	5.36	2.38	0.24	0.75	0.82	-3.74	-439.56	870.43
1220	24.34	244.39	137.45	15.43	0.68	0.75	0.69	8.86	4.70	4.38	2.02	-0.08	1.10	-0.56	2.93	-202.50	409.71
1221	30.47	419.14	198.07	16.23	0.67	0.76	0.72	10.12	4.93	4.35	2.33	0.16	1.05	-0.56	-41.11	-354.52	620.23
1222	36.47	668.69	248.39	15.97	0.70	0.76	0.73	11.41	4.74	4.42	2.58	0.17	1.06	-0.67	-76.50	-495.79	800.93
1223	43.11	1000.58	339.13	16.33	0.70	0.76	0.75	12.69	4.89	4.38	2.90	0.21	1.08	-0.52	-106.95	-513.86	786.57
1224	79.05	483.77	237.15	21.60	0.61	0.65	0.67	10.08	6.55	5.09	1.98	0.30	-0.62	0.78	33.82	-375.85	843.51
1225	141.52	982.30	401.01	25.85	0.62	0.69	0.70	11.90	7.11	5.28	2.26	-0.39	-1.08	0.32	-5.99	-438.05	861.77
1226	128.40	567.06	203.41	26.76	0.61	0.64	0.58	10.12	6.33	6.58	1.60	0.33	-0.51	0.93	141.29	-288.63	1016.20
1227	34.19	669.24	266.26	15.36	0.70	0.75	0.71	11.14	4.68	4.35	2.56	-0.01	2.51	-0.60	-152.07	-644.14	858.97

	<b>62</b>	<b>63</b>	<b>66</b>	<b>68</b>	<b>70</b>	<b>71</b>	<b>72</b>	<b>73</b>	<b>74</b>	<b>75</b>	<b>76</b>	<b>78</b>	<b>79</b>	<b>80</b>	<b>84</b>	<b>86</b>	<b>87</b>
1228	122.84	821.62	194.12	19.91	0.68	0.61	0.70	11.53	6.22	5.25	2.19	2.84	-2.14	-2.11	79.15	-370.66	956.55
1230	45.63	1346.34	435.69	15.87	0.72	0.76	0.76	13.63	4.71	4.44	3.07	0.00	-1.83	0.66	-180.48	-621.94	837.45
1231	157.15	429.49	251.68	23.60	0.63	0.70	0.71	9.79	7.05	4.81	2.04	0.27	1.08	0.57	231.31	-73.44	508.17
1240	29.89	369.39	223.35	16.58	0.66	0.75	0.70	9.58	4.99	4.41	2.17	3.95	-1.58	0.85	96.75	-137.52	426.98
1241	34.13	592.88	310.21	17.03	0.65	0.76	0.73	10.84	5.12	4.38	2.48	4.07	-1.42	0.89	4.84	-282.67	574.49
1242	47.57	1287.32	491.79	17.23	0.68	0.76	0.75	13.41	5.08	4.44	3.02	4.24	-1.31	0.87	-29.15	-395.74	733.83
1243	134.72	780.24	270.67	26.70	0.63	0.65	0.58	10.82	6.18	6.63	1.75	4.40	-0.50	1.00	138.05	-306.44	1023.92
1250	73.80	74.44	45.59	21.54	0.65	0.70	0.65	6.24	6.55	4.72	1.39	0.08	0.08	-0.97	-83.77	-125.13	185.52
1251	112.16	114.19	51.77	24.35	0.66	0.72	0.64	7.25	6.72	5.05	1.44	-0.28	0.15	0.81	73.83	-93.40	260.30
1260	114.99	222.01	77.79	24.34	0.67	0.70	0.64	7.91	6.61	5.28	1.50	-1.60	-0.03	-0.24	83.29	-194.63	560.82
1261	116.45	221.65	82.17	24.94	0.65	0.73	0.65	8.06	6.47	5.30	1.52	-1.42	-1.65	0.49	35.56	-228.93	525.64
1262	129.09	376.50	128.81	25.15	0.63	0.68	0.65	9.30	6.89	5.39	1.73	0.25	-0.65	0.14	162.26	-118.65	508.36
1263	126.45	376.50	145.62	24.48	0.63	0.68	0.68	9.42	6.92	5.19	1.82	0.00	-1.05	0.18	34.43	-264.06	596.11
1264	129.36	651.35	249.90	24.45	0.64	0.69	0.70	10.73	6.87	5.14	2.09	0.07	1.14	1.58	58.72	-262.83	639.60
1265	438.84	466.82	152.50	36.40	0.59	0.64	0.70	9.08	8.68	6.53	1.39	-1.24	-0.41	-0.68	240.83	-234.26	1414.73
1270	103.21	109.34	51.81	23.48	0.71	0.71	0.61	6.47	6.58	5.04	1.30	-1.35	-0.75	-0.01	189.23	-31.96	265.66
1271	170.59	278.95	96.81	23.44	0.63	0.62	0.69	9.03	7.32	5.17	1.75	1.08	-0.65	-0.36	244.32	-71.24	697.97

## 9. Molecular descriptors

	<b>88</b>	<b>92</b>	<b>93</b>	<b>96</b>	<b>97</b>	<b>98</b>	<b>99</b>	<b>100</b>	<b>102</b>	<b>103</b>	<b>104</b>	<b>105</b>	<b>106</b>	<b>108</b>	<b>110</b>	<b>111</b>	<b>112</b>
1200	14.84	0.63	0.072	-0.040	39.58	26.49	3.05	2.51	-1.68	0.52	1.00	13.01	12.25	168.12	0.82	10.71	7.21
1201	18.49	0.86	0.069	-0.049	50.01	60.83	4.93	21.01	-3.46	0.28	0.62	5.87	7.42	226.74	0.85	10.78	6.78
1202	13.90	0.70	0.047	-0.035	63.65	60.00	4.08	22.55	-3.04	0.37	0.77	7.43	8.40	262.44	0.89	10.83	6.78
1203	10.54	0.94	0.032	-0.033	69.31	100.83	3.46	38.34	-3.56	0.23	0.55	1.95	2.55	306.07	0.93	10.92	6.35
1204	23.61	1.36	0.091	-0.047	51.87	91.12	6.11	15.22	-3.13	0.31	0.43	0.00	2.93	222.34	0.86	10.94	6.22
1205	12.12	0.67	0.039	-0.025	54.62	65.53	3.79	43.03	-2.44	0.31	0.65	0.00	4.54	288.66	0.92	10.90	6.26
1210	23.33	0.93	0.071	-0.033	82.75	100.08	7.67	25.18	-3.52	0.23	0.43	4.67	1.61	291.96	0.89	9.69	6.52
1211	25.61	1.22	0.071	-0.039	88.47	156.07	9.18	39.96	-5.00	0.21	0.33	0.26	0.29	318.14	0.89	9.78	6.11
1212	31.59	1.15	0.084	-0.086	69.46	161.40	11.83	70.86	-12.02	0.20	0.32	0.10	0.21	287.03	0.77	8.84	6.12
1220	22.74	0.81	0.089	-0.116	32.70	52.69	5.78	31.96	-7.49	0.26	0.51	7.64	4.32	166.36	0.65	9.84	6.81
1221	21.72	0.93	0.076	-0.116	35.32	76.30	6.24	47.13	-9.57	0.24	0.43	0.17	2.36	198.61	0.69	9.86	6.43
1222	23.90	0.95	0.074	-0.114	39.36	98.07	7.68	63.95	-11.79	0.25	0.40	0.12	2.10	232.08	0.72	9.86	6.39
1223	20.24	0.78	0.058	-0.099	42.19	95.13	7.06	79.50	-12.03	0.26	0.42	0.13	2.10	268.84	0.77	9.99	6.36
1224	30.32	1.50	0.098	-0.103	53.56	145.35	9.42	43.04	-9.91	0.23	0.36	0.00	1.10	222.70	0.72	10.01	5.80
1225	20.62	1.17	0.057	-0.076	64.47	153.43	7.47	66.64	-9.92	0.25	0.45	0.18	1.46	287.66	0.79	9.91	5.85
1226	30.77	2.22	0.094	-0.097	76.62	238.01	10.07	30.40	-10.34	0.27	0.34	0.00	0.82	237.54	0.73	10.23	5.46
1227	29.80	0.71	0.098	-0.177	23.15	65.37	9.07	69.42	-16.42	0.20	0.37	0.10	1.93	164.63	0.54	8.86	6.45

	<b>88</b>	<b>92</b>	<b>93</b>	<b>96</b>	<b>97</b>	<b>98</b>	<b>99</b>	<b>100</b>	<b>102</b>	<b>103</b>	<b>104</b>	<b>105</b>	<b>106</b>	<b>108</b>	<b>110</b>	<b>111</b>	<b>112</b>
1228	30.34	1.67	0.086	-0.110	75.78	206.09	10.67	47.94	-13.61	0.17	0.23	0.00	4.49	239.16	0.68	8.87	6.12
1230	11.37	0.58	0.031	-0.070	35.59	80.15	4.23	102.71	-9.72	0.23	0.45	0.06	2.27	318.38	0.86	8.60	6.33
1231	21.73	1.34	0.067	-0.041	90.56	141.44	7.07	15.30	-4.32	0.23	0.35	2.88	1.99	282.84	0.87	8.94	5.87
1240	24.53	1.06	0.090	-0.132	50.12	78.70	6.67	23.81	-9.76	0.26	0.46	4.93	3.58	164.25	0.60	7.96	6.77
1241	21.10	0.96	0.070	-0.121	46.77	88.55	6.40	45.30	-11.18	0.22	0.43	0.16	1.99	198.26	0.65	8.10	6.39
1242	19.12	0.91	0.052	-0.104	63.36	125.38	7.09	74.17	-14.31	0.23	0.42	0.06	1.73	270.44	0.73	8.05	6.32
1243	30.25	2.09	0.088	-0.111	82.86	246.73	10.40	35.39	-13.17	0.27	0.32	0.00	0.63	234.63	0.68	8.31	5.41
1250	10.38	0.25	0.043	-0.039	18.76	14.50	2.49	38.87	-2.23	0.42	0.92	10.62	10.41	197.09	0.82	11.17	8.01
1251	12.59	0.64	0.048	-0.030	43.84	43.64	3.29	24.53	-2.06	0.34	0.76	8.29	6.30	228.87	0.88	11.04	7.18
1260	23.24	1.34	0.085	-0.097	48.41	99.71	6.33	25.73	-7.18	0.29	0.38	0.00	2.81	184.19	0.68	9.96	6.85
1261	21.04	1.08	0.076	-0.116	42.91	81.81	5.80	33.11	-8.83	0.20	0.45	4.85	5.66	186.47	0.68	9.67	7.23
1262	24.31	1.28	0.080	-0.075	70.99	118.59	7.40	21.61	-6.96	0.25	0.46	7.22	3.64	217.15	0.71	10.37	6.79
1263	22.80	1.10	0.076	-0.077	50.73	100.21	6.88	40.34	-7.00	0.24	0.45	0.00	2.96	222.69	0.74	10.06	6.43
1264	22.87	1.14	0.069	-0.080	63.97	124.16	7.54	44.62	-8.68	0.20	0.40	5.67	2.28	246.18	0.75	10.41	6.38
1265	34.03	3.28	0.095	-0.080	108.18	425.06	12.25	21.47	-10.32	0.20	0.26	0.00	0.29	277.85	0.77	9.93	4.36
1270	17.78	0.94	0.071	-0.056	54.62	58.23	4.43	7.47	-3.48	0.33	0.67	7.99	6.28	194.74	0.78	8.50	7.29
1271	31.15	2.04	0.101	-0.059	84.62	192.40	9.56	9.62	-5.57	0.17	0.36	0.04	3.22	250.61	0.82	8.46	6.84

## 9. Molecular descriptors

### 9.4 Values of molecular descriptors for tertiary amines

Table IX-23. Values of the 68 retained descriptors for tertiary amines. The numbers of the left column indicate the number of the amine. The numbers of the top line indicate the number of the descriptor.

	1	2	5	6	8	9	10	11	12	13	14	15	16	18	20	21	24
1300	-0.2191	-0.0112	52.6	293.5	-0.0110	-0.2212	1.03	-3.29	9.57	0	0	1	0	0.32	1.28	2.17	12
1301	-0.2180	-0.0105	77.4	278.3	-0.0100	-0.2217	1.00	-2.96	9.87	2	0	1	0	1.19	3.14	2.52	20
1302	-0.2175	-0.0090	77.6	270.3	-0.0087	-0.2215	1.05	-2.75	9.97	2	0	1	0	1.02	3.14	2.63	20
1310	-0.2375	-0.0186	102.2	51.4	-0.0121	-0.2251	2.17	-19.68	8.44	9	3	4	0	-1.30	6.84	3.10	36
1311	-0.2242	-0.0165	86.4	-71.5	-0.0124	-0.2233	3.81	-15.98	8.70	6	2	3	0	-0.76	4.95	2.74	28
1312	-0.2221	-0.0141	69.4	-79.4	-0.0112	-0.2232	1.74	-9.73	9.03	3	1	2	0	-0.22	3.08	2.47	20
1313	-0.2187	-0.0134	94.6	-77.1	-0.0102	-0.2205	1.62	-9.16	9.55	5	1	2	0	0.48	5.01	2.93	28
1314	-0.2137	-0.0164	91.3	-4.9	-0.0140	-0.2122	1.65	-8.23	9.59	3	1	2	0	0.36	2.44	3.55	34
1315	-0.2152	-0.0172	121.2	8.1	-0.0134	-0.2116	2.82	-15.67	9.55	7	2	3	0	0.17	4.65	3.71	46
1316	-0.2205	-0.0142	82.3	238.8	-0.0107	-0.2219	3.08	-9.99	9.16	4	1	2	0	-0.16	4.04	2.54	24
1320	-0.2228	-0.0143	100.5	207.2	-0.0116	-0.2232	1.46	-12.37	8.87	6	1	3	0	-0.35	5.93	2.55	32
1321	-0.2406	-0.0206	78.5	-44.8	-0.0129	-0.2254	5.35	-8.44	6.92	3	0	2	0	0.30	3.35	2.74	24
1330	-0.2179	-0.0097	84.1	245.9	-0.0096	-0.2217	1.03	-2.71	9.81	0	0	1	0	1.24	1.69	2.06	30
1331	-0.2189	-0.0104	71.8	258.9	-0.0108	-0.2202	1.07	-2.68	10.08	0	1	1	0	0.70	1.51	1.96	24
1340	-0.2231	-0.0134	89.1	231.9	-0.0094	-0.2246	3.22	-9.69	9.03	1	1	2	0	-0.25	1.86	2.11	36
1341	-0.2218	-0.0135	88.7	-41.3	-0.0104	-0.2235	2.15	-9.41	9.18	1	1	2	1	0.27	1.86	2.14	36

	<b>1</b>	<b>2</b>	<b>5</b>	<b>6</b>	<b>8</b>	<b>9</b>	<b>10</b>	<b>11</b>	<b>12</b>	<b>13</b>	<b>14</b>	<b>15</b>	<b>16</b>	<b>18</b>	<b>20</b>	<b>21</b>	<b>24</b>
1342	-0.2208	-0.0143	100.3	-3.7	-0.0103	-0.2247	1.77	-8.98	9.47	2	1	2	1	0.73	2.49	2.22	40
1343	-0.2223	-0.0136	88.7	-52.5	-0.0112	-0.2230	1.97	-9.05	9.66	3	1	2	0	0.24	2.30	1.97	34
1344	-0.2202	-0.0132	101.2	-101.5	-0.0106	-0.2229	1.78	-9.20	9.46	3	1	2	0	0.70	3.01	2.00	38
1345	-0.2119	-0.0147	113.6	-74.1	-0.0109	-0.2071	1.96	-5.31	9.87	3	1	2	0	1.15	3.76	2.08	42
1346	-0.2129	-0.0176	104.9	24.6	-0.0143	-0.2073	2.27	-8.92	9.70	1	1	2	2	0.27	1.46	2.03	54
1350	-0.2266	-0.0101	76.6	100.1	-0.0086	-0.2289	1.98	-6.88	7.51	0	0	2	0	0.01	1.65	1.99	30
1351	-0.2236	-0.0221	111.2	229.7	-0.0142	-0.2255	4.68	-18.56	6.90	5	2	4	1	-1.04	3.79	2.01	48
1352	-0.2345	-0.0324	110.6	-0.6	-0.0443	-0.1946	4.72	-8.91	7.53	2	0	2	0	0.96	2.87	2.12	44
1353	-0.2379	-0.0186	110.8	-93.4	-0.0118	-0.2259	5.62	-7.83	7.40	0	0	1	0	0.78	1.10	2.11	26

## 9. Molecular descriptors

	<b>25</b>	<b>27</b>	<b>34</b>	<b>35</b>	<b>37</b>	<b>40</b>	<b>42</b>	<b>43</b>	<b>44</b>	<b>46</b>	<b>47</b>	<b>48</b>	<b>51</b>	<b>55</b>	<b>56</b>	<b>57</b>	<b>60</b>
1300	4.0	0.0	0	1	1.73	0.58	1.34	1.34	0.00	0.81	0.51	1.19	23.26	56.05	14.82	0.00	0.797
1301	6.0	5.3	3	1	2.77	0.41	2.42	1.80	0.67	2.25	0.97	0.33	104.38	170.70	21.00	2.47	0.810
1302	6.0	3.0	4	1	2.81	0.29	2.49	1.49	1.08	1.92	0.83	0.67	105.07	171.36	21.00	2.33	0.810
1310	10.0	5.5	9	1	4.85	0.20	3.40	2.01	1.25	1.90	0.60	1.43	485.58	630.43	37.23	1.75	0.996
1311	8.0	5.0	6	1	3.81	0.29	2.71	1.75	0.96	2.25	0.80	0.75	255.09	359.17	30.52	1.61	0.957
1312	6.0	5.3	3	1	2.77	0.41	2.03	1.53	0.55	2.25	0.97	0.33	104.38	170.70	23.43	1.02	0.898
1313	8.0	3.7	7	1	3.85	0.20	3.18	1.75	1.31	2.16	0.77	0.84	256.63	360.65	29.93	3.17	0.882
1314	8.0	2.2	9	5	3.50	1.34	2.79	2.86	1.60	2.50	0.89	0.50	258.64	363.73	29.93	0.21	0.891
1315	11.0	4.4	12	5	5.02	1.51	3.99	3.61	1.69	2.48	0.75	0.98	632.17	800.40	40.50	1.56	0.925
1316	7.0	6.0	4	1	3.27	0.41	2.53	1.88	0.76	2.52	0.98	0.29	169.91	254.60	26.72	2.17	0.889
1320	9.0	8.0	6	1	4.27	0.41	3.10	2.14	0.92	2.42	0.81	0.75	356.63	480.42	33.93	2.19	0.940
1321	7.0	6.0	4	1	3.27	0.41	2.29	1.71	0.67	2.52	0.84	0.29	169.91	254.60	22.66	1.50	0.907
1330	5.1	1.5	8	1	3.39	0.29	3.08	2.36	1.58	1.84	0.66	0.96	258.01	257.49	22.82	6.91	0.874
1331	4.2	1.3	6	0	3.00	0.00	2.71	1.81	1.21	0.00	0.00	2.58	172.16	172.16	19.82	6.72	0.880
1340	6.1	1.8	10	2	3.79	0.58	3.15	2.53	1.69	1.50	0.50	1.50	362.69	361.57	28.62	4.02	0.944
1341	6.1	1.8	10	2	3.79	0.58	3.15	2.56	1.60	2.25	0.75	0.75	363.53	362.48	28.62	4.15	0.944
1342	7.1	1.7	13	2	4.34	0.40	3.65	2.81	2.13	2.73	0.86	0.44	488.82	487.41	31.78	5.25	0.933

	<b>25</b>	<b>27</b>	<b>34</b>	<b>35</b>	<b>37</b>	<b>40</b>	<b>42</b>	<b>43</b>	<b>44</b>	<b>46</b>	<b>47</b>	<b>48</b>	<b>51</b>	<b>55</b>	<b>56</b>	<b>57</b>	<b>60</b>
1343	6.1	1.8	10	1	3.93	0.20	3.26	2.27	1.61	2.16	0.72	0.84	360.28	359.58	28.62	6.22	0.940
1344	7.1	2.4	11	1	4.43	0.20	3.76	2.63	1.86	2.11	0.67	1.06	485.80	484.06	31.78	7.60	0.932
1345	8.1	3.1	12	1	4.93	0.20	4.26	2.98	2.11	2.05	0.62	1.28	631.37	630.49	34.90	8.98	0.925
1346	6.7	1.0	21	4	4.77	0.81	4.17	3.68	3.07	2.52	0.73	0.80	805.47	635.23	33.49	4.62	0.976
1350	5.1	1.5	8	1	3.39	0.29	2.66	1.92	1.23	1.84	0.66	0.96	258.01	257.49	25.40	4.02	0.956
1351	9.1	3.3	14	2	5.33	0.49	3.92	2.75	1.78	2.85	0.82	0.61	796.73	795.61	39.20	3.58	1.037
1352	8.1	2.7	13	2	4.83	0.49	4.07	2.88	1.95	2.65	0.76	0.68	630.16	628.27	33.49	5.90	0.943
1353	4.2	1.0	7	1	2.89	0.29	2.58	2.01	1.33	1.92	0.74	0.67	172.93	172.66	19.82	5.47	0.875

## 9. Molecular descriptors

	<b>62</b>	<b>63</b>	<b>66</b>	<b>68</b>	<b>70</b>	<b>71</b>	<b>72</b>	<b>73</b>	<b>74</b>	<b>75</b>	<b>76</b>	<b>78</b>	<b>79</b>	<b>80</b>	<b>84</b>	<b>86</b>	<b>87</b>
1300	58.26	58.27	40.82	18.81	0.66	0.71	0.71	6.56	6.19	4.28	1.53	0.06	-0.01	-0.57	167.80	-35.47	254.98
1301	69.90	284.09	132.13	21.40	0.65	0.64	0.67	9.03	6.43	5.16	1.75	0.05	-0.08	-0.47	191.82	-59.53	343.80
1302	105.54	209.76	105.40	23.51	0.67	0.67	0.66	8.42	6.63	5.27	1.60	0.15	-0.04	-0.52	171.83	-76.73	378.38
1310	326.74	700.07	259.88	29.60	0.59	0.68	0.62	10.98	7.55	5.76	1.91	-0.82	0.91	0.14	148.02	-261.42	905.38
1311	108.72	657.94	360.08	21.32	0.64	0.67	0.66	10.90	6.03	5.30	2.06	0.02	2.29	1.15	-32.27	-412.79	750.10
1312	67.64	281.36	136.99	21.63	0.63	0.64	0.63	8.76	6.44	5.24	1.67	0.03	-1.10	-0.36	98.86	-141.99	441.34
1313	222.14	413.25	196.92	31.73	0.58	0.70	0.66	9.20	8.36	5.40	1.71	-0.57	0.01	-0.92	95.08	-276.16	778.15
1314	171.65	344.76	122.35	28.90	0.66	0.66	0.63	8.69	7.05	6.25	1.39	-0.06	1.04	-0.19	218.52	-111.35	776.71
1315	545.64	583.12	208.17	40.34	0.56	0.66	0.64	9.68	9.60	6.38	1.52	-0.46	0.10	1.97	102.49	-558.65	1530.5 6
1316	73.86	491.12	223.68	20.87	0.64	0.66	0.67	10.09	6.31	5.05	2.00	0.24	-1.52	-0.97	83.01	-197.01	540.41
1320	82.67	1100.47	479.62	21.68	0.64	0.64	0.67	12.31	6.36	5.29	2.33	0.35	-0.61	-0.72	4.37	-444.18	899.19
1321	71.44	431.45	217.99	22.08	0.63	0.64	0.63	9.49	6.47	5.34	1.78	3.92	1.98	0.33	133.42	-126.18	463.57
1330	114.26	220.21	74.70	24.39	0.68	0.72	0.68	8.22	6.72	5.05	1.63	0.03	0.03	0.47	165.34	-52.92	248.60
1331	112.16	114.19	51.77	24.35	0.66	0.72	0.64	7.25	6.72	5.05	1.44	0.26	-0.19	0.81	72.93	-95.16	262.92
1340	114.78	368.50	118.40	24.31	0.68	0.71	0.68	8.99	6.69	5.09	1.77	-1.42	-0.43	-1.19	183.44	-106.84	540.02
1341	163.62	299.70	125.76	25.51	0.64	0.67	0.67	8.86	7.29	5.22	1.70	-1.28	-0.58	0.26	213.33	-63.20	436.02

	<b>62</b>	<b>63</b>	<b>66</b>	<b>68</b>	<b>70</b>	<b>71</b>	<b>72</b>	<b>73</b>	<b>74</b>	<b>75</b>	<b>76</b>	<b>78</b>	<b>79</b>	<b>80</b>	<b>84</b>	<b>86</b>	<b>87</b>
1342	228.24	373.93	137.31	29.66	0.61	0.71	0.68	9.39	8.17	5.12	1.83	0.09	1.13	-0.29	215.19	-87.08	515.51
1343	90.36	511.68	221.24	23.62	0.64	0.69	0.66	9.89	6.45	5.31	1.86	0.33	-1.22	-0.26	163.27	-89.56	369.21
1344	130.23	633.65	244.09	26.35	0.63	0.69	0.66	10.56	6.95	5.47	1.93	-0.23	1.03	0.57	63.99	-183.94	454.70
1345	233.10	608.50	207.02	30.33	0.69	0.67	0.67	9.45	7.45	6.07	1.56	0.03	-0.93	0.86	140.88	-132.70	445.90
1346	274.70	416.48	149.26	33.82	0.61	0.70	0.69	8.10	7.34	6.60	1.23	-0.53	-0.94	-0.94	145.70	-170.83	617.89
1350	105.38	216.86	71.50	23.57	0.72	0.72	0.67	7.43	6.57	5.01	1.48	1.12	-0.67	0.31	200.00	-42.77	315.56
1351	176.60	1082.04	327.77	26.92	0.63	0.68	0.67	11.14	6.90	5.72	1.95	-2.54	-1.53	-1.39	189.27	-186.91	786.74
1352	134.49	832.83	281.23	26.34	0.65	0.70	0.67	11.31	6.89	5.43	2.08	-3.11	-1.42	-0.52	124.25	-222.18	680.87
1353	76.41	161.16	64.97	21.88	0.68	0.71	0.72	7.17	6.53	4.69	1.53	-0.05	-0.06	0.55	220.41	-17.66	195.96

## 9. Molecular descriptors

	<b>88</b>	<b>92</b>	<b>93</b>	<b>96</b>	<b>97</b>	<b>98</b>	<b>99</b>	<b>100</b>	<b>102</b>	<b>103</b>	<b>104</b>	<b>105</b>	<b>106</b>	<b>108</b>	<b>110</b>	<b>111</b>	<b>112</b>
1300	24.48	0.94	0.105	-0.039	46.53	51.03	5.69	7.52	-2.09	0.12	0.28	2.75	2.18	207.36	0.89	9.75	5.71
1301	20.36	0.97	0.069	-0.030	71.20	83.42	5.97	14.91	-2.60	0.16	0.27	0.16	2.19	264.55	0.90	9.98	4.68
1302	17.85	1.04	0.062	-0.026	66.61	87.20	5.16	16.94	-2.14	0.20	0.30	0.14	0.65	265.38	0.92	10.35	4.93
1310	34.25	1.84	0.098	-0.159	87.28	225.57	12.00	35.43	-19.52	0.15	0.25	4.41	7.06	190.81	0.54	7.77	4.24
1311	30.01	1.05	0.094	-0.136	46.25	108.18	9.62	56.60	-14.00	0.17	0.29	4.88	8.39	193.00	0.60	8.56	4.92
1312	27.15	1.08	0.098	-0.094	52.15	83.00	7.53	24.74	-7.20	0.25	0.43	7.48	12.52	198.19	0.71	9.25	5.40
1313	23.43	1.53	0.072	-0.087	69.25	164.47	7.68	38.10	-9.38	0.21	0.32	0.10	0.00	255.03	0.78	9.80	4.27
1314	33.32	2.17	0.109	-0.066	80.40	203.84	10.21	13.46	-6.22	0.32	0.25	0.00	4.21	233.39	0.76	10.26	4.50
1315	39.73	2.56	0.105	-0.132	91.50	368.93	15.08	52.59	-19.08	0.22	0.26	0.00	0.00	245.15	0.65	9.07	3.27
1316	29.09	1.12	0.095	-0.088	59.70	105.26	8.92	34.26	-8.23	0.23	0.39	6.64	11.49	225.62	0.74	9.45	4.61
1320	28.00	1.25	0.077	-0.100	67.05	165.63	10.19	65.46	-13.32	0.23	0.28	0.17	8.56	272.52	0.75	8.99	5.18
1321	28.15	1.15	0.096	-0.117	62.41	98.80	8.24	23.34	-10.05	0.22	0.30	4.37	17.62	193.32	0.66	7.08	5.18
1330	15.90	0.68	0.055	-0.016	65.24	56.33	4.58	17.64	-1.29	0.16	0.38	3.60	2.87	275.80	0.96	10.08	5.40
1331	12.64	0.64	0.048	-0.032	44.51	44.31	3.34	25.25	-2.21	0.34	0.76	8.41	6.80	230.53	0.87	10.31	5.62
1340	28.66	1.43	0.094	-0.076	73.92	131.50	8.70	18.24	-7.02	0.24	0.38	0.00	10.38	237.80	0.78	9.10	5.36
1341	24.54	1.24	0.082	-0.073	77.18	112.01	7.37	13.08	-6.56	0.27	0.46	6.36	12.30	237.86	0.79	8.81	4.97
1342	23.72	1.32	0.073	-0.054	87.78	139.24	7.71	17.84	-5.74	0.25	0.40	7.34	9.10	269.18	0.83	9.67	5.23

	<b>88</b>	<b>92</b>	<b>93</b>	<b>96</b>	<b>97</b>	<b>98</b>	<b>99</b>	<b>100</b>	<b>102</b>	<b>103</b>	<b>104</b>	<b>105</b>	<b>106</b>	<b>108</b>	<b>110</b>	<b>111</b>	<b>112</b>
1343	16.44	0.88	0.052	-0.070	76.16	88.68	5.21	24.39	-7.02	0.34	0.57	9.90	17.38	252.79	0.80	9.73	5.27
1344	16.76	0.81	0.050	-0.064	66.97	90.81	5.62	45.51	-7.24	0.30	0.50	8.59	14.34	274.54	0.82	9.51	4.82
1345	17.09	0.90	0.049	-0.035	85.10	109.02	5.95	36.06	-4.29	0.29	0.47	8.34	8.36	299.33	0.86	9.97	3.70
1346	23.93	1.37	0.073	-0.077	76.84	145.69	7.80	29.36	-8.23	0.34	0.38	0.00	10.04	264.55	0.81	10.18	4.94
1350	21.15	0.99	0.077	-0.044	65.08	74.85	5.80	10.20	-3.35	0.12	0.31	2.71	7.07	238.88	0.87	7.50	5.38
1351	31.22	1.66	0.087	-0.111	99.16	216.32	11.26	30.90	-14.45	0.19	0.29	5.48	6.77	243.49	0.68	6.78	2.08
1352	16.89	1.28	0.047	-0.087	86.22	164.10	6.04	41.77	-11.18	0.33	0.28	1.10	13.23	290.23	0.81	8.24	4.34
1353	16.24	0.66	0.060	-0.016	65.78	47.94	4.37	6.52	-1.19	0.20	0.51	4.81	3.56	255.76	0.95	7.57	5.10

## 10. Nitrogen accessible surface

### 10 Nitrogen accessible surface

#### 10.1 Algorithm to calculate the nitrogen accessible surface

This algorithm have been directly inspired from calculation of accessible area of MOF according to the work of Düren *et al.* (Düren *et al.*, 2007; Düren, 2013).

```
Program accessible_surface_area
!
! This program calculates the accessible surface area by using a simple
Monte
! Carlo integration. To run the program the following files are needed:
! 1) an input file containing the name of the file containing the diameters
of
! the atoms, the name of the file containing the coordinates of the
! framework atoms, the diameter of the probe, the number of random
trials
! around each framework atom, the lenghts of the unit cells (a, b, c)
and
! the crystal density.
! 2) A file containing the diameters of the framework atoms. The program is
! written to read in a file that contains the coordinates in the format
of
! a music molecule file (compare
! http://zeolites.cqe.northwestern.edu/Music/music.html). It can easily
be
! adapted to read in any cartesian coordinates by changing the
read(10,*)
! comments.
!
! Things that you might have to change:
! - The program uses double precision (real) variables. Depending on your
! compiler, you might have to change the value for realkind (E.g. 8 is
the
! value for the intel compiler, 2 is another widely used definition)
! - The maximum number of framework atoms 5000 at the moment. Change the
value
! of max_no if your unit cells contains more atoms.
!
IMPLICIT NONE

Integer, parameter      :: realkind = 8
Integer, parameter      :: max_no = 5000
Real, parameter         :: pi=3.14159

Integer                 :: izeed
Integer                 :: N, ntypes, nsample, ncount
Integer                 :: i1, i2, i3
Integer                 :: i, j, k, ndprobe

Character(len = 3)      :: atom
Character(len = 10)     :: atomname(1:max_no), atomtype(1:max_no)
Character(len = 50)     :: atom_file, coord_file
Character(len = 10)     :: word, trashchar

Real(kind = realkind)  :: sigmatype(1:max_no), atomsigma(1:max_no)
Real(kind = realkind)  :: x(1:max_no), y(1:Max_no), z(1:max_no)
Real(kind = realkind)  :: xl, yl, zl, rho_crys
Real(kind = realkind)  :: xpoint, ypoint, zpoint
```

```

Real(kind = realkind) :: dx, dy, dz, dist2
Real(kind = realkind) :: phi, theta, costheta
Real(kind = realkind) :: dprobe,dprobe0
Real(kind = realkind) :: stotal, sfrac, sjreal, stotalreduced
Real(kind = realkind) :: trash
real(kind = realkind) :: ran0

Logical          :: deny, match
Logical          :: read_atom

!
! Seed for random number generator, change if you want to start from a
! different random number
!
iseed=23904890

! =====
! Read input file
! =====

Read(*,*) atom_file
atom_file=trim(atom_file)
Read(*,*) coord_file
coord_file=trim(coord_file)
Open(9, file=atom_file, status='old')
!Open(10, file=coord_file, status='old')

Read(*,*) dprobe0 ! diameter of the probe
Read(*,*) Nsample ! Number of samples per sphere
Read(*,*) XL, YL, ZL ! Cell parameters in A
Read(*,*) rho_crys ! chrystal density in g / cm3

! =====
! Read force field file (Dreiding)
! =====

ntypes = 0
DO
  Read(9,*) atom
  IF(Trim(atom) == 'EOF') EXIT
  ntypes = ntypes + 1
END DO

REWIND(9)

! =====
! Read coordinates file (*.pdb)
! =====

DO i = 1, ntypes
  read(9,*) atomtype(i), sigmatype(i)
  atomtype(i)=Trim(atomtype(i))
  ! write(*,*) atomtype(i), sigmatype(i)
END DO
!
! The first line of the coordinate file contains the number of molecules
!
```

## 10. Nitrogen accessible surface

```
DO ndprobe = 1,1
  dprobe = dprobe0 + (ndprobe-1)*0.1

Open(10, file=coord_file, status='old')

read_atom = .true.

read(10,*)
read(10,*)

do while (read_atom)

read(10,*)word
word=Trim(word)

if (word.eq.'ATOM') then
  backspace (10)
  read(10,*) word,i,trashchar,trashchar,i2,x(i), y(i), z(i),      &
    trash, trash,atomname(i)
  N=i
endif

if (word.eq.'TER') then
  read_atom=.FALSE.
endif

!
=====
===
! Attribute force field type to the atoms and apply periodic boundary
conditions
!
=====
===

!
! The format of the coordinate file corresponds to a music molecule file.
! Therefore there is some information that is not necessary for the surface
! area program.
! i1: continuous integer (not important for this program)
! x(i), y(i), z(i): x,y,z coordinates in Angstrom
! atomname(i): name of framework atom. Note that this is the name
!           not the chemical symbol
! trash: a real number that doesn't play a role in this program
! i2, i3: two integer numbers that don't play a role in this program
!
! Change the following read statement if you want to use a different
! file format. But ensure that you end up with the coordinates in A and
! the name of the framework atoms!
!
!
! Shift unit cell so that it lies at the origin
```

```

!
  if(x(i)<0.0) x(i)=x(i)+XL
  if(x(i)>=XL) x(i)=x(i)-XL
  if(y(i)<0.0) y(i)=y(i)+YL
  if(y(i)>=YL) y(i)=y(i)-YL
  if(z(i)<0.0) z(i)=z(i)+ZL
  if(z(i)>=ZL) z(i)=z(i)-ZL

  atomname(i)=Trim(atomname(i))
  match=.False.
  DO j = 1, ntypes
    IF(atomname(i) == atomtype(j)) Then
      atomsigma(i)=sigmatype(j)+dprobe
      match=.True.
      exit
    END IF
  END DO

  IF(.Not.match) then
!     write(*,*) 'Could not find match for atom: ', i, ' ', atomname(i)
!     write(*,*) 'The name is either read in incorrectly or does not
exist'
!     Write(*,*) 'in the list of available atoms in ', TRIM(atom_file)
      stop
    END IF
  END DO

!
!Write(*,*)
!Write(*,*) 'Calculating the accessible surface area for the following
input parameters'
!Write(*,*) '-----'
!Write(*,*) 'File with framework coordinates: ',TRIM(coord_file)
!Write(*,*) 'File with atom diameters: ', atom_file
!Write(*,*) 'Probe diameter in A: ',dprobe

close (10)

!
! Main sampling cycle
!
stotal=0.0

open (15,file='surface_vs_dprobe.dat')

DO i = 1, 1 ! Only loop for the N atom

!   write(*,*)'Testing atom',i,'Dprobe=', dprobe

  ncount=0

  DO j = 1, Nsample ! Number of random trials around each framework atom
!
! Generate random vector of length 1
!
! First generate phi 0:+2pi
!

```

## 10. Nitrogen accessible surface

```
      phi = pi - ran0(iseed)*2.0*pi
!
! Generate Theta -pi:pi
!
      costheta = 1 - ran0(iseed) * 2.0
      theta = Acos(costheta)
      xpoint = sin(theta)*cos(phi)
      ypoint = sin(theta)*sin(phi)
      zpoint = costheta

! Make this vector of length (sigma+probe_diameter)/2.0

      xpoint = xpoint*atomsigma(i)/2.0
      ypoint = ypoint*atomsigma(i)/2.0
      zpoint = zpoint*atomsigma(i)/2.0

! Translate the center of coordinate to the particle i center and apply PBC

      xpoint = xpoint + x(i)
      ypoint = ypoint + y(i)
      zpoint = zpoint + z(i)

      if(xpoint < 0.0) xpoint = xpoint + XL
      if(xpoint >= XL) xpoint = xpoint - XL
      if(ypoint < 0.0) ypoint = ypoint + YL
      if(ypoint >= YL) ypoint = ypoint - YL
      if(zpoint < 0.0) zpoint = zpoint + ZL
      if(zpoint >= ZL) zpoint = zpoint - ZL

! Test for overlap

      deny = .False.

      DO k = 1, N

          if(k == i) cycle

          dx = xpoint - x(k)
          dx = dx - XL*int(2.0*dx/XL)
          dy = ypoint - y(k)
          dy = dy - YL*int(2.0*dy/YL)
          dz = zpoint - z(k)
          dz = dz - ZL*int(2.0*dz/ZL)

          dist2 = dx*dx+dy*dy+dz*dz

          IF(sqrt(dist2) < 0.999*atomsigma(k)/2.0) THEN
              deny=.True.
              exit
          END IF
      END DO

      IF(deny) cycle

      ncount = ncount + 1

      END DO
```

```

! Fraction of the accessible surface area for sphere i
      sfrac = real(ncount) / real(Nsample)

! Surface area for sphere i in real units (A^2)
      sjreal = pi*atomsigma(i)*atomsigma(i)*sfrac

      write (15,*)dprobe,sjreal
      stotal = stotal + sjreal
    END DO
  END DO

! Converting stotal on Surface per Volume

close (15)

stotalreduced = stotal/(XL*YL*ZL)*1.E4

! Report results

Write(*,'(A30,F12.2,F6.3)')coord_file,stotal,dprobe
!Write(*,'(A,F12.2)') 'Accessible surface area in A^2: ', stotal
!Write(*,'(A,F12.2)') 'Accessible surface area per volume in m^2/cm^3: ',
stotalreduced
!Write(*,'(A,F12.2)') 'Accessible surface area per mass in m^2/g: ', &
!
      stotalreduced / rho_crys

END PROGRAM accessible_surface_area

!-----FUNCTIONS-----

FUNCTION ran0(idum)
!
! Random number generator from W.H. Press et al, Numerical Recipes in
! FORTRAN, Cambridge University Press, 1992
!
  INTEGER idum,IA,IM,IQ,IR,NTAB,NDIV
  REAL(kind = 8) ran0,AM,EPS,RNMX
  PARAMETER (IA=16807,IM=2147483647,AM=1./IM,IQ=127773,IR=2836, &
    NTAB=32,NDIV=1+(IM-1)/NTAB,EPS=1.2e-7,RNMX=1.-EPS)
  INTEGER j,k,iv(NTAB),iy

  SAVE iv,iy
  DATA iv /NTAB*0/, iy /0/
  if (idum.le.0.or.iy.eq.0) then
    idum=max(-idum,1)
    do 11 j=NTAB+8,1,-1
      k=idum/IQ
      idum=IA*(idum-k*IQ)-IR*k
      if (idum.lt.0) idum=idum+IM
      if (j.le.NTAB) iv(j)=idum
11  continue
    iy=iv(1)
  endif
  k=idum/IQ

```

## 10. Nitrogen accessible surface

```
idum=IA*(idum-k*IQ)-IR*k
if (idum.lt.0) idum=idum+IM
j=1+iy/NDIV
iy=iv(j)
iv(j)=idum
ran0=min(AM*iy,RNMX)
return
```

```
END FUNCTION ran0
```

## 10.2 Values of nitrogen accessible surface of studied monoamines

Table IX-24. Value of nitrogen accessible surface (NAS) of studied amines.

Number	NAS (Å <sup>2</sup> )	Number	NAS (Å <sup>2</sup> )	Number	NAS (Å <sup>2</sup> )
1100	8.91	1200	7.21	1300	5.71
1101	8.49	1201	6.78	1301	4.68
1102	8.17	1202	6.78	1302	4.93
1103	7.84	1203	6.35	1310	4.24
1104	8.00	1204	6.22	1311	4.92
1105	7.62	1205	6.26	1312	5.40
1106	7.82	1210	6.52	1313	4.27
1110	8.24	1211	6.11	1314	4.50
1111	7.70	1212	6.12	1315	3.27
1112	7.65	1220	6.81	1316	4.61
1113	8.46	1221	6.43	1320	5.18
1120	8.52	1222	6.39	1321	5.18
1121	8.48	1223	6.36	1330	5.40
1122	8.48	1224	5.80	1331	5.62
1123	8.49	1225	5.85	1340	5.36
1124	8.44	1226	5.46	1341	4.97
1125	8.16	1227	6.45	1342	5.23
1126	7.44	1228	6.12	1343	5.27
1127	7.75	1230	6.33	1344	4.82
1128	7.63	1231	5.87	1345	3.70
1129	7.55	1240	6.77	1346	4.94
1130	8.04	1241	6.39	1350	5.38
1131	8.52	1242	6.32	1351	2.08
1132	8.50	1243	5.41	1352	4.34
1140	8.47	1250	8.01	1353	5.10
		1251	7.18		
		1260	6.85		
		1261	7.23		
		1262	6.79		
		1263	6.43		
		1264	6.38		
		1265	4.36		
		1270	7.29		
		1271	6.84		

## 11 QSPR model

### 11.1 Justification of the proportion of data in each set

As we explain previously the value of each coefficient determined by the PLS-GLR regression for each model depend on the nature and the number of the individual used to build in the relation. Moreover, it seems obvious that results obtained in the validation and prediction set will also depend on the nature and the number of individuals which constitute them. Indeed, if the nature of molecules of the validation and prediction set is quite different of the nature of molecules used in the training set, the value of the corresponding error can be very important. This explains the trend of the distribution of the RMSEP of validation of the Figure VI-9. For all these reasons it is important to determine the proportion of data in each set.

Among the different set, the training set is by far the most important because it must take into account of the diversity of all molecules and kinetic properties to determine the coefficient of each descriptors to be a representative PLS-GLR model. For this reason we choose to use 75 % of individuals in each training set.

Then, the validation set is the second most important set because it helps to compare the performance of the modelling in different conditions and it is used to determine the QSPR model. We choose to assign around 15 % of individuals in each validation set.

Finally we select around 10 % of individuals in the prediction set. In this set of data, we only select molecules of different series which are numerous enough. For example, we never select sterically hindered amines which are only three or secondary cyclic amines. In the case of primary and secondary amines, we select the same molecules for kinetic constants  $k_1$  and  $k_2$ . Finally we try to select molecules of most various classes as possible.

## 11.2 Justification of the number of model used

It seems obvious that there is a minimal number of models to use. In order to be sure to use an optimal number of models we determine the RMSEP of the validation set for the modelling the  $\log_{10}(k_1)$  of amines which form carbamates for 250 models (black line), 500 models (blue line), 750 models (green line) and 1,000 models (red line) as indicated in Figure IX-3 (a). We notice that if we normalize the abscissa axis, all curves can be superposed as indicated in Figure IX-3 (b).

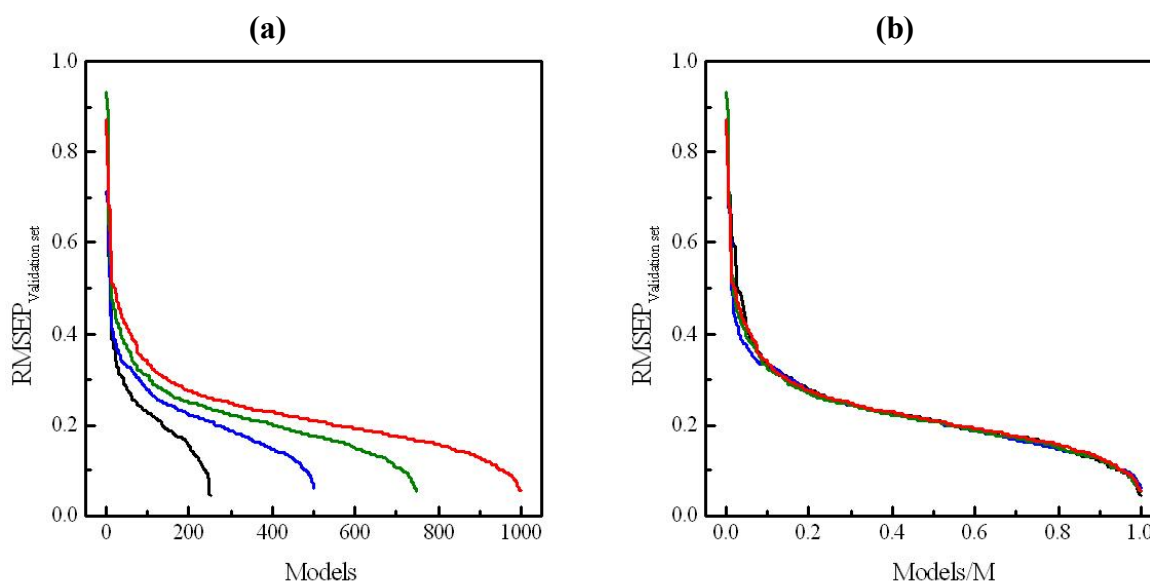


Figure IX-3. (a) Distribution of RMSEP of prediction for modelling of  $\log_{10}(k_1)$  of amines which form carbamates with 68 descriptors with 250 models (black line), 500 models (blue line), 750 models (green models) and 1,000 models (red line). (b) Same plot with normalized abscissa axis.

Corresponding RMSEP of the validation set of each series are represented as a function of the number of model used in Figure IX-4. This figure does not show obvious correlation between the average error and the number of model used. The biggest difference is between the average RMSEP of 500 and 1,000 models. This difference corresponds to  $(0.2251-0.2187) 0.0064$ . In a kinetic scale it corresponds to  $10^{0.0064}$  or 1.01 which corresponds to 1 % of deviation. In other words, the difference of performance between the "best" and the "worst" number of model lead to a difference of 1 % in the scale of kinetic constant which is not significant. This result indicates that we can use any number of model M superior to 250. We choose to use 500 models in order to have a good compromise between robustness and calculation time.

## 11. QSPR model

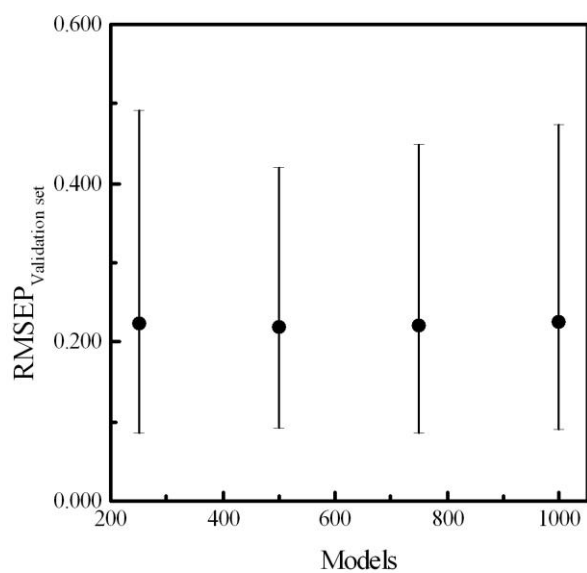


Figure IX-4. Distribution of RMSEP of the the validation set as a function of the number of models.

## 12 Coefficients of the second order models

### 12.1 Kinetic constant $k_1$ tertiary and sterically hindered amines

Table IX-25. Coefficients and coefficients of standardized variables of the second order QSPR model for  $k_1$  of tertiary and sterically hindered amines.

Descriptor	Coefficients	Coefficients of standardized variables	Weight (%)	Cumulative weight (%)
Intercept	$-5.76 \times 10^0$	-	-	-
RPCG*RotBonds	$4.45 \times 10^{-1}$	$2.42 \times 10^{-1}$	13.50	13.50
RotBonds*WNSA1	$1.66 \times 10^{-3}$	$2.29 \times 10^{-1}$	12.74	26.24
pka_exp	$1.44 \times 10^{-1}$	$1.89 \times 10^{-1}$	10.52	36.76
pka_exp^2	$8.11 \times 10^{-3}$	$1.86 \times 10^{-1}$	10.38	47.14
HOMOG^2	$-3.55 \times 10^1$	$-1.81 \times 10^{-1}$	10.10	57.24
HOMOG	$1.62 \times 10^1$	$1.81 \times 10^{-1}$	10.07	67.31
pka_exp*HOMOG	$-7.45 \times 10^{-1}$	$-1.71 \times 10^{-1}$	9.56	76.87
Dipoleaq*RPCG	$-3.42 \times 10^{-1}$	$-1.64 \times 10^{-1}$	9.15	86.02
pka_exp*RPCG	$1.34 \times 10^{-1}$	$1.13 \times 10^{-1}$	6.33	92.34
pka_exp*BETA	$-2.31 \times 10^{-5}$	$-4.02 \times 10^{-2}$	2.24	94.59
BETA^2	$-7.19 \times 10^{-7}$	$-2.76 \times 10^{-2}$	1.54	96.13
BETA	$-1.29 \times 10^{-4}$	$-2.34 \times 10^{-2}$	1.30	97.43
BETA*RPCG	$-4.80 \times 10^{-4}$	$-1.84 \times 10^{-2}$	1.03	98.46
Dipoleaq*BETA	$-4.05 \times 10^{-5}$	$-1.81 \times 10^{-2}$	1.01	99.47
BETA*RotBonds	$1.11 \times 10^{-5}$	$6.48 \times 10^{-3}$	0.36	99.83
RPCG	$2.49 \times 10^{-2}$	$1.93 \times 10^{-3}$	0.11	99.94
HOMOG*RPCG	$-6.42 \times 10^{-2}$	$-1.02 \times 10^{-3}$	0.06	99.99
RPCG^2	$2.32 \times 10^{-4}$	$1.03 \times 10^{-4}$	0.01	100.00

## 12. Coefficients of the second order models

### 12.2 Kinetic constant $k_1$ primary and secondary amines

Table IX-26. Coefficients and coefficients of standardized variables of the second order QSPR model for  $k_1$  of primary and secondary amines.

Descriptor	Coefficients	Coefficients of standardized variables	Weight (%)	Cumulative weight (%)
Intercept	$-4.72 \times 10^0$	-	-	-
Surf_acces*pk <sub>a</sub> _exp	$5.15 \times 10^{-3}$	$6.23 \times 10^{-2}$	2.50	2.50
HOMOLUMOaq <sup>2</sup>	$-1.09 \times 10^1$	$-5.96 \times 10^{-2}$	2.39	4.89
HOMOLUMOaq	$5.22 \times 10^0$	$5.96 \times 10^{-2}$	2.39	7.28
Surf_acces*ShdwAreaFrZXplane	$7.87 \times 10^{-2}$	$5.93 \times 10^{-2}$	2.38	9.65
DPSA2*RNCG	$-1.06 \times 10^{-3}$	$-5.70 \times 10^{-2}$	2.29	11.94
DPSA1*BETA	$8.14 \times 10^{-6}$	$5.58 \times 10^{-2}$	2.24	14.18
pk <sub>a</sub> _exp	$6.64 \times 10^{-2}$	$5.44 \times 10^{-2}$	2.18	16.36
pk <sub>a</sub> _exp <sup>2</sup>	$3.33 \times 10^{-3}$	$5.23 \times 10^{-2}$	2.10	18.45
Surf_acces*ShdwAreaFrYZ	$5.69 \times 10^{-2}$	$4.93 \times 10^{-2}$	1.98	20.43
Surf_acces	$4.78 \times 10^{-2}$	$4.81 \times 10^{-2}$	1.93	22.36
Surf_acces <sup>2</sup>	$3.27 \times 10^{-3}$	$4.65 \times 10^{-2}$	1.86	24.22
SssCH2*ChiralCenter	$3.06 \times 10^{-2}$	$4.24 \times 10^{-2}$	1.70	25.93
Surf_acces*Kappa1	$4.07 \times 10^{-3}$	$3.84 \times 10^{-2}$	1.54	27.47
RNCG*HAccept	$-1.54 \times 10^{-1}$	$-3.80 \times 10^{-2}$	1.52	28.99
pk <sub>a</sub> _exp*ShdwAreaFrXY	$5.78 \times 10^{-2}$	$3.67 \times 10^{-2}$	1.47	30.46
pk <sub>a</sub> _exp*ShdwAreaFrYZ	$4.50 \times 10^{-2}$	$3.62 \times 10^{-2}$	1.45	31.91
Dipoleaq*DPSA2	$-3.05 \times 10^{-5}$	$-3.49 \times 10^{-2}$	1.40	33.31
RotBonds*HAccept	$-7.07 \times 10^{-3}$	$-3.45 \times 10^{-2}$	1.38	34.69
SubgCnts0cluster*EllipsVolume	$-1.32 \times 10^{-4}$	$-3.45 \times 10^{-2}$	1.38	36.08
WPSA2*DipMomX	$-1.60 \times 10^{-4}$	$-3.35 \times 10^{-2}$	1.34	37.42
RNCG*PNSA2	$5.85 \times 10^{-4}$	$3.22 \times 10^{-2}$	1.29	38.71
Chi3cluster*EllipsVolume	$-3.66 \times 10^{-4}$	$-3.21 \times 10^{-2}$	1.29	40.00
Chi3cluster*DipMomX	$-2.71 \times 10^{-2}$	$-3.12 \times 10^{-2}$	1.25	41.25
ShdwLenLZ*RotBonds	$-3.53 \times 10^{-3}$	$-3.11 \times 10^{-2}$	1.25	42.50
Surf_acces*DPSA2	$2.37 \times 10^{-5}$	$3.09 \times 10^{-2}$	1.24	43.74
DipMomX*FPSA3	$-2.60 \times 10^{-1}$	$-2.97 \times 10^{-2}$	1.19	44.93
Surf_acces*ShdwAreaFrXY	$3.83 \times 10^{-2}$	$2.96 \times 10^{-2}$	1.19	46.12
Dipoleaq*RPCG	$-1.10 \times 10^{-1}$	$-2.94 \times 10^{-2}$	1.18	47.29
RNCG*DipMomY	$5.71 \times 10^{-2}$	$2.84 \times 10^{-2}$	1.14	48.43
SssCH2*LUMOaq	$-1.21 \times 10^0$	$-2.79 \times 10^{-2}$	1.12	49.55
SssCH2*HAccept	$7.47 \times 10^{-3}$	$2.74 \times 10^{-2}$	1.10	50.65

Descriptor	Coefficients	Coefficients of standardized variables	Weight (%)	Cumulative weight (%)
Chi3cluster*RotBonds	$-1.82 \times 10^{-2}$	$-2.63 \times 10^{-2}$	1.05	51.70
ChiralCenter*Chi2ValModif	$2.35 \times 10^{-2}$	$2.61 \times 10^{-2}$	1.05	52.75
DPSA2*RotBonds	$-1.62 \times 10^{-5}$	$-2.55 \times 10^{-2}$	1.02	53.77
SssCH2*EllipsVolume	$4.17 \times 10^{-5}$	$2.54 \times 10^{-2}$	1.02	54.79
Dipoleaq*Chi2ValModif	$-8.18 \times 10^{-3}$	$-2.54 \times 10^{-2}$	1.02	55.81
Dipoleaq*ShdwLenLZ	$-3.98 \times 10^{-3}$	$-2.43 \times 10^{-2}$	0.98	56.79
ShdwLenLZ*EllipsVolume	$-3.94 \times 10^{-5}$	$-2.42 \times 10^{-2}$	0.97	57.76
pka_exp*ShdwLenLZ	$3.34 \times 10^{-3}$	$2.42 \times 10^{-2}$	0.97	58.73
RotBonds^2	$-2.08 \times 10^{-3}$	$-2.30 \times 10^{-2}$	0.92	59.65
ChiralCenter*WPSA2	$2.81 \times 10^{-4}$	$2.30 \times 10^{-2}$	0.92	60.57
PNSA2*BETA	$1.47 \times 10^{-6}$	$2.27 \times 10^{-2}$	0.91	61.48
SssCH2*Kappa1	$1.56 \times 10^{-3}$	$2.21 \times 10^{-2}$	0.89	62.37
SubgCnts0cluster*LUMOAq	$9.83 \times 10^{-1}$	$2.21 \times 10^{-2}$	0.89	63.25
Chi3cluster*PNSA2	$1.73 \times 10^{-4}$	$2.19 \times 10^{-2}$	0.88	64.13
RNCG*RotBonds	$-2.89 \times 10^{-2}$	$-2.16 \times 10^{-2}$	0.87	65.00
RotBonds	$-1.15 \times 10^{-2}$	$-2.13 \times 10^{-2}$	0.85	65.85
HOMOLUMOAq*RPCG	$1.38 \times 10^0$	$2.12 \times 10^{-2}$	0.85	66.70
DPSA2*RPCG	$-4.36 \times 10^{-4}$	$-2.10 \times 10^{-2}$	0.84	67.54
SssCH2*RPCS	$1.62 \times 10^{-3}$	$2.07 \times 10^{-2}$	0.83	68.37
Dipoleaq*RNCG	$-4.03 \times 10^{-2}$	$-2.04 \times 10^{-2}$	0.82	69.19
Chi3cluster*Kappa1	$-4.86 \times 10^{-3}$	$-2.03 \times 10^{-2}$	0.81	70.01
HOMOLUMOAq*RotBonds	$4.49 \times 10^{-2}$	$1.96 \times 10^{-2}$	0.79	70.79
RPCS*Chi2ValModif	$4.02 \times 10^{-3}$	$1.93 \times 10^{-2}$	0.77	71.57
Surf_acces*DipMomY	$2.40 \times 10^{-3}$	$1.91 \times 10^{-2}$	0.76	72.33
WPSA2*EllipsVolume	$-9.29 \times 10^{-7}$	$-1.89 \times 10^{-2}$	0.76	73.09
Dipoleaq*ShdwAreaFrYZ	$-2.18 \times 10^{-2}$	$-1.86 \times 10^{-2}$	0.75	73.83
Chi3cluster*ShdwLenLZ	$-5.22 \times 10^{-3}$	$-1.79 \times 10^{-2}$	0.72	74.55
Dipoleaq	$-1.52 \times 10^{-2}$	$-1.77 \times 10^{-2}$	0.71	75.26
pka_exp*RPCS	$5.08 \times 10^{-4}$	$1.72 \times 10^{-2}$	0.69	75.95
Dipoleaq*SubgCnts0cluster	$-3.68 \times 10^{-3}$	$-1.72 \times 10^{-2}$	0.69	76.64
SubgCnts0cluster*PNSA2	$4.63 \times 10^{-5}$	$1.70 \times 10^{-2}$	0.68	77.32
SubgCnts0cluster*DipMomY	$1.48 \times 10^{-2}$	$1.70 \times 10^{-2}$	0.68	78.01
Dipoleaq*Chi3cluster	$-9.58 \times 10^{-3}$	$-1.69 \times 10^{-2}$	0.68	78.68
HAccept*DPSA1	$8.05 \times 10^{-5}$	$1.62 \times 10^{-2}$	0.65	79.33
ChiralCenter*SubgCnts0cluster	$1.90 \times 10^{-2}$	$1.61 \times 10^{-2}$	0.65	79.98
DPSA2^2	$-4.82 \times 10^{-8}$	$-1.57 \times 10^{-2}$	0.63	80.61

## 12. Coefficients of the second order models

Descriptor	Coefficients	Coefficients of standardized variables	Weight (%)	Cumulative weight (%)
Chi3cluster*LUMOaq	$1.98 \times 10^0$	$1.52 \times 10^{-2}$	0.61	81.21
SubgCnts0cluster*Kappa1	$-1.20 \times 10^{-3}$	$-1.49 \times 10^{-2}$	0.60	81.81
DPSA2*ShdwLenLZ	$-1.01 \times 10^{-5}$	$-1.47 \times 10^{-2}$	0.59	82.40
Dipoleaq*HOMOLUMOaq	$5.15 \times 10^{-2}$	$1.46 \times 10^{-2}$	0.59	82.99
RotBonds*ShdwAreaFrXY	$-1.18 \times 10^{-2}$	$-1.45 \times 10^{-2}$	0.58	83.57
Chi3cluster*RNCG	$-7.81 \times 10^{-2}$	$-1.43 \times 10^{-2}$	0.57	84.14
Chi3cluster*RPCG	$-9.96 \times 10^{-2}$	$-1.39 \times 10^{-2}$	0.56	84.70
Chi3cluster*DPSA2	$-2.51 \times 10^{-5}$	$-1.37 \times 10^{-2}$	0.55	85.25
Chi3cluster	$-2.45 \times 10^{-2}$	$-1.34 \times 10^{-2}$	0.54	85.79
RNCG*EllipsVolume	$-2.77 \times 10^{-4}$	$-1.31 \times 10^{-2}$	0.53	86.31
Chi3cluster*ShdwAreaFrYZ	$-3.74 \times 10^{-2}$	$-1.31 \times 10^{-2}$	0.53	86.84
Chi3cluster*HOMOLUMOaq	$1.02 \times 10^{-1}$	$1.31 \times 10^{-2}$	0.52	87.36
DPSA2*WPSA2	$-1.45 \times 10^{-7}$	$-1.24 \times 10^{-2}$	0.50	87.86
RotBonds*DPSA1	$3.60 \times 10^{-5}$	$1.20 \times 10^{-2}$	0.48	88.34
WPSA2*DipMomY	$1.09 \times 10^{-4}$	$1.18 \times 10^{-2}$	0.47	88.81
ShdwLenLZ*SubgCnts0cluster	$-1.20 \times 10^{-3}$	$-1.17 \times 10^{-2}$	0.47	89.28
SubgCnts0cluster*RPCG	$-3.06 \times 10^{-2}$	$-1.13 \times 10^{-2}$	0.45	89.73
WPSA2*PNSA2	$5.10 \times 10^{-7}$	$1.12 \times 10^{-2}$	0.45	90.18
ShdwLenLZ*BETA	$4.75 \times 10^{-5}$	$1.12 \times 10^{-2}$	0.45	90.63
Chi3cluster*WPSA2	$-7.40 \times 10^{-5}$	$-1.04 \times 10^{-2}$	0.42	91.05
pka_exp*BETA	$2.32 \times 10^{-5}$	$1.02 \times 10^{-2}$	0.41	91.45
WPSA2^2	$-4.46 \times 10^{-7}$	$-1.00 \times 10^{-2}$	0.40	91.86
DPSA2*SubgCnts0cluster	$-5.82 \times 10^{-6}$	$-9.48 \times 10^{-3}$	0.38	92.24
RNCG*Kappa1	$-1.81 \times 10^{-2}$	$-9.47 \times 10^{-3}$	0.38	92.62
Chi3cluster*Chi2ValModif	$-5.23 \times 10^{-3}$	$-9.46 \times 10^{-3}$	0.38	93.00
Chi3cluster*ShdwAreaFrXY	$-2.72 \times 10^{-2}$	$-9.39 \times 10^{-3}$	0.38	93.37
RPCG*BETA	$7.59 \times 10^{-4}$	$9.33 \times 10^{-3}$	0.37	93.75
Chi3cluster^2	$-8.08 \times 10^{-3}$	$-9.28 \times 10^{-3}$	0.37	94.12
HOMOLUMOaq*DPSA2	$1.74 \times 10^{-4}$	$9.11 \times 10^{-3}$	0.37	94.48
DipMomY^2	$-5.65 \times 10^{-3}$	$-9.05 \times 10^{-3}$	0.36	94.85
Dipoleaq*BETA	$5.00 \times 10^{-5}$	$8.80 \times 10^{-3}$	0.35	95.20
Chi3cluster*SubgCnts0cluster	$-2.74 \times 10^{-3}$	$-8.29 \times 10^{-3}$	0.33	95.53
SubgCnts0cluster^2	$-1.05 \times 10^{-3}$	$-8.19 \times 10^{-3}$	0.33	95.86
ShdwLenLZ*WPSA2	$-1.84 \times 10^{-5}$	$-7.89 \times 10^{-3}$	0.32	96.18
DPSA2	$-3.39 \times 10^{-5}$	$-7.85 \times 10^{-3}$	0.31	96.49
pka_exp*RotBonds	$-4.55 \times 10^{-4}$	$-7.73 \times 10^{-3}$	0.31	96.80

Descriptor	Coefficients	Coefficients of standardized variables	Weight (%)	Cumulative weight (%)
EllipsVolume*Chi2ValModif	$-2.42 \times 10^{-5}$	$-7.36 \times 10^{-3}$	0.30	97.10
WPSA2*SubgCnts0cluster	$-1.62 \times 10^{-5}$	$-7.16 \times 10^{-3}$	0.29	97.38
SubgCnts0cluster*Chi2ValModif	$-1.21 \times 10^{-3}$	$-6.66 \times 10^{-3}$	0.27	97.65
RNCG*SubgCnts0cluster	$-1.24 \times 10^{-2}$	$-6.20 \times 10^{-3}$	0.25	97.90
Chi3cluster*SssCH2	$-6.76 \times 10^{-3}$	$-5.43 \times 10^{-3}$	0.22	98.12
RotBonds*BETA	$-2.81 \times 10^{-5}$	$-5.14 \times 10^{-3}$	0.21	98.32
SubgCnts0cluster	$-2.77 \times 10^{-3}$	$-4.76 \times 10^{-3}$	0.19	98.51
ChiralCenter*DipMomX	$4.96 \times 10^{-3}$	$4.15 \times 10^{-3}$	0.17	98.68
Chi3cluster*DPSA1	$-2.85 \times 10^{-5}$	$-3.68 \times 10^{-3}$	0.15	98.83
DipMomX*BETA	$4.39 \times 10^{-5}$	$3.33 \times 10^{-3}$	0.13	98.96
RPCS*DipMomY	$9.73 \times 10^{-4}$	$3.27 \times 10^{-3}$	0.13	99.09
ShdwAreaFrXY <sup>2</sup>	$-7.43 \times 10^{-2}$	$-3.13 \times 10^{-3}$	0.13	99.22
ShdwAreaFrXY*BETA	$9.83 \times 10^{-5}$	$3.00 \times 10^{-3}$	0.12	99.34
ShdwAreaFrXY	$-9.54 \times 10^{-2}$	$-2.99 \times 10^{-3}$	0.12	99.46
pka_exp*Chi3cluster	$-4.25 \times 10^{-4}$	$-2.90 \times 10^{-3}$	0.12	99.58
DipMomX*RPCS	$1.31 \times 10^{-3}$	$2.77 \times 10^{-3}$	0.11	99.69
SubgCnts0cluster*DPSA1	$-6.97 \times 10^{-6}$	$-2.68 \times 10^{-3}$	0.11	99.79
Dipoleaq*SssCH2	$-3.65 \times 10^{-4}$	$-2.11 \times 10^{-3}$	0.08	99.88
ChiralCenter*DipMomY	$-2.21 \times 10^{-3}$	$-1.53 \times 10^{-3}$	0.06	99.94
BETA <sup>2</sup>	$3.62 \times 10^{-7}$	$1.50 \times 10^{-3}$	0.06	100.00

## 12. Coefficients of the second order models

### 12.3 Kinetic constant $k_2$ primary and secondary amines

Table IX-27. Coefficients and coefficients of standardized variables of the second order QSPR model for  $k_1$  of primary and secondary amines.

Descriptor	Coefficients	Coefficients of standardized variables	Weight (%)	Cumulative weight (%)
Intercept	$3.77 \times 10^0$	-	-	-
HOMOLUMOaq <sup>2</sup>	$-1.74 \times 10^1$	$-8.11 \times 10^{-2}$	5.35	5.35
HOMOLUMOaq	$8.21 \times 10^0$	$7.99 \times 10^{-2}$	5.28	10.63
HOMOLUMOaq*HOMOG	$-1.89 \times 10^1$	$-7.90 \times 10^{-2}$	5.21	15.84
HOMOLUMOaq*MolecDensity	$5.76 \times 10^0$	$7.44 \times 10^{-2}$	4.91	20.75
pka_exp*MolecDensity	$1.38 \times 10^{-1}$	$6.68 \times 10^{-2}$	4.41	25.16
pka_exp <sup>2</sup>	$4.94 \times 10^{-3}$	$6.67 \times 10^{-2}$	4.40	29.56
pka_exp	$9.37 \times 10^{-2}$	$6.58 \times 10^{-2}$	4.34	33.90
DipMomZ*FPSA2	$-4.51 \times 10^{-2}$	$-4.12 \times 10^{-2}$	2.72	36.63
HOMOLUMOaq*LUMOG	$-4.53 \times 10^1$	$-3.49 \times 10^{-2}$	2.30	38.93
HOMOLUMOaq*HAccept	$2.36 \times 10^{-1}$	$3.17 \times 10^{-2}$	2.09	41.02
HOMOLUMOaq*DipMomZ	$1.79 \times 10^{-1}$	$3.06 \times 10^{-2}$	2.02	43.05
LUMOG	$9.45 \times 10^0$	$2.88 \times 10^{-2}$	1.90	44.94
DPSA2*BalabanJX	$-5.94 \times 10^{-5}$	$-2.75 \times 10^{-2}$	1.81	46.76
pka_exp*DipMomZ	$-3.88 \times 10^{-3}$	$-2.72 \times 10^{-2}$	1.79	48.55
HOMOLUMOaq*FPSA2	$3.24 \times 10^{-1}$	$2.48 \times 10^{-2}$	1.64	50.19
DPSA2*HOMOLUMOaq	$6.09 \times 10^{-4}$	$2.33 \times 10^{-2}$	1.54	51.73
DPSA2 <sup>2</sup>	$-1.25 \times 10^{-7}$	$-2.29 \times 10^{-2}$	1.51	53.24
BalabanJX*LUMOG	$2.00 \times 10^0$	$2.22 \times 10^{-2}$	1.47	54.71
DPSA2*LUMOG	$6.41 \times 10^{-3}$	$2.17 \times 10^{-2}$	1.43	56.14
BalabanJX*MolecDensity	$-6.32 \times 10^{-2}$	$-2.09 \times 10^{-2}$	1.38	57.52
LUMOG*Kappa1	$6.39 \times 10^{-1}$	$2.07 \times 10^{-2}$	1.37	58.89
HOMOG*BalabanJX	$2.36 \times 10^{-1}$	$2.05 \times 10^{-2}$	1.35	60.24
pka_exp*RPCS	$6.82 \times 10^{-4}$	$2.05 \times 10^{-2}$	1.35	61.60
HOMOLUMOaq*BalabanJX	$2.49 \times 10^{-1}$	$2.03 \times 10^{-2}$	1.34	62.94
LUMOG*MolecDensity	$6.42 \times 10^0$	$2.03 \times 10^{-2}$	1.34	64.27
LUMOG*FPSA2	$2.91 \times 10^0$	$1.99 \times 10^{-2}$	1.31	65.59
DPSA2*MolecDensity	$-1.22 \times 10^{-4}$	$-1.97 \times 10^{-2}$	1.30	66.88
DPSA2*HAccept	$-3.51 \times 10^{-5}$	$-1.95 \times 10^{-2}$	1.29	68.17
BalabanJX <sup>2</sup>	$-1.27 \times 10^{-2}$	$-1.88 \times 10^{-2}$	1.24	69.41
DPSA2	$-1.14 \times 10^{-4}$	$-1.87 \times 10^{-2}$	1.23	70.65
DPSA2*Dipoleaq	$-2.17 \times 10^{-5}$	$-1.86 \times 10^{-2}$	1.23	71.88

Descriptor	Coefficients	Coefficients of standardized variables	Weight (%)	Cumulative weight (%)
BalabanJX	$-5.65 \times 10^{-2}$	$-1.84 \times 10^{-2}$	1.22	73.09
Kappa1*Dipoleaq	$-2.10 \times 10^{-3}$	$-1.77 \times 10^{-2}$	1.17	74.26
HAccept^2	$-8.56 \times 10^{-3}$	$-1.76 \times 10^{-2}$	1.16	75.43
DPSA2*HOMOG	$4.40 \times 10^{-4}$	$1.75 \times 10^{-2}$	1.16	76.58
EllipsVolume	$-1.65 \times 10^{-4}$	$-1.72 \times 10^{-2}$	1.13	77.72
DPSA2*DipMomZ	$-3.75 \times 10^{-5}$	$-1.69 \times 10^{-2}$	1.12	78.83
RPCS^2	$6.21 \times 10^{-4}$	$1.69 \times 10^{-2}$	1.12	79.95
pka_exp*HOMOG	$-1.11 \times 10^{-1}$	$-1.69 \times 10^{-2}$	1.12	81.07
BalabanJX*FPSA2	$-1.63 \times 10^{-2}$	$-1.68 \times 10^{-2}$	1.11	82.18
RPCS	$5.65 \times 10^{-3}$	$1.64 \times 10^{-2}$	1.08	83.26
HAccept*EllipsVolume	$-6.26 \times 10^{-5}$	$-1.62 \times 10^{-2}$	1.07	84.33
pka_exp*HOMOLUMOaq	$-8.43 \times 10^{-2}$	$-1.60 \times 10^{-2}$	1.06	85.38
Dipoleaq*EllipsVolume	$-4.04 \times 10^{-5}$	$-1.59 \times 10^{-2}$	1.05	86.43
HOMOG*LUMOG	$-1.83 \times 10^1$	$-1.55 \times 10^{-2}$	1.02	87.45
EllipsVolume*SubgCnts0cluster	$-1.19 \times 10^{-4}$	$-1.54 \times 10^{-2}$	1.02	88.47
RPCS*MolecDensity	$5.98 \times 10^{-3}$	$1.54 \times 10^{-2}$	1.01	89.49
HOMOG*FPSA2	$1.91 \times 10^{-1}$	$1.54 \times 10^{-2}$	1.01	90.50
RPCS*Dipoleaq	$2.45 \times 10^{-3}$	$1.51 \times 10^{-2}$	1.00	91.50
LUMOG^2	$-1.40 \times 10^2$	$-1.46 \times 10^{-2}$	0.97	92.46
pka_exp*LUMOG	$6.37 \times 10^{-1}$	$1.46 \times 10^{-2}$	0.96	93.43
HOMOLUMOaq*Kappa1	$4.87 \times 10^{-2}$	$1.46 \times 10^{-2}$	0.96	94.39
BalabanJX*RPCS	$2.45 \times 10^{-3}$	$1.43 \times 10^{-2}$	0.95	95.33
MolecDensity^2	$-1.70 \times 10^{-1}$	$-1.43 \times 10^{-2}$	0.94	96.28
MolecDensity	$-2.94 \times 10^{-1}$	$-1.40 \times 10^{-2}$	0.92	97.20
DPSA2*EllipsVolume	$-1.48 \times 10^{-7}$	$-1.39 \times 10^{-2}$	0.92	98.12
pka_exp*HAccept	$-2.94 \times 10^{-3}$	$-1.38 \times 10^{-2}$	0.91	99.03
LUMOG*EllipsVolume	$6.75 \times 10^{-3}$	$1.38 \times 10^{-2}$	0.91	99.94
LUMOG*Chi3cluster	$2.14 \times 10^0$	$1.33 \times 10^{-2}$	0.88	100.82
BalabanJX*SubgCnts0cluster	$-5.23 \times 10^{-3}$	$-1.33 \times 10^{-2}$	0.88	101.70
HOMOLUMOaq*RPCS	$-1.89 \times 10^{-2}$	$-1.30 \times 10^{-2}$	0.86	102.55
LUMOG*RPCS	$-3.29 \times 10^{-1}$	$-1.28 \times 10^{-2}$	0.85	103.40
BalabanJX*Chi3cluster	$-1.26 \times 10^{-2}$	$-1.24 \times 10^{-2}$	0.82	104.22
HOMOG*Chi3cluster	$1.51 \times 10^{-1}$	$1.23 \times 10^{-2}$	0.81	105.03
SubgCnts0cluster^2	$-3.84 \times 10^{-3}$	$-1.21 \times 10^{-2}$	0.80	105.84
HOMOLUMOaq*Chi3cluster	$1.47 \times 10^{-1}$	$1.21 \times 10^{-2}$	0.80	106.63
BalabanJX*EllipsVolume	$-4.55 \times 10^{-5}$	$-1.20 \times 10^{-2}$	0.79	107.43

## 12. Coefficients of the second order models

Descriptor	Coefficients	Coefficients of standardized variables	Weight (%)	Cumulative weight (%)
Kappa1*RPCS	$8.66 \times 10^{-4}$	$1.20 \times 10^{-2}$	0.79	108.22
MolecDensity*EllipsVolume	$-1.16 \times 10^{-4}$	$-1.19 \times 10^{-2}$	0.79	109.01
Chi3cluster	$-3.57 \times 10^{-2}$	$-1.19 \times 10^{-2}$	0.78	109.79
HOMOLUMOaq*EllipsVolume	$4.63 \times 10^{-4}$	$1.15 \times 10^{-2}$	0.76	110.55
Kappa1*EllipsVolume	$-1.13 \times 10^{-5}$	$-1.14 \times 10^{-2}$	0.75	111.30
pka_exp*Chi3cluster	$-3.29 \times 10^{-3}$	$-1.08 \times 10^{-2}$	0.71	112.02
FPSA2*EllipsVolume	$-9.47 \times 10^{-5}$	$-1.07 \times 10^{-2}$	0.71	112.72
SubgCnts0cluster*Chi3cluster	$-8.50 \times 10^{-3}$	$-1.06 \times 10^{-2}$	0.70	113.43
DPSA2*Kappa1	$-6.05 \times 10^{-6}$	$-1.01 \times 10^{-2}$	0.67	114.09
EllipsVolume^2	$-1.49 \times 10^{-7}$	$-9.12 \times 10^{-3}$	0.60	114.69
Chi3cluster^2	$-1.60 \times 10^{-2}$	$-8.20 \times 10^{-3}$	0.54	115.23
RPCS*EllipsVolume	$1.77 \times 10^{-5}$	$6.72 \times 10^{-3}$	0.44	115.68
Kappa1^2	$2.85 \times 10^{-4}$	$4.60 \times 10^{-3}$	0.30	115.98
RPCS*Chi3cluster	$-1.24 \times 10^{-2}$	$-4.51 \times 10^{-3}$	0.30	116.28
HOMOG*EllipsVolume	$1.40 \times 10^{-4}$	$4.40 \times 10^{-3}$	0.29	116.57
FPSA2	$-8.90 \times 10^{-3}$	$-4.33 \times 10^{-3}$	0.29	116.85
BalabanJX*Kappa1	$-1.01 \times 10^{-3}$	$-4.25 \times 10^{-3}$	0.28	117.14
RPCS*SubgCnts0cluster	$-2.08 \times 10^{-3}$	$-3.38 \times 10^{-3}$	0.22	117.36
pka_exp*DPSA2	$-1.74 \times 10^{-6}$	$-2.61 \times 10^{-3}$	0.17	117.53
Kappa1*MolecDensity	$1.60 \times 10^{-3}$	$2.27 \times 10^{-3}$	0.15	117.68
DipMomZ*RPCS	$6.43 \times 10^{-4}$	$1.59 \times 10^{-3}$	0.11	117.79
pka_exp*EllipsVolume	$5.38 \times 10^{-7}$	$6.22 \times 10^{-4}$	0.04	117.83

## 13 Results of the QSPR modelling

### 13.1 Tertiary and sterically hindered amines

Table IX-28. Experimental and modelled with the first and second order QSPR models kinetic constants  $k_1$  and  $k_2$  for tertiary and sterically hindered amines. Molecules in bold are used in the prediction set.

Molecules	Exp, $k_1$	Mod, $k_1$ (1 <sup>st</sup> order)	Mod, $k_1$ (2 <sup>nd</sup> order)
1226	$5.37 \times 10^{-7}$	$2.23 \times 10^{-7}$	$4.33 \times 10^{-7}$
1243	$4.79 \times 10^{-9}$	$4.59 \times 10^{-9}$	$8.06 \times 10^{-9}$
1265	$6.76 \times 10^{-8}$	$1.16 \times 10^{-7}$	$1.11 \times 10^{-7}$
1300	$9.44 \times 10^{-8}$	$5.80 \times 10^{-8}$	$4.76 \times 10^{-8}$
1301	$1.06 \times 10^{-7}$	$1.38 \times 10^{-7}$	$1.17 \times 10^{-7}$
1302	$9.86 \times 10^{-8}$	$1.99 \times 10^{-7}$	$2.14 \times 10^{-7}$
1310	$2.47 \times 10^{-8}$	$4.82 \times 10^{-8}$	$3.48 \times 10^{-8}$
1311	$8.92 \times 10^{-8}$	$1.38 \times 10^{-7}$	$1.29 \times 10^{-7}$
1312	$1.70 \times 10^{-7}$	$1.61 \times 10^{-7}$	$1.32 \times 10^{-7}$
1313	$5.86 \times 10^{-7}$	$6.26 \times 10^{-7}$	$5.92 \times 10^{-7}$
1314	$8.06 \times 10^{-7}$	$3.86 \times 10^{-7}$	$7.62 \times 10^{-7}$
<b>1315</b>	<b><math>2.93 \times 10^{-7}</math></b>	<b><math>5.23 \times 10^{-7}</math></b>	<b><math>7.84 \times 10^{-7}</math></b>
1316	$1.23 \times 10^{-7}$	$9.26 \times 10^{-8}$	$1.28 \times 10^{-7}$
1320	$1.00 \times 10^{-6}$	$4.37 \times 10^{-7}$	$4.24 \times 10^{-7}$
1321	$2.45 \times 10^{-9}$	$1.88 \times 10^{-9}$	$1.71 \times 10^{-9}$
1330	$6.66 \times 10^{-8}$	$1.19 \times 10^{-7}$	$8.66 \times 10^{-8}$
1331	$1.59 \times 10^{-7}$	$1.77 \times 10^{-7}$	$1.52 \times 10^{-7}$
1340	$2.77 \times 10^{-8}$	$2.18 \times 10^{-8}$	$2.28 \times 10^{-8}$
1341	$3.40 \times 10^{-8}$	$4.80 \times 10^{-8}$	$3.53 \times 10^{-8}$
1342	$2.37 \times 10^{-7}$	$1.37 \times 10^{-7}$	$1.40 \times 10^{-7}$
<b>1343</b>	<b><math>3.95 \times 10^{-7}</math></b>	<b><math>1.99 \times 10^{-7}</math></b>	<b><math>3.08 \times 10^{-7}</math></b>
1344	$2.75 \times 10^{-7}$	$4.23 \times 10^{-7}$	$3.11 \times 10^{-7}$
1345	$1.03 \times 10^{-6}$	$6.73 \times 10^{-7}$	$6.93 \times 10^{-7}$
1346	$2.02 \times 10^{-7}$	$3.10 \times 10^{-7}$	$3.15 \times 10^{-7}$

### 13. Results of the QSPR modelling

<b>1350</b>	<b><math>2.70 \times 10^{-9}</math></b>	<b><math>7.95 \times 10^{-9}</math></b>	<b><math>3.50 \times 10^{-9}</math></b>
1351	$3.43 \times 10^{-9}$	$6.45 \times 10^{-9}$	$5.22 \times 10^{-9}$
1352	$9.14 \times 10^{-9}$	$1.16 \times 10^{-8}$	$8.78 \times 10^{-9}$
1353	$2.00 \times 10^{-9}$	$1.11 \times 10^{-9}$	$1.42 \times 10^{-9}$

### 13.2 Primary and secondary amines

Table IX-29. Experimental and modelled with the first and second order QSPR models kinetic constants  $k_1$  and  $k_2$  for primary and secondary amines. Molecules in bold are used in the prediction set.

Molecules	Exp, $k_1$	Mod, $k_1$ (1 <sup>st</sup> order)	Mod, $k_1$ (2 <sup>nd</sup> order)	Exp, $k_2$	Mod, $k_2$ (1 <sup>st</sup> order)	Mod, $k_2$ (2 <sup>nd</sup> order)
1100	$4.03 \times 10^{-4}$	$6.73 \times 10^{-4}$	$4.84 \times 10^{-4}$	$5.46 \times 10^{-1}$	$1.38 \times 10^0$	$9.31 \times 10^{-1}$
1101	$2.30 \times 10^{-4}$	$3.68 \times 10^{-4}$	$3.23 \times 10^{-4}$	$3.61 \times 10^{-1}$	$2.67 \times 10^{-1}$	$2.09 \times 10^{-1}$
1102	$9.38 \times 10^{-5}$	$1.23 \times 10^{-4}$	$1.04 \times 10^{-4}$	$6.20 \times 10^{-3}$	$3.99 \times 10^{-2}$	$4.09 \times 10^{-2}$
<b>1103</b>	<b><math>9.64 \times 10^{-5}</math></b>	<b><math>1.32 \times 10^{-4}</math></b>	<b><math>1.07 \times 10^{-4}</math></b>	<b><math>7.48 \times 10^{-2}</math></b>	<b><math>6.07 \times 10^{-2}</math></b>	<b><math>7.80 \times 10^{-2}</math></b>
1104	$9.92 \times 10^{-5}$	$2.43 \times 10^{-4}$	$1.98 \times 10^{-4}$	$4.38 \times 10^{-2}$	$1.24 \times 10^{-1}$	$1.48 \times 10^{-1}$
1105	$1.61 \times 10^{-4}$	$1.12 \times 10^{-4}$	$9.17 \times 10^{-5}$	$8.86 \times 10^{-2}$	$4.86 \times 10^{-2}$	$4.97 \times 10^{-2}$
1106	$2.07 \times 10^{-5}$	$1.32 \times 10^{-5}$	$2.29 \times 10^{-5}$	$4.51 \times 10^{-3}$	$5.57 \times 10^{-3}$	$5.77 \times 10^{-3}$
1110	$1.07 \times 10^{-4}$	$1.59 \times 10^{-4}$	$1.17 \times 10^{-4}$	$1.99 \times 10^{-2}$	$3.25 \times 10^{-2}$	$4.09 \times 10^{-2}$
1111	$4.87 \times 10^{-5}$	$3.78 \times 10^{-5}$	$5.37 \times 10^{-5}$	$3.48 \times 10^{-3}$	$5.32 \times 10^{-3}$	$5.25 \times 10^{-3}$
1112	$4.80 \times 10^{-5}$	$5.56 \times 10^{-5}$	$6.87 \times 10^{-5}$	$4.94 \times 10^{-3}$	$9.35 \times 10^{-3}$	$7.98 \times 10^{-3}$
1113	$1.52 \times 10^{-4}$	$9.94 \times 10^{-5}$	$1.11 \times 10^{-4}$	$3.69 \times 10^{-2}$	$3.00 \times 10^{-2}$	$3.58 \times 10^{-2}$
1120	$9.68 \times 10^{-5}$	$1.25 \times 10^{-4}$	$8.41 \times 10^{-5}$	$1.38 \times 10^{-2}$	$9.50 \times 10^{-2}$	$8.38 \times 10^{-2}$
1121	$1.46 \times 10^{-4}$	$1.02 \times 10^{-4}$	$1.24 \times 10^{-4}$	$1.23 \times 10^{-1}$	$4.42 \times 10^{-2}$	$6.97 \times 10^{-2}$
1122	$1.82 \times 10^{-4}$	$2.05 \times 10^{-4}$	$1.94 \times 10^{-4}$	$8.08 \times 10^{-2}$	$4.97 \times 10^{-2}$	$4.90 \times 10^{-2}$
1123	$1.91 \times 10^{-4}$	$1.42 \times 10^{-4}$	$1.74 \times 10^{-4}$	$2.32 \times 10^{-1}$	$4.39 \times 10^{-2}$	$5.19 \times 10^{-2}$
1124	$9.99 \times 10^{-5}$	$1.13 \times 10^{-4}$	$9.37 \times 10^{-5}$	$2.05 \times 10^{-2}$	$3.05 \times 10^{-3}$	$4.15 \times 10^{-3}$
1125	$3.23 \times 10^{-5}$	$7.86 \times 10^{-5}$	$4.28 \times 10^{-5}$	$6.46 \times 10^{-3}$	$6.69 \times 10^{-3}$	$6.39 \times 10^{-3}$
1126	$2.81 \times 10^{-5}$	$6.58 \times 10^{-5}$	$3.31 \times 10^{-5}$	$3.45 \times 10^{-3}$	$1.52 \times 10^{-2}$	$1.69 \times 10^{-2}$
1127	$5.14 \times 10^{-6}$	$2.72 \times 10^{-6}$	$3.53 \times 10^{-6}$	$8.45 \times 10^{-4}$	$1.24 \times 10^{-3}$	$1.41 \times 10^{-3}$
1128	$7.61 \times 10^{-7}$	$1.06 \times 10^{-6}$	$8.81 \times 10^{-7}$	$2.14 \times 10^{-4}$	$1.63 \times 10^{-4}$	$1.37 \times 10^{-4}$
<b>1129</b>	<b><math>3.78 \times 10^{-7}</math></b>	<b><math>2.79 \times 10^{-7}</math></b>	<b><math>7.62 \times 10^{-7}</math></b>	<b><math>2.40 \times 10^{-5}</math></b>	<b><math>2.58 \times 10^{-5}</math></b>	<b><math>1.80 \times 10^{-5}</math></b>
1130	$6.06 \times 10^{-5}$	$4.08 \times 10^{-5}$	$6.94 \times 10^{-5}$	$2.37 \times 10^{-2}$	$8.72 \times 10^{-3}$	$1.18 \times 10^{-2}$
1131	$9.67 \times 10^{-5}$	$1.14 \times 10^{-4}$	$9.49 \times 10^{-5}$	$1.29 \times 10^{-2}$	$4.22 \times 10^{-2}$	$4.15 \times 10^{-2}$
1132	$9.43 \times 10^{-5}$	$3.03 \times 10^{-5}$	$5.41 \times 10^{-5}$	$2.74 \times 10^{-2}$	$2.22 \times 10^{-3}$	$2.21 \times 10^{-3}$
1140	$2.82 \times 10^{-5}$	$2.11 \times 10^{-5}$	$2.15 \times 10^{-5}$	$1.81 \times 10^{-3}$	$6.41 \times 10^{-4}$	$4.94 \times 10^{-4}$
1200	$5.18 \times 10^{-4}$	$2.49 \times 10^{-4}$	$5.01 \times 10^{-4}$	$2.28 \times 10^1$	$1.04 \times 10^1$	$8.79 \times 10^0$

### 13. Results of the QSPR modelling

1201	$3.61 \times 10^{-4}$	$3.18 \times 10^{-4}$	$2.75 \times 10^{-4}$	$6.48 \times 10^0$	$2.91 \times 10^0$	$2.45 \times 10^0$
<b>1202</b>	<b><math>3.48 \times 10^{-4}</math></b>	<b><math>3.26 \times 10^{-4}</math></b>	<b><math>3.38 \times 10^{-4}</math></b>	<b><math>6.86 \times 10^0</math></b>	<b><math>4.51 \times 10^0</math></b>	<b><math>4.76 \times 10^0</math></b>
1203	$1.94 \times 10^{-4}$	$1.76 \times 10^{-4}$	$1.68 \times 10^{-4}$	$1.56 \times 10^0$	$5.27 \times 10^{-1}$	$5.55 \times 10^{-1}$
1204	$1.70 \times 10^{-4}$	$9.56 \times 10^{-5}$	$1.12 \times 10^{-4}$	$1.05 \times 10^0$	$5.86 \times 10^{-1}$	$5.49 \times 10^{-1}$
1205	$1.53 \times 10^{-4}$	$1.46 \times 10^{-4}$	$1.44 \times 10^{-4}$	$1.13 \times 10^0$	$4.46 \times 10^{-1}$	$5.74 \times 10^{-1}$
1210	$8.77 \times 10^{-5}$	$1.18 \times 10^{-4}$	$1.21 \times 10^{-4}$	$1.54 \times 10^{-1}$	$1.87 \times 10^{-1}$	$2.00 \times 10^{-1}$
1211	$3.95 \times 10^{-5}$	$4.47 \times 10^{-5}$	$4.58 \times 10^{-5}$	$5.01 \times 10^{-2}$	$6.51 \times 10^{-2}$	$5.44 \times 10^{-2}$
1212	$4.95 \times 10^{-6}$	$5.35 \times 10^{-6}$	$4.78 \times 10^{-6}$	$2.70 \times 10^{-3}$	$3.60 \times 10^{-3}$	$1.95 \times 10^{-3}$
1220	$7.88 \times 10^{-5}$	$1.03 \times 10^{-4}$	$8.67 \times 10^{-5}$	$9.75 \times 10^{-2}$	$3.81 \times 10^{-1}$	$3.80 \times 10^{-1}$
1221	$2.83 \times 10^{-5}$	$4.34 \times 10^{-5}$	$3.88 \times 10^{-5}$	$4.30 \times 10^{-2}$	$9.93 \times 10^{-2}$	$7.41 \times 10^{-2}$
<b>1222</b>	<b><math>2.18 \times 10^{-5}</math></b>	<b><math>1.98 \times 10^{-5}</math></b>	<b><math>2.46 \times 10^{-5}</math></b>	<b><math>2.33 \times 10^{-2}</math></b>	<b><math>5.27 \times 10^{-2}</math></b>	<b><math>3.62 \times 10^{-2}</math></b>
1223	$2.31 \times 10^{-5}$	$2.08 \times 10^{-5}$	$2.07 \times 10^{-5}$	$3.44 \times 10^{-2}$	$4.55 \times 10^{-2}$	$3.25 \times 10^{-2}$
1224	$6.31 \times 10^{-6}$	$9.26 \times 10^{-6}$	$7.52 \times 10^{-6}$	$3.16 \times 10^{-3}$	$1.84 \times 10^{-2}$	$1.52 \times 10^{-2}$
1225	$8.67 \times 10^{-6}$	$1.05 \times 10^{-5}$	$7.79 \times 10^{-6}$	$2.30 \times 10^{-3}$	$1.55 \times 10^{-2}$	$1.22 \times 10^{-2}$
1226	$5.37 \times 10^{-7}$	$5.81 \times 10^{-7}$	$4.67 \times 10^{-7}$	-	-	-
1227	$1.85 \times 10^{-6}$	$3.41 \times 10^{-6}$	$3.76 \times 10^{-6}$	$9.86 \times 10^{-4}$	$5.92 \times 10^{-3}$	$4.17 \times 10^{-3}$
1228	$7.00 \times 10^{-7}$	$7.63 \times 10^{-7}$	$6.20 \times 10^{-7}$	$6.35 \times 10^{-4}$	$6.17 \times 10^{-4}$	$7.51 \times 10^{-4}$
1230	$1.56 \times 10^{-6}$	$3.49 \times 10^{-6}$	$1.34 \times 10^{-6}$	$5.28 \times 10^{-4}$	$3.94 \times 10^{-3}$	$3.22 \times 10^{-3}$
1231	$1.83 \times 10^{-5}$	$1.18 \times 10^{-5}$	$1.45 \times 10^{-5}$	$9.52 \times 10^{-3}$	$8.86 \times 10^{-3}$	$1.15 \times 10^{-2}$
<b>1240</b>	<b><math>1.28 \times 10^{-5}</math></b>	<b><math>3.18 \times 10^{-6}</math></b>	<b><math>5.21 \times 10^{-6}</math></b>	<b><math>3.66 \times 10^{-3}</math></b>	<b><math>2.66 \times 10^{-3}</math></b>	<b><math>3.70 \times 10^{-3}</math></b>
1241	$2.26 \times 10^{-6}$	$1.65 \times 10^{-6}$	$2.90 \times 10^{-6}$	$1.24 \times 10^{-3}$	$1.24 \times 10^{-3}$	$1.14 \times 10^{-3}$
1242	$1.84 \times 10^{-6}$	$6.95 \times 10^{-7}$	$1.44 \times 10^{-6}$	$9.96 \times 10^{-4}$	$5.27 \times 10^{-4}$	$3.40 \times 10^{-4}$
1243	$4.79 \times 10^{-9}$	$1.37 \times 10^{-8}$	$6.18 \times 10^{-9}$	-	-	-
1250	$1.14 \times 10^{-3}$	$9.69 \times 10^{-4}$	$1.03 \times 10^{-3}$	$1.33 \times 10^1$	$1.13 \times 10^1$	$9.80 \times 10^0$
1251	$9.80 \times 10^{-4}$	$7.62 \times 10^{-4}$	$1.05 \times 10^{-3}$	$3.98 \times 10^0$	$2.80 \times 10^0$	$3.33 \times 10^0$
1260	$2.20 \times 10^{-4}$	$1.09 \times 10^{-4}$	$1.19 \times 10^{-4}$	$8.31 \times 10^{-1}$	$1.21 \times 10^{-1}$	$1.53 \times 10^{-1}$
1261	$1.40 \times 10^{-4}$	$1.52 \times 10^{-4}$	$1.21 \times 10^{-4}$	$4.67 \times 10^{-1}$	$6.41 \times 10^{-2}$	$8.98 \times 10^{-2}$
1262	$5.96 \times 10^{-4}$	$3.75 \times 10^{-4}$	$4.29 \times 10^{-4}$	$3.63 \times 10^{-1}$	$5.10 \times 10^{-1}$	$7.17 \times 10^{-1}$
1263	$9.50 \times 10^{-5}$	$1.38 \times 10^{-4}$	$9.82 \times 10^{-5}$	$2.05 \times 10^{-1}$	$7.97 \times 10^{-2}$	$9.32 \times 10^{-2}$
1264	$1.05 \times 10^{-4}$	$9.38 \times 10^{-5}$	$1.69 \times 10^{-4}$	$5.14 \times 10^{-2}$	$3.88 \times 10^{-2}$	$7.59 \times 10^{-2}$

1265	$6.76 \times 10^{-8}$	$4.65 \times 10^{-8}$	$5.56 \times 10^{-8}$	-	-	-
1270	$7.44 \times 10^{-5}$	$8.54 \times 10^{-5}$	$9.98 \times 10^{-5}$	$5.81 \times 10^{-2}$	$1.68 \times 10^{-1}$	$1.56 \times 10^{-1}$
1271	$5.72 \times 10^{-5}$	$3.73 \times 10^{-5}$	$4.76 \times 10^{-5}$	$3.87 \times 10^{-2}$	$1.01 \times 10^{-2}$	$1.06 \times 10^{-2}$

## 14 French detailed summary (résumé détaillé en français)

### Contexte

Depuis plusieurs années de nombreuses études ont montré que si l'effet de serre est un phénomène naturel bénéfique et complexe qui permet de préserver une température moyenne de la planète aux alentours de 18 °C, la hausse des émissions anthropiques de gaz à effet de serre dans l'atmosphère est responsable de nombreux changements climatiques observés au cours de ces dernières décennies. Parmi les 6 principaux gaz à effet de serre (méthane, monoxyde de diazote, fluorocarbures, chlorofluorocarbures et hexafluorure de soufre et CO<sub>2</sub>) la part de dioxyde de carbone (CO<sub>2</sub>) totale représentait en 2004 plus de 76 % de la part de tous les gaz à effet de serre rapportée en CO<sub>2</sub> équivalent. Or ce gaz trouvait en 2009 son origine à plus de 61 % dans les différentes activités industrielles à source fixe (production d'électricité, métallurgie, raffinage, *etc.*)<sup>1</sup>

A l'heure actuelle, le procédé de captage du CO<sub>2</sub> en postcombustion basé sur le principe d'absorption utilisant des solvants est la technique la plus mature pour purifier les rejets gazeux industriels. Ce procédé se déroule en deux grandes étapes. Le gaz issu des fumées est d'abord injecté dans une colonne d'absorption dans laquelle une solution aqueuse d'amine circule à contre-courant. L'amine et le CO<sub>2</sub> réagissent pour former un produit, ce qui permet de relâcher dans l'atmosphère des fumées appauvries en dioxyde de carbone. Le produit de la réaction, lui, est ensuite entraîné dans une colonne de régénération qui reforme l'amine et le CO<sub>2</sub>. Ce dernier est comprimé en tête de colonne pour ensuite être stocké alors que l'amine régénérée est renvoyée dans la colonne d'absorption pour réagir à nouveau.<sup>1</sup>

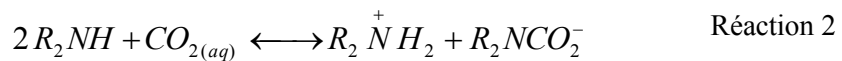
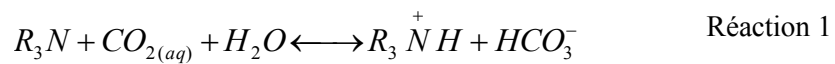
Le procédé de référence, utilisant la monoéthanolamine, fonctionne actuellement avec un coût de traitement compris entre 30 et 50 €. Ce coût s'explique principalement par trois paramètres importants du procédé de captage : la thermodynamique, la cinétique et la stabilité chimique du solvant employé.<sup>1</sup> De nombreuses études ayant été réalisées sur l'aspect thermodynamique<sup>2</sup>, nous nous intéressons dans le cadre de ce travail à la cinétique de réaction entre l'amine et le dioxyde de carbone qui intervient dans le dimensionnement de la colonne d'absorption (entre 30 et 50 % des coûts d'investissement du procédé) et l'optimisation du débit de solvant circulant et de l'énergie de régénération (entre 55 et 70 % des coûts de fonctionnement). Compte-tenu du nombre d'amines candidates pour ce procédé (plusieurs centaines) nous proposons de mettre en place une relation structure-propriété afin de prédire la cinétique de la réaction amine-CO<sub>2</sub>. Parmi la diversité d'amines qu'il est possible de trouver, nous limitons notre étude à celles constituées d'atomes de carbone, d'hydrogène, d'azote et d'oxygène.

---

<sup>1</sup> Lecomte F. *et al.* (2010) *Le captage du CO<sub>2</sub>, des technologies pour réduire les émissions de gaz à effet de serre*, Technip (ed(s)/éd.), Paris.

<sup>2</sup> Porcheron F. *et al.*, (2011), "High throughput screening of amine thermodynamic properties applied to post-combustion CO<sub>2</sub> capture process evaluation", *Energy Procedia*, **Volume 4**, Pages 15-22.

Nous présentons d'abord les différentes réactions mises en œuvre au cours du procédé de captage du CO<sub>2</sub>. Dans un premier temps nous indiquons celles qui sont considérées à l'équilibre thermodynamique à chaque instant. Il s'agit de la réaction d'autoprotolyse de l'eau, et des réactions de dissociation des ions hydrogénocarbonate, de l'acide carbonique et de l'amine protonée. Les réactions qui ont une cinétique « limitée » peuvent être regroupées en trois catégories : celles qui se produisent quelle que soit la nature de l'amine, celles qui se produisent en présence d'amines tertiaires (R<sub>3</sub>N) (Réaction 1) et celles qui se produisent avec des amines primaires ou secondaires (R<sub>2</sub>NH) (Réaction 2). Lorsque la fonction amine porte un proton labile, un carbamate (R<sub>2</sub>NCO<sub>2</sub><sup>-</sup>) peut se former. Cependant, les amines tertiaires qui ne portent pas de proton labile ne forment pas de carbamates. Pour les amines primaires, secondaires et tertiaires, plusieurs mécanismes (termoléculaire, zwitterion, acide carbamique) sont proposés dans la littérature afin d'expliquer les données expérimentales.<sup>3</sup>



Nous présentons également les moyens existants pour étudier la cinétique. D'après les données de la littérature, la technique d'écoulement bloqué (stopped-flow) est la plus adaptée pour caractériser des cinétiques ayant des vitesses de réaction variées dans l'optique de mettre en place une relation structure-propriété. Pour les auteurs utilisant la technique d'écoulement bloqué nous avons vu que la plupart d'entre eux caractérisent la constante cinétique apparente  $k_0$  avec une relation analytique. Fort de ce constat nous avons réalisé une étude approfondie des données de la littérature obtenues par la technique d'écoulement bloqué et en avons extrait les propriétés cinétiques avec la relation analytique afin de faire ressortir les principales tendances permettant de préciser les objectifs de cette étude.

## Revue critique des données de la littérature

A partir des données de la littérature, nous avons d'abord comparé la cinétique apparente des différentes amines pour une concentration donnée et vérifié que les amines primaires et secondaires réagissent généralement bien plus rapidement que les amines tertiaires. Nous avons aussi remarqué que la technique d'écoulement bloqué ne permet pas d'étudier des solutions concentrées (concentration supérieure à 1 mol.dm<sup>-3</sup>) en raison du temps de mélange qui ne permet pas de mesurer des constantes cinétiques apparentes supérieures à 500 s<sup>-1</sup>.

Nous avons ensuite étudié l'effet de la concentration sur la constante cinétique apparente de premier ordre à partir d'une loi puissance. Celle-ci a permis de mettre en évidence que toutes les amines tertiaires ont un ordre de réaction de 1 par rapport à l'amine alors que celui-ci est compris entre 1 et 2 pour les amines primaires et secondaires. Le comportement de certaines amines secondaires encombrées montre qu'il est plus judicieux de distinguer les amines qui

<sup>3</sup> Vaidya P.D. and Kenig E.Y., (2007), "CO<sub>2</sub>-alkanolamine reaction kinetics: A review of recent studies", *Chemical Engineering & Technology*, **Volume 30**, Issue 11, Pages 1467-1474.

#### 14. French detailed summary (résumé détaillé en français)

forment des carbamates et celles qui n'en forment pas. Dans le cas des amines ne formant pas de carbamates nous avons vu que la réaction entre les ions hydroxydes et le dioxyde de carbone n'est pas négligeable contrairement aux hypothèses formulées par certains auteurs. Toutefois, quelle que soit la catégorie de l'amine, à partir des données expérimentales il n'a pas été possible d'identifier le mécanisme réactionnel qui se produit. De plus nous avons prouvé qu'il y a une indétermination mathématique pour les trois constantes cinétiques du modèle du zwitterion de telle sorte qu'il est impossible de déterminer un jeu de données univoque. Ceci montre cependant la nécessité de mettre en place un modèle cinétique pour caractériser les propriétés cinétiques des amines.

Dans le cas des amines ne formant pas de carbamates, les auteurs ont obtenu une corrélation entre la constante de la réaction d'ordre 1 vis-à-vis de l'amine et la constante de dissociation de l'amine. Dans le cas des amines formant des carbamates, certains auteurs ont montré que les propriétés cinétiques sont reliées à la basicité de l'amine et à l'encombrement stérique.

Nous avons également montré l'influence de la température. Nous avons observé un phénomène de compensation sur la constante de la réaction d'ordre 1 vis-à-vis de l'amine du modèle termoléculaire. Ce phénomène montre qu'il y a une certaine corrélation entre l'enthalpie d'activation et l'entropie d'activation des molécules concernées.

A partir de ces observations nous avons défini deux objectifs pour cette étude. D'abord, il est question de mesurer la cinétique de réaction amine-CO<sub>2</sub> en phase aqueuse avec la technique d'écoulement à flux bloqué en régime dilué et à 25 °C pour des amines de structures variées. Le choix des molécules se fera de façon à améliorer notre compréhension du ou des mécanismes de réaction entre l'amine et le dioxyde de carbone. Il consiste à choisir des séries d'amines représentatives dans lesquelles on fera varier le pKa, l'encombrement ou d'autres paramètres structuraux. Outre le fait de mieux comprendre le lien existant entre les propriétés cinétiques et la structure d'une amine, ces mesures permettront de constituer une base de données. Ensuite, le but ultime est de modéliser et prédire la cinétique des amines de manière à identifier des molécules potentiellement intéressantes pour le procédé de captage du CO<sub>2</sub>. Pour cela, on utilisera les valeurs des constantes précédemment déterminées et on les reliera à leur structure grâce à des descripteurs moléculaires par un modèle statistique.

### **Méthodologie**

Avant d'étudier à proprement parler la cinétique de réaction nous avons décrit la méthode suivie. Nous avons d'abord présenté les deux techniques expérimentales utilisées : la technique d'écoulement bloqué avec détection conductimétrique et les dosages acido-basiques. La technique d'écoulement bloqué a été exclusivement utilisée pour mesurer le signal conductimétrique représentatif de l'évolution de l'avancement de la réaction amine - CO<sub>2</sub>. C'est à partir des courbes conductimétriques qui en découlent qu'il a été possible de caractériser les propriétés cinétiques de chaque amine étudiée. Les dosages acido-basiques ont été utilisés pour trois raisons : pour doser la quantité d'amine présente dans des solutions, pour doser la quantité de CO<sub>2</sub> présente dans des solutions et pour déterminer la constante de dissociation des amines.

Nous avons ensuite présenté les méthodes utilisées pour déterminer les constantes cinétiques apparentes. Pour cela nous d'abord mis en place une méthode numérique de traitement des données basée sur la mise en équation de l'ensemble des réactions qui se produisent et exprimée en activité selon le formalisme de Debye-Hückel. L'eau est utilisée comme composé de référence. Parmi tous les équilibres considérés, seule la constante de dissociation de l'amine est à déterminer expérimentalement. En résolvant le système des équations différentielles et algébriques issues des différents bilans matière, équilibres et lois cinétiques, on calcule à chaque instant la concentration des différentes espèces de manière à simuler la conductance selon la loi de Kohlrausch. Une méthode d'optimisation permet d'obtenir les constantes cinétiques apparentes intrinsèques à l'amine. Une autre méthode permet d'obtenir une expression analytique indiquée par l'Équation 1. Dans cette relation R correspond à la résistance électrique ( $\Omega$ ), G est la conductance (S), A est l'amplitude (S) de sa variation,  $k_0$  est la constante cinétique apparente ( $s^{-1}$ ) et C est la valeur de la conductance en fin de réaction lorsque le plateau est atteint (S). Pour obtenir celle-ci il faut formuler trois hypothèses et se placer dans des conditions expérimentales telles que l'on puisse les respecter. D'abord, on considère que les valeurs des conductibilités molaires sont constantes au cours de la réaction, ensuite on s'assure que l'amine est en large excès par rapport au dioxyde de carbone, enfin on considère comme négligeable la contribution cinétique de réactions parallèles ou inverses.

$$\frac{1}{R(t)} = G(t) = -A \times \exp(-k_0 \times t) + C \quad \text{Équation 1}$$

Comme le modèle numérique nécessite un certain nombre de paramètres qui sont autant de sources d'erreurs potentielles nous avons choisi d'utiliser le modèle analytique autant que possible dès lors que les hypothèses le permettant sont vérifiées. Dans ce sens nous avons développé deux nouvelles méthodes expérimentales pour faciliter l'interprétation des données cinétiques issues de la technique d'écoulement bloqué. La première pré-acidifie les solutions aqueuses d'amines avec de l'acide chlorhydrique afin de maîtriser voire neutraliser la contribution cinétique des ions hydroxydes. La seconde pré-acidifie les solutions aqueuses d'amines avec de l'acide formique afin d'améliorer le signal conductimétrique obtenu.

A partir des constantes cinétiques apparentes, les propriétés cinétiques de chaque amine ont été caractérisées à partir d'un modèle semi-empirique basé sur l'observation des données expérimentales. Ce modèle est indiqué par l'Équation 2. Dans cette équation  $k_1$  est une constante d'ordre 1 vis-à-vis de l'amine que l'on détermine quelle que soit la nature de l'amine,  $k_2$  est une constante d'ordre 2 vis-à-vis de l'amine que l'on détermine uniquement lorsque les amines forment des carbamates, et  $\varepsilon$  est le résidu d'une réaction parallèle qui n'aurait pas été complètement retiré qui survient uniquement pour les amines qui ne forment pas de carbamates.

$$k_0 = k_1 \cdot [Am] \cdot [H_2O] + k_2 \cdot [Am]^2 + \varepsilon \quad \text{Équation 2}$$

#### 14. French detailed summary (résumé détaillé en français)

Pour l'étude, 25 amines primaires, 24 amines secondaires acycliques, 10 amines secondaires acycliques et 25 amines tertiaires ont été choisies de manière à être les plus représentatives possible des molécules envisageables pour le procédé de post-combustion. Nous avons également pu étudier 3 multi-amines.

### **Interprétation des données expérimentales**

A partir de la méthode présentée dans la partie précédente, nous avons caractérisé les constantes cinétiques des 89 molécules étudiées. Nous avons réalisé la comparaison des données en raisonnant par degré de substitution. D'abord nous avons pu vérifier que les amines tertiaires sont les amines les plus lentes. Comme cela a été observé dans la littérature, nous avons vérifié que la basicité des amines est le facteur qui influe de manière prépondérante sur la constante cinétique de la réaction d'ordre 1 par rapport à l'amine. Nous avons pu mettre ce phénomène en évidence pour d'autres séries de molécules que celles des alkanolamines. Nous avons également montré que l'accessibilité des fonctions alcools a un rôle important dans la cinétique. Celui-ci peut s'expliquer par la possibilité des liaisons hydrogène favorisant l'interaction avec la molécule d'eau dans le mécanisme réactionnel. Nous avons aussi identifié trois amines secondaires fortement encombrées qui ne forment pas de carbamates et suivent les tendances obtenues par les amines tertiaires. Cela confirme le fait que le degré de substitution de l'amine n'est pas une façon convenable de différencier les mécanismes. Enfin le rôle de l'effet inductif donneur (+I) ou attracteur (-I) a été observé.

Ensuite nous nous sommes intéressés aux amines primaires. Nous avons montré que pour des séries d'amines ayant le même encombrement stérique, les constantes cinétiques  $k_1$  et  $k_2$  sont corrélées linéairement à la basicité de l'amine. De la même façon, pour une série de molécules ayant la même basicité, on remarque que les constantes cinétiques  $k_1$  et  $k_2$  varient de manière continue avec l'encombrement stérique du doublet de l'azote de la fonction amine. Pour estimer cet encombrement stérique, nous avons utilisé les constantes de Taft qui peuvent être employées pour une série de molécules avec une mono-substitution. Nous avons également remarqué que l'effet de la basicité sur les constantes cinétiques est plus ou moins marqué selon l'encombrement stérique et inversement. On remarque que la contribution de la déprotonation par l'amine, réaction d'ordre 2 par rapport à l'amine est importante est d'autant plus marquée que la basicité est importante et que l'encombrement stérique est faible.

Nous avons aussi étudié les amines secondaires acycliques. Nous avons d'abord remarqué qu'il y a une nette différence de comportement entre une amine primaire et la méthylamine secondaire correspondante à cette amine primaire. Cette différence s'explique par l'apport électronique et stérique de ce groupement méthyle. On remarque que ce changement de degré de substitution, avec l'ajout d'un groupement méthyle, augmente la constante cinétique pour une amine primaire très basique ( $pK_a$  d'environ 10,5) alors qu'il diminue la constante cinétique pour une amine primaire faiblement basique ( $pK_a$  d'environ 8,0). Cependant, dans la majorité des cas, les amines secondaires acycliques ont de meilleures propriétés cinétiques que les amines primaires. De même que pour les amines primaires, nous avons observé des tendances linéaires entre les constantes cinétiques  $k_1$  et  $k_2$  et la basicité ou l'encombrement de

séries de molécules. Nous avons également pu constater que la basicité et l'encombrement ont un effet couplé sur les constantes cinétiques des amines secondaires acycliques.

Nous avons aussi observé que la basicité peut être reliée de manière linéaire avec les constantes cinétiques d'une série d'amines secondaires cycliques. Nous avons pu voir l'effet de l'encombrement sur ces propriétés cinétiques.

Finalement l'étude des multi-amines nous a permis de les classer parmi deux catégories : d'une part celles qui sont symétriques et d'autre part celles qui sont asymétriques. Les deux multi-amines symétriques étudiées ont une constante cinétique de l'ordre de deux fois celle de la mono-amine correspondante, cette observation pouvant être liée à un effet entropique. En effet, comme la molécule est symétrique, il y a deux sites identiques qui peuvent potentiellement réagir et donc, deux fois plus de chances d'obtenir un contact actif. Dans le cas de la seule molécule asymétrique étudiée, celle-ci se comporte comme une mono-amine ayant une fonction amine équivalente.

## **Modèle Q.S.A.R.**

A partir des données obtenues précédemment nous avons mis en place un modèle structure-propriété pour les mono-amines étudiées. Un modèle a été réalisé avec la constante cinétique  $k_1$  pour les amines qui ne forment pas de carbamates. Deux modèles ont été ensuite réalisés, un pour la constante  $k_1$  pour les amines primaires et secondaires et un autre pour la constante  $k_2$  pour les amines qui forment des carbamates. Pour cela nous avons d'abord décrit les molécules sous forme de descripteurs moléculaires qui nous informent de leurs différents paramètres électroniques et géométriques. Ainsi nous avons d'abord calculé 108 descripteurs génériques théoriques par modélisation moléculaire. Une étude de corrélation statistique basée sur une classification hiérarchique ascendante a permis de conserver les 66 qui sont les moins corrélés entre eux. Nous avons en sus introduit un nouveau descripteur que nous avons appelé « surface accessible de l'azote ». Ce descripteur est également issu de modélisation moléculaire. Enfin nous avons ajouté comme descripteur la valeur expérimentale du  $pK_a$ .

Ensuite nous avons montré que la prédiction ne peut être réalisée qu'avec les valeurs logarithmiques des constantes cinétiques du fait la dispersion de nos données s'étendant sur 9 décades. Nous avons justifié d'utiliser une régression de type Partial Least Square (PLS) pour relier ces 68 descripteurs à la propriété à modéliser. Parmi les différents algorithmes, nous avons choisi la Partial Least Square Generalised Linear Regression (PLS-GLR) qui permet de construire le modèle uniquement à partir des descripteurs les plus corrélés à la propriété. Nous utilisons trois jeux de données : une base d'apprentissage, une base de validation et une base de prédiction. Pour chaque modèle nous attribuons 77 % des molécules à la base d'apprentissage, 14 % à celles de la base de validation et 9 % à celles de la base de prédiction. La base d'apprentissage permet de déterminer les coefficients d'un modèle. La base de validation permet de déterminer la performance du modèle établi sur la base d'apprentissage. Comme les coefficients du modèle PLS-GLR dépendent des molécules utilisés dans l'apprentissage nous justifions le fait d'utiliser 500 modèles pour chaque modélisation dans lesquels on répartit de manière aléatoire les molécules de la base d'apprentissage et de

#### 14. French detailed summary (résumé détaillé en français)

validation. Le « modèle QSPR » correspond au modèle dont la valeur de chaque coefficient est égale à la moyenne des coefficients des 500 modèles PLS-GLR obtenus à partir des 500 bases d'apprentissage. La base de prédiction, qui est utilisée pour estimer la performance du modèle QSPR, comporte toujours les mêmes molécules. L'optimisation de chaque « modèle QSPR » est réalisée en choisissant le modèle optimal en termes de nombre de descripteurs et de l'ordre du modèle. Le critère d'optimisation est la moyenne de l'erreur de prédiction de la base de validation des 500 modèles.

A partir de cette méthode, nous avons déterminé pour chaque prédiction deux modèles : un modèle de premier ordre, un peu moins précis mais qui compte « peu » de descripteurs du premier ordre, et un modèle du second ordre qui compte d'avantage de termes du second ordre. Dans le cas de la modélisation de la constante  $k_1$  pour les amines qui ne forment pas de carbamates, nous avons obtenu une erreur relative moyenne de prédiction de 107 % pour le modèle de premier ordre (7 descripteurs de premier ordre) et de 73 % pour le modèle de second ordre (18 termes de second ordre issu de 7 descripteurs). Nous avons montré que le faible nombre de molécules dans la base de prédiction utilisé pour évaluer l'erreur du modèle peut être une source de sous estimation des performances de ce modèle. Dans le cas de la prédiction de la constante  $k_1$  des amines primaires et secondaires, on obtient une erreur relative moyenne de prédiction de 31 % pour le modèle de premier ordre (16 descripteurs de premier ordre) et de 37 % pour le modèle de second ordre (123 termes de second ordre issus de 29 descripteurs). Dans le cas de la prédiction de  $k_2$ , on obtient une erreur relative moyenne de prédiction de 43 % pour le modèle de premier ordre (16 descripteurs de premier ordre) et de 23 % pour le modèle de second ordre (89 termes de second ordre de 16 descripteurs).

Finalement une discussion de la corrélation de certains descripteurs dans le cas des amines qui ne forment pas de carbamates est réalisée. Ensuite la performance de la surface accessible de l'azote, qui est un descripteur clef, est étudiée plus en profondeur en montrant ces forces et ces faiblesses et en proposant des voies d'amélioration de celui-ci notamment par des méthodes de calcul de modélisation dynamique.

A Nancy, le 03 octobre 2013

No étudiant : 31001171

COUCHAUX GABRIEL  
30 grande rue de la guillotière  
69007 LYON

Monsieur,

Par décision en date du 01 octobre 2013, vous avez été autorisé à présenter en soutenance vos travaux en vue de l'obtention du diplôme :

**Doctorat Génie des Procédés et des Produits**

La soutenance aura lieu le 24 octobre 2013 à 14h00 à l'adresse suivante :

Amphi A ENSIC - 1, rue Grandville 54000 NANCY

La soutenance sera publique.

Je vous prie d'agréer, Monsieur, l'expression de mes salutations distinguées.

Le Président



Pierre MUTZENHARDT

---

**TITRE:** Relation Structure-Propriété pour la Cinétique de la Réaction Amine-CO<sub>2</sub> en Solutions Aqueuses

---

**RESUME:** Les objectifs de ces travaux portent sur l'étude et la compréhension de la cinétique de réaction amine-CO<sub>2</sub> et de la mise en place d'un modèle structure-propriété prédictif. Cette démarche est adaptée au grand nombre d'amines envisageables pour le procédé

Dans un premier temps nous avons étudié cinq types d'amines (primaires, secondaires acycliques, secondaires cycliques, tertiaires et multi-amines) représentatifs des molécules candidates. Parmi ces molécules deux comportements peuvent être distingués : d'une part les amines qui forment des carbamates et d'autre part celles qui n'en forment pas. Des mesures réalisées sur des solutions diluées d'amine, à différentes concentrations et à 25°C, obtenues par la technique d'écoulement bloqué ont permis de caractériser la cinétique intrinsèque de chacune des 87 amines par deux constantes cinétiques. Pour chaque type d'amine les principaux facteurs structuraux, électroniques et géométriques influant sur la cinétique de réaction ont été identifiés.

Un modèle statistique utilisant des descripteurs moléculaires pour décrire les différents paramètres de chaque amine a permis d'établir une relation structure –propriété pour différentes constantes cinétiques. Un nouveau descripteur de l'encombrement stérique de l'azote a également été calculé pour décrire les résultats et prédire la réactivité des amines.

---

**TITLE:** Structure-Property Relationship for Kinetics of Reaction between Amines and Carbon Dioxide in Aqueous Solutions

---

**ABSTRACT:** The post-combustion process by amine scrubbing is currently the most mature to reduce carbon dioxide emissions from industry. However, if there are numerous demonstrators, the investment and operating cost of this process are still too important to develop it in a large scale. The kinetics of reaction between the amine and the carbon dioxide is one of the major factor which influence the costs.

The objectives of this work are to study and understand the kinetics of the amine-CO<sub>2</sub> reaction and to set up of a predictive structure-property model. This approach is adapted to the large number of possible amines which can be candidates for the process.

In a first time we study five kinds of amines (primary, acyclic secondary, cyclic secondary, tertiary and multi-amines) representatives of candidate molecules. Among those molecules, two behaviours can be distinguished: one the one hand amines which form carbamates and on the other hand those which do not form carbamates. Measurements have been realised at 25 °C in diluted solutions by stopped-flow technique to characterize the intrinsic kinetics of each of the 87 studied amines using two kinetic constants. For each kind of amine, the main structural factors, electronic and geometric, which impact the kinetics of reaction have been identified.

Then, from a statistical model using molecular descriptors to describe the different parameters of each amine, a structure-property relationship has been set up with the different kinetic constants. A descriptor of the steric hindrance has been developed.

---

**DISCIPLINE:** Génie des procédés et des produits, physico-chimie

---

**MOTS-CLES :** Cinétique – Amines – Dioxyde de carbone – Ecoulement bloqué – QSPR

---

**KEYWORDS :** Kinetics – Amines – Carbon dioxide – Stopped-flow – QSPR

---

**INTITULE ET ADRESSE DU LABORATOIRE :** IFP Energies nouvelles  
Direction Catalyse et Séparation / Département Sséparation  
Rond-Point de l'échangeur de Solaize, BP3, 69360 Solaize